# IDENTIFICATION OF GENES INVOLVED IN MACROPHAGE ACTIVATION AND EFFECTOR FUNCTIONS AGAINST INTRACELLULAR PATHOGENS

**Anita Ruth Schwegmann**

*B.Sc., B.Sc.(Hons.), M.Sc.*

**Thesis submitted to the University of Cape Town in fulfilment of the degree**

**Doctor of Philosophy**

**Division of Immunology**

**Faculty of Health Sciences**

**University of Cape Town**

**December 2006**

## DECLARATION

I Anita Ruth Schwegmann, hereby declare that the work on which this thesis is based, is my original work (except where acknowledgements indicate otherwise) and that neither the whole work or any part thereof has been, or is submitted for another degree in this or any other University.

I empower the University of Cape Town to reproduce for the purpose of research either the whole or any portion of the contents in any manner whatsoever.

Signed by candidate
Anita Ruth Schwegmann

## DEDICATION

This thesis is dedicated to my mother, my sister Leonie and to my beloved Nikolay.

**ACKNOWLEDGMENTS**

I am deeply grateful to the people below who have helped shaped and develop my scientific career. My sincerest gratitude goes to my supervisor, Professor Frank Brombacher for his guidance and motivation during this work. His knowledge and vision have been a great inspiration. My co-supervisor, Dr. Reto Guler, has been an excellent teacher who made sure my hands were never idle at the bench! His enthusiasm and guidance has been a great source of encouragement. A special thanks to Dr. Guler for his help with the animal work and critical reading of this dissertation.

Thank you to Dr. A Cutler for his help with FACs. Thanks to Berenice Arendse and Alexandra Hölscher who have taught me all the animal work and cell culture I know today. Thank you to Lizette Fick, Marilyn Tyler and Zoë Lotz for their excellent histology services. To the University of Cape Town Animal Unit staff, Reagon Pieterse, Wendy Green and Erica Smit, thank you for breeding and genotyping the mice. Thank you to Mohammed Jaffer at the Electron Microscope Unit for his excellent training in transmission electron microscopy. Thank you to Tsion Tabhara and Rachel van Dyk at the capar Microarray Unit for their guidance in performing the microarray experiments.

The support of the National Bioinformatics Network (NBN) has been invaluable during this thesis. I would like to thank the NBN for giving me the opportunity to attend their training courses and for their excellent advice and support. I would especially like to thank Dr. Cathal Seioghe and Dr. Wiesner Vos for their help with microarray statistics and analysis in R. A very special thank you goes to Professor Dan Jacobson, whose mentorship has guided me through challenging circumstances.

My deepest gratitude to Dr. De'Broski Herbert, Dr. Sharon Nicholson-Herbert, Professor Dan Jacobson, Dr. Barbara Nurse, Dr. Christoph Hölscher, Mark Barkhuizen, Marquard Simpson and Alexandra Höslcher who always made time to listen me and for their kind words of encouragement. Thank you to my colleagues in the lab for making the lab a vibrant and stimulating environment. A very special thank you goes to Dhuraiyah and Gloria for their excellent administrative support. Thank you to George and Sandra fro keeping the lab so clean and organized.

I would like to acknowledge and thank the Stella and Paul Lowenstein Trust, Medical Research Council, National Research Foundation and National Bioinformatics Network for their financial support during the course of this study.

I would like to send a special thank you to my family, especially my mother, father and sisters Leonie and Cecilia for their unwavering love, support and belief in me. Also, thank you to Uncle John, Aunty Cecilia and my cousin Mark for taking such a genuine interest in my scientific career. Thank you to all my friends who have persevered with me in travelling down the very long road to a Ph.D. Thank you Tigger for being such an angel. A special thanks to Cisca Vennard for cooking countless meals while I was writing up the thesis. My deepest love and gratitude go to Nikolay Mavrodinov who has encouraged and supported me unconditionally.

Lastly, I would like to give acknowledgement to all the mice that were sacrificed in the name of science.

## TABLE OF CONTENTS

## LIST OF FIGURES

**CHAPTER 1**

**CHAPTER 2**



**CHAPTER 3**



**CHAPTER 4**

**CHAPTER 5**

## LIST OF TABLES

## LIST OF SYMBOLS AND ABBREVIATIONS

| Abbreviation or Symbol | Description |
|---|---|
| Agtr1a | Angiotensin receptor 1 |
| AIDS | Acquired immunodeficieny syndrome |
| App | Amyloid beta (A4) precursor protein |
| Arf6 | ADP-ribosylation factor 6 (Arf6) |
| ARHGAP10 | Rho GTPase activating protein 10 |
| aRNAs | amplified RNA |
| Arp2/3 | Actin related protein 2/3 complex |
| ASC | Apoptosis-associated speck-like protein containing a C-terminal caspase recruitment domain |
| Bglap1 | Bone gamma carboxyglutamate protein 1 |
| BK(Ca) | Large conductance, calcium- and voltage-activated potassium channels |
| BMDMs | Bone marrow derived macrophages |
| BR-PLC | Broad range PLC |
| C/EBPa, | C/CAAT Enhancer Binding Protein alpha |
| C/EBPb | C/CAAT Enhancer Binding Protein beta |
| C/EBPβ | C/CAAT/enhancer binding protein beta |
| C1q | Complement component C1q |
| C1qR | C1q complement receptor |
| C3bi | Complement component C3bi |
| CARD | Caspase-recruitment domain |
| Cbl | Casitas B-lineage lymphoma |
| CCR2 | CC-chemokine receptor 2 |
| CDC42 | Cell division cycle 42 homolog |
| cDNA | complementary DNA |
| CFU | Colony Forming Unit |
| Chat | Choline acetyltransferase |
| CIAS1 | Cold autoinflammatory syndrome 1 |
| CLECSF9 | C-type lectin domain family 4 member e |
| Col4a2 | Alpha-2 type IV collagen |
| CR3 | Complement receptor 3 |
| Csrp2 | Cysteine and glycine-rich protein 2 |
| DAG | Diacylglycerol |
| DC | Dendritic cell |
| DE | Differentially expressed |
| DNA | Deoxyribonucleic acid |
| Dscr6 | Down syndrome critical region homolog 6 |
| E-cadherin | Epithelial cadherin |
| ECM | Extracellular matrix |
| EEA1 | Early endosome antigen 1 |
| ELISA | Enzyme linked immuno-sorbant assay |
| Elk-1 | ETS oncogene family 1 |
| Ena/VASP | Enabled homologue/vasodilator-stimulated phosphoprotein |
| Ep300 | E1A binding protein p300 |
| ER | Endoplasmic reticulum |
| ERK | Extracellular-signal-regulated kinase |

| | |
|---|---|
| F- actin | Filamentous actin |
| FcγR | Fc gamma receptor |
| FDR | False Discovery Rate |
| FOI | Frequency of incorporation |
| Fth1 | Ferritin heavy chain 1 |
| FWER | Family Wise Error Rate |
| G | Glycine |
| Gab1 | Growth factor receptor bound protein 2-associated protein 1 |
| G-actin | Globular actin |
| GAGs | Glucosaminoglycans |
| GAPs | GTPase activating proteins |
| GAS | IFN-γ-activated site |
| GATE | IFN-γ-activated transcriptional element |
| gC1qR | Globular C1q complement receptor |
| G-CSF | Granulocyte colony stimulating factor |
| G-CSFR | G-CSF Receptor |
| GDIs | Guanine diphosphate (GDP) dissociation inhibitors |
| GEFs | Guanine nucleotide exchange factors |
| GM-CSF | Granulocyte-macrophage colony stimulating factor |
| Gna13 | Guanine nucleotide binding protein alpha 13 |
| Gnb2rs1 | Guanine nucleotide binding protein beta 2 related sequence 1 |
| GO | Gene Ontology |
| GPCRs | G protein coupled receptors (GPCRs) |
| GPI | Glycosylphosphatidylinositol |
| Gpr119 | G-protein coupled receptor 119 |
| Grp78 | Glucose-regulated protein 78 kDa |
| Gsn | Gelsolin |
| H | hour |
| H28 | Histocompatibility 28 |
| Hbb-b1 | Hemoglobin beta adult major chain |
| HGF | Hepatocyte growth factor |
| HIV | Human Immunodeficieny Virus |
| Hmga2 | High mobility group AT-hook 2 |
| Hmox1 | Heme oxygenase 1 |
| HPFV | High Power Field View |
| Hpt | *L. monocytogenes* sugar-uptake system |
| HSPG | Heparan sulfate proteoglycans |
| i.p. | Intraperitoneal |
| ICSBP | Interferon Consensus Sequence Binding Protein |
| iE-DAP | Dipeptide or tripeptide motifs |
| Ifi202b | Interferon activated gene 202B |
| Ifi203 | Interferon activated gene 203 |
| Ifi35 | Interferon-induced protein 35 |
| Ifit2 | Interferon-induced protein with tetratricopeptide repeats 2 |
| Ifit3 | Interferon-induced protein with tetratricopeptide repeats 3 |
| IFN-α | Interferon beta |
| IFN-β | Interferon alpha |
| IFN-γ | Interferon gamma |
| IFN-γR | IFN-γ Receptor |
| IgG | Immunoglobulin G |

| | |
|---|---|
| IKDCs | Interferon producing killer DCs |
| IKK | NF-kB (IκB)-kinase |
| IKKγ | NF-kB (IκB)-kinase-γ |
| IL-1 | Interleukin 1 |
| IL-12 | Interleukin 12 |
| IL-12p35 | Interleukin 12 p35 subunit |
| IL-18bp | Interleukin 18 binding protein |
| Il1f6 | Interleukin 1 family member 6 |
| IL-1β | Interleukin 1 beta |
| IL-6 | Interleukin 6 |
| IL6st | Interleukin 6 signal transducer |
| InlA | Internalin A |
| InlB | Internalin B |
| iNOS | inducible Nitric Oxide Synthase |
| Ins2 | Insulin II |
| Insr | Insulin receptor |
| IRF2 | Interferon regulatory factor 2 |
| IP | Inositol-Phosphate |
| IP3 | Inositol-1,4,5-P3 |
| IRAK | Interleukin-1 receptor (IL-1R)-associated kinase |
| Irs1 | Insulin receptor substrate 1 |
| ISGF3γ | IFN-stimulated gene factor 3 gamma |
| ISRE | IFN-stimulated response element |
| IVT | in vitro transcription |
| LAMP1 | Lysosomal membrane glycoprotein 1 |
| LAMP2 | Lysosomal membrane glycoprotein 2 |
| LBPA | Lysobisphosphatidic acid |
| Lipg | Endothelial lipase |
| LLO | Listeriolysin O |
| LOWESS | Locally weighted scatter plot smoothing |
| LplA1 | Lipoate protein ligase A1 |
| LPS | Lipopolysaccharide |
| LRR | Leucine rich repeat domain |
| Lrrc6 | Leucine rich repeat containing 6 |
| mAb | Monoclonal antibodies |
| MAPK | Mitogen-activated protein kinase |
| MCH class I | Major Histocompatibility (MHC) complex class I |
| MCP-1 | Monocyte chemoattractant protein 1 |
| MDP | Muramyl dipeptide |
| MEK1 | MAP kinase 1 |
| MEKK1 | MAP kinase kinase 1 |
| MHC class II | Major Histocompatibility (MHC) complex class II |
| MIAME | Minimum Information about Microarray Experiments (MIAME) |
| min | minute |
| MIP-1a | Macrophage inflammatory protein 1 alpha |
| MIP-1b | Macrophage inflammatory protein 1 beta |
| MIP-2 | Macrophage inflammatory protein 2 |
| MLK3 | Mixed-lineage kinase 3 |
| MLKs | Mixed-lineage kinases |
| MOI | Multiplicity of infection |

| | |
|---|---|
| Mpa2 | Macrophage activation 2 |
| MPR | Mannose-6-phosphate receptor |
| Muc1 | Mucin 1 |
| Myd88 | Myeloid differentiation primary response gene 88 |
| NACHT | NAIP, CIITA, HET-E and TP1 |
| NALP | NACHT (domain present in NAIP, CIITA, HET-E and TP1)-LRR - and pyrin-domain-containing (NALP) proteins |
| NF-kB | Nuclear Factor kappa B |
| NFκB(p50) | NFκB subunit p50 |
| NF-κB(p65) | NFκB subunit p65 |
| NK | Natural killer |
| NLRs | Nucleotide-binding oligomerization domain (NOD)-like receptors |
| NOD | Nucleotide-binding and oligomerization domain |
| NOD1 | Nucleotide-binding and oligomerization domain protein 1 |
| NOD2 | Nucleotide-binding and oligomerization domain protein 2 |
| Nqo1 | NADPH dehydrogenase quinone 1 |
| N-WASP | Neural Wiskott–Aldrich syndrome protein (WASP) f |
| p.i. | post infection |
| PAMPs | Pathogen associated molecular patterns |
| PDH | Pyruvate-dehydrogenase |
| PEST | P for proline, E for glutamic acid, S for serine and T for threonine |
| PGN | Peptidoglycan |
| PI(3)P | Phosphatidylinositol 3-phosphate |
| PI3K | Phosphatidylinositol 3-kinase |
| PIP2 | PI-4,5-P2 |
| PI-PLC | Phosphatidylinositol (PI) specific PLC |
| PKA | Protein kinase A |
| PKC | Protein kinase C |
| PKCβI | PKC beta I isoform |
| PKCβII | PKC beta II isoform |
| PKCδ | PKC delta isoform |
| PLC | Phospholipase C |
| PLD | Phospholipase D |
| PMT | Photo-multiplier-tube |
| PRRs | Pattern recognition receptors |
| Ptk2b | Protein tyrosine kinase 2 beta |
| PYR | Pyrin domain |
| Rab5a | Ras related protein 5a |
| Rab9 | RAS oncogene family member 9 |
| Rabgef1 | RAB guanine nucleotide exchange factor 1 |
| Rabep1 | RAB GTPase binding effector protein 1 |
| Rac1 | Very small GTP binding RAS-related C3 botulinum substrate 1 |
| RANTES | Regulated on activation normal T cell expressed and secreted |
| Rasa1 | RAS p21 protein activator 1 |
| RD1 | Regulatory domain 1 |
| RD2 | Regulatory domain 2 |
| Rgs5 | G-protein signalling 5 |
| RIP2 | Receptor-interacting protein 2 |
| RNA | Ribonucleic acid |
| RNI | Reactive nitrogen intermediates |

| | |
|---|---|
| ROI | Reactive oxygen intermediates |
| rRNA | ribosomal RNA |
| RSK | Ribosomal S6 kinase |
| RT-PCR | Reverse Transcription Polymerase Chain Reaction |
| Runx1 | Runt related transcription factor 1 |
| SAA1 | Serum amyloid A1 |
| SAA2 | Serum amyloid A2 |
| SAA3 | Serum amyloid A3 |
| SAGE | Serial analysis of gene expression |
| SCID | Severe Combined Immunodeficient |
| SD | Standard deviation |
| SEM | Standard error mean |
| Shc | Src homology 2 domain-containing transforming protein C1 |
| Slc25a3 | Solute carrier family 25 member 36 |
| Smyd4 | SET and MYND domain containing 4 |
| SNARE | Soluble N-ethylmaleimide-sensitive factor-attachment protein receptor |
| Sp1 | Trans-acting transcription factor 1 |
| Src | Rous sarcoma oncogene |
| Srf | Serum response factor |
| STAT3 | Signal transducer and activator of transcription 3 |
| Stx7 | Syntaxin 7 |
| SSH-PCR | Suppressive subtractive PCR |
| TAB1 | Transforming-growth-factor-β activated kinase 1 (TAK1) binding protein 1 |
| TAB2 | Transforming-growth-factor-β activated kinase 1 (TAK1) binding protein 2 |
| TAK1 | Transforming-growth-factor-β activated kinase 1 |
| TAP1 | Transporter 1 ATP-binding cassette, sub-family B member 1 |
| TAP2 | Transporter 2, ATP-binding cassette, sub-family B member 2 |
| Tcfap2c | Transcription factor AP-2 gamma |
| TH1 | T Helper 1 |
| TipDCs | TNF- and iNOS-producing DCs |
| TIR | Toll/IL-1 receptor |
| Tirap | TIR domain-containing adaptor protein |
| TLRs | Toll-like receptors |
| TNF | Tumor necrosis factor |
| TNFRp55 | TNF Receptor p55 |
| Tnfrsf5 | TNF receptor superfamily member 5 |
| Tnfsf10 | TNF ligand superfamily member 10 |
| Tnfsf4 | TNF ligand superfamily member 4 |
| TRAF6 | TNF receptor associated factor 6 |
| TRAM | Toll-like receptor adaptor molecule 2 |
| TRIF | Toll-like receptor adaptor molecule 1 |
| Tsc2 | Tuberous sclerosis 2 |
| UDPGT | UDP-glucuronosyltransferase |
| Vamp3 | Vesicle-associated membrane protein 3 |
| VAP33 | Vascular adhesion protein 33 |
| Vcam1 | Vascular cell adhesion molecule 1 |
| V1rB4 | Vomeronasal 1 receptor B4 |
| W | Tryptophan |
| WAVE | WASP verprolin homologue |
| Ywhag | 14-3-3 gamma |

## PUBLICATIONS

In addition to the work in this dissertation, the candidate has made significant contributions to the publications below:

Schwegmann, A.R., Guler, R., Cutler, A., Arendse, B., Kottman, A.H., Ryan, G., Hide, W., Leitges, M., Seioghe, C. and Brombacher, F. PKCδ is critical for confinement of *Listeria* within macrophage phagosomes. JEM *submitted.*

Herbert DR, Hölscher C, Mohrs M, Arendse B, Schwegmann A, Radwanska M, Leeto M, Kirsch R, Hall P, Mossmann H, Claussen B, Förster I, Brombacher F. Alternative Macrophage Activation Is Essential For Survival During Schistosomiasis And Down modulates T Helper 1 Responses And Immunopathology. Immunity. 2004; 20:623-635.

Hölscher C, Arendse B, Schwegmann A, Myburgh E, Brombacher F. Impairment of alternative macrophage activation delays cutaneous leishmaniasis in nonhealing BALB/c mice. J Immunol. 2006 Jan 15;176(2):1115-21.

Herbert, D.R., Leeto, M., Marillier, R., Joseph, S., Myburgh, E., Arendse, B., Schwegmann, A., Hünig, T. and Brombacher, F. (2006). Infection-induced increase of Foxp3+ T regulatory cells in the gut is dependent upon CD4+ T cell independent IL-4Ra expression and protects against ileitis during schistosomiasis. J. Immunol. Submitted

Leeto, M., Herbert, D.R., Mariller, R., Schwegmann, A., Fick, L. and Brombacher, F. (2006). CD4+ T cell specific IL-4Ra deficient mice develop exacerbated granulomatous pathology in response to S. mansoni eggs. J. Immunol. In revision

## ABSTRACT

This dissertation addressed the hypothesis that macrophages have an alternative killing mechanism that is independent of superoxide and nitric oxide but dependent on IFN-γ, TNF and C/EBPβ. Since the mechanism and the genes involved in this alternative pathway are mostly unknown, the aim of this dissertation was to identify these macrophage effector genes and to functionally characterize their role during infection utilizing gene deficient mouse models. Since mice deficient for C/EBPβ (C/EBPβ$^{-/-}$) expressed normal levels of IFN-γ and TNF during *Listeria monocytogenes* infection, the macrophage effector genes involved in confinement and killing of *L. monocytogenes* were postulated to be downstream of C/EBPβ. Furthermore, C/EBPβ$^{-/-}$ mice are highly susceptible *L. monocytogenes* due to impaired listericidal activity. Comparison of the gene expression profiles of WT and C/EBPβ$^{-/-}$ macrophages infected with *L. monocytogenes* was postulated to increase the probability of identifying these effector genes, which would be differentially expressed between the two groups. Comparative gene expression profiling by DNA microarrays between *L. monocytogenes* infected WT and C/EBPβ$^{-/-}$ macrophages, successfully identified 1268 genes to be differentially expressed between the two groups. A focussed functional clustering strategy reduced the number of candidate genes to 220. PKCδ was selected for further study since it was involved in humoral defense, immune signalling, production of superoxide, regulation of transcription and may be putatively transcriptionally regulated by C/EBPβ. Furthermore, PKCδ was indirectly shown to promote *L. monocytogenes* escape from the phagosome and to negatively regulate transcription activity of C/EBPβ. In addition, since PKCδ was up-regulated, as shown by microarray and confirmed by RT-PCR, in *L. monocytogenes* infected C/EBPβ$^{-/-}$ macrophages, it was therefore thought to play a detrimental role during *L. monocytogenes*. However, since this premise has never been investigated directly, the role PKCδ during innate immunity against *L. monocytogenes* was examined using the PKCδ deficient (PKCδ$^{-/-}$) mouse model. Data in this dissertation provides new insight into the role of PKCδ during innate immunity to *L. monocytogenes*. PKCδ$^{-/-}$ mice were highly susceptible to *L. monocytogenes* due to enhanced listerial escape and impaired listericidal activity. Despite full macrophage activation and production of nitric oxide, PKCδ$^{-/-}$ mice displayed uncontrolled bacterial growth and dissemination of *L. monocytogenes*, which led to early death of the mice. In contrast, PKCδ$^{-/-}$ mice were able to control *Mycobacterium* infection as well as WT mice, suggesting that the activity of PKCδ may be negatively

regulated by *L. monocytogenes*. A systems biology approach generated the hypothesis that PKCδ may promote Rab5a activation, which together with localized release of superoxide into the phagosome and activation of C/EBPβ by PKCδ, resulted in the confinement of the *L. monocytogenes* within the phagosome. Alternatively, PKCδ may act in a separate pathway that confines *L. monocytogenes* within the phagosome, by activating and/or synergizing with unidentified proteins to neutralize that activity of listerial LLO and PI-PLC. Data in this dissertation clearly demonstrates that PKCδ is critical for confinement of *L. monocytogenes* within phagosomes and may be part of a listericidal mechanism that is independent of nitric oxide, superoxide and pro-inflammatory cytokines.

"The way of progress is neither swift nor easy. "

*Marie Curie*

# CHAPTER 1

## INTRODUCTION

The aim of the current study was identify genes involved in macrophage effector functions against intracellular pathogens. In this study, *Listeria monocytogenes* was used as a model intracellular pathogen to study host macrophage-mediated immunity and to identify macrophage effector genes against intracellular pathogens. *L. monocytogenes* is widely used as a model organism to study bacterial pathogenesis and pathophysiology due to its ability to invade non-phagocytic cells and to survive and multiply within phagocytic cells. In addition, *L. monocytogenes* crosses several host defense barriers such as the intestinal, the blood–brain and the placental barriers and can therefore infect a wide variety of organs (1). Furthermore, *L. monocytogenes* is easily manipulated and grows well *in vitro* and in tissue cultured cells. This literature review comprises three parts, the first part will review the pathogenesis and survival strategy of *L. monocytogenes*, the second part the will review the host's innate immune response and the third part will discuss the research aims and strategy undertaken in this study.

## A. THE PATHOGENESIS OF *L. MONOCYTOGENES* INFECTIONS

*L. monocytogenes* is a Gram-positive, facultative intracellular bacterium that is found in soil, water, effluents, human and animal faeces and a large variety of foods. *L. monocytogenes* is pathogenic and causes the infectious disease termed listeriosis in humans and domesticated animals. In domesticated livestock, *L. monocytogenes* infection is transmitted by the ingestion of contaminated silage, resulting in herd outbreaks (2). Similarly, in humans infection occurs through ingestion of contaminated foods, such as industrially produced, refrigerated ready-to-eat products that do not require cooking or reheating e.g. soft cheeses, dairy products, patês, sausages, smoked fish and salads (2). Since *L. monocytogenes* can tolerate high concentrations of salt, relatively low pHs and can multiply at refrigeration temperatures, it can survive most food processing technologies and therefore is a threat to food safety (2). The clinical manifestations of listeriosis include encephalitis, gastroenteritis, meningitis, mother-to-foetus infections and septicaemia. Although listeriosis is a rare disease, when infection does occur it is usually a very severe and has a mean mortality rate in humans of 30% or higher despite early antibiotic treatment (2, 3). The clinical outcome of *L. monocytogenes* infection depends on three major variables: (i) the number of bacteria ingested with food, (ii) the virulence properties of the strain and (iii) the health status of the host. Individuals most at

risk include pregnant females, unborn foetuses, the elderly (55 years and older), and immunocompromised or debilitated adults with underlying diseases such as HIV/AIDS, lupus, leukaemia, lymphoma, sarcoma, chronic liver disease, kidney disease and diabetes (2). In addition adults undergoing anti-cancer chemotherapy or immunosuppressant therapy (for organ transplantation) are also at risk (2). The immune systems of immunocompromised and debilitated individuals are unable to mount a strong enough response even at low dose infections. As a consequence, they are unable to control bacterial proliferation resulting in invasive disease. Uncontrolled bacterial growth in the liver, the primary target organ of *L. monocytogenes*, results in the release of bacteria into the bloodstream and subsequent infection and septicaemia in secondary target organs such as the brain and placenta. Furthermore, *L. monocytogenes* also has the potential to infect immunocompetent individuals (4). In immunocompetent individuals, ingestion of low doses of *L. monocytogenes* usually has no clinical manifestations other than boosting protective anti-listerial immunity. However, ingestion of large doses may result in gastroenteritis and fever, and in rare cases, invasive disease depending on the virulence of the strain. These diverse clinical manifestation of listeriosis highlights its ability to cross three very important host barriers: (i) the intestinal barrier via invasion of the intestinal epithelium and thereby gaining access to the bloodstream and organs, (ii) the blood –brain barrier resulting in meningitis and (iii) the foetal-placental barrier in pregnant women resulting in foetal infection and/or abortion.

**1. Internalization into target host cells by molecular mimicry**

Entry of *L. monocytogenes* into mammalian cells is a dynamic process whereby *L. monocytogenes* manipulates host-cell signaling and endocytic pathways to induce remodelling of the actin cytoskeleton and plasma membrane facilitating its uptake into target cells. *L. monocytogenes* is able to induce its own internalization into professional phagocytes (e.g. macrophages and dendritic cells) and non-professional phagocytes (e.g. epithelial cells, fibroblasts, enterocytes, hepatocytes, endothelial cells and neurons) (2). The invasion of professional phagocytes is a passive process, whereas entry into non-professional phagocytes is induced by a "zipper mechanism" involving direct interactions between bacterial surface proteins and host cell surface receptors, resulting in the engulfment of the bacterium by the plasma membrane (5). Regardless of the mechanism used by the bacterium for invasion, the interactions between the bacteria and the host cell result in re-organization of the cell's actin cytoskeleton induced by cellular signaling cascades, culminating in bacterial uptake (5, 6).

The ability of *L. monocytogenes* to infect such as wide variety of cell types is facilitated by interactions of its surface proteins, internalin (Inl) A, InlB and p60 with several host cell surface receptors including E-cadherin, the Met receptor for hepatocyte growth factor (HGF), the C1q complement fraction receptor, macrophage scavenger receptor and components of the extracellular matrix (ECM) such as heparan sulfate proteoglycans (HSPG) and fibronectin (2). More recently, several other *L. monocytogenes* proteins have been implicated in the adhesion and invasion process. For example, *L. monocytogenes* expresses lectin-like ligands that are involved in adherence to eukaryotic cells (7, 8). Bacterial surface protein, Lap is involved in attachment to Caco-2 cells and the autolysin Ami has a cell wall-anchoring domain similar to InlB at its C-terminal (9, 10). Expression of an adhesin protein containing a D-galactose moiety induces *L. monocytogenes* uptake into mouse dendritic cells (11). More recently, genetic studies utilizing the genome sequence of *L. monocytogenes* has enabled the identification of other listerial proteins involved invasion of eukaryotic cells. With respect to virulence, the *L. monocytogenes* genome contains a significantly large percentage (4.7% of all predicted genes) (12) of genes encoding surface proteins, which may potentially interact with host cells and may therefore be virulence factors. Similarly, global interference RNA studies in Drosophila S2 macrophage-like cells, have identified several new host genes involved during the invasion (13, 14). The natural route of infection for *L. monocytogenes* is through the gastrointestinal tract, where the bacterium infects the intestinal epithelial cells via the interaction between InlA and epithelial cadherin (E-cadherin) (15). *L. monocytogenes* then crosses the epithelial-cell layer and disseminates into the bloodstream and lymph to mesenteric lymph nodes and other organs such as the liver and spleen, where they are internalized by hepatocytes and resident macrophages.

### 1.1. Invasion of phagocytic cells

*L. monocytogenes* internalization into phagocytic cells such as macrophages and dendritic cells occurs either via the opsonin-dependent pathway mediated by Fc gamma receptor (FcγR) and C3bi and C1q complement receptors (16-19) and/or via the opsonin-independent pathway mediated macrophage scavenger receptors (20, 21) (Fig. 1). In the opsonin-dependent pathway, dissemination of *L. monocytogenes* in the blood stream results in the bacilli becoming coated (opsonized) with host opsonins such as IgG antibodies and complement fragments C3bi and C1q. The IgG molecules recognize and attach to specific bacterial surface proteins, whereas the complement fragments bind non-specifically to the bacterium's cell wall (22). IgG-opsonized *L. monocytogenes* are recognized and engaged by the FC gamma receptor (FcγR). The C3bi-opsonized bacteria are recognized and engaged by complement

receptor 3 (CR3 ; also known as CD11b, CD18 or Mac-1) or complement receptor of the immunoglobulin superfamily (CRIg) (23). C1q-opsonized bacteria are bound by the C1q complement receptor (C1qR; also known as Ly68). In the non-opsonic pathway, *L. monocytogenes* surface proteins bind to host receptors that then trigger the engulfment of the bacterium into the cell. For example, the invasion of dendritic cells by *L monocytogenes* into dendritic cells involves a bacterial adhesion protein containing α-D-galactose (11) and non-opsonic uptake by macrophages is mediated by the macrophage scavenger receptor and components of the extracellular matrix (ECM) such as heparan sulfate proteoglycans (HSPG) (2). In addition, *L. monocytogenes* binds to the globular C1qR (gC1qR), the receptor for the globular part of complement component C1q, via its surface protein Internalin B (InlB) (24). The crosslinking of these receptors upon binding *L. monocytogenes* initiates waves of signal transduction events that require kinase activation, alterations in phospholipid metabolism, remodelling of the actin cytoskeleton and acceleration of membrane traffic (25) leading to the internalization of the bacteria into a primary phagosome (26, 27). Several proteins are implicated in the phagocytosis process, and the list is continually growing longer, and at present includes protein kinases, phosphatases, GTPases, lipid-modifying enzymes, adaptor complexes, actin-binding proteins and membrane fusion and scission mediators (22).

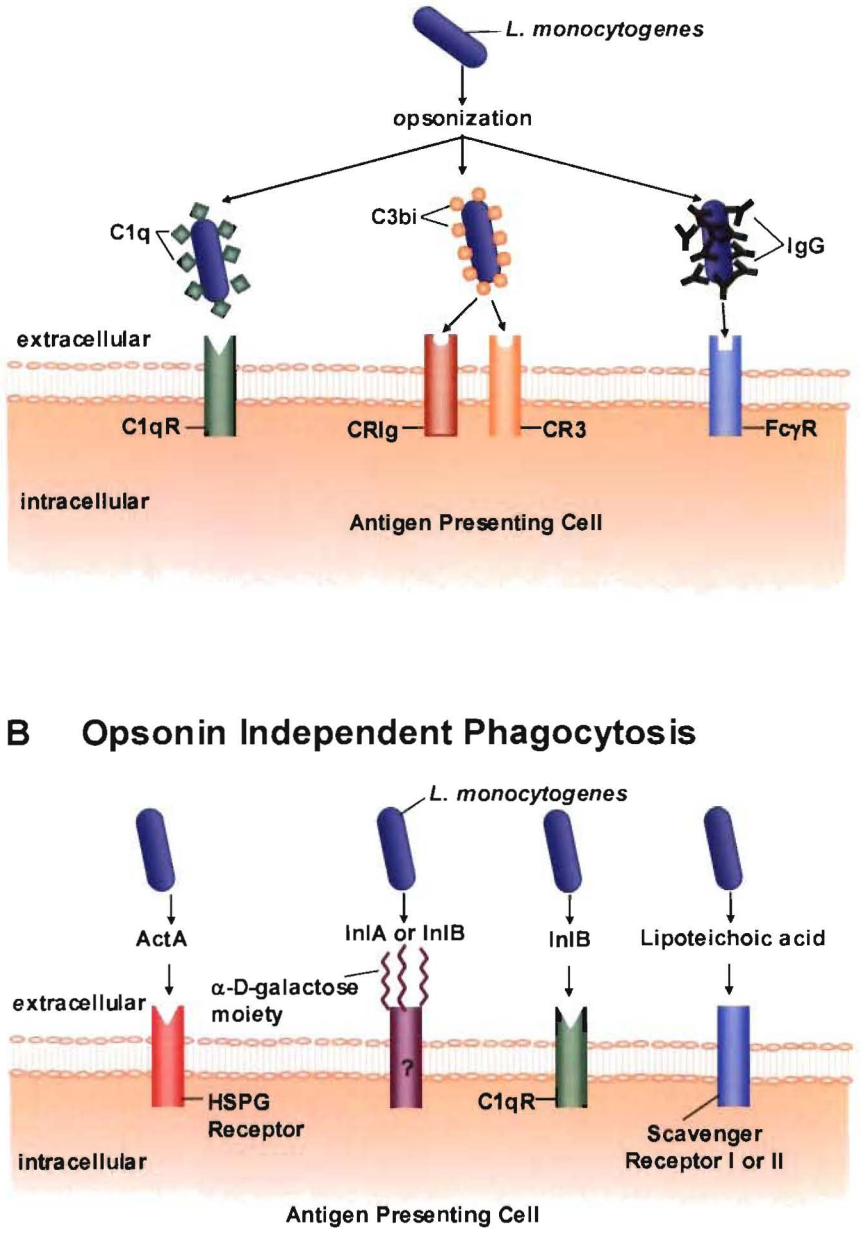


**Figure 1. Internalization of *L. monocytogenes* into antigen presenting cells.** (A) *L. monocytogenes* opsonized with IgG antibodies and/or complement proteins such as C3bi and C1q are recognized by the FcγR, CR3, CRIg and C1qR and internalized by receptor-mediated phagocytosis. (B) *L. monocytogenes* surface molecules such as ActA, InlB and lipoteichoic acid are recognized by macrophage HSPG receptors, gC1qR and macrophage scavenger receptors I and II. On dendritic cells, InlB is recognized by glycolyslated receptors containing a-D galactose moieties. Attachment of *L. monocytogenes* to its target cells by either pathway results in receptor-mediated phagocytosis involving kinase activation, alterations in phospholipid metabolism, remodelling of the actin cytoskeleton and acceleration of membrane traffic.

### 1.2. Invasion of non-phagocytic cells

Invasion of non-phagocytic cells by *L. monocytogenes* occurs "zipper" mechanism, where listerial surface proteins Internalin A (InlA) and InlB interact with E-cadherin and the Met receptors on the host cell respectively, resulting in the localized remodeling of the actin cytoskeleton that culminates in the engulfment and internalization of the bacterium in a zipper-like manner by the plasma membrane (5). Internalization into non-phagocytic cell also involves kinase activation, alterations in phospholipid metabolism, remodeling of the actin cytoskeleton and acceleration of membrane traffic (25).

***InlA exploits intercellular adherens junction complexes to cross host defense barriers.***

InlA is anchored covalently to the cell wall of *L. monocytogenes* by an LPTTG (L for leucine, P for proline, T for threonine and G for glycine) motif in its C-terminal domain. The binding of InlA to E-cadherin induces local cytoskeletal rearrangements in host epithelial cells to induce the internalization of *L. monocytogenes* (28) (Fig. 2). InlA does not share any structural homology to E-cadherin and binds to a different E-cadherin domain other than that involved in homophilic interactions (29). E-cadherin is a transmembrane glycoprotein that belongs to a large family of cell–cell adhesion molecules that are required for the calcium dependent stabilization of adherens junctions between host epithelial cells. E-cadherin is localized at these cellular junctions, where its intracellular domain forms a complex with the cytoskeleton through protein-protein interactions with α-catenin and β-catenin, whereas its extra-cellular domain is involved in homophilic interactions with other E-cadherin molecules on adjacent cells (30). InlA binds to the extracellular domain of E-cadherin and triggers the recruitment of several molecules that establish a functional link between the InlA/E-cadherin complex and the actin cytoskeleton (31) (Fig. 2). For example, once InlA has bound to E-cadherin, β-catenin bound at the distal domain of the intracytoplasmic tail of E-cadherin recruits α-catenin which in turn binds to actin. Since both α-catenin and β-catenin are usually present in adherence junctions, this suggests that *L. monocytogenes* exploits the molecular machinery involved in the formation of adherens junctions to induce its entry into target cells. The exact mechanism of how the cytoskeleton is remodeled is not yet fully understood. However, several proteins involved adherens junction complexes have been shown to be important for *L. monocytogenes* invasion into non-phagocytic cells. For example, Rho GTPase activating (GAP) protein, ARHGAP10, binds to α-catenin and is essential for recruitment of α-catenin to cellular junctions (32). ADP-ribosylation factor 6 (Arf6) tethers ARHGAP10 to Vezatin, another ubiquitous cell junction protein, anchors the motor myosin

VIIA to the E-cadherin/catenin complex, thereby creating a tension force between cell junctions and the actin cytoskeleton. The tension generated beneath the plasma membrane by the E-cadherin-catenin-actin complex in adherence junctions is counteracted by an opposite equal force exerted by neighbouring cells and therefore strengthens the cell-cell adhesion. Both myosin VIIA and Vezatin were found to be important for cell invasion by *L. monocytogenes* and most likely also creates a tension force that is used by the bacterium to propel itself forward into its target cell membrane to trigger its internalization (33). The interaction between E-cadherin and InlA results in phagocytosis and not to adherence, because the *L. monocytogenes* bacilli is not attached to a substratum and therefore does not counteract the link of α-catenin to the cytoskeleton. In addition the shape of the bacterium itself induces a "zippering" of the plasma membrane around the bacterial body due to the interaction of InlA with E-cadherin. Once *L. monocytogenes* has penetrated the epithelial-cell layer and crossed the intestinal barrier, it travels via the bloodstream and lymph to mesenteric lymph nodes and other organs such as the liver and spleen, where they are internalized by hepatocytes and resident macrophages. Since E-cadherin is present on the surface of hepatocytes, dendritic cells, brain microvascular endothelial cells and the epithelial cells lining the choroid plexus and placental chorionic villi, *L. monocytogenes* is able to cross host physiological barriers such as the intestinal barrier, blood-brain barrier and placental barrier by exploiting the molecular machinery of the intercellular adherens junctions.

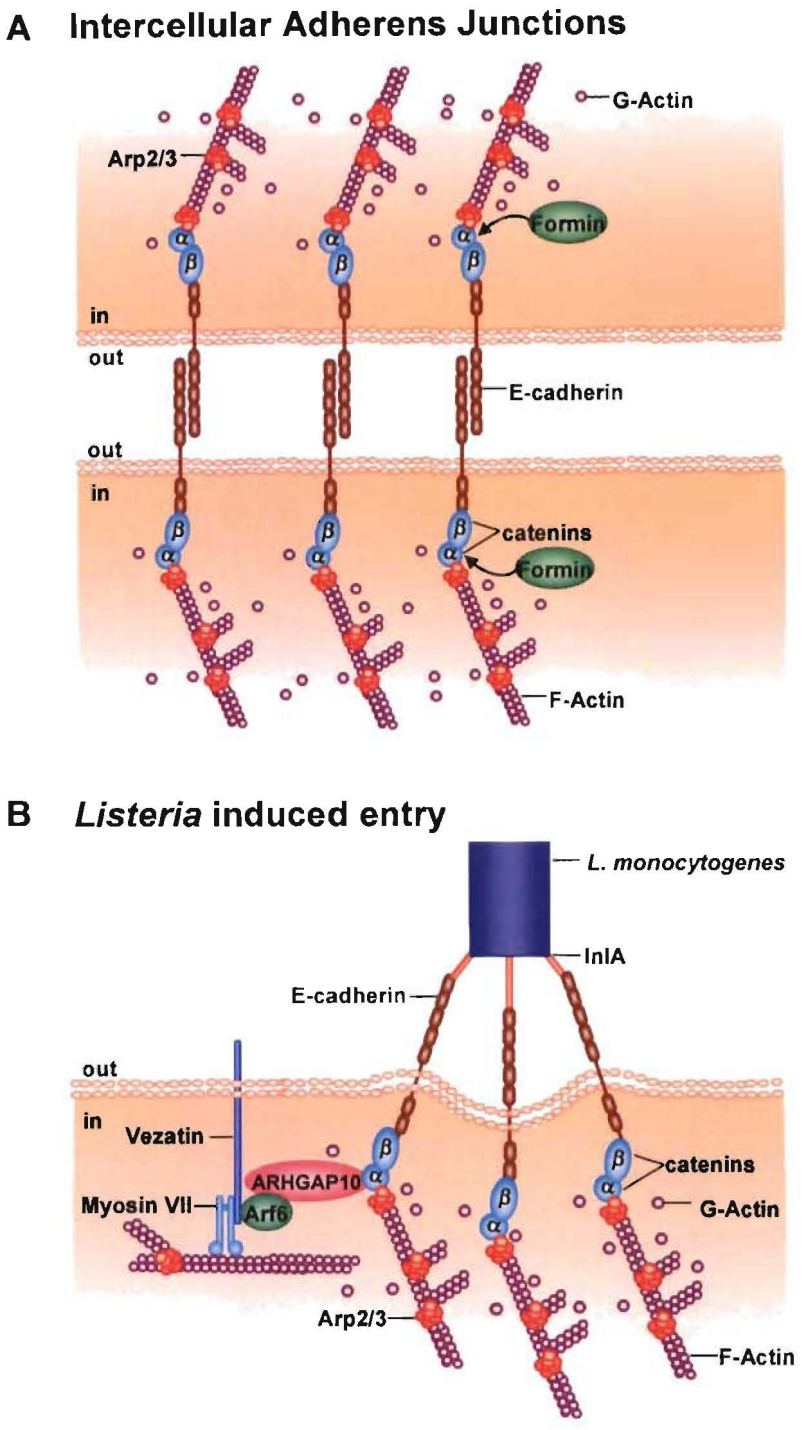


**Figure 2. Invasion by InlA exploits intercellular adherens junction complexes to cross host barriers.** (A) Adherens junctions hold neighbouring together via homophilic interactions between epithelial E-cadherin, which is anchored to the actin cytoskeleton via its interaction with α-catenin. Formins interact directly with α-catenin and form actin filaments that connect the adherens junction machinery to the cytoskeleton. (B) *L. monocytogenes* InlA binds to E-cadherin and recruits proteins involved in adherens junctions assembly and actin cytoskeletal remodeling to induce its internalization. Figure modified and redrawn from reference (3).

***InlB subverts host cellular-signaling and endocytic pathways to invade hepatocytes***

InlB is a listerial surface protein that is loosely attached to the lipoteichoic acids of the bacteria's cell wall via its glycine (G)-tryptophan(W) rich domains (9) InlB contains leucine rich repeats (34, 35) which induces the internalization of *L. monocytogenes* into a much broader range of target cells than InlA (15, 36). The main signaling receptor for InlB is the hepatocyte growth factor (HGF) receptor, Met, (37) which is a tyrosine kinase receptor present on many cell types. The activation of Met by HGF, its natural ligand, activates cellular survival and proliferation signals and cytoskeletal rearrangements that functionally contribute to cellular motility and differentiation. The binding of InlB to Met activates the receptor's protein-tyrosine-kinase activity and the phosphatidylinositol 3-kinase (PI3K) and Ras–mitogen-activated protein kinase (MAPK) pathways which synergize to internalize *L. monocytogenes* into the host cell (37-39) (Fig. 3). Since InlB does not share any structural similarity to HGF (40, 41), it does not compete with HGF for binding with Met suggesting that these molecules bind to different sites on the receptor (37). Although InlB and HGF both bind and activate Met, InlB does not strictly mimic signaling induced by HGF since the kinetics of InlB-induced signaling are different from those induced by HGF (37). In addition equal concentration of InlB induces more potent activation of the Ras–MAPK pathway than does HGF (42). These differences in signaling may be due to the ability of InlB to also bind to gC1qR, the receptor for the globular part of complement component C1q (24). The gC1qR may therefore act as a co-receptor for InlB and thereby enhance Ras–MAPK pathway signaling in addition to signaling induced by activated Met. However, there are some similarities in signaling mediated by InlB and HGF that induces parallel morphological changes in target cells (43). For example HGF requires interactions with extracellular oligosaccharide glucosaminoglycans (GAGs) in order to activate Met (44, 45). Similarly, *L. monocytogenes* interacts with GAGs via the GW domains of InlB resulting in strong activation of Met. Similar to HGF, InlB is also able to induce tyrosine auto-phosphorylation of Met and the recruitment of several adaptor molecules such as farp2f(46). The signaling pathways activated by InlB ultimately result in cytoskeletal rearrangements downstream of Met that facilitate entry of *L. monocytogenes* into its target cells. The remodelling of actin at the InlB attachment site requires the recruitment and activation of the Actin related protein 2/3 (Arp2/3) actin-nucleation complex, which promotes actin nucleation and polymerization (discussed later). The activation of Arp2/3 involves a combination of proteins such Rac1, Cell division cycle 42 homolog (CDC42) and Wiskott–Aldrich syndrome protein (WASP) family proteins such as neural WASP (N-WASP) and WASP verprolin homologue (WAVE (47).

In addition, Ena/VASP (enabled homologue/vasodilator-stimulated phosphoprotein) proteins promote actin-filament elongation, whereas cofilin depolymerizes actin filaments and functions as both a stimulator and a repressor of actin rearrangements that occur during the internalization process (46, 47). More recently, *L. monocytogenes* has been shown to invade epithelial cells by exploiting clathrin-mediated endocytosis (48) (Fig. 3). Both HGF and InlB induce the ubiquination and internalization of Met by a clathrin-mediated endocytosis mechanism (49) leading to degradation of the receptor and internalization of the bacterium that is bound to Met. In addition to taking advantage of the host's endocytic machinery, *L. monocytogenes* may exploit other mechanisms for cellular invasion, since inhibitors of endocytosis reduced bacterial entry but did not completely abolish it (48). For example, plasma-membrane microdomains known as lipid rafts have also been shown to be important for the entry of *L. monocytogenes* (50). Furthermore, Recent studies in Drosophila S2 cells, which are macrophage-like, revealed that about 295 host proteins are important for bacterial invasion and survival and many of these still need to be characterized (14). Therefore by mimicking the activity of host molecules, *L. monocytogenes* is able to exploit several host cellular-signaling and endocytic pathways to induce its entry into target cells.

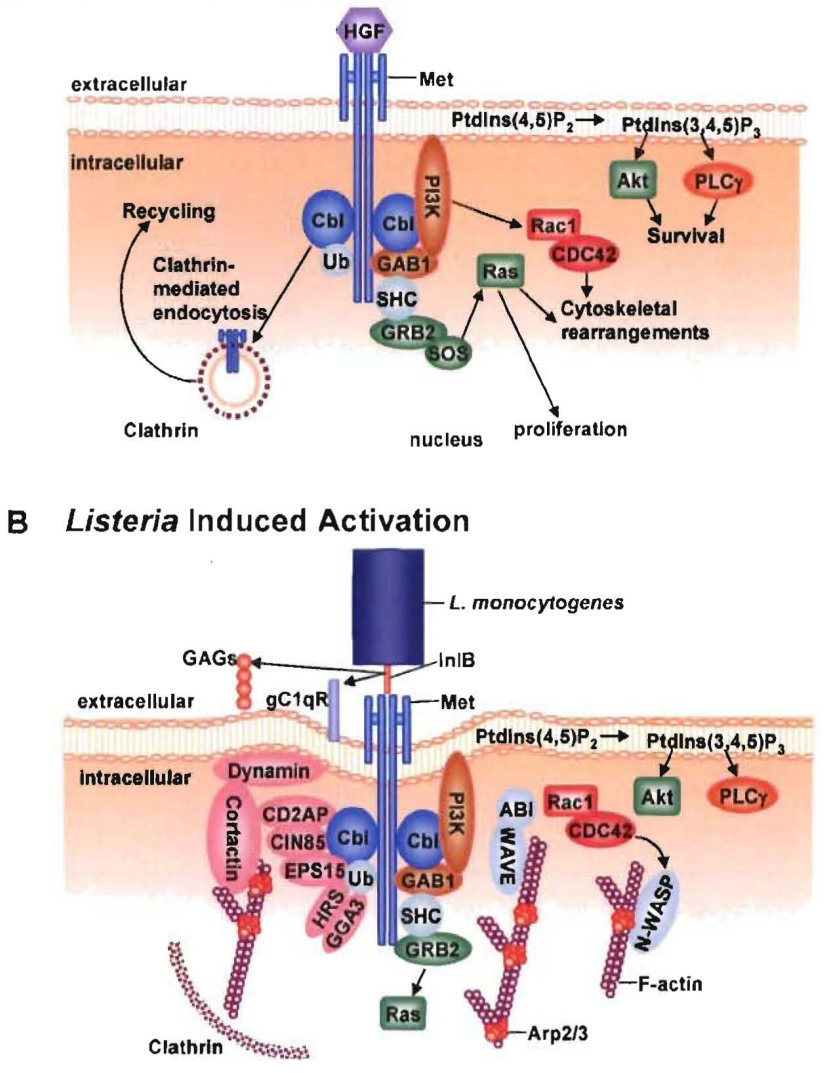


**Figure 3. InlB subverts host cellular-signaling and endocytic pathways to invade hepatocytes.** (A) HGF activates Met by inducing its tyrosine auto-phosphorylation. Activated Met recruits signal transducing adaptor proteins and cytosolic signaling proteins, which activate survival and proliferation signals and induces cytoskeletal rearrangements needed for cellular motility and differentiation. Regulation of HGF signaling is mediated by clathrin-mediated endocytosis of activated Met. (B) InlB bound to Met activates the receptor by inducing its tyrosine auto-phosphorylation. In addition, interaction of InlB with GAGs results in strong activation of Met. Activated Met recruits adaptor molecules Shc, Cbl and Gab1 which activate PI3K, MAPK and Rac1, which mediate actin remodeling via Arp2/3, Rac, CDC42, N-WASP, WAVE, Ena/VASP and cofilin, which together facilitate internalization of *L. monocytogenes* into its target cells. InlB also induces the ubiquination and internalization of Met by a clathrin-mediated endocytosis mechanism. In addition to signaling induced by activated Met, InlB interaction with gC1qR enhances Ras–MAPK pathway signaling. Figure modified and redrawn from reference (3).

**2. Escape from the phagosome**

After invasion and internalization into its target cells, *L. monocytogenes* escapes into the cytoplasm from the phagosome by secreting the pore-forming toxin listeriolysin O (LLO) and two phospholipases (PLC), phosphatidylinositol (PI) specific PLC (PI-PLC) and broad range PLC (BR-PLC). Escape from the primary vacuole (phagosome) formed upon invasion is dependent on LLO and PI-PLC, whereas escape from the secondary vacuole formed upon cell-to cell spread, requires LLO, PI-PLC and BR-PLC (1, 6, 51). The essential role of these proteins in bacterial escape was demonstrated by the failed or defective phagosomal escape of *L. monocytogenes* mutants lacking LLO or both PLCs. PI-PLC is encoded by the bacterium's plcA gene and is a highly specific bacterial PLC that hydrolyzes PI- and glycosylphosphatidylinositol (GPI)- anchored phosphoglyerolipids, by cleaving the PI and GPI anchors. Purified PI-PLC from *L. monocytogenes* is highly active on PI, but not on GPI-anchored proteins (52). BR-PLC is encoded by the plcB gene and is a broad range PLC that that hydrolyzes phosphoglyerolipids as well as sphingomyelin (53). LLO is encoded by the hly gene and is a member of a large family of cholesterol-dependent cytolysins that are secreted by numerous Gram-positive bacteria. Once LLO has bound cholesterol, LLO monomers insert into the phagosome membrane and polymerize to form pores of varying sizes depending on the concentration of the monomers. During the invasion of host cells, LLO synthesis is increased in the phagosome (54, 55) and is further increased in the cytoplasm after bacterial escape from the phagosome (55). Since LLO secreted into the host cytoplasm is free to interact with the host cell membrane, LLO activity is therefore tightly regulated in order to balance efficient bacterial escape from the phagosome, while preventing host-cell damage and thereby ensuring the bacterium's intracellular survival. The compartmentalization of LLO activity is achieved through its optimal activity at acidic pH (<6), where it is fully active in the acidic environment of the phagosome but is inactive at the neutral pH of the host-cell cytoplasm. At acidic pH, LLO monomers oligomerize into large complexes that form pores in the phagosome membrane by extending transmembrane β-hairpins (56). At neutral pH, the acidic amino-acid residues in the transmembrane domain initiate irreversible denaturation of the β-hairpins, resulting in permanent inactivation of the pore-forming activity of LLO (57). The complex structure of LLO therefore enables it to sense and respond to its environment. Indeed, *L. monocytogenes* containing phagosomes gradually acidify to an average pH of 5.9 during the maturation process (58) and inhibition of acidification, by bafilomycin, resulted in inhibition of vacuolar perforation and bacterial escape (59-61). Another mechanism regulating the activity of LLO is the presence of a PEST-like sequence (P for proline, E for glutamic acid, S for serine and T for threonine) near its N-terminal that is

rich in proline, glutamic acid, serine and threonine (62, 63) residues, which promotes LLO degradation in the cytoplasm in a proteasome-dependent manner (64). Removal of the PEST-like sequence from LLO resulted in a listerial strain that was extremely toxic to infected host cells, since the mutant LLO accumulated in the host cytosol and subsequently permeabilized and killed the host cell (62). In addition, *L. monocytogenes* expressing LLO mutants lacking the PEST-like sequence was strongly impaired in its ability to escape from the phagosomal vacuole, suggesting that the PEST-like sequence may play a role in phagosomal escape (63). Indeed, LLO's PEST-like sequence has recently been reported to control LLO production in the cytosol (64). In addition to its pore-forming ability, LLO is also a potent signaling molecule in the host cell and has been shown to activate nuclear factor kappa B (NF-κB) (65), MAPK (66), phosphatidylinositol (67, 68), calcium (69-71) and protein kinase C (72) signaling pathways (discussed later).

The precise mechanism by which *L. monocytogenes* outwits the host's immune defenses and escapes from the phagosome is not clear. The primary defense strategy employed by the host is to restrict the *L. monocytogenes* bacilli within phagosomes and promote fusion with lysosomes. The lysosome is highly bactericidal and contains many hydrolytic enzymes which damage and digest the bacilli (25, 26). The process of phagosome maturation, phago-lysosome fusion and subsequent bacterial killing is regulated by the Ras related protein 5a (Rab5a) in an IFN-γ dependent manner (73, 74). Active Rab5a causes remodeling of the phagosomal environment, facilitating localized production of superoxide and nitric oxide into the phagosome which has been shown to decrease listerial phagosomal escape (75). *L. monocytogenes* counteracts these host defense responses by delaying phagosome maturation in order to "buy time" for itself so that it can escape from the phagosome via the activity of LLO, PI-PLC and BR-PLC. *L. monocytogenes* has been shown to delay phagosomal maturation by inhibiting the activity of Rab5a by preventing the exchange of inactive GDP-bound Rab5a for active GTP-bound Rab5a (76). This manipulation of Rab5a activity occurs possibly via modulation of Rab5a regulating proteins such as guanine nucleotide exchange factors (GEFs), GTPase activating proteins (GAPs) and guanine diphosphate (GDP) dissociation inhibitors (GDIs). However, the mechanism of how LLO, PI-PLC and BR-PLC activity enables phagosomal escape still remains elusive. Studies by Wadsworth and Goldfine addressed this issue using *in vitro* infection of the J774 macrophage cell line with various *L. monocytogenes* mutants deficient for LLO, PI-PLC, BR-PLC and/or both PI-PLC and BR-PLC (51, 71, 72, 77, 78). Data from their studies suggests that *L. monocytogenes* manipulates the macrophage's calcium and protein kinase C (PKC) signaling cascades via its virulence

proteins LLO, PI-PLC and BR-PLC (51, 71, 72, 77, 78). Infection of J774 macrophages with *L. monocytogenes* was shown to induce three calcium influxes (71). Using calcium channel blockers SK&F96365 and thaspigargin, it was shown that the first calcium elevation resulted from an influx of extracellular calcium through an unidentified channel in the cell membrane, whereas the second and third intracellular calcium elevations resulted from release of calcium from intracellular stores. Inhibition of both extracellular and intracellular calcium mobilization resulted in increased phagocytosis of *L. monocytogenes* into the cells and greatly decreased escape of WT *L. monocytogenes* from the primary phagocytic vacuole (71). Concurrent with these three calcium influxes, was the activation of host phospholipases C and D which together with the activity of PI-PLC and BR-PLC activated the host's PKC signalling pathway (72, 78). Activation of host PKC in turn modulated the uptake and escape of *L. monocytogenes* from the phagosome (72). LLO, PI-PLC and BR-PLC were shown to activate host polyphosphoinositide-specific phospholipase C (PLC) (78), which hydrolyzes host PI-4,5-$P_2$ ($PIP_2$) in a calcium dependent manner into diacylglycerol (DAG) and inositol-1,4,5-$P_3$ ($IP_3$) (79), which in turn activated PKC and calcium release from the endoplasmic reticulum respectively (51, 80). In addition, infection of macrophages with *L. monocytogenes* also resulted in the activation of host phospholipase D (PLD) in a LLO dependent manner (PLD) (78) and coincided with the internalization of WT *L. monocytogenes* into host cells and the beginning of phagosome maturation (71). Moreover, inhibition of PLD by 2,3-diphosphoglycerate decreased the efficiency *L. monocytogenes* of escape from the primary vacuole (78) indicating that PLD plays a role in phagosomal escape. However, the mechanism by which PLD achieves this is unknown, although phosphatidic acid, a product of PLD activity, has been implicated in regulating intracellular vesicle trafficking (79, 81). Furthermore, the combined activity of listerial LLO and PI-PLC hydrolyzed host phosphatidyl inositol (PI) into DAG and inositol-phosphate (IP) (78), whereas the activity of listerial BR-PLC hydrolyzed host sphingomyelin, resulting in the release of ceramide and sphingosine-phosphate, the latter of which has been shown to release intracellular calcium stores (82, 83). The elevated levels of DAG generated by the combined activities of bacterial and host PLCs, resulted in the activation PKC signalling within the cells (72). Using a combination of pharmacological inhibitors specific for different PKC isoforms, it was shown that the first calcium influx upon *L. monocytogenes* infection was mediated by PKCδ in a calcium independent manner (72). Since PKCδ been has been implicated in phosphorylation and opening of L-type calcium channel calcium channels (84, 85) and large conductance, calcium- and voltage-activated potassium (BK(Ca)) channels (86, 87), the calcium channel activated by PKCδ in macrophages infected with *L. monocytogenes* may belong to either one of these

calcium channel families. In addition, DAG also activated calcium-dependent PKCβI and PKCβII isoforms, which upon the first calcium influx translocated to the early endosome. Blocking the activity of PKCδ by rottlerin, a putative specific inhibitor of PKCδ, prevented the first calcium influx. The consequent lack of calcium prevented full activation of PKCβII, even though DAG was present, resulting in failure to translocate to early endosomes. Surprisingly, PKCβI was able to translocate to the endosomes. In separate experiments, blocking the activity of PKCβII by hispidin, prevented PKCβII translocation to endosomes and resulted in decreased escape of *L. monocytogenes* from the phagosome. Taken together, these experiments suggested that *L. monocytogenes* manipulates the activity of PKCδ to induce elevated intracellular calcium levels, in order to facilitate its escape from the phagosome via an unknown mechanism that requires elevated calcium levels, PKCβII, LLO, PI-PLC, BR-PLC and PLD (72). In addition, the first calcium influx mediated by PKCδ and translocation of PKCβI and PKCβII occurred prior to *L. monocytogenes* adherence and/or internalization into the cells.

Based on their findings Wadsworth and Goldfine proposed a model (Fig. 4) in which PI-PLC initially enters the macrophage's cytosol from outside the cell (68) via pores formed by LLO in the macrophage cell membrane (72). PI-PLC generates DAG through hydrolysis of PI in the macrophage membranes in an LLO dependent manner. The induction of DAG leads to the calcium independent activation of PKCδ which then translocates to the macrophage cell membrane where it activates an unknown calcium channel(s) resulting in the first calcium influx into the cell. PKCβI and PKCβII become activated by DAG and the elevated intracellular calcium levels and translocate to early endosomes. Once internalized into the phagosome, the expression of LLO, PI-PLC and BR-PLC is increased. In the acidic pH of the phagosome LLO monomers integrate into the phagosome membrane and form pores that allow the passage of PI-PLC and possibly other phagosomal proteins into the host cytoplasm. In the cytoplasm PI-PLC continues to hydrolyze PI in host membranes, generating DAG which sustains activation of PKCδ, PKCβI and PKCβII from the time of entry until the escape of *L. monocytogenes* from the vacuole (72, 88). In addition, sustained activation of PKCδ in turn activates the host's PLD (78), which together with PKCβI, PKCβII, LLO and PI-PLC orchestrate the permeablization of the primary phagosome membrane and escape of *L. monocytogenes* into the cytoplasm. Similarly escape from the secondary phagosome formed upon cell to cell spread is also mediated by a the proposed sequence of events, except that BR-PLC is secreted together with LLO and PI-PLC from the secondary phagosome into the host cytoplasm, where it also hydrolyzes PI in host membranes to generate DAG. In addition,

the hydrolysis of sphingomyelin by BR-PLC generates sphingosine-phosphate which mediates the release of intracellular calcium stores form the endoplasmic reticulum, thereby mediating the second and third (prolonged) intracellular calcium levels (51, 72), which sustains activation of PKCδ, PKCβI and PKCβII (72, 88). The mechanism of how the membrane permeabilization and escape is still unknown. However, PLD activity is induced in *L. monocytogenes* infected macrophages (78) and a by-product of its activity, phosphatidic acid, has been implicated in regulating intracellular vesicle trafficking. Moreover, PKCβI and PKCβII mobilize to early endosomes during *L. monocytogenes* infection (72) and early endosomes have been shown to traffic through sorting endosomes with other organelles including lysosomes and phagosomes (26, 89). Therefore phosphorylation of proteins on early endosomes by PKCβI and PKCβII, together with increased PLD activity and phosphatidic acid levels, may therefore "buy time" for LLO and PI-PLC to permeabilize the phagosomal membrane. However, this proposed pathway still needs to be investigated

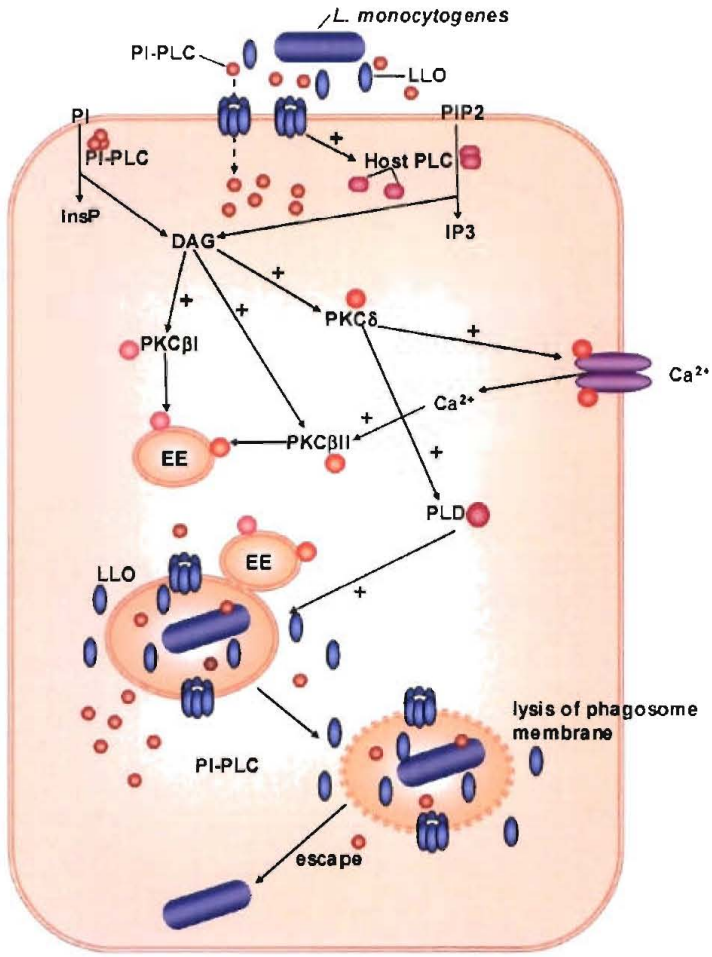


**Figure 4. Proposed signaling pathway mediating escape of *L. monocytogenes* from J774 macrophages.** Upon infection, *L. monocytogenes* secretes LLO and PI-PLC, which enters the macrophage cytosol via pores formed in the macrophage cell membrane by LLO. PI-PLC hydrolyzes PI in host cell membranes to generate DAG which activates PKCδ. Activated PKCδ translocates to the cell membrane where it activates an unknown calcium channel(s) resulting in a calcium influx into the cell. Elevated levels of DAG and calcium activate PKCβI and PKCβII which translocated to early endosomes (EE), which then fuse with pathogen containing phagosomes. In the acidic phagosome, LLO monomers form pores in the phagosome membrane that allow transport of LLO, PI-PLC and other phagosomal proteins into the cytoplasm. In the cytoplasm, LLO activates host PLC, which together with PI-PLC generate DAG by hydrolysis of PI in host membranes. Host PLC also generates IP3 which stimulates calcium release from the endoplasmic reticulum. The consequent elevated levels of DAG and calcium sustains activation of PKCδ, PKCβI, PKCβII and activates host PLD, which together orchestrate the permeabilization of the primary phagosome membrane and escape of *L. monocytogenes* in to the cytoplasm. Escape from the secondary phagosome involves the same proposed pathway and requires BR-PLC in addition to LLO and PI-PLC. Figure modified and redrawn from reference (51).

### 3. Cytosolic growth and replication

Optimal cytosolic growth of *L. monocytogenes* within the cytoplasm of many types of host cells is a unique characteristic of *L. monocytogenes*. Other intracellular pathogens, such as *M. tuberculosis* normally reside inside the phagosome and are unable to replicate in the cytosol of the host cell (90), highlighting that *L. monocytogenes* has evolved specific mechanisms to grow in the host-cell cytosol. The ability of *L. monocytogenes* to thrive inside the cytosol is reflected in its genome, which contains a large number of regulatory and transport proteins (11.6% of all predicted genes) (91). For example, 25% of the transport proteins encoded by the *L. monocytogenes* genome are dedicated to carbohydrate transport as compared to only 2.4% of the *M. tuberculosis* genome (92). In addition, the *L. monocytogenes* genome contains 16 putative two-component regulatory systems, which is is two fold greater than found in the *M. tuberculosis* genome(92). Inactivation of several of these two-component regulatory systems revealed their importance for the resistance of *L. monocytogenes* to various stresses and for survival in the host. Although the intracytosolic survival of *L. monocytogenes* is not well understood, two key proteins for intracellular growth have been identified: the sugar-uptake system (Hpt) and lipoate protein ligase A1 (LplA1). The listerial Hpt protein is a homologue of the mammalian glucose-6-phosphate translocase and it is essential for optimal intracellular bacterial replication. Expression of Hpt allows the bacterium to use glucose-1-phosphate in the host cytoplasm as a carbon source for growth (93). LplA1 catalyses the lipoylation of the bacteria's pyruvate-dehydrogenase enzyme (PDH) complex which is required for full PDH activity. Since the host cytosol lacks lipoic acid, LplA1 scavenges lipoyl groups from host molecules which is then used to activate the bacteria's pyruvate-dehydrogenase. A mutant lacking LplA1 was unable to replicate in the cytoplasm of macrophages and displayed 300-fold decrease in virulence, due to loss of pyruvate-dehydrogenase activity (94). Recently, two studies using whole genome DNA arrays, has revealed that *L. monocytogenes* activates approximately 500 genes for its survival within the host cytoplasm (95, 96) and further investigation of these genes may provide new insight into the mechanism employed by *L. monocytogenes* to adapt and survive within the host cell cytoplasm.

**4. Actin-based motility and cell to cell spread**

Shortly after entry into the mammalian cytosol, *L. monocytogenes* polymerizes actin asymmetrically along its surface, producing an actin tail that propels the bacterium through the cytoplasm and then into neighbouring cells (97, 98).

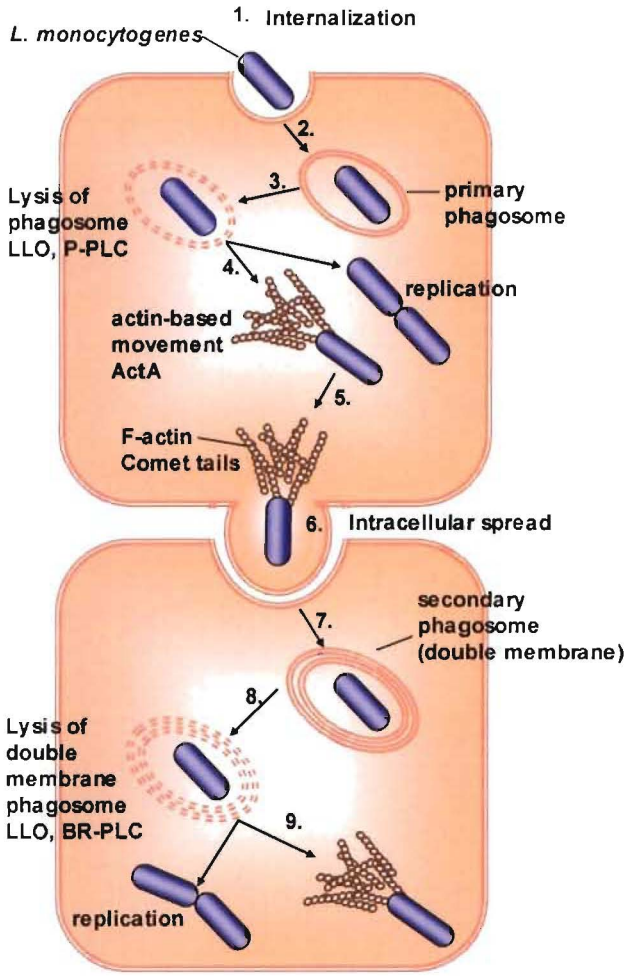


**Figure 5. Pathogenesis of cellular *L. monocytogenes* infection.** *L. monocytogenes* induces its internalization into phagocytic cells and non-phagocytic cells and is engulfed by receptor-mediated phagocytosis into a primary vacuole (phagosome). Escape from the primary phagosome is facilitated by lysis of the phagosome membrane mediated by the combined activities of LLO and PI-PLC. In the cytoplasm, *L. monocytogenes* is able to survive, replicate and move by polymerizing actin as observed by the formation of actin tails. Actin-based motility is mediated by the bacterial ActA protein and allows the bacterium to invade neighbouring cells, where they are confined within a double membrane secondary phagosome. Escape from the secondary phagosome is mediated by the combined actions of LLO, PI-PLC and BR-PLC. The ability to spread from cell to cell allows *L. monocytogenes* to avoid contact with circulating antibodies or other extracellular bactericidal compounds. Figure modified and redrawn from reference (3).

The listerial surface protein ActA is responsible for inducing actin polymerization, actin-based motility and pathogenicity (99, 100). *L. monocytogenes* mutants deficient in ActA efficiently escaped from the primary phagosome, but were unable to spread from cell to cell and grew as micro-colonies in the host cytosol (101-103). The amino terminal end of ActA binds to monomeric actin and acts as a constitutively active nucleation promoting factor by stimulating the intrinsic actin nucleation activity of the Arp2/3 complex by a mechanism similar to that proposed for host neural Wiskott–Aldrich syndrome protein (N-WASP) and WASP verprolin homologue (WAVE) proteins (104-108). By mimicking the activity of N-WASP and WAVE, *L. monocytogenes* has therefore successfully been able to harness the actin polymerization machinery in the host cytoplasm to facilitate its intracellular and intercellular movement. (104-108).

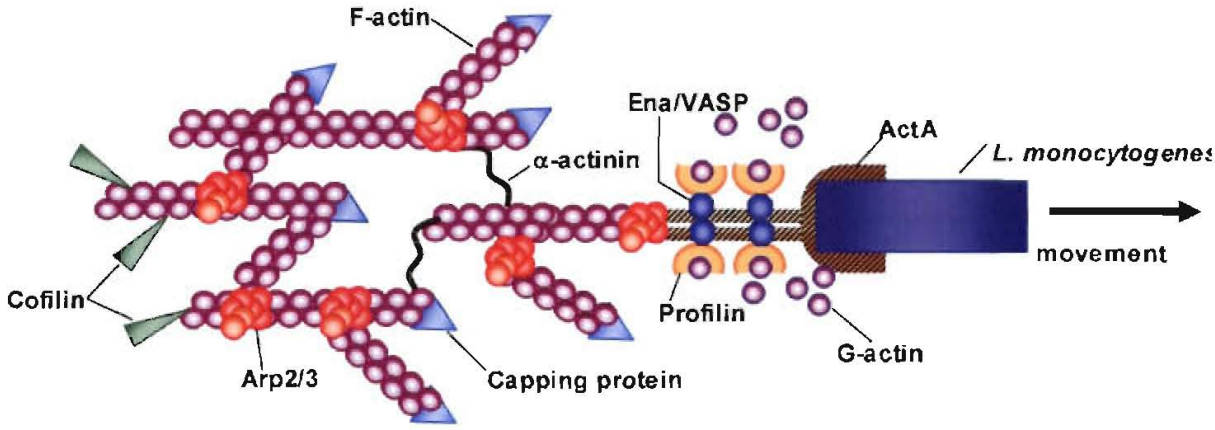


**Figure 6. Model of *L. monocytogenes* actin-based motility.** ActA mediates actin-based motility of *L. monocytogenes* by mimicking the eukaryotic N-WASP and WAVE actin nucleating proteins. The polar distribution of ActA is represented as a hatched area and its N-terminal activates the Arp2/3 complex. Profilin and Ena/VASP bound at the N-terminal tail deliver actin monomers to Arp2/3 complex which nucleates actin monomer into filaments. Profilin increases the elongation rate of nucleated actin filaments and Ena/VASP proteins interact with the barbed ends of growing filaments, preventing the binding of capping proteins. The growth of actin filaments is stopped by the Arp2/3 complex which caps the pointed ends of filaments. The rapidly growing barbed ends (protected from capping protein by Ena/VASP) are concentrated at the site necessary for force generation, thereby propelling the bacterium forward. The bacterium is moving from left to right as indicated by the arrow. Figure adapted and redrawn from (109).

## B. HOST IMMUNE REPSONSES TO *L. MONOCYTOGENES* INFECTION

### 1. The Murine Listeriosis Infection Model

For many years, the murine model of listeriosis has been used to study basic aspects of innate and acquired cellular immunity due to the similarity of the pathogenesis between humans and rodents (110, 111). Although natural infections with *L. monocytogenes* are acquired through the gastrointestinal tract, most experimental studies use either intravenous or intraperitoneal inoculation to initiate infection. The reason for this "unnatural" route of infection was that mice are relatively resistant to oral inoculation due to a single amino-acid difference between human and mouse E-cadherin, which prevented listerial InlA binding and consequent inefficient invasion of epithelial cells (112) (Fig. 7). Most studies over the past four decades have therefore focused on immune responses to systemic *L. monocytogenes* infection. However, a transgenic mouse model expressing human E-cadherin on the surface of enterocytes, has been recently developed enabling investigation of process involved in crossing the intestinal barrier (113).

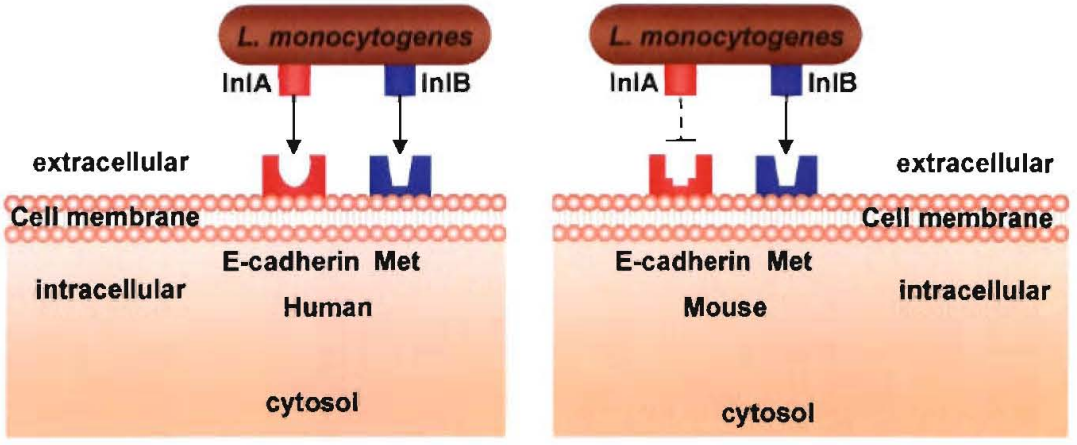


**Figure 7. Host specificity for entry of *L. monocytogenes* into non-phagocytic cells.**
*L. monocytogenes* induces it own internalization into non-phagocytic cells cell via the interaction of its surface proteins InlA and InlB with the host receptors E-cadherin and Met respectively. However, *L. monocytogenes* is unable to invade mouse epithelial cells due to a single amino acid change in the mouse E-cadherin receptor, which prevents InlA from binding. Figure adapted and redrawn from (3).

## 2. Cellular Immune Responses to *L. monocytogenes* Infection

Early control of *L. monocytogenes* infection requires the non-specific, innate immune response which plays a crucial role in controlling the initial bacterial burden, thereby allowing time for the adaptive cellular immune response to develop which eliminates the bacteria and confers sterilizing immunity. The innate immune response to *L. monocytogenes* occurs independently of T cells and is dominated by resident macrophages (Kupffer cells), neutrophils, natural killer (NK) cells and activated macrophages. The effectiveness of the innate immune response to *L. monocytogenes* was demonstrated in Severe Combined Immunodeficient (SCID) mice and Nude mice (114), which lack T-, B-cells and humoral immunity. At early time points these mutant mice were resistant to *L. monocytogenes* infection, but were unable to clear bacteria in the long term. The adaptive immune response is entirely cell mediated and largely dependent on cytotoxic CD8+ T-cells that recognize and lyse *L. monocytogenes* infected cells (111, 114).

The first step in the innate immune response is to control the growth of *L. monocytogenes* in the liver, which is the primary target organ for *L. monocytogenes*, in order to prevent dissemination to other organs and overwhelming sepsis. Upon infection, most *L. monocytogenes* bacilli are rapidly cleared from the bloodstream by resident macrophages in the spleen and liver (115-117). In the liver, resident macrophages called Kupffer cells, line the liver sinusoids and are most dense at the periportal region, the area where the portal vein from the gut enters the liver. The Kupffer cells are therefore optimally located for response to systemic bacteria and bacterial products transported from gut via the portal vein. Mice depleted of Kupffer cells and infected with *L. monocytogenes* had increased numbers of bacilli in the blood and decreased bacterial load in the liver at 10 minutes after infection as compared to controls (118). In addition, Kupffer cells are also important for the secretion of cytokines and chemokines such as interleukin (IL)-1, granulocyte-macrophage colony stimulating factor 2 (GM-CSF), IL-6, interferon (IFN)-γ, macrophage inflammatory protein (MIP)-1α, MIP-1β and MIP-2 early during infection and for inducing antigen-dependent proliferation of T cells (119). However, not all *L. monocytogenes* bacilli that are engulfed by Kupffer cells are destroyed by phago-lysosome fusion, and the surviving bacteria are able to replicate in the liver for 2 to 5 days after infection (115, 120-125). Contrary to the long-held idea that macrophages are the major niche for *L. monocytogenes* in the liver, the principal site of bacterial multiplication is the hepatocyte (116, 126-130). *L. monocytogenes* therefore gains access to the liver parenchyma via two routes: the first is via uptake by Kupffer cells and subsequent cell to cell spread, and the second route is by direct invasion of hepatocytes via the

interaction of InlB with the Met receptor present on hepatocytes (36, 37). The consequent cell to cell spread of *L. monocytogenes* in the liver (127, 131) results in the formation of infectious foci without the bacterium coming into contact with the humoral effectors of the immune system. This may explain why antibodies generated by the adaptive immune response play no major role in anti-Listeria immunity (132). However, a protective role for Listeria-specific natural antibodies and anti-LLO monoclonal antibodies (mAb) has been demonstrated, where they were shown to reduce the dissemination of the bacilli into organs and to enhance antigen-trapping in secondary lymphoid organs (133). In addition, mice treated passively with an anti-LLO mAb had significantly lower bacterial burden in the spleen and liver and increased survival time after a challenge with a lethal dose of *L. monocytogenes* (134).

During the first 48 hours after infection neutrophils play a critical role in resolving early *L. monocytogenes* infection, especially in the liver (135-139). Hepatocytes respond to *L. monocytogenes* infection by undergoing apoptosis, thereby releasing neutrophil chemoattractants. In addition, hepatocytes up-regulate expression of adhesion molecules resulting in increased adhesion to neutrophils (135). The recruited neutrophils appear at the sites of infection within 24 hours, forming discrete microabscesses where they destroy *L. monocytogenes* infected hepatocytes and released bacteria (140). The importance of neutrophils was demonstrated in neutrophil-depleted mice which died early in infection and had large bacteria laden foci in the liver parenchyma (135-140). Two to four days after infection, neutrophils are gradually replaced by monocytes and lymphocytes that infiltrate the sites of infection and contribute to the formation of early granulomatous lesions that are composed of granulocytes and activated macrophages (122). These granulomatous lesions act as physical barriers to confine the infectious foci, and therefore prevent further bacterial dissemination by direct cell to cell spread (141). NK cells are activated during this phase and become the major source of interferon–gamma (IFNγ) (142, 143), which is essential for full macrophage activation and anti-listerial immunity (discussed later) (141). Moreover, IFN-γ activation of hepatocytes also impairs the replication of *L. monocytogenes* within these cells, especially if co-stimulated with IL-6 and tumor necrosis factor (TNF) (144, 145). Thereafter, between days 5 and 7 post infection, IFN-γ activated macrophages in the granulomatous lesions destroy the bacteria and present the bacterial peptides (antigens) on their surface together with either major histocompatibility complex (MCH) class I or MHC class II molecules to CD8+ or CD4+ T cells respectively (2, 114, 129, 132, 146-148). The activation and recruitment of macrophages is essential for bacterial clearance and listericidal activity as shown by experiments where depletion or inhibition of either CR3 or CC-chemokine receptor

2 (CCR2) in mice resulted in dramatically enhanced susceptibility to *L. monocytogenes* infection (130, 149). CR3 is the major receptor on the surface of macrophages that mediates phagocytosis of *L. monocytogenes* into the cell (17) and is important for listericidal activity (18). Activated macrophages express CCR2 which binds monocyte chemoattractant protein-1 (MCP-1; also known as CC-chemokine ligand 2 (CCL2)), which is secreted *L. monocytogenes* infected macrophages. Mice that lack CCR2 were extremely susceptible to *L. monocytogenes*, since they failed to recruit activated macrophages resulting in markedly decreased levels of inducible nitric oxide synthase (iNOS) and TNF in the splees during the first 2 days after infection (149). IFN-γ activated macrophages become a rich source of cytokines and chemokines, resulting in a transition of the macrophage being a habitat supporting bacterial growth, into an effector-cell, terminating or restricting microbial survival (116, 132). In addition, pro-inflammatory cytokines and chemokines also trigger the maturation of immature dendritic cells (DCs) that were recruited to the microabscesses. For example, a novel DC population which produced high levels of TNF and iNOS, termed TNF- and iNOS-producing DCs (TipDCs), were shown to be critical to control *L. monocytogenes* growth during the early stages of infection (150).

The primary function of activated macrophages and dendritic cells is to engulf, destroy and present listerial antigenic peptides to T cells, thereby initiating the adaptive immune response. *L. monocytogenes* is internalized into macrophages and dendritic cells via opsonic dependent or independent receptor mediated phagocytosis (2, 11, 16-24). During phagocytosis, the endoplasmic reticulum (ER) and not the plasma membrane, is the major reservoir of membrane for primary phagosome formation (26, 151, 152). Since the newly formed phagosome is relatively inert and are unable to kill and digest the *L. monocytogenes* bacilli, its has to undergo a transformation process in which it acquires proteins that mediate its fusion with the lysosome. The lysosome is highly bactericidal and contains many hydrolytic enzymes which fatally damage and digest the bacilli (25, 26). After its scission from the plasmalemma, the phagosome fuses sequentially with early endosomes, late endosomes and finally with lysosomes, by a maturation process which is regulated by Rab and soluble N-ethylmaleimide-sensitive factor-attachment protein receptor (SNARE) proteins (26, 153-155) (Fig. 8)

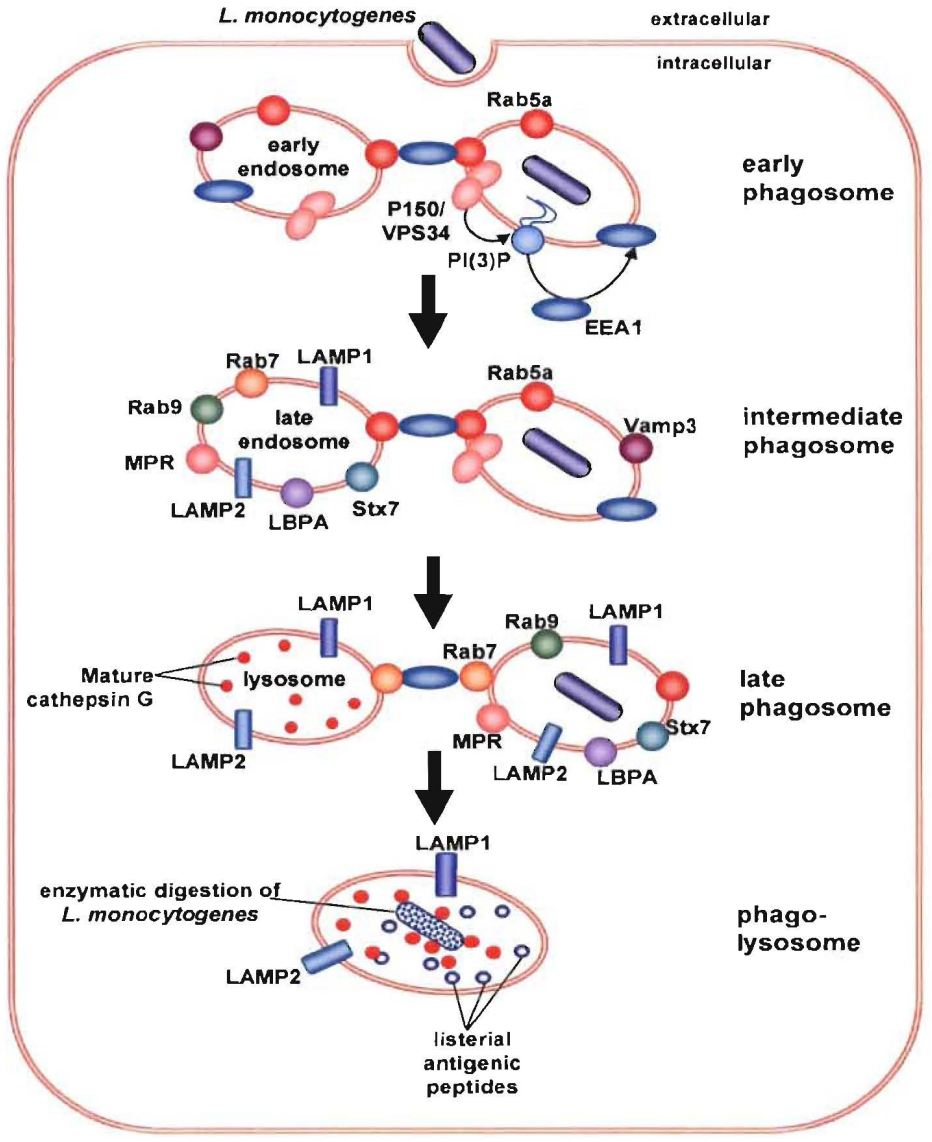


**Figure 8. Schematic outline of phagosome maturation and phago-lysosome fusion.**

The newly formed phagosome containing the *L. monocytogenes* bacilli acquires Rab5a from the plasmalemma or cytosol. Rab5 recruits p150/VPS34 to generate PI(3)P and attracts EEA1, which in turn facilitates tethering and fusion to early endosomes. During the transient fusion, the early phagosome acquires early endosomal marker proteins such as Vamp3. Subsequently, the intermediate phagosome fuses with late endosomes and acquires Rab7, Rab9, MPR, Stx7, LAMP1, LAMP2 and LBPA either from the cytosol and/or along with late endosomes. Rab7 on the late phagosome promotes fusion with lysosomes, leading to the killing and enzymatic digestion of the bacilli by proteases such as cathespin G. The resulting listerial peptides are then processed via the MHC class II antigen presentation pathway and presented to CD4+ T cells.

The fusion between phagosomes and endo/ lysosomes does not result in amalgamation of the organelles, but rather forms transient hybrid organelles connected by fusion pores that allow selective exchange of some membranes and luminal components, followed by scission. The age of the phagosome (i.e. the time elapsed after scission of the phagosome from the plasmalemma) dictates which individual sub-compartments of the endocytic pathway it will fuse with. Generally, early phagosomes selectively fuse with early endosomes (also termed sorting or recycling endosomes), intermediate phagosomes with late endosomes and late phagosomes with lysosomes (26, 153-158). At each fusion step, the phagosome acquires particular proteins which are characteristic of the age of the phagosome (Table 1). For example, early endosomes contain early endosome antigen 1 (EEA1), Rab5a, phosphatidylinositol 3-phosphate (PI(3)P), syntaxin-13 (Stx13), transferrin receptor (TF) and vesicle-associated membrane protein 3 (VAMP3).

**Table 1. Molecular markers of endomembrane organelles that interact with *L. monocytogenes* containing phagosomes**

| organelle | markers |
|---|---|
| early endosome; early phagosome | EEA-1, Rab5a, PI(3)P, Stx13, TF, Vamp3 |
| Late endosome; late phagosome | Rab7, Rab9, MPR, Stx7, LAMP1, LAMP2, LBPA |
| Lysosome; phago-lysosome | LAMPs, mature cathepsin D; .fluid-phase markers chased for +/- 2 hours |
| Endoplasmic reticulum | Calnexin, calreticulin, GRP78, UDPGT, VAP33 |

early endosome antigen 1, EEA1; RAS oncogene family member 5a, Rab5a; phosphatidylinositol-3-kinase, PI(3)P; syntaxin 13, Stx13; transferrin receptor, TF; vesicle-associated membrane protein 3, Vamp3; RAS oncogene family member 7, Rab7; RAS oncogene family member 9, Rab9; mannose-6-phosphate receptor, MPR; syntaxin 7, Stx7; lysosomal membrane glycoprotein 1, LAMP1; lysosomal membrane glycoprotein 2 , LAMP2; lysobisphosphatidic acid (LBPA); glucose-regulated protein 78 kDa, GRP78; UDP-glucuronosyltransferase, UDPGT; vascular adhesion protein 33, VAP33.

As a result of these fusion events the phagosomal lumen becomes a highly acidic and oxidizing environment, and contains a variety of hydrolytic enzymes that fatally damage and digest the *L. monocytogenes* bacilli (25, 26, 153, 155, 159-161). After degradation within the phagosome, listerial peptides are processed via the MHC class II antigen presentation pathway and are presented to CD4+ T cells, which primes the development of T Helper 1 (TH1) CD4+ T cells which produce IFN-γ (162) and protective type 1 immune responses (163, 164) that activates macrophages to become more bactericidal (165) (Fig. 9). In addition, listerial proteins in the cytosol such as LLO (166-171), the metalloprotease Mpl (172) and the listerial surface protein p60 (163, 173-175) are degraded by the proteosome and presented via the MHC class I antigen processing pathway to CD8+ T cells.

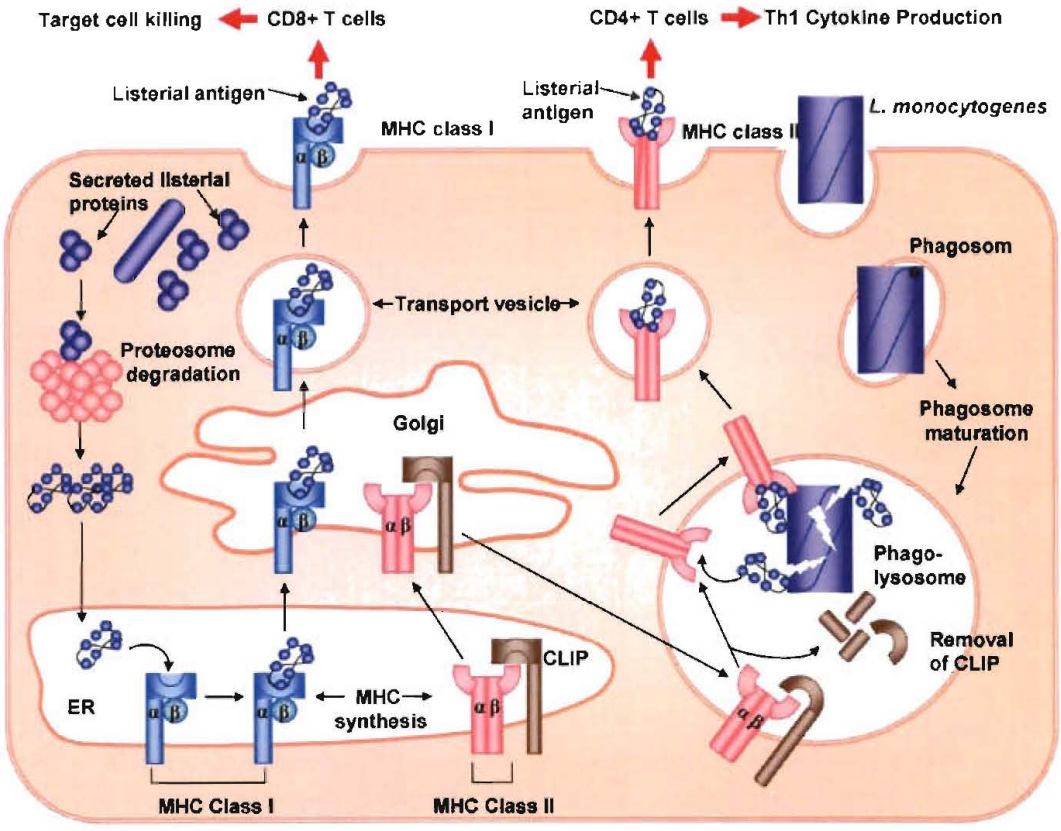


**Figure 9. Schematic outline of antigen processing.** Proteins secreted by cytosolic *L. monocytogenes* are degraded by the proteosome into peptides, which are transported across the endoplasmic reticulum (ER) membrane by transporter 1 ATP-binding cassette sub-family B member 1 (TAP1) and TAP2. Synthesis and assembly of MHC class I heavy chain (α) and β-2-microglobulin (β) occurs in the ER, where the listerial peptides form a stable complex that is transported through the Golgi and trans-Golgi apparatus to the cell surface. Similarly, *L. monocytogenes* containing phago-lysosomes kill and enzymatically digest the bacilli into peptides. In the ER, the invariant chain (Ii) associates with newly synthesized MHC class II α and β chains via its CLIP domain. The newly assembled MHC class II complex is then transported through the Golgi and trans-Golgi apparatus to reach the phago-lysosome, where the invariant chain is digested and the listerial peptide fragments are able to bind to the MHC class II molecules. The antigen bound MHC class II complex is transported to the cell surface by transport vesicles. At the cell surface, listerial peptides bound to MHC class I and MHC class II molecules are presented to CD8+ T cells and CD4+ T cells respectively. Antigen stimulation of CD8+ T cells leads to killing of cells infected with *L. monocytogenes*, whereas activated CD4+ T cells secrete pro-inflammatory cytokines and IFN-γ thereby augmenting the listercidal activity of macrophages, neutrophils and IKDCs. Figure modified and redrawn from reference (176).

The end of the innate phase is marked by an influx of T cells to the sites of infection on days 4 to 5 (177), where clearance of *L. monocytogenes* is mediated primarily by cytotoxic CD8+ T cells which destroy *L. monocytogenes*-infected cells (114, 147, 167). However, interferon producing killer DCs (IKDCs ) have also been recently shown to kill *L. monocytogenes* infected cells by utilizing NK-activating receptors (178). In summary, the above course of events in the immunocompetent host results in the rapid elimination of *L. monocytogenes* from the liver and acquired anti-listerial immunity. However, if the infection is not controlled in the liver due to an inadequate immune response, as with immunocompromised hosts, unlimited listerial growth in the liver results in the dissemination of the bacteria via the bloodstream and systemic infection of other organs, the central nervous system and/or placenta.

### 3. Recognition of *L. monocytogenes* and signaling by TLRs and NLRs

Activated macrophages, dendritic cells, neutrophils and NK are major cell types of the innate immune system that act immediately to control *L. monocytogenes* growth upon infection. These different cell types communicate with each other by producing and/or responding to pro-inflammatory cytokines and chemokines, which in turn activate and mobilize effector cell populations to the site of infection. At the cellular level, neutrophils and macrophages are considered the major effector cells important for mediating listericidal activity. Depletion of neutrophils in mice using antibodies specific for GR1 (136, 138, 140) markedly enhanced their susceptibility to infection with *L. monocytogenes*. Similarly, blocking CR3 or CCR2 with neutralizing antibodies or by gene targeting also dramatically enhanced susceptibility to *L. monocytogenes* (130, 149). During the early stage of infection, macrophages are recruited to the site of infection (microabscesses) where they encounter bacilli released by infected hepatocytes and Kupffer cells that were lysed by neutrophils or underwent apoptosis.

Macrophages recognize the *L. monocytogenes* bacilli via pattern recognition receptors (PRRs), such as Toll-like receptors (TLRs) and nucleotide-binding oligomerization domain (NOD)-like receptors (NLRs), which sense conserved pathogen associated molecular patterns (PAMPs) via a leucine rich domain (LRR) (179-182). TLRs are transmembrane proteins whose LLR ligand-binding domains extend towards the extracellular milieu or to a topologically equivalent lumen of membrane-enclosed intracellular compartments (182) (Fig. 10). TLRs therefore recognize either extracellular or phagosome restricted *L. monocytogenes*. In contrast, NLRs are soluble proteins that recognize microbial components in the cytosol, rather than at the cell surface or in vesicles (183, 184) (Fig. 10). Upon ligand binding, TLRs and NLRs dimerize with adaptor proteins and recruit additional signaling proteins and triggers the activation of NF-κB, which results in the induction of antimicrobial peptides, pro-inflammatory chemokines, and cytokines, adhesion molecules and enzymes that catalyze production of secondary inflammatory mediators and bactericidal molecules.

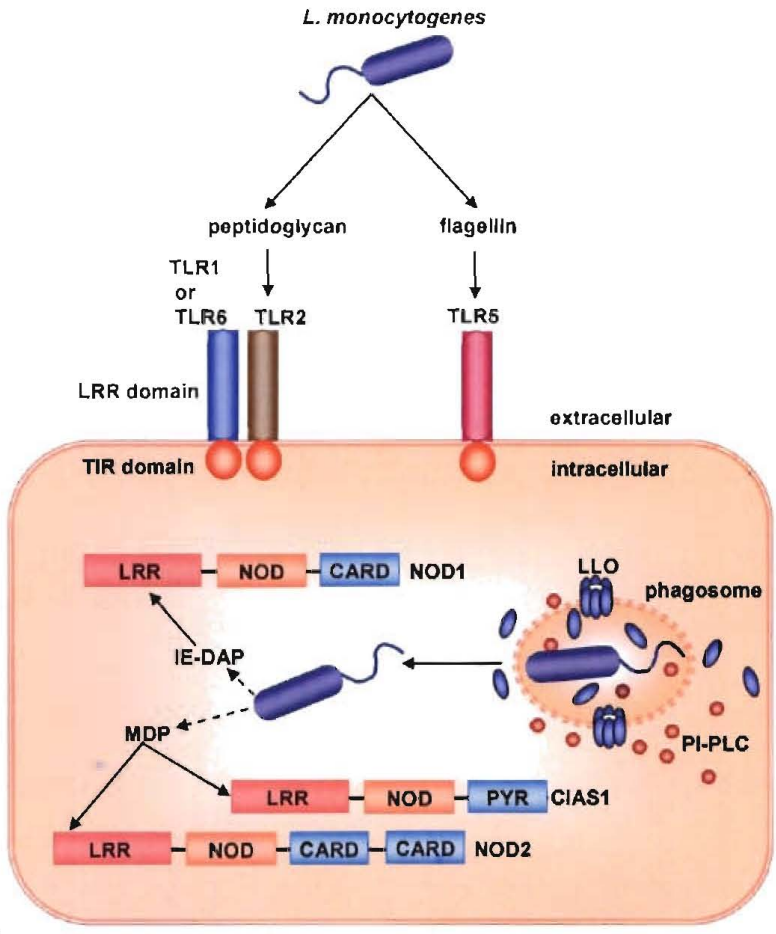


**Figure 10. The structure and cellular location of TLRs and NLRs involved in recognition of *L. monocytogenes*.** TLRs contains an intracellular Toll/IL-1 receptor (TIR) domain and an extracellular leucine rich repeat (LRR) domain. At the macrophage cell surface TLR2, TLR4 and TLR5 recognize *L. monocytogenes* via their LRR domains. TLR2 recognizes peptidoglycan, lipoteichoic acid and lipoproteins and TLR5 recognizes listerial flagellin. TLR2 forms a heterodimer with either TLR1 or TLR6 depending on the identity of the ligand, and CD14 acts in synergy with TLR4 to bind LPS. NLRs are cytosolic proteins that recognize listerial proteins in the cytosol. NLRs contain a caspase-recruitment domain (CARD) or a pyrin (PYR) effector domain, a nucleotide-binding and oligomerization domain (NOD) and a LRR domain that detects degradation production of listerial peptidoglycan. NOD1 and NOD2 detect dipeptide or tripeptide motifs (iE-DAP) while NOD2 detects muramyl dipeptide (MDP). Cold autoinflammatory syndrome 1 (CIAS1) is structurally similar to NOD2 except that it contains a PYR domain instead of a CARD domain, and also recognizes listerial MDP. Upon ligand binding, the TLRs and NLRs initiate downstream signalling events that activate NF-κB leading to the production of pro-inflammatory cytokines, chemokines and antimicrobial peptides. Figure modified and redrawn from reference (185).

TLRs contain two distinct domains, a leucine rich repeat (LRR) domain in their extracellular region, which recognize and bind specific PAMPs, and a Toll/IL-1 receptor (TIR) domain in their intracellular region (Fig 10). To date, 11 different TLRs have been identified and each TLR recognizes different PAMPs and mediate distinctive pathways by associating with different combinations of adaptor proteins such as Myeloid differentiation primary response gene 88 (MyD88), TIR domain-containing adaptor protein (Tirap), Toll-like receptor adaptor molecule 1 (TRIF, also known as Ticam1) and Toll-like receptor adaptor molecule 2 (TRAM, also known as Ticam2) (182). Macrophages express most TLRs except TLR3 (186) and the expression of TLRs is highly up-regulated in these cells (187). In contrast, the expression of TLRs in DCs is differentially expressed depending on the DC subset and maturation stage (186, 188-198). TLR2 and TLR5 have been implicated in recognition of *L. monocytogenes* (199-202). Generally, TLR2 is a receptor for bacterial peptidoglycan, lipoteichoic acid and lipoproteins, whereas TLR5 recognizes bacterial flagellins (182). *L.monocytogenes* of mice deficient for TLR2 ($TRL2^{-/-}$) revealed that TLR2 was important for macrophage production of TNF, IL-12, IL-18, IFN-γ and nitric oxide (NO). In addition, IL-12 and IL-18 synergistically induced IFN-γ production, leading to normal clearance of *L. monocytogenes* (200). Although *in vivo* data about the role of TLR5 has not yet been investigated in $TLR5^{-/-}$ mice, *in vitro* data has shown that intravenous or oral infection of mice with a *L. monocytogenes* strain lacking flagellins resulted in impaired macrophage activation as shown by a 50% reduction in TNF production by of macrophages (202). In addition MyD88, the intracellular adaptor protein that transmits many, but not all, TLR-mediated signals, was shown to be critical for innate immunity against *L. monocytogenes* (200, 203). Mice that lack MyD88 ($Myd88^{-/-}$) were more susceptible to infection with *L. monocytogenes* than mice that lack either IFN-γ or both IL-12 and IL-18 (200). However macrophage-mediated killing of bacteria did not require MyD88 (203).

The binding of *L. monocytogenes* to TRL2, TRL4 and TLR5 stimulates the receptors to dimerize Myd88 and to recruit interleukin-1 receptor (IL-1R)-associated kinase (IRAK) 4 and IRAK1. (Fig. 11) TNF receptor associated factor 6 (TRAF6) binds to IRAK1 and then dissociates to form a complex with transforming-growth-factor-β activated kinase 1 (TAK1), TAK1-binding protein 1 (TAB1) and TAB2. This complex is required for the ubiquitylation of TRAF6 and for the activation of the kinase activity of TAK1, which then leads to the phosphorylation of components of the inhibitor of NF-κB (IκB)-kinase (IKK) complex which results in the activation of NF-κB. In addition, TAK1 activates MAP kinase kinase (MKK)-3/6 and MKK4 which in turn activate p38 kinase and c-Jun N-terminal kinase (JNK)

respectively, which in turn activate the transcription factor AP1. Activation of NF-κB and AP-1 results in the up-regulation of genes encoding pro-inflammatory cytokines such as TNF, IL-1β, IL-6, IL-12 and chemokines MIP-1α, MIP-1β and RANTES (regulated on activation normal T cell expressed and secreted) (Fig. 11). Myd88-independent signaling by TLR4 through the adaptor proteins TRAM and TRIF to activate NF-κB to up-regulate expression of co-stimulatory molecules CD40, CD80 and CD86 at the macrophage cell surface which initiates T cell activation. *L. monocytogenes* has been shown to induce up-regulation of type I interferons such as IFN-α and IFN-β via a TLR4-Myd88-independent pathway that is mediated by IRF3. Type I IFNs have been shown to sensitize lymphocytes to LLO-mediated apoptosis, thereby disrupting the innate immune response and reducing resistance to *L. monocytogenes* (204-208). In addition, cytosolic invasion of *L. monocytogenes* and membrane permeabilization by LLO has been shown to activate NF-κB in a MyD88- and IRAK-independent, most likely via the NLR pathways (209, 210).

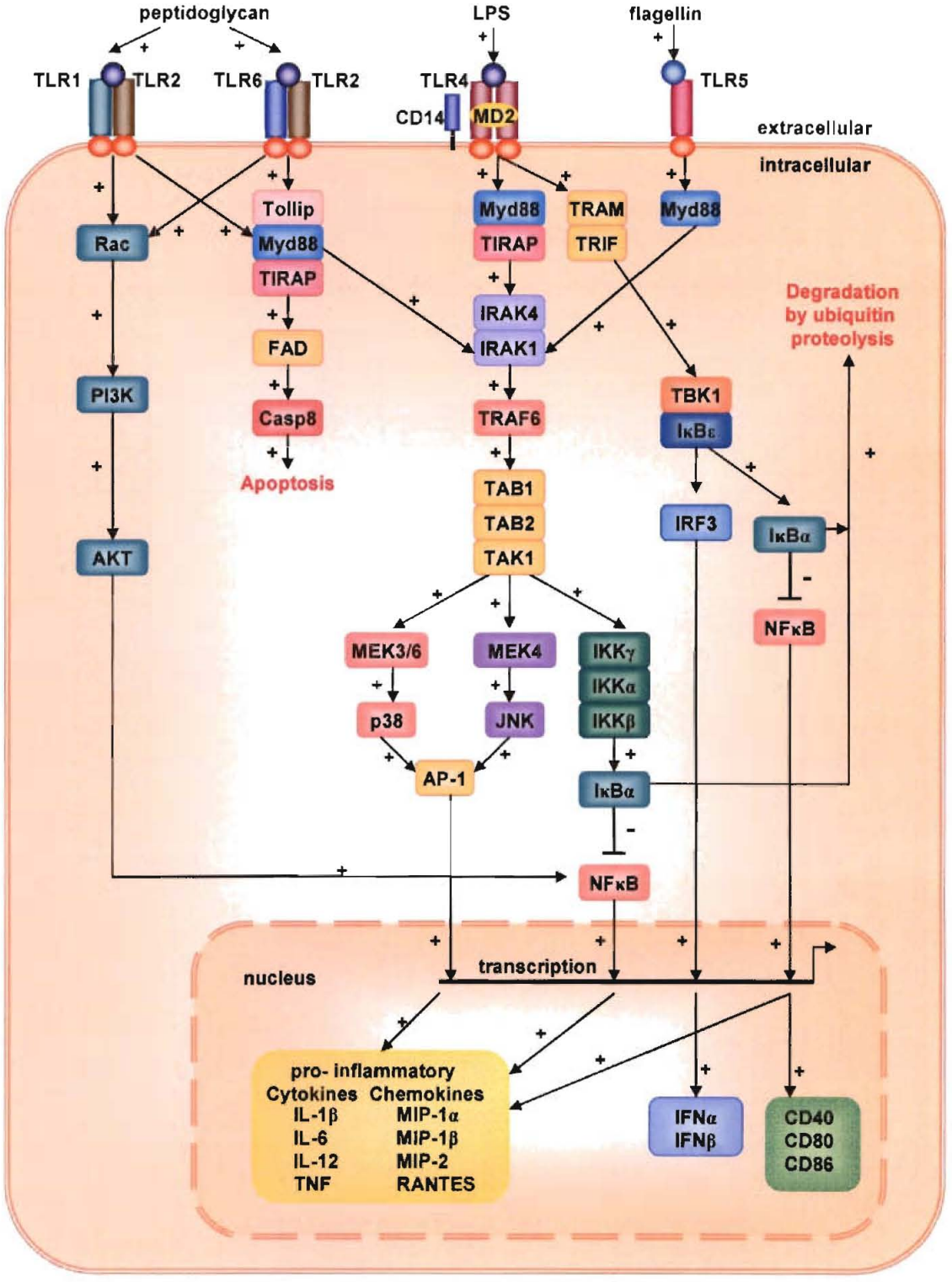


**Figure 11. TLR signalling in macrophages in response to *L. monocytogenes* infection.** Solid black lines with plus signs represent activation; blunt-ended solid lines with minus signs represent inhibition. Figure modified and redrawn from reference(185).

The NLR family are soluble proteins that survey the cytosol for microbial PAMPs which they recognize via a LRR domain. The NLR family includes the NOD proteins and NACHT (domain present in NAIP, CIITA, HET-E and TP1)-LRR - and pyrin-domain-containing (NALP) proteins (183, 184). NLRs contain three distinct domains: (i) an amino-terminal caspase-recruitment domain (CARD) or pyrin effector domain, (ii) a nucleotide-binding and oligomerization domain ('NACHT' domain) and (iii) a variable number of LRRs at the carboxy-terminal (Fig. 10). To date, 22 NLRs have been identified (179, 185) however, only NOD1 (also known as CARD4), NOD2 (also known as CARD15) and CIAS1 (also known as cryopyrin or NALP3) have been found to recognize *L. monocytogenes* (211-217). NOD1 and NOD2 detect peptides derived from the degradation of *L. monocytogenes* peptidoglycan (PGN) released by the listerial hydrolases during cell-wall biosynthesis and remodeling, and/or after phago-lysosome degradation. NOD1 recognizes diaminopimelic acid-containing dipeptide or tripeptide motifs (iE-DAP) while NOD2 detects muramyl dipeptide (MDP), which is a common component of bacterial cell walls (214, 218-220). Both NOD1 and NOD2 are mainly expressed in epithelial cells, macrophages and DCs (184, 221, 222). NOD1 expression is up-regulated by IFN-γ only (223), whereas NOD2 is up-regulated by TNF which is further augmented by IFN-γ (224). Upon ligand binding NOD1 and NOD2 recruit downstream adaptor protein, receptor-interacting protein 2 (RIP2; also known as RICK and CARDIAK), that drives the activation of mitogen-activated protein kinases (MAPKs) and NF-κB (218, 225, 226) (Fig. 12). Activated NOD2 recruits RIP2 which mediates polyubiquitylation of an inhibitor of NF-κB (IκB)-kinase-γ (IKKγ; also known as NEMO) at the lysine residue at position 285 (227). This is followed by the phosphorylation of IKKβ and IκB resulting in the release NF-κB for translocation to the nucleus where it transcribes its target genes (228). In the case of NOD1, ubiquitylation of IKKγ by RIP2 has not been investigated and the mechanism of NOD1 mediated activation of NF-κB is not clear. Furthermore, NOD1 and NOD2 signaling activate MAPKs such as JNK, extracellular-signal-regulated kinase (ERK) and p38 MAPK by an, as yet, unidentified mechanism (211, 216). In addition, NOD2 has been shown to bind to procaspase-1, and induces IL-1β secretion (229). Since caspase-1 is required for processing pro- IL-1β into mature IL-1β (230), the binding of NOD2 to pro-caspase 1 via CARD–CARD interactions, may convert the pro-caspase into a caspase. However, this putative NOD2 function still needs to be investigated *in vivo*. Both NOD1 and NOD2 have been shown to be important is defense against *L. monocytogenes*. (211, 231). Inhibition of NOD1 by interference RNA, revealed that NOD1 is critical for the *L.*

*monocytogenes* induced activation of NF-κB and p38 MAPK resulting in IL-8 production (231).

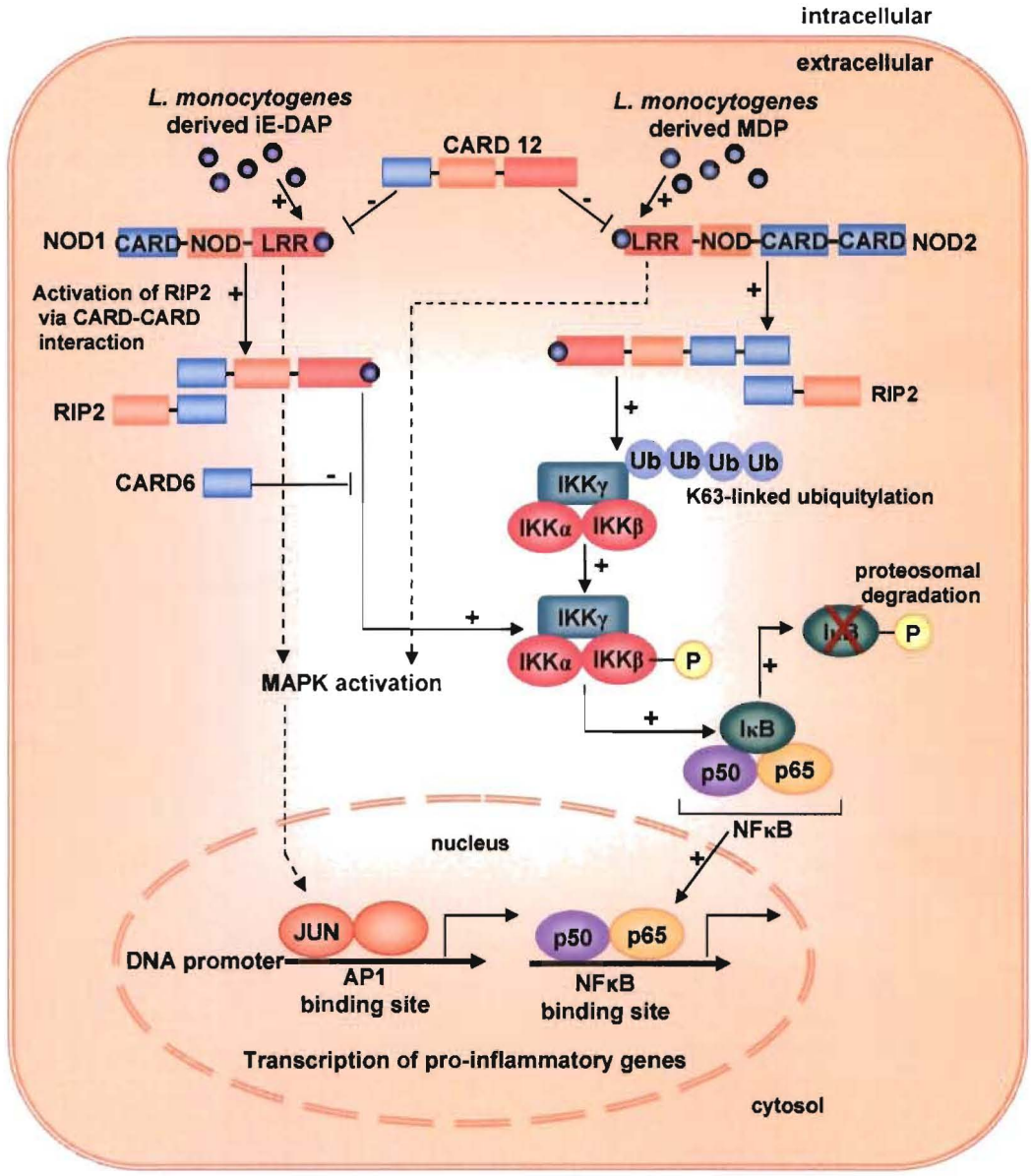


**Figure 12. NOD1 and NOD2 signalling in macrophages in response to *L. monocytogenes* infection.** Solid black lines with plus signs represent activation; blunt-ended solid lines with minus signs represent inhibition, dashed lines represent activation by unknown mechanisms. Figure modified and redrawn from reference (185).

NOD2 is involved in mucosal defense against *L. monocytogenes* and is required for the expression intestinal antimicrobial peptides, known as cryptdins. NOD2 deficient mice were susceptible to *L. monocytogenes* infection due to impaired expression cryptdins (211). Moreover, mouse deficient for the adaptor molecule RIP2, has profoundly increased susceptibility to *L. monocytogenes* and RIP2 deficient ($RIP2^{-/-}$) mice succumb to infection within 8 days of inoculation (232). $RIP2^{-/-}$ macrophages infected with *L. monocytogenes* or treated with LPS had decreased activation of NF-κB and impaired production of IL-12, IL-6 and IFN-γ production. Although RIP2 is a component of the NOD1 and TLR4 signalling pathways, $RIP2^{-/-}$ mice seem to be less immunocompromised than MyD88-deficient mice with respect to infection with *L. monocytogenes* (233). In addition to NOD1 and NOD2, the NLR protein CIAS1 (also known as cryopyrin and NALP3) detects *L. monocytogenes* and induces production of L-1β and IL-18. CIAS1 is structurally similar to NOD2 except that it contains a pyrin domain in place of a CARD at its amino-terminal domain and is also activated by MDP (234). Upon ligand binding, CIAS1 together with apoptosis-associated speck-like protein containing a C-terminal caspase recruitment domain protein (ASC) activates pro-caspase-1 and assembles with together with CARDINAL and mature caspase 1 to form a multi-protein complex termed the NALP3 inflammasome, which controls the processing and activation of pro-inflammatory cytokines IL-1β and IL-18 (179, 212, 213) (Fig. 13). Consequently, mice deficient for CIAS1 ($CIAS^{-/-}$) had increased susceptibility to *L. monocytogenes* due to impaired production of mature IL1-β and IL-18.

The TLR and NLR pathways in macrophages therefore co-operate during *L. monocytogenes* infection to activate the transcription factors NF-κB and AP-1 which induce the expression of pro-inflammatory chemokines such as MIP-1α, MIP-1β and RANTES and cytokines such as, IL-1, IL-6, TNF and IL-12, which is pivotal in controlling innate immune responses to *L. monocytogenes* (116, 132, 179, 182, 185, 235).

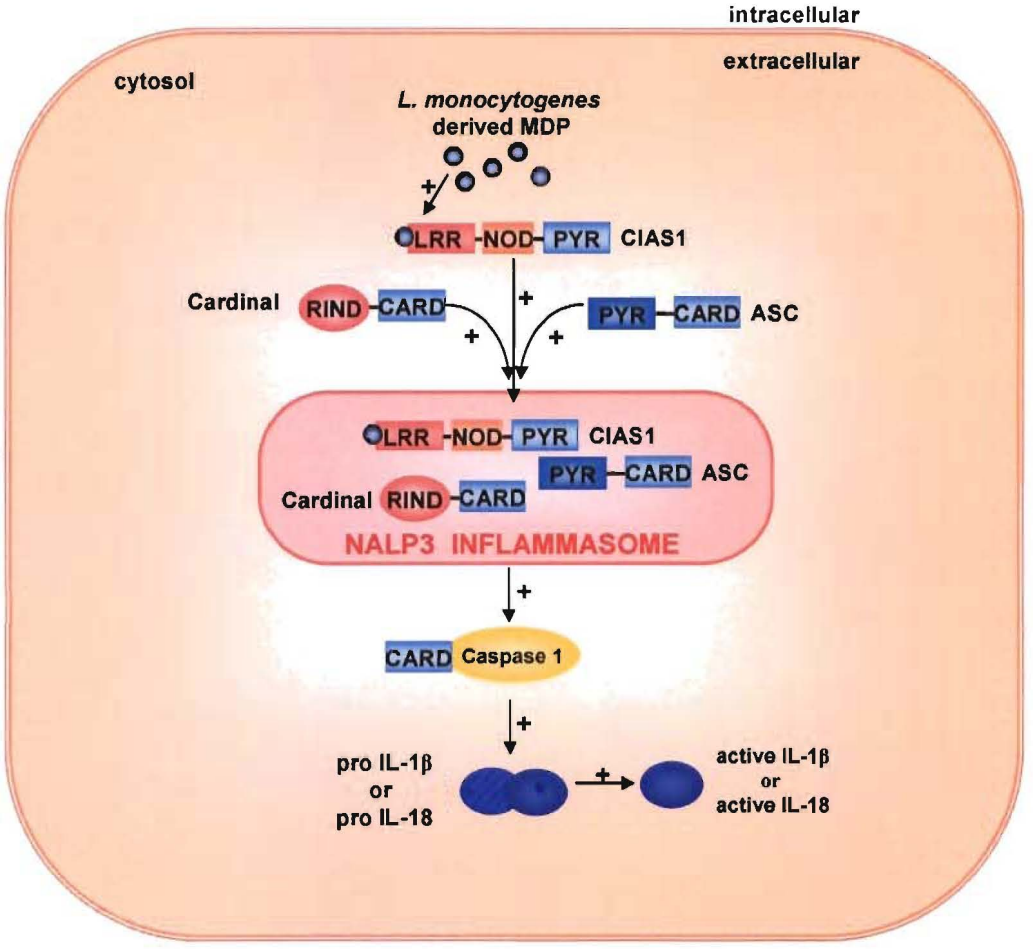


**Figure 13. CIAS1 signalling in macrophages in response to *L. monocytogenes* infection.** Solid black lines with plus signs represent activation; blunt-ended solid lines with minus signs represent inhibition. Figure modified and redrawn from reference (179).

**4. Role of Chemokines and Cytokines during *L. monocytogenes* infection**

Chemokines are low molecular weight cytokines whose chemoattractant activities are critical during innate immunity to *L. monocytogenes*: Chemokines are essential for trafficking and recruiting effector cells such as neutrophils, macrophages, DCS and NK cells to the site of infection, which confine the infection within microabscesses and destroy the bacteria. Within 3 hours after infection with *L. monocytogenes*, Kupffer cells, hepatocytes, macrophages and neutrophils up-regulate expression of MIP-1α, MIP-1β, MIP-2, RANTES, KC and IFN-γ inducible protein-10 (IP-10) in the liver, which is the primary target organ of *L. monocytogenes* (236-240). The initial secretion of MIP-2 by infected Kupffer cells and hepatocytes recruit neutrophils, which become activated and secrete MIP-1α and MIP-1β which in turn recruits and co-localizes macrophages, NK cells and T cells at the site of infection (241). However, MCP-1 is the most important chemokine that is critical for defense against *L. monocytogenes*. MCP-1 in induced by LLO secreted by cytosolic *L. monocytogenes* (65) and is indispensable for the recruitment of macrophages (149). Mice lacking CCR2, receptor for MCP-1, are highly susceptible to *L. monocytogenes* due to impaired emigration of monocytes from bone marrow, resulting in accumulation of activated macrophages in the bone marrow rather than at the site of infection (242, 243). In addition to recruiting effector cells, chemokines also play a role in macrophage activation and have direct antimicrobial activity. For example, MIP-1α, MIP-1β, RANTES, and ATAC/lymphotactin secreted by NK cells were shown to act in synergy with IFN-γ as "type 1 cytokines" to activate macrophages (241). Moreover, chemokines such as monokine induced by IFN-γ (MIG or CXCL9), IFN-γ inducible protein of 10 kDa (IP-10 or CXCL10) and IFN-γ inducible T cell alpha chemoattractant (I-TAC or CXCL11) share structural homology with antimicrobial peptides called defensins, and posses antimicrobial activity against *Escherichia coli* and *L. monocytogenes* which is augmented by IFN-γ (244).

Both IL-6 and IL-1 are required for resistance to *L. monocytogenes* early during infection and are important for regulating the neutrophil responses at the sites of infection (245-248). Kupffer and macrophages are the primary source of IL-6 produced in the livers of mice during *L. monocytogenes* infection, and the production of IL-6 by is independent on IFN-γ and TNF and correlates with disease severity (249). Mice deficient for IL-6 (IL-$6^{-/-}$) are highly susceptible to *L. monocytogenes* and have increased bacterial load in the liver and spleen that correlates with inefficient peripheral blood neutrophilia (246). However, at low doses IL-$6^{-/-}$ mice are able to clear *L. monocytogenes* infection (250). The protective function of IL-6 during *L. monocytogenes* infection is not completely understood, probably due to pleiotropic

effects on diverse systemic and tissue specific biological responses (251). IL-1α and IL-1β belong to the IL-1 family of potent inflammatory cytokines that contribute to a number of normal physiologic processes and to the development of a number of inflammatory diseases. IL-1 is essential for the activation of and neutrophils during *L. monocytogenes* infection (245, 247) and primes neutrophils to produce bactericidal molecules such as reactive oxygen intermediates (ROI) (252). In addition, although IL-1 is not chemotactic, it up-regulates the expression of chemokines and adhesion molecules (253, 254) thereby promoting the recruitment of effector cells to infectious foci (245, 247). Although, IL-1β deficient (IL-1β$^{-/-}$) mice showed equivalent resistance to *L. monocytogenes* as WT controls, complete inhibition of IL-1 signaling via blockade of the type I IL-1R by mAb or by gene targeting greatly increased the susceptibility of the mice injected with a sub-lethal dose of *L. monocytogenes*, and was accompanied with enhanced bacterial growth in the livers and spleens (248, 255).

TNF, IL-12 and IL-18 produced via the TLR and NLR pathways, synergize to stimulate the production of IFN-γ by NK cells (256-259), CD8+ T cells (260-263), dendritic cells (264), Th1 cells (265) and IKDCs (178). TNF is critical for innate antibacterial defenses and macrophage activation during *L. monocytogenes* infection (266, 267). Blockade of TNF signaling by the genetic deletion of the TNF receptor I or by the depletion of TNF using monoclonal antibodies (268) rendered mice highly susceptible to sub-lethal doses of *L. monocytogenes* (266-270). Induction of TNF during *L. monocytogenes* infection is dependent on TLR2 and Myd88 signaling pathway (200), and together with IL-12 activates NK cells to produce IFN-γ (259). Moreover, TNF has phagocytic and bactericidal/bacteriostatic functions (271) and synergizes with IFN-γ to activate the listericidal activity of macrophages (272). Recently, the soluble form of TNF was shown to be required for the control of listerial growth and cellular inflammation during primary high-dose infections, whereas the membrane bound form of TNF was required for resolution of a secondary high-dose infection and for T cell memory (273, 274). IL-12 is also critical for innate immune responses against *L. monocytogenes* (275) and is produced by Kupffer cells, macrophages, neutrophils and dendritic cells (276-280). Neutralization of IL-12 in mice decreased macrophage activation resulting in enhanced susceptibility, bacterial overgrowth and early death (275, 281). Administration of recombinant IFN-γ was able to restore the deleterious effect of anti-IL-12 treatment, thereby demonstrating a role for IL-12 in the production of IFN-γ early during *L. monocytogenes* infection (275). Moreover, mice deficient for IFN-γR (IFN-γR$^{-/-}$) expressed normal levels of IL-12 as compared to controls, confirming the that the initial production of IL-12 is independent of IFN-γ (282). However, *in vivo* infection of IL-12 deficient mice (IL-

$12^{-/-}$) showed that IL-12 was only crucial for effective innate immune responses at higher infective doses of *L. monocytogenes*, but not at low infective doses when residual activity of IL-18 could compensate for IL-12 (283). In addition to TNF, IL-12 can also synergize with IL-18 to stimulate the production of IFN-γ in NK cells (256-258), CD8+ T cells (261), Th1 cells (265) and dendritic cells (264). IL-18 is a pro-inflammatory cytokine that belongs to the IL-1 cytokine family and is a pleiotropic factor involved in the regulation of both innate and acquired immune responses. IL-18 is expressed via a Myd88-dependent pathway in antigen-presenting cells and is produced as a precursor requiring caspase-1 for cleavage into an active IL-18 molecule (284). Indeed mice deficient for IL-18 ($IL\text{-}18^{-/-}$) or caspase 1 ($Casp1^{-/-}$) were mildly susceptible to *L. monocytogenes*, since they were able to produce IL-12 and TNF (200, 285). However, mice doubly deficient for 12 and IL-18 were highly susceptible to *L. monocytogenes*, but not to the same extent as $Myd88^{-/-}$ or IFN-$\gamma^{-/-}$ mice (200). In addition, the activation of IL-18 is also dependent on the NALP3 inflammasome proteins NALP3 and ASC, which activate caspase 1 in response to cytosolic invasion by *L. monocytogenes* (286). Besides its IFN-γ enhancing capacity, IL-18 also augments the cytotoxic activity of both NK and T cells (257, 287-290) and can enhance production of other pro-inflammatory mediators in these cells (257, 291-294). Moreover, IL-18 plays an important in both innate and adaptive immune responses to *L. monocytogenes* involving the production of TNF and nitric oxide (NO) as well as IFN-γ (295). During *L. monocytogenes* infection, the pro-inflammatory responses are themselves regulated by anti-inflammatory cytokine IL-10, which is also produced by activated macrophages with kinetics similar to those for the pro-inflammatory mediators (259, 296). The suppressive role of IL-10 early in *L. monocytogenes* infections was demonstrated by *in vivo* neutralization (297), administration of recombinant IL-10 administration (298) or by IL-10 deficient ($IL\text{-}10^{-/-}$) mice (299).

### 5. Role of IFN-γ during *L. monocytogenes* Infection

The production of IFN-γ is crucial for full macrophage activation, which produce pro-inflammatory cytokines and chemokines which in turn further induce further production of IFN-γ and enhanced macrophage activation in a positive feedback loop (114). During the innate immune response to *L. monocytogenes*, IFN-γ is crucial for controlling bacterial growth by activating the antimicrobial and antigen-presenting properties of macrophages (142, 143, 300-305). IFN-γ is produced by multiple cell types upon synergistic activation by a combination of TNF, IL-12 and/or IL-18 (142, 143, 178, 257-259, 261, 264, 270, 301, 306-310). More recently, other IFN-γ inducing cytokines such as IL-21, IL-23, and IL-27 have been described and may play overlapping and/or redundant roles in the innate immune

response against *L. monocytogenes* (311-313). Evidence that IFN-γ is critically important in the innate immune responses to *L. monocytogenes* comes from experiments using mice deficient for either IFN-γ (IFN-$\gamma^{-/-}$) (277, 314), or the IFN-γ receptor (IFN-γ $R^{-/-}$) (277, 282) or cell specific deletion of IFN-γRα in recently activated macrophages (315). These mice have multiple defects and do not survive the first 5 days of *L. monocytogenes* infection, even when injected with a very low dose of 70 *L. monocytogenes* bacilli (282). Early *in vitro* studies by Portnoy indicated that TNF acted synergistically with IFN-γ to promote the listericidal activity of macrophages, and that the primary role of IFN-γ was to prevent access of *L. monocytogenes* to the macrophage cytoplasm and to enhance phago-lysosome digestion of the bacilli (165). Indeed, electron microscopy of macrophages from *L. monocytogenes* infected IFN-$\gamma^{-/-}$ or IFN-γ$R^{-/-}$mice showed that these mice were unable to restrict *L. monocytogenes* bacilli to the phagosomes resulting in increased escape into the cytoplasm leading to uncontrolled bacterial growth and early death (277, 282, 314). However, the mechanism whereby IFN-γ mediates confinement and bacterial killing is only partially understood. Two general antimicrobial mechanisms implemented by activated macrophages include (i) the production of reactive oxygen intermediates (ROI) by the phagocyte NADPH oxidase (phox) and reactive nitrogen intermediates (RNI) by inducible nitric oxide synthase (iNOS) and (ii) enzymatic degradation of the pathogen mediated by phago-lysosome fusion. Both these pathways synergize to rapidly confine and restrict/terminate listerial growth within the liver.

At the phagosome level, listericidal activity of IFN-γ is mediated by the small GTPase Rab5a, which co-ordinates confinement of the *L. monocytogenes* bacilli within the phagosome, phagosome maturation, phago-lysosome fusion and subsequent killing by lysosomal enzymes (73, 316). Confinement of *L. monocytogenes* within the phagosome is dependent on active GTP-bound Rab5a (76) and the localized release of nitric oxide and superoxide into the phagosomal space (73, 75). However the actual mechanisms of how this is achieved are not fully elucidated. IFN-γ up-regulates the expression and activation of Rab5a into its active GTP-bound from (316), which directly accelerates maturation of *L. monocytogenes*-containing phagosomes, phago-lysosome fusion and consequent bacterial killing (316). The release of nitric oxide and superoxide into the small space of the phagosome is generally considered to cause fatal oxidative damage to the bacilli (132, 317, 318). However, recent studies have indicated that phagocyte NADPH oxidase, is involved in an additional pathway that promotes bacterial killing via potassium ion influx. High concentrations of superoxide in the phagosome was shown to result in the accumulation of anionic charge, which was compensated for by an influx of potassium ions across the phagosome membrane in a pH-

dependent manner. The consequent rise in ionic strength and alkalinity facilitated the release of cationic granule proteins elastase and cathepsin G from the anionic sulphated proteoglycan matrix, which resulted in bacterial destruction. (319-322). Furthermore, the alkaline conditions within the phagosome would most likely neutralize the activity of LLO by preventing its integration into the phagosome membrane and thereby confine *L. monocytogenes* within the phagosome (56). *L. monocytogenes* competes with the above defense pathway by delaying of phagosome maturation, thereby "buying time" for its escape from the phagosome and consequently avoiding phago-lysosome fusion and digestion by lytic enzymes (3, 6). *L. monocytogenes* achieves this by preventing the exchange of inactive GDP-bound Rab5a for active GTP-bound Rab5a (76) via modulation of Rab5a regulating proteins such as guanine nucleotide exchange factors (GEFs), GTPase Activating proteins (GAPs) and guanine diphosphate (GDP) dissociation inhibitors (GDIs) (76).

**6. Role of RNI and ROI during *L. monocytogenes* infection**

Although, several studies using gene deficient mice have shown that nitric oxide and superoxide are important for pathogen killing, these molecules are not essential (75, 323-325). Mice deficient for inducible nitric oxide genes ($iNOS^{-/-}$) had significantly increased susceptibility to pathogens such as *Mycobacterium tuberculosis* (326), *Leishmania major* (327) and ectromelia virus (328), but were able to adequately clear and recover from *L. monocytogenes* (110, 278, 324) and *Toxoplasma gondii* (329, 330) infections. Similarly, mice deficient for the p47phox ($p47phox^{-/-}$) (323) and gp91phox ($gp91phox^{-/-}$) (325) components of the phagocyte NADPH phagocyte oxidase, efficiently cleared and recovered from *L. monocytogenes* infections. Furthermore, studies using $gp91phox^{-/-}/NOS2^{-/-}$ double gene deficient mice, indicated that phagocyte NADPH oxidase and iNOS could substantially compensate for each other's deficiency (324).

Taken together, these studies demonstrated that although nitric oxide and superoxide were are important for pathogen killing, they were not essential. Moreover, studies using mice deficient for specific innate immune receptors or components of innate immune signaling pathways have underscored the hypothesis that macrophages have an alternative listericidal pathway that is independent of nitric oxide (110, 278, 324), superoxide (323-325) TLR2 (203) and MyD88 (203) (Table 2). Mice deficient for TNF Receptor p55 ($TNFRp55^{-/-}$) (266, 267), IFN-γ ($IFN\text{-}\gamma^{-/-}$) (277, 314), IFN-γ-Receptor ($IFN\text{-}\gamma R^{-/-}$) (277, 282), Interferon Consensus Sequence Binding Protein ($ICSBP^{-/-}$) (331), Interferon Regulatory Factor 2 ($IRF2^{-/-}$) (331), RelB (332) and CCAAT/enhancer binding protein beta ($C/EBP\beta^{-/-}$) (333) are all severely

susceptible to *L. monocytogenes*, even when infected with very low doses. Since IFN-γ activates the cytocidal or cytostatic potential of macrophages (271, 282) and TNF has phagocytic and bactericidal/bacteriostatic functions (271), this hypothetical killing pathway is most likely activated by these cytokines. IFN-γ would be the first component in the pathway, since the IFN-$\gamma^{-/-}$ (277, 314) and IFN-$\gamma R^{-/-}$ (277, 282) mice had impaired induction of TNF. Similarly RelB would be downstream of IFN-γ, since mice deficient in this transcription factor efficiently produced IFN-γ but have impaired macrophage activation due to defective induction of TNF (334). Consequently TNF would be downstream of IFN-γ and RelB. The most downstream molecule in this hypothetical pathway would be C/EBPβ, since the C/EBP$\beta^{-/-}$ mice expressed normal levels of IFN-γ and TNF (333). Moreover, experiments by Pizarro-Cerda et al (335) using C/EBP$\beta^{-/-}$ mice infected with *Brucella abortus*, indicated that C/EBPβ promoted endocytosis and membrane fusion between endosomes and pathogen-containing phagosomes in a G-CSF-dependent manner (335). Since IFN-γ stimulation results in the enhanced expression (336, 337) and activation of C/EBPβ (338, 339), and TNF promotes the translocation of C/EBPβ to the nucleus in response to pro-inflammatory cytokine signalling (340), it can therefore be envisaged that IFN-γ and TNF signalling converge on C/EBPβ to transcribe genes required for confinement of *L. monocytogenes* within the phagosome, leading to phago-lysosome fusion and consequent bacterial killing (Fig. 14). Alternatively, a third pathway mediated by IFN-γ and/or TNF activation and independent of iNOS , superoxide and C/EBPβ may be possible.

**Table 2. Gene deficient mouse strain responses to *L. monocytogenes* infection**

| Mouse strain | Response to *L. monocytogenes* infection | Reference |
|---|---|---|
| C/EBPβ$^{-/-}$ | Very susceptible, early lethality | (333) |
| ICSBP | Very susceptible, early lethality | (331) |
| IFN-γ$^{-/-}$ | Very susceptible, early lethality | (314) |
| IFN-γR | Very susceptible, early lethality | (277, 282) |
| IRF2 | Very susceptible, early lethality | (331) |
| Myd88$^{-/-}$ | Very susceptible, early lethality | (200, 203, 243) |
| RelB$^{-/-}$ | Very susceptible, early lethality | (334) |
| TNFRp55$^{-/-}$ | Very susceptible, early lethality | (266, 267) |
| CCR2$^{-/-}$ | Highly susceptible, early lethality | (149, 150) |
| IL-1R$^{-/-}$ | Highly susceptible, early lethality | (248) |
| IL-6 | Highly susceptible, early lethality | (246) |
| CIAS1$^{-/-}$ | Moderately increased susceptibility | (212) |
| IL-12 | Moderately increased susceptibility | (283) |
| iNOS$^{-/-}$ | Moderately increased susceptibility | (150, 278, 324) |
| MCP-1$^{-/-}$ | Moderately increased susceptibility | (243) |
| CASP1$^{-/-}$ | Mildly increased susceptibility | (203, 285) |
| p47phox$^{-/-}$ | Mildly increased susceptibility | (323) |
| RIP2$^{-/-}$ | Mildly increased susceptibility, delayed lethality | (232) |
| IL-1β$^{-/-}$ | Normal resistance | (341) |
| IRF1 | Normal resistance | (331) |
| TLR2 $^{-/-}$ | Normal resistance | (200, 203, 243) |
| TLR4$^{-/-}$ | Normal resistance | (200, 243) |
| IFN-αR$^{-/-}$ | Increased resistance | (204-206) |
| IL-10 | Increased resistance | (299) |
| IRF3$^{-/-}$ | Increased resistance | (206) |

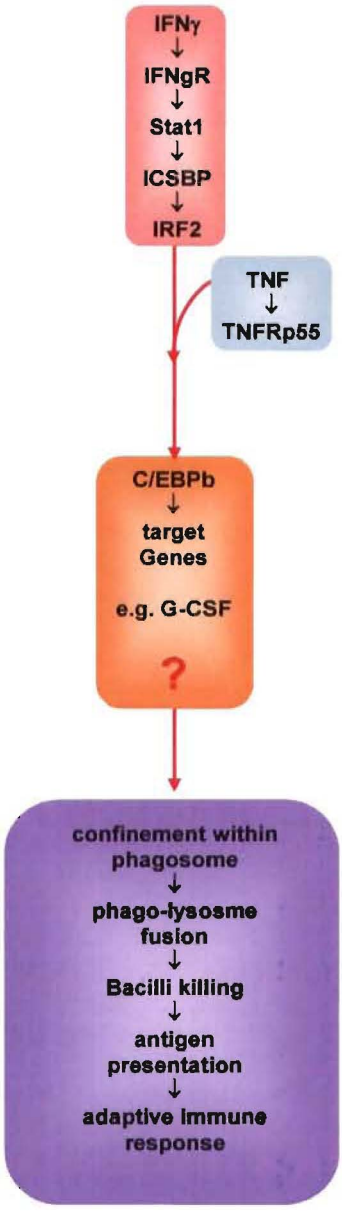


**Figure 14. Hypothetical listericidal pathway independent of nitric oxide and superoxide.** Mice deficient for IFN-γ, IFN-γ-R, ICSBP, IRF2 and C/EBPβ have underscored the hypothesis that macrophages have an alternative listericidal pathway that is independent of nitric oxide, superoxide, TLR2 and MyD88. In this hypothetical pathway, IFN-γ and TNF signalling via their receptors converge on the transcription factor C/EBPβ, resulting in its activation and translocation to the nucleus respectively. In response to IFN-γ and TNF stimulation, activated C/EBPβ transcribes granulocyte colony stimulating factor (G-SCF) and other, as yet, unknown (designated as ?) genes required for confinement of *L. monocytogenes* within the phagosome leading to phago-lysosome fusion and consequent bacterial killing and enzymatic digestion.

## 6. Role of C/EBPβ in IFN-γ signal transduction

C/EBPβ is a transcription factor that is also known as Nuclear Factor IL-6 (NF-IL-6), IL-6 induced DNA binding protein (IL-6- DBP) and C-reactive protein 2 (CRP2). In this dissertation, the current gene name, C/EBPβ, as stipulated by Mouse Genomic Nomenclature Committee (MGNC) (342), will be used. C/EBPβ belongs to the bZIP transcription factor family which includes C/EBPα, C/EBPγ, C/EBPδ, C/EBPε, and is involved in many physiologic processes such as carbohydrate metabolism, lipid storage, differentiation, cellular, Th1 immune responses, macrophage-mediated antibacterial, anti-tumour defenses and female fertility (339). C/EBPβ contains a bZIP domain at its C-terminal end which is comprised of a leucine zipper and a basic region (217, 343) (Fig. 15). The bZIP domain is essential for DNA binding and for mediating homodimeric and heterodimeric interactions with other C/EBP isoforms. The dimerization domain, also known as the leucine zipper, contains seven leucine repeats that intercalate with the leucine repeats of the dimerizing partner (344). In the centre of the protein are two regulatory domains (RD), RD1 and RD2, which contain sites that can be phosphorylated by protein kinases. At the N-terminal end of the protein is the transcription activation domain. Dimerization between C/EBPβ and different C/EBP isoforms allows the expression of C/EBPβ target genes to be finely regulated in particular tissues and in response to various divergent stimuli (345).

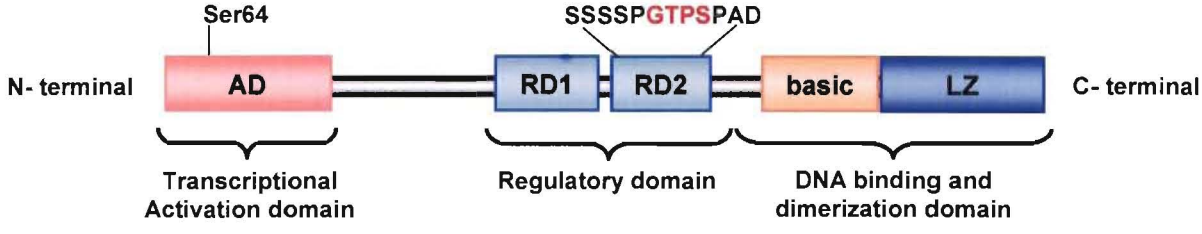


**Figure 15. Schematic diagram showing structure of C/EBPβ.** C/EBPβ contains three structural modules, the N-terminal transcriptional activation domain (AD), the intracellular regulatory domains (RD) and the bZIP domain that consists of a leucine zipper and a basic region. Activation of C/EBPβ requires dephosphorylation at serine 64 in the AD and phosphorylation at the GTPS consensus site in RD2. The leucine zipper mediates dimerization with other transcription factors while the basic domain, which rich in basic amino acids, dictates DNA-binding specificity. The amino acid sequence phosphorylated by ERK1/2 is indicated in red. Figure modified and redrawn from reference (339).

C/EBPβ is expressed as two isoforms, which are generated from a single mRNA by a leaky ribosomal scanning mechanism. The first isoform encodes the full-length C/EBPβ protein (346) and the second isoform a truncated protein termed liver inhibitory protein (LIP), which contains only the DNA-binding and leucine zipper domains (347, 348). Heterodimerization between LIP and full-length C/EBPβ inhibits transcriptional activity in sub-stoichiometric amounts, suggesting a naturally occurring dominant negative mechanism of transcriptional regulation (349). C/EBPζ (also known as CHOP or GADD153) is expressed only under conditions of stress (349, 350) and its dimerization with C/EBPβ also inhibits transcription (349). The expression of C/EBPβ is strongly up-regulated by LPS, IFN-γ, IL-6, IL-1, dexamethasone and glucagon (336, 337). Moreover, TNF promotes nuclear localization of C/EBPβ in response to inflammatory stress (340). Cytokine treatment further increases C/EBPβ transcriptional activity via enhanced DNA binding (348). The activation of C/EBPβ at the post-transcriptional level involves phosphorylation by protein kinases such as PKA, PKC, ribosomal S6 kinase (RSK), and extracellular signal-related kinase (ERK) at conserved serine and threonine residues (338, 351-356). Once activated, C/EBPβ forms heterodimeric complexes with other transcription factors, such as Retinoblastoma 1 (pRB), NF-κB, trans-acting transcription factor 1 (Sp1) and myeloblastosis oncogene (Myb) and binds to a variety of response elements (339). For example the C/EBPβ:NF-κB heterodimer synergizes to transcribe genes encoding the acute-phase response proteins such as serum amyloid (SA)A1, SAA2, SAA3 and α1-acid glycoprotein, as well as cytokines IL-6, IL-12, grnaulocyte colony stimulating factor (G-CSF) and MIP2 (357-363). In some instances, other C/EBP isoforms are able to compensate for C/EBPβ, thereby preventing impaired transcription of C/EBPβ target genes in absence of C/EBPβ. For example, the promoter for iNOS contains a C/EBPβ binding site, yet C/EBPβ$^{-/-}$ mice efficiently produce nitric oxide in response to infection by *L. monocytogenes* (333). On the other hand, C/EBPβ is indispensable for the transcription of genes such as C-type lectin domain family 4 member e (CLECSF9), IFN-stimulated gene factor 3 gamma (ISGF3γ), G-CSF and IL-12p35 in response LPS stimulation (364-366).

Moreover, studies using C/EBPβ$^{-/-}$ mice have shown that C/EBPβ is critical for killing intracellular pathogens such as *Listeria* (333), *Salmonella* (333), *Brucella* (335), *Mycobacterium* (367) and *Candida* (368). The mortality kinetics of C/EBPβ$^{-/-}$ mice infected with a low dose of *L. monocytogenes* infection is comparable to that of TNFRp55$^{-/-}$ (266, 267), (IFN-γ$^{-/-}$ (277, 314), IFN-γR$^{-/-}$ (277, 282), ICSBP$^{-/-}$ (331), IRF2$^{-/-}$ (331) and RelB (332) mice suggesting that C/EBPβ$^{-/-}$ is a downstream effector molecule of IFN-γ signalling.

Moreover, C/EBPβ is also involved in regulating transcription of genes stimulated by IFN-α and IFN-β. Generally, IFN-γ stimulated genes contain a IFN-γ-activated site (GAS) in their promoters, whereas IFN-α/β stimulated genes contain IFN-stimulated response element ISRE. More recently, a novel IFN-γ-response element termed IFN-γ-activated transcriptional element (GATE) was discovered (369), through which C/EBPβ links the IFN-γ and IFN-α/β signalling pathways (339, 352, 369-371). In the IFN-α/β induced signalling pathway, Janus kinase 1 (JAK1) and Tyrosine kinase 2 (TYK2) induces tyrosine phosphorylation of Signal transducer and activator of transcription (STAT) 1 and STAT2 respectively, which in association with ISGF3γ (also known as IFN gene regulatory factor-9; IRF-9) forms the multimeric transcription factor termed IFN-stimulated gene factor 3 (ISGF3). The ISGF3 transcription factor complex initiates transcription of genes containing an the IFN-stimulated response element (ISRE) in their promoters e.g. MHC class I genes. ISGF3γ is critical for driving antiviral defenses and acts in synergy with IRF-1 to drive transcription in response to both IFN-γ and IFN-α/β signalling (372). The transcription of ISGF3γ is mediated by C/EBPβ though the GATE in the ISGF3γ promoter (373-376). Both IL-6 and IFN-γ augment IFN-α/β signalling by inducing the expression of C/EBPβ (336, 337) and consequently that of ISGF3γ (370, 373-376)s.

Recent studies have shown that at least two IFN-γ-induced MAPK signals converge on to C/EBPβ for inducing transcription of IFN-γ responsive genes (338, 339) (Fig. 16). The first pathway is driven by extracellular signal-regulated kinases (ERKs), which phosphorylates C/EBPβ in its RD2 and the second pathway is driven by the mixed-lineage kinases (MLKs), which induces a dephosphorylation leading to the recruitment of transcriptional co-activators. Both these pathways act in concert to mediate transcription of genes in response to IFN-γ signalling. In the first pathway, IFN-γ binding to its receptor IFN-γR results in the phosphorylation of STAT1, which in turn activates an unknown factor that phosphorylates and activates MAP kinase kinase 1 (MEKK1) (352). Activated MEKK1 recruits MAP kinase kinase 1 (MEK1) and ERK1/2 to its N-terminal domain (377). Activated MEKK1 phosphorylates MEK1 on the same residue as does Raf (378). Activated MEK1 in turn activates ERK1/2 (379), which phosphorylates C/EBPβ at threonine residue 189 in the ERK consensus GTPS phosphorylation site located in the RD2 domain (380). Phosphorylation at the GTPS site induces a conformational change that allows C/EBPβ to dimerize with other transcription factors (381). In the second pathway, IFN-γ signals through the IFN-γR to activate an unknown factor which in turn activates MLK3. Activated MLK3 indirectly mediates the dephosphorylation of C/EBPβ at a conserved serine residue at position 64 (338),

which results in recruitment of transcriptional co-activators such as p300 (338). The convergence of the ERK1/2 and MLK3 pathways on C/EBPβ and the recruitment of transcriptional co-activators therefore sets the stage for activation of the IFN-stimulated genes containing ISRE, GAS and GATE motifs in their promoters (Fig. 4). Due to its severe susceptibility to *L. monocytogenes*, despite efficient production of nitric oxide and superoxide, together with its role in mediating IFN-γ stimulated transcription of innate defense genes, the C/EBPβ$^{-/-}$ mouse model was therefore considered a useful tool to identify the genes involved in IFN-γ mediated listericidal activity.

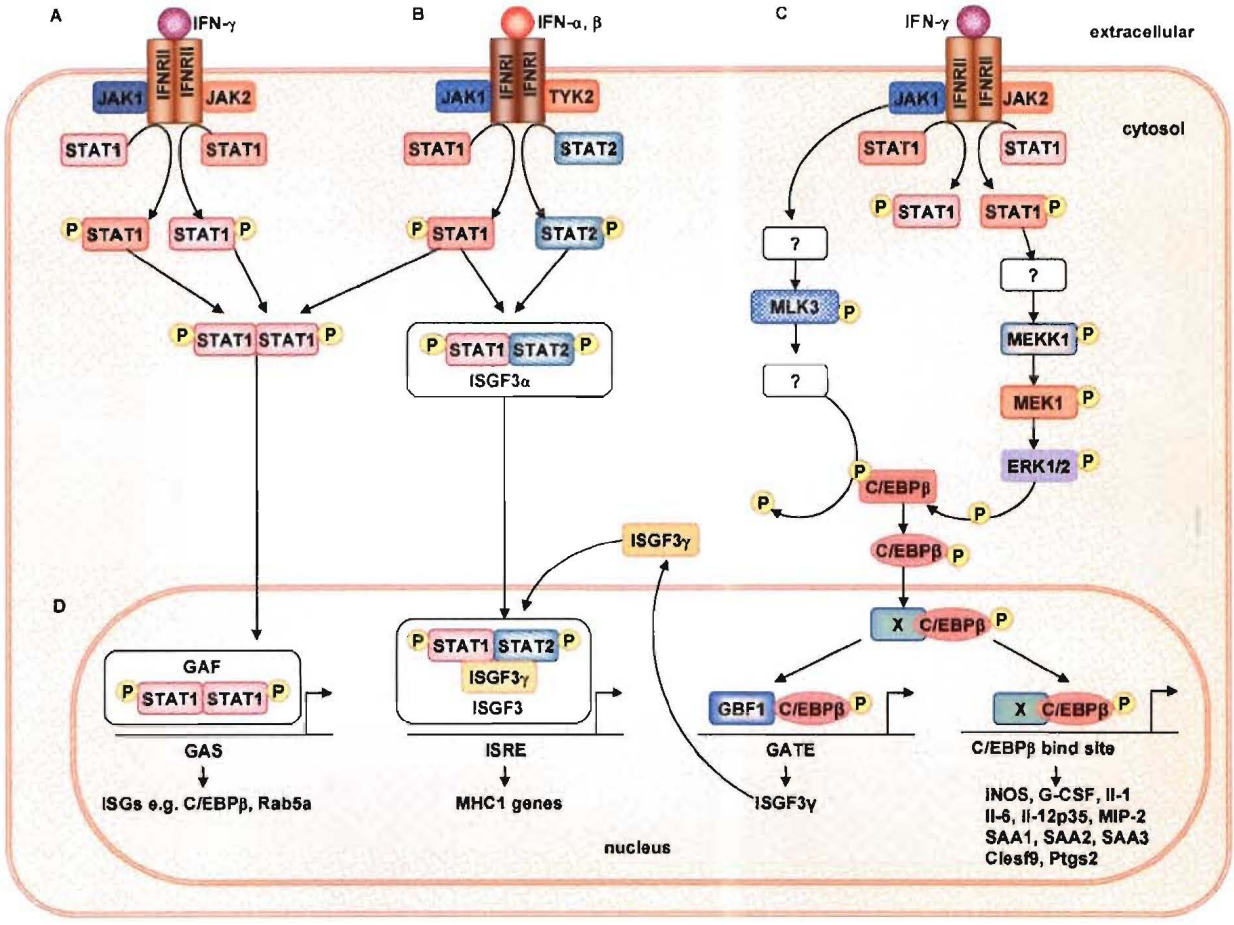


**Figure 16. Regulation of C/EBPβ-mediated transcription by IFN-γ.** (A) IFN-γ signalling via the IFN receptor II triggers tyrosine phosphorylation of STAT1via JAK1 and JAK2. The STAT1 dimer migrates to the nucleus and initiates the transcription of genes that possess the GAS in their promoter. (B) Similarly, IFN-α,β signalling via IFN receptor I triggers phosphorylation of STAT1 and STAT2 via JAK1 and TYK2 respectively. In the nucleus the STAT1:STAT2 heterodimer binds with ISGF3γ to form the ISGF3 complex that initiates transcription of genes containing an ISRE. (C) IFN-γ signalling via IFN receptor II triggers activation of MAPK pathways that converge on C/EBPβ resulting in its activation by phosphorylation of threonine[189] in the GTPS motif of RD2 and dephosphorylation of serine[64] in the AD. Activation of C/EBPβ induces a conformational change that allows C/EBPβ to dimerize with other transcription factors (designated as X) and recruit transcriptional co-activators, such as p300, in order to transcribe genes containing either a consensus C/EBPβ binding site or GATE motif in their promoters e.g. transcription of ISGF3γ by C/EBPβ through GATE links the IFN-γ and IFN-α,β signalling pathways. Transcription of C/EBPβ itself is induced by IFN-γ. Figure modified and redrawn from reference (339).

## C. RESEARCH HYPOTHESIS AND STRATEGY

The aim of the current study was was to identify the genes involved in the hypothetical listericidal pathway that is independent of nitric oxide and superoxide. Based on the hypothetical pathway outlined in (Fig. 17), genes involved in mediating listericidal activity would most likely be downstream of C/EBPβ. Since activated macrophages and neutrophils are the major cell types involved in T cell independent killing of *L. monocytogenes* (114), it was therefore postulated that comparison of the gene expression profiles between activated WT and C/EBPβ$^{-/-}$ macrophages infected with *L. monocytogenes* would increase the probability of identifying the listericidal genes. Moreover, the bone marrow from WT and C/EBPβ$^{-/-}$ mice would provide a plentiful source of quiescent bone marrow derived macrophages (BMDMs) for *in vitro* infection experiments.

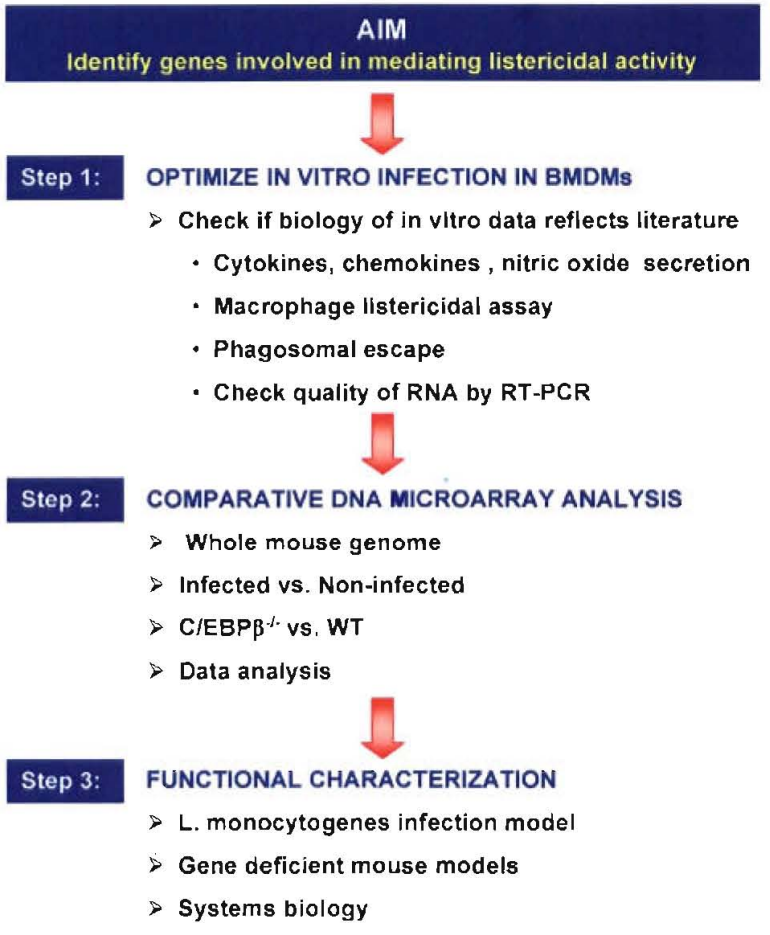


**Figure 17. Research strategy employed to identify genes involved in macrophage effector functions against *L. monocytogenes* that is independent nitric oxide and superoxide.**

The first part of the research strategy was to establish and optimize *in vitro* infection of WT and C/EBPβ$^{-/-}$ bone marrow derived macrophages (BMDMs) with *L. monocytogenes* so that the biology of the *in vitro* infection faithfully represented that of *in vivo* infections as reported in literature (333, 364, 366, 370). Furthermore, RNA extracted from *L. monocytogenes* infected WT and C/EBPβ$^{-/-}$ BMDMs was stringently tested to ensure that it was of high quality and that it represented the expected gene expression profile for genes known to be differentially expressed in macrophages deficient for C/EBPβ (333, 364, 366, 370). These controls thereby provided a solid foundation on which to base the gene expression profiling experiments. The second part of strategy was to identify the listericidal genes, which were postulated to be differentially expressed between the infected WT and C/EBPβ$^{-/-}$ macrophages. A comparative gene expression profiling strategy using whole mouse genome oligonucleotide DNA microarrays, rather than suppressive subtractive PCR (SSH PCR) (382-385) or serial analysis of gene expression (SAGE) (386-388) was followed, since DNA microarrays involved shorter experimental time scales, were more cost effective and required relatively simple technical expertise. In contrast, both SSH PCR and SAGE are technically very demanding and the protocols are extremely time consuming due to a multitude of PCR and cloning steps. Moreover, both these methods requires extensive DNA sequencing for the identification of the cloned genes, which makes these methods much more expensive than DNA microarrays. The third part of the research strategy was to functionally characterized the roles of candidate genes involved in defense against *L. monocytogenes* infection using appropriate gene deficient mouse models. Moreover a systems biology approach would be used to investigate the mechanism whereby the candidate genes mediated protection against *L. monocytogenes* during infection.

## CONCLUSION

In the current study, *L. monocytogenes* was used as a model intracellular pathogen to identify genes involved in mediating macrophage bactericidal effector activity. *L. monocytogenes* has developed many molecular adaptations to invade and proliferate within the intracellular environment of many different cell types, thereby enabling it to cross the intestinal-, blood-brain- and placental defense barriers. Several virulence factors mimic the activity of eukaryotic molecules and thereby exploit the biological functions of the infected cell to favour bacterial survival. These molecular adaptations and elaborate mimicries used by *L. monocytogenes*, has made it an excellent tool for the study of cellular processes such as actin-based motility, growth-factor mediated signalling, endocytosis and cellular adhesion. In addition, due to its ability to cross protective defense barriers and induce strong macrophage and T cell responses, *L. monocytogenes* has emerged as an excellent model to study the pathophysiology of a complex bacterial infection in animals. Furthermore, the availability of the genome sequence of five *L. monocytogenes* serovars (91, 389, 390) has provided an excellent platform in which to unravel the genetic basis of *L. monocytogenes* virulence, by whole genome comparison with its closely related non-pathogenic species *L. monocytogenes*. In the immunocompetent host, protective immunity against *L. monocytogenes* evolves through several phases, each of which is controlled by different cell types, cytokines and cytocidal molecules. These different cells and effector molecules do not participate equivalently at all stages of the infection and their importance depends on the time of infection, the host's immunologic status, and the site of infection (147, 167, 317). Activated macrophages, dendritic cells, neutrophils and NK cells are critical for immediate control of *L. monocytogenes* proliferation and they communicate with each other by producing and/or responding to pro-inflammatory cytokines and chemokines, which in turn activate and mobilize effector cell populations to the site of infection. The current study has addressed the hypothesis that macrophages have an alternative killing mechanism that is independent of superoxide and nitric oxide (323-325) but dependent on IFN-γ (277, 282, 314), TNF (266, 267) and C/EBPβ$^{-/-}$ (333). Since the mechanism and the genes involved in this alternative pathway are largely unknown, the aim of this thesis was to identify these macrophage effector genes and to functionally characterize their role during infection by utilizing gene deficient mouse models.

## REFERENCES


1. Lecuit, M. 2005. Understanding how Listeria monocytogenes targets and crosses host barriers. *Clin Microbiol Infect 11:430.*
2. Vazquez-Boland, J. A., M. Kuhn, P. Berche, T. Chakraborty, G. Dominguez-Bernal, W. Goebel, B. Gonzalez-Zorn, J. Wehland, and J. Kreft. 2001. Listeria pathogenesis and molecular virulence determinants. *Clin Microbiol Rev 14:584.*
3. Hamon, M., H. Bierne, and P. Cossart. 2006. Listeria monocytogenes: a multifaceted model. *Nat Rev Microbiol 4:423.*
4. Schlech, W. F., 3rd, P. M. Lavigne, R. A. Bortolussi, A. C. Allen, E. V. Haldane, A. J. Wort, A. W. Hightower, S. E. Johnson, S. H. King, E. S. Nicholls, and C. V. Broome. 1983. Epidemic listeriosis--evidence for transmission by food. *N Engl J Med 308:203.*
5. Cossart, P., and P. J. Sansonetti. 2004. Bacterial invasion: the paradigms of enteroinvasive pathogens. *Science 304:242.*
6. Pizarro-Cerda, J., and P. Cossart. 2006. Subversion of cellular functions by Listeria monocytogenes. *J Pathol 208:215.*
7. Cottin, J., O. Loiseau, R. Robert, C. Mahaza, B. Carbonnelle, and J. M. Senet. 1990. Surface Listeria monocytogenes carbohydrate-binding components revealed by agglutination with neoglycoproteins. *FEMS Microbiol Lett 56:301.*
8. Facinelli, B., E. Giovanetti, G. Magi, F. Biavasco, and P. E. Varaldo. 1998. Lectin reactivity and virulence among strains of Listeria monocytogenes determined in vitro using the enterocyte-like cell line Caco-2. *Microbiology 144 ( Pt 1):109.*
9. Braun, L., S. Dramsi, P. Dehoux, H. Bierne, G. Lindahl, and P. Cossart. 1997. InlB: an invasion protein of Listeria monocytogenes with a novel type of surface association. *Mol Microbiol 25:285.*
10. McLaughlan, A. M., and S. J. Foster. 1998. Molecular characterization of an autolytic amidase of Listeria monocytogenes EGD. *Microbiology 144 ( Pt 5):1359.*
11. Guzman, C. A., M. Rohde, T. Chakraborty, E. Domann, M. Hudel, J. Wehland, and K. N. Timmis. 1995. Interaction of Listeria monocytogenes with mouse dendritic cells. *Infect Immun 63:3665.*
12. Cabanes, D., P. Dehoux, O. Dussurget, L. Frangeul, and P. Cossart. 2002. Surface proteins and the pathogenic potential of Listeria monocytogenes. *Trends Microbiol 10:238.*
13. Cheng, L. W., J. P. Viala, N. Stuurman, U. Wiedemann, R. D. Vale, and D. A. Portnoy. 2005. Use of RNA interference in Drosophila S2 cells to identify host pathways controlling compartmentalization of an intracellular pathogen. *Proc Natl Acad Sci U S A 102:13646.*
14. Agaisse, H., L. S. Burrack, J. A. Philips, E. J. Rubin, N. Perrimon, and D. E. Higgins. 2005. Genome-wide RNAi screen for host factors required for intracellular bacterial infection. *Science 309:1248.*
15. Gaillard, J. L., P. Berche, C. Frehel, E. Gouin, and P. Cossart. 1991. Entry of L. monocytogenes into cells is mediated by internalin, a repeat protein reminiscent of surface antigens from gram-positive cocci. *Cell 65:1127.*
16. Alvarez-Dominguez, C., E. Carrasco-Marin, and F. Leyva-Cobian. 1993. Role of complement component C1q in phagocytosis of Listeria monocytogenes by murine macrophage-like cell lines. *Infect Immun 61:3664.*
17. Drevets, D. A., and P. A. Campbell. 1991. Roles of complement and complement receptor type 3 in phagocytosis of Listeria monocytogenes by inflammatory mouse peritoneal macrophages. *Infect Immun 59:2645.*

18. Drevets, D. A., P. J. Leenen, and P. A. Campbell. 1993. Complement receptor type 3 (CD11b/CD18) involvement is essential for killing of Listeria monocytogenes by mouse macrophages. *J Immunol 151:5431.*
19. Kolb-Maurer, A., S. Pilgrim, E. Kampgen, A. D. McLellan, E. B. Brocker, W. Goebel, and I. Gentschev. 2001. Antibodies against listerial protein 60 act as an opsonin for phagocytosis of Listeria monocytogenes by human dendritic cells. *Infect Immun 69:3100.*
20. Dunne, D. W., D. Resnick, J. Greenberg, M. Krieger, and K. A. Joiner. 1994. The type I macrophage scavenger receptor binds to gram-positive bacteria and recognizes lipoteichoic acid. *Proc Natl Acad Sci U S A 91:1863.*
21. Greenberg, J. W., W. Fischer, and K. A. Joiner. 1996. Influence of lipoteichoic acid structure on recognition by the macrophage scavenger receptor. *Infect Immun 64:3318.*
22. Kwiatkowska, K., and A. Sobota. 1999. Signaling pathways in phagocytosis. *Bioessays 21:422.*
23. Helmy, K. Y., K. J. Katschke, Jr., N. N. Gorgani, N. M. Kljavin, J. M. Elliott, L. Diehl, S. J. Scales, N. Ghilardi, and M. van Lookeren Campagne. 2006. CRIg: a macrophage complement receptor required for phagocytosis of circulating pathogens. *Cell 124:915.*
24. Braun, L., B. Ghebrehiwet, and P. Cossart. 2000. gC1q-R/p32, a C1q-binding protein, is a receptor for the InlB invasion protein of Listeria monocytogenes. *Embo J 19:1458.*
25. Vieira, O. V., R. J. Botelho, and S. Grinstein. 2002. Phagosome maturation: aging gracefully. *Biochem J 366:689.*
26. Desjardins, M. 2003. ER-mediated phagocytosis: a new membrane for new functions. *Nat Rev Immunol 3:280.*
27. Jutras, I., and M. Desjardins. 2005. Phagocytosis: at the crossroads of innate and adaptive immunity. *Annu Rev Cell Dev Biol 21:511.*
28. Mengaud, J., H. Ohayon, P. Gounon, R. M. Mege, and P. Cossart. 1996. E-cadherin is the receptor for internalin, a surface protein required for entry of L. monocytogenes into epithelial cells. *Cell 84:923.*
29. Schubert, W. D., C. Urbanke, T. Ziehm, V. Beier, M. P. Machner, E. Domann, J. Wehland, T. Chakraborty, and D. W. Heinz. 2002. Structure of internalin, a major invasion protein of Listeria monocytogenes, in complex with its human receptor E-cadherin. *Cell 111:825.*
30. Perez-Moreno, M., C. Jamora, and E. Fuchs. 2003. Sticky business: orchestrating cellular signals at adherens junctions. *Cell 112:535.*
31. Lecuit, M., R. Hurme, J. Pizarro-Cerda, H. Ohayon, B. Geiger, and P. Cossart. 2000. A role for alpha-and beta-catenins in bacterial uptake. *Proc Natl Acad Sci U S A 97:10008.*
32. Sousa, S., D. Cabanes, C. Archambaud, F. Colland, E. Lemichez, M. Popoff, S. Boisson-Dupuis, E. Gouin, M. Lecuit, P. Legrain, and P. Cossart. 2005. ARHGAP10 is necessary for alpha-catenin recruitment at adherens junctions and for Listeria invasion. *Nat Cell Biol 7:954.*
33. Sousa, S., D. Cabanes, A. El-Amraoui, C. Petit, M. Lecuit, and P. Cossart. 2004. Unconventional myosin VIIa and vezatin, two proteins crucial for Listeria entry into epithelial cells. *J Cell Sci 117:2121.*
34. Braun, L., F. Nato, B. Payrastre, J. C. Mazie, and P. Cossart. 1999. The 213-amino-acid leucine-rich repeat region of the listeria monocytogenes InlB protein is sufficient for entry into mammalian cells, stimulation of PI 3-kinase and membrane ruffling. *Mol Microbiol 34:10.*

35. Braun, L., H. Ohayon, and P. Cossart. 1998. The InlB protein of Listeria monocytogenes is sufficient to promote entry into mammalian cells. *Mol Microbiol 27:1077.*
36. Dramsi, S., I. Biswas, E. Maguin, L. Braun, P. Mastroeni, and P. Cossart. 1995. Entry of Listeria monocytogenes into hepatocytes requires expression of inlB, a surface protein of the internalin multigene family. *Mol Microbiol 16:251.*
37. Shen, Y., M. Naujokas, M. Park, and K. Ireton. 2000. InlB-dependent internalization of Listeria is mediated by the Met receptor tyrosine kinase. *Cell 103:501.*
38. Tang, P., C. L. Sutherland, M. R. Gold, and B. B. Finlay. 1998. Listeria monocytogenes invasion of epithelial cells requires the MEK-1/ERK-2 mitogen-activated protein kinase pathway. *Infect Immun 66:1106.*
39. Ireton, K., B. Payrastre, H. Chap, W. Ogawa, H. Sakaue, M. Kasuga, and P. Cossart. 1996. A role for phosphoinositide 3-kinase in bacterial invasion. *Science 274:780.*
40. Marino, M., L. Braun, P. Cossart, and P. Ghosh. 1999. Structure of the InlB leucine-rich repeats, a domain that triggers host cell invasion by the bacterial pathogen L. monocytogenes. *Mol Cell 4:1063.*
41. Chirgadze, D. Y., J. P. Hepple, H. Zhou, R. A. Byrd, T. L. Blundell, and E. Gherardi. 1999. Crystal structure of the NK1 fragment of HGF/SF suggests a novel mode for growth factor dimerization and receptor binding. *Nat Struct Biol 6:72.*
42. Copp, J., M. Marino, M. Banerjee, P. Ghosh, and P. van der Geer. 2003. Multiple regions of internalin B contribute to its ability to turn on the Ras-mitogen-activated protein kinase pathway. *J Biol Chem 278:7783.*
43. Cossart, P. 2001. Met, the HGF-SF receptor: another receptor for Listeria monocytogenes. *Trends Microbiol 9:105.*
44. Lyon, M., J. A. Deakin, and J. T. Gallagher. 2002. The mode of action of heparan and dermatan sulfates in the regulation of hepatocyte growth factor/scatter factor. *J Biol Chem 277:1040.*
45. Lyon, M., J. A. Deakin, D. Lietha, E. Gherardi, and J. T. Gallagher. 2004. The interactions of hepatocyte growth factor/scatter factor and its NK1 and NK2 variants with glycosaminoglycans using a modified gel mobility shift assay. Elucidation of the minimal size of binding and activatory oligosaccharides. *J Biol Chem 279:43560.*
46. Bierne, H., E. Gouin, P. Roux, P. Caroni, H. L. Yin, and P. Cossart. 2001. A role for cofilin and LIM kinase in Listeria-induced phagocytosis. *J Cell Biol 155:101.*
47. Bierne, H., H. Miki, M. Innocenti, G. Scita, F. B. Gertler, T. Takenawa, and P. Cossart. 2005. WASP-related proteins, Abi1 and Ena/VASP are required for Listeria invasion induced by the Met receptor. *J Cell Sci 118:1537.*
48. Veiga, E., and P. Cossart. 2005. Listeria hijacks the clathrin-dependent endocytic machinery to invade mammalian cells. *Nat Cell Biol 7:894.*
49. Li, N., G. S. Xiang, H. Dokainish, K. Ireton, and L. A. Elferink. 2005. The Listeria protein internalin B mimics hepatocyte growth factor-induced receptor trafficking. *Traffic 6:459.*
50. Seveau, S., H. Bierne, S. Giroux, M. C. Prevost, and P. Cossart. 2004. Role of lipid rafts in E-cadherin-- and HGF-R/Met--mediated entry of Listeria monocytogenes into host cells. *J Cell Biol 166:743.*
51. Goldfine, H., and S. J. Wadsworth. 2002. Macrophage intracellular signaling induced by Listeria monocytogenes. *Microbes Infect 4:1335.*
52. Gandhi, A. J., B. Perussia, and H. Goldfine. 1993. Listeria monocytogenes phosphatidylinositol (PI)-specific phospholipase C has low activity on glycosyl-PI-anchored proteins. *J Bacteriol 175:8014.*
53. Geoffroy, C., J. Raveneau, J. L. Beretti, A. Lecroisey, J. A. Vazquez-Boland, J. E. Alouf, and P. Berche. 1991. Purification and characterization of an extracellular 29-kilodalton phospholipase C from Listeria monocytogenes. *Infect Immun 59:2382.*

54. Bubert, A., Z. Sokolovic, S. K. Chun, L. Papatheodorou, A. Simm, and W. Goebel. 1999. Differential expression of Listeria monocytogenes virulence genes in mammalian host cells. *Mol Gen Genet 261:323.*
55. Moors, M. A., B. Levitt, P. Youngman, and D. A. Portnoy. 1999. Expression of listeriolysin O and ActA by intracellular and extracellular Listeria monocytogenes. *Infect Immun 67:131.*
56. Shatursky, O., A. P. Heuck, L. A. Shepard, J. Rossjohn, M. W. Parker, A. E. Johnson, and R. K. Tweten. 1999. The mechanism of membrane insertion for a cholesterol-dependent cytolysin: a novel paradigm for pore-forming toxins. *Cell 99:293.*
57. Schuerch, D. W., E. M. Wilson-Kubalek, and R. K. Tweten. 2005. Molecular basis of listeriolysin O pH dependence. *Proc Natl Acad Sci U S A 102:12537.*
58. Alvarez-Dominguez, C., R. Roberts, and P. D. Stahl. 1997. Internalized Listeria monocytogenes modulates intracellular trafficking and delays maturation of the phagosome. *J Cell Sci 110 ( Pt 6):731.*
59. Conte, M. P., G. Petrone, C. Longhi, P. Valenti, R. Morelli, F. Superti, and L. Seganti. 1996. The effects of inhibitors of vacuolar acidification on the release of Listeria monocytogenes from phagosomes of Caco-2 cells. *J Med Microbiol 44:418.*
60. Beauregard, K. E., K. D. Lee, R. J. Collier, and J. A. Swanson. 1997. pH-dependent perforation of macrophage phagosomes by listeriolysin O from Listeria monocytogenes. *J Exp Med 186:1159.*
61. Glomski, I. J., M. M. Gedde, A. W. Tsang, J. A. Swanson, and D. A. Portnoy. 2002. The Listeria monocytogenes hemolysin has an acidic pH optimum to compartmentalize activity and prevent damage to infected host cells. *J Cell Biol 156:1029.*
62. Decatur, A. L., and D. A. Portnoy. 2000. A PEST-like sequence in listeriolysin O essential for Listeria monocytogenes pathogenicity. *Science 290:992.*
63. Lety, M. A., C. Frehel, I. Dubail, J. L. Beretti, S. Kayal, P. Berche, and A. Charbit. 2001. Identification of a PEST-like motif in listeriolysin O required for phagosomal escape and for virulence in Listeria monocytogenes. *Mol Microbiol 39:1124.*
64. Schnupf, P., D. A. Portnoy, and A. L. Decatur. 2006. Phosphorylation, ubiquitination and degradation of listeriolysin O in mammalian cells: role of the PEST-like sequence. *Cell Microbiol 8:353.*
65. Kayal, S., A. Lilienbaum, C. Poyart, S. Memet, A. Israel, and P. Berche. 1999. Listeriolysin O-dependent activation of endothelial cells during infection with Listeria monocytogenes: activation of NF-kappa B and upregulation of adhesion molecules and chemokines. *Mol Microbiol 31:1709.*
66. Tang, P., I. Rosenshine, P. Cossart, and B. B. Finlay. 1996. Listeriolysin O activates mitogen-activated protein kinase in eucaryotic cells. *Infect Immun 64:2359.*
67. Sibelius, U., F. Rose, T. Chakraborty, A. Darji, J. Wehland, S. Weiss, W. Seeger, and F. Grimminger. 1996. Listeriolysin is a potent inducer of the phosphatidylinositol response and lipid mediator generation in human endothelial cells. *Infect Immun 64:674.*
68. Sibelius, U., T. Chakraborty, B. Krogel, J. Wolf, F. Rose, R. Schmidt, J. Wehland, W. Seeger, and F. Grimminger. 1996. The listerial exotoxins listeriolysin and phosphatidylinositol-specific phospholipase C synergize to elicit endothelial cell phosphoinositide metabolism. *J Immunol 157:4055.*
69. Dramsi, S., and P. Cossart. 2003. Listeriolysin O-mediated calcium influx potentiates entry of Listeria monocytogenes into the human Hep-2 epithelial cell line. *Infect Immun 71:3614.*
70. Tsuchiya, K., I. Kawamura, A. Takahashi, T. Nomura, C. Kohda, and M. Mitsuyama. 2005. Listeriolysin O-induced membrane permeation mediates persistent interleukin-6

production in Caco-2 cells during Listeria monocytogenes infection in vitro. *Infect Immun 73:3869.*

71. Wadsworth, S. J., and H. Goldfine. 1999. Listeria monocytogenes phospholipase C-dependent calcium signaling modulates bacterial entry into J774 macrophage-like cells. *Infect Immun 67:1770.*
72. Wadsworth, S. J., and H. Goldfine. 2002. Mobilization of protein kinase C in macrophages induced by Listeria monocytogenes affects its internalization and escape from the phagosome. *Infect Immun 70:4650.*
73. Prada-Delgado, A., E. Carrasco-Marin, G. M. Bokoch, and C. Alvarez-Dominguez. 2001. Interferon-gamma listericidal action is mediated by novel Rab5a functions at the phagosomal environment. *J Biol Chem 276:19059.*
74. Alvarez-Dominguez, C., and P. D. Stahl. 1999. Increased expression of Rab5a correlates directly with accelerated maturation of Listeria monocytogenes phagosomes. *J Biol Chem 274:11459.*
75. Myers, J. T., A. W. Tsang, and J. A. Swanson. 2003. Localized reactive oxygen and nitrogen intermediates inhibit escape of Listeria monocytogenes from vacuoles in activated macrophages. *J Immunol 171:5447.*
76. Prada-Delgado, A., E. Carrasco-Marin, C. Pena-Macarro, E. Del Cerro-Vadillo, M. Fresno-Escudero, F. Leyva-Cobian, and C. Alvarez-Dominguez. 2005. Inhibition of Rab5a exchange activity is a key step for Listeria monocytogenes survival. *Traffic 6:252.*
77. Goldfine, H., C. Knob, D. Alford, and J. Bentz. 1995. Membrane permeabilization by Listeria monocytogenes phosphatidylinositol-specific phospholipase C is independent of phospholipid hydrolysis and cooperative with listeriolysin O. *Proc Natl Acad Sci U S A 92:2979.*
78. Goldfine, H., S. J. Wadsworth, and N. C. Johnston. 2000. Activation of host phospholipases C and D in macrophages after infection with Listeria monocytogenes. *Infect Immun 68:5735.*
79. Singer, W. D., H. A. Brown, and P. C. Sternweis. 1997. Regulation of eukaryotic phosphatidylinositol-specific phospholipase C and phospholipase D. *Annu Rev Biochem 66:475.*
80. Ron, D., and M. G. Kazanietz. 1999. New insights into the regulation of protein kinase C and novel phorbol ester receptors. *Faseb J 13:1658.*
81. Exton, J. H. 1997. New developments in phospholipase D. *J Biol Chem 272:15579.*
82. Ghosh, T. K., J. Bian, and D. L. Gill. 1994. Sphingosine 1-phosphate generated in the endoplasmic reticulum membrane activates release of stored calcium. *J Biol Chem 269:22628.*
83. Mattie, M., G. Brooker, and S. Spiegel. 1994. Sphingosine-1-phosphate, a putative second messenger, mobilizes calcium from internal stores via an inositol trisphosphate-independent pathway. *J Biol Chem 269:3181.*
84. Wang, Y., and M. Ashraf. 1999. Role of protein kinase C in mitochondrial KATP channel-mediated protection against Ca2+ overload injury in rat myocardium. *Circ Res 84:1156.*
85. Gerstin, E. H., Jr., T. McMahon, J. Dadgar, and R. O. Messing. 1998. Protein kinase Cdelta mediates ethanol-induced up-regulation of L-type calcium channels. *J Biol Chem 273:16409.*
86. Zhu, S., R. E. White, and S. A. Barman. 2006. Effect of PKC isozyme inhibition on forskolin-induced activation of BKCa channels in rat pulmonary arterial smooth muscle. *Lung 184:89.*
87. Barman, S. A., S. Zhu, and R. E. White. 2004. PKC activates BKCa channels in rat pulmonary arterial smooth muscle via cGMP-dependent protein kinase. *Am J Physiol Lung Cell Mol Physiol 286:L1275.*

88. Poussin, M. A., and H. Goldfine. 2005. Involvement of Listeria monocytogenes phosphatidylinositol-specific phospholipase C and host protein kinase C in permeabilization of the macrophage phagosome. *Infect Immun 73:4410.*
89. Duclos, S., R. Corsini, and M. Desjardins. 2003. Remodeling of endosomes during lysosome biogenesis involves 'kiss and run' fusion events regulated by rab5. *J Cell Sci 116:907.*
90. Pieters, J. 2001. Entry and survival of pathogenic mycobacteria in macrophages. *Microbes Infect 3:249.*
91. Glaser, P., L. Frangeul, C. Buchrieser, C. Rusniok, A. Amend, F. Baquero, P. Berche, H. Bloecker, P. Brandt, T. Chakraborty, A. Charbit, F. Chetouani, E. Couve, A. de Daruvar, P. Dehoux, E. Domann, G. Dominguez-Bernal, E. Duchaud, L. Durant, O. Dussurget, K. D. Entian, H. Fsihi, F. Garcia-del Portillo, P. Garrido, L. Gautier, W. Goebel, N. Gomez-Lopez, T. Hain, J. Hauf, D. Jackson, L. M. Jones, U. Kaerst, J. Kreft, M. Kuhn, F. Kunst, G. Kurapkat, E. Madueno, A. Maitournam, J. M. Vicente, E. Ng, H. Nedjari, G. Nordsiek, S. Novella, B. de Pablos, J. C. Perez-Diaz, R. Purcell, B. Remmel, M. Rose, T. Schlueter, N. Simoes, A. Tierrez, J. A. Vazquez-Boland, H. Voss, J. Wehland, and P. Cossart. 2001. Comparative genomics of Listeria species. *Science 294:849.*
92. Pruess, M., P. Kersey, and R. Apweiler. 2005. The Integr8 project--a resource for genomic and proteomic data. *In Silico Biol 5:179.*
93. Chico-Calero, I., M. Suarez, B. Gonzalez-Zorn, M. Scortti, J. Slaghuis, W. Goebel, and J. A. Vazquez-Boland. 2002. Hpt, a bacterial homolog of the microsomal glucose-6-phosphate translocase, mediates rapid intracellular proliferation in Listeria. *Proc Natl Acad Sci U S A 99:431.*
94. O'Riordan, M., M. A. Moors, and D. A. Portnoy. 2003. Listeria intracellular growth and virulence require host-derived lipoic acid. *Science 302:462.*
95. Chatterjee, S. S., H. Hossain, S. Otten, C. Kuenne, K. Kuchmina, S. Machata, E. Domann, T. Chakraborty, and T. Hain. 2006. Intracellular gene expression profile of Listeria monocytogenes. *Infect Immun 74:1323.*
96. Joseph, B., K. Przybilla, C. Stuhler, K. Schauer, J. Slaghuis, T. M. Fuchs, and W. Goebel. 2006. Identification of Listeria monocytogenes genes contributing to intracellular replication by expression profiling and mutant screening. *J Bacteriol 188:556.*
97. Tilney, L. G., and D. A. Portnoy. 1989. Actin filaments and the growth, movement, and spread of the intracellular bacterial parasite, Listeria monocytogenes. *J Cell Biol 109:1597.*
98. Dabiri, G. A., J. M. Sanger, D. A. Portnoy, and F. S. Southwick. 1990. Listeria monocytogenes moves rapidly through the host-cell cytoplasm by inducing directional actin assembly. *Proc Natl Acad Sci U S A 87:6068.*
99. Domann, E., J. Wehland, M. Rohde, S. Pistor, M. Hartl, W. Goebel, M. Leimeister-Wachter, M. Wuenscher, and T. Chakraborty. 1992. A novel bacterial virulence gene in Listeria monocytogenes required for host cell microfilament interaction with homology to the proline-rich region of vinculin. *Embo J 11:1981.*
100. Welch, M. D., A. Iwamatsu, and T. J. Mitchison. 1997. Actin polymerization is induced by Arp2/3 protein complex at the surface of Listeria monocytogenes. *Nature 385:265.*
101. Goossens, P. L., and G. Milon. 1992. Induction of protective CD8+ T lymphocytes by an attenuated Listeria monocytogenes actA mutant. *Int Immunol 4:1413.*
102. Kocks, C., J. B. Marchand, E. Gouin, H. d'Hauteville, P. J. Sansonetti, M. F. Carlier, and P. Cossart. 1995. The unrelated surface proteins ActA of Listeria monocytogenes and IcsA of Shigella flexneri are sufficient to confer actin-based motility on Listeria innocua and Escherichia coli respectively. *Mol Microbiol 18:413.*

103. Kocks, C., E. Gouin, M. Tabouret, P. Berche, H. Ohayon, and P. Cossart. 1992. L. monocytogenes-induced actin assembly requires the actA gene product, a surface protein. *Cell 68:521.*
104. Stevens, J. M., E. E. Galyov, and M. P. Stevens. 2006. Actin-dependent movement of bacterial pathogens. *Nat Rev Microbiol 4:91.*
105. Krause, M., E. W. Dent, J. E. Bear, J. J. Loureiro, and F. B. Gertler. 2003. Ena/VASP proteins: regulators of the actin cytoskeleton and cell migration. *Annu Rev Cell Dev Biol 19:541.*
106. Portnoy, D. A., V. Auerbuch, and I. J. Glomski. 2002. The cell biology of Listeria monocytogenes infection: the intersection of bacterial pathogenesis and cell-mediated immunity. *J Cell Biol 158:409.*
107. Sechi, A. S., and J. Wehland. 2004. ENA/VASP proteins: multifunctional regulators of actin cytoskeleton dynamics. *Front Biosci 9:1294.*
108. Welch, M. D., A. H. DePace, S. Verma, A. Iwamatsu, and T. J. Mitchison. 1997. The human Arp2/3 complex is composed of evolutionarily conserved subunits and is localized to cellular regions of dynamic actin filament assembly. *J Cell Biol 138:375.*
109. Cossart, P., and H. Bierne. 2001. The use of host cell machinery in the pathogenesis of Listeria monocytogenes. *Curr Opin Immunol 13:96.*
110. North, R. J., P. L. Dunn, and J. W. Conlan. 1997. Murine listeriosis as a model of antimicrobial defense. *Immunol Rev 158:27.*
111. Unanue, E. R. 1997. Studies in listeriosis show the strong symbiosis between the innate cellular system and the T-cell response. *Immunol Rev 158:11.*
112. Lecuit, M., S. Dramsi, C. Gottardi, M. Fedor-Chaiken, B. Gumbiner, and P. Cossart. 1999. A single amino acid in E-cadherin responsible for host specificity towards the human pathogen Listeria monocytogenes. *Embo J 18:3956.*
113. Lecuit, M., S. Vandormael-Pournin, J. Lefort, M. Huerre, P. Gounon, C. Dupuy, C. Babinet, and P. Cossart. 2001. A transgenic model for listeriosis: role of internalin in crossing the intestinal barrier. *Science 292:1722.*
114. Bancroft, G. J., R. D. Schreiber, and E. R. Unanue. 1991. Natural immunity: a T-cell-independent pathway of macrophage activation, defined in the scid mouse. *Immunol Rev 124:5.*
115. Conlan, J. W., and R. J. North. 1991. Neutrophil-mediated dissolution of infected host cells as a defense strategy against a facultative intracellular bacterium. *J Exp Med 174:741.*
116. Cousens, L. P., and E. J. Wing. 2000. Innate defenses in the liver during Listeria infection. *Immunol Rev 174:150.*
117. Mackaness, G. B. 1962. Cellular resistance to infection. *J Exp Med 116:381.*
118. Gregory, S. H., and E. J. Wing. 1998. Neutrophil-Kupffer-cell interaction in host defenses to systemic infections. *Immunol Today 19:507.*
119. Gregory, S. H., and E. J. Wing. 1990. Accessory function of Kupffer cells in the antigen-specific blastogenic response of an L3T4+ T-lymphocyte clone to Listeria monocytogenes. *Infect Immun 58:2313.*
120. Cheers, C., I. F. McKenzie, H. Pavlov, C. Waid, and J. York. 1978. Resistance and susceptibility of mice to bacterial infection: course of listeriosis in resistant or susceptible mice. *Infect Immun 19:763.*
121. de Chastellier, C., and P. Berche. 1994. Fate of Listeria monocytogenes in murine macrophages: evidence for simultaneous killing and survival of intracellular bacteria. *Infect Immun 62:543.*
122. Mandel, T. E., and C. Cheers. 1980. Resistance and susceptibility of mice to bacterial infection: histopathology of listeriosis in resistant and susceptible strains. *Infect Immun 30:851.*

123. Mitsuyama, M., K. Takeya, K. Nomoto, and S. Shimotori. 1978. Three phases of phagocyte contribution to resistance against Listeria monocytogenes. *J Gen Microbiol 106:165.*
124. Lepay, D. A., R. M. Steinman, C. F. Nathan, H. W. Murray, and Z. A. Cohn. 1985. Liver macrophages in murine listeriosis. Cell-mediated immunity is correlated with an influx of macrophages capable of generating reactive oxygen intermediates. *J Exp Med 161:1503.*
125. Fleming, S. D., and P. A. Campbell. 1997. Some macrophages kill Listeria monocytogenes while others do not. *Immunol Rev 158:69.*
126. Conlan, J. W., and R. J. North. 1992. Early pathogenesis of infection in the liver with the facultative intracellular bacteria Listeria monocytogenes, Francisella tularensis, and Salmonella typhimurium involves lysis of infected hepatocytes by leukocytes. *Infect Immun 60:5164.*
127. Gaillard, J. L., F. Jaubert, and P. Berche. 1996. The inlAB locus mediates the entry of Listeria monocytogenes into hepatocytes in vivo. *J Exp Med 183:359.*
128. Gregory, S. H., L. K. Barczynski, and E. J. Wing. 1992. Effector function of hepatocytes and Kupffer cells in the resolution of systemic bacterial infections. *J Leukoc Biol 51:421.*
129. Gregory, S. H., and C. C. Liu. 2000. CD8+ T-cell-mediated response to Listeria monocytogenes taken up in the liver and replicating within hepatocytes. *Immunol Rev 174:112.*
130. Rosen, H., S. Gordon, and R. J. North. 1989. Exacerbation of murine listeriosis by a monoclonal antibody specific for the type 3 complement receptor of myelomonocytic cells. Absence of monocytes at infective foci allows Listeria to multiply in nonphagocytic cells. *J Exp Med 170:27.*
131. Siddique, I. H., B. E. McKenzie, W. J. Sapp, and P. Rich. 1978. Light and electron microscopic study of the livers of pregnant mice infected with Listeria monocytogenes. *Am J Vet Res 39:887.*
132. Pamer, E. G. 2004. Immune responses to Listeria monocytogenes. *Nat Rev Immunol 4:812.*
133. Ochsenbein, A. F., T. Fehr, C. Lutz, M. Suter, F. Brombacher, H. Hengartner, and R. M. Zinkernagel. 1999. Control of early viral and bacterial distribution and disease by natural antibodies. *Science 286:2156.*
134. Edelson, B. T., P. Cossart, and E. R. Unanue. 1999. Cutting edge: paradigm revisited: antibody provides resistance to Listeria infection. *J Immunol 163:4087.*
135. Rogers, H. W., M. P. Callery, B. Deck, and E. R. Unanue. 1996. Listeria monocytogenes induces apoptosis of infected hepatocytes. *J Immunol 156:679.*
136. Rogers, H. W., and E. R. Unanue. 1993. Neutrophils are involved in acute, nonspecific resistance to Listeria monocytogenes in mice. *Infect Immun 61:5090.*
137. Czuprynski, C. J., J. F. Brown, N. Maroushek, R. D. Wagner, and H. Steinberg. 1994. Administration of anti-granulocyte mAb RB6-8C5 impairs the resistance of mice to Listeria monocytogenes infection. *J Immunol 152:1836.*
138. Czuprynski, C. J., J. F. Brown, R. D. Wagner, and H. Steinberg. 1994. Administration of antigranulocyte monoclonal antibody RB6-8C5 prevents expression of acquired resistance to Listeria monocytogenes infection in previously immunized mice. *Infect Immun 62:5161.*
139. Rakhmilevich, A. L. 1995. Neutrophils are essential for resolution of primary and secondary infection with Listeria monocytogenes. *J Leukoc Biol 57:827.*
140. Conlan, J. W., and R. J. North. 1994. Neutrophils are essential for early anti-Listeria defense in the liver, but not in the spleen or peritoneal cavity, as revealed by a granulocyte-depleting monoclonal antibody. *J Exp Med 179:259.*

141. Portnoy, D. A. 1992. Innate immunity to a facultative intracellular bacterial pathogen. *Curr Opin Immunol 4:20.*
142. Dunn, P. L., and R. J. North. 1991. Early gamma interferon production by natural killer cells is important in defense against murine listeriosis. *Infect Immun 59:2892.*
143. Teixeira, H. C., and S. H. Kaufmann. 1994. Role of NK1.1+ cells in experimental listeriosis. NK1+ cells are early IFN-gamma producers but impair resistance to Listeria monocytogenes infection. *J Immunol 152:1873.*
144. Gregory, S. H., and E. J. Wing. 1993. IFN-gamma inhibits the replication of Listeria monocytogenes in hepatocytes. *J Immunol 151:1401.*
145. Szalay, G., J. Hess, and S. H. Kaufmann. 1995. Restricted replication of Listeria monocytogenes in a gamma interferon-activated murine hepatocyte line. *Infect Immun 63:3187.*
146. Harty, J. T., R. D. Schreiber, and M. J. Bevan. 1992. CD8 T cells can protect against an intracellular bacterium in an interferon gamma-independent fashion. *Proc Natl Acad Sci U S A 89:11612.*
147. Kaufmann, S. H. 1993. Immunity to intracellular bacteria. *Annu Rev Immunol 11:129.*
148. Mielke, M., S. Ehlers, and H. Hahn. 1988. The role of T cell subpopulations in cell mediated immunity to facultative intracellular bacteria. *Infection 16 Suppl 2:S123.*
149. Kurihara, T., G. Warr, J. Loy, and R. Bravo. 1997. Defects in macrophage recruitment and host defense in mice lacking the CCR2 chemokine receptor. *J Exp Med 186:1757.*
150. Serbina, N. V., T. P. Salazar-Mather, C. A. Biron, W. A. Kuziel, and E. G. Pamer. 2003. TNF/iNOS-producing dendritic cells mediate innate immune defense against bacterial infection. *Immunity 19:59.*
151. Gagnon, E., S. Duclos, C. Rondeau, E. Chevet, P. H. Cameron, O. Steele-Mortimer, J. Paiement, J. J. Bergeron, and M. Desjardins. 2002. Endoplasmic reticulum-mediated phagocytosis is a mechanism of entry into macrophages. *Cell 110:119.*
152. Gagnon, E., J. J. Bergeron, and M. Desjardins. 2005. ER-mediated phagocytosis: myth or reality? *J Leukoc Biol 77:843.*
153. Desjardins, M. 1995. Biogenesis of phagolysosomes: the 'kiss and run' hypothesis. *Trends Cell Biol 5:183.*
154. Desjardins, M., J. E. Celis, G. van Meer, H. Dieplinger, A. Jahraus, G. Griffiths, and L. A. Huber. 1994. Molecular characterization of phagosomes. *J Biol Chem 269:32194.*
155. Desjardins, M., M. Houde, and E. Gagnon. 2005. Phagocytosis: the convoluted way from nutrition to adaptive immunity. *Immunol Rev 207:158.*
156. Mayorga, L. S., F. Bertini, and P. D. Stahl. 1991. Fusion of newly formed phagosomes with endosomes in intact cells and in a cell-free system. *J Biol Chem 266:6511.*
157. Pitt, A., L. S. Mayorga, A. L. Schwartz, and P. D. Stahl. 1992. Transport of phagosomal components to an endosomal compartment. *J Biol Chem 267:126.*
158. Desjardins, M., N. N. Nzala, R. Corsini, and C. Rondeau. 1997. Maturation of phagosomes is accompanied by changes in their fusion properties and size-selective acquisition of solute materials from endosomes. *J Cell Sci 110 ( Pt 18):2303.*
159. Hampton, M. B., A. J. Kettle, and C. C. Winterbourn. 1998. Inside the neutrophil phagosome: oxidants, myeloperoxidase, and bacterial killing. *Blood 92:3007.*
160. Underhill, D. M. 2005. Phagosome maturation: steady as she goes. *Immunity 23:343.*
161. Mullins, C., and J. S. Bonifacino. 2001. The molecular machinery for lysosome biogenesis. *Bioessays 23:333.*
162. Nakane, A., A. Numata, Y. Chen, and T. Minagawa. 1991. Endogenous gamma interferon-independent host resistance against Listeria monocytogenes infection in CD4+ T cell- and asialo GM1+ cell-depleted mice. *Infect Immun 59:3439.*

163. Geginat, G., M. Lalic, M. Kretschmar, W. Goebel, H. Hof, D. Palm, and A. Bubert. 1998. Th1 cells specific for a secreted protein of Listeria monocytogenes are protective in vivo. *J Immunol 160:6046.*
164. Daugelat, S., and S. H. Kaufmann. 1996. Role of Th1 and Th2 cells in bacterial infections. *Chem Immunol 63:66.*
165. Portnoy, D. A., R. D. Schreiber, P. Connelly, and L. G. Tilney. 1989. Gamma interferon limits access of Listeria monocytogenes to the macrophage cytoplasm. *J Exp Med 170:2141.*
166. Brunt, L. M., D. A. Portnoy, and E. R. Unanue. 1990. Presentation of Listeria monocytogenes to CD8+ T cells requires secretion of hemolysin and intracellular bacterial growth. *J Immunol 145:3540.*
167. Harty, J. T., L. L. Lenz, and M. J. Bevan. 1996. Primary and secondary immune responses to Listeria monocytogenes. *Curr Opin Immunol 8:526.*
168. Hess, J., I. Gentschev, D. Miko, M. Welzel, C. Ladel, W. Goebel, and S. H. Kaufmann. 1996. Superior efficacy of secreted over somatic antigen display in recombinant Salmonella vaccine induced protection against listeriosis. *Proc Natl Acad Sci U S A 93:1458.*
169. Sirard, J. C., C. Fayolle, C. de Chastellier, M. Mock, C. Leclerc, and P. Berche. 1997. Intracytoplasmic delivery of listeriolysin O by a vaccinal strain of Bacillus anthracis induces CD8-mediated protection against Listeria monocytogenes. *J Immunol 159:4435.*
170. Villanueva, M. S., A. J. Sijts, and E. G. Pamer. 1995. Listeriolysin is processed efficiently into an MHC class I-associated epitope in Listeria monocytogenes-infected cells. *J Immunol 155:5227.*
171. Bouwer, H. G., C. S. Nelson, B. L. Gibbins, D. A. Portnoy, and D. J. Hinrichs. 1992. Listeriolysin O is a target of the immune response to Listeria monocytogenes. *J Exp Med 175:1467.*
172. Busch, D. H., H. G. Bouwer, D. Hinrichs, and E. G. Pamer. 1997. A nonamer peptide derived from Listeria monocytogenes metalloprotease is presented to cytolytic T lymphocytes. *Infect Immun 65:5326.*
173. Geginat, G., T. Nichterlein, M. Kretschmar, S. Schenk, H. Hof, M. Lalic-Multhaler, W. Goebel, and A. Bubert. 1999. Enhancement of the Listeria monocytogenes p60-specific CD4 and CD8 T cell memory by nonpathogenic Listeria innocua. *J Immunol 162:4781.*
174. Harty, J. T., and E. G. Pamer. 1995. CD8 T lymphocytes specific for the secreted p60 antigen protect against Listeria monocytogenes infection. *J Immunol 154:4642.*
175. Sijts, A. J., A. Neisig, J. Neefjes, and E. G. Pamer. 1996. Two Listeria monocytogenes CTL epitopes are processed from the same antigen with different efficiencies. *J Immunol 156:683.*
176. BioCarta. Antigen Processing and Presentation Pathway. *http://www.biocarta.com/pathfiles/h_mhcPathway.asp.*
177. Goossens, P. L., H. Jouin, and G. Milon. 1991. Dynamics of lymphocytes and inflammatory cells recruited in liver during murine listeriosis. A cytofluorimetric study. *J Immunol 147:3514.*
178. Chan, C. W., E. Crafton, H. N. Fan, J. Flook, K. Yoshimura, M. Skarica, D. Brockstedt, T. W. Dubensky, M. F. Stins, L. L. Lanier, D. M. Pardoll, and F. Housseau. 2006. Interferon-producing killer dendritic cells provide a link between innate and adaptive immunity. *Nat Med 12:207.*
179. Meylan, E., J. Tschopp, and M. Karin. 2006. Intracellular pattern recognition receptors in the host response. *Nature 442:39.*
180. Meylan, E., and J. Tschopp. 2006. Toll-like receptors and RNA helicases: two parallel ways to trigger antiviral responses. *Mol Cell 22:561.*

181. Eckmann, L. 2006. Sensor molecules in intestinal innate immunity against bacterial infections. *Curr Opin Gastroenterol 22:95.*
182. Takeda, K., and S. Akira. 2005. Toll-like receptors in innate immunity. *Int Immunol 17:1.*
183. Martinon, F., and J. Tschopp. 2005. NLRs join TLRs as innate sensors of pathogens. *Trends Immunol 26:447.*
184. Inohara, N., and G. Nunez. 2003. NODs: intracellular proteins involved in inflammation and apoptosis. *Nat Rev Immunol 3:371.*
185. Strober, W., P. J. Murray, A. Kitani, and T. Watanabe. 2006. Signalling pathways and molecular interactions of NOD1 and NOD2. *Nat Rev Immunol 6:9.*
186. Muzio, M., D. Bosisio, N. Polentarutti, G. D'Amico, A. Stoppacciaro, R. Mancinelli, C. van't Veer, G. Penton-Rol, L. P. Ruco, P. Allavena, and A. Mantovani. 2000. Differential expression and regulation of toll-like receptors (TLR) in human leukocytes: selective expression of TLR3 in dendritic cells. *J Immunol 164:5998.*
187. Zarember, K. A., and P. J. Godowski. 2002. Tissue expression of human Toll-like receptors and differential regulation of Toll-like receptor mRNAs in leukocytes in response to microbes, their products, and cytokines. *J Immunol 168:554.*
188. Kadowaki, N., S. Ho, S. Antonenko, R. W. Malefyt, R. A. Kastelein, F. Bazan, and Y. J. Liu. 2001. Subsets of human dendritic cell precursors express different toll-like receptors and respond to different microbial antigens. *J Exp Med 194:863.*
189. Visintin, A., A. Mazzoni, J. H. Spitzer, D. H. Wyllie, S. K. Dower, and D. M. Segal. 2001. Regulation of Toll-like receptors in human monocytes and dendritic cells. *J Immunol 166:249.*
190. Krug, A., A. Towarowski, S. Britsch, S. Rothenfusser, V. Hornung, R. Bals, T. Giese, H. Engelmann, S. Endres, A. M. Krieg, and G. Hartmann. 2001. Toll-like receptor expression reveals CpG DNA as a unique microbial stimulus for plasmacytoid dendritic cells which synergizes with CD40 ligand to induce high amounts of IL-12. *Eur J Immunol 31:3026.*
191. Rissoan, M. C., V. Soumelis, N. Kadowaki, G. Grouard, F. Briere, R. de Waal Malefyt, and Y. J. Liu. 1999. Reciprocal control of T helper cell and dendritic cell differentiation. *Science 283:1183.*
192. Liu, Y. J., H. Kanzler, V. Soumelis, and M. Gilliet. 2001. Dendritic cell lineage, plasticity and cross-regulation. *Nat Immunol 2:585.*
193. Jarrossay, D., G. Napolitani, M. Colonna, F. Sallusto, and A. Lanzavecchia. 2001. Specialization and complementarity in microbial molecule recognition by human myeloid and plasmacytoid dendritic cells. *Eur J Immunol 31:3388.*
194. Ito, T., R. Amakawa, T. Kaisho, H. Hemmi, K. Tajima, K. Uehira, Y. Ozaki, H. Tomizawa, S. Akira, and S. Fukuhara. 2002. Interferon-alpha and interleukin-12 are induced differentially by Toll-like receptor 7 ligands in human blood dendritic cell subsets. *J Exp Med 195:1507.*
195. Mellman, I., and R. M. Steinman. 2001. Dendritic cells: specialized and regulated antigen processing machines. *Cell 106:255.*
196. Tsuji, S., M. Matsumoto, O. Takeuchi, S. Akira, I. Azuma, A. Hayashi, K. Toyoshima, and T. Seya. 2000. Maturation of human dendritic cells by cell wall skeleton of Mycobacterium bovis bacillus Calmette-Guerin: involvement of toll-like receptors. *Infect Immun 68:6883.*
197. Michelsen, K. S., A. Aicher, M. Mohaupt, T. Hartung, S. Dimmeler, C. J. Kirschning, and R. R. Schumann. 2001. The role of toll-like receptors (TLRs) in bacteria-induced maturation of murine dendritic cells (DCS). Peptidoglycan and lipoteichoic acid are inducers of DC maturation and require TLR2. *J Biol Chem 276:25680.*

198. Hertz, C. J., S. M. Kiertscher, P. J. Godowski, D. A. Bouis, M. V. Norgard, M. D. Roth, and R. L. Modlin. 2001. Microbial lipopeptides stimulate dendritic cell maturation via Toll-like receptor 2. *J Immunol 166:2444.*
199. Torres, D., M. Barrier, F. Bihl, V. J. Quesniaux, I. Maillet, S. Akira, B. Ryffel, and F. Erard. 2004. Toll-like receptor 2 is required for optimal control of Listeria monocytogenes infection. *Infect Immun 72:2131.*
200. Seki, E., H. Tsutsui, N. M. Tsuji, N. Hayashi, K. Adachi, H. Nakano, S. Futatsugi-Yumikura, O. Takeuchi, K. Hoshino, S. Akira, J. Fujimoto, and K. Nakanishi. 2002. Critical roles of myeloid differentiation factor 88-dependent proinflammatory cytokine release in early phase clearance of Listeria monocytogenes in mice. *J Immunol 169:3863.*
201. Hayashi, F., K. D. Smith, A. Ozinsky, T. R. Hawn, E. C. Yi, D. R. Goodlett, J. K. Eng, S. Akira, D. M. Underhill, and A. Aderem. 2001. The innate immune response to bacterial flagellin is mediated by Toll-like receptor 5. *Nature 410:1099.*
202. Way, S. S., L. J. Thompson, J. E. Lopes, A. M. Hajjar, T. R. Kollmann, N. E. Freitag, and C. B. Wilson. 2004. Characterization of flagellin expression and its role in Listeria monocytogenes infection and immunity. *Cell Microbiol 6:235.*
203. Edelson, B. T., and E. R. Unanue. 2002. MyD88-dependent but Toll-like receptor 2-independent innate immunity to Listeria: no role for either in macrophage listericidal activity. *J Immunol 169:3869.*
204. Carrero, J. A., B. Calderon, and E. R. Unanue. 2004. Type I interferon sensitizes lymphocytes to apoptosis and reduces resistance to Listeria infection. *J Exp Med 200:535.*
205. Auerbuch, V., D. G. Brockstedt, N. Meyer-Morse, M. O'Riordan, and D. A. Portnoy. 2004. Mice lacking the type I interferon receptor are resistant to Listeria monocytogenes. *J Exp Med 200:527.*
206. O'Connell, R. M., S. K. Saha, S. A. Vaidya, K. W. Bruhn, G. A. Miranda, B. Zarnegar, A. K. Perry, B. O. Nguyen, T. F. Lane, T. Taniguchi, J. F. Miller, and G. Cheng. 2004. Type I interferon production enhances susceptibility to Listeria monocytogenes infection. *J Exp Med 200:437.*
207. Stockinger, S., T. Materna, D. Stoiber, L. Bayr, R. Steinborn, T. Kolbe, H. Unger, T. Chakraborty, D. E. Levy, M. Muller, and T. Decker. 2002. Production of type I IFN sensitizes macrophages to cell death induced by Listeria monocytogenes. *J Immunol 169:6522.*
208. Stockinger, S., B. Reutterer, B. Schaljo, C. Schellack, S. Brunner, T. Materna, M. Yamamoto, S. Akira, T. Taniguchi, P. J. Murray, M. Muller, and T. Decker. 2004. IFN regulatory factor 3-dependent induction of type I IFNs by intracellular bacteria is mediated by a TLR- and Nod2-independent mechanism. *J Immunol 173:7416.*
209. Kayal, S., A. Lilienbaum, O. Join-Lambert, X. Li, A. Israel, and P. Berche. 2002. Listeriolysin O secreted by Listeria monocytogenes induces NF-kappaB signalling by activating the IkappaB kinase complex. *Mol Microbiol 44:1407.*
210. Hauf, N., W. Goebel, F. Fiedler, Z. Sokolovic, and M. Kuhn. 1997. Listeria monocytogenes infection of P388D1 macrophages results in a biphasic NF-kappaB (RelA/p50) activation induced by lipoteichoic acid and bacterial phospholipases and mediated by IkappaBalpha and IkappaBbeta degradation. *Proc Natl Acad Sci U S A 94:9394.*
211. Kobayashi, K. S., M. Chamaillard, Y. Ogura, O. Henegariu, N. Inohara, G. Nunez, and R. A. Flavell. 2005. Nod2-dependent regulation of innate and adaptive immunity in the intestinal tract. *Science 307:731.*
212. Mariathasan, S., D. S. Weiss, K. Newton, J. McBride, K. O'Rourke, M. Roose-Girma, W. P. Lee, Y. Weinrauch, D. M. Monack, and V. M. Dixit. 2006. Cryopyrin activates the inflammasome in response to toxins and ATP. *Nature 440:228.*

213. Kanneganti, T. D., N. Ozoren, M. Body-Malapel, A. Amer, J. H. Park, L. Franchi, J. Whitfield, W. Barchet, M. Colonna, P. Vandenabeele, J. Bertin, A. Coyle, E. P. Grant, S. Akira, and G. Nunez. 2006. Bacterial RNA and small antiviral compounds activate caspase-1 through cryopyrin/Nalp3. *Nature 440:233.*
214. Chamaillard, M., M. Hashimoto, Y. Horie, J. Masumoto, S. Qiu, L. Saab, Y. Ogura, A. Kawasaki, K. Fukase, S. Kusumoto, M. A. Valvano, S. J. Foster, T. W. Mak, G. Nunez, and N. Inohara. 2003. An essential role for NOD1 in host recognition of bacterial peptidoglycan containing diaminopimelic acid. *Nat Immunol 4:702.*
215. Inohara, Chamaillard, C. McDonald, and G. Nunez. 2005. NOD-LRR proteins: role in host-microbial interactions and inflammatory disease. *Annu Rev Biochem 74:355.*
216. Pauleau, A. L., and P. J. Murray. 2003. Role of nod2 in the response of macrophages to toll-like receptor agonists. *Mol Cell Biol 23:7531.*
217. Kanazawa, N., I. Okafuji, N. Kambe, R. Nishikomori, M. Nakata-Hizume, S. Nagai, A. Fuji, T. Yuasa, A. Manki, Y. Sakurai, M. Nakajima, H. Kobayashi, I. Fujiwara, H. Tsutsumi, A. Utani, C. Nishigori, T. Heike, T. Nakahata, and Y. Miyachi. 2005. Early-onset sarcoidosis and CARD15 mutations with constitutive nuclear factor-kappaB activation: common genetic etiology with Blau syndrome. *Blood 105:1195.*
218. Inohara, N., Y. Ogura, A. Fontalba, O. Gutierrez, F. Pons, J. Crespo, K. Fukase, S. Inamura, S. Kusumoto, M. Hashimoto, S. J. Foster, A. P. Moran, J. L. Fernandez-Luna, and G. Nunez. 2003. Host recognition of bacterial muramyl dipeptide mediated through NOD2. Implications for Crohn's disease. *J Biol Chem 278:5509.*
219. Girardin, S. E., I. G. Boneca, L. A. Carneiro, A. Antignac, M. Jehanno, J. Viala, K. Tedin, M. K. Taha, A. Labigne, U. Zahringer, A. J. Coyle, P. S. DiStefano, J. Bertin, P. J. Sansonetti, and D. J. Philpott. 2003. Nod1 detects a unique muropeptide from gram-negative bacterial peptidoglycan. *Science 300:1584.*
220. Girardin, S. E., I. G. Boneca, J. Viala, M. Chamaillard, A. Labigne, G. Thomas, D. J. Philpott, and P. J. Sansonetti. 2003. Nod2 is a general sensor of peptidoglycan through muramyl dipeptide (MDP) detection. *J Biol Chem 278:8869.*
221. Gutierrez, O., C. Pipaon, N. Inohara, A. Fontalba, Y. Ogura, F. Prosper, G. Nunez, and J. L. Fernandez-Luna. 2002. Induction of Nod2 in myelomonocytic and intestinal epithelial cells via nuclear factor-kappa B activation. *J Biol Chem 277:41701.*
222. Ogura, Y., N. Inohara, A. Benito, F. F. Chen, S. Yamaoka, and G. Nunez. 2001. Nod2, a Nod1/Apaf-1 family member that is restricted to monocytes and activates NF-kappaB. *J Biol Chem 276:4812.*
223. Hisamatsu, T., M. Suzuki, and D. K. Podolsky. 2003. Interferon-gamma augments CARD4/NOD1 gene and protein expression through interferon regulatory factor-1 in intestinal epithelial cells. *J Biol Chem 278:32962.*
224. Rosenstiel, P., M. Fantini, K. Brautigam, T. Kuhbacher, G. H. Waetzig, D. Seegert, and S. Schreiber. 2003. TNF-alpha and IFN-gamma regulate the expression of the NOD2 (CARD15) gene in human intestinal epithelial cells. *Gastroenterology 124:1001.*
225. Viala, J., C. Chaput, I. G. Boneca, A. Cardona, S. E. Girardin, A. P. Moran, R. Athman, S. Memet, M. R. Huerre, A. J. Coyle, P. S. DiStefano, P. J. Sansonetti, A. Labigne, J. Bertin, D. J. Philpott, and R. L. Ferrero. 2004. Nod1 responds to peptidoglycan delivered by the Helicobacter pylori cag pathogenicity island. *Nat Immunol 5:1166.*
226. Kobayashi, K., N. Inohara, L. D. Hernandez, J. E. Galan, G. Nunez, C. A. Janeway, R. Medzhitov, and R. A. Flavell. 2002. RICK/Rip2/CARDIAK mediates signalling for receptors of the innate and adaptive immune systems. *Nature 416:194.*
227. Abbott, D. W., A. Wilkins, J. M. Asara, and L. C. Cantley. 2004. The Crohn's disease protein, NOD2, requires RIP2 in order to induce ubiquitinylation of a novel site on NEMO. *Curr Biol 14:2217.*

228. Zhou, H., I. Wertz, K. O'Rourke, M. Ultsch, S. Seshagiri, M. Eby, W. Xiao, and V. M. Dixit. 2004. Bcl10 activates the NF-kappaB pathway through ubiquitination of NEMO. *Nature 427:167.*
229. Damiano, J. S., V. Oliveira, K. Welsh, and J. C. Reed. 2004. Heterotypic interactions among NACHT domains: implications for regulation of innate immune responses. *Biochem J 381:213.*
230. Martinon, F., and J. Tschopp. 2004. Inflammatory caspases: linking an intracellular innate immune system to autoinflammatory diseases. *Cell 117:561.*
231. Opitz, B., A. Puschel, W. Beermann, A. C. Hocke, S. Forster, B. Schmeck, V. van Laak, T. Chakraborty, N. Suttorp, and S. Hippenstiel. 2006. Listeria monocytogenes activated p38 MAPK and induced IL-8 secretion in a nucleotide-binding oligomerization domain 1-dependent manner in endothelial cells. *J Immunol 176:484.*
232. Chin, A. I., P. W. Dempsey, K. Bruhn, J. F. Miller, Y. Xu, and G. Cheng. 2002. Involvement of receptor-interacting protein 2 in innate and adaptive immune responses. *Nature 416:190.*
233. Way, S. S., T. R. Kollmann, A. M. Hajjar, and C. B. Wilson. 2003. Cutting edge: protective cell-mediated immunity to Listeria monocytogenes in the absence of myeloid differentiation factor 88. *J Immunol 171:533.*
234. Martinon, F., L. Agostini, E. Meylan, and J. Tschopp. 2004. Identification of bacterial muramyl dipeptide as activator of the NALP3/cryopyrin inflammasome. *Curr Biol 14:1929.*
235. Mocci, S., S. A. Dalrymple, R. Nishinakamura, and R. Murray. 1997. The cytokine stew and innate resistance to L. monocytogenes. *Immunol Rev 158:107.*
236. Seebach, J., D. Bartholdi, K. Frei, K. S. Spanaus, E. Ferrero, U. Widmer, S. Isenmann, R. M. Strieter, M. Schwab, H. Pfister, and A. Fontana. 1995. Experimental Listeria meningoencephalitis. Macrophage inflammatory protein-1 alpha and -2 are produced intrathecally and mediate chemotactic activity in cerebrospinal fluid of infected mice. *J Immunol 155:4367.*
237. Baggiolini, M., B. Moser, and I. Clark-Lewis. 1994. Interleukin-8 and related chemotactic cytokines. The Giles Filley Lecture. *Chest 105:95S.*
238. Shiratori, Y., H. Takada, Y. Hikiba, K. Okano, Y. Niwa, M. Matsumura, Y. Komatsu, and M. Omata. 1993. Increased release of KC/gro protein, intercrine cytokine family, from hepatocytes of the chronically ethanol fed rats. *Biochem Biophys Res Commun 197:319.*
239. Thornton, A. J., J. Ham, and S. L. Kunkel. 1991. Kupffer cell-derived cytokines induce the synthesis of a leukocyte chemotactic peptide, interleukin-8, in human hepatoma and primary hepatocyte cultures. *Hepatology 14:1112.*
240. Barsig, J., I. E. Flesch, and S. H. Kaufmann. 1998. Macrophages and hepatocytic cells as chemokine producers in murine listeriosis. *Immunobiology 199:87.*
241. Dorner, B. G., A. Scheffold, M. S. Rolph, M. B. Huser, S. H. Kaufmann, A. Radbruch, I. E. Flesch, and R. A. Kroczek. 2002. MIP-1alpha, MIP-1beta, RANTES, and ATAC/lymphotactin function together with IFN-gamma as type 1 cytokines. *Proc Natl Acad Sci U S A 99:6181.*
242. Serbina, N. V., and E. G. Pamer. 2006. Monocyte emigration from bone marrow during bacterial infection requires signals mediated by chemokine receptor CCR2. *Nat Immunol 7:311.*
243. Serbina, N. V., W. Kuziel, R. Flavell, S. Akira, B. Rollins, and E. G. Pamer. 2003. Sequential MyD88-independent and -dependent activation of innate immune responses to intracellular bacterial infection. *Immunity 19:891.*
244. Cole, A. M., T. Ganz, A. M. Liese, M. D. Burdick, L. Liu, and R. M. Strieter. 2001. Cutting edge: IFN-inducible ELR- CXC chemokines display defensin-like antimicrobial activity. *J Immunol 167:623.*

245. Rogers, H. W., C. S. Tripp, R. D. Schreiber, and E. R. Unanue. 1994. Endogenous IL-1 is required for neutrophil recruitment and macrophage activation during murine listeriosis. *J Immunol 153:2093.*
246. Dalrymple, S. A., L. A. Lucian, R. Slattery, T. McNeil, D. M. Aud, S. Fuchino, F. Lee, and R. Murray. 1995. Interleukin-6-deficient mice are highly susceptible to Listeria monocytogenes infection: correlation with inefficient neutrophilia. *Infect Immun 63:2262.*
247. Rogers, H. W., K. C. Sheehan, L. M. Brunt, S. K. Dower, E. R. Unanue, and R. D. Schreiber. 1992. Interleukin 1 participates in the development of anti-Listeria responses in normal and SCID mice. *Proc Natl Acad Sci U S A 89:1011.*
248. Havell, E. A., L. L. Moldawer, D. Helfgott, P. L. Kilian, and P. B. Sehgal. 1992. Type I IL-1 receptor blockade exacerbates murine listeriosis. *J Immunol 148:1486.*
249. Havell, E. A., and P. B. Sehgal. 1991. Tumor necrosis factor-independent IL-6 production during murine listeriosis. *J Immunol 146:756.*
250. Brombacher, F., and M. Kopf. 1996. Innate versus acquired immunity in listeriosis. In *67 FORUM IN IMMUNOLOGY*, p. 505
251. Kishimoto, T. 2006. Interleukin-6: discovery of a pleiotropic cytokine. *Arthritis Res Ther 8 Suppl 2:S2.*
252. Sullivan, G. W., H. T. Carper, J. A. Sullivan, T. Murata, and G. L. Mandell. 1989. Both recombinant interleukin-1 (beta) and purified human monocyte interleukin-1 prime human neutrophils for increased oxidative activity and promote neutrophil spreading. *J Leukoc Biol 45:389.*
253. Bevilacqua, M. P., J. S. Pober, M. E. Wheeler, R. S. Cotran, and M. A. Gimbrone, Jr. 1985. Interleukin 1 acts on cultured human vascular endothelium to increase the adhesion of polymorphonuclear leukocytes, monocytes, and related leukocyte cell lines. *J Clin Invest 76:2003.*
254. Furie, M. B., and D. D. McHugh. 1989. Migration of neutrophils across endothelial monolayers is stimulated by treatment of the monolayers with interleukin-1 or tumor necrosis factor-alpha. *J Immunol 143:3309.*
255. Labow, M., D. Shuster, M. Zetterstrom, P. Nunes, R. Terry, E. B. Cullinan, T. Bartfai, C. Solorzano, L. L. Moldawer, R. Chizzonite, and K. W. McIntyre. 1997. Absence of IL-1 signaling and reduced inflammatory response in IL-1 type I receptor-deficient mice. *J Immunol 159:2452.*
256. Nomura, T., I. Kawamura, K. Tsuchiya, C. Kohda, H. Baba, Y. Ito, T. Kimoto, I. Watanabe, and M. Mitsuyama. 2002. Essential role of interleukin-12 (IL-12) and IL-18 for gamma interferon production induced by listeriolysin O in mouse spleen cells. *Infect Immun 70:1049.*
257. Takeda, K., H. Tsutsui, T. Yoshimoto, O. Adachi, N. Yoshida, T. Kishimoto, H. Okamura, K. Nakanishi, and S. Akira. 1998. Defective NK cell activity and Th1 response in IL-18-deficient mice. *Immunity 8:383.*
258. Leite-De-Moraes, M. C., A. Hameg, A. Arnould, F. Machavoine, Y. Koezuka, E. Schneider, A. Herbelin, and M. Dy. 1999. A distinct IL-18-induced pathway to fully activate NK T lymphocytes independently from TCR engagement. *J Immunol 163:5871.*
259. Tripp, C. S., S. F. Wolf, and E. R. Unanue. 1993. Interleukin 12 and tumor necrosis factor alpha are costimulators of interferon gamma production by natural killer cells in severe combined immunodeficiency mice with listeriosis, and interleukin 10 is a physiologic antagonist. *Proc Natl Acad Sci U S A 90:3725.*
260. Lertmemongkolchai, G., G. Cai, C. A. Hunter, and G. J. Bancroft. 2001. Bystander activation of CD8+ T cells contributes to the rapid production of IFN-gamma in response to bacterial pathogens. *J Immunol 166:1097.*

261. Berg, R. E., C. J. Cordes, and J. Forman. 2002. Contribution of CD8+ T cells to innate immunity: IFN-gamma secretion induced by IL-12 and IL-18. *Eur J Immunol 32:2807.*
262. Berg, R. E., E. Crossley, S. Murray, and J. Forman. 2003. Memory CD8+ T cells provide innate immune protection against Listeria monocytogenes in the absence of cognate antigen. *J Exp Med 198:1583.*
263. Berg, R. E., E. Crossley, S. Murray, and J. Forman. 2005. Relative contributions of NK and CD8 T cells to IFN-gamma mediated innate immune protection against Listeria monocytogenes. *J Immunol 175:1751.*
264. Stober, D., R. Schirmbeck, and J. Reimann. 2001. IL-12/IL-18-dependent IFN-gamma release by murine dendritic cells. *J Immunol 167:957.*
265. Yoshimoto, T., K. Takeda, T. Tanaka, K. Ohkusu, S. Kashiwamura, H. Okamura, S. Akira, and K. Nakanishi. 1998. IL-12 up-regulates IL-18 receptor expression on T cells, Th1 cells, and B cells: synergism with IL-18 for IFN-gamma production. *J Immunol 161:3400.*
266. Rothe, J., W. Lesslauer, H. Lotscher, Y. Lang, P. Koebel, F. Kontgen, A. Althage, R. Zinkernagel, M. Steinmetz, and H. Bluethmann. 1993. Mice lacking the tumour necrosis factor receptor 1 are resistant to TNF-mediated toxicity but highly susceptible to infection by Listeria monocytogenes. *Nature 364:798.*
267. Pfeffer, K., T. Matsuyama, T. M. Kundig, A. Wakeham, K. Kishihara, A. Shahinian, K. Wiegmann, P. S. Ohashi, M. Kronke, and T. W. Mak. 1993. Mice deficient for the 55 kd tumor necrosis factor receptor are resistant to endotoxic shock, yet succumb to L. monocytogenes infection. *Cell 73:457.*
268. Havell, E. A. 1989. Evidence that tumor necrosis factor has an important role in antibacterial resistance. *J Immunol 143:2894.*
269. Nakane, A., T. Minagawa, and K. Kato. 1988. Endogenous tumor necrosis factor (cachectin) is essential to host resistance against Listeria monocytogenes infection. *Infect Immun 56:2563.*
270. Bancroft, G. J., K. C. Sheehan, R. D. Schreiber, and E. R. Unanue. 1989. Tumor necrosis factor is involved in the T cell-independent pathway of macrophage activation in scid mice. *J Immunol 143:127.*
271. Mielke, M. E., S. Ehlers, and H. Hahn. 1993. The role of cytokines in experimental listeriosis. *Immunobiology 189:285.*
272. Drevets, D. A., P. J. Leenen, and P. A. Campbell. 1996. Complement receptor type 3 mediates phagocytosis and killing of Listeria monocytogenes by a TNF-alpha- and IFN-gamma-stimulated macrophage precursor hybrid. *Cell Immunol 169:1.*
273. Musicki, K., H. Briscoe, S. Tran, W. J. Britton, and B. M. Saunders. 2006. Differential requirements for soluble and transmembrane tumor necrosis factor in the immunological control of primary and secondary Listeria monocytogenes infection. *Infect Immun 74:3180.*
274. Torres, D., L. Janot, V. F. Quesniaux, S. I. Grivennikov, I. Maillet, J. D. Sedgwick, B. Ryffel, and F. Erard. 2005. Membrane tumor necrosis factor confers partial protection to Listeria infection. *Am J Pathol 167:1677.*
275. Tripp, C. S., M. K. Gately, J. Hakimi, P. Ling, and E. R. Unanue. 1994. Neutralization of IL-12 decreases resistance to Listeria in SCID and C.B-17 mice. Reversal by IFN-gamma. *J Immunol 152:1883.*
276. Bancroft, G. J., M. J. Bosma, G. C. Bosma, and E. R. Unanue. 1986. Regulation of macrophage Ia expression in mice with severe combined immunodeficiency: induction of Ia expression by a T cell-independent mechanism. *J Immunol 137:4.*
277. Huang, S., W. Hendriks, A. Althage, S. Hemmi, H. Bluethmann, R. Kamijo, J. Vilcek, R. M. Zinkernagel, and M. Aguet. 1993. Immune response in mice that lack the interferon-gamma receptor. *Science 259:1742.*

278. MacMicking, J. D., C. Nathan, G. Hom, N. Chartrain, D. S. Fletcher, M. Trumbauer, K. Stevens, Q. W. Xie, K. Sokol, N. Hutchinson, and et al. 1995. Altered responses to bacterial infection and endotoxic shock in mice lacking inducible nitric oxide synthase. *Cell 81:641.*
279. Merrick, J. C., B. T. Edelson, V. Bhardwaj, P. E. Swanson, and E. R. Unanue. 1997. Lymphocyte apoptosis during early phase of Listeria infection in mice. *Am J Pathol 151:785.*
280. Cassatella, M. A., L. Meda, S. Gasperini, A. D'Andrea, X. Ma, and G. Trinchieri. 1995. Interleukin-12 production by human polymorphonuclear leukocytes. *Eur J Immunol 25:1.*
281. Wagner, R. D., H. Steinberg, J. F. Brown, and C. J. Czuprynski. 1994. Recombinant interleukin-12 enhances resistance of mice to Listeria monocytogenes infection. *Microb Pathog 17:175.*
282. Dai, W. J., W. Bartens, G. Kohler, M. Hufnagel, M. Kopf, and F. Brombacher. 1997. Impaired macrophage listericidal and cytokine activities are responsible for the rapid death of Listeria monocytogenes-infected IFN-gamma receptor-deficient mice. *J Immunol 158:5297.*
283. Brombacher, F., A. Dorfmuller, J. Magram, W. J. Dai, G. Kohler, A. Wunderlin, K. Palmer-Lehmann, M. K. Gately, and G. Alber. 1999. IL-12 is dispensable for innate and adaptive immunity against low doses of Listeria monocytogenes. *Int Immunol 11:325.*
284. Seki, E., H. Tsutsui, H. Nakano, N. Tsuji, K. Hoshino, O. Adachi, K. Adachi, S. Futatsugi, K. Kuida, O. Takeuchi, H. Okamura, J. Fujimoto, S. Akira, and K. Nakanishi. 2001. Lipopolysaccharide-induced IL-18 secretion from murine Kupffer cells independently of myeloid differentiation factor 88 that is critically involved in induction of production of IL-12 and IL-1beta. *J Immunol 166:2651.*
285. Tsuji, N. M., H. Tsutsui, E. Seki, K. Kuida, H. Okamura, K. Nakanishi, and R. A. Flavell. 2004. Roles of caspase-1 in Listeria infection in mice. *Int Immunol 16:335.*
286. Ozoren, N., J. Masumoto, L. Franchi, T. D. Kanneganti, M. Body-Malapel, I. Erturk, R. Jagirdar, L. Zhu, N. Inohara, J. Bertin, A. Coyle, E. P. Grant, and G. Nunez. 2006. Distinct roles of TLR2 and the adaptor ASC in IL-1beta/IL-18 secretion in response to Listeria monocytogenes. *J Immunol 176:4337.*
287. Tsutsui, H., K. Nakanishi, K. Matsui, K. Higashino, H. Okamura, Y. Miyazawa, and K. Kaneda. 1996. IFN-gamma-inducing factor up-regulates Fas ligand-mediated cytotoxic activity of murine natural killer cell clones. *J Immunol 157:3967.*
288. Hyodo, Y., K. Matsui, N. Hayashi, H. Tsutsui, S. Kashiwamura, H. Yamauchi, K. Hiroishi, K. Takeda, Y. Tagawa, Y. Iwakura, N. Kayagaki, M. Kurimoto, H. Okamura, T. Hada, H. Yagita, S. Akira, K. Nakanishi, and K. Higashino. 1999. IL-18 up-regulates perforin-mediated NK activity without increasing perforin messenger RNA expression by binding to constitutively expressed IL-18 receptor. *J Immunol 162:1662.*
289. Dao, T., K. Ohashi, T. Kayano, M. Kurimoto, and H. Okamura. 1996. Interferon-gamma-inducing factor, a novel cytokine, enhances Fas ligand-mediated cytotoxicity of murine T helper 1 cells. *Cell Immunol 173:230.*
290. Kagi, D., B. Ledermann, K. Burki, R. M. Zinkernagel, and H. Hengartner. 1996. Molecular mechanisms of lymphocyte-mediated cytotoxicity and their role in immunological protection and pathogenesis in vivo. *Annu Rev Immunol 14:207.*
291. Okamura, H., K. Nagata, T. Komatsu, T. Tanimoto, Y. Nukata, F. Tanabe, K. Akita, K. Torigoe, T. Okura, S. Fukuda, and et al. 1995. A novel costimulatory factor for gamma interferon induction found in the livers of mice causes endotoxic shock. *Infect Immun 63:3966.*

292. Ushio, S., M. Namba, T. Okura, K. Hattori, Y. Nukada, K. Akita, F. Tanabe, K. Konishi, M. Micallef, M. Fujii, K. Torigoe, T. Tanimoto, S. Fukuda, M. Ikeda, H. Okamura, and M. Kurimoto. 1996. Cloning of the cDNA for human IFN-gamma-inducing factor, expression in Escherichia coli, and studies on the biologic activities of the protein. *J Immunol 156:4274.*
293. Micallef, M. J., T. Ohtsuki, K. Kohno, F. Tanabe, S. Ushio, M. Namba, T. Tanimoto, K. Torigoe, M. Fujii, M. Ikeda, S. Fukuda, and M. Kurimoto. 1996. Interferon-gamma-inducing factor enhances T helper 1 cytokine production by stimulated human T cells: synergism with interleukin-12 for interferon-gamma production. *Eur J Immunol 26:1647.*
294. Kohno, K., J. Kataoka, T. Ohtsuki, Y. Suemoto, I. Okamoto, M. Usui, M. Ikeda, and M. Kurimoto. 1997. IFN-gamma-inducing factor (IGIF) is a costimulatory factor on the activation of Th1 but not Th2 cells and exerts its effect independently of IL-12. *J Immunol 158:1541.*
295. Neighbors, M., X. Xu, F. J. Barrat, S. R. Ruuls, T. Churakova, R. Debets, J. F. Bazan, R. A. Kastelein, J. S. Abrams, and A. O'Garra. 2001. A critical role for interleukin 18 in primary and memory effector responses to Listeria monocytogenes that extends beyond its effects on Interferon gamma production. *J Exp Med 194:343.*
296. Flesch, I. E., and S. H. Kaufmann. 1994. Role of macrophages and alpha beta T lymphocytes in early interleukin 10 production during Listeria monocytogenes infection. *Int Immunol 6:463.*
297. Wagner, R. D., N. M. Maroushek, J. F. Brown, and C. J. Czuprynski. 1994. Treatment with anti-interleukin-10 monoclonal antibody enhances early resistance to but impairs complete clearance of Listeria monocytogenes infection in mice. *Infect Immun 62:2345.*
298. Kelly, J. P., and G. J. Bancroft. 1996. Administration of interleukin-10 abolishes innate resistance to Listeria monocytogenes. *Eur J Immunol 26:356.*
299. Dai, W. J., G. Kohler, and F. Brombacher. 1997. Both innate and acquired immunity to Listeria monocytogenes infection are increased in IL-10-deficient mice. *J Immunol 158:2259.*
300. Buchmeier, N. A., and R. D. Schreiber. 1985. Requirement of endogenous interferon-gamma production for resolution of Listeria monocytogenes infection. *Proc Natl Acad Sci U S A 82:7404.*
301. Bancroft, G. J., R. D. Schreiber, G. C. Bosma, M. J. Bosma, and E. R. Unanue. 1987. A T cell-independent mechanism of macrophage activation by interferon-gamma. *J Immunol 139:1104.*
302. Beller, D. I., J. M. Kiely, and E. R. Unanue. 1980. Regulation of macrophage populations. I. Preferential induction of Ia-rich peritoneal exudates by immunologic stimuli. *J Immunol 124:1426.*
303. Bancroft, G. J., R. D. Schreiber, and E. R. Unanue. 1989. T cell-independent macrophage activation in scid mice. *Curr Top Microbiol Immunol 152:235.*
304. Bancroft, G. J. 1993. The role of natural killer cells in innate resistance to infection. *Curr Opin Immunol 5:503.*
305. Shtrichman, R., and C. E. Samuel. 2001. The role of gamma interferon in antimicrobial immunity. *Curr Opin Microbiol 4:251.*
306. Ferrick, D. A., M. D. Schrenzel, T. Mulvania, B. Hsieh, W. G. Ferlin, and H. Lepper. 1995. Differential production of interferon-gamma and interleukin-4 in response to Th1- and Th2-stimulating pathogens by gamma delta T cells in vivo. *Nature 373:255.*
307. Yang, J., T. L. Murphy, W. Ouyang, and K. M. Murphy. 1999. Induction of interferon-gamma production in Th1 CD4+ T cells: evidence for two distinct pathways for promoter activation. *Eur J Immunol 29:548.*

308. Yang, J., H. Zhu, T. L. Murphy, W. Ouyang, and K. M. Murphy. 2001. IL-18-stimulated GADD45 beta required in cytokine-induced, but not TCR-induced, IFN-gamma production. *Nat Immunol 2:157.*
309. Hunter, C. A., J. Timans, P. Pisacane, S. Menon, G. Cai, W. Walker, M. Aste-Amezaga, R. Chizzonite, J. F. Bazan, and R. A. Kastelein. 1997. Comparison of the effects of interleukin-1 alpha, interleukin-1 beta and interferon-gamma-inducing factor on the production of interferon-gamma by natural killer. *Eur J Immunol 27:2787.*
310. Robinson, D., K. Shibuya, A. Mui, F. Zonin, E. Murphy, T. Sana, S. B. Hartley, S. Menon, R. Kastelein, F. Bazan, and A. O'Garra. 1997. IGIF does not drive Th1 development but synergizes with IL-12 for interferon-gamma production and activates IRAK and NFkappaB. *Immunity 7:571.*
311. Strengell, M., S. Matikainen, J. Siren, A. Lehtonen, D. Foster, I. Julkunen, and T. Sareneva. 2003. IL-21 in synergy with IL-15 or IL-18 enhances IFN-gamma production in human NK and T cells. *J Immunol 170:5464.*
312. Oppmann, B., R. Lesley, B. Blom, J. C. Timans, Y. Xu, B. Hunte, F. Vega, N. Yu, J. Wang, K. Singh, F. Zonin, E. Vaisberg, T. Churakova, M. Liu, D. Gorman, J. Wagner, S. Zurawski, Y. Liu, J. S. Abrams, K. W. Moore, D. Rennick, R. de Waal-Malefyt, C. Hannum, J. F. Bazan, and R. A. Kastelein. 2000. Novel p19 protein engages IL-12p40 to form a cytokine, IL-23, with biological activities similar as well as distinct from IL-12. *Immunity 13:715.*
313. Pflanz, S., J. C. Timans, J. Cheung, R. Rosales, H. Kanzler, J. Gilbert, L. Hibbert, T. Churakova, M. Travis, E. Vaisberg, W. M. Blumenschein, J. D. Mattson, J. L. Wagner, W. To, S. Zurawski, T. K. McClanahan, D. M. Gorman, J. F. Bazan, R. de Waal Malefyt, D. Rennick, and R. A. Kastelein. 2002. IL-27, a heterodimeric cytokine composed of EBI3 and p28 protein, induces proliferation of naive CD4(+) T cells. *Immunity 16:779.*
314. Harty, J. T., and M. J. Bevan. 1995. Specific immunity to Listeria monocytogenes in the absence of IFN gamma. *Immunity 3:109.*
315. Dighe, A. S., D. Campbell, C. S. Hsieh, S. Clarke, D. R. Greaves, S. Gordon, K. M. Murphy, and R. D. Schreiber. 1995. Tissue-specific targeting of cytokine unresponsiveness in transgenic mice. *Immunity 3:657.*
316. Alvarez-Dominguez, C., and P. D. Stahl. 1998. Interferon-gamma selectively induces Rab5a synthesis and processing in mononuclear cells. *J Biol Chem 273:33901.*
317. Unanue, E. R. 1997. Inter-relationship among macrophages, natural killer cells and neutrophils in early stages of Listeria resistance. *Curr Opin Immunol 9:35.*
318. Brombacher, F., and M. Kopf. 1996. Innate versus acquired immunity in listeriosis. *Res Immunol 147:505.*
319. Reeves, E. P., H. Lu, H. L. Jacobs, C. G. Messina, S. Bolsover, G. Gabella, E. O. Potma, A. Warley, J. Roes, and A. W. Segal. 2002. Killing activity of neutrophils is mediated through activation of proteases by K+ flux. *Nature 416:291.*
320. Ahluwalia, J., A. Tinker, L. H. Clapp, M. R. Duchen, A. Y. Abramov, S. Pope, M. Nobles, and A. W. Segal. 2004. The large-conductance Ca2+-activated K+ channel is essential for innate immunity. *Nature 427:853.*
321. Rada, B. K., M. Geiszt, K. Kaldi, C. Timar, and E. Ligeti. 2004. Dual role of phagocytic NADPH oxidase in bacterial killing. *Blood 104:2947.*
322. Wagner, D., J. Maser, I. Moric, S. Vogt, W. V. Kern, and L. E. Bermudez. 2006. Elemental analysis of the Mycobacterium avium phagosome in Balb/c mouse macrophages. *Biochem Biophys Res Commun 344:1346.*
323. Endres, R., A. Luz, H. Schulze, H. Neubauer, A. Futterer, S. M. Holland, H. Wagner, and K. Pfeffer. 1997. Listeriosis in p47(phox-/-) and TRp55-/- mice: protection despite absence of ROI and susceptibility despite presence of RNI. *Immunity 7:419.*

324. Shiloh, M. U., J. D. MacMicking, S. Nicholson, J. E. Brause, S. Potter, M. Marino, F. Fang, M. Dinauer, and C. Nathan. 1999. Phenotype of mice and macrophages deficient in both phagocyte oxidase and inducible nitric oxide synthase. *Immunity 10:29.*
325. Dinauer, M. C., M. B. Deck, and E. R. Unanue. 1997. Mice lacking reduced nicotinamide adenine dinucleotide phosphate oxidase activity show increased susceptibility to early infection with Listeria monocytogenes. *J Immunol 158:5581.*
326. MacMicking, J. D., R. J. North, R. LaCourse, J. S. Mudgett, S. K. Shah, and C. F. Nathan. 1997. Identification of nitric oxide synthase as a protective locus against tuberculosis. *Proc Natl Acad Sci U S A 94:5243.*
327. Wei, X. Q., I. G. Charles, A. Smith, J. Ure, G. J. Feng, F. P. Huang, D. Xu, W. Muller, S. Moncada, and F. Y. Liew. 1995. Altered immune responses in mice lacking inducible nitric oxide synthase. *Nature 375:408.*
328. Karupiah, G., J. H. Chen, C. F. Nathan, S. Mahalingam, and J. D. MacMicking. 1998. Identification of nitric oxide synthase 2 as an innate resistance locus against ectromelia virus infection. *J Virol 72:7703.*
329. Khan, I. A., J. D. Schwartzman, T. Matsuura, and L. H. Kasper. 1997. A dichotomous role for nitric oxide during acute Toxoplasma gondii infection in mice. *Proc Natl Acad Sci U S A 94:13955.*
330. Scharton-Kersten, T. M., G. Yap, J. Magram, and A. Sher. 1997. Inducible nitric oxide is essential for host control of persistent but not acute infection with the intracellular pathogen Toxoplasma gondii. *J Exp Med 185:1261.*
331. Fehr, T., G. Schoedon, B. Odermatt, T. Holtschke, M. Schneemann, M. F. Bachmann, T. W. Mak, I. Horak, and R. M. Zinkernagel. 1997. Crucial role of interferon consensus sequence binding protein, but neither of interferon regulatory factor 1 nor of nitric oxide synthesis for protection against murine listeriosis. *J Exp Med 185:921.*
332. Weih, F., S. K. Durham, D. S. Barton, W. C. Sha, D. Baltimore, and R. Bravo. 1996. Both multiorgan inflammation and myeloid hyperplasia in RelB-deficient mice are T cell dependent. *J Immunol 157:3974.*
333. Tanaka, T., S. Akira, K. Yoshida, M. Umemoto, Y. Yoneda, N. Shirafuji, H. Fujiwara, S. Suematsu, N. Yoshida, and T. Kishimoto. 1995. Targeted disruption of the NF-IL6 gene discloses its essential role in bacteria killing and tumor cytotoxicity by macrophages. *Cell 80:353.*
334. Weih, F., G. Warr, H. Yang, and R. Bravo. 1997. Multifocal defects in immune responses in RelB-deficient mice. *J Immunol 158:5211.*
335. Pizarro-Cerda, J., M. Desjardins, E. Moreno, S. Akira, and J. P. Gorvel. 1999. Modulation of endocytosis in nuclear factor IL-6(-/-) macrophages is responsible for a high susceptibility to intracellular bacterial infection. *J Immunol 162:3519.*
336. Akira, S., H. Isshiki, T. Sugita, O. Tanabe, S. Kinoshita, Y. Nishio, T. Nakajima, T. Hirano, and T. Kishimoto. 1990. A nuclear factor for IL-6 expression (NF-IL6) is a member of a C/EBP family. *Embo J 9:1897.*
337. Roy, S. K., S. J. Wachira, X. Weihua, J. Hu, and D. V. Kalvakolanu. 2000. CCAAT/enhancer-binding protein-beta regulates interferon-induced transcription through a novel element. *J Biol Chem 275:12626.*
338. Roy, S. K., J. D. Shuman, L. C. Platanias, P. S. Shapiro, S. P. Reddy, P. F. Johnson, and D. V. Kalvakolanu. 2005. A role for mixed lineage kinases in regulating transcription factor CCAAT/enhancer-binding protein-{beta}-dependent gene expression in response to interferon-{gamma}. *J Biol Chem 280:24462.*
339. Kalvakolanu, D. V., and S. K. Roy. 2005. CCAAT/enhancer binding proteins and interferon signaling pathways. *J Interferon Cytokine Res 25:757.*

340. Yin, M., S. Q. Yang, H. Z. Lin, M. D. Lane, S. Chatterjee, and A. M. Diehl. 1996. Tumor necrosis factor alpha promotes nuclear localization of cytokine-inducible CCAAT/enhancer binding protein isoforms in hepatocytes. *J Biol Chem 271:17974.*
341. Zheng, H., D. Fletcher, W. Kozak, M. Jiang, K. J. Hofmann, C. A. Conn, D. Soszynski, C. Grabiec, M. E. Trumbauer, A. Shaw, and et al. 1995. Resistance to fever induction and impaired acute-phase response in interleukin-1 beta-deficient mice. *Immunity 3:9.*
342. MGNC. Mouse Genomic Nomenclature Committee. *http://www.informatics.jax.org/mgihome/nomen/#mgnc*.
343. Williams, S. C., M. Baer, A. J. Dillner, and P. F. Johnson. 1995. CRP2 (C/EBP beta) contains a bipartite regulatory domain that controls transcriptional activation, DNA binding and cell specificity. *Embo J 14:3170.*
344. Landschulz, W. H., P. F. Johnson, and S. L. McKnight. 1988. The leucine zipper: a hypothetical structure common to a new class of DNA binding proteins. *Science 240:1759.*
345. Williams, S. C., C. A. Cantwell, and P. F. Johnson. 1991. A family of C/EBP-related proteins capable of forming covalently linked leucine zipper dimers in vitro. *Genes Dev 5:1553.*
346. Descombes, P., M. Chojkier, S. Lichtsteiner, E. Falvey, and U. Schibler. 1990. LAP, a novel member of the C/EBP gene family, encodes a liver-enriched transcriptional activator protein. *Genes Dev 4:1541.*
347. Descombes, P., and U. Schibler. 1991. A liver-enriched transcriptional activator protein, LAP, and a transcriptional inhibitory protein, LIP, are translated from the same mRNA. *Cell 67:569.*
348. Poli, V., F. P. Mancini, and R. Cortese. 1990. IL-6DBP, a nuclear protein involved in interleukin-6 signal transduction, defines a new family of leucine zipper proteins related to C/EBP. *Cell 63:643.*
349. Ron, D., and J. F. Habener. 1992. CHOP, a novel developmentally regulated nuclear protein that dimerizes with transcription factors C/EBP and LAP and functions as a dominant-negative inhibitor of gene transcription. *Genes Dev 6:439.*
350. Wang, X. Z., M. Kuroda, J. Sok, N. Batchvarova, R. Kimmel, P. Chung, H. Zinszner, and D. Ron. 1998. Identification of novel stress-induced genes downstream of chop. *Embo J 17:3619.*
351. Buck, M., V. Poli, T. Hunter, and M. Chojkier. 2001. C/EBPbeta phosphorylation by RSK creates a functional XEXD caspase inhibitory box critical for cell survival. *Mol Cell 8:807.*
352. Roy, S. K., J. Hu, Q. Meng, Y. Xia, P. S. Shapiro, S. P. Reddy, L. C. Platanias, D. J. Lindner, P. F. Johnson, C. Pritchard, G. Pages, J. Pouyssegur, and D. V. Kalvakolanu. 2002. MEKK1 plays a critical role in activating the transcription factor C/EBP-beta-dependent gene expression in response to IFN-gamma. *Proc Natl Acad Sci U S A 99:7945.*
353. Liu, J. S., E. A. Park, A. L. Gurney, W. J. Roesler, and R. W. Hanson. 1991. Cyclic AMP induction of phosphoenolpyruvate carboxykinase (GTP) gene transcription is mediated by multiple promoter elements. *J Biol Chem 266:19095.*
354. Trautwein, C., C. Caelles, P. van der Geer, T. Hunter, M. Karin, and M. Chojkier. 1993. Transactivation by NF-IL6/LAP is enhanced by phosphorylation of its activation domain. *Nature 364:544.*
355. Nakajima, T., S. Kinoshita, T. Sasagawa, K. Sasaki, M. Naruto, T. Kishimoto, and S. Akira. 1993. Phosphorylation at threonine-235 by a ras-dependent mitogen-activated protein kinase cascade is essential for transcription factor NF-IL6. *Proc Natl Acad Sci U S A 90:2207.*

356. Buck, M., V. Poli, P. van der Geer, M. Chojkier, and T. Hunter. 1999. Phosphorylation of rat serine 105 or mouse threonine 217 in C/EBP beta is required for hepatocyte proliferation induced by TGF alpha. *Mol Cell 4:1087.*
357. Ray, A., and B. K. Ray. 1995. Lipopolysaccharide-mediated induction of the bovine interleukin-6 gene in monocytes requires both NF-kappa B and C/EBP binding sites. *DNA Cell Biol 14:795.*
358. Betts, J. C., J. K. Cheshire, S. Akira, T. Kishimoto, and P. Woo. 1993. The role of NF-kappa B and NF-IL6 transactivating factors in the synergistic activation of human serum amyloid A gene expression by interleukin-1 and interleukin-6. *J Biol Chem 268:25624.*
359. Matsusaka, T., K. Fujikawa, Y. Nishio, N. Mukaida, K. Matsushima, T. Kishimoto, and S. Akira. 1993. Transcription factors NF-IL6 and NF-kappa B synergistically activate transcription of the inflammatory cytokines, interleukin 6 and interleukin 8. *Proc Natl Acad Sci U S A 90:10193.*
360. Plevy, S. E., J. H. Gemberling, S. Hsu, A. J. Dorner, and S. T. Smale. 1997. Multiple control elements mediate activation of the murine and human interleukin 12 p40 promoters: evidence of functional synergy between C/EBP and Rel proteins. *Mol Cell Biol 17:4572.*
361. Dunn, S. M., L. S. Coles, R. K. Lang, S. Gerondakis, M. A. Vadas, and M. F. Shannon. 1994. Requirement for nuclear factor (NF)-kappa B p65 and NF-interleukin-6 binding elements in the tumor necrosis factor response region of the granulocyte colony-stimulating factor promoter. *Blood 83:2469.*
362. Lee, Y. M., L. H. Miau, C. J. Chang, and S. C. Lee. 1996. Transcriptional induction of the alpha-1 acid glycoprotein (AGP) gene by synergistic interaction of two alternative activator forms of AGP/enhancer-binding protein (C/EBP beta) and NF-kappaB or Nopp140. *Mol Cell Biol 16:4257.*
363. Vietor, I., I. C. Oliveira, and J. Vilcek. 1996. CCAAT box enhancer binding protein alpha (C/EBP-alpha) stimulates kappaB element-mediated transcription in transfected cells. *J Biol Chem 271:5595.*
364. Matsumoto, M., T. Tanaka, T. Kaisho, H. Sanjo, N. G. Copeland, D. J. Gilbert, N. A. Jenkins, and S. Akira. 1999. A novel LPS-inducible C-type lectin is a transcriptional target of NF-IL6 in macrophages. *J Immunol 163:5039.*
365. Gorgoni, B., M. Caivano, C. Arizmendi, and V. Poli. 2001. The transcription factor C/EBPbeta is essential for inducible expression of the cox-2 gene in macrophages but not in fibroblasts. *J Biol Chem 276:40769.*
366. Gorgoni, B., D. Maritano, P. Marthyn, M. Righi, and V. Poli. 2002. C/EBP beta gene inactivation causes both impaired and enhanced gene expression and inverse regulation of IL-12 p40 and p35 mRNAs in macrophages. *J Immunol 168:4055.*
367. Sugawara, I., S. Mizuno, H. Yamada, M. Matsumoto, and S. Akira. 2001. Disruption of nuclear factor-interleukin-6, a transcription factor, results in severe mycobacterial infection. *Am J Pathol 158:361.*
368. Screpanti, I., L. Romani, P. Musiani, A. Modesti, E. Fattori, D. Lazzaro, C. Sellitto, S. Scarpa, D. Bellavia, G. Lattanzio, and et al. 1995. Lymphoproliferative disorder and imbalanced T-helper response in C/EBP beta-deficient mice. *Embo J 14:1932.*
369. Weihua, X., V. Kolla, and D. V. Kalvakolanu. 1997. Interferon gamma-induced transcription of the murine ISGF3gamma (p48) gene is mediated by novel factors. *Proc Natl Acad Sci U S A 94:103.*
370. Weihua, X., J. Hu, S. K. Roy, S. B. Mannino, and D. V. Kalvakolanu. 2000. Interleukin-6 modulates interferon-regulated gene expression by inducing the ISGF3 gamma gene using CCAAT/enhancer binding protein-beta(C/EBP-beta). *Biochim Biophys Acta 1492:163.*

371. Meng, Q., A. Raha, S. Roy, J. Hu, and D. V. Kalvakolanu. 2005. IFN-gamma-stimulated transcriptional activation by IFN-gamma-activated transcriptional element-binding factor 1 occurs via an inducible interaction with CAAAT/enhancer-binding protein-beta. *J Immunol 174:6203.*
372. Kimura, T., Y. Kadokawa, H. Harada, M. Matsumoto, M. Sato, Y. Kashiwazaki, M. Tarutani, R. S. Tan, T. Takasugi, T. Matsuyama, T. W. Mak, S. Noguchi, and T. Taniguchi. 1996. Essential and non-redundant roles of p48 (ISGF3 gamma) and IRF-1 in both type I and type II interferon responses, as revealed by gene targeting studies. *Genes Cells 1:115.*
373. Bandyopadhyay, S. K., D. V. Kalvakolanu, and G. C. Sen. 1990. Gene induction by interferons: functional complementation between trans-acting factors induced by alpha interferon and gamma interferon. *Mol Cell Biol 10:5055.*
374. Levy, D. E., D. J. Lew, T. Decker, D. S. Kessler, and J. E. Darnell, Jr. 1990. Synergistic interaction between interferon-alpha and interferon-gamma through induced synthesis of one subunit of the transcription factor ISGF3. *Embo J 9:1105.*
375. Xiao, W., L. Wang, X. Yang, T. Chen, D. Hodge, P. F. Johnson, and W. Farrar. 2001. CCAAT/enhancer-binding protein beta mediates interferon-gamma-induced p48 (ISGF3-gamma ) gene transcription in human monocytic cells. *J Biol Chem 276:23275.*
376. Lewis, J. A., A. Huq, and B. Shan. 1989. Beta and gamma interferons act synergistically to produce an antiviral state in cells resistant to both interferons individually. *J Virol 63:4569.*
377. Karandikar, M., S. Xu, and M. H. Cobb. 2000. MEKK1 binds raf-1 and the ERK2 cascade components. *J Biol Chem 275:40120.*
378. Xu, S., D. Robbins, J. Frost, A. Dang, C. Lange-Carter, and M. H. Cobb. 1995. MEKK1 phosphorylates MEK1 and MEK2 but does not cause activation of mitogen-activated protein kinase. *Proc Natl Acad Sci U S A 92:6808.*
379. Lewis, T. S., P. S. Shapiro, and N. G. Ahn. 1998. Signal transduction through MAP kinase cascades. *Adv Cancer Res 74:49.*
380. Hu, J., S. K. Roy, P. S. Shapiro, S. R. Rodig, S. P. Reddy, L. C. Platanias, R. D. Schreiber, and D. V. Kalvakolanu. 2001. ERK1 and ERK2 activate CCAAAT/enhancer-binding protein-beta-dependent gene transcription in response to interferon-gamma. *J Biol Chem 276:287.*
381. Mo, X., E. Kowenz-Leutz, H. Xu, and A. Leutz. 2004. Ras induces mediator complex exchange on C/EBP beta. *Mol Cell 13:241.*
382. Wang, X., and G. Z. Feuerstein. 2000. Suppression subtractive hybridisation: application in the discovery of novel pharmacological targets. *Pharmacogenomics 1:101.*
383. Rebrikov, D., S. Desai, Y. N. Kogan, A. M. Thornton, and L. Diatchenko. 2002. Subtractive cloning: new genes for studying inflammatory disorders. *Ann Periodontol 7:17.*
384. Diatchenko, L., Y. F. Lau, A. P. Campbell, A. Chenchik, F. Moqadam, B. Huang, S. Lukyanov, K. Lukyanov, N. Gurskaya, E. D. Sverdlov, and P. D. Siebert. 1996. Suppression subtractive hybridization: a method for generating differentially regulated or tissue-specific cDNA probes and libraries. *Proc Natl Acad Sci U S A 93:6025.*
385. Diatchenko, L., S. Lukyanov, Y. F. Lau, and P. D. Siebert. 1999. Suppression subtractive hybridization: a versatile method for identifying differentially expressed genes. *Methods Enzymol 303:349.*
386. Tuteja, R., and N. Tuteja. 2004. Serial analysis of gene expression (SAGE): unraveling the bioinformatics tools. *Bioessays 26:916.*

387. Velculescu, V. E. 1999. Essay: Amersham Pharmacia Biotech & Science prize. Tantalizing transcriptomes--SAGE and its use in global gene expression analysis. *Science 286:1491.*

388. Yamamoto, M., T. Wakatsuki, A. Hada, and A. Ryo. 2001. Use of serial analysis of gene expression (SAGE) technology. *J Immunol Methods 250:45.*

389. Doumith, M., C. Cazalet, N. Simoes, L. Frangeul, C. Jacquet, F. Kunst, P. Martin, P. Cossart, P. Glaser, and C. Buchrieser. 2004. New aspects regarding evolution and virulence of Listeria monocytogenes revealed by comparative genomics and DNA arrays. *Infect Immun 72:1072.*

390. Nelson, K. E., D. E. Fouts, E. F. Mongodin, J. Ravel, R. T. DeBoy, J. F. Kolonay, D. A. Rasko, S. V. Angiuoli, S. R. Gill, I. T. Paulsen, J. Peterson, O. White, W. C. Nelson, W. Nierman, M. J. Beanan, L. M. Brinkac, S. C. Daugherty, R. J. Dodson, A. S. Durkin, R. Madupu, D. H. Haft, J. Selengut, S. Van Aken, H. Khouri, N. Fedorova, H. Forberger, B. Tran, S. Kathariou, L. D. Wonderling, G. A. Uhlich, D. O. Bayles, J. B. Luchansky, and C. M. Fraser. 2004. Whole genome comparisons of serotype 4b and 1/2a strains of the food-borne pathogen Listeria monocytogenes reveal new insights into the core genome components of this species. *Nucleic Acids Res 32:2386.*

# CHAPTER 2

# MATERIALS AND METHODS

## METHODS

### 1. Culture of *Listeria monocytogenes*

Virulent *L. monocytogenes* (EGD strain) were grown in tryptose-soy broth (Difco, Detroit, MI, USA) until early to mid log-phase of growth ($OD_{600}$=0.2). DMSO was added to a final concentration of 10% and aliquots made and stored at –70°C until use. For each experiment, a vial was thawed and mixed thoroughly to disperse clumps. For each experiment, the titre of the inoculum was checked by plating 100µl of 10-fold serial dilutions of the thawed *L. monocytogenes* stock on tryptose-soy agar plates. The plates were incubated overnight at 37°C and the next day the number of colonies was counted and the colony forming units (CFU)/ml calculated. All experiments were performed in the BSL 2 laboratories at the University of Cape Town, South Africa.

### 2. Culture of *Mycobacterium tuberculosis*

*Mycobacterium tuberculosis* (H37Rv) was grown in Middlebrook 7H9 broth (Difco, Detroit, MI, USA) supplemented with Middlebrook OADC enrichment medium (Life Technologies, Gaithersburg, MI, USA), 0.002 % glycerol, and 0.05 % Tween 80. Mid log-phase cultures were harvested, aliquoted, and frozen at –80°C. After thawing, viable cell counts were determined by plating 100µl of 10-fold serial dilutions of the cultures on Middlebrook 7H10 agar plates. The plates were incubated at 37°C for 21 days and the CFU/ml enumerated. All experiments were performed in the BSL 3 laboratories at the University of Cape Town, South Africa.

### 3. Mice

C/EBPβ$^{+/-}$ on a C57BL/6x129/sv background were obtained from V. Poli (Department of Genetics, Biology and Biochemistry, University of Turin, Turin, Italy). A null mutation in the C/EBPPβ gene was generated by inserting a neo cassette into the carboxy-terminal part of the gene, coding for the leucine zipper and a portion of the basic domain (Fig. 1 A). This mutation inactivated the full length C/EBPPβ protein and its truncated amino-terminal isoform, LIP.

PKCδ$^{+/-}$ mice on a 129/SvxOla background were obtained from M. Leitges (Department of Experimental Endocrinology, Medical University, Hanover, Germany). A LacZ/neo cassette was inserted into the first transcribed exon of the PKCδ gene resulting in a null allele and abolished transcription (Fig. 1 B) All mice were bred in specific pathogen-free conditions at the Animal unit at the University of Cape Town, South Africa. For *L. monocytogenes* infections, mice were kept in filter-cap cages in a biohazard level 2 physical containment facility. For *M. tuberculosis* infections, mice were kept in individually ventilated cages in a biohazard level 3 physical containment facility. In any given experiment, mice were matched for age (6–10 weeks) and sex. All experiments performed were in accordance with the Animal Research Ethics Committee of the University of Cape Town.

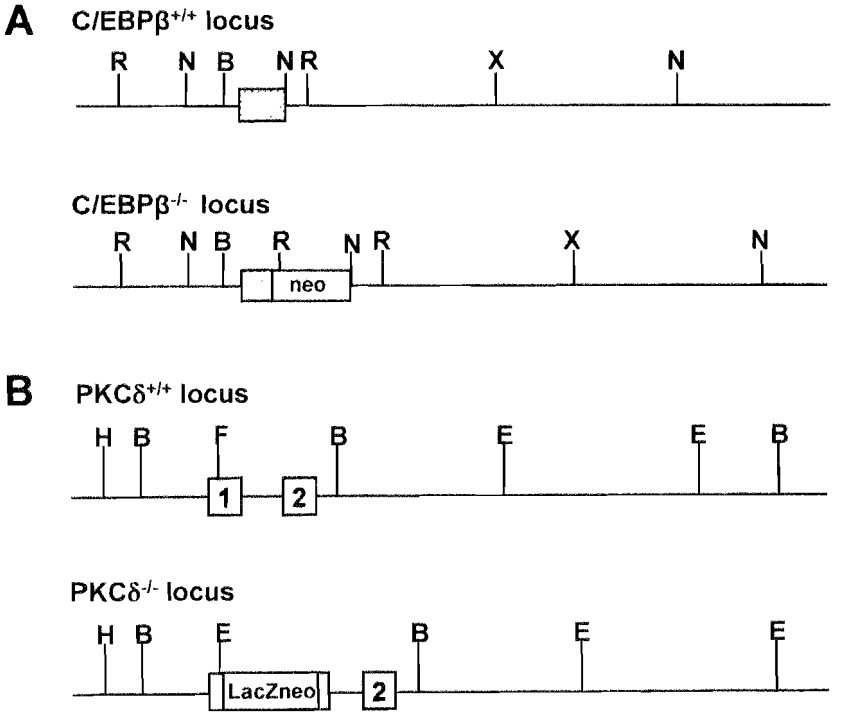


**Figure 1. Generation of C/EBPβ$^{-/-}$ and PKCδ$^{-/-}$ mice.** (A) C/EBPβ$^{-/-}$ mice were generated by V. Poli by inserting a neo cassette (open box) into the BZIP (grey hatched box) domain of the C/EBPβ gene via homologous recombination. B, *Bam*HI; N, *Nhe*I; R, *Rsa*I; X, *Xba*I. (B) PKCδ$^{-/-}$ mice were generate by M. Leitges via homologous recombination which inserted a LacZ/neo cassette (open box) into exon 1 (grey box labeled 1) of the PKCδ gene. B, *Bam*HI; E, *Eco*RI; F, *Fsp*1; H, *Hind*III.

**4. Genomic DNA extraction**

1cm mouse tail cuttings were digested overnight in digestion buffer (50mM TRIS-HCL, pH8; 100mM EDTA; 100mM NaCl, 1% SDS, 0.5mg/ml Proteinase K) at 56°C with gentle shaking. The samples were centrifuged at 14000 rpm for 15 minutes and the clear supernatant transferred to a clean microcentrifuge tube. An equal volume isopropanol was added and thoroughly mixed. The genomic DNA was allowed to precipitate out of solution by incubating at room temperature for 30 minutes and centrifuged at 14000 rpm at 4°C for 30 minutes. The genomic DNA pellet was washed in 1ml 70% ethanol, air dried and resuspended in 500µl sterile water. The quantity and quality of the genomic DNA was checked by spectroscopy by reading the absorbance at $A_{260}$ and $A_{280}$.

**5. Genotyping PCR**

All mice used in this thesis were genotyped prior to experiments to confirm their genotype using gene specific primers. 2µl of genomic DNA was added to 48µl of PCR cocktail (1 X Supertherm PCR Buffer, 1.5mM $MgCl_2$, 0.2mM dNTPs, 0.125U/µl Supertherm Taq, 0.25µM forward primer and 0.25µM reverse primer). Control reactions included a (i) no template/water control, (ii) positive control and (iii) negative control. The PCR products were amplified on a MJ thermocycler (Biozym, Hessisch Oldendorf, Frankfurt, Germany). C/EBPβ$^{-/-}$ mice were genotyped using a common primer 5'-TGGACAAGCTGAGCGAC-3' and a primer specific for either the WT (5'-GGGCTGCTTGAACA-3') or targeted C/EBPβ locus (5'-GCCGATTGTCTGTTGTGCCC-3'). The PCR products for the WT allele was 200bp and 450bp for the C/EBPβ targeted allele. The PCR cycle for CEBPβ PCR was: 1 cycle at 94°C for 3 minutes; 45 cycles of 94°C for 30 seconds, 59°C for 30 seconds, 72°C for 30 seconds; 1 cycle at 72°C for 3 minutes. For PKCδ$^{-/-}$ genotyping, a common reverse primer (5'-AACAGCTGTGATGGGATCGAA-3') and a forward primer specific for either the WT (5'-ACCCTTCCTGCGCATCTCCT-3') or targeted PKCδ locus (5'-GAGGATCTCGTCGTGACCCA- 3') were used. The PCR products for the WT allele was 621bp and 872bp for the PKCδ targeted allele. The PCR cycle for was: 1 cycle at 94°C for 3 minutes; 40 cycles of 94°C for 30 seconds, 55°C for 30 seconds, 72°C for 45 seconds; 1 cycle at 72°C for 5 minutes. The PCR products were analysed by gel electrophoresis.

**6. Generation Of C/EBPβ$^{-/-}$ Bone Marrow Derived Macrophages (BMDMs)**

Mice were sacrificed by cervical dislocation and the femur and tibia bones collected. The bone marrow cells were flushed from the bones using DMEM (Gibco, Invitrogen Corporation, Carlsbad, CA, USA) containing 10% FCS, 100U/ml penicillin G and 100µg/ml streptomycin. The cells were washed and concentrated by centrifuging at 1200 rpm at 4°C for 10 minutes. The bone marrow cells were added at a final concentration of 1 x $10^6$ cells/ml in PLUTZNIK media (DMEM containing 10% FCS, 5% horse serum, 2mM L-glutamine, 1mM Na-pyruvate, 0.1mM 2-β-Mercaptoethanol, 30% L929 cell-conditioned medium, 100U/ml penicillin G, 100µg/ml streptomycin) and transferred into a special gas-permeable 15cm x 6cm Teflon coated-bag (Max Planck Institute for Immunobiology, Max Planck, Freiberg, Germany). The L929 conditioned medium contained GM-CSF and M-CSF, which stimulated the differentiation and growth of bone marrow stem cells into macrophages. The open end of the bag was heat-sealed and bone marrow stem cells incubated at 37°C under 5% $CO_2$ for 10 days. The supernatant was discarded and the adherent cells were massaged from the Teflon-coated bags into DMEM containing 10% FCS, 100U/ml penicillin G, 100µg/ml streptomycin. The BMDMs were washed twice in DMEM containing 10% FCS, 100U/ml penicillin G, 100µg/ml streptomycin to get rid of residual GM-CSF from the L929 conditioned medium. The BMDMs were plated at a density of 5 x $10^5$ BMDMs/ml and incubated overnight at 37°C under 5% $CO_2$. If activated macrophages were required for infection the next day, IFN-γ (BD Pharmigen, BD Biosciences, San Jose, CA, USA) was added at 100U/ml to the BMDMs for 16-24 hours before infection.

**7. L929 conditioned medium**

L929 cells were maintained in DMEM (Gibco, Invitrogen Corporation, Carlsbad, CA, USA) containing 10% FCS, 100U/ml penicillin G and 100µg/ml streptomycin until 90% confluence. The growth media was removed and the cells washed in 10ml 1 x PBS. Cells were removed from the plastic surface of the flask by incubation in 5ml Trypsin/EDTA (Gibco, Invitrogen Corporation, Carlsbad, CA, USA) at room temperature for 4 minutes. The cells were washed in 50ml DMEM (Gibco, Invitrogen Corporation, Carlsbad, CA, USA) containing 10% FCS, 100U/ml penicillin G, 100µg/ml streptomycin and seeded at 2 x $10^4$cells/ml in 100ml DMEM (Gibco, Invitrogen Corporation, Carlsbad, CA, USA) containing 10% FCS, 100U/ml penicillin G, 100µg/ml streptomycin. The L929 cells were grown in 162cm2 tissue culture grade flasks (Corning Costar Corporation, Cambridge, MA, USA) at 37°C under 5% $CO_2$ for

7 days. The supernatant was harvested and centrifuged at 2500 rpm for 15 minutes at 4°C to get rid of cell debris. The clear supernatants were stored in 50ml aliquots at –20°C.

**8. *In vitro* Infection with *L. monocytogenes***

Before each infection experiment, the BMDM cultures were washed three times in DMEM containing 10% FCS but without antibiotics. These washing steps ensured that any residual antibiotics were washed away. The BMDM monolayers were then simultaneously stimulated with 100U/ml IFN-γ (BD Pharmigen, BD Biosciences, San Jose, CA, USA) and infected with *L. monocytogenes* at a multiplicity of infection (MOI) of 10:1 (10 bacilli : 1 macrophage). After 1 hour, gentamycin (Sigma-Aldrich, Munich, Germany) was added at 50μg/ml to kill extracellular bacteria. At 2, 4, 8 and 12 hours after infection, RNA and supernatant samples were taken and stored at –80°C.

**9. *In vivo* Infection with *L. monocytogenes***

For each experiment, a vial of frozen *L. monocytogenes* stock was thawed and diluted in PBS before injection. Mice were injected into the peritoneal cavity with 200μl PBS containing 2 x $10^4$ *L. monocytogenes* bacilli or without bacteria. The number of viable bacteria in the inoculum was determined by plating 10-fold serial dilutions on trypticase soy agar plates. Plates were incubated at 37°C and the CFU counted after 24 hours. The actual infectious dose was then calculated.

**10. Secondary *in vivo* Challenge with *L. monocytogenes***

Mice were immunized by a sub-lethal dose (for WT mice) of 2 x $10^3$ *L. monocytogenes* injected into the intraperitoneal cavity. Surviving mice were challenged 8 weeks later with a secondary i.p. infection of 2 x $10^4$ *L. monocytogenes*. Bacterial load (CFU) was measured in the liver and spleen 2 days after secondary infection.

**11. *In vivo* Aerosol Infection with *Mycobacterium tuberculosis***

All *M. tuberculosis* experiments were performed in the BSL 3 laboratories at the University of Cape Town, South Africa. Pulmonary infection of mice was performed using an inhalation exposure system (system model A4224, Glas-Col, Terre-Haute, IN). Stock solutions of *M. tuberculosis* were thawed and diluted in sterile distilled water. To infect mice with a natural dose of 100 CFU/lung, animals were exposed for 40 minutes to an aerosol generated by nebulizing approximately 5.5 ml of a suspension containing $10^7$ live bacteria. Inoculum size

was checked 24 hours after infection by determining the bacterial load in the lung of infected mice. Mice were weighed weekly before and after infection. In accordance with the Animal Research Ethics Committee of the University of Cape Town, mice that lost 25% of their original weight during the course of infection were sacrificed. Moribund CEBPβ$^{-/-}$ and IFN-γR$^{-/-}$ mice were sacrificed at 6 and 7 weeks post infection respectively and their CFUs determined in lung, liver and spleen. Surviving WT, PKCδ$^{+/-}$ and PKCδ$^{-/-}$ were sacrificed 10 weeks post infection and their bacterial load in lung, liver and spleen determined

**12. Determination of Bacterial Load in Organs**

Bacterial loads in lung, liver and spleen of infected mice were evaluated at different time points after infection with *L. monocytogenes* or *M. tuberculosis*. Organs from sacrificed mice were removed aseptically and divided into 2 pieces, one for histology and one for bacterial load determination. The piece for bacterial burden was weighed and homogenized in 0.05% Tween-80 made in PBS. Ten-fold serial dilutions of the organ lysate was made in 1 x PBS and 100µl plated in duplicate on tryptose-soy agar plates (for *L. monocytogenes*) or Middlebrook 7H10 agar plates containing 10 % OADC (for *M. tuberculosis)*. The *L. monocytogenes* plates were incubated at 37°C overnight and the colonies counted the next day. The *M. tuberculosis* plates were incubated at 37°C for 19-21 days and the colonies counted. The CFU/organ was calculated and expressed as $\log_{10}$ CFU per organ.

**13. Histology**

One lung lobe, a piece of liver and spleen per mouse were fixed in 4 % phosphate-buffered formalin and paraffin-embedded. Sections (2 to 3 µm) were stained with hematoxylin and eosin and a modified Ziehl-Nielsen method as described (1). Standard Gram positive staining was used to detect *L. monocytogenes* bacilli. All observations were done with a Nikon E400 microscope and the diameter of 250 granulomas was determined using Scion Image, Software (Scion, Frederick, MD, USA).

**14. FACS analysis of Peritoneal Exudate Cells (PECs).**

Mice were inoculated i.p. with 2 x $10^4$ *L. monocytogenes* and sacrificed 2 days after infection. PECs were harvested by flushing the peritoneal cavity with 10 ml of sterile Iscoves's-Modified Dulbecco's Medium (IMDM) supplemented with 10% FCS, 100 U/ml penicillin and 100 µg/ml streptomycin (All Gibco, Invitrogen Corporation, Carlsbad, CA, USA). Harvested cells were centrifuged at 1200 rpm for 8 minutes and resuspended in 2ml complete IMDM supplemented with 10% FCS, 100 U/ml penicillin and 100µg/ml streptomycin (all Gibco). Cells in single cell suspension were counted using an improved neubauer haemocytometer. 5 x $10^5$ cells were pooled for each experimental mouse group and were washed in FACS buffer (PBS supplemented with 0.1% BSA and 0.05% Sodium Azide) by centrifugation at 1200 rpm for 5 minutes. Cells were then stained for 15 minutes on ice in 100µl of FACS buffer with a saturating amount of anti-Gr-1-FITC (mAb clone RB6-8G5), anti-I-$A^b$-biotin (mAb clone KH74), anti-CD11b-PE (mAb clone M1/70) (all from BD Pharmigen, BD Biosciences, San Jose, CA, USA) or F4/80-PE mAb (Caltag Laboratories, Burlingame, CA, USA) in the presence of 1% normal rat serum. Unbound antibody was removed by centrifugation in 1ml FACS buffer. Pelleted cells were resuspended and incubated for a further 15 minutes on ice with 100µl of a saturating amount of streptavidin-APC (BD) in FACs buffer. Cells were washed for a final time and resuspended in 500µl FACs buffer supplemented with 7-AAD (Sigma, St. Louis, USA). Stained cells were acquired using a FACSCalibur flow cytometer and cells analyzed using CellQuest software (both BD). Dead cells stained with 7-AAD were excluded from analysis.

**15. ELISA**

The levels of cytokines and chemokines in culture supernatants and sera was measured by sandwich ELISA as previously described (2). The coating and biotinylated detection antibody pairs, stepavidin-alkaline-phosphatase, stepavidin-horseradsish peroxidase, and recombinant protein standards were purchased from BD Pharmigen (BD Pharmigen, BD Biosciences, San Jose, CA, USA). *In vitro* Supernatant samples from triplicate wells at 2, 4, 8 and 12 hours after infection were collected and stored at –20°C. Sera samples were collected from infected mice and stored at –20°C. Maxisorb 96 well ELISA plates (Nalge Nunc International, Naperville, IKL,USA) were coated overnight at 4°C with 50µl of "coating antibody" diluted in coating buffer (1 X PBS, 0.02% sodium azide) at the recommended concentration. For TNF ELISAs, the plates were coated in carbonate coating buffer (15mM $NaCO_3$, 35mM $NaHCO_3$, 72mM NaCl). Plates were washed, blocked 2 hours at 37°C in 250µl blocking buffer (2% fat

free milk powder, 0.1% sodium azide in 1xPBS) and then washed again. Samples (serum or supernatant) were serially diluted two-fold in dilution buffer (4% BSA (fraction V), 0.02% sodium azide in 1 X PBS) and 50µl added to each well. Similarly, the appropriate recombinant protein standard was diluted to the recommended concentration, then serially diluted three-fold in dilution buffer (4% BSA (fraction V), 0.02% sodium azide in 1 X PBS) and 50µl added to designated control wells. The plates were incubated overnight at 4°C and washed. 50µl of the appropriate biotinylated antibody was diluted to the recommended concentration in dilution buffer (4% BSA (fraction V), 0.02% sodium azide in 1 X PBS) and 50µl was added to each well. The plates were incubated at 37°C for 3h, washed and 50µl of streptavidin-alkaline phosphatase diluted 1:1000 in dilution buffer (4% BSA (fraction V), 0.02% sodium azide in 1 X PBS) was added to each well. The plates were incubated for 60 minutes at 37°C, washed and 50µl substrate solution (1mg/ml p-nitrophenol-phospahte, 0.2mM $MgCl_2$, 10% diethanolamine, 0.01% sodium azide) added to each well. The enzymatic reactions were developed at room temperature and was stopped when the most concentrated standard reached 1.0 to 1.5 $A_{405nm}$ OD units. The developing reaction was stopped by adding 50µl of 1M NaOH to each well. The plates were plates read at $A_{405nm}$ using a VersaMax microplate reader (Molecular Devices Corporation, Sunnyvale, CA, U.S.A). For the wash steps above, each well was washed 4 times with 300µl of wash buffer (2.68mM KCl, 1.47mM $KH_2PO_4$, 8.09mM $Na_2HPO_4.2H_2O$, 136mM NaCl, 0.05% Tween-20, 0.01% sodium azide). For IL-10 ELISA reaction development, streptavidin-horseradish peroxidase and TMB Substrate Solutions (Roche Diagnostics GmbH, Mannheim, Germany) were used as per the manufacturer's instructions.

**16. Measurement of nitric oxide in culture supernatants**

Cell culture supernatants were analyzed for the production of NO using the Griess reaction assay, which measures the concentration of nitrite, a stable product of the reaction of NO with $O_2$ (3). BMDM were infected as described and supernatant samples collected at 2, 4, 8 and 12 hours after infection and stored at –20°C until analysis. Supernatant samples and standards (1mM $NO_2$ solution) were serially diluted three-fold in DMEM containing 10% FCS, 100U/ml penicillin G, 100µg/ml streptomycin (all Gibco, Invitrogen Corporation, Carlsbad, CA, USA) and 50µl added to designated wells in a flat bottomed 96 well plate. 25µl of Griess Reagent 1 (1% sulfanilamide in 2.5% phosphoric acid) and then 25µl of Griess Reagent (2 0.1% napthyl-ethylene-diamine in 2.5 % phosphoric acid) were sequentially added to each well. The plate was incubated at room temperature for 5 minutes to allow the reaction to

develop. The purple-pink colour of the reactions were read at $A_{540nm}$ and the reference at $A_{690nm}$ using VersaMax microplate reader (Molecular Devices Corporation, Sunnyvale, CA, U.S.A).

**17. Macrophage Bacterial Killing Assay**

BMDMs (2.5 x $10^5$ cells) were plated at 1ml per well in a 24-well tissue-culture grade plate. The BMDMs were stimulated overnight with 100U/ml IFN-γ and the BMDMs infected with *L. monocytogenes* as described. At 2, 4, 8 and 12 hours after infection, the BMDMs were washed three times with 1ml cold 1 X PBS containing 0.68mM $CaCl_2$ and 0.49mM $MgCl_2$ to get rid of extracellular bacteria and residual gentamycin. The BMDMs were lysed by repetitive pipetting in 1ml of 0.05% Triton-X100. Ten-fold serial dilutions of the lysate was made in 1 X PBS and 100µl plated on tryptose-soy agar plates. The plates were incubated at 37°C for 24 hours and the number of colonies counted and the CFU/ml for each sample calculated.

**18. Electron microscopy with low temperature fixation in cacodylate buffer**

BMDMs were stimulated and infected with *L. monocytogenes* as described. 4 hours after infection, the BMDMs were washed twice with 1 X cold PBS containing 0.68mM $CaCl_2$ and 0.49mM $MgCl_2$ to remove extracellular bacteria. The BMDMs were washed once cacodylate buffer (0.1M sodium cacodylate, 5mM $CaCl_2$, 5mM $MgCl_2$, 0.1M sucrose pH7.2) and fixed overnight at 4°C in 2.5% gluteraldehyde made up in cacodylate buffer lacking sucrose. The BMDMs were washed twice in cacodylate buffer (lacking sucrose) and stained with freshly prepared osmium staining buffer (1% osmium tetroxide, 0.05M ferric cyanide in cacodylate buffer (devoid of sucrose)) for 1-2 hours at room temperature in the dark. The BMDMs were then washed twice in cacodylate buffer (lacking sucrose) and scraped from the culture dish. The BMDMs were centrifuged at 1200 rpm for 20 minutes and the cell pellet resuspended in 20µl of 2% low-melting-point-agarose prepared in cacodylate buffer (lacking sucrose). The agar cell pellet was cut into 1mM cubes and dehydrated in a series of ethanol and embedded in Spurr's resin. Ultra thin sections (90µM) were cut with a glass knife on a Reichert Ultracut S (Leica) ultramicrotome. The ultra thin sections were picked up on uncoated copper grids (300 mesh) and stained with uranyl acetate and Reynolds lead(4). The sections were examined using a Zeiss 109 transmission electron microscope at 4400X and 20000X magnification.

**19. Fluorescent Microscopy**

BMDM from WT, PKCδ$^{+/-}$ and PKCδ$^{-/-}$ mice were generated as described and grown on acid-cleaned 12-mm circular glass coverslips at density of 2.5 x $10^5$ cells/coverslip. BMDMs were activated with 100U/ml IFN-γ overnight and infected at MOI of 30:1 (30 bacilli : 1 macrophage) as described. At 90 minutes, 180 minutes and 240 minutes post-infection, BMDMs were washed twice with PBS containing 0.68mM $CaCl_2$ and 0.49mM $MgCl_2$ to remove extracellular bacteria. The BMDMs were fixed at room temperature for 15 minutes in 3.7% formaldehyde (vol/vol in PBS) and washed twice in pre-warmed PBS. The cells were permeabilized in 0.2% Triton X-100 (vol/vol in PBS) for 10 minutes at 37°C and washed twice in PBS and blocked in 1% BSA (fraction V) (vol/vol in PBS) for 30 minutes at room temperature. The BMDMs were washed twice with PBS and incubated in 1/1000 diluted polyclonal rabbit anti-*Listeria antibody* (Capricorn Products LLC, Portland, ME, USA) for 30 minutes at room temperature. The BMDMS were washed twice with PBS and incubated in 1/1000 diluted goat anti-rabbit IgG-FITC antibody (Sigma-Aldrich, Munich, Germany) for 30 minutes at room temperature. The BMDMS were washed twice with PBS and incubated in actin staining solution (10.3nM rhodamine phalloidin (Molecular Probes, Invitrogen Corporation, Carlsbad, CA, USA) in 1% BSA(fraction V) for 30 minutes. The coverslips were washed twice, air dried and mounted onto glass slides using Prolong AntiFade Mounting media (Molecular Probes, Invitrogen Corporation, Carlsbad, CA, USA). BMDMs were visualized using deconvoluting fluorescent microscope (Zeiss Axiovert 200M, Carl Zeiss, Göttingen, Germany) under 100X oil immersion. Images in both the red and green channels were saved for 15 non-overlapping random high power field views (HPFV). Images were analysed using Axiovision version 3.1 (Carl Zeiss, Göttingen, Germany). The total number of bacteria in each HPFV was scored in the green channel. In the merged red and green image, the number of bacteria associated with actin (red-orange-yellow) and trapped in the phagosome (green) was scored. Percentage escape is calculated as total number of bacteria associated with actin in all HPFV divided by the total number of bacteria in all the HPFV.

**20. Total RNA Isolation**

Total RNA was extracted from BMDMs using TriReagent (Molecular Research Company, Cincinnati, USA) as per the manufacture's instructions. Briefly, 5 x $10^5$ cells were lysed directly in the culture dish in 1ml of TriReagent. 200µl of chloroform was added for every 1ml of lysate and vortexed thoroughly. The samples were incubated at room temperature for 15 minutes and centrifuged at 13500 rpm for 15 minutes at 4°C. The top aqueous layer was transferred to a new tube and an equal volume of 100% isopropanol added and mixed. The RNA was precipitated out of solution by incubating overnight at –80°C and centrifuging at 13500 rpm for 30 minutes at 4°C. The RNA pellet was washed twice in 800µl 70% ethanol, air-dried and resuspended in 50µl -100µl of DEPC-treated water. Total RNA was extracted from organs as described by Chomczynski et al (5). Organs were homogenized on ice in 3ml RNA denaturing solution (4M guanidinium thiocyanate, 25mM sodium citrate, 0.5% (w/v) sodium lauryl sarcosinate, 0.1M β–mercaptoethanol) for every 100mg of tissue. An equal volume of phenol pH4.0 was added and thoroughly mixed with the lysate. For every 1ml of volume lysate 0.05ml 3M sodium acetate (pH 4.0) and 0.1ml chloroform-isoamyl alcohol (49:1) were sequentially added. The samples were mixed thoroughly for 30 seconds and incubated on ice for 15 minutes. The samples were centrifuged 14000 rpm for 20 minutes at 4°C and the top aqueous layer transferred to a new tube. An equal volume of 100% isopropanol was added and mixed thoroughly. The RNA was precipitated by incubating for 1 hour at -80°C and centrifuging at 14000 rpm for 30 minutes at 4°C. The RNA pellet was dissolved in 0.3 ml of Solution D and an equal volume of 100% isopropanol added. The samples were incubated for 1 hour at -80°C and centrifuged at 14000 rpm for 30 minutes at 4°C. The RNA pellet was washed twice in 800µl 75% ethanol, air dried and resuspended in 100µl DEPC-treated $H_2O$. All purified RNA samples were DNAseI treated, "cleaned up" and stored at -80°C. The quality of the RNA was checked by determining the ratio of the absorbance at $A_{260}/A_{280}$ and by running 1µg of RNA on a 1% agarose gel that contained 2.2M formaldehyde. The concentration of the RNA was determined by measuring the $A_{260}$. All solutions, except TRIS-containing buffers, used for the RNA work were treated with DEPC to destroy any endogenous RNAses. To each solution, DEPC was added to a final concentration of 0.1% and gently shaken overnight at 37°C. The solutions were then autoclaved for 30 minutes to remove any traces of DEPC. For TRIS-containing buffers, solutions were prepared using DEPC-treated water and an ultra-pure TRIS stock designated for RNA work only.

**21. DNAseI treatment and "cleanup"**

The RNA was DNAse I treated to get rid of contaminating genomic DNA. 1-10µg of total RNA was incubated with DNAseI cocktail (1 X DNAseI buffer (Promega, Madison, WI, USA), 10U/µl DNAseI (Roche Diagnostics GmbH, Mannheim, Germany), 1U/µl RNAsin (Promega, Madison, WI, USA) for 60 minutes at 37°C. The DNAseI-treated RNA was "cleaned up" using the Qiagen MiniElute RNA cleanup kit (Qiagen, Valencia, CA, USA) as per the manufacturer's instructions. This "clean up" step helped remove contaminating genomic DNA, proteins, residual phenol and salts. Briefly, the volume of the total RNA was adjusted to 100µl by adding RNAse-free water. β-mercaptoethanol was added to Buffer RLT before use as per the manufacturer's instructions. 350µl of Buffer RLT was added to the RNA and vortexed. 250µl of 96% ethanol was added and vigorously vortexed to precipitate the RNA out of solution. Each sample was then applied to a single RNeasy mini-column and centrifuged at 10 000 rpm for 15 seconds at room temperature. The flow-through was discarded and the RNeasy mini-column transferred to a new 2ml collection tube. The mini-column was washed with 500µl Buffer RPE and centrifuged at 10 000 rpm for 15 seconds at room temperature. The wash step was repeated and the mini-column centrifuged at 10 000 rpm for 2 minutes. The mini-column transferred to a new 2ml collection tube and centrifuged at 10 000 rpm for 2 minutes at room temperature to dry the membrane. The mini-column transferred to a new 1.5ml elution tube and 30µl of RNAse-free water was added directly on to the membrane and incubated for 5 minutes at room temperature. The mini-column was then centrifuged at 10 000 rpm for 1 minute at room temperature to elute the RNA. The elution step was repeated and both 30µl RNA eluates pooled. The elimination of contaminating genomic DNA was confirmed by RT-PCR using primers that bound to genomic DNA. The quality and quantity of the RNA was checked by spectroscopy and denaturing gel electrophoresis using standard methods (6). The $A_{260}/A_{280}$ ratio was measured and an aliquot was run on a 1% agarose gel containing 2.2M formaldehyde. The RNA was stored at –80°C until used.

**22. cDNA synthesis**

The genomic DNA free RNA was reverse transcribed into cDNA using the ImProm-II™ Reverse Transcription System (Promega, Madison, WI, USA) as per the manufacturer's instructions. 0.5µg of Oligo(dT)15 primer was added to 1-10µg of genomic DNA free RNA in a final volume of 20µl. The sample was denaturing at 70°C for 10 minutes, then cooled on ice for 5 minutes. 20µl of cDNA synthesis cocktail (ImProm-II™ 5X Reaction Buffer, 4mM

$MgCl_2$, 0.5mM each dNTP, 1U/µl RNAsin, 2.0µl ImProm-II™ Reverse Transcriptase) was added and the samples incubated at 25°C for 5 minutes to anneal the primers. cDNA synthesis was extended at 50°C for 60 minutes. The reaction was heat deactivated at 75°C for 5 minutes and cooled on ice. The samples were divided into aliquots and stored at –20°C.

**23. Quantitative RT-PCR**

The cDNA was diluted 1:10 in 0.1mg/ml molecular grade BSA (Roche Diagnostics GmbH, Mannheim, Germany) and 2µl added to 18µl PCR cocktail (1 X Sensimix d(T) (Quantace, Neutral Bay, NSW, Australia) containing 1 X SYBR GreenI, 4.0mM $MgCl_2$, 0.5µM forward primer, 0.5µM reverse primer, 0.1mg/ml molecular grade BSA). PCR products were amplified on the Lightcycler (Roche Diagnostics GmbH, Mannheim, Germany) using the generic programme:1 cycle at 95°C for 10 minutes, 50 cycles of 95°C for 5 seconds, 60°C for 15 seconds, 72°C for 10-60 seconds depending on PCR product size. Extension time was calculated based on the fact that DNA Taq Polymerase can cover 25 base pairs (bp) per second: $Temperature_{extend}$ = (PCR product size in bp)/(25bp/second). Data was acquired at 80°C for 1 second. A melting curve analysis was performed at the end of the amplification program: 95°C for 0 seconds, 75°C for 15 seconds, 65°C for 15 seconds and 95°C for 0 seconds with a ramping time of 0.1°C/seconds. Quantitative data was analyzed using the "Fit Points" and "Standard Curve Method". The β-2-microglubulin gene was used as the housekeeping gene for data normalization. Primer sequences and product sizes are given in Table 1.

**Table 1. Primer Sequences and Product Sizes**

| Name | Forward Sequence | Reverse Sequence | Product size (bp) |
|---|---|---|---|
| MCP-1 | 5'-CAG CTC TCT CTT CCT CCA C-3' | 5'-ATT TAC GGG TCA ACT TCA CA-3' | 390 |
| β-Actin* | 5'-TGG AAT CCT GTG GCA TCC AG AAA C -3' | 5'-TAA AAC GCA GCT CAG TAA CAG TCC G-3' | 348 |
| β2mg | 5'-TGA CCG GCT TGT ATG CTA TC-3' | 5'-CAG TGT GAG CCA GGA TAT AG-3' | 222 |
| IL-18 | 5'-TGG TTC CAT GCT TTC TGG -3' | 5'-TCC GTA TTA CTG CGG TTG T -3' | 279 |
| TNF | 5'-TCT CAT CAG TTC TAT GGC CC-3' | 5'-GGG AGT AGA CAA GGT ACA AC -3' | 212 |
| IFN-γ | 5'-GCT CTG AGA CAA TGA ACG CT-3' | 5'-AAA GAG ATA ATC TGG CTC TGC-3' | 227 |
| IL-6 | 5'-GTT CTC TGG GAA ATC GTG GA -3' | 5'-TGT ACT CCA GGT AGC TAT GG-3' | 208 |
| IL-10 | 5'-AGC CGG GAA GAC AAT AAC TG -3' | 5'-CAT TTC CGA TAA GGC TTG G -3' | 189 |
| IL-12p35 | 5'-GAT GAC ATG GTG AAG ACG GCC -3' | 5'-GGA GGT TTC TGG CGC AGA GT -3' | 402 |
| IL-12p40 | 5'- CTG GCC AGT ACA CCT GCC AC-3' | 5'-GTG CTT CCA ACG CCA GTT C -3' | 384 |
| INOS | 5'-AGC TCC TCC CAG GAC CAC AC -3' | 5'-ACG CTG AGT ACC TCA TTG GC -3' | 481 |
| PKCδ | 5'-CGGGCTACGTTTTATGC -3' | 5'-TCCAACGGGGATAGTG -3' | 367 |
| CLECSF9 | 5'-GGA AGA ATG AAT TCA ACC AAA T-3' | 5'-AAA GGT GTA TCA TCC ACC CA-3' | 486 |
| ISGF3γ | 5'-CAT ATT CAA GGC TTG GGC AC-3' | 5'-GCC ACC ATA GAT GAA GGT GA-3' | 496 |
| C/EBPβ | 5'-CCC ATG GAA GTG GCC AAC T-3' | 5'-GCG AAG AGG TCG GAG AGG AA-3' | 382 |
| G-CSF | 5'-TCCCAAACTGGGTTCT -3' | 5'-CTTTATTATCCGCAAGCT -3' | 278 |
| * binds to genomic DNA and cDNA | | | |

**24. Microarray Design and Overview**

A 2 x 2 factorial experimental design was used to compare the gene expression patterns of treated vs. non-treated BMDMs for WT and CEBPβ$^{-/-}$ mice. A 2 x 2 factorial design means that comparison between 2 factors (treatment vs. untreated) are being also compared with another 2 factors, namely the WT and CEBPβ$^{-/-}$ mice genetic backgrounds. An outline of the design shown in Figure 2. "Treated" refers to BMDMs that were simultaneously stimulated with 100U/ml IFN-γ and infected with *L. monocytogenes* at a MOI of 10:1 (10 bacilli : 1 macrophage) for 4 hours. "Untreated" refers to media controls. Due to budget limitations, biological replicates were done instead of technical repeats and a "balanced dye" approach used instead of dye-swaps to compensate for dye-labelling bias. "Dye balance" means that each condition is measured equally often with the Cy3 dye as with the Cy5 dye. Therefore, the "treated" samples for each biological repeat was labelled with the opposite Cy-dye than in the previous biological repeat. The same principle was applied to "untreated" controls and is outlined in Figure 2. There were 4 biological repeat experiments which were analysed over 8 individual arrays (Fig. 2). Each biological experiment was analyzed using 2 microarrays: the first microarray compared $WT_{treated}$ vs. $WT_{untreated}$ and the second microarray compared $KO_{treated}$ vs. $KO_{untreated}$. None of the samples from the biological repeat experiments were pooled. Each biological infection experiment was done independently of each other. The RNA for each biological replicate was extracted separately at 4 hours post-infection using TriReagent (Molecular Research Company, Cincinnati, USA) and DNAseI treated and cleaned up using the RNeasy Mini Kit (Qiagen, Valencia, CA, USA) as per the manufacturer's instructions. The mRNA was linearly amplified and labelled using the Amino Allyl MessageAmp™ II CyDye aRNA Amplification (Ambion, Austin, Texas, USA) as per the manufacturer's instructions. The labelled cDNA was purified and hybridized to spotted Mouse Exonic Evidence Based Oligonucleotide (Illumina, San Diego, CA, USA) microarrays printed at the capar Microarray Facility (University of Cape Town, South Africa). The microarrays were processed in batches of 2 or 4 over a period of 4 weeks. Table 2 summarizes the information for all samples and hybridization experiments for the four independent biological experiments.

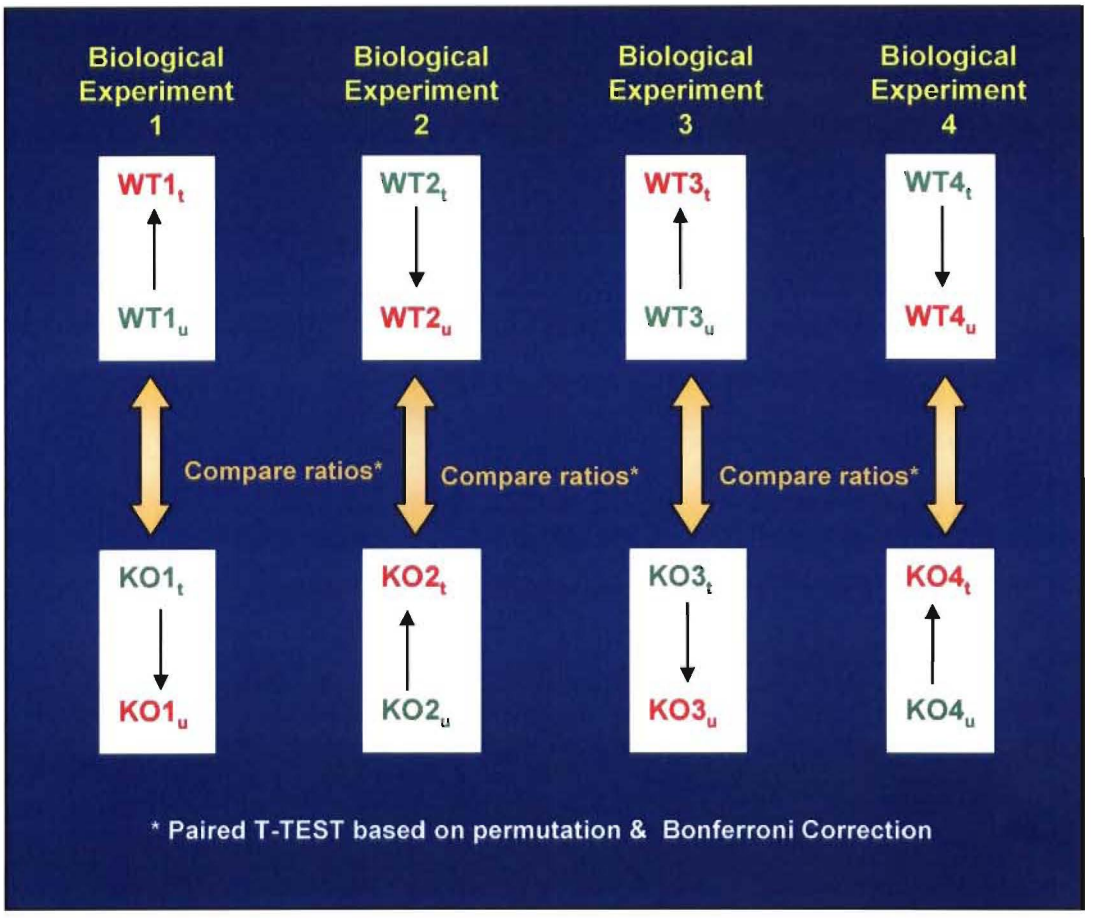


**Figure 2. Microarray Design**: The gene expression patterns of treated vs. untreated BMDMs within each genotype were compared. The "treated" and "untreated" samples are denoted by a subscripted "t" and "u" respectively. Each white rectangle represents a two channel microarray. The back of the black arrow represents sample labelled with Cy3 (green) and the front of the arrow represents labelling with Cy5 (red). "Treated" refers to BMDMs that were simultaneously stimulated with 100U/ml IFN-γ and infected with *L. monocytogenes* at a MOI of 10:1 at 4 hours post-infection. "Untreated" refers to media controls. For each biological experiment there were 2 microarray slides, one for the C/EBPβ$^{+/+}$ (WT) samples and the second for the C/EBPβ$^{-/-}$ (KO) samples. There were 4 independent biological repeat experiments which were analysed over 8 individual arrays. Differentially expressed genes between the WT and C/EBPβ$^{-/-}$ were identified by a paired T-Test based on permutation and Bonferroni Correction.

**Table 2. RNA samples, treatments, labelling, and microarrays.** Four independent biological infection experiments were analysed over 8 individual arrays. In the treatment column "+" refers to BMDMs simultaneously stimulated with IFN-γ and infected with *L. monocytogenes* at a MOI of 10:1 (10 bacilli : 1 macrophage)and "-" refers to untreated media controls. RNA was purified at 4 hours post-infection and the mRNA linearly amplified and labelled with either Cy5 (red) or Cy3 (green) fluorescent dyes. The labelled samples were hybridised to spotted MEEBO oligonucleotide arrays which were printed at the "capar" Microarray Facility at the University of Cape Town, South Africa. Microarray slides were identified by their unique barcode numbers.

| Biological experiment | Sample label | Treatment | Cy-dye label | Hybridization to Slide (Barcode #) |
|---|---|---|---|---|
| 1 | $KO1_{treated}$ | + | Cy3 | 12301884 |
| 1 | $KO1_{untreated}$ | - | Cy5 | 12301884 |
| 1 | $WT1_{treated}$ | + | Cy5 | 12301864 |
| 1 | $WT1_{untreated}$ | - | Cy3 | 12301864 |
| 2 | $KO2_{treated}$ | + | Cy5 | 12301883 |
| 2 | $KO2_{untreated}$ | - | Cy3 | 12301883 |
| 2 | $WT2_{treated}$ | + | Cy3 | 12301862 |
| 2 | $WT2_{untreated}$ | - | Cy5 | 12301862 |
| 3 | $KO3_{treated}$ | + | Cy3 | 12301878 |
| 3 | $KO3_{untreated}$ | - | Cy5 | 12301878 |
| 3 | $WT3_{treated}$ | + | Cy5 | 12301881 |
| 3 | $WT3_{untreated}$ | - | Cy3 | 12301881 |
| 4 | $KO4_{treated}$ | + | Cy5 | 12301882 |
| 4 | $KO4_{untreated}$ | - | Cy3 | 12301882 |
| 4 | $WT4_{treated}$ | + | Cy3 | 12301856 |
| 4 | $WT4_{untreated}$ | - | Cy5 | 12301856 |

**25. Microarray Total RNA Isolation**

BMDMs were generated from C/EBPβ-deficient (C/EBPβ$^{-/-}$) and wild-type (WT) mice as described in section 6. The BMDMs were IFN-γ-activated and infected with *L. monocytogenes* at a MOI 10:1 as described in section 8. At 4 hours post-infection, RNA was extracted and using TriReagent (Molecular Research Company, Cincinnati, USA) and DNAseI treated and cleaned up using the RNeasy Mini Kit (Qiagen, Valencia, CA, USA) as described in sections 20 and 21.

**26. Generation And Labelling Of cDNA**

The mRNA was linearly amplified and labelled using the Amino Allyl MessageAmp™ II CyDye aRNA Amplification (Ambion, Austin, Texas, USA) as per the manufacturer's instructions. Since the MessageAmp II procedure was very sensitive to temperature, all thermocyclers and incubators were preheated to ensure that the correct temperature had been reached and stabilized. Tube holders were also pre-warmed in the incubator before placing the reaction tubes in them. For all enzymatic reactions, a hybridization oven was used to avoid the formation of condensation in the reaction tubes. Condensation would change the composition of reaction mixtures and therefore greatly reduce yield.

**27. Reverse Transcription to Synthesize First Strand cDNA**

In a 0.5µl tube, 1µl T7 Oligo(dT) Primer was added to 1µg of total RNA and the volume adjusted to 12µl with RNAse-free water. The reactions were incubated at 70°C for minutes in a thermocycler and snap-cooled on ice for 5 minutes. The reactions were centrifuged at 13000 rpm for 30 seconds to bring down the contents of the tube and placed on ice. The reverse transcription master mix (1 X First Strand Buffer, dNTP mix, RNAse Inhibitor and ArrayScript reverse Transcriptase) was made at room temperature as per the manufacturer's instructions. The master mix was gently mixed by pipetting and 8µl added to each sample and incubated at 42°C in a hybridization oven. The samples were then briefly centrifuged at 13000 rpm for 30 seconds to bring down the contents of the tube and placed on ice until ready to proceed with second strand synthesis.

**28. Second Strand cDNA Synthesis**

The second strand master mix (1 X Second Strand Buffer, dNTP mix, DNA Polymerase, RNAse H) was assembled on ice as per the manufacturer's instructions and mixed by gentle pipetting. 80µl of second strand master mix was added to each sample. The sample and master mix was mixed by gentle pipetting up and down 2 to 3 times, then flicking 2 to 3 times. The samples were centrifuged at 13000 rpm for 30 seconds to bring down the contents of the tube. The samples were incubated at 16°C in a pre-cooled thermocycler for 2 hours. The cDNA samples were immediately purified using the spin columns provided in the kit.

**29. cDNA Purification**

250µl of cDNA Binding Buffer was added to each sample and mixed thoroughly by pipetting up and down 2 to 3 times and flicking 3 to 4 times. The samples were centrifuged at 13000 rpm for 30 seconds to bring down the contents of the tube. The cDNA sample\cDNA Binding Buffer mixture was added onto the center of the cDNA filter cartridge and centrifuged for 1 minute at 10000 rpm at room temperature. The flow-through was discarded and the cDNA filter cartridge placed in a new wash tube. 500µl of wash buffer was added to each cDNA filter cartridge and centrifuged for 1 minute at 10000 rpm at room temperature. The flow-through was discarded and the cDNA filter cartridge centrifuged for an extra 1 minute to remove trace amounts of wash buffer. The cDNA filter cartridge was placed in a new cDNA elution tube and 10µl of pre-warmed (50–55°C) nuclease-free water was added directly onto the membrane and incubated at room temperature for 5 minutes. The cDNA filter cartridge was centrifuged for 1.5 minutes at 10000 rpm at room temperature. The elution step was repeated and the cDNA eluates pooled (~16 µl). The cDNA was used immediately for mRNA amplification by *in vitro* transcription.

**30. *In Vitro* Transcription to Synthesize aRNA (single round amplification)**

The *in vitro* transcription (IVT) master mix (aaUTP, ATP, CTP, GTP, UTP, 1 X T4 Reaction Buffer, T7 Enzyme Mix) was made up at room temperature as per the manufacturer's instructions. The ratio of aaUTP:UTP used was 1:1. The IVT master mix was gently vortexed and centrifuged at 13000 rpm for 30 seconds to bring down the contents of the tube. 26µl of the IVT master mix was added to each reaction and thoroughly mixed by pipetting up and down 2 to 3 times, then flicking the tube 3 to 4 times. The samples were centrifuged at 13000 rpm for 30 seconds to bring down the contents of the tube. The samples were incubated 37°C in a

hybridization oven for 14 hours. 60µl nuclease-free water was added to each aRNA sample (final volume equaled 100 µl) to stop the IVT reaction. The aRNA samples were immediately purified using the spin columns provided in the kit.

**31. aRNA Purification**

350µl of aRNA Binding Buffer was added to each sample and mix thoroughly by pipetting up and down 2 to 3 times and flicking 3 to 4 times. 250 µl of analytical grade 96% ethanol was added to each aRNA sample and pipetted up and down 3 times. The sample was then immediately added onto the center of the aRNA filter cartridge and centrifuged for 1 minute at 10000 rpm at room temperature. The flow-through was discarded and the aRNA filter cartridge placed in a new 2.0ml collection tube. 650µl of Wash Buffer was added to each aRNA filter cartridge and centrifuged for 1 minute at 10000 rpm at room temperature. The flow-through was discarded and the aRNA filter cartridge centrifuged for an extra 1 minute to remove trace amounts of wash buffer. The aRNA filter cartridge was placed in a new aRNA elution tube. 100µl of pre-warmed (55°C) nuclease-free water was added directly onto the membrane and incubated at room temperature for 5 minutes. The aRNA filter cartridge was centrifuged for 1.5 minutes at 10000 rpm at room temperature. The elution step was repeated and the aRNA eluates pooled (200µl). The purified aRNA was quantitated by spectrophotometric analysis at $A_{260}$, $A_{280}$ and $A_{230}$ using a NanoDrop® ND-1000A UV-Vis Spectrophotometer (NanoDrop Technologies, Wilmington, DE, USA). The size distribution of aRNA was analyzed by denaturing agarose gel analysis. The remaining purified aRNA was vacuum dried until completion using a SpeedVac (Savant Instruments Inc, Holbrook, NY, USA) set at medium for 10 minutes. The dried aRNA was resuspended in 9µl Coupling Buffer and used immediately for dye coupling.

**32. aRNA:Dye Coupling Reaction**

For this procedure, all reactions were carried out in the dark because the Cy3 and Cy5 dyes were light sensitive. All reagents and reaction tubes were wrapped in foil. The Cy3 or Cy5 dye was resuspended in 11µl ultra-pure DMSO and gently vortexed. The 11µl of resuspended dye was added to the aRNA that was resuspended in Coupling Buffer and gently vortexed. The dye coupling reaction was incubated at room temperature for 30 minutes in a dark closed drawer. To quench the coupling reaction, 4.5µl of 4M hydroxylamine was added to each reaction and gently vortexed. The quenching reaction was incubated in the dark at room temperature for 15 minutes.

During this reaction, the large molar excess of hydroxylamine quenched the amine-reactive groups on un-reacted dye molecules. The volume of the reactions was brought up to 30µl by adding 5.5µl RNAse-free water to each sample. The dye-coupled aRNA was immediately purified using the aRNA filter cartridge supplied in the kit.

**33. Dye Labelled aRNA Purification**

105µl of aRNA Binding Buffer was added to each sample and mix thoroughly by pipetting up and down 2 to 3 times and flicking 3 to 4 times. 75µl of analytical grade 96% ethanol was added to each labeled aRNA sample and pipetted up and down 3 times. The sample was then immediately added onto the center of the labeled aRNA filter cartridge and centrifuged for 1 minute at 10000 rpm at room temperature. The flow-through was discarded and the labeled aRNA filter cartridge placed in a new 2ml collection tube. 500µl of Wash Buffer was added to each labeled aRNA filter cartridge and centrifuged for 1 minute at 10000 rpm at room temperature. The flow-through was discarded and the labeled aRNA filter cartridge centrifuged for an extra 1 minute to remove trace amounts of Wash Buffer. The labeled aRNA filter cartridge was placed in a new labeled aRNA elution tube. 10µl of pre-warmed (55°C) nuclease-free water was added directly onto the membrane and incubated at room temperature for 5 minutes. The labeled aRNA filter cartridge was centrifuged for 1.5 minutes at 10000 rpm at room temperature. The elution step was repeated and the aRNA eluates pooled (~20µl). The quantity of the labeled aRNA and the number of dye molecules incorporated was measured by spectrophotometric using the NanoDrop® ND-1000A UV-Vis Spectrophotometer (NanoDrop Technologies, Wilmington, DE, USA) For labeled aRNA quantitation the absorbance at 260nm, 280nm and 230nm were measured. The success of the aRNA labeling was determined successful if the frequency of dye incorporation (FOI) into the aRNA was between 30-60 dye molecules per 1000bp of aRNA. The frequency of dye incorporation (FOI) was determined by measuring the absorbances at 550nm (Cy3) and 650nm (Cy5) and the FOI calculated using the equation below. 4µg of each pure labeled aRNA was mixed together and RNAse-free water added to 30µl. The aRNA probe mixture was placed on ice until ready for hybridization.

$$\textbf{Frequency of incorporation} = \frac{\textbf{\# dye molecules}}{\textbf{1000 base pairs}} = \frac{A_{dye}}{A_{260}} \times \frac{9010 cm^{-1} M^{-1}}{\textbf{Dye Extinction Coefficient}} \times 1000$$

**Where:**

| Dye | Absorbance Maximum | Extinction Coefficient* |
|---|---|---|
| Cy3 | 550nm | 150000 |
| Cy5 | 650nm | 250000 |

* Extinction Coefficient at $\lambda_{max}$ in $cm^{-1}M^{-1}$

**34. Hybridization Coverslip preparation**

Coverslips (Erie Scientific Company, Portsmouth, NH, USA) were washed in 100% acetone for 1 hour, in 0.2 % SDS for 10 minutes, then twice in double distilled water for 10 minutes for each wash. All wash steps were done at room temperature with gentle agitation. The coverslips were dried in an oven at 42°C for 10 minutes.

**35. Prehybridization**

The Mouse Exonic Evidence Based Oligonucleotide(MEEBO) (Illumina, San Diego, CA, USA) spotted microarrays were printed at the capar Microarray Facility (University of Cape Town, South Africa). The pre-hybridization buffer (5X SSC, 0.1% SDS, 1% BSA) and 2 X hybridisation buffer (50% formamide, 10 X SSC, 0.2% SDS) were made fresh and preheated to 42°C for 30 minutes just before use. Only 2 or 4 microarray slides were processed in one batch. Each MEEBO microarray slide was placed in a hybridisation chamber (ArrayIt, Sunnyvale, CA ,USA) with the gene spots facing up. The cleaned coverslip was placed over the slide and 200µl of the pre-hybridization solution gently pipetted under the coverslip. The chamber was sealed and submerged in a plastic container containing water preheated to 42°C. The plastic container was placed in a hybridisation preheated to 42°C and the slides were pre-hybridized for 30 minutes. The slides were washed 5 times in double distilled water. Each wash was done at room temperature for 30-60 seconds. The slides were then dipped in 100% isopropanol and dried by centrifugation in swinging bucket rotor for 5 minutes at 1000 rpm at room temperature. The dried slides were placed in a hybridization chamber and the cleaned hybridization coverslip carefully placed over the array. The microarray slides were used immediately for hybridization.

**36. Hybridization**

The 2 X hybridisation buffer (50% formamide, 10 X SSC, 0.2% SDS) was made fresh and preheated to 42°C for 30 minutes just before use. 28µl of the heated 2 X hybridization buffer was mixed with the 30µl aRNA probe mixture. The probe was then heat denatured at 90°C for 3 minutes and then cooled to 42°C. The denatured probe was added very carefully to the pre-hybridized microarray slide at the bottom end of coverslip. Any air bubbles were worked toward the edge by gently tapping the coverslip surface. The hybridization chamber was sealed wrapped in foil to keep out light. The chamber was then submerged in a plastic container containing water tub preheated to 42°C. The hybridization reactions were incubated at 42°C in a hybridization oven for 16-20 hours. The plastic container was also wrapped with foil to retain humidity and block out light.

**37. Post-hybridization Washing**

The low stringency wash buffer (2 X SSC, 0.1% SDS), medium-stringency wash buffer (1.0X SSC) and high-stringency wash buffer (0.02X SSC) were made fresh. All staining dishes were covered with foil to make them light tight and the laboratory lights were turned off, in order to minimize the exposure of the microarray slides to light. The hybridization chamber was unsealed, the microarray slide gently removed from the chamber. The microarray slide was submerged into a dish containing low stringency wash buffer (2 X SSC, 0.1% SDS) and gently agitated at to remove the coverslip. The microarray slide was washed in the low stringency wash buffer for 4 minutes at room temperature with gentle agitation. The microarray slide was then washed twice in medium stringency wash buffer (1.0X SSC) at room temperature for 4 minutes. The microarray was washed in high-stringency wash buffer (0.02X SSC) slide for each wash. The slides were then dipped 5 times in 100% isopropanol and dried by centrifugation in swinging bucket rotor for 5 minutes at 1000 rpm at room temperature. The slides were kept in a light-tight container and scanned immediately.

**38. Scanning and Image Analysis**

The microarray slides were scanned using an Axon GenePix 4000A (Axon Instruments/Molecular Devices Corporation, Sunnyvale, CA, U.S.A) scanner and GenePix Pro 5.1.0.19 software running on a Windows XP operating system. The scan power was set to 100100, the resolution to 10um and the pixel size to 10. The internal scanner temperature

averaged between 37°C to 38°C. The number of lines averaged during the scanning process was set to 2. The microarray slides were scanned at 635nm and 532nm wavelengths and the gene/spot ratios were set for 635nm/532nm. No normalization or background subtraction was done at this stage. Each microarray slide was initially scanned in the "Preview Mode" to optimise the photo-multiplier (PMT) settings so that the overall fluorescence in the red and green channels were balanced. The channels were considered balanced when the ratio of overall fluorescence in the green and read channels were equal to 1. The microarray slide was then scanned at the optimized PMT settings and the image saved as atiff file. Each slide was scanned a maximum of 3 times to avoid damaging the dye molecules resulting in subsequent loss of quantitative florescence data. The array list and grid was loaded over the tiff images using the GenePix 5.1.0.19 software. Individual spots were aligned using the single irregular and /or regular feature tool. Each spot was individually checked for quality and to see if it was aligned to the grid. Spots were flagged as bad if they were (1) printed on top of each other, (2) dilated, (3) looked like doughnuts, (4) were irregular in morphology, (5) had a comet tail or (6) contained particles or scratches. Once the grids were aligned, the settings were saved and the quantitative gene expression data exported as a "GenePix Results" (.gpr) file.

**39. Microarray Image and Data Analysis**

All image and data analysis was conducted in the R environment for statistical computing and programming using the following packages (7), BioConductor (8), Limma (9-11) and Smida (12). R version 2.2.0. was downloaded from http://cbio.uct.ac.za/CRAN/ and BioConductor, LIMMA and SMIDA from http://www.bioconductor.org/. R was run on a Windows XP operating system. The gpr files, Targets file, SpotTypes file and R-script were placed in the same working directory. The Targets file was used by R to identify the gpr files and which samples (reference or treated) were labelled with Cy3 or Cy5. The SpotTypes file identified which genes on the array were experimental and which were controls. The gpr. files were read by the Limma programme and genes that were flagged as "bad" during the gridding process were given a weighting 0.1. This meant that the "bad" spots would not be excluded from further analyses, but only 10% of their values would be used. The layout of the array was composed of 4 x 8 grids, where each grid was composed of 35 rows x 35 columns. This layout was entered into the Limma programme which was then used for subsequent image plots. The background for each array was corrected using a "probabilistic" method rather than subtraction (12). The variation in background, foreground and log-ratios (treated vs. untreated; also called M-values) for each array was assessed using image plots. The balance of the densities of the red and green channels was evaluated by density plots. Systematic bias and print-tip artifacts were identified by whole array and print-group Ratio-Intensity plots (also called MA-plots) before normalization. Evaluation of these plots helped decide which normalization method would be best to use. The data within each array was normalized using print-group LOWESS. The effectiveness of normalization in removing the systematic and printing biases was assessed by image plots of the spatially normalized M values and MA plots and box plots for each array and its print-tip groups. The data between arrays were normalized using the slide-scale normalization method and the effectiveness of the normalization was assessed by density plots and box plots. The duplicate spots in the normalized data were merged and averaged, taking into account gene weights for bad spots. The M and A values of the normalized and averaged data was saved and read into the TM4 Multi-experiment Viewer (MeV) Software Package (13). Differentially expressed (DE) genes were identified by a paired T-Test where *p*-values were calculated based on 100 permutations per gene. Significance was determined by Standard Bonferroni Correction (14, 15). The T-Test used Welch approximation since unequal variances between samples was assumed. The alpha value (the overall threshold *p*-value) was set to 0.01 and the false discovery control rate was to set to "fast but conservative". The differentially

expressed genes were hierarchically clustered using using Euclidian distance and average link clustering.

**40. Reproducibility of Microarray Experiments**

Reproducibility between arrays was assessed by linear regression analysis. The M-values of one array was plotted against its biological replicate value in another array. The more reproducible the data was between the arrays, the closer the $R^2$ value was to 1. Biological replicates were considered reproducible if the $R^2 \geq 0.3$, since Churchill et al found that reproducibility between biological replicates can be as low as $R^2 = 0.3$ (16). Reproducibility within each array was assessed by calculating the standard deviation for each replicate gene on the array. Those replicate genes with a standard deviation greater than 0.2 were questionable and unreliable. The standard deviation value of >0.2 was chosen since this was the cut-off value used by many researcher to define questionable data (17). However, a standard deviation cut-off of 0.2 was too stringent for the data from this study (discussed in chapter 4), therefore the less conservative value of 0.3, was used in this study to trim unreliable data from the microarray data set. Statistical analyses were performed in Microsoft Excel.

**41. Functional Clustering and Promoter Analysis**

The DE genes were functionally clustered according to their functional annotations using the FatiGOplus program (18). The Unigene gene symbols for the DE genes were submitted into FatiGOPlus web page found at http://babelomics.bioinfo.cipf.es/fatigoplus/cgi-bin/fatigoplus.cgi. Annotations for SwissProt keywords, InterPro motifs, KEGG signalling pathways and Gene Ontology (GO) levels 1 to 9 for Biological Processes, Molecular Functions and Cellular Component, were included in the analysis. The results were saved and the annotation data parsed into Microsoft Excel.

**42. Promoter Analysis**

The P-MATCH (19) program was used to identify putative transcription factor binding sites in the promoters of DE genes. The first 1000bp of the promoter sequences were downloaded from the University of California Santa Cruz RefSeq Gene Table Browser found at http://www.genome.ucsc.edu/cgi-bin/hgTables?command=start. The RefSeq gene accession numbers for each DE gene was pasted as a list and submitted into the Gene Table Browser and the following options selected: "genomic DNA", "promoter region only", "1000bp upstream of transcriptional start site". The promoter sequences were saved as text files and parsed into the P-MACTH programme that searches for potential binding sites for transcription factors in any given sequence. A customized set of transcription factor matrices were selected to analyze the promoter sequences of the DE genes. The immune cell-specific profile provided by P-MATCH contains the matrices for transcription factors that are known to be active during immune responses in T-, B-, mast, myeloid, natural killer cells and macrophages. This profile was further customized by adding matrices for transcription factors that interact with C/EBPβ (Table 3). Only high quality matrices were used for the analysis and the "minimize false positives" option was selected. High quality matrices are defined as those matrices that give the lowest frequency of false positive matches.

**Table 3. Transcription Factors Included in the Promoter Analysis**

| | | | | |
|---|---|---|---|---|
| AML1 | HMG I | NF-κB1 | RARα2 | TCF-1(P) |
| AML1a | HMG I(Y) | NF-κB2 | RARβ | TCF-1A |
| AML1b | HMG Y | oct-B2 | RARβ1 | TCF-1B |
| AML1c | Ik-1 | p300 | RARβ2 | TCF-1C |
| AP-1 | Ik-2 | PEBP2 | RARβ3 | TCF-2 |
| ATF-4 | Ik-3 | PEBP2α | RARγ | TCF-3 |
| C/EBPα | Ik-4 | PEBP2αA1 | RARγ1 | TCFβ1 |
| C/EBPβ | Ik-5 | PEBP2αA2 | RARγ2 | VDR |
| C/EBPδ | IRF-1 | PEBP2αB1 | Rc | |
| C/EBPε | IRF-2 | PEBP2αB2 | RXRα | |
| C/EBPγ | JunB | PEBP2β | RXRβ | |
| c-Ets-1 | JunD | PEBP2β1 | RXRβ1 | |
| c-Ets-2 | LEF-1 | PEBP2β2 | RXRβ2 | |
| c-Fos | LyF-1 | POU2F1 | RXRγ | |
| CHOP-10 | Lyl-1 | POU2F1α | Sox4 | |
| c-Jun | MAF | POU2F2 (Oct-2.1) | Sp1 | |
| c-Maf | MAZR | POU2F2 (Oct-2.3) | SRF | |
| EGR1 | MZF-1 | POU2F2 (Oct-2.4) | STAT1 | |
| EGR2 | NF-AT | POU2F2 (Oct-2.6) | STAT1α | |
| EGR3 | NFAT-1 | POU2F2C | STAT1β | |
| Elf-1 | NF-AT3 | POU3F1 | STAT2 | |
| Elk-1 | NF-ATc | POU4F1(I) | STAT3 | |
| FosB | NF-ATp | pRb | STAT4 | |
| FOXO4 | NF-ATx | PU.1 | STAT6 | |
| GATA-3 | NF-EM5 | RAR | Tal-1 | |
| GATA-4 | NF-JUN | RARα | TBP | |
| HEB | NF-κB | RARα1 | TCF-1 | |

### 43. Literature Profiling

The literature profiling strategy used to select candidate genes for further study is outlined in Figure 3. The Milano Literature mining tool (20) was used to search the PubMed (21) database to see if any of the differentially expressed genes has been shown to play a role in infectious diseases caused by intracellular pathogens such as *Listeria monocytogenes*, *Mycobacterium tuberculosis*, *Brucella abortus*, *Salmonella typhimurium* and *Leishmania major*. In addition, searches were done to determine if the differentially expressed genes played a role in innate immunity, bactericidal functions, phagocytosis, endocytosis, phagosome maturation and phago-lysosome fusion. Furthermore, any links to immune signalling pathways regulated by cytokines, Rab GTPases, C/EBPβ and NF-κB were investigated. Nested keyword searches using gene aliases coupled to the search terms were done. Manual literature searches were done for a smaller set of candidate genes using PubMed (21), AceView (22), OMIM (23) and Entrez Gene (24) databases. The ISMR (25, 26), BayGenomics (26), DeltaOne (27) and Entrez Gene (24) databases were searched to find transgenic and gene deficient mouse models for candidate genes. The Milano Literature mining tool can be accessed at http://milano.md.huji.ac.il.

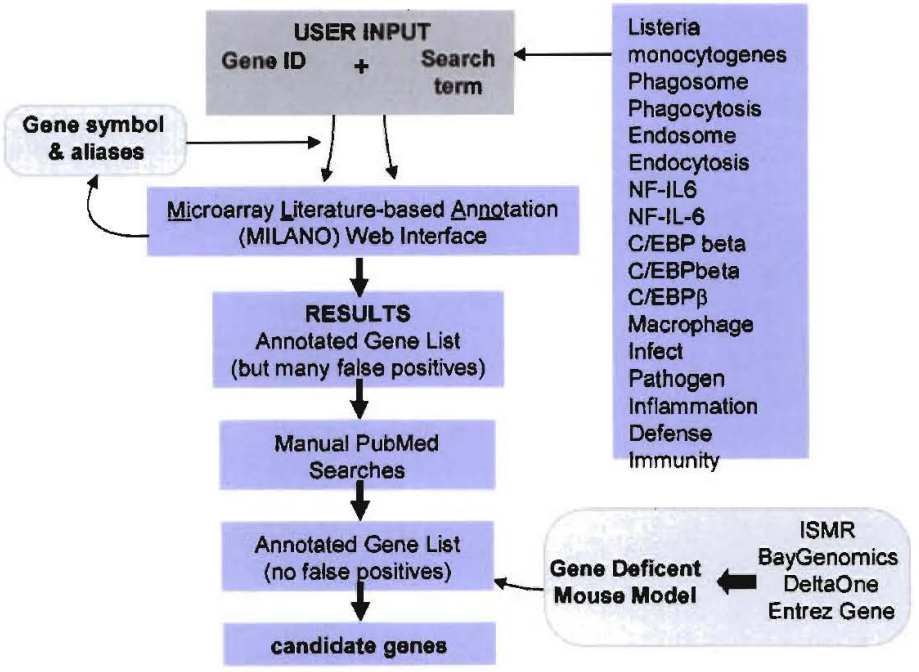


**Figure 3. Literature Mining Strategy to identify candidate genes for further investigation.**

**44. Systems Biology Protein-Protein Interaction Network**

Protein-protein interaction data for genes of interest were downloaded from Entrez Gene, Human Protein Reference Database (HPRD) and Biomolecular Interaction Network Database (BIND). The network was created by downloading the interaction data for all the first, second and third "neighbours" of Rab5a, PKCδ and G-CSF. The term "first neighbours" refers to proteins that interact directly with the protein of interest, while "second neighbours" are those proteins that interact with the "first neighbour" proteins and "third neighbours" are proteins that interact with the "second neighbour" proteins: e.g. in Figure 4 A the first neighbours of protein A are coloured in blue and the second neighbours in pink. It possible that two different proteins have the same first and/or second neighbour (Fig. 4 B) thereby creating a small network. The protein-protein interaction data was saved in simple interaction file (sif) format, visualized and analyzed using the Cytoscape 2.2 software programme (28).

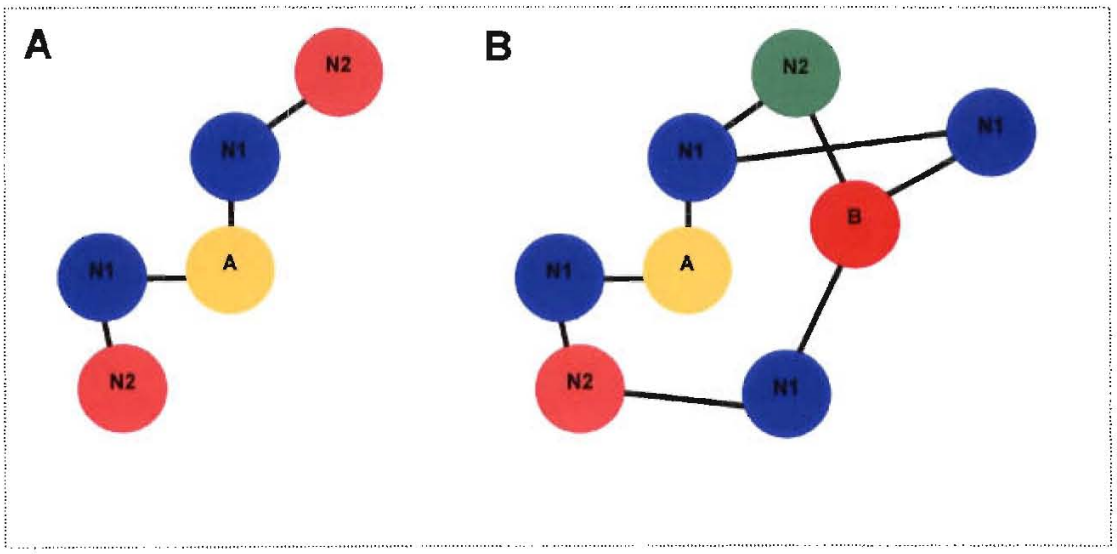


**Figure 4. Creation of Protein-Protein Interaction Networks.** Proteins are depicted as coloured circles and protein-protein interactions as black lines. (A) The first neighbours (N1, blue circles) of protein A interact directly with protein A. The second neighbours of protein A (N2, pink circles) interact with the first neighbours of protein A, hence they are two interactions away from protein A. (B) The first neighbour of protein B is also the second neighbour of protein A (green, circle), and protein B is the third neighbour of protein A. Similarly protein-protein interactions occur between the first, second and third neighbours of protein A and protein B, thus creating an interaction network.

**45. MIAME Compliance and Public Database submission**

In accordance with Minimum Information about Microarray Experiments (MIAME) compliance (29), the microarray design, methodology and data has been deposited in the MIAME compliant Gene Expression Omnibus database. The data can be accessed at the website below using the accession number GSE6256: http://www.ncbi.nlm.nih.gov/geo/

**46. Statistical analysis.**

All *in vitro* and *in vivo* data, was statistically analyzed using Student's T-tests (two-tailed with unequal variance) and values of $p<0.05$ were considered significant. Survival data was analyzed by Kaplan-Meier using the log-rank test to compare survival data. Each experiment was repeated at least once to ensure reproducibility. Differentially expressed (DE) genes were identified by a paired T-Test using Welch approximation where *p*-values were calculated based on 100 permutations per gene. Significance was determined by Standard Bonferroni Correction (14, 15). The alpha value (the overall threshold *p*-value) was set to 0.01 and the false discovery control rate was to set to "fast but conservative".

**REAGENTS AND SUPPLIERS:**

| Reagent or Kit | Supplier |
|---|---|
| 3,3',5,5'-tetramethylbenzidine (TMB) | Roche Diagnostics GmbH, Mannheim, Germany |
| 7-Amino Actinomycin D (AAD) | Sigma-Aldrich, Munich, Germany |
| Acetone | Sigma-Aldrich, Munich, Germany |
| Amino Allyl MessageAmp™ II CyDye aRNA Amplification Kit | Ambion, Austin, Texas, USA |
| ammonium chloride | BDH Chemicals Ltd., Poole, England |
| anti-CD11b (clone M1/70) | BD Pharmigen, BD Biosciences, San Jose, CA, USA |
| anti-F4/80 | Caltag Laboratories, Burlingame, CA, USA |
| anti-Gr-1 (clone RB6-8G5) | BD Pharmigen, BD Biosciences, San Jose, CA, USA |
| anti-I-Ab (clone KH74) | BD Pharmigen, BD Biosciences, San Jose, CA, USA |
| anti-rabbit IgG-FITC | Sigma-Aldrich, Munich, Germany |
| b-Mercaptoethanol | Sigma-Aldrich, Munich, Germany |
| Bovine Serum Albumin (fraction V) | Roche Diagnostics GmbH, Mannheim, Germany |
| Bovine Serum Albumin(BSA) (molecular grade at 20mg/ml) | Roche Diagnostics GmbH, Mannheim, Germany |
| calcium chloride | BDH Chemicals Ltd., Poole, England |
| Chloroform | BDH Chemicals Ltd., Poole, England |
| circular glass coverslips (12-mm) | Merck Laboratory Supplies, South Africa |
| Concanavalin A (ConA) | Sigma-Aldrich, Munich, Germany |
| diethanolamine | Merck Laboratory Supplies, South Africa |
| Diethylpyrocarbonate (DEPC) | Sigma-Aldrich, Munich, Germany |
| dimethylsulphoxide (DMSO) | Sigma-Aldrich, Munich, Germany |
| DNAse1 (10U/µl) | Roche Diagnostics GmbH, Mannheim, Germany |
| dNTPs (100µM) | Promega, Madison, WI, USA |
| Dulbecco's Modified Eagle's Medium (DMEM) for Cell Culture | Gibco, Invitrogen Corporation, Carlsbad, CA, USA |
| EDTA | BDH Chemicals Ltd., Poole, England |

| Reagent or Kit | Supplier |
|---|---|
| eosin stain | Sigma-Aldrich, Munich, Germany |
| Ethanol (absolute) | BDH Chemicals Ltd., Poole, England |
| Fat free milk powder (Spar House Brand) | Spar Grocery Store Franchise, South Africa |
| ferric cyanide | Sigma-Aldrich, Munich, Germany |
| Fetal Calf Serum (FCS | Delta Bioproducts, Johannesburg, Gauteng Province, South Africa |
| Fetal Calf Serum (FCS | Gibco, Invitrogen Corporation, Carlsbad, CA, USA |
| formaldehyde | BDH Chemicals Ltd., Poole, England |
| Formamide | Sigma-Aldrich, Munich, Germany |
| Formamide, redistilled (microarray) | Life Technologies, Gaithersburg, MI, USA |
| gluteraldehyde (electron microscopy grade) | Sigma-Aldrich, Munich, Germany |
| glycerol | BDH Chemicals Ltd., Poole, England |
| guanidinium thiocyanate | BDH Chemicals Ltd., Poole, England |
| hematoxylin stain | Sigma-Aldrich, Munich, Germany |
| horse serum | Gibco, Invitrogen Corporation, Carlsbad, CA, USA |
| hybridisation chamber | Arraylt, Sunnyvale, CA ,USA |
| Hybridization Coverslips | Erie Scientific Company, Portsmouth, NH, USA |
| Hybridization Coverslips (Hybrislip) | Sigma-Aldrich, Munich, Germany |
| hydrogen peroxide | Merck Laboratory Supplies, South Africa |
| IFN-γ (recombinant protein for stimulation) | BD Pharmigen, BD Biosciences, San Jose, CA, USA |
| IFN-γ Biotinylated antibody | BD Pharmigen, BD Biosciences, San Jose, CA, USA |
| IFN-γ Coating antibody | BD Pharmigen, BD Biosciences, San Jose, CA, USA |
| IFN-γ Recombinant Protein Standard | BD Pharmigen, BD Biosciences, San Jose, CA, USA |
| IL-12p35 Biotinylated antibody | BD Pharmigen, BD Biosciences, San Jose, CA, USA |
| IL-12p35 Coating antibody | BD Pharmigen, BD Biosciences, San Jose, CA, USA |
| IL-12p35 Recombinant Protein Standard | BD Pharmigen, BD Biosciences, San Jose, CA, USA |
| IL12p40 Biotinylated antibody | BD Pharmigen, BD Biosciences, San Jose, CA, USA |
| IL12p40 Coating antibody | BD Pharmigen, BD Biosciences, San Jose, CA, USA |
| IL12p40 Recombinant Protein Standard | BD Pharmigen, BD Biosciences, San Jose, CA, USA |
| IL-18 Biotinylated antibody | BD Pharmigen, BD Biosciences, San Jose, CA, USA |
| IL-18 Coating antibody | BD Pharmigen, BD Biosciences, San Jose, CA, USA |
| IL-18 Recombinant Protein Standard | BD Pharmigen, BD Biosciences, San Jose, CA, USA |
| IL-6 Biotinylated antibody | BD Pharmigen, BD Biosciences, San Jose, CA, USA |
| IL-6 Coating antibody | BD Pharmigen, BD Biosciences, San Jose, CA, USA |
| IL-6 Recombinant Protein Standard | BD Pharmigen, BD Biosciences, San Jose, CA, USA |

| Reagent or Kit | Supplier |
|---|---|
| ImProm-II™ Reverse Transcription System | Promega, Madison, WI, USA |
| Iscoves's Modified Dulbecco's Modified Eagle's Medium (IMDMM) for Cell Culture | Gibco, Invitrogen Corporation, Carlsbad, CA, USA |
| isoamyl alcohol | Sigma-Aldrich, Munich, Germany |
| isopropanol | BDH Chemicals Ltd., Poole, England |
| Isopropanol (microarray) | Fisher Scientific |
| L-glutamine | Gibco, Invitrogen Corporation, Carlsbad, CA, USA |
| Lipopolysaccharide (LPS) | Sigma-Aldrich, Munich, Germany |
| low melting point agarose | Promega, Madison, WI, USA |
| magnesium chloride | BDH Chemicals Ltd., Poole, England |
| magnesium chloride | BDH Chemicals Ltd., Poole, England |
| MCP-1 Biotinylated antibody | BD Pharmigen, BD Biosciences, San Jose, CA, USA |
| MCP-1 Coating antibody | BD Pharmigen, BD Biosciences, San Jose, CA, USA |
| MCP-1 Recombinant Protein Standard | BD Pharmigen, BD Biosciences, San Jose, CA, USA |
| MEEBO Oligonucleotide Array Spotted Arrays | capar Microarray Facility, University of Cape Town, South Africa |
| Microarray Slide (GAPSII Coated Slides) | Corning Costar Corporation, Cambridge, MA, USA |
| Middlebrook 7H9 broth | Difco, Detroit, MI, USA |
| Middlebrook ADC enrichment medium | Difco, Detroit, MI, USA |
| Middlebrook OADC enrichment medium | Life Technologies, Gaithersburg, MI, USA |
| Mouse Exonic Evidence Based Oligonucleotide(MEEBO) Set | Illumina, San Diego, CA, USA |
| *n*-1-napthylethylenediamide | Sigma-Aldrich, Munich, Germany |
| normal rat serum | BD Pharmigen, BD Biosciences, San Jose, CA, USA |
| odium lauryl sarcosinate | BDH Chemicals Ltd., Poole, England |
| Oligonucleotide Primers | DNA Synthesis Laboratory, Dept. Molecular and Cellular Biology, University of Cape Town , South Africa |
| osmium tetroxide | Sigma-Aldrich, Munich, Germany |
| p-aminobenzene-sulfonamide | Sigma-Aldrich, Munich, Germany |
| Penicillin G and Streptomycin Solution (100X) | Gibco, Invitrogen Corporation, Carlsbad, CA, USA |
| Peroxidase Substrate (Solution B) | Roche Diagnostics GmbH, Mannheim, Germany |
| phenol pH4.0 | Sigma-Aldrich, Munich, Germany |
| phosphoric acid | BDH Chemicals Ltd., Poole, England |
| Polyacrylcarrier | Molecular Research Company, Cincinnati, USA |

| Reagent or Kit | Supplier |
|---|---|
| polyclonal rabbit anti-*Listeria antibody* | Capricorn Products LLC, Portland, ME, USA |
| potassium chloride | BDH Chemicals Ltd., Poole, England |
| potassium dihydrogen phosphate | BDH Chemicals Ltd., Poole, England |
| Prolong Antifade Mounting Media | Molecular Probes, Invitrogen Corporation, Carlsbad, CA, USA |
| Proteinase K | Roche Diagnostics GmbH, Mannheim, Germany |
| Qiagen MiniElute RNA cleanup kit | Qiagen, Valencia, CA, USA |
| Reynolds lead | Electron Microscopy Sciences, Fort Washington, PA, USA |
| rhodamine phalloidin | Molecular Probes, Invitrogen Corporation, Carlsbad, CA, USA |
| RNasin (1U/µl) | Promega, Madison, WI, USA |
| RNeasy Midi Kit | Qiagen, Valencia, CA, USA |
| RNeasy RNA Extraction Mini Kit | Qiagen, Valencia, CA, USA |
| RQ1 DNAse1 buffer (10 X) | Promega, Madison, WI, USA |
| Saline Sodium Citrate (SSC) Solution (20 X) | Sigma-Aldrich, Munich, Germany |
| Sensimix d(T) Mastermix Kit | Quantace, Neutral Bay, NSW, Australia |
| sodium acetate | BDH Chemicals Ltd., Poole, England |
| Sodium Azide | BDH Chemicals Ltd., Poole, England |
| sodium bicarbonate | BDH Chemicals Ltd., Poole, England |
| Sodium cacodylate | BDH Chemicals Ltd., Poole, England |
| sodium carbonate | BDH Chemicals Ltd., Poole, England |
| Sodium Chloride | BDH Chemicals Ltd., Poole, England |
| sodium citrate | BDH Chemicals Ltd., Poole, England |
| Sodium Dodecyl Sulfate (SDS), 10% | BDH Chemicals Ltd., Poole, England |
| Sodium Pyruvate | Gibco, Invitrogen Corporation, Carlsbad, CA, USA |
| stepavidin-alkaline-phosphatase | BD Pharmigen, BD Biosciences, San Jose, CA, USA |
| Streptavidin-APC | BD Pharmigen, BD Biosciences, San Jose, CA, USA |
| sucrose | BDH Chemicals Ltd., Poole, England |
| sulfanilamide | Sigma-Aldrich, Munich, Germany |
| SYBR Green1 | Roche Diagnostics GmbH, Mannheim, Germany |
| Teflon coated-bag | Max Planck Institute for Immunobiology, Max Planck, Freiberg, Germany |
| TMB Peroxidase Substrate (Solution A) | Roche Diagnostics GmbH, Mannheim, Germany |
| TNF Biotinylated antibody | BD Pharmigen, BD Biosciences, San Jose, CA, USA |

| Reagent or Kit | Supplier |
|---|---|
| TNF Coating antibody | BD Pharmigen, BD Biosciences, San Jose, CA, USA |
| TNF Recombinant Protein Standard | BD Pharmigen, BD Biosciences, San Jose, CA, USA |
| TriReagent | Molecular Research Company, Cincinnati, USA |
| TRIS-HCl | BDH Chemicals Ltd., Poole, England |
| Triton-X100 | BDH Chemicals Ltd., Poole, England |
| Trypsin/EDTA Solution (10 X) | Gibco, Invitrogen Corporation, Carlsbad, CA, USA |
| tryptose-soy broth | Difco, Detroit, MI, USA |
| Tween 80 | BDH Chemicals Ltd., Poole, England |
| Tween-20 | Merck Laboratory Supplies, South Africa |
| uncoated copper grids (300 mesh) | Sigma-Aldrich, Munich, Germany |
| uranyl acetate | Electron Microscopy Sciences, Fort Washington, PA, USA |
| β-mercaptoethanol | Sigma-Aldrich, Munich, Germany |

**SOFTWARE RESOURCES**

| Software | Supplier/URL |
|---|---|
| AceView Database | http://www.ncbi.nlm.nih.gov/IEB/Research/Acembly/index.html |
| Axiovision version 3.1 | Carl Zeiss, Göttingen, Germany |
| BayGenomics Database | http://baygenomics.ucsf.edu/cgi-bin/BayDbAccess.py?TYPE=search |
| BioConductor (BioCLite) | http://www.bioconductor.org/. |
| Capar Microarray Facility Website | http://www.capar.uct.ac.za/default.html |
| CellQuest | Becton-Dickinson, BD Biosciences, San Jose, CA, USA |
| CyDye Incorporation Calculator | http://www.prontosystems.com/technical_support/calculator. |
| DeltaOne Database | http://www.deltagen.com/deltaone/blast.html |
| DNAMAN version4.1.3. | Lynnon BioSoft, USA |
| Entrez Gene Database | http://www.ncbi.nlm.nih.gov/entrez/query.fcgi?db=gene |
| FatiGOplus | http://babelomics.bioinfo.cipf.es/fatigoplus/cgi-bin/fatigoplus.cgi |
| GenePix Pro 5.1 | Molecular Devices Corporation, Sunnyvale, CA, U.S.A |
| ISMR Database | http://www.informatics.jax.org/imsr/index.jsp |
| Limma | http://www.bioconductor.org/. |
| Milano Literature Mining Tool | http://milano.md.huji.ac.il. |
| OMIM Database | http://www.ncbi.nlm.nih.gov/entrez/query.fcgi?db=OMIM |
| PubMed Database | http://www.ncbi.nlm.nih.gov/entrez/query.fcgi?db=PubMed |
| R version 2.2.0 | http://cbio.uct.ac.za/CRAN/ |
| Scion Image Software | Scion, Frederick, MD, USA |
| Smida | http://www.bioconductor.org/. |
| TM4 Multi-experiment Viewer (MeV) version 3.1 | http://www.tm4.org/ |
| University of Southern California's RefSeq Gene Table Brower | http://www.genome.ucsc.edu/cgi-bin/hgTables?command=start |

**SOFTWARE SCRIPTS WRITTEN FOR IMAGE ANALYSIS USING LIMMA**

```
setwd("C:\\Anita\\New_MEEBO_mouse_oligo_microarray\\R Data Analysis")
library(limma)

## Read Targets
targets <- readTargets()

## Read GPR files into R. Give weight 0.1 to flags with GenePix flag less than 0
RG <- read.maimages(targets$FileName, source = "genepix", wt.fun=wtflags(0.1))

## Set print layout
RG$printer <- getLayout(RG$genes)
spottypes<-readSpotTypes()
RG$genes$Status<-controlStatus(spottypes,RG)
RG$printer

#RG2<-RG
library(smida)
RG$R[,1]<-bkg.norm(xpr=RG$R[,1],empty=200,method="probabilistic",dat.log.scale=FALSE)
RG$R[,2]<-bkg.norm(xpr=RG$R[,2],empty=200,method="probabilistic",dat.log.scale=FALSE)
RG$R[,3]<-bkg.norm(xpr=RG$R[,3],empty=200,method="probabilistic",dat.log.scale=FALSE)
RG$R[,4]<-bkg.norm(xpr=RG$R[,4],empty=200,method="probabilistic",dat.log.scale=FALSE)
RG$R[,5]<-bkg.norm(xpr=RG$R[,5],empty=200,method="probabilistic",dat.log.scale=FALSE)
RG$R[,6]<-bkg.norm(xpr=RG$R[,6],empty=200,method="probabilistic",dat.log.scale=FALSE)
RG$R[,7]<-bkg.norm(xpr=RG$R[,7],empty=200,method="probabilistic",dat.log.scale=FALSE)
RG$R[,8]<-bkg.norm(xpr=RG$R[,8],empty=200,method="probabilistic",dat.log.scale=FALSE)
RG$G[,1]<-bkg.norm(xpr=RG$G[,1],empty=200,method="probabilistic",dat.log.scale=FALSE)
RG$G[,2]<-bkg.norm(xpr=RG$G[,2],empty=200,method="probabilistic",dat.log.scale=FALSE)
RG$G[,3]<-bkg.norm(xpr=RG$G[,3],empty=200,method="probabilistic",dat.log.scale=FALSE)
RG$G[,4]<-bkg.norm(xpr=RG$G[,4],empty=200,method="probabilistic",dat.log.scale=FALSE)
RG$G[,5]<-bkg.norm(xpr=RG$G[,5],empty=200,method="probabilistic",dat.log.scale=FALSE)
RG$G[,6]<-bkg.norm(xpr=RG$G[,6],empty=200,method="probabilistic",dat.log.scale=FALSE)
RG$G[,7]<-bkg.norm(xpr=RG$G[,7],empty=200,method="probabilistic",dat.log.scale=FALSE)
RG$G[,8]<-bkg.norm(xpr=RG$G[,8],empty=200,method="probabilistic",dat.log.scale=FALSE)

# Plot densities of Raw Data
MA.b<-normalizeWithinArrays(RG,method="none",bc.method="none")
plotDensities(MA.b)

# Look at the variation of background values over each array.
for (i in 1:8)
{
x11()
imageplot(log2(RG$Rb[,i]+0.1), RG$printer, low="white", high="red")
x11()
imageplot(log2(RG$Gb[,i]+0.1), RG$printer, low="white", high="green")
```

```
}

#Image plots of the red and green foreground for each array:
for (i in 1:8){
x11()
imageplot(log2(RG$R[,i]+0.1), RG$printer, low="white", high="red")
x11()
imageplot(log2(RG$G[,i]+0.1), RG$printer, low="white", high="green")
}

# Image plot of the un-normalized log-ratios or M-values for each array:
for (i in 1:8){
x11()
imageplot(MA.b$M[,i], RG$printer, zlim=c(-3,3))

}

## MA Plots for each whole array before dye normalization
for (i in 1:8){
x11()
plotMA(MA.b,array=i,main=paste("Array",format(i),sep=" "))
lines(lowess(x=MA.b$A[,i],y=MA.b$M[,i]),col=2)
}

## MA Plots for each array by printtipgroup before before dye normalization
for (i in 1:8){
plotPrintTipLoess(MA.b,array=i)
x11()
}

## Normalize within arrays using print-tip loess
MA.p<-normalizeWithinArrays(RG,method="printtiploess",bc.method="none")
plotDensities(MA.p)

# Image plot of the spatially normalized log-ratios(M-values
for (i in 1:8){
x11()
imageplot(MA.p$M[,i], RG$printer, zlim=c(-3,3))
}

## MA Plots for each whole array after print-tip normalization
for (i in 1:8){
plotMA(MA.p,array=i,main=paste("Array",format(i),sep=" "))
lines(lowess(x=MA.p$A[,i],y=MA.p$M[,i]),col=2)
x11()
}
boxplot(MA.p$M~col(MA.p$M),names=colnames(MA.p$M))
```

```
## Normalize between Arrays
MA.ps<-normalizeBetweenArrays(MA.p,method="scale")
plotDensities(MA.ps)


## Identify and merge replicates. Sort by gene ID to get spacing regular and average over duplicate spots
i <- order(MA.pAq$genes$ID)
MA.pAq.o<- MA.pAq[i,]
aveM<-matrix(0,ncol=8,nrow=length(unique(MA.pAq.o$genes$ID)))
aveA<-matrix(0,ncol=8,nrow=length(unique(MA.pAq.o$genes$ID)))
for (j in 1:8)
{
aveM[,j]<-unlist(lapply(split(MA.pAq.o$M[,j],MA.pAq.o$genes$ID),mean))
aveA[,j]<-unlist(lapply(split(MA.pAq.o$A[,j],MA.pAq.o$genes$ID),mean))
}

MA.pAq.o$M<-aveM
MA.pAq.o$A<-aveA
MA.pAq.o$weights<-MA.pAq.o$weights[!duplicated(MA.pAq.o$genes$ID),]
MA.pAq.o$genes<-MA.pAq.o$genes[!duplicated(MA.pAq.o$genes$ID),]

## MA plots of normalized and averaged data
for (i in 1:8){
plotMA(MA.pAq.o,array=1,main=paste("Array",format(i),sep=" "),cex=0.3)
lines(lowess(x=MA.pAq.o$A[,i],y=MA.pAq.o$M[,i]),col=2)
x11()
}

# save M-values to file on C:drive
Mvals<-cbind(MA.pAq.o$genes$ID,MA.pAq.o$genes$Name,MA.pAq.o$M)
write.table(Mvals,file="c:\\Mvals",sep="\t",row.names=FALSE)
#END OF SCRIPT
```

**SPECIALIZED EQUIPEMENT**

| Equipment | Supplier |
|---|---|
| Axiovert 200M Deconvoluting Fluorescent Microscope | Carl Zeiss, Göttingen, Germany |
| Axon GenePix 4000A Scanner | Axon Instruments/Molecular Devices Corporation, Sunnyvale, CA, U.S.A |
| FACSCalibur | Becton-Dickinson, BD Biosciences, San Jose, CA, USA |
| Lightcycler | Roche Diagnostics GmbH, Mannheim, Germany |
| MJ thermocycler | Biozym, Hessisch Oldendorf, Frankfurt, Germany |
| NanoDrop ND-1000A UV-Vis Spectrophotometer | NanoDrop Technologies, Wilmington, DE, USA |
| Nikon E400 microscope | Nikon E400 microscope |
| SpeedVac | Savant Instruments Inc, Holbrook, NY, USA |
| Zeiss 109 transmission electron microscope. | Carl Zeiss, Göttingen, Germany |
| VersaMax microplate reader | Molecular Devices Corporation, Sunnyvale, CA, U.S.A |

## RECIPES

### General Lab Solutions

**Mouse Tail Digestion Buffer**

12.5ml 1M TRIS-HCL, pH8

50ml 500mM EDTA, pH8.0

12.5ml 1M NaCl

25ml 10% SDS

2.5ml 10mg/ml Proteinase K

Add 12.5ml of 1M TRIS-HCL (pH8), 50ml of 500mM EDTA (pH8.0), 12.5ml of 1M NaCl and 25ml of 10% SDS to 140ml of $ddH_2O$. Bring up the final volume to 250ml and filter sterilize with a 0.22µM filter (Millipore Corporation, Bedford, USA). Aliquot into sterile tubes and store at -20°C. Thaw buffer and add 10mg/ml Proteinase K at a 1:100 dilution.

**10mg/ml Proteinase K**

1g Proteinase K

Weigh out 1g of Proteinase K and dissolve in 100ml of $ddH_2O$. Filter sterilize with a 0.22µM filter (Millipore Corporation, Bedford, USA) and aliquot into sterile tubes. Store at -20°C and use at a 1:100 dilution in Mouse Tail Digestion Buffer.

**0.5M EDTA, pH 8.0**

93.06g EDTA

Weigh out 93.06g of EDTA and dissolve in 450ml $ddH_2O$. Adjust pH to 8.0 and bring final volume to 500ml. Autoclave and store at room temperature.

**2M NaCl**

11.688g NaCl

Weigh out 11.688g of NaCl and dissolve in 90ml of $ddH_2O$. Bring final volume to 100ml and autoclave. Store at room temperature.

**10% SDS**

10g SDS

Weigh out 10g of SDS and dissolve in 90ml of $ddH_2O$. Bring final volume to 100ml and autoclave. Store at room temperature.

**1M TRIS-HCl, pH8.0**

60.55g TRIS-HCl

Weigh out 60.55g of TRIS-HCl and dissolve in 450ml$ddH_2O$. Adjust pH to 8.0 and bring final volume to 500ml. Autoclave and store at room temperature.

**1 X Phosphate Buffered Saline (PBS)**

8g NaCl

0.2g KCl

1.44g Na2HPO4

0.24g KH2PO4

Weigh out chemicals and dissolve in 900ml of $ddH_2O$ and adjust pH to 7.4. Bring final volume to 1000ml and filter sterilize with a 0.22µM filter (Millipore Corporation, Bedford, USA). Store at 4°C or room temperature.

**1 X PBS (with $CaCl_2$ and $MgCl_2$)**

8g NaCl

0.2g KCl

1.44g $Na_2HPO_4.2H_2O$

0.24g $KH_2PO_4$

100mg $CaCl_2 2H_2O$

100mg $MgCl_2 \cdot 6H_2O$

Weigh out chemicals and dissolve in 900ml of $ddH_2O$ and adjust pH to 7.4. Bring final volume to 1000ml and filter sterilize with a 0.22µM filter (Millipore Corporation, Bedford, USA). Store at 4°C or room temperature.

**3.7% formaldehyde (vol/vol in PBS)**

48.68ml 38% formaldehyde

500ml 1 X PBS

Mix together 48.68ml of 38% formaldehyde and 400ml of 1 X PBS. Bring up volume to 500ml and filter sterilize with a 0.22μM filter (Millipore Corporation, Bedford, USA). Aliquot into sterile tubes and store at 4°C.

**4 % phosphate-buffered formalin**

52.63ml 38% formaldehyde

500ml 1 X PBS

Mix together 52.63ml of 38% formaldehyde and 400ml of 1 X PBS. Bring up volume to 500ml and filter sterilize with a 0.22μM filter (Millipore Corporation, Bedford, USA). Aliquot into sterile tubes and store at 4°C.

**10% glycerol**

10ml 100% Glycerol

90ml 1 X PBS

Mix together 10ml of 100% of Glycerol and 90ml of 1 X PBS. Autoclave and store at temperature.

**10 % Tween-80**

10ml 100% Tween-80

90ml 1 X PBS

Mix together 10ml of 100% Tween-80 and 90ml of 1 X PBS. Autoclave and store at temperature.

**10% Triton-X100**

10ml 100% Triton-X100

90ml 1 X PBS

Mix together 10ml of 100% Triton-X100 and 90ml of 1 X PBS. Autoclave and store at temperature.

**0.2% Triton-X100**

2ml 10% Triton-X100

98ml 1 X PBS

Mix together 2ml of 10% Triton-X100 and 98ml of 1 X PBS. Autoclave and store at temperature.

**1% BSA (Fraction V)**

1g BSA (fraction V)

100ml 1 X PBS

Weigh out 1g of BSA (fraction V) and dissolve in 95ml of 1 X PBS. Bring up the final volume to 100ml and filter sterilize with a 0.22μM filter (Millipore Corporation, Bedford, USA). Aliquot into sterile tubes and store at -20°C.

**Bacterial Solutions**

**Tryptose-Soy Agar Plates.**

30g Tryptose-Soy Broth

25g Bacto Agar

Weigh out 30g of Tryptose-Soy Broth and 25g of Bacto Agar and dissolve in 1000ml of $ddH_2O$. Autoclave and pour into sterile bacterial grade plastic petridishes in a sterile laminar flow hood and allow the agar to set. Invert the plates and incubate overnight at 37°C. Pack plates in sterile plastic bags and store in the inverted position at 4°C.

**Tryptose-Soy Broth**

30g Tryptose-Soy Broth

Weigh out 30g of Tryptose-Soy Broth and dissolve in 1000ml of $ddH_2O$. Autoclave and store at room temperature.

**Middlebrook 7H10 agar plates**

19g Middlebrook 7H10 agar

100ml Middlebrook OADC enrichment medium

5ml glycerol

Weigh out 19g of Middlebrook 7H10 agar and dissolve in 900ml of $ddH_2O$ containing 5ml of 100% glycerol. Autoclave at 121°C for 10 minutes only and cool agar to 50-55°C. Aseptically add 100ml Middlebrook OADC enrichment medium. Pour into sterile bacterial grade plastic petridishes with 2 compartments under a sterile laminar flow hood and allow the agar to set. Pack the plates in sterile plastic bags and store in the inverted position at 4°C.

**Middlebrook 7H10 Broth**

4.7g Middlebrook 7H10 Broth

100ml Middlebrook ADC enrichment medium

2ml 100% glycerol

0.5g Tween-80

Weigh out 4.7g Middlebrook 7H10 broth and dissolve in 900ml of $ddH_2O$ containing 2ml 100% glycerol and 0.5g Tween-80. Autoclave for 10 minutes at 121oC and cool to 50-55°C and aseptically add 100ml Middlebrook ADC enrichment medium. Store at room temperature.

**0.05% Triton-X100 in 1 X PBS**

500µl 10% Triton-X100

99.5 1 X PBS

Mix together 10ml of 10% Triton-X100 and 95ml of 1 X PBS. Bring up the final volume to 100ml and autoclave. Store at temperature.

## Cell Culture Solutions

### Fetal Calf Serum (FCS)

500ml FCS

Thaw one 500ml bottle of FCS at 37°C and heat inactivate at 56°C for 30 minutes with intermittent agitation. Make 25ml aliquots and store at -20°C.

### Horse Serum

500ml Horse Serum

Thaw one 500ml bottle of horse serum at 37°C and heat inactivate at 56°C for 30 minutes with intermittent agitation. Make 25ml aliquots and store at -20°C.

### Dulbecco's Modified Eagle's Medium (DMEM)

13.38g DMEM powder

100ml Fetal calf serum

10ml 100X Penicillin G and Streptomycin Solution

Weigh out 13.38g of DMEM powder and 3.7g of sodium bicarbonate and dissolve in 800ml dd$H_2O$. Add 100ml heat decomplemented fetal calf serum and 10ml of 100X Penicillin G and Streptomycin Solution. Bring the final volume to 1000ml and filter sterilize with a 0.22μM filter (Millipore Corporation, Bedford, USA). Store at 4°C.

### Iscoves's Modified DMEM (IMDM)

17.66g IMDM powder

100ml Fetal calf serum

10ml 100X Penicillin G and Streptomycin Solution

Weigh out 17.66g of IMDM powder and 3.024g of sodium bicarbonate and dissolve in 800ml dd$H_2O$. Adjust pH to between 7.2 – 7.4 with 1M NaOH. Add 100ml heat decomplemented fetal calf serum and 10ml of 100X Penicillin G and Streptomycin Solution. Bring the final volume to 1000ml and filter sterilize with a 0.22μM filter (Millipore Corporation, Bedford, USA). Store at 4°C.

**Plutznik Media**

264ml DMEM (with 100U/ml penicillin G, 100µg /ml streptomycin)

50ml FCS (heat decomplemented)

25ml Horse serum (heat decomplemented)

5ml 200mM L-glutamine

5ml 100mM Na-pyruvate

1ml 1000X 2-β-Mercaptoethanol

150ml L929 cell-conditioned medium

Add all the reagents together and filter sterilize with a 0.22µM filter (Millipore Corporation, Bedford, USA). Always make fresh just before use.

**200mM L-Glutamine**

2.922g L-Glutamine

Weigh out 2.922g L-Glutamine and dissolve in 100ml of $ddH_2O$ and filter sterilize with a 0.22µM filter (Millipore Corporation, Bedford, USA). Make 5ml aliquots and store at -20°C.

**1000X 2-β-Mercaptoethanol**

698µl 2-β-Mercaptoethanol

Add 698µl of 2-β-Mercaptoethanol to 100ml of $ddH_2O$. Filter sterilize with a 0.22µM filter (Millipore Corporation, Bedford, USA) and store at 4°C.

**100mM Sodium Pyruvate**

1.1g Sodium Pyruvate

Weigh out 1.1g sodium pyruvate and dissolve in 100ml $ddH_2O$. Filter sterilize with a 0.22µM filter (Millipore Corporation, Bedford, USA) and store at 4°C.

**Red cell lysis Buffer**

8.34g $NH_4CL$

0.037g EDTA

1.00g $NaHCO_3$

Weigh out chemicals and dissolve in 1000ml of $ddH_2O$. Filter sterilize with a 0.22µM filter (Millipore Corporation, Bedford, USA) and store at 4°C.

**1 X Trypsin/EDTA Solution**

10 X Trypsin/EDTA Solution (Gibco, Invitrogen Corporation, Carlsbad, CA, USA)

Add 10ml of 10 X Trypsin/EDTA Solution to 90ml of $ddH_20$, filter sterilize with a 0.22 µM filter (Millipore Corporation, Bedford, USA) and store at 4°C.

**Immunology Solutions**

**ELISA Coating Buffer**

0.2g $NaN_3$

Weigh out $NaN_3$ and dissolve in 900ml of 1 X PBS, bring the final volume to 1000ml and store at room temperature.

**ELISA Carbonate Coating Buffer**

1.6g $Na_2CO_3$

2.9g $NaHCO_3$

4.2g NaCl

Weigh out chemicals and dissolve in 900ml of $ddH_2O$. Adjust pH to 9.5 with 1M Citric Acid. Bring the final volume to 1000ml and filter sterilize with a 0.22µM filter (Millipore Corporation, Bedford, USA) and store at 4°C.

**ELISA Blocking Buffer**

20g Powder Milk

0.2g $NaN_3$

Weigh out chemicals and dissolve in 900ml of 1 X PBS, bring the final volume to 1000ml and store at 4°C.

**ELISA Dilution Buffer**

10g BSA

0.2g $NaN_3$

Weigh out chemicals and dissolve in 900ml of 1 X PBS, bring the final volume to 1000ml and store at 4°C.

**ELISA Washing Buffer (20 X)**

20g KCL

20g $KH_2HPO_4.2H_2O$

800g NaCl

50ml Tween-20

100ml 10% $NaN_3$

Weigh out chemicals and dissolve in 4500ml double distilled water ($ddH_2O$). Add 50ml of Tween-20 and 100ml of 10% $NaN_3$. Bring final volume to 5000ml and store at room temperature. Dilute 1:20 in $ddH_2O$ for a 1 X working concentration buffer.

**ELISA Substrate Buffer (for alkaline phosphatase conjugates)**

0.2g $NaN_3$

97ml diethanolamine

0.8g $MgCl_2.6H_2O$

Weigh out chemicals and dissolve in 700ml of $ddH_2O$. Add 97ml of liquefied diethanolamine and adjust pH to 9.8. Bring the final volume to 1000ml and store at 4°C.

ELISA Substrate Buffer (for horseradish peroxidase conjugates)

TMB Peroxidase Substrate Solution A (Roche Diagnostics GmbH, Mannheim, Germany)

Peroxidase Substrate Solution B (Roche Diagnostics GmbH, Mannheim, Germany)

1M $H_3PO_4$

Just before use, mix equal volumes of TMB Peroxidase Substrate (Solution A) with Peroxidase Substrate Solution B. Add 50µl per well and let the reaction develop at room temperature for 5 minutes. Stop the reaction by adding 50µl of 1M $H_3PO_4$

**Griess Reagent Standard (1mM $NaNO_2$)**

6.899mg $NaNO_2$

Weigh out 6.899mg of $NaNO_2$ and dissolve in 100ml of $ddH_2O$ and store at 4°C.

**Griess Reagent 1**

1g sulfanilamide

100ml 2.5% phosphoric acid

Weigh out 1g sulfanilamide and dissolve in 100ml of 2.5 % phosphoric acid. Cover bottle in foil to protect from light and store at 4°C.

**Griess Reagent 2**

0.1g napthyl-ethylene-diamine

100ml 2.5 %phosphoric acid

Weigh out 0.1g napthyl-ethylene-diamine and dissolve in 100ml of 2.5 % phosphoric acid. Cover bottle in foil to protect from light and store at 4°C.

**2.5% phosphoric acid**

3ml 85% phosphoric acid

Add 3ml of 85% phosphoric acid slowly to 90ml of $ddH_2O$. Bring up volume to 100ml and store at room temperature.

## Microscopy Solutions

### 6.6μM Rhodamine Phalloidin Stock

1 vial rhodamine phalloidin (300Units)

1.5ml methanol (ultra pure)

Dissolve 1 vial of rhodamine phalloidin (300Units) in 1.5 ml methanol. Make 10μl aliquots and wrap in foil to protect from light. Store in the dark at –20°C. Do not free/thaw more than once.

### Cacodylate Buffer (with or without sucrose)

5.35g sodium cacodylate

254mg $CaCl_2 2H_2O$

184mg $MgCl_2\ 6H_2O$

8.5g sucrose

Weigh out 5.35g of sodium cacodylate and dissolve in 220ml ddH20. Adjust pH to 7.2 with 1M HCl and adjust volume to 250ml. Add the $MgCl_2$ and $CaCl_2$ If required, add 8.5g sucrose and bring volume to 250ml. Store at 4°C.

### 0.5M Ferric Cyanide

2.112g ferric cyanide

Weigh out and dissolve 2.112g of ferric cyanide in ddH20. Make Always make fresh just before use. This solution is highly toxic. Use it under the flow hood at all times. Adhere to all University Health and Safety precautions relevant to this solution.

### 2.5% Gluteraldehyde in Cacodylate Buffer

25% gluteraldehyde stock (electron microscopy grade)

Add 2ml of 25% gluteraldehyde to 18ml cacodylate buffer containing sucrose. Always make fresh just before use.

**4% Osmium Tetroxide**

1g $OsO_4$

Weigh out and dissolve 1g of $OsO_4$ in 25ml $ddH_2O$. Cover in foil to protect the solution from light and store at 4°C. The solution can be kept for several months at 4°C, and can be used so long as it has not turned black during storage. This solution is highly toxic. Use it under the flow hood at all times. Adhere to all University Health and Safety precautions relevant to this solution.

**1% $OsO_4$ and 0.05M Ferric Cyanide Staining Solution**

4% Osmium Tetroxide

0.5M Ferric Cyanide (freshly made)

Prepare this solution just prior to use. Add 2ml of 4% $OsO_4$ solution and 200µl of 0.05M ferric cyanide (freshly prepared) to 6ml of cacodylate buffer pH7.0 devoid of sucrose (the solution will turn brown). Use the solution immediately.

**Reynolds Lead Solution**

1.33g lead nitrate

1.76g sodium citrate

8ml 1M sodium hydroxide

Boil 750ml of $ddH_2O$ for at least 30 minutes in order to boil off carbon dioxide. Weigh out 1.33g of lead nitrate and carefully add to a 50ml volumetric flask. Add 30ml of the boiled water to the 50ml volumetric flask and shake. Add 1.76g of sodium citrate to 50ml volumetric flask and shake vigorously for 2 minutes. The solution will turn milky white.Let solution stand for 30 minutes with occasional shaking by inversion. Add 8ml of 1M sodium hydroxide solution (freshly made) and mix by inversion. The solution should clear. Bring up the volume to 50ml. Aliquot into 10ml portions using a syringe into air-tight bottles that contain a rubber or cork stopper in the bottle neck. Store at 4°C.

**Uranyl Acetate Solution**

6.25g uranyl acetate

Weigh out 6.25 grams of uranyl acetate powder into an amber glass bottle. Add 100ml $ddH_2O$ into the amber bottle and sonicate the uranyl acetate solution for 1 hour under a fume hood. When sonication is complete, wrap some Parafilm around the cover of the amber bottle and store at 4°C.

## RNA and Microarray Solutions

**DEPC-treated $H_2O$**

1000ml $ddH_2O$

1ml Diethylpyrocarbonate (DEPC)

Add 1ml of DEPC to 1000ml of $ddH_2O$ and incubate overnight at 37°C with agitation. Autoclave to sterilize and heat deactivate the DEPC. Aliquot in RNAse-free tubes and store at room temperature.

**70% Ethanol**

70ml absolute ethanol

30ml DEPC-treated $H_2O$

Add 30ml of DEPC-treated $H_2O$ to 70ml absolute ethanol and mix well. Aliquot in RNAse-free tubes and store at room temperature.

**75% Ethanol**

75ml absolute ethanol

25ml DEPC-treated $H_2O$

Add 25ml of DEPC-treated $H_2O$ to 75ml absolute ethanol and mix well. Aliquot in RNAse-free tubes and store at room temperature.

**Chloroform-Isoamyl Alcohol (49:1)**

1ml isoamyl alcohol

49ml chloroform

Add 1ml of isoamyl alcohol to 49ml of chloroform in a in RNAse-free glass bottle. Cover bottle in foil and store at 4°C.

**3M Sodium Acetate**

408.3g sodium acetate.$3H_2O$

glacial acetic acid

1.0ml DEPC

Weigh and dissolve 408.3g of sodium acetate.$3H_2O$ in 700 ml of $ddH_2O$. Adjust the pH to 5.2 with glacial acetic acid and bring the final volume to 1000ml. Add 1ml of DEPC and incubate overnight at 37°C with agitation. Autoclave to sterilize and heat deactivate the DEPC. Aliquot in RNAse-free tubes and store at room temperature.

**0.75M Sodium Citrate Ph7.0**

110.29g of sodium citrate

Weigh 110.29g of sodium citrate and dissolve in 450ml of $ddH_2O$. Adjust the pH to 7.0 and bring the final volume to 500ml. Add 0.5ml of DEPC and incubate overnight at 37°C with agitation. Autoclave to sterilize and heat deactivate the DEPC. Aliquot in RNAse-free tubes and store at room temperature.

**0.5% Sodium Lauryl Sarcosinate**

5g sodium lauryl sarcosinate

Weigh out 5g of sodium lauryl sarcosinate and dissolve in 950ml of $ddH_2O$ and bring the final volume to 1000ml. Add 1ml of DEPC and incubate overnight at 37°C with agitation. Autoclave to sterilize and heat deactivate the DEPC. Aliquot in RNAse-free tubes and store at room temperature.

**RNA Denaturing Solution "Solution D"**

250g guanidinium thiocyanate

17.6ml 0.75M sodium citrate pH7.0

26.4ml 0.5% (w/v) sodium lauryl sarcosinate

360µl 14.4M 2-β-mercaptoethanol

Weigh out and dissolve 250g of guanidinium thiocyanate in 293 ml of dd$H_2O$, 17.6 ml of 0.75M sodium citrate (pH 7.0) and 26.4 ml of 10% sodium lauryl sarcosinate. Dissolve using a heated magnetic stirrer set at 65°C. Cover the bottle in foil as this solution is sensitive to light. Solution D may be stored for months at 4°C but the guanidinium will precipitate out of solution, therefore pre-warm the solution before using it to dissolve the crystals. Add 360µl 14.4M 2-β-mercaptoethanol per 50 ml of Solution D just before use.

**RNA Loading Buffer**

14.0µl 12.3M Formaldehyde

50.0µl 100% Formamide

10.0µl 10 X MEA Buffer

1µl 10mg/ml Ethidium Bromide

Make up the buffer fresh each time. Add all reagents together and mix well. Add 7.4µl of loading buffer to 2.6µl of RNA. This recipe is enough for 10 samples

**10 X MEA Electrophoresis Buffer**

0.2 M MOPS, pH 7.0

6.67ml 3M sodium acetate, pH5.2

0.5M EDTA pH 8.0

Weigh out and dissolve 41.8 g of MOPS in 700 ml of sterile DEPC-treated $H_2O$. Adjust the pH to 7.0 with 1M NaOH. Add 6.67ml of DEPC-treated 3M sodium acetate and 20ml of DEPC-treated 0.5M EDTA (pH 8.0). Adjust the volume of the solution to 1000ml with DEPC-treated $H_2O$. Add 1ml DEPC and incubate overnight at 37°C with shaking. Autoclave to heat deactivate the DEPC and to sterilize (autoclaving turns the solution yellow but does not affect the pH). Store at 4°C wrapped in foil to protect from light.

**Pre-Hybridization Buffer**

50µl 20 X SSC

1µl 20% SDS

20µl 1% BSA

129µl $ddH_2O$

Mix together 50µl of 20 X SSC, 1µl of 20% SDS, 20µl of 1% BSA and 129µl of $ddH_2O$. Make buffer fresh each time and incubate at 42°C until use. This recipe is enough for 1 microarray slide.

**2 X Hybridisation Buffer**

100µl 50% formamide

100µl 20 X SSC

2µl 20% SDS

Mix together in sequential order100µl of 50% formamide, 100µl of 20 X SSC and 2µl of 20% SDS. Make buffer fresh each time and incubate at 42°C until use. This recipe is enough for 1 microarray slide.

**Low Stringency Wash Buffer**

20ml 20 X SSC

1ml 20% SDS

179ml $ddH_2O$

Mix together 20ml of 20 X SSC, 1ml of 20% SDS and 179ml of $ddH_2O$. Make buffer fresh each time.

**Medium-Stringency Wash Buffer**

10ml 20 X SSC

190ml $ddH_2O$

Mix together10ml of 20 X SSC and 190ml of $ddH_2O$. Make buffer fresh each time.

**High-Stringency Wash Buffer**

2ml 20 X SSC

198ml $ddH_2O$

Mix together 2ml of 20 X SSC and 198ml of $ddH_2O$. Make buffer fresh each time.

## REFERENCES


1. Jacobs, M., M. W. Marino, N. Brown, B. Abel, L. G. Bekker, V. J. Quesniaux, L. Fick, and B. Ryffel. 2000. Correction of defective host response to Mycobacterium bovis BCG infection in TNF-deficient mice by bone marrow transplantation. *Lab Invest 80:901.*
2. Mohrs, M., B. Ledermann, G. Kohler, A. Dorfmuller, A. Gessner, and F. Brombacher. 1999. Differences between IL-4- and IL-4 receptor alpha-deficient mice in chronic leishmaniasis reveal a protective role for IL-13 receptor signaling. *J Immunol 162:7302.*
3. Ding, A. H., C. F. Nathan, and D. J. Stuehr. 1988. Release of reactive nitrogen intermediates and reactive oxygen intermediates from mouse peritoneal macrophages. Comparison of activating cytokines and evidence for independent production. *J Immunol 141:2407.*
4. Diaz, R., L. S. Mayorga, L. E. Mayorga, and P. Stahl. 1989. In vitro clustering and multiple fusion among macrophage endosomes. *J Biol Chem 264:13171.*
5. Chomczynski, P., and N. Sacchi. 1987. Single-step method of RNA isolation by acid guanidinium thiocyanate-phenol-chloroform extraction. *Anal Biochem 162:156.*
6. Sambrook, J., and D. W. Russell. 2001. *Molecular cloning : a laboratory manual.* Cold Spring Harbor Laboratory Press, Cold Spring Harbor, N.Y.
7. R. Development Core Team: R: A language and environment for statistical computing.http://www.R-project.org.
8. Gentleman, R. C., V. J. Carey, D. M. Bates, B. Bolstad, M. Dettling, S. Dudoit, B. Ellis, L. Gautier, Y. Ge, J. Gentry, K. Hornik, T. Hothorn, W. Huber, S. Iacus, R. Irizarry, F. Leisch, C. Li, M. Maechler, A. J. Rossini, G. Sawitzki, C. Smith, G. Smyth, L. Tierney, J. Y. Yang, and J. Zhang. 2004. Bioconductor: open software development for computational biology and bioinformatics. *Genome Biol 5:R80.*
9. Wettenhall, J. M., and G. K. Smyth. 2004. limmaGUI: a graphical user interface for linear modeling of microarray data. *Bioinformatics 20:3705.*
10. Smyth, G. K., J. Michaud, and H. S. Scott. 2005. Use of within-array replicate spots for assessing differential expression in microarray experiments. *Bioinformatics 21:2067.*
11. Smyth, G. K. 2004. Linear models and empirical bayes methods for assessing differential expression in microarray experiments. *Stat Appl Genet Mol Biol 3:Article3.*
12. Wit, E., and J. D. McClure. 2004. *Statistics for microarrays : design, analysis, and inference.* John Wiley & Sons, Chichester, England ; Hoboken, NJ, USA.
13. Saeed, A. I., V. Sharov, J. White, J. Li, W. Liang, N. Bhagabati, J. Braisted, M. Klapa, T. Currier, M. Thiagarajan, A. Sturn, M. Snuffin, A. Rezantsev, D. Popov, A. Ryltsov, E. Kostukovich, I. Borisovsky, Z. Liu, A. Vinsavich, V. Trush, and J. Quackenbush. 2003. TM4: a free, open-source system for microarray data management and analysis. *Biotechniques 34:374.*
14. Pan, W. 2002. A comparative review of statistical methods for discovering differentially expressed genes in replicated microarray experiments. *Bioinformatics 18:546.*
15. Dudoit, S., and T. P. Speed. 2000. A score test for the linkage analysis of qualitative and quantitative traits based on identity by descent data from sib-pairs. *Biostatistics 1:1.*
16. Churchill, G. A. 2002. Fundamentals of experimental design for cDNA microarrays. *Nat Genet 32 Suppl:490.*
17. Quackenbush, J. 2002. Microarray data normalization and transformation. *Nat Genet 32 Suppl:496.*

18. Al-Shahrour, F., P. Minguez, J. M. Vaquerizas, L. Conde, and J. Dopazo. 2005. BABELOMICS: a suite of web tools for functional annotation and analysis of groups of genes in high-throughput experiments. *Nucleic Acids Res 33:W460.*
19. Chekmenev, D., C. Haid, and A. Kel 2001. P-Match (Public). In *German Conference on Bioinformatics*. Biobase, Germany.
20. Rubinstein, R., and I. Simon. 2005. MILANO--custom annotation of microarray results using automatic literature searches. *BMC Bioinformatics 6:12.*
21. PubMed. http://www.ncbi.nlm.nih.gov/entrez/query.fcgi?db=PubMed.
22. Aceview. http://www.ncbi.nlm.nih.gov/IEB/Research/Acembly/index.html.
23. OMIM. http://www.ncbi.nlm.nih.gov/entrez/query.fcgi?db=OMIM.
24. Gene. http://www.ncbi.nlm.nih.gov/entrez/query.fcgi?db=gene.
25. IMSR. http://www.informatics.jax.org/imsr/index.jsp.
26. BayGenomics. http://baygenomics.ucsf.edu/cgi-bin/BayDbAccess.py?TYPE=search.
27. DeltaOne. http://www.deltagen.com/deltaone/blast.html.
28. Cytoscape. 2005. http://www.cytoscape.org.
29. Brazma, A., P. Hingamp, J. Quackenbush, G. Sherlock, P. Spellman, C. Stoeckert, J. Aach, W. Ansorge, C. A. Ball, H. C. Causton, T. Gaasterland, P. Glenisson, F. C. Holstege, I. F. Kim, V. Markowitz, J. C. Matese, H. Parkinson, A. Robinson, U. Sarkans, S. Schulze-Kremer, J. Stewart, R. Taylor, J. Vilo, and M. Vingron. 2001. Minimum information about a microarray experiment (MIAME)-toward standards for microarray data. *Nat Genet 29:365.*

## CHAPTER 3

# GENERATION AND INFECTION OF BONE MARROW DERIVED MACROPHAGES WITH *LISTERIA MONOCYTOGENES*

## SUMMARY

The chief aims of this chapter were to establish *in vitro* infection of bone marrow derived macrophages (BMDMs) with *L. monocytogenes* and to compare the subsequent innate immune responses between infected WT macrophages and macrophages genetically deficient for C/EBPβ (C/EBPβ$^{-/-}$). *L. monocytogenes* was used in the current study as a model intracellular pathogen to identify genes involved in mediating macrophage bactericidal effector activity. Host protection to *L. monocytogenes* involves the activation of cellular immune responses resulting in the activation of macrophage bactericidal effector functions, granuloma formation and protective Th1-type responses. IFN-γ and TNF are key cytokines essential for full macrophage activation (1, 2), resulting in enhanced production of cytokines, chemokines and bactericidal molecules such as reactive oxygen intermediates (ROI) and reactive nitrogen intermediates (RNI). Several *in vivo* infection studies using mice deficient for iNOS or various components of NADPH phagocyte oxidase, showed that bacterial killing took place despite the lack of ROI and RNI (3-7). These studies suggested that macrophages have an alternative killing mechanism that is independent of ROI and RNI. Furthermore, studies using mice deficient for genes involved in TNF and/or IFN-γ signalling emphasized the existence of an alternative unknown killing mechanism that is independent of ROI or RNI (3-7), but dependent on IFN-γ, TNF and C/EBPβ (8-10). The most downstream molecule in this hypothetical pathway would be C/EBPβ, since the C/EBPβ$^{-/-}$ mice induced IFN-γ and TNF at levels equivalent to WT mice during *L. monocytogenes* infection (10). Macrophage genes involved in mediating listericidal activity would therefore most likely be downstream of C/EBPβ in this unknown killing pathway. Comparison of the gene expression profiles of WT and C/EBPβ$^{-/-}$activated macrophages infected with *L. monocytogenes* would therefore increase the probability of identifying these listericidal effector genes. However, before RNA was extracted and the gene expression profiling experiments executed, several biological parameters were compared to literature to ensure that the *in vitro* infection experiments reflected the" biology" of *in vivo* infections. Only if all the results concurred with literature, was the *in vitro* experiment judged successful and the RNA used for gene expression analysis. Furthermore, in order to mimick as closely as possible the biology of *in vivo* infections,

macrophages were only stimulated with IFN-γ upon infection with *L. monocytogenes*.

Both WT and C/EBPβ$^{-/-}$ infected macrophages were fully activated and secreted equivalent amounts of pro-inflammatory mediators such as IL-6, IL-12, IL-18, TNF, MCP-1 and nitric oxide. However, despite full macrophage activation C/EBPβ$^{-/-}$ macrophages had 30% more escaped *Listeria* bacilli in the cytoplasm than the WT macrophages at 4 hours p.i.. Consequently, the C/EBPβ$^{-/-}$ macrophages displayed uncontrolled bacilli growth and at 12 hours after of infection contained 6-fold more bacteria than the WT macrophages. Furthermore, the C/EBPβ$^{-/-}$ macrophages had impaired induction of G-CSF, CLECSF9, IL-12p35 and ISGF3γ genes, whose transcription is dependent on C/EBPβ (10-13). Altogether, these results demonstrated that the observed phenotype of C/EBPβ$^{-/-}$ macrophages were representative of those reported in the literature and confirmed that the "biology" of the *in vitro* infection experiments reflected that of *in vivo* infections. The infection experiment was repeated four times independently of each other and RNA extracted at 4 hours p.i. for microarray analysis, since this was the earliest time point where a significant difference between WT and C/EBPβ$^{-/-}$ macrophage listericidal activity was observed. The increased bacterial load and impaired killing in the C/EBPβ$^{-/-}$ macrophages was considered a consequence of differential expression of genes, between the WT and C/EBPβ$^{-/-}$ macrophages, that were required for mediating listericidal activity. The quality and purity of the RNA was high and was biologically relevant as shown by quantitative RT-PCR for C/EBPβ target genes. Although the yield of RNA was low for some experiments, there was sufficient RNA for linear mRNA amplification which would generate enough sample for microarray analysis.

## RESULTS

### 1. Efficient Activation of C/EBPβ$^{-/-}$ BMDMs

Bone marrow derived macrophages (BMDMs) were successfully generated from the WT and C/EBPβ$^{-/-}$ mice. The yield of bone marrow stem cells per mouse prior to differentiation was comparable for both WT and C/EBPβ$^{-/-}$ However, after 10 days of *in vitro* differentiation in conditioned medium containing granulocyte macrophage colony stimulating factor (GM-CSF) and macrophage colony stimulating factor (M-CSF), the yield of differentiated macrophages was significantly lower for the C/EBPβ$^{-/-}$ mice (Fig. 1). Macrophages from WT and C/EBPβ$^{-/-}$ mice were simultaneously stimulated with IFN-γ and infected with *L. monocytogenes* at a MOI of 10 bacilli : 1 macrophage. Macrophage activation was assessed by measuring the levels of pro-inflammatory mediators (Fig. 2) in the cell culture supernatants. Both WT and C/EBPβ$^{-/-}$ macrophages efficiently induced TNF, IL-12, IL-6, IL-18, and MCP-1 which increased until the last time-point in the assay. As expected from the literature, there was no significant difference in the level of induction of these mediators between the WT and C/EBPβ$^{-/-}$ macrophages during *L. monocytogenes* infection (10). The only exception was for IL-18, which at 4 hours p.i. was >10 fold lower in the C/EBPβ$^{-/-}$ macrophages as compared to WT. Although not statistically significant, the levels for TNF, IL-6 and IL-18 were generally lower, whereas IL-10 was higher in the C/EBPβ$^{-/-}$ macrophages than the WT. These results demonstrated that C/EBPβ$^{-/-}$ macrophages were fully activated as compared to WT, since they produced protective, pro-inflammatory mediators at levels comparable to WT.

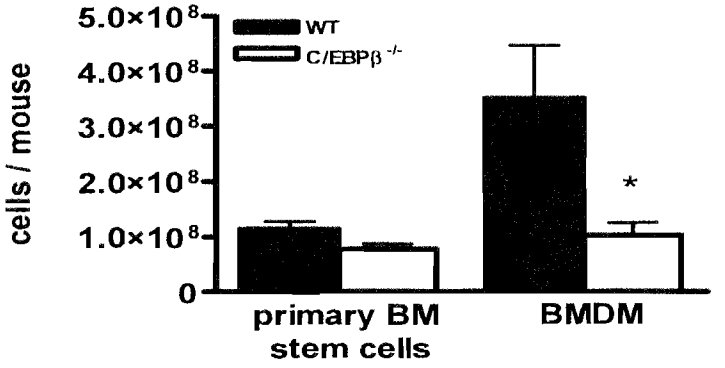


**Figure 1. Decreased *in vitro* differentiation of C/EBPβ$^{-/-}$ bone marrow stem cells into macrophages.** Bone marrow stem cells were grown for 10 days in 30% L929 conditioned media containing GM-CSF which stimulated the differentiation of the stem cells into macrophages. Data are represented as averages and SEM of 8 independent experiments (* $p$ <0.05).

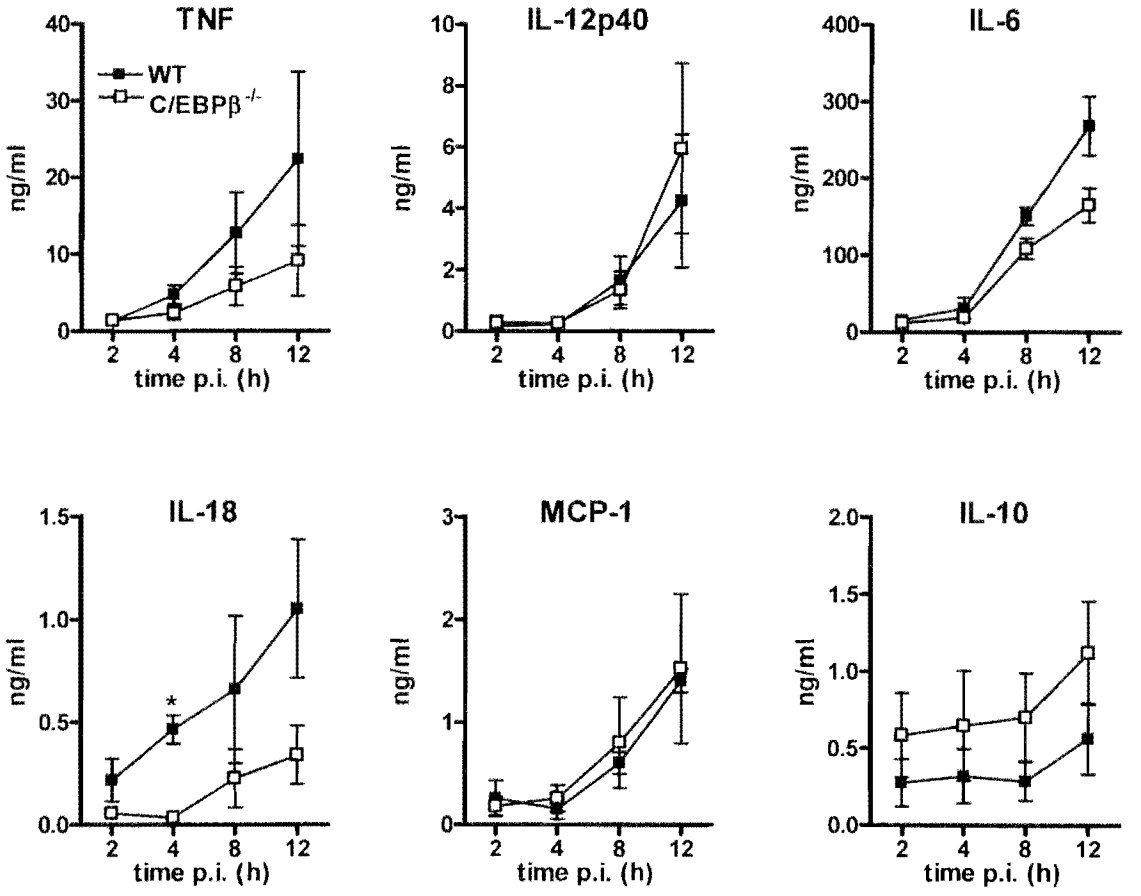


**Figure 2. Efficient induction of pro-inflammatory mediators in C/EBPβ$^{-/-}$ macrophages during *in vitro L. monocytogenes* infection.** Macrophages from WT (filled squares) and C/EBPβ$^{-/-}$ (open squares) were generated and infected with *L. monocytogenes* at MOI of 10 bacilli : 1 macrophage. Supernatants from triplicate wells were collected at 2, 4, 8 and 12 hours post-infection and levels of cytokines and chemokine MCP-1 was measured by ELISA. Data are represented as averages and SEM of 3 independent experiments done in triplicate (* $p<0.05$).

**2. Enhanced bacterial growth and increased bacterial escape from C/EBPβ$^{-/-}$ phagosomes following *L. monocytogenes* infection.**

WT and C/EBPβ$^{-/-}$ macrophages were simultaneously stimulated with IFN-γ and infected with *L. monocytogenes* for 2, 4, 8 and 12 hours. Despite having levels of nitrite, which is indicative of nitric oxide production, that were equivalent to WT (Fig. 3 A), C/EBPβ$^{-/-}$ macrophages had significantly increased bacterial growth at 4, 8 and 12 hours p.i. (Fig. 3 B). In contrast, WT macrophages were able to restrict bacterial growth and maintained a steady state plateau during the 12 hour period. Both WT and C/EBPβ$^{-/-}$ macrophages contained equivalent numbers of bacteria at 2 hours p.i., indicating no significant defect with respect to phagocytosis in the C/EBPβ$^{-/-}$ macrophages. To determine if the increased bacterial growth was due to enhanced bacterial escape from phagosomes, macrophages were infected with *Listeria* and bacterial escape measured by electron microscopy (Fig. 4). The number of bacteria in the cytoplasm or enclosed by a double membrane (phagosome) were scored and the percentage of escape calculated as described in the methods. The majority of the bacteria in the WT macrophages were confined within phagosomes (Fig. 4 A), whereas many bacilli in the C/EBPβ$^{-/-}$ macrophages were free in the cytoplasm and in the process of moving as shown by the actin "comet tails" (Fig. 4 B). Furthermore, several bacilli in the C/EBPβ$^{-/-}$ macrophages were in the process of cell division (Fig. 4 C). The C/EBPβ$^{-/-}$macrophages had significantly 30% more escaped *L. monocytogenes* in the cytoplasm than the WT (Fig. 4 D). These results demonstrated that although C/EBPβ$^{-/-}$ macrophages were activated and produced protective, pro-inflammatory mediators and nitric oxide, they were nevertheless unable to control *Listeria* growth due to their inability to confine *Listeria* within the phagosome.

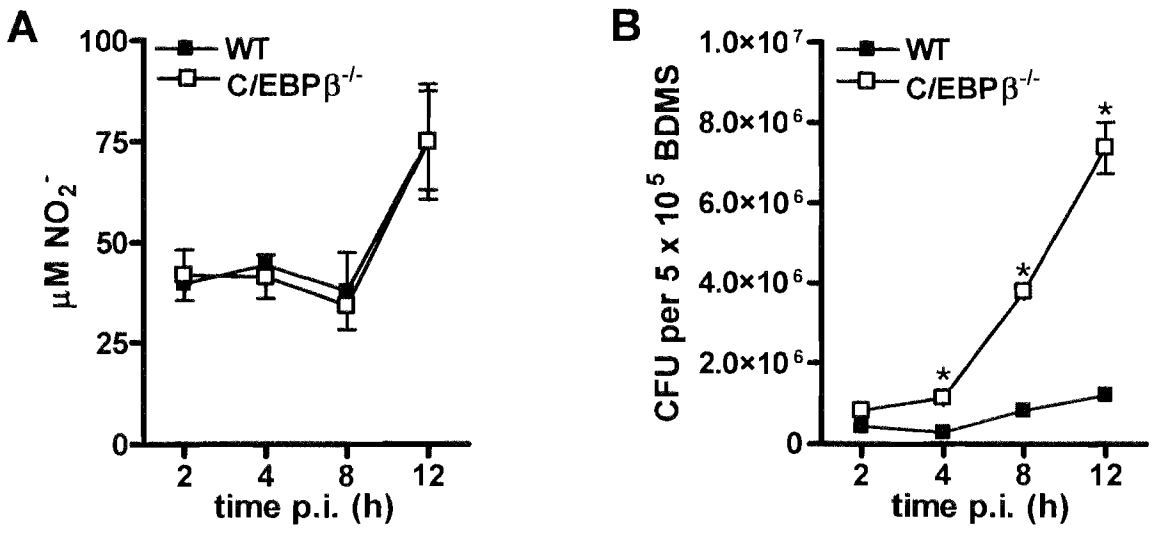


**Figure 3. Impaired bacterial killing in C/EBPβ$^{-/-}$ macrophages despite efficient induction of bactericidal mediators.** Macrophages from WT (filled squares), C/EBPβ$^{-/-}$ (open squares) were generated and infected with *L. monocytogenes*. At 2, 4, 8 and 12 hours after infection the (A) levels of nitrite, which is indicative of nitric oxide production and the (B) bacterial load were measured. Data is representative of three independent experiments (* $p<0.05$).

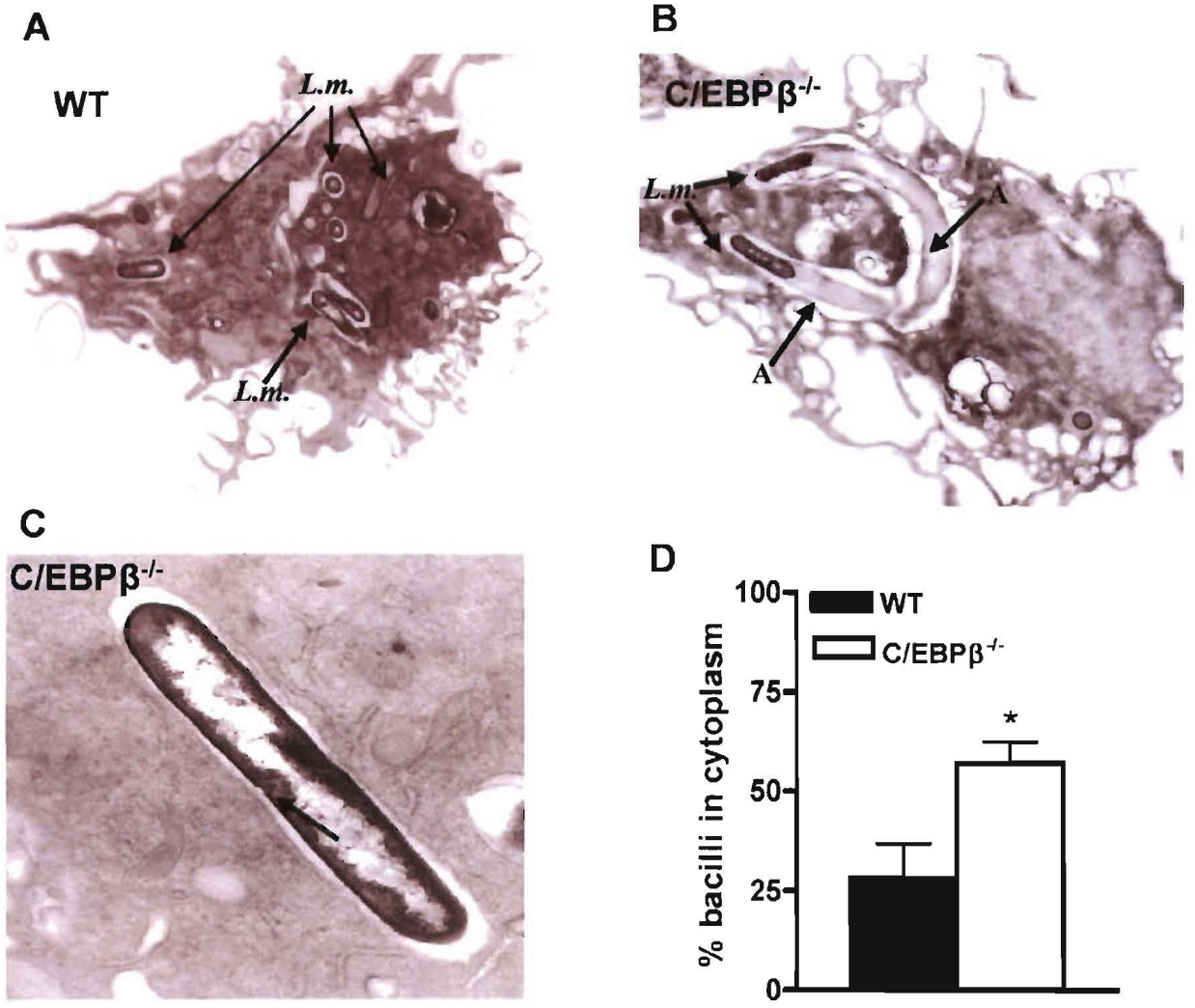


**Figure 4. Increased escape of *L. monocytogenes* from C/EBPβ$^{-/-}$ phagosomes.** WT and C/EBPβ$^{-/-}$ macrophages were infected with *L. monocytogenes* and were processed for electron microscopy at 4 hours p.i.. *L. monocytogenes* bacilli are indicated by arrows labelled *L.m.* (A) The majority of the bacilli in the WT macrophages were confined within phagosomes, whereas (B) many bacilli in C/EBPβ$^{-/-}$ macrophages were free in the cytoplasm and in the process of moving as shown by the actin "comet tails" (arrows labelled A). (C) Many of the bacilli in the C/EBPβ$^{-/-}$ macrophages were in the process of cell division, as shown by the dividing membrane (black arrow). (D) The C/EBPβ$^{-/-}$ (open bars) macrophages had significantly greater *L. monocytogenes* phagosomal escape as compared to the WT (filled bars). Electron micrographs are representative of 3 independent experiments. Data in graph (D) is the average and SEM of 3 independent experiments (* $p<0.05$). Magnification for (A) and (B) is 4400X, (C) is 20000X.

**3. Purification of total RNA from activated BMDMs infected with *L. monocytogenes***

WT and C/EBPβ$^{-/-}$ macrophages were simultaneously stimulated with IFN-γ and infected with *L. monocytogenes*. RNA extracted at 4 hours p.i. for microarray analysis, since this was earliest instance time point where a significant difference between WT and C/EBPβ$^{-/-}$ macrophage listericidal activity was observed (Fig. 3 B). Since the difference in listericidal activity was a consequence of differential expression of listericidal genes in the C/EBPβ$^{-/-}$ macrophages as compared to WT, RNA was collected for comparative microarray analysis in order to identify the listericidal genes. RNA was isolated from four independent biological experiments and DNAseI treated to get rid of contaminating genomic DNA (Fig. 5 A). The quality and quantity of the RNA was checked by denaturing gel electrophoresis (Fig. 5 B) and spectroscopy (Table 1.). The ratio of 28S to 18S eukaryotic ribosomal RNA bands were visually estimated to be approximately 2:1, indicating that the RNA was intact and of high integrity. The purity of the RNA was high for all samples as indicated by $A_{260}/A_{280}$ ratios, which for pure RNA is equal to 2.0 (14). The yield of RNA for each experiment differed and ranged from 8.2μg to 115μg. Since the standard protocols at the capar Microarray Facility required at least 50μg of total RNA for each microarray hybridization, the mRNA in each sample would have to be linearly amplified in order to generate enough sample for microarray hybridization (discussed in chapter 4).


**Figure 5. Denaturing 1% agarose gel electrophoresis of total RNA purified for microarray analysis.** WT and C/EBPβ$^{-/-}$ macrophages were activated and infected with *L. monocytogenes* and total RNA purified at 4 hours p.i.. (A) Total RNA contaminated with genomic DNA (gDNA); (B) DNAse I-treated and purified total RNA. The 28S and 18S ribosomal RNA bands are indicated. WT1 and KO1 denote the RNA extracted from WT and C/EBPβ$^{-/-}$ (KO) macrophages for the first infection experiment. The same labelling scheme applies for infection experiments 2, 3, and 4.

**Table 1. Quantification and purity of total RNA purified for microarray analysis.**

Total RNA was purified from *L. monocytogenes* infected WT and C/EBPβ$^{-/-}$ activated macrophages at 4 hours p.i.. The RNA was DNAse I treated to get rid of contaminating genomic DNA. WT1 and KO1 represent the RNA extracted from WT and C/EBPβ$^{-/-}$ (KO) macrophages for the first infection experiment. The same labelling scheme applies for infection experiments 2, 3, and 4; In the treatment column "-" refers to media controls and "+" to samples activated by IFN-γ and infected with *L. monocytogenes*.

| Experiment | Treatment | $A_{260}$ | $A_{280}$ | $A_{260}/A_{280}$ | RNA conc. (μg/μl) | yield (μg) |
|---|---|---|---|---|---|---|
| WT1 | - | 10.66 | 5.08 | 2.1 | 0.43 | 24.15 |
| WT1 | + | 8.88 | 4.21 | 2.1 | 0.36 | 19.95 |
| KO1 | - | 11.73 | 5.56 | 2.1 | 0.47 | 26.68 |
| KO1 | + | 3.90 | 1.84 | 2.1 | 0.16 | 8.20 |
| WT2 | - | 27.40 | 12.93 | 2.1 | 1.10 | 63.67 |
| WT2 | + | 32.88 | 15.51 | 2.1 | 1.32 | 76.60 |
| KO2 | - | 41.04 | 19.45 | 2.1 | 1.64 | 95.85 |
| KO2 | + | 40.66 | 19.27 | 2.1 | 1.63 | 94.96 |
| WT3 | - | 22.60 | 10.71 | 2.1 | 0.90 | 52.33 |
| WT3 | + | 11.90 | 5.67 | 2.1 | 0.48 | 27.09 |
| KO3 | - | 26.37 | 12.44 | 2.1 | 1.05 | 61.23 |
| KO3 | + | 17.93 | 8.50 | 2.1 | 0.72 | 41.32 |
| WT4 | - | 0.38 | 0.22 | 1.7 | 0.30 | 64.23 |
| WT4 | + | 0.33 | 0.18 | 1.8 | 0.26 | 55.67 |
| KO4 | - | 0.68 | 0.36 | 1.9 | 0.54 | 115.07 |
| KO4 | + | 0.49 | 0.27 | 1.8 | 0.39 | 82.89 |

In order to determine if the RNA was "biologically representative" of *in vivo* and *in vitro* data reported for C/EBPβ$^{-/-}$ mice, the induction of C/EBPβ target genes G-CSF, CLECSF9, IL-12p35 and ISGF3γ was measured by quantitative real-time RT-PCR. An aliquot of the RNA that was to be used for RNA analysis was used to make cDNA for the RT-PCR analysis. C/EBPβ was shown to be essential for the induction of G-CSF during innate immunity against *L. monocytogenes* (10), *Mycobacterium tuberculosis* (15) and *Brucella abortus* (16). G-CSF was found to be important for bactericidal killing by promoting membrane fusion between

pathogen-containing phagosomes and endosomes (16). Similarly, C/EBPβ was shown to be essential for induction of CLECSF9 in response to LPS, TNF, IL-6, and IFN-γ stimulation (12) and for IL-12p35 induction during *Candida albicans* infection (11). In addition, C/EBPβ was shown to transcriptionally induce ISGF3γ, a component of the ISGF3 protein complex that is essential for IFN signaling (13). As expected, the C/EBPβ$^{-/-}$ macrophages had impaired induction of G-CSF, CLECSF9, IL-12p35 and ISGF3γ (Fig. 6). Furthermore, the amplification of the RT-PCR products was very efficient and robust, indicating that the quality of the RNA to be used for microarray was of high quality.

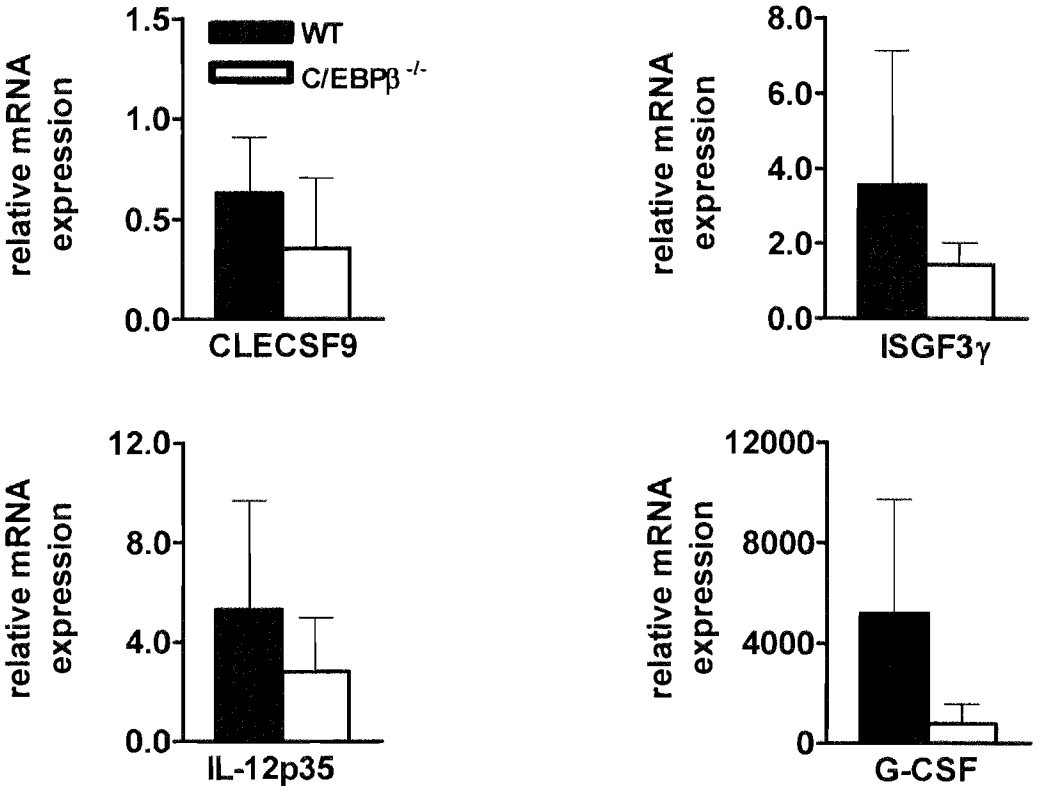


**Figure 6. Impaired induction of C/EBPβ target genes in C/EBPβ$^{-/-}$ macrophages during *L. monocytogenes* infection.** Quantitative RT-PCR of C/EBPβ target genes in WT (filled bars) and C/EBPβ$^{-/-}$ (open bars) activated macrophages at 4 hours p.i. cDNA was generated from the same batch of total RNA that was used for microarray analysis. Data represents the averages and SEM of 3 independent experiments.

**DISCCUSION**

The aims of this chapter were to establish and evaluate the *in vitro* infection of BMDMs with *L. monocytogenes*, compare the innate immune responses between infected WT and C/EBPβ$^{-/-}$ macrophages and to purify RNA from the infected WT and C/EBPβ$^{-/-}$ macrophages for comparative gene expression profiling. In this study *L. monocytogenes* was used as a model intracellular pathogen to identify macrophage genes involved in mediating listericidal activity. Host protection to *L. monocytogenes* involves the activation of macrophage bactericidal effector functions, granuloma formation and protective Th1-type responses. Key cytokines required during the innate immune phase are IFN-γ and TNF, which promote macrophage activation and production pro-inflammatory mediators and anti-microbial molecules such as ROI and RNI.

Several *in vivo* infection studies using mice deficient for iNOS, p47phox, gp91phox or both gp91phox and iNOS, showed that bacterial killing took place despite the lack of ROI and RNI (3-7). Furthermore, studies using mice deficient for genes such as IFN-γ (17, 18), IFN-γR (8, 17), ICSBP (19), IRF2 (19), RelB (20), TNFRp55 (21, 22), and C/EBPβ (10) also demonstrated that that macrophages have an alternative unknown killing mechanism that is independent of ROI or RNI. This unknown mechanism is most likely driven by IFN-γ and TNF, since these cytokines are essential for the cytocidal/cytostatic and bactericidal/bacteriostatic activity of macrophages respectively (8, 9). The most downstream molecule in this alternative killing pathway would be C/EBPβ, since the C/EBPβ$^{-/-}$ macrophages expressed normal levels of IFN-γ and TNF as compared to WT (10, 15). Furthermore, since the macrophage effector genes would most likely be downstream of C/EBPβ in the unknown killing pathway, comparative gene expression analysis between WT and C/EBPβ$^{-/-}$ macrophages infected with *Listeria* would therefore increase the probability of identifying these effector genes. However, before proceeding with the RNA extractions and the microarray experiments, several parameters of the infection experiment needed to be checked to (1) determine if the biology of the *in vitro* infection was equivalent to that of the *in vivo* infections, (2) determine the best time-point at which to extract RNA for microarray analysis and (3) purify and assess the quality of RNA to be used for microarray analysis. In order to mimic the biology of the *in vivo* infection experiments, macrophages were not pre-activated with IFN-γ prior to infection with *L. monocytogenes*. Instead, macrophages were stimulated with IFN-γ and infected with *L. monocytogenes* at the same time. This particular infection protocol was used since it reflected more closely the biology of natural infections,

where macrophages do not exist in a pre-activated state, but rather undergo activation upon infection. The biology of the *in vitro* data was assessed by measuring the production of pro-inflammatory mediators, nitric oxide, transcription of C/EBPβ target genes, phagosomal escape and listericidal activity. The generation of BMDMs from stem cells was successfully optimized, although the yield was 3 times lower for the C/EBPβ$^{-/-}$ mice. This was not unexpected, since C/EBPβ has been shown to be important for macrophage differentiation and is highly up-regulated during the differentiation process (23). Moreover, the lack of G-CSF in the C/EBPβ$^{-/-}$ bone marrow stem cells may also account for the decreased yield of bone marrow derived macrophages. Studies using G-CSF deficient (G-CSF$^{-/-}$) mice demonstrated that G-CSF is required for the differentiation of bone marrow stem cells into macrophages(24). In the G-CSF$^{-/-}$ mice, the frequency of bone marrow progenitor macrophage colony forming cells were significantly reduced as compared to WT mice, resulting in marked decreased yield of macrophages (24).

Both WT and C/EBPβ$^{-/-}$ macrophages were equivalently activated during *L. monocytogenes* infection since they both induced significantly high levels of IL-6, IL-12, IL-18, TNF and MCP-1 as compared to their media controls. Moreover, in spite of slightly higher levels of IL-10, the C/EBPβ$^{-/-}$ macrophages were activated to the same extent as WT, since there was no significant difference in the levels of induction of these pro-inflammatory mediators between these two groups. However, IL-18 levels were significantly lower in the C/EBPβ$^{-/-}$ macrophages at 4 hours p.i., but reached levels comparable to WT at later time points. Furthermore, the levels of nitrite, which is indicative of nitric oxide, were equivalent for both C/EBPβ$^{-/-}$ and WT macrophages. However, despite full macrophage activation, the C/EBPβ$^{-/-}$ macrophages had 30% greater listerial escape from the phagosome and uncontrolled bacilli growth. Kinetic analyses of macrophage activation and listericidal activity were performed at 2, 4, 8 and 12 hours after infection in order to determine the best time point to collect RNA for microarray analysis. No significant differences between the WT and C/EBPβ$^{-/-}$ macrophage activation were observed over a 12 hour period, since both groups efficiently induced protective pro-inflammatory cytokines, chemokine MCP-1 and nitric oxide. However, significant differences in listericidal activity were observed between the two groups at 4, 8 and 12 hours p.i.. Since the increased bacterial load and impaired killing in the C/EBPβ$^{-/-}$ macrophages was a consequence of differential expression of listericidal genes in C/EBPβ$^{-/-}$ macrophages as compared to WT, total RNA was therefore purified from infected samples and controls at 4 hours p.i.. The quality of the RNA was excellent, since cDNA

generated from it robustly amplified in several quantitative RT-PCR reactions using the Lightcycler, which is a real-time RT-PCR instrument that is highly sensitive to impurities and requires a high quality cDNA template. In addition, quantitative RT-PCR confirmed that C/EBPβ$^{-/-}$ macrophages had impaired induction of C/EBPβ target genes as reported in literature (10-13). All together, these results demonstrated and confirmed the phenotype of C/EBPβ$^{-/-}$ macrophages infected *in vitro* with *L. monocytogenes* was the same as reported in the literature (10-13) and therefore provided a solid foundation on which to base the gene expression profiling experiments. The infection experiment was repeated four times independently of each other and RNA extracted at 4 hours p.i. for microarray analysis.

## REFERENCES


1. Buchmeier, N. A., and R. D. Schreiber. 1985. Requirement of endogenous interferon-gamma production for resolution of Listeria monocytogenes infection. *Proc Natl Acad Sci U S A 82:7404.*
2. Havell, E. A. 1989. Evidence that tumor necrosis factor has an important role in antibacterial resistance. *J Immunol 143:2894.*
3. Endres, R., A. Luz, H. Schulze, H. Neubauer, A. Futterer, S. M. Holland, H. Wagner, and K. Pfeffer. 1997. Listeriosis in p47(phox-/-) and TRp55-/- mice: protection despite absence of ROI and susceptibility despite presence of RNI. *Immunity 7:419.*
4. Jackson, S. H., J. I. Gallin, and S. M. Holland. 1995. The p47phox mouse knock-out model of chronic granulomatous disease. *J Exp Med 182:751.*
5. Shiloh, M. U., J. D. MacMicking, S. Nicholson, J. E. Brause, S. Potter, M. Marino, F. Fang, M. Dinauer, and C. Nathan. 1999. Phenotype of mice and macrophages 4*10:29.*
6. Dinauer, M. C., M. B. Deck, and E. R. Unanue. 1997. Mice lacking reduced nicotinamide adenine dinucleotide phosphate oxidase activity show increased susceptibility to early infection with Listeria monocytogenes. *J Immunol 158:5581.*
7. MacMicking, J. D., C. Nathan, G. Hom, N. Chartrain, D. S. Fletcher, M. Trumbauer, K. Stevens, Q. W. Xie, K. Sokol, N. Hutchinson, and et al. 1995. Altered responses to bacterial infection and endotoxic shock in mice lacking inducible nitric oxide synthase. *Cell 81:641.*
8. Dai, W. J., W. Bartens, G. Kohler, M. Hufnagel, M. Kopf, and F. Brombacher. 1997. Impaired macrophage listericidal and cytokine activities are responsible for the rapid death of Listeria monocytogenes-infected IFN-gamma receptor-deficient mice. *J Immunol 158:5297.*
9. Mielke, M. E., S. Ehlers, and H. Hahn. 1993. The role of cytokines in experimental listeriosis. *Immunobiology 189:285.*
10. Tanaka, T., S. Akira, K. Yoshida, M. Umemoto, Y. Yoneda, N. Shirafuji, H. Fujiwara, S. Suematsu, N. Yoshida, and T. Kishimoto. 1995. Targeted disruption of the NF-IL6 gene discloses its essential role in bacteria killing and tumor cytotoxicity by macrophages. *Cell 80:353.*
11. Gorgoni, B., D. Maritano, P. Marthyn, M. Righi, and V. Poli. 2002. C/EBP beta gene inactivation causes both impaired and enhanced gene expression and inverse regulation of IL-12 p40 and p35 mRNAs in macrophages. *J Immunol 168:4055.*
12. Matsumoto, M., T. Tanaka, T. Kaisho, H. Sanjo, N. G. Copeland, D. J. Gilbert, N. A. Jenkins, and S. Akira. 1999. A novel LPS-inducible C-type lectin is a transcriptional target of NF-IL6 in macrophages. *J Immunol 163:5039.*
13. Weihua, X., J. Hu, S. K. Roy, S. B. Mannino, and D. V. Kalvakolanu. 2000. Interleukin-6 modulates interferon-regulated gene expression by inducing the ISGF3 gamma gene using CCAAT/enhancer binding protein-beta(C/EBP-beta). *Biochim Biophys Acta 1492:163.*
14. Sambrook, J., and D. W. Russell. 2001. *Molecular cloning : a laboratory manual.* Cold Spring Harbor Laboratory Press, Cold Spring Harbor, N.Y.
15. Sugawara, I., S. Mizuno, H. Yamada, M. Matsumoto, and S. Akira. 2001. Disruption of nuclear factor-interleukin-6, a transcription factor, results in severe mycobacterial infection. *Am J Pathol 158:361.*
16. Pizarro-Cerda, J., M. Desjardins, E. Moreno, S. Akira, and J. P. Gorvel. 1999. Modulation of endocytosis in nuclear factor IL-6(-/-) macrophages is responsible for a high susceptibility to intracellular bacterial infection. *J Immunol 162:3519.*

17. Huang, S., W. Hendriks, A. Althage, S. Hemmi, H. Bluethmann, R. Kamijo, J. Vilcek, R. M. Zinkernagel, and M. Aguet. 1993. Immune response in mice that lack the interferon-gamma receptor. *Science 259:1742.*
18. Harty, J. T., and M. J. Bevan. 1995. Specific immunity to Listeria monocytogenes in the absence of IFN gamma. *Immunity 3:109.*
19. Fehr, T., G. Schoedon, B. Odermatt, T. Holtschke, M. Schneemann, M. F. Bachmann, T. W. Mak, I. Horak, and R. M. Zinkernagel. 1997. Crucial role of interferon consensus sequence binding protein, but neither of interferon regulatory factor 1 nor of nitric oxide synthesis for protection against murine listeriosis. *J Exp Med 185:921.*
20. Weih, F., D. Carrasco, S. K. Durham, D. S. Barton, C. A. Rizzo, R. P. Ryseck, S. A. Lira, and R. Bravo. 1995. Multiorgan inflammation and hematopoietic abnormalities in mice with a targeted disruption of RelB, a member of the NF-kappa B/Rel family. *Cell 80:331.*
21. Pfeffer, K., T. Matsuyama, T. M. Kundig, A. Wakeham, K. Kishihara, A. Shahinian, K. Wiegmann, P. S. Ohashi, M. Kronke, and T. W. Mak. 1993. Mice deficient for the 55 kd tumor necrosis factor receptor are resistant to endotoxic shock, yet succumb to L. monocytogenes infection. *Cell 73:457.*
22. Rothe, J., W. Lesslauer, H. Lotscher, Y. Lang, P. Koebel, F. Kontgen, A. Althage, R. Zinkernagel, M. Steinmetz, and H. Bluethmann. 1993. Mice lacking the tumour necrosis factor receptor 1 are resistant to TNF-mediated toxicity but highly susceptible to infection by Listeria monocytogenes. *Nature 364:798.*
23. Natsuka, S., S. Akira, Y. Nishio, S. Hashimoto, T. Sugita, H. Isshiki, and T. Kishimoto. 1992. Macrophage differentiation-specific expression of NF-IL6, a transcription factor for interleukin-6. *Blood 79:460.*
24. Lieschke, G. J., D. Grail, G. Hodgson, D. Metcalf, E. Stanley, C. Cheers, K. J. Fowler, S. Basu, Y. F. Zhan, and A. R. Dunn. 1994. Mice lacking granulocyte colony-stimulating factor have chronic neutropenia, granulocyte and macrophage progenitor cell deficiency, and impaired neutrophil mobilization. *Blood 84:1737.*

## CHAPTER 4

## IDENTIFICATION OF GENES INVOVLED IN MACROPHAGE EFFECTOR FUNCTIONS AGAINST *L. MONOCYTOGENES* BY DNA MICROARRAY.


### SUMMARY

The anti-listerial transcriptional response of IFN-γ-activated macrophages from WT and C/EBPβ$^{-/-}$ mice infected with *L. monocytogenes* was successfully profiled at 4h post-infection using oligonucleotide microarrays. Image analysis revealed that there were several quality and printing defects which resulted in systematic variation within and between the arrays. A sequential normalization procedure within and between arrays was used to remove, as much as possible, systematic variation from the data. However, statistical evaluation of the normalized microarray data showed that the technical reproducibility within each array and between replicate experiments was poor. Removal of questionable and unreliable data increased the reproducibility and reliability of the microarray data, although it did necessitate trimming 49% of the genes from the data set. Despite the poor performance on statistical level, the microarray data still contained biologically meaningful data. For example, genes encoding several pro-inflammatory cytokines, chemokines, iNOS and genes important for macrophage activation and MHC class II presentation were significantly up-regulated in both the WT and C/EBPβ$^{-/-}$ infected macrophages. Moreover, the induction of C/EBPβ and its target genes, G-CSF, CLECSF9, IL-12p35 and ISGF3γ was impaired in the C/EBPβ$^{-/-}$ macrophages. Differentially expressed (DE) genes were identified by a two sample paired T-Test based on permutation rather than distribution. A Bonferroni correction was applied to the p values to adjust for multiple testing. Five percent (1268 genes) of the mouse genome was differentially expressed between the WT and C/EBPβ$^{-/-}$ activated macrophages infected with *L. monocytogenes*. Functional clustering of genes showed that 2.0% of the DE genes were involved in host immunity and defense, 3.1% in the production of ROI, 4.6% in the regulation of transcription, 16.1% in signalling and 8.9% were involved in phagosome maturation, phago-lysosome fusion. Moreover, promoter analysis identified that 18.0% of the DE genes had putative binding sites for C/EBPβ and 47.3% had binding sites for transcription factors that interacted with C/EBPβ. A focused functional clustering strategy was used to reduce the number of candidate genes from 1268 down to 220 genes. Literature profiling of these 220 candidate genes revealed that several were already published in literature to play a role in defense against *L. monocytogenes*. Since the aim of the microarray experiment was to identify

listericidal genes in the activation and killing pathway downstream of C/EBPβ, PKCδ was considered the most promising candidate gene since it is involved in humoral defense, immune signalling and production of superoxide. Moreover, PKCδ is involved in the regulation of transcription and promoter analysis revealed that it may itself be a transcriptionally regulated by C/EBPβ. In B cells stimulated with LPS, PKCδ was shown to negatively regulate C/EBPβ transcriptional activity. Studies by Wadsworth and Goldfine using rottlerin, a putative specific PKCδ inhibitor, indirectly suggested that PKCδ promoted phagosomal escape however no direct evidence showing a correlation between the listerial phagosomal escape and PKCδ activity was presented. Furthermore, the up-regulation of PKCδ in the highly susceptible C/EBPβ$^{-/-}$ macrophages infected with *L. monocytogenes* was validated by quantitative RT-PCR. Taken together, these data suggested that PKCδ may be detrimental to the host during *L. monocytogenes* infection, however this premise has never been tested. Since the role of PKCδ in innate immunity to intracellular pathogens has not been directly investigated to date, the PKCδ gene deficient mouse model was used in the current study to functionally characterize the role of PKCδ during *L. monocytogenes* infection. PKCδ gene deficient mice were used rather than rottlerin, since this putative PKCδ specific inhibitor has been reported to non-specifically inhibit several other kinases and non-kinase enzymes (1, 2).

## RESULTS

### 1. RNA Amplification, Labelling and hybridization to MEEBO Oligonucleotide Microarrays

Total RNA was purified from *L. monocytogenes* infected WT and C/EBPβ$^{-/-}$ activated macrophages at 4 hours p.i. The total RNA was DNAseI treated and re-purified to get rid of contaminating genomic DNA, salts and phenol which may inhibit cDNA synthesis. Although the quality of the RNA was excellent as discussed in Chapter 3, the yield was too low for standard microarray protocols used at the capar Microarray Facility, which required at least 50μg total RNA for each hybridization. This is a common problem with gene expression profiling by microarray. Routinely 10 to 100∝g of total RNA or 2 to 5∝g of mRNA for each sample is required for a single labeling and hybridization reaction. To overcome this limitation, especially in the case of gene expression analysis of small biopsies, fine needle aspiration or laser capture microdissection samples, a linear RNA amplification method was developed by van Gelder et al (3). In this method, the mRNA in the total RNA sample is reverse transcribed into double stranded DNA using oligo-d(T) primers that contain a T7 RNA polymerase promoter 5' to the polythymidyate (d(T)) region. After second-strand cDNA synthesis, a T7 RNA polymerase is used to generate amplified anti-sense RNA (aRNA). However, one major concern of this procedure is the fidelity of the amplification process, since not all mRNAs may amplify equally well. Unequal amplification of RNA could lead to the erroneous identification of genes as being differentially expressed when in fact their differential expression is due to biased RNA amplification rather than biology. Hypothetically, there may be two kinds of biases during the RNA amplification procedure. The first bias may be sequence-dependent which is caused by the complicated secondary structure of RNA, the full length of the mRNA, the length of polyA tail and/or the sequence-specific efficiency of the T7 RNA polymerase. These sequence-dependent biases could change the relative mRNA abundance for some genes in the amplified RNA. The second bias may be abundance-dependent and is caused by the copy number of the RNA. Since the mRNA copy numbers are different between the test sample and the reference sample, the resulting ratios may not depict the true expression profile of the two samples. A study by Li et al showed that biases introduced in the processes of RNA amplification were minimal and were sequence-dependent but not abundance-dependent (4). Several groups have also shown that the biases introduced during the RNA amplification procedure are minimal (5, 6). In one of these studies, the differential expression of only 3-4 % of genes identified as being outliers,

could not be validate by quantitative RT-PCR (6). Moreover, RNA amplification has been reported to improve the reproducibility of microarray expression profiles for a wide range of RNA inputs (5, 6). However, it is prudent to test if linear amplification has taken place by spiking the RNA amplification reactions with different doses of control RNAs e.g. Lucidea doping controls from Amersham Biosciences. Furthermore, to ensure that genes identified as outliers are truly differentially expressed, it is important to quantitate their expression levels in the unamplified RNA from the same batch of RNA that was used for RNA amplification and microarray hybridization. Therefore, in this study, the mRNA fraction of the total RNA was linearly amplified to generate enough probe for microarray analysis. However, at the time of the microarray experiments in this study, these doping RNA controls were not available. Therefore the linearity of the RNA amplification procedure could not be assessed.

First strand cDNA was successfully reversed transcribed using oligo d(T) primers that contained a T7 promoter sequence. Second strand cDNA synthesis converted the single-stranded cDNA into double-stranded cDNA that was then *in vitro* transcribed using T7 RNA polymerase to synthesize aRNA. During the *in vitro* transcription (IVT) amplification reaction, amino allyl modified dUTP (aaUTP) was incorporated into the aRNA at a ratio of 1 UTP:1 aaUTP. The aaUTP contained a reactive primary amino group on the C5 position of the uracil that could be chemically coupled to N-hydroxysuccinimidyl ester-derivatized dyes (NHS dyes) such as Cy3 and Cy5. The amplification of the RNA samples was highly successful as shown by the excellent yields, quality and purity: the amplified RNA (aRNA) appeared as a smear extending above the 28S rRNA band to just above the 5S rRNA band, and was of high quality since no degradation was observed (Fig. 1). The purity of the aRNA was excellent as revealed by $A_{260}/A_{280}$ ratios that were close to 2.0 (Table 1). Furthermore, the yield of aRNA was exceptionally good, since >100µg aRNA was generated from 1µg of total RNA (Table 1). The purified aRNA was successfully labelled with either Cy3 or Cy5 via a coupling reaction between the amino ally modified UTP residues on the aRNA and the amine reactive Cy-dyes. The frequency of dye incorporation (FOI) into the purified aRNA was excellent and between 39-57 dye molecules were incorporated per 1000 nucleotides of aRNA (Table 2). The yield, quality and dye-labelling of the aRNA probes was first-rate, and the microarray hybridization step was proceeded with confidence.

Before hybridization of the labelled aRNA, the arrays were prehybridized to wash away any unbound oligonucleotides that did not bind to the slide during to the printing process. In addition, the prehybridization step reduced non-specific background hybridization by

blocking the reactive groups on the surface of the slide which could have bound labelled aRNA. Furthermore, in order to reduce evaporation of the labelled aRNA, the hybridizations were carried out at 42°C. However, it was later discovered that the hybridization apparatus used was inadequate as it did not maintain the temperature at 42°C throughout the hybridization step. Instead, the hybridization apparatus, a plastic container filled with water pre-warmed to 42°C placed in a hybridization oven heated to 42°C, cooled to 35°C. Unfortunately since, half of the experiment (4 microarrays) had already been processed using the faulty system and economic constraints did not allow for repeat hybridizations, it was decided to process the remaining experiments under the same conditions to maintain consistency. Moreover, since the hybridization buffer contained 50% formamide, it was hoped that any non-specific hybridization due to the lower temperature would be prevented by the high percentage of formamide in the hybridization buffer. Consequently a calibrated waterbath set at 42°C was set up for future hybridizations in the capar microarray facility.

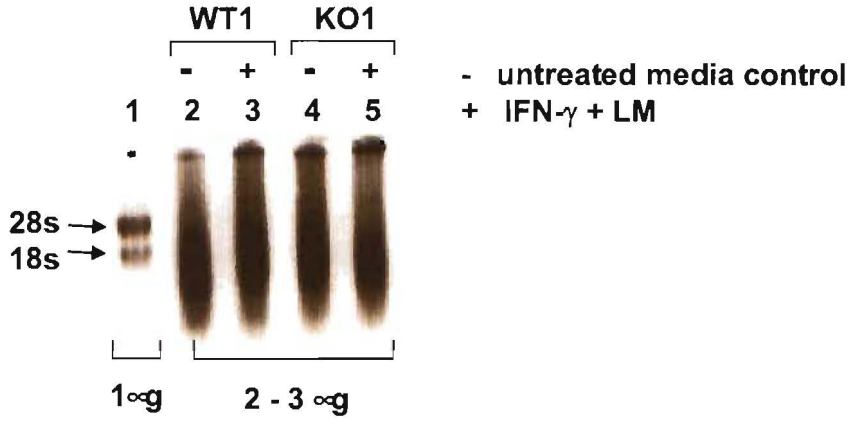


**Figure 1. Denaturing 1% agarose gel electrophoresis of purified aRNA.**

Shown is an example of high quality aRNA that is representative of all samples used in the microarray experiment. Lane 1 contains 1μg total RNA; lanes 2 – 5 contains 2-3μg of aRNA generated from RNA isolated from WT and C/EBPβ$^{-/-}$ (KO) macrophages from the first biological experiment that were either untreated media controls (-) or activated with IFN-γ and infected with *L. monocytogenes* (+). Arrows indicate the position of the rRNA bands

**Table 1. Quality and yield of purified unlabelled aRNA.** Purified total RNA (1μg) was reversed transcribed using oligo d(T) primers that contained a T7 promoter sequence. Second strand cDNA synthesis converted the single-stranded cDNA into double-stranded cDNA that was then *in vitro* transcribed (IVT) using T7 RNA polymerase to synthesize aRNA. WT1 and KO1 represent aRNA samples from the first biological infection experiment. The same labelling scheme applies for infection experiments 2, 3, and 4. In the treatment column "-" refers to untreated media controls and "+" refers to samples activated by IFN-γ and infected with *L. monocytogenes*.

| Sample | Treatment | $A_{260}$ | $A_{280}$ | $A_{260}/A_{280}$ | Conc. (μg/μl) | Yield (μg) |
|---|---|---|---|---|---|---|
| KO1 | + | 16.76 | 8.14 | 2.06 | 0.67 | 134.10 |
| KO1 | - | 19.38 | 9.50 | 2.04 | 0.78 | 155.06 |
| WT1 | + | 34.57 | 16.78 | 2.06 | 1.73 | 172.86 |
| WT1 | - | 29.54 | 14.20 | 2.08 | 1.48 | 147.71 |
| KO2 | + | 19.98 | 9.65 | 2.07 | 0.80 | 159.80 |
| KO2 | - | 16.33 | 7.96 | 2.05 | 0.65 | 130.62 |
| WT2 | + | 23.40 | 11.36 | 2.06 | 0.94 | 187.20 |
| WT2 | - | 15.28 | 7.31 | 2.09 | 0.61 | 122.24 |
| KO3 | + | 20.55 | 10.08 | 2.04 | 0.82 | 164.42 |
| KO3 | - | 18.17 | 8.95 | 2.03 | 0.73 | 145.32 |
| WT3 | + | 19.41 | 9.56 | 2.03 | 0.78 | 155.24 |
| WT3 | - | 19.35 | 9.53 | 2.03 | 0.77 | 154.84 |
| KO4 | + | 10.83 | 5.44 | 1.99 | 0.43 | 86.66 |
| KO4 | - | 14.00 | 7.11 | 1.97 | 0.56 | 112.00 |
| WT4 | + | 20.54 | 10.27 | 2.00 | 0.82 | 164.34 |
| WT4 | - | 15.77 | 7.88 | 2.00 | 0.63 | 126.14 |

**Table 2. Frequency of Cy-dye incorporation into purified labelled aRNA.** Purified aRNA from WT and C/EBPβ$^{-/-}$ (KO) macrophages were labelled with either Cy3 or Cy5 via a coupling reaction between the amino ally modified UTP residues on the aRNA and the amine reactive Cy-dyes. WT1 and KO1 represent aRNA samples from the first biological infection experiment. The same labelling scheme applies for infection experiments 2, 3, and 4. In the treatment column "-" refers to untreated media controls and "+" refers to samples activated by IFN-γ and infected with *L. monocytogenes*. The frequency of incorporation (FOI) represents the number of Cy dye molecules incorporated per 1000 nucleotides. (nd = not determined)

| Sample | Treatment | Dye Label | $A_{260}/A_{280}$ | $A_{260}$ | $A_{550}$ (Cy3) | $A_{650}$ (Cy5) | aRNA (µg) | FOI |
|---|---|---|---|---|---|---|---|---|
| KO1 | + | Cy3 | 2.06 | 0.259 | 0.238 | nd | 19.17 | 55 |
| KO1 | - | Cy5 | 2.04 | 0.263 | nd | 0.323 | 19.46 | 44 |
| WT1 | + | Cy5 | 2.06 | 0.286 | nd | 0.321 | 21.16 | 40 |
| WT1 | - | Cy3 | 2.08 | 0.273 | 0.227 | nd | 20.20 | 50 |
| KO2 | + | Cy5 | 2.07 | 0.252 | nd | 0.309 | 18.65 | 44 |
| KO2 | - | Cy3 | 2.05 | 0.281 | 0.24 | nd | 20.79 | 51 |
| WT2 | + | Cy3 | 2.06 | 0.279 | 0.241 | nd | 20.65 | 52 |
| WT2 | - | Cy5 | 2.09 | 0.26 | nd | 0.347 | 19.24 | 48 |
| KO3 | + | Cy3 | 1.74 | 0.235 | 0.175 | nd | 17.39 | 45 |
| KO3 | - | Cy5 | 1.78 | 0.281 | nd | 0.309 | 20.79 | 40 |
| WT3 | + | Cy5 | 1.85 | 0.245 | nd | 0.268 | 18.13 | 39 |
| WT3 | - | Cy3 | 1.76 | 0.284 | 0.194 | nd | 21.02 | 41 |
| KO4 | + | Cy5 | 1.86 | 0.115 | nd | 0.138 | 8.51 | 43 |
| KO4 | - | Cy3 | 1.69 | 0.106 | 0.097 | nd | 7.84 | 55 |
| WT4 | + | Cy3 | 1.73 | 0.106 | 0.1 | nd | 7.84 | 57 |
| WT4 | - | Cy5 | 1.92 | 0.106 | nd | 0.128 | 7.84 | 44 |

**2. Scanning and Image Analysis**

After washing away unbound labelled aRNA probe, the microarray arrays were scanned using optimized photo-multiplier-tube (PMT) settings so that the overall fluorescence in the red and green channels were balanced. Scanned microarray images were saved and analyzed using GenePix 5.1 software. The image analysis process consisted of three general steps: (i) the addressing/gridding step where the co-ordinates and identity of each spot on the array were defined, (ii) segmentation step where pixels were classified as either foreground (within the printed spot) or background and (iii) intensity extraction where the red and green fluorescence foreground and background intensity pairs were calculated for each spot.

The addressing for each spot was difficult, because many of the grids were printed slightly "skew" resulting in displacement of spots from the expected location. These displacements and irregular spacing of spots were most likely caused by misalignment of the gridding robot and/or bent damaged pins. Furthermore, only 50% to 60% of the spots on the arrays gave a detectable fluorescent signal. Consequently the "missing" spots were flagged as "not found" during the addressing step. Segmentation for each spot on the arrays was done by manual alignment using the single irregular and/or the regular feature tool. This method was chosen because it allowed the diameter of the "circle" that defined the foreground of the spot to be estimated independently of other spots. Moreover, the segmentation algorithm implemented by this feature did not place restrictions on the shape of the spot, and efficiently allowed spots that were oval or irregularly shaped to be defined. The intensity extraction step was automatically carried out by the GenePix software, and was based on the principle that (i) each pixel in a scanned image represented the level of hybridization at a specific location on the slide and (ii) that the total amount of hybridization for a particular spotted DNA sequence was proportional to the total fluorescence at the spot. The natural measure of spot intensity was therefore the sum of pixel intensities within the spot. The background fluorescence for each spot was estimated by measuring the local background intensity in the region that was furtherest away from all four surrounding spots. In addition, the GenePix software also calculated other quality control metrics for spot size, morphology and flags.

Visual inspection of the scanned fluorescent microarray images revealed several quality and printing defects summarized in Table 3. For example, several bright spots on the arrays had comet tails that masked the true signal of surrounding spots (Fig. 2 A). About 10% of the spots on the array were either printed on top of each other or merged into each other (Fig. 2 B, C), resulting in significant loss of data. This was particularly bad in grid number 31 for all arrays, where spots within the first 8 rows had merged (Fig. 2 C), most likely due to misalignment of the gridding robot and/or bent/damaged printing pins. The general size and morphology of the spots were inconsistent over the whole array and several dilated spots were observed (Fig. 2. D). Furthermore, several grids were printed skew, resulting in irregular spot-to-spot spacing within the 35x35 array, which made the assignment of gene IDs difficult.

**Table 3. Summary of visual quality and printing issues for all arrays.** Visual inspection of fluorescent microarray images revealed several quality and printing defects. The severity of each problem was rated by + signs, where + is present, + + bad and + + + very bad.

| | WT1 | WT2 | WT3 | WT4 | KO1 | KO2 | KO3 | KO4 |
|---|---|---|---|---|---|---|---|---|
| Comet tails | + + + | + + | + + | + | + + | + + | + | + |
| Merged spots | + + + | + + + | + + + | + + + | + + + | + + + | + + + | + + + |
| Spots on top of each other | + + + | + + + | + + + | + + + | + + + | + + + | + + + | + + + |
| Missing spots | + | + | + | + | + | + | + | + |
| Dilated spots | + | + | + | + | + | + | + | + |
| Displaced spots | + | + | + | + | + | + | + | + |
| Particle contamination | + | + | + + | + | + | + + + | + | + + + |
| Irregular morphology | + | + | + | + | + | + | + | + |

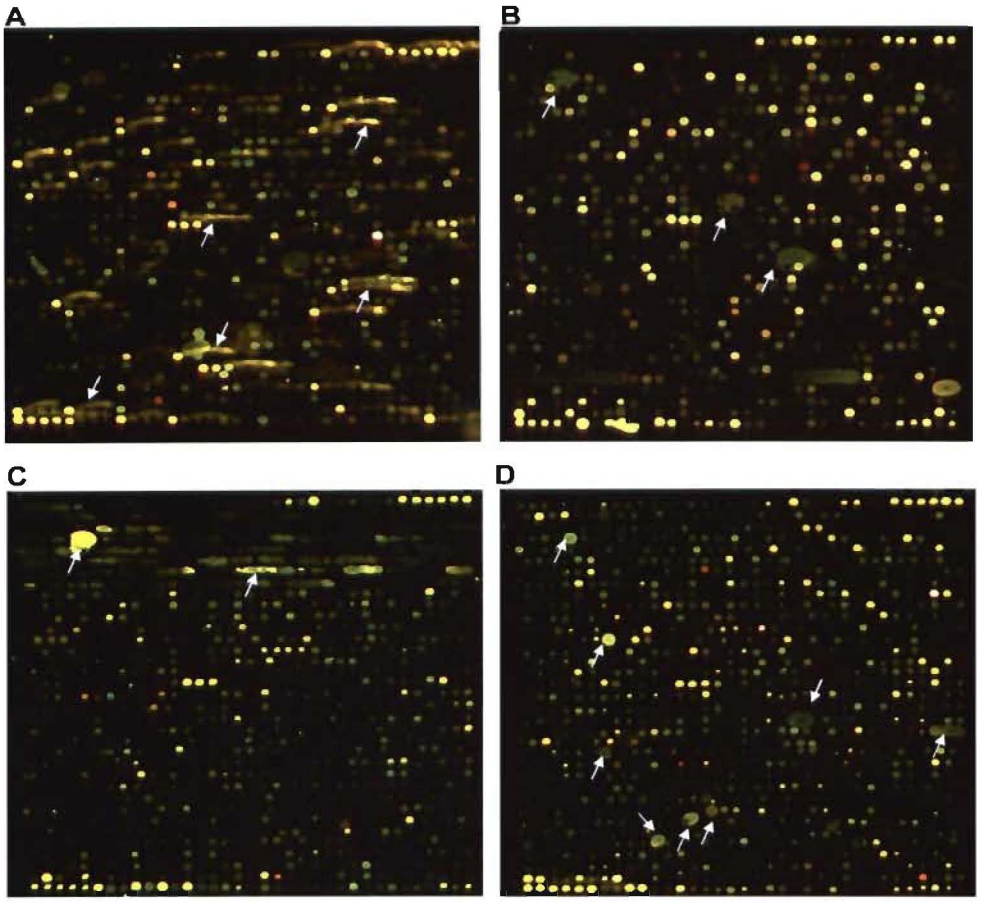


**Figure 2. Microarray Printing and Quality Issues.** Visual inspection of the fluorescent images revealed that the arrays had several quality and printing defects (arrows) as demonstrated by (A) comet tails that streak out from bright spots, (B) spots printed on top of each other that consequently spread out (C) spots that merged into each other and (D) dilated spots. Shown here are grids from the array for the third biological experiment where the aRNA from WT macrophages untreated (media controls; labelled with green Cy3) or activated with IFN-γ and infected with *L. monocytogenes* (labelled with red Cy5) was compared. Each square represents a grid of genes that were printed in 35 x 35 array and each microarray contained 32 grids. Each fluorescent spot represents an individual gene. Spots that appear yellow indicate that the particular gene is expressed in both the untreated macrophages and IFN-γ activated and *L. monocytogenes* infected macrophages. Green or red spots indicate that the gene is expressed only in the untreated macrophages or the IFN-γ and infected macrophages respectively. Shown in A, B, C and D are grids 5, 25, 32 and 4 respectively for array WT3.

The reasons for the observed printing defects can only be speculated since the arrays were printed by the capar Microarray facility and the physical printing process was not part of this dissertation. The comet tails may have been caused by (i) printing too high a concentration of DNA resulting in overloading the binding capacity of the slide, (ii) inadequate fixation of DNA to the slide due to poor UV cross-linking or inadequate baking, (iii) poor post-print washing technique and/or (iv) damaged and/or defective printing pins which delivered an excessive amount of DNA during the printing process. In addition, some of the above defects may also have been worsened by the hybridization of very highly expressed genes in the samples or by accidental movement of the coverslip while adding the labelled probes to the array. Misalignment of the gridding robot and bent/damaged printing pins may have accounted for spots being printed with irregular spacing resulting in "skew grids", as well as causing spots to be printed on top of each other and merging together. Moreover, damaged, bent and/or blocked printing pins may have delivered excessive amount of DNA to spots, causing them to "bleed out" due to capillary action resulting in dilated spots. In addition, some of the spots could not be addressed (i.e. given a gene ID) since they were not printed in the expected location. Consequently several spots could not be confidently identified and were classified as "missing". However, several "displaced" spots that were printed in a position other than their expected location could still be confidently identified. For example, a spot printed equidistantly between the expected location for gene A and gene B can not confidently be given the identity of either gene A or B. However, a spot printed off centre from the expected location of gene A can be confidently addressed as gene A. Furthermore, some of the above defects may also have been worsened by "human handling techniques" where particle contamination from dust in the work area, gloves or particulates in the wash buffers may have been introduced.

Although hybridization of the labelled probes was performed at 35°C instead of 42°C, no noticeable non-specific hybridization was observed by eye. Open "non-fluorescent" areas indicated that not every spot on the array had bound labelled probe, which would be expected if non-specific binding had taken place. Moreover, several bright green or red spots were observed, indicating that differentially expressed RNAs had bound specifically to their oligonucleotide target spot on the array (Fig. 3.). Had non-specific binding taken place, the background fluorescence may have been high and the majority of the spots on the array would have fluoresced yellow. Although there were several quality issues, the array still contained biologically meaningful data, since induction of pro-inflammatory genes was clearly up-regulated in the "treated" samples and appeared as bright green or red spots depending on the

Cy-dye label of the treated sample (Fig. 3). Moreover, since most of the negative control genes did not have any significant fluorescent signal above background, the specificity of the hybridization reaction, despite the low temperature of 35°C, appeared to be reliable. Once the grids were aligned for each spot, the fluorescent intensity for each spot and its estimated background fluorescence was measured and exported as a "GenePix Results" (.gpr) file for analysis.

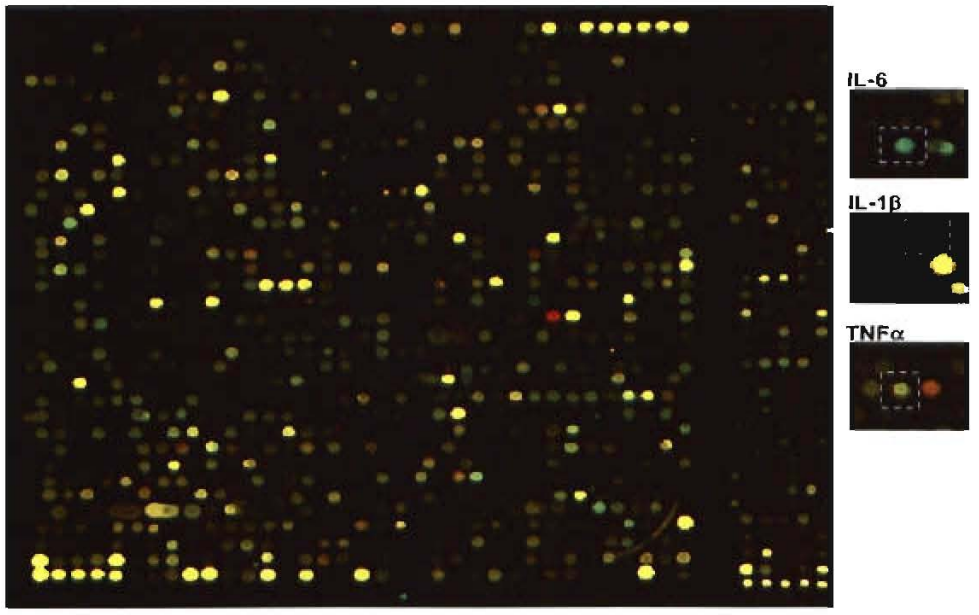


**Figure 3. Apparent specific hybridization at 35°C.** Although hybridization of the labelled probes was performed at 35°C instead of 42°C, no noticeable non-specific hybridization was observed. Several bright green or red spots can be seen, indicating that differentially expressed aRNAs have bound specifically to their oligonucleotide target spot on the array. Differential hybridization of pro-inflammatory genes known to be induced in activated macrophages during *L. monocytogenes* infection can be seen: the levels of mRNA for IL-6, IL-β and TNF in macrophages activated with IFN-γ and infected with *L. monocytogenes* (labelled with green Cy3) was much higher than in the untreated macrophages (labelled red with Cy5), and these spots therefore appeared bright green. Shown is a grid 10 of 32 from the WT2 array for the second biological experiment where the aRNA from WT macrophages untreated or activated with IFN-γ and infected with *L. monocytogenes* was compared. The insets for IL-6, IL-β and TNF are taken from grids 24, 25 and 16 respectively from WT2 array.

### 3. Identification and Normalization of Systematic Bias

Visual inspection of the fluorescent images revealed that there were several quality issues and systematic biases. In order to accurately and precisely measure gene expression changes, it was important to remove any systematic variation in the microarray data that may obscure the true experimental variation between the WT and C/EBPβ$^{-/-}$ infected macrophages. If the systematic variation was not removed, it may have resulted in the failure to identify truly differentially expressed genes (false negatives), as well as in the identification of genes not truly differentially expressed between the two samples (false positives). The goal of normalization was to identify and remove these systematic variations while retaining the biological information. However, complex normalization procedures may also remove biological information. To avoid this, a simple sequential normalization procedure was followed as recommended by Wit and McClure (7): first the data within each array was normalized followed by normalization of data between all the arrays. Furthermore, a specific sequence of steps was followed for the within-array normalization: first spatial effects were removed, then the background corrected and lastly dye bias effects were removed. Thereafter between-array normalization re-scaled the data across all arrays. All image and normalization procedures were conducted in the R version 2.2.0. environment for statistical computing and programming (8) using packages BioConductor (9), Limma (10-12) and Smida (7).

Sources of systematic variation (not related with variation due to biological causes) include: (i) differences in the labelling (i.e. dye biases), (ii) differences in the sample preparation, (iii) differences in the hybridization, (iv) differences in the photo-detection and (v) auto-fluorescence. The most common systematic variation is caused by dye bias, where the red channel intensities tend to be lower than the green channel intensities. The Cy3 and Cy5 dyes used for labeling the aRNA probes have slightly different physical properties with respect to their quantum yield, size, half-life, heat- and light-sensitivity. These differences resulted in differential incorporation of the dyes into the labeled aRNA and differential hybridization of the labeled aRNA probes onto the array. Furthermore, the imbalance between the red and green spot intensities was not constant for all spots within and between arrays. Red (Cy5) and green (Cy3) spot intensities varied as a result in differences of location of the spot on the array, the arraying pins used and experimental variation in the hybridization process. As a consequence the red and green channels of the array had slightly different efficiencies, which made direct comparison of the gene expression data unfeasible.

Dye-swap normalization is often used to normalize for dye biases, where hybridizations are repeated twice with dyes swapped and the expression value for each spot over the Cy3 and Cy5 channel are averaged. However, the dye bias effects often differ from array to array and there is no guarantee that dye swap normalization effectively removes the dye bias. Moreover, dye swap experiments were not economically feasible. Therefore in this study, a "balanced dye" approach was used, where each treatment condition for all four biological replicates were labelled equally often with the Cy3 dye as with the Cy5 dye (Fig. 4). In this manner the dye labelling bias was compensated for.

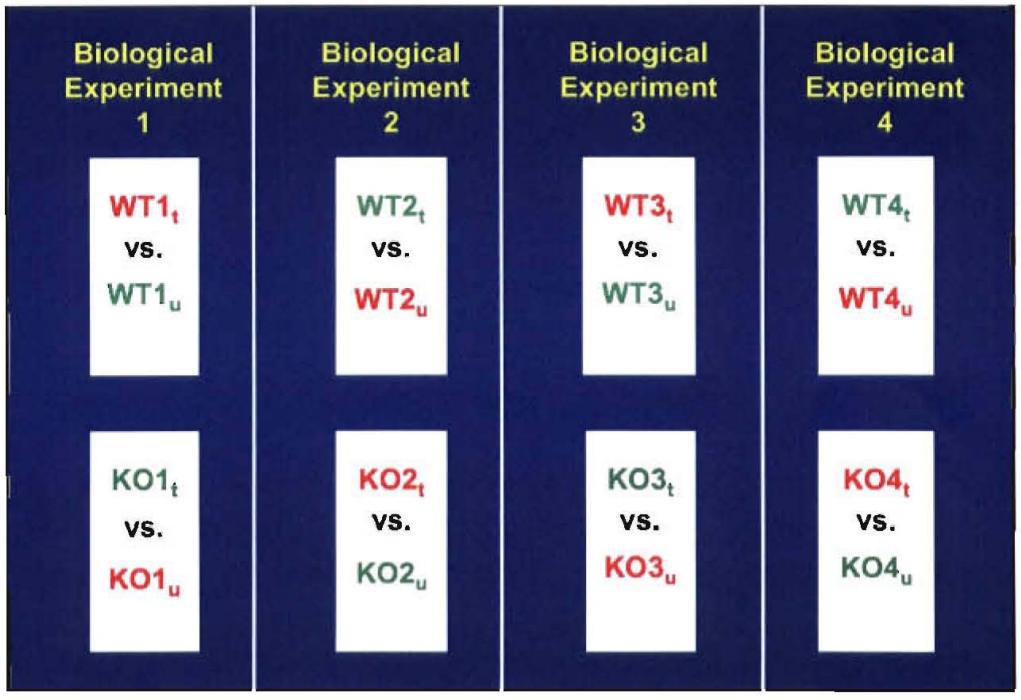


**Figure 4. Balanced dye labeling strategy to compensate for dye bias.** In the balanced dye labelling strategy, each treatment condition for all four biological replicates were labelled equally often with the Cy3 dye as with the Cy5 dye. Each white rectangle represents a two colour DNA microarray where the aRNA form IFN-γ activated macrophages infected *L. monocytogenes* ("treated") is compared to aRNA from untreated macrophages. Samples labelled with Cy3 are shown in green and samples labelled with Cy5 are shown in red. The "treated" and "untreated" samples are denoted by a subscripted "t" and "u" respectively. For each biological experiment there were 2 microarray slides, one for the C/EBPβ$^{+/+}$ (WT) samples and the second for the C/EBPβ$^{-/-}$ (KO) samples.

Other widely used normalization methods are (i) global intensity-independent normalization, (ii) global intensity-dependent *lo*cally *we*ighted *s*catter plot *s*moothing (LOWESS) normalization and (iii) print-group LOWESS normalization (local intensity-dependent). Global normalization assumes that the efficiencies of Cy5 and Cy3 dye differ by a constant value and that most of the genes on the array are not differentially expressed. The average of the log ratios for all the genes on the array is therefore assumed to be zero. If this was the case, then the summed intensity values for each channel should be equal, and where they differed, a normalization factor could be calculated and used to rescale the intensity values for each gene on the array (13). However, this method did not correct for spatial differences or for intensity biases of the dye. For example the Cy3 dye may incorporate into the aRNA more efficiently at lower intensities than the Cy5 dye. Global LOWESS normalization acknowledges that the variation between the red and green channels is not always constant and can change as a function of the signal intensity (i.e. is intensity-dependent). In this method, the intensity variation can be corrected by generating a best fit curve through the middle of a Ratio-Intensity plot of the microarray data and this line becomes the new zero line for the vertical axis (14). In the Ratio-Intensity plot, the ratio of the red (R) and green (G) intensities ($\log_2(R/G)$; also called the M value) for each spot is plotted against the average signal intensity ($0.5*(\log_2 R + \log_2 G)$; also called the A value) for each spot. In this analysis, the M value in the (M, A) pair is shifted by a quantity $c=c(A)$ depending on the A value. This constant, $c(A)$ is estimated by using the LOWESS function (15), which acts as a kind of regression analysis, and performs robust linear fits by calculating a moving average along the A axis, using data from an unselected set of genes on the array. Robust in this context means that the curve is not affected by a small to moderate percentage of differentially expressed genes. The fraction of data to be used for smoothing at each point can be defined by the researcher. This method assumes that (i) relatively few genes are differentially expressed and (ii) that no systematic relationship exists between the differential gene expression and the location of spots on the array. However, in practice this is not true since spatial bias is a very common problem and is often caused by hybridization artifacts, print tip and/or plate effects that occurred during array printing. Print-group LOWESS normalization can correct for both intensity-dependent bias and spatial bias, by performing LOWESS fits for the data within each print group. The basic assumptions of this method are that (i) the majority of the genes are not differentially expressed and (ii) that the number of up-regulated genes is approximately equal to the number of down regulated genes. Therefore, all the genes on the microarray are used for print-group LOWESS normalization. Moreover, print-group LOWESS normalization is only effective if the print-group is greater than 1000 spots per

print-group and that the above assumptions holds true for each print-group. Normalization between arrays adjusts the M values across all of the arrays so that they are on the same scale. This essentially prevents one or more arrays having undue weight when averaging thelog ratio across arrays. However, normalization between arrays is only effective if the data does not contain "missing values", which can result from excluding flagged data and using background subtraction.

Image plots of the red and green background helped identify damaged arrays, spatial patterns and/or miscellaneous strange patterns. Although not detected by visual inspection of the fluorescent images, the image plots clearly showed that all the arrays except WT4 had high background levels in both the red and green channels (Figs. 5, 6). Moreover, within each array, the level of red and green background hybridization appeared uniform, except for small areas/patches that appeared darker. Since these dark patches were localized to small areas, they were most likely caused by printing defects rather than uneven hybridization, which would have affected larger areas of the array. Since the high background may mask/bias the true intensity value of spots, the microarray data needed to be corrected to remove the bias attributed by the high background. Background subtraction is the most common method for background correction, where the local background fluorescence is subtracted from the total spot intensity. However, background subtraction was found to actually increase the variance in the data, which is evident by the wide spreading of points at the low fluorescent intensities (Figs. 7, 8 "subtraction" panel). In contrast, global background normalization using the probabilistic method (16), stabilized the variance, which can be seen by the tight clustering of data points at low intensities (Figs. 7, 8 "probabilistic" panel). The "probabilistic" method calculated the conditional expectation of the true signal given the observed signal using the equation: $E(si \mid si + bi)$, where the observed signal was considered to be the sum of the true signal ($si$) and the background ($bi$), which are assumed to follow exponential and normal distributions respectively. Estimates of the background distribution's mean and standard deviation were calculated from the fluorescent values of a defined set of empty spots over the array.

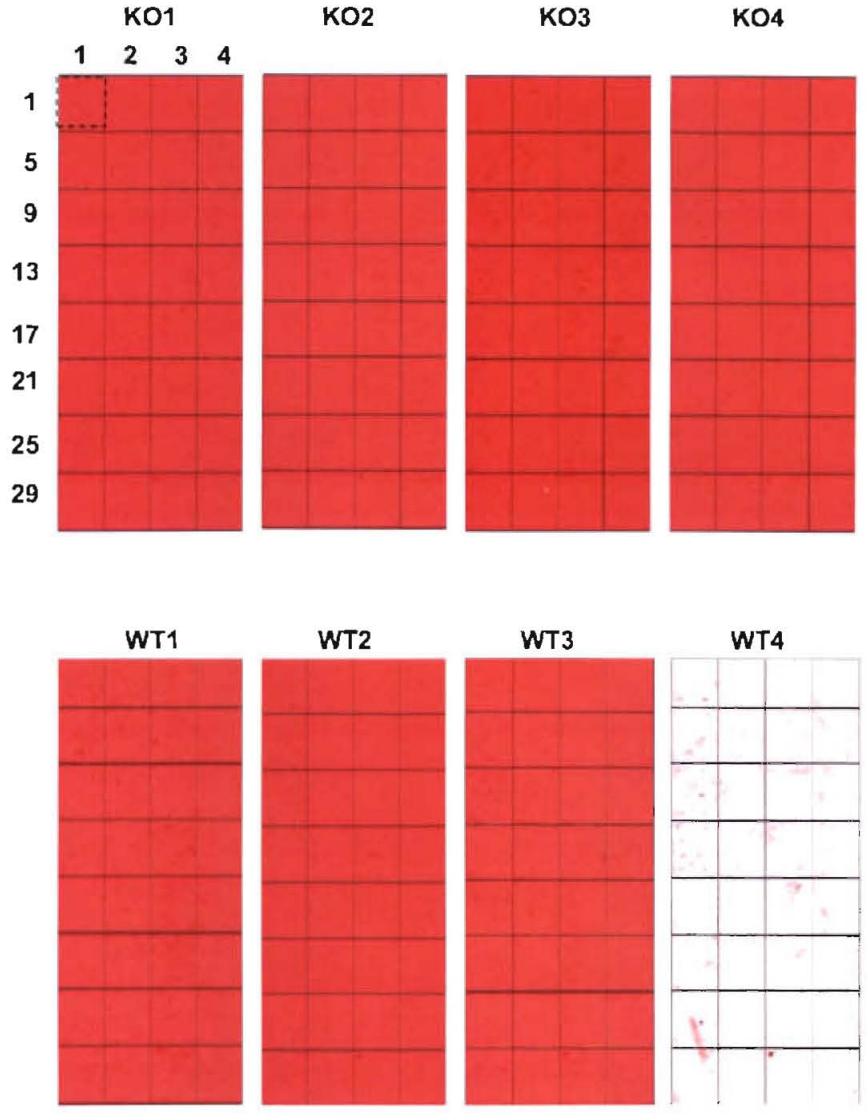


**Figure 5. Image plots of the background fluorescence in the red channel.** Shown here are image plots of the red background fluorescence for each individual array which is made up of 4 x 8 grids. Each rectangle represents a DNA microarray slide and the smaller squares represent the grids. The grids for array KO1 are numbered from left to right and grid number 1 is highlighted within the dashed box. The same grid numbering scheme applies for all the arrays. The level of brightness is proportional to the level of background fluorescence. WT1 and KO1 represent DNA microarray slides from the first biological infection experiment. KO represents C/EBPβ$^{-/-}$. The same labelling scheme applies for infection experiments 2, 3, and 4.

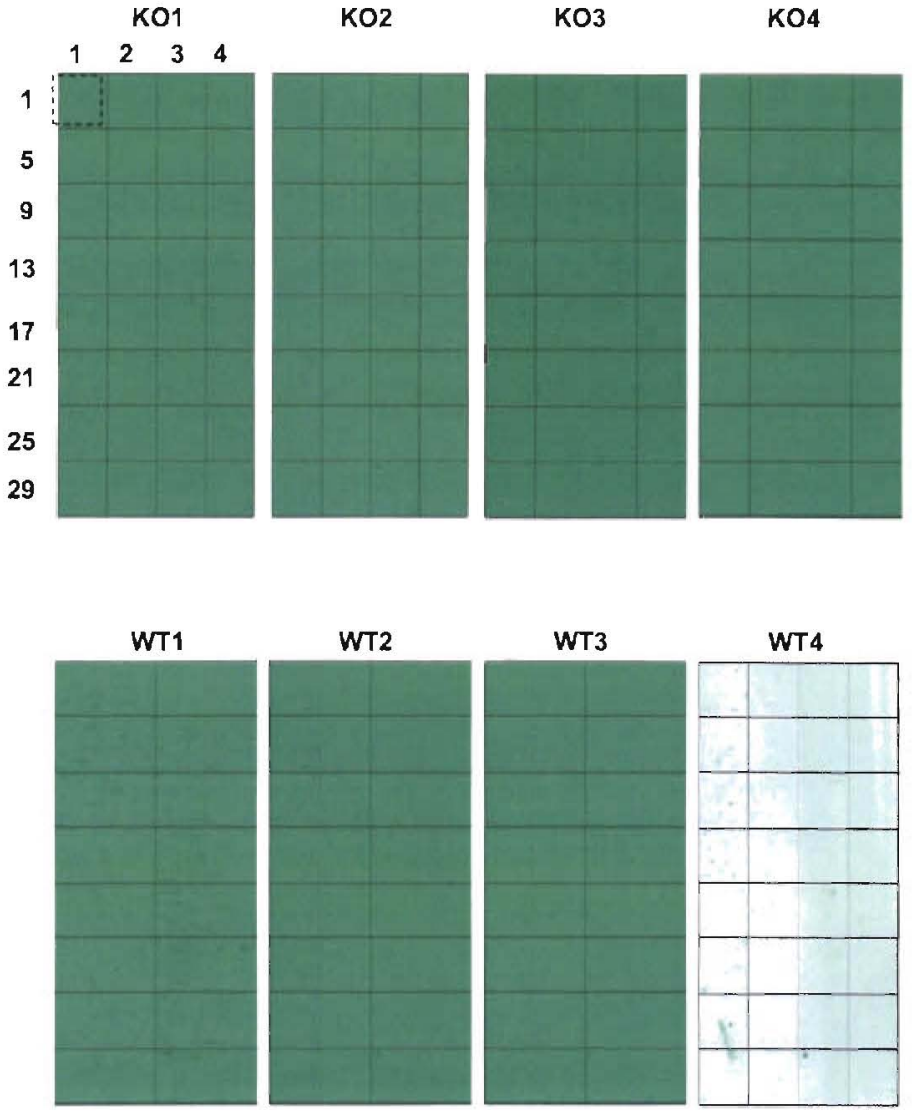


**Figure 6. Image plots of the background fluorescence in the green channel.** Shown here are image plots of the green background fluorescence for each individual array which is made up of 4 x 8 grids. Each rectangle represents a DNA microarray slide and the smaller squares represent the grids. The grids for array KO1 are numbered from left to right and grid number 1 is highlighted within the dashed box. The same grid numbering scheme applies for all the arrays. The level of brightness is proportional to the level of background fluorescence. WT1 and KO1 represent DNA microarray slides from the first biological infection experiment. KO represents C/EBP$\beta^{-/-}$. The same labelling scheme applies for infection experiments 2, 3, and 4.

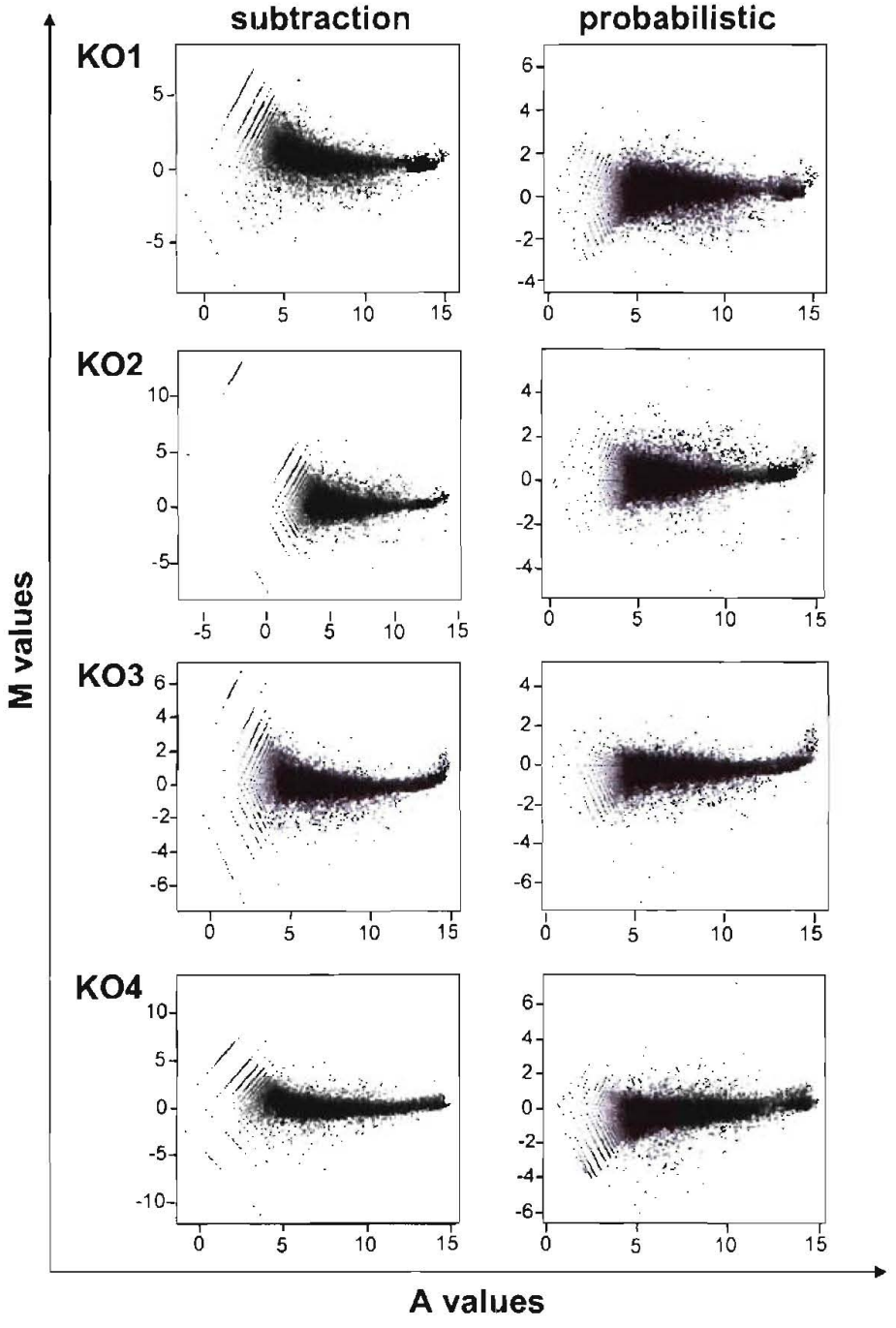


**Figure 7. Comparison of background correction methods for C/EBPβ$^{-/-}$ arrays.** Shown here are Ratio-Intensity plots of microarray data from the C/EBPβ$^{-/-}$ arrays that were background corrected by subtraction (left panel) or by probabilistic adjustment (right panel). The average signal intensity (represented as an "A value") represents A = [0.5 * ($\log_2$R + $\log_2$G)]. The M values represent the differential ratio of $\log_2$(R/G). R and G represented the background corrected Red and Green intensities respectively.

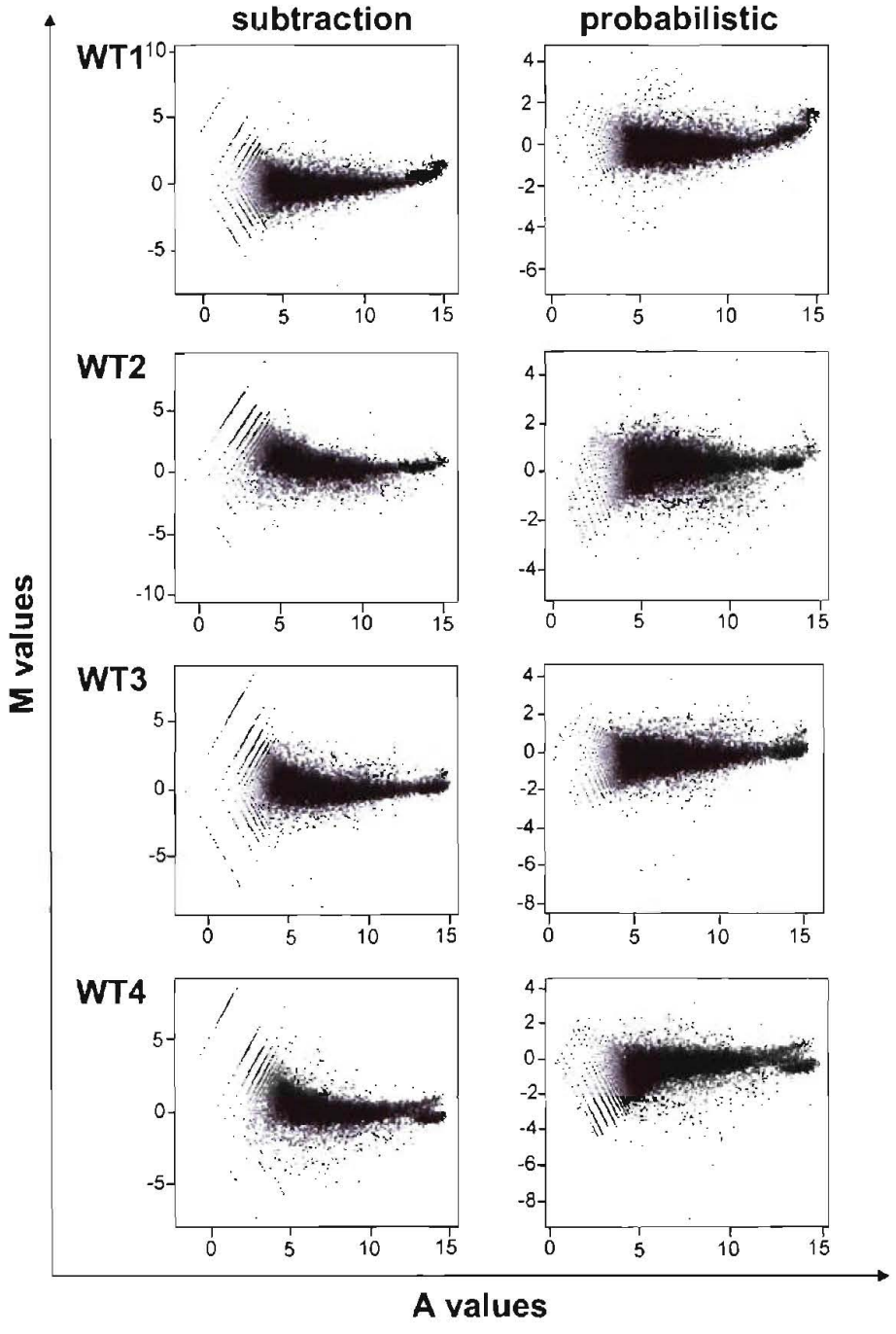


**Figure 8. Comparison of background correction methods for WT arrays.** Shown here are Ratio-Intensity plots of microarray data from the WT arrays that were background corrected by subtraction (left panel) or by probabilistic adjustment (right panel). The M values represent the differential ratio of $\log_2(R/G)$. The average signal intensity (represented as an "A value") represents $A = [0.5 * (\log_2 R + \log_2 G)]$. R and G represented the background corrected Red and Green intensities respectively.

Although probabilistic global background normalization removed the high background, Ratio-Intensity plots revealed that there was significant dye bias, especially at the lower intensities. The intensity-dependent relationship between the "average signal" (A value) and expression ratio (M value) for each array can be seen by the curvature of the data and dipping of the LOWESS line at lower intensities, which was particularly bad for KO1, KO2, KO4, WT2 and WT4 arrays (Figs. 9, 10 "Background corrected" panel). The marked decreased background fluorescence for the WT4 and KO4 arrays, as compared to the other arrays, may be due fragmentation of the aRNA in the WT and KO4 aRNA samples. For this pair of samples, the microarray slides were accidentally broken in the swinging bucket centrifuge during the post-hybridization washing steps. Consequently, the "back-up" labelled aRNA for WT4 and KO4 samples, which had been stored at -20°C, were thawed and used for hybridization on new MEEBO arrays. The single freeze thaw cycle of the labelled aRNA for these samples may have partially fragmented the aRNA. Interestingly, the fragmentation of aRNA has been shown to actually improve hybridization kinetics on oligonucleotide printed microarrays (17). Therefore the shorter aRNA sequences in the WT4 and KO4 samples my have bound more specifically to their target probes and less non-specifically to the background of microarray slides. Consequently, the background fluorescence for the WT4 and KO4 microarrays were much lower than the other microarrays in this study. Moreover density plots of the background corrected data confirmed the presence of significant dye bias (Fig. 11 A), as demonstrated by the spread between green and red density lines for each array. Had there been no dye bias, the density lines for the red and green channels would have been superimposed on each other. Furthermore, the mean pixel intensities (log 2) of the red and green foregrounds ranged from 0 to 16, and centred around 5, which indicated that the hybridization worked well and that there was no saturation of signal during the scanning process. Had either of these conditions occurred, the pixel intensity values would have clustered either at the high or low end of the scale respectively. Since the assumption was made that the majority of the genes on the arrays, representing the entire mouse genome, were not differentially expressed during infection, the mean M values were expected to be centered around zero. However, differential dye bias affecting the arrays resulted in different spreads of M values for each array, resulting in their median M values deviating around zero (Fig. 12 A). In addition, the degree of intensity-dependent dye bias was not consistent over the array, and varied by print group, as shown by the deviation from zero and the differing degree of curvature of the LOWESS lines for each print group (Figs. 13, 14). This was particularly noticeable in arrays KO1, KO4, WT2 and WT4.

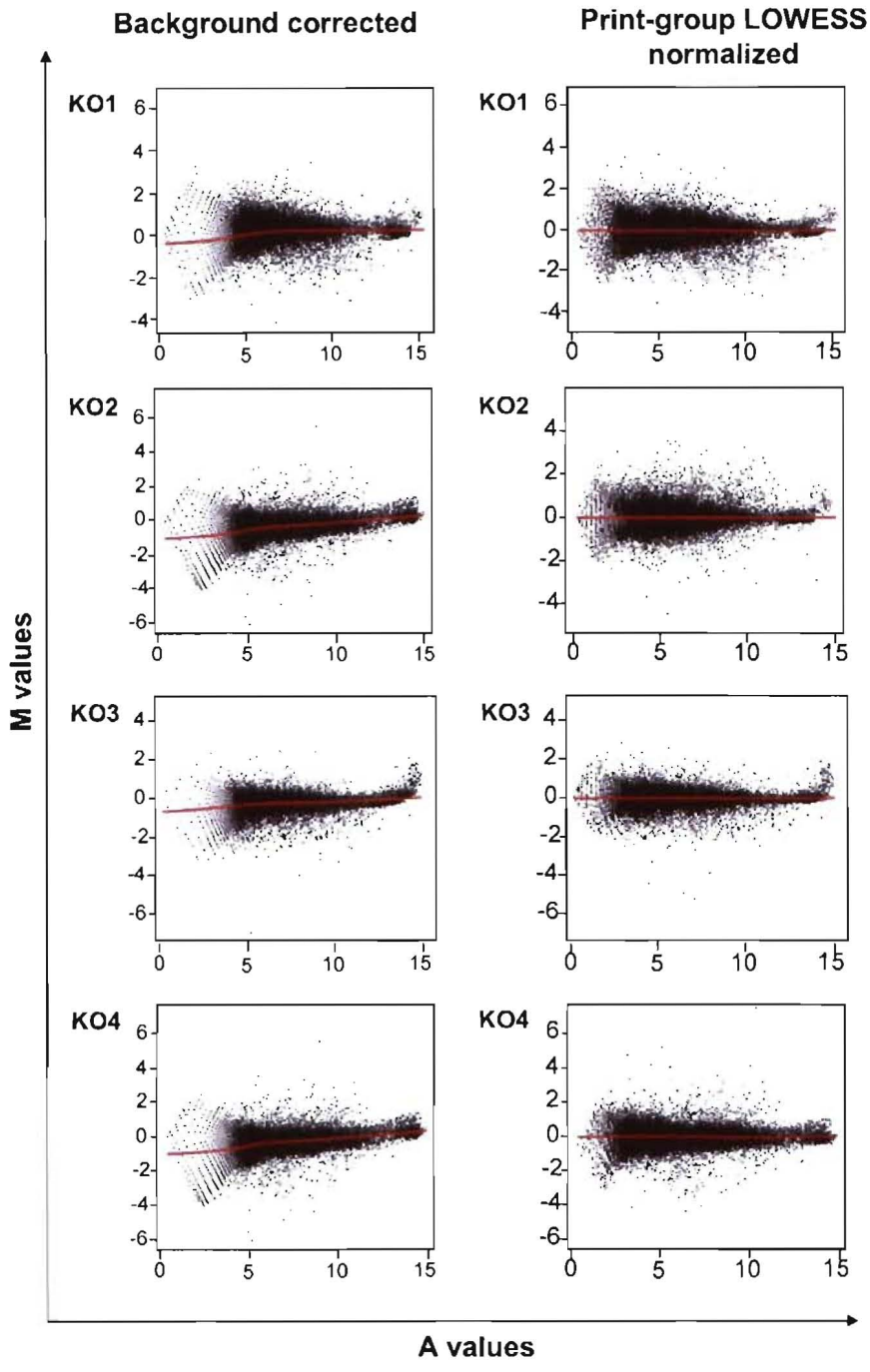


**Figure 9. Identification of intensity-dependent dye biases in C/EBPβ$^{-/-}$ arrays.** Shown here are Ratio-Intensity plots of background corrected C/EBPβ$^{-/-}$ microarrays before and after print-group LOWESS normalization. The "best fit" LOWESS line is shown in red. The M values represent the differential ratio of $\log_2(R/G)$. The average signal intensity is represented as "A values", where $A = [0.5 * (\log_2 R + \log_2 G)]$. R and G represent the background corrected Red and Green intensities respectively. KO1 represents data the KO (C/EBPβ$^{-/-}$) array from the first biological experiment. The same labelling scheme applies for infection experiments 2, 3, and 4.

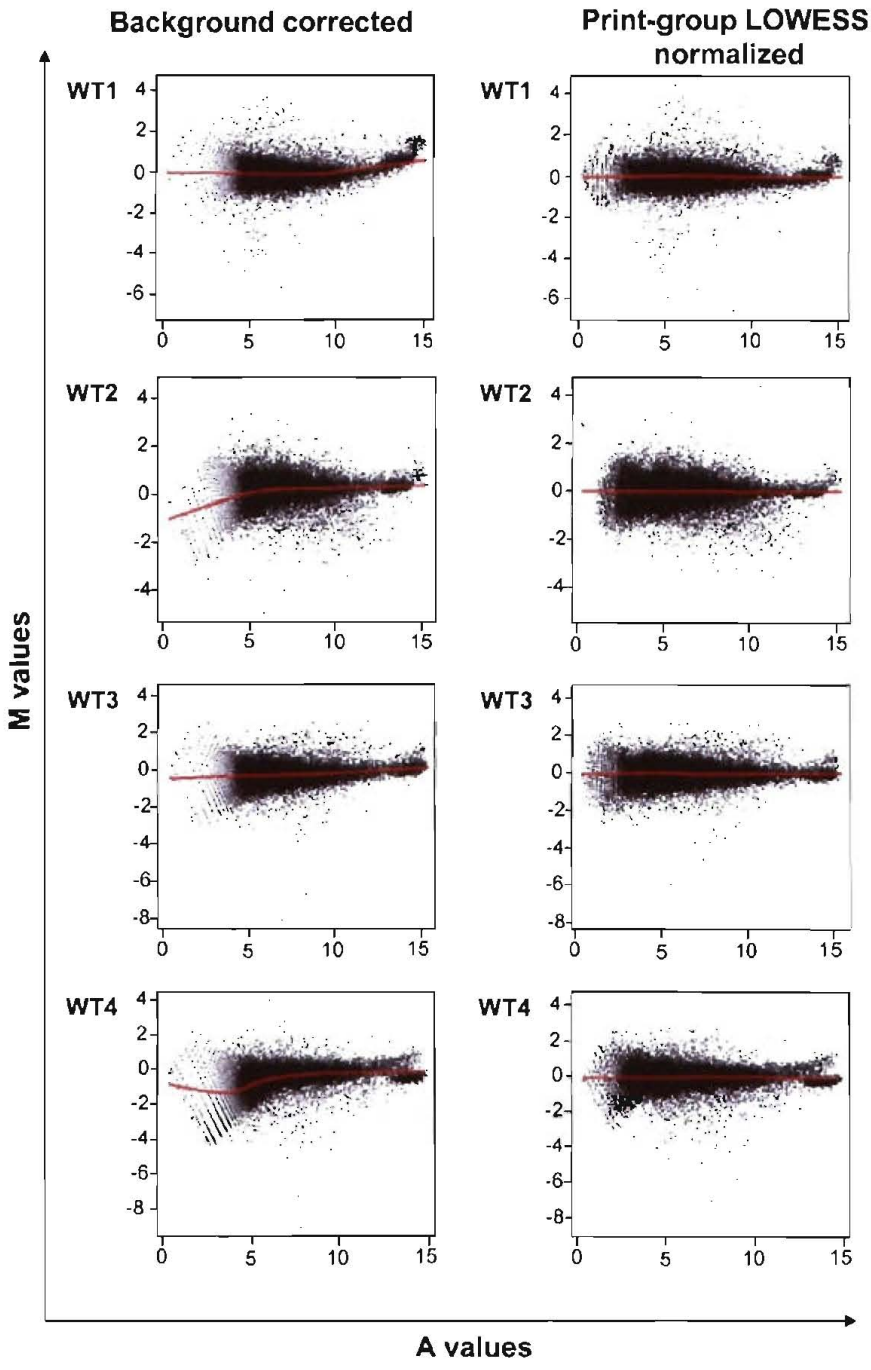


**Figure 10. Identification of intensity-dependent dye biases in WT arrays.** Shown here are Ratio-Intensity plots of background corrected C/EBPβ$^{-/-}$ microarrays before and after print-group LOWESS normalization. The "best fit" LOWESS line is shown in red. The M values represent the differential ratio of $\log_2(R/G)$. The average signal intensity is represented as "A values", where $A = [0.5 * (\log_2 R + \log_2 G)]$. R and G represent the background corrected Red and Green intensities respectively. KO1 represents data from the KO (C/EBPβ$^{-/-}$) array for the first biological experiment. The same labelling scheme applies for infection experiments 2, 3, and 4.

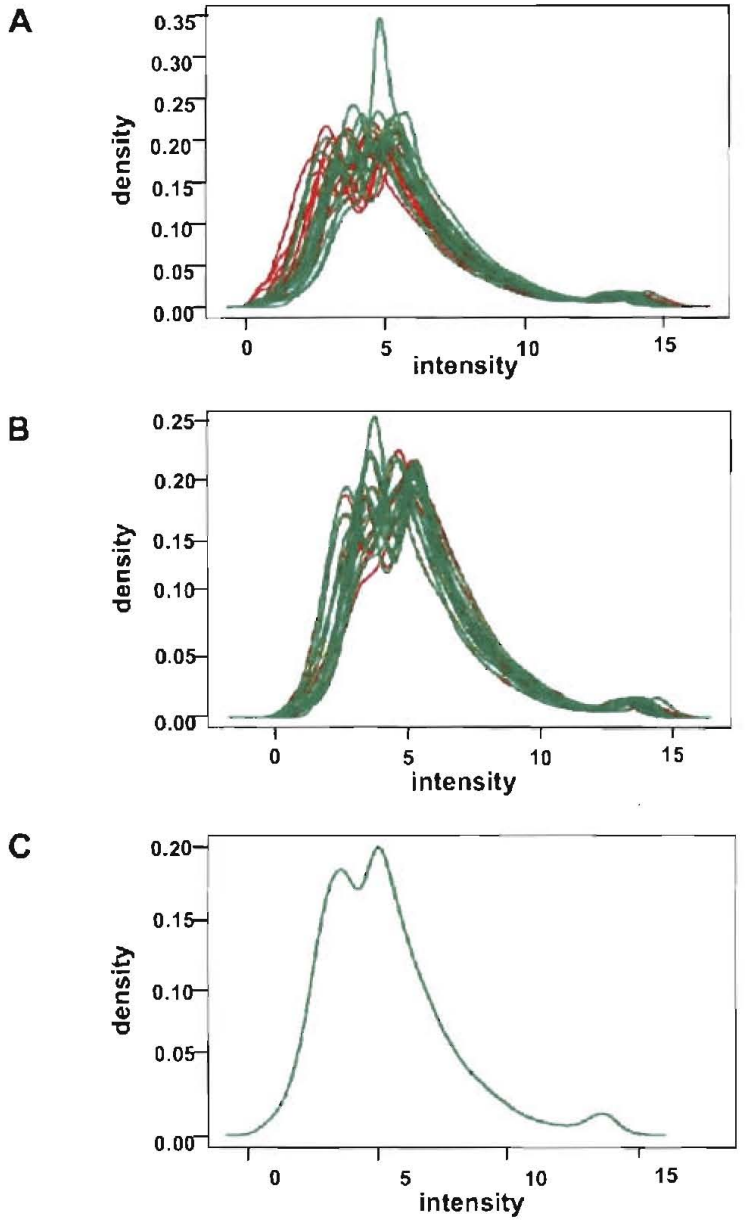


**Figure 11. Identification and correction of dye bias in microarray data.** Shown here are density plots of the smoothed empirical densities for the individual green (green line) and red (red line) channels (A) after background correction, (B) after print-group LOWESS normalization and (C) after slide scale normalization between microarray slides.

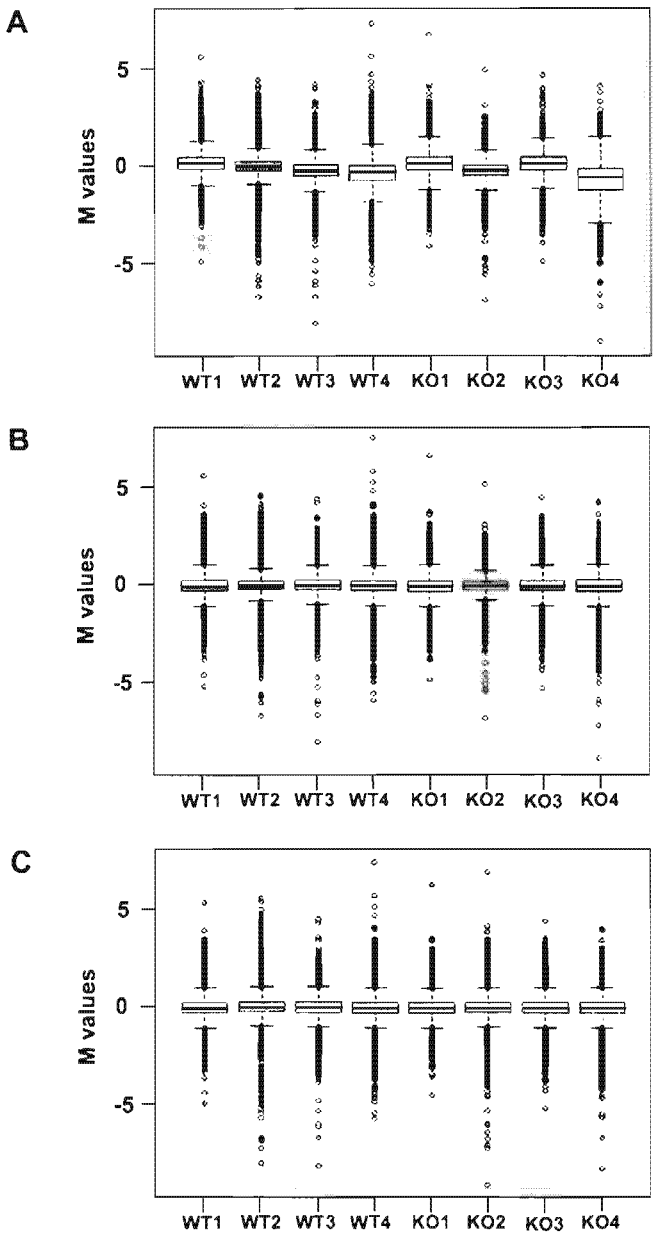


**Figure 12. Box plots of Ratio-Intensity plots of arrays after within slide and between slide normalization.** Shown here are box plots of the M values which are (A) background corrected only, (B) normalized by print-group LOWESS and (C) normalized across all arrays using a slide-scale re-scaling algorithm.The central box represents the inter-quartile range (IQR), which is the difference between the 75th percentile (upper quartile) and 25th percentile (lower quartile). The line in the middle of the box represents the median. Extreme values (>75th percentile and <25th percentile) are plotted individually. WT1 and KO1 represent microarray data from the first biological infection experiment. WT and KO represent wild-type (C/EBPβ$^{+/+}$) and C/EBPβ$^{-/-}$respectively. The same labelling scheme applies for infection experiments 2, 3, and 4.

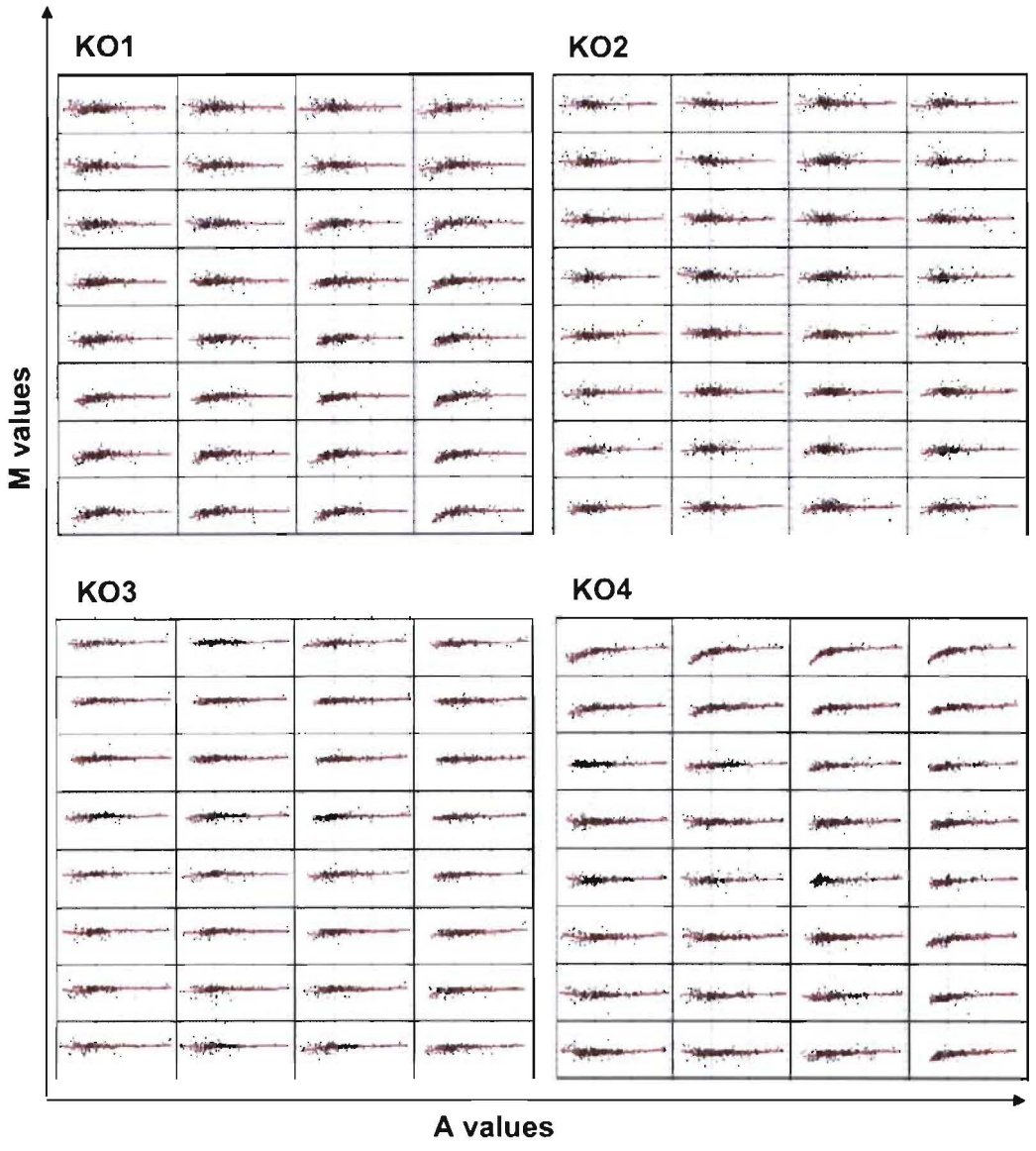


**Figure. 13. Identification of intensity-dependent spatial dye biases in C/EBPβ$^{-/-}$ arrays.** Shown here are Ratio-Intensity plots of background corrected data by print-group before normalization. Each large square represents an individual array that is composed of 4 x 8 grids which are represented as smaller squares. The "best fit" LOWESS line for data in each print-group (grid) is shown is red. The M values represent the differential ratio of $\log_2(R/G)$. The average signal intensity is represented as "A values", where $A = [0.5 * (\log_2 R + \log_2 G)]$. R and G represent the background corrected Red and Green intensities respectively. KO1 represents data from the KO (C/EBPβ$^{-/-}$) array for the first biological experiment. The same labelling scheme applies for infection experiments 2, 3, and 4.

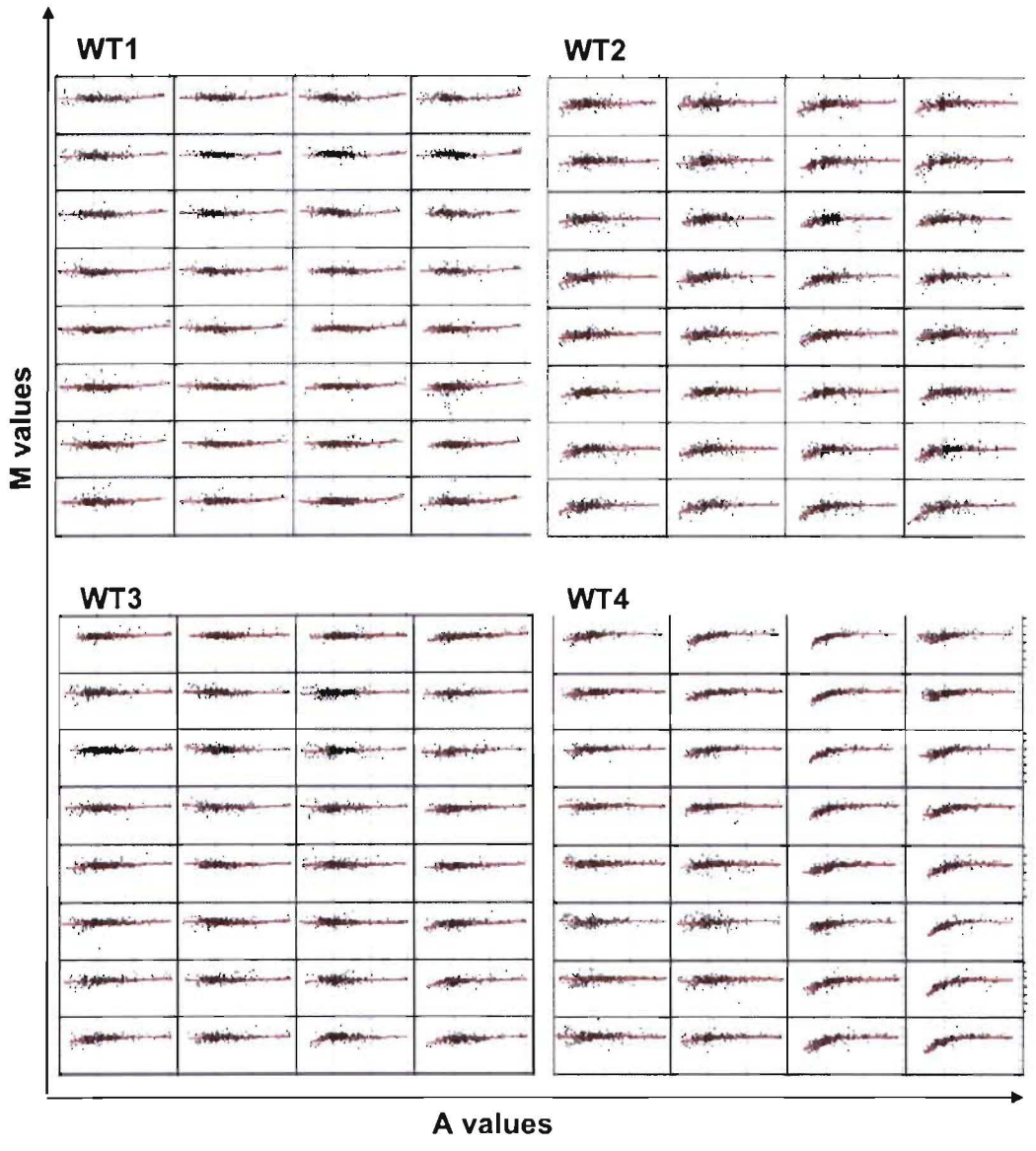


**Figure. 14. Identification of intensity-dependent spatial dye biases in WT arrays.** Shown here sare Ratio-Intensity plots of background corrected data by print-group before normalization. Each large square represents an individual array that is composed of 4 x 8 grids which are represented as smaller squares. The "best fit" LOWESS line for data in each print-group (grid) is shown is red. The M values represent the differential ratio of $\log_2(R/G)$. The average signal intensity is represented as "A values", where $A = [0.5 * (\log_2 R + \log_2 G)]$. R and G represent the background corrected Red and Green intensities respectively. WT1 represents data from the WT array for the first biological experiment. The same labelling scheme applies for infection experiments 2, 3, and 4.

Data shown in the diagnostic plots in figures 9 and 10 indicate that there were significant spatial and dye biases that needed to be removed from the microarray data before any quantitative analysis could be done. Print-group LOWESS normalization was considered the best method to use to remove these systematic biases, since it corrects for both spatial bias and smoothes the dependence of log ratios on intensities. However, this method was only reliable if (i) the majority of the genes were not differentially expressed and (ii) that each print-group consisted of at least 1000 genes. Since most of the genes on the fluorescent images appeared yellow (not differentially expressed) and the print-groups were composed of 1225 genes, all the assumptions of print-group LOWESS normalization were satisfied and the data within each array were normalized using print-group LOWESS. Furthermore, spots that were flagged as bad were given a weighting of 0.1, normalized and retained in the data set, thereby avoiding the generation of "missing data". Print-group LOWESS normalization successfully removed the spatial and dye biases within each array. Density plots showed that the distributions of the red and green intensities essentially became the same for each array (Fig. 11 B) and box plots of the M values showed that the median of the M values was centered on zero for all arrays (Fig. 12 B). Moreover, Ratio-Intensity plots of the data no longer had the previously observed curvature and was more tightly clustered along the LOWESS line which was linear and centered around zero (Figs. 9, 10 "Print-group LOWESS normalized" panel). However, differences in scale and spread of the M values existed between the arrays, indicating that the data between arrays needed to be normalized. Since probabilistic background correction and gene weighting had been used during the normalization procedure, the microarray data did not contain any "missing values", a requirement for between array normalization. The M values between the arrays were therefore normalized using a sliding scale normalization, which effectively divided the M values in every array by the Median Absolute Deviation (MAD). Normalization between the arrays resulted in the density of the red and green channels being the same for all arrays (Fig. 11 C) and the M values having the same median and spread (Fig. 12 C). The sequential normalization procedure implemented had therefore effectively removed, as much as possible, the systematic biases and "non-biological" differences from the microarray data.

**4. Reproducibility of Microarray Experiments**

Although sequential normalization of the microarray data removed as much systematic biases as possible, there was still considerable "non-biological" variability due to the inclusion of questionable or inconsistent data. In order to reduce the probability of erroneously classifying non-differentially expressed genes as being differential expressed, it was therefore important to remove the questionable data before proceeding with the quantitative gene expression analysis. Usually, technical replicate or biological replicate experiments are performed to identify and reduce the variability of microarray data. Biological replicate experiments use RNA isolated from the independent biological sources and measures both the natural biological variability and the random variation introduced during the RNA preparation. Technical replicate experiments measures the natural and systematic variability introduced during the experiment. Technical replicates include replicated spots within a single array, multiple alternatively spliced cDNAs/oligos for a particular gene within a single array, or repeated hybridizations using the same RNA sample. For example, dye-swap experiments are commonly used to compensate for technical variation and dye biases that occurred during labeling or hybridization. However, due to budget limitations, technical replicate hybridizations and dye-swap experiments were not done in this study. Instead, multiple replicate spots within each array were used to assess the technical reproducibility of the arrays and a balanced dye-labelling approach was used to compensate for dye labelling variation. Moreover, since it is the reproducibility of biological replicates that is important for biological inference, biological replicate experiments were chosen over technical repeat experiments.

Reproducibility within each array was assessed by calculating the standard deviation (SD) of the M values for each replicated gene on the array. Genes with SD>0.2 were considered questionable/unreliable and therefore not reproducible. The SD value of 0.2 was chosen since it is the SD cut off value that many researchers use to define questionable data (18). A total of 41 different genes were randomly spotted multiple times across the array. The number of replicates per gene varied from 2 to 20 and the total number of replicate spots was 728. The reproducibility within all the arrays was poor, where >50% of the replicate genes failed the SD<0.2 criteria of reproducibility (Table 4). The only exceptions were for arrays KO3 and WT1 which respectively had 39% and 49% reproducibility among replicated genes. This poor reproducibility indicated that there were significant technical sources of variation within the experiments, which may include unequal hybridization kinetics across the individual arrays and/or variability within the printed arrays.

**Table 4. Technical reproducibility assessed by replicate genes within each array.** The Standard deviation of the M values for each replicated gene was calculated. M values with a SD<0.2 were "passed" and considered reproducible. Similarly, M values with a SD>0.2 were "failed" and considered to questionable/unreliable.

| | KO1 | KO2 | KO3 | KO6 | WT1 | WT2 | WT3 | WT4 |
|---|---|---|---|---|---|---|---|---|
| Total replicate spots | 728 | 728 | 728 | 728 | 728 | 728 | 728 | 728 |
| # genes replicated | 41 | 41 | 41 | 41 | 41 | 41 | 41 | 41 |
| # passes | 11 | 10 | 16 | 7 | 20 | 11 | 15 | 10 |
| # fails | 30 | 31 | 25 | 34 | 21 | 30 | 26 | 31 |
| total replicates | 41 | 41 | 41 | 41 | 41 | 41 | 41 | 41 |
| **% pass** | **27** | **24** | **39** | **17** | **49** | **27** | **37** | **24** |
| **% fail** | **73** | **76** | **61** | **83** | **51** | **73** | **63** | **76** |

In order to reduce the variance and complexity of the microarray gene expression data, the M values for the replicate spots were merged and averaged over all four biological replicate experiments. The reproducibility between biological duplicates was measured by linear regression. Biological replicates were considered reproducible if the correlation between their M values was greater than 0.3, since Churchill et al found that reproducibility between biological replicates can be as low as $R^2 \geq 0.3$ (19). Comparison of "like-treatment" samples, e.g. $WT1_{untreated}$ vs. $WT3_{untreated}$ within the red (Cy5) or green (Cy3) channel, showed that the reproducibility within each treatment group was satisfactory ($R^2$=0.62) (Fig. 15). However, when the ratio of the intensities, comparing treated vs. untreated samples (M values) were calculated, the reproducibility was poor ($R^2$= 0.000001 – 0.13) (Fig. 16). This may have been due the fact that the individual treatment groups already had a considerable amount of variation ($R^2$<0.7, Fig 15) and the direct comparison between the treatment groups introduced even more variation, due to the additive nature of their inherent variances. Ratio-Intensity plots of the biological replicate experiments showed that the majority of the data was not reproducible between experiments, as shown by the "outliers" which had standard deviations (SD) greater than 0.2 (blue data in Fig. 17) or SD greater than 0.3 (blue data in Fig. 18) . Therefore to improve the reliability and confidence of the microarray data, unreliable or questionable data was removed from the microarray data set. As reviewed by Quackenbusch et al (18), many researchers define questionable data as those genes which have SD>0.2 between biological or technical replicate experiments. However, since a SD>0.2 cut-off would require trimming 60% of the genes from the data set, it was considered too stringent.

Moreover, using the SD>0.2 cut off criteria would result in the exclusion of key immunological genes, such as TNFRp55 (20), IL-1β (21, 22), p47phox (23), Pld2 (24), Rabgef (25), Zfp198 (26, 27) and Cyp2b9 (28), which play a significant role during the innate inflammatory immune response against *L. monocytogenes*. Since the microarray experiments were considered an exploratory study, it was more important to include biologically significant genes in the data for future analyses. Elimination of known and other, as yet, unidentified biologically relevant genes, would decrease the probability of fulfilling the aims of the study, which were to identify genes involved in mediating listericidal activity. Therefore a less conservative value of SD>0.3, which is used as a yardstick by several data analysis software e.g. GenePix 5.1 to define reliable data, was used to trim unreliable data from the microarray data set. Removal of these inconsistent/unreliable "outliers" with SD>0.3 required 49% of the genes to be trimmed from the data set. However it did result in better correlation and reproducibility between the biological replicates ($R^2$= 0.3 – 0.4, Fig. 17), but not to the same extent when a SD>0.2 cut off was used ($R^2$= 0.2 – 0.4, Fig. 18). Had there been no budget limitations, the microarray experiments would have been repeated using commercial, high quality microarray slides in order to obtain statistically reliable data.

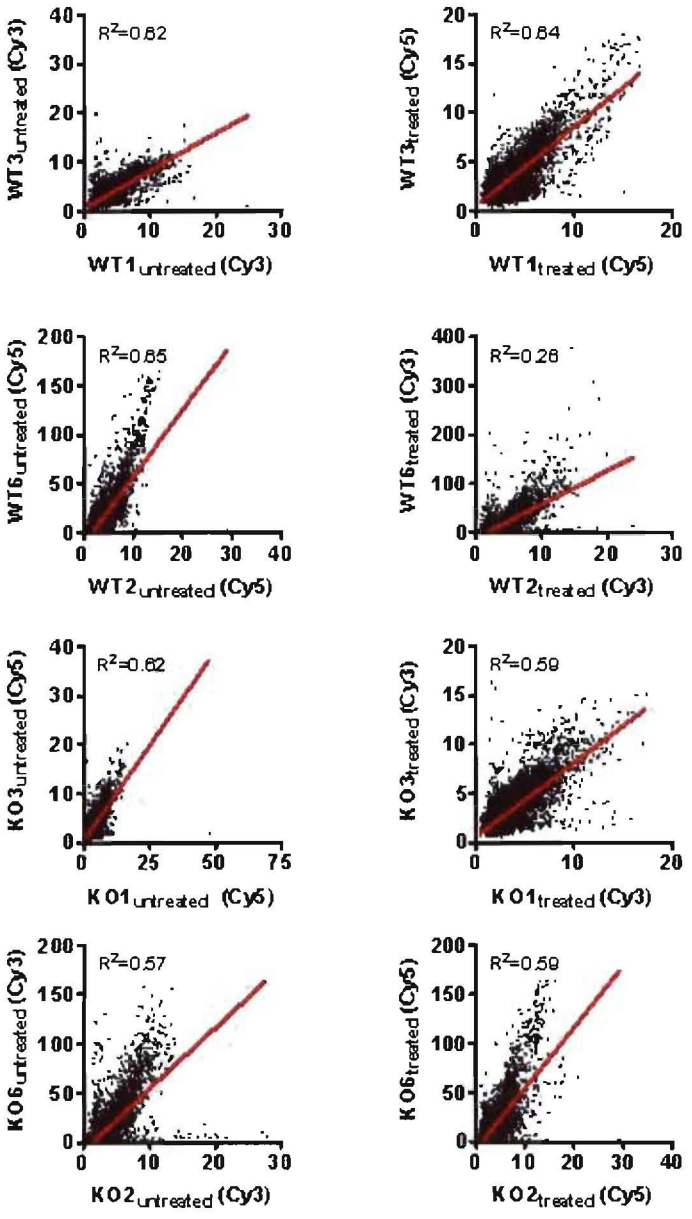


**Figure 15. Reproducibility of fluorescent intensities between biological replicate experiments.** The normalized red (Cy5) or green (Cy3) fluorescent intensities for "like" treatments labelled with the same dye were plotted against each other for each biological experiment. Reproducibility of the fluorescent intensities between the biological experiments was measured by linear regression (red line). Biological replicates were considered reproducible only if the correlation between the fluorescent intensities was $R^2 \geq 0.3$. Treated refers to aRNA generated from IFN-γ activated macrophages infected with *L. monocytogenes*. Untreated refers to aRNA generated from media control macrophages. WT1 and KO1 represent data from the WT or KO (C/EBPβ$^{-/-}$) arrays for the first biological experiment. The same labelling scheme applies for infection experiments 2, 3, and 4.

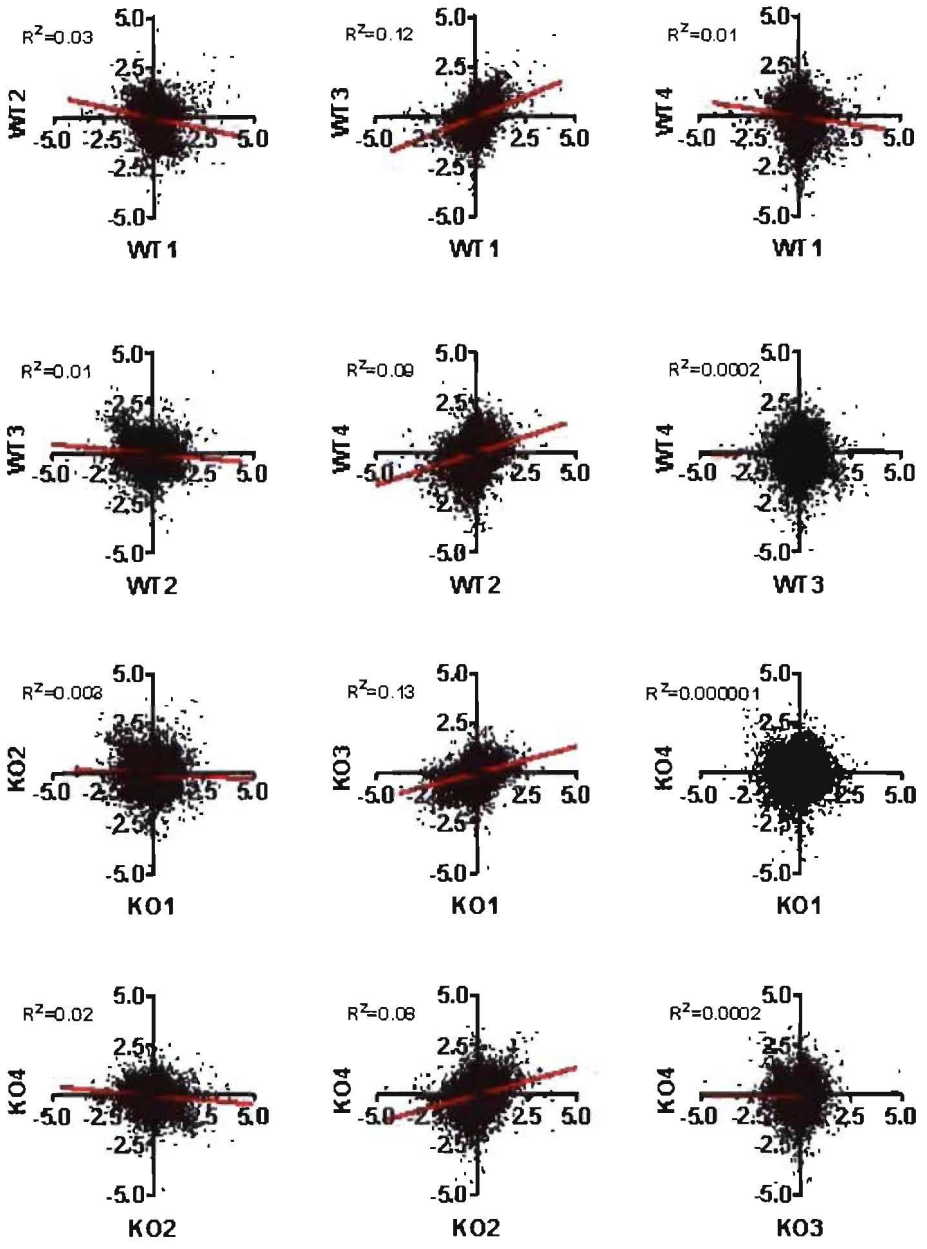


**Figure 16. Reproducibility of gene expression ratios between biological replicate experiments.** The normalized M values for each spot was plotted against each other for each biological experiment. Reproducibility of the M values between the biological experiments was measured by linear regression (red line). Biological replicates were considered reproducible only if the correlation between the M values was $R^2 \geq 0.3$. The M value represents the ratio of the fluorescent intensities for treated vs. untreated aRNA bound to each spot. Treated refers to aRNA generated from IFN-γ activated macrophages infected with *L. monocytogenes*. Untreated refers to aRNA generated from media control macrophages. WT1 and KO1 represent data from the WT or KO (C/EBPβ$^{-/-}$) arrays for the first biological experiment. The same labelling scheme applies for infection experiments 2, 3, and 4.

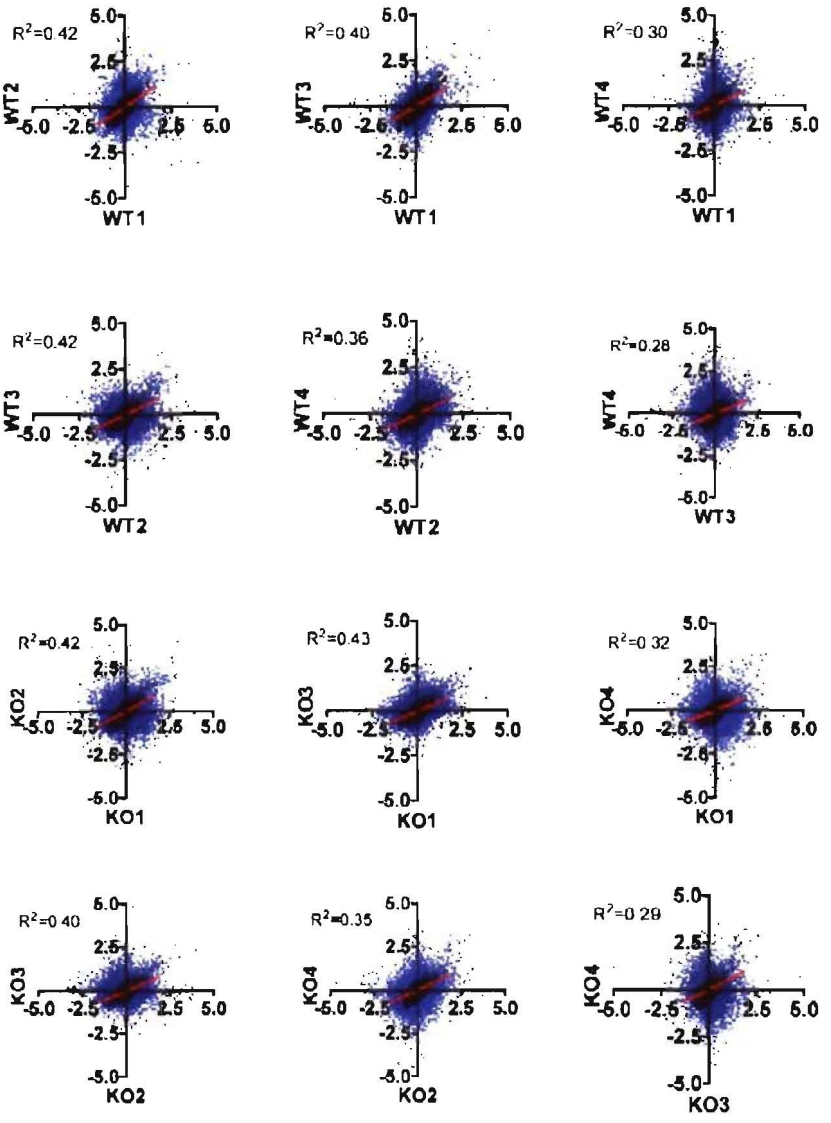


**Figure 17. Reproducibility of gene expression ratios between "trimmed" biological replicate experiments (SD<0.2).** The normalized M values for each spot was plotted against each other for each biological experiment. M values with SD>0.2 (blue) were considered questionable and were removed from the data. Reproducibility between the biological experiments was measured by linear regression (red line) of the remaining M values (black). Biological replicates were considered reproducible only if the correlation between the M values was $R^2 \geq 0.3$. The M value represents the ratio of the fluorescent intensities for treated vs. untreated aRNA bound to each spot. Treated refers to aRNA generated from IFN-γ activated macrophages infected with *L. monocytogenes*. Untreated refers to aRNA generated from media control macrophages. WT1 and KO1 represent data from the WT or KO (C/EBPβ$^{-/-}$) arrays for the first biological experiment. The same labelling scheme applies for infection experiments 2, 3, and 4.

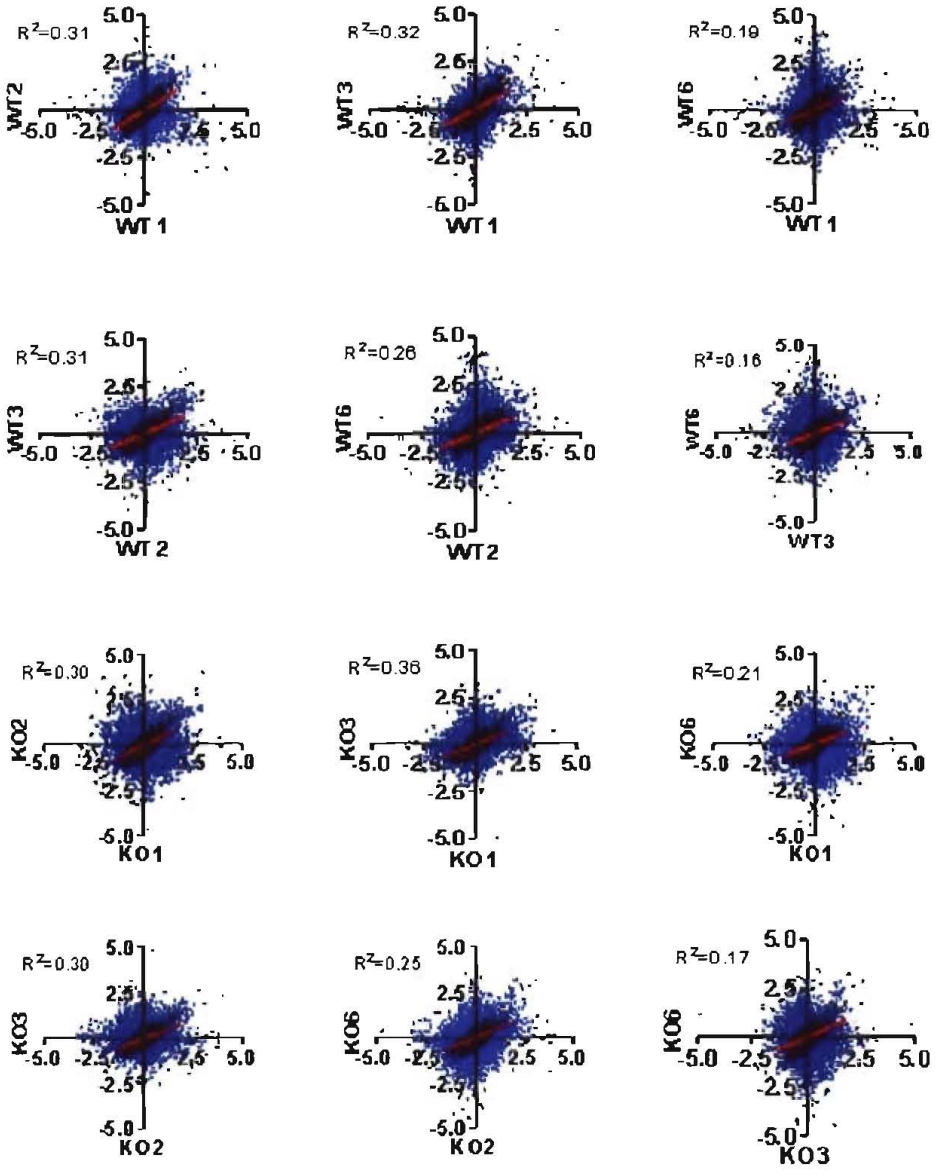


**Figure 18. Reproducibility of gene expression ratios between "trimmed" biological replicate experiments.** The normalized M values for each spot was plotted against each other for each biological experiment. M values with SD>0.3 (blue) were considered questionable and were removed from the data. Reproducibility between the biological experiments was measured by linear regression (red line) of the remaining M values (black). Biological replicates were considered reproducible only if the correlation between the M values was $R^2 \geq 0.3$. The M value represents the ratio of the fluorescent intensities for treated vs. untreated aRNA bound to each spot. Treated refers to aRNA generated from IFN-γ activated macrophages infected with *L. monocytogenes*. Untreated refers to aRNA generated from media control macrophages. WT1 and KO1 represent data from the WT or KO (C/EBPβ$^{-/-}$) arrays for the first biological experiment. The same labelling scheme applies for infection experiments 2, 3, and 4.

**5. Biological Relevance of Microarray Data**

Despite the poor reproducibility within and across the microarrays, biologically relevant data could still be extracted. Several genes involved in host defense and immune responses were significantly up-regulated in both the WT and C/EBPβ$^{-/-}$ macrophages during *L. monocytogenes* infection (Fig. 19 A). For example, the pro-inflammatory cytokines IL-1α, IL-β, IL-6, IL-12p40, IL-18, TNF and chemokines MIP-1α, MIP-1β, MIP-2, MCP-1, MCP-3, MIG and ITAC were significantly up-regulated in both the WT and C/EBPβ$^{-/-}$ macrophages. Similarly, inducible nitric oxide synthase (iNOS), which catalyzes the formation of bactericidal nitric oxide, was efficiently induced in both WT and C/EBPβ$^{-/-}$ macrophages. Moreover, several genes involved in mediating IFN-γ and TNF signalling were highly up-regulated in both WT and C/EBPβ$^{-/-}$ macrophages. For example, ICSBP, IRF1, Interferon-induced protein with tetratricopeptide repeats 2 (Ifit2), Ifit3, Interferon-induced protein 35 (Ifi35), Interferon activated gene 203 (Ifi203) and Interferon activated gene 202B (Ifi202b) are important for IFN-γ-mediated signalling, whereas TNFRp55, TNF receptor superfamily member 5 (Tnfrsf5), TNF ligand superfamily member 10 (Tnfsf10) and TNF ligand superfamily member 4 (Tnfsf4) are important for TNF signalling. In addition, Myd88, the adaptor protein essential for integrating TLR signalling to downstream effectors, was also highly up-regulated in both genotypes. Similarly the genes for Macrophage activation 2 (Mpa2) and Histocompatibility 28 (H28), which are important for macrophage activation and MHC class II expression respectively, were also induced in WT and C/EBPβ$^{-/-}$ macrophages. More importantly, C/EBPβ was up-regulated only in WT macrophages (Fig. 19 B) and the induction of C/EBPβ target genes such as G-CSF, CLECSF9, IL-12p35 and ISGF3γ were impaired in the C/EBPβ$^{-/-}$ macrophages (Fig. 19 B). C/EBPβ was shown to be essential for the induction of G-CSF during innate immunity against *L. monocytogenes* (29), *Mycobacterium tuberculosis* (30) and *Brucella abortus* (31). Similarly, C/EBPβ was found to be necessary for the induction of CLECSF9 in response to LPS, TNF, IL-6, and IFN-γ stimulation (32) and IL-12p35 during *Candida albicans* infection (33). In addition, C/EBPβ was shown to play an important role in IFN-γ signaling transduction via its transcriptional regulation of ISGF3γ, a component of the ISGF3 protein complex that is essential for IFN signaling (34). Since the microarray gene expression patterns for several immunologically relevant genes were as expected from the literature, it was concluded that although the microarray gene expression data did not have good reproducibility on a statistical level, it did contain biologically relevant data. Therefore the decision was made to go ahead and continue with the analysis in order to identify the genes involved mediating listericidal activity.

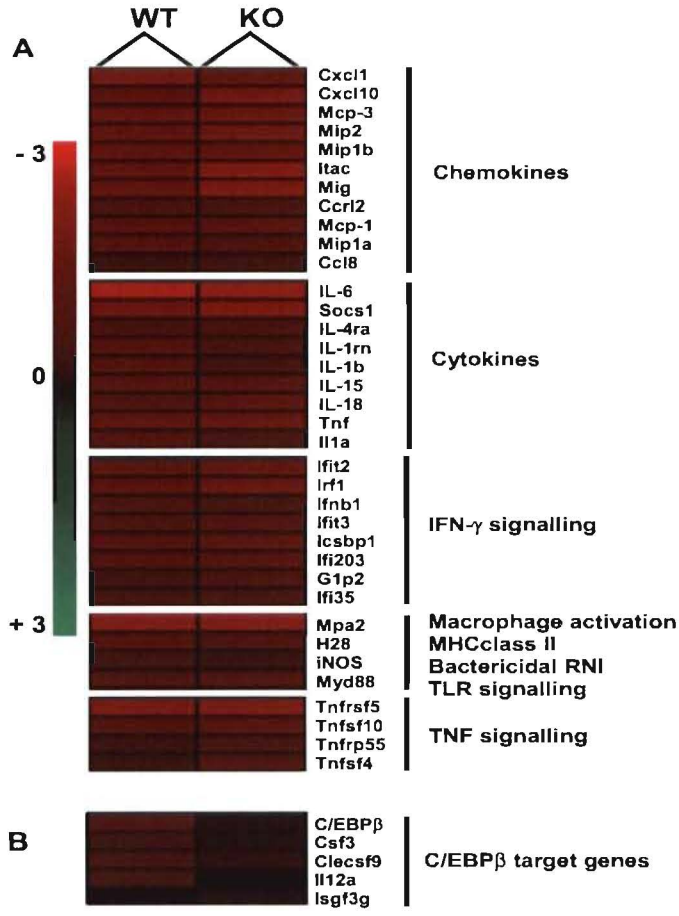


**Figure 19. Microarrays contained biologically relevant data despite poor reproducibility.** (A) Efficient induction of pro-inflammatory cytokines, chemokines and genes involved in host immune responses during *L. monocytogenes* infection in both the WT and C/EBPβ$^{-/-}$ macrophages. (B) Impaired induction of C/EBPβ target genes in C/EBPβ$^{-/-}$ macrophages. Shown are Eisen plots where columns represent the average of four WT and C/EBPβ$^{-/-}$ (KO) microarray experiments. Rows represent the average expression ratios of individual genes, which is the ratio of the mRNA levels for the gene in IFN-γ activated macrophages infected with *L. monocytogenes* as compared to untreated macrophages. Genes which have higher levels of their encoding mRNA in IFN-γ activated macrophages infected with *L. monocytogenes* than in the untreated macrophages are defined as up-regulated and are coloured red. Conversely, genes which have lower levels of their encoding mRNA in IFN-γ activated macrophages infected with *L. monocytogenes* than in the untreated macrophages are defined as down-regulated and are coloured green. The intensity of red or green shading is proportional to the level of gene up-regulation or down-regulation respectively.

**6. Identification of differentially expressed genes**

The aim of the microarray experiment was to identify macrophage genes downstream of C/EBPβ that are involved in mediating listericidal activity. Differentially expressed (DE) genes were identified by a paired T-Test that was based on permutation rather than distribution, in order to directly control the Type I Family Wise Error Rate (FWER) and thereby reduce the probability of erroneously identifying genes to be differentially expressed. The Type I error rate is the probability of rejecting the null hypothesis when the null is in fact true. The null hypothesis in this case was that there was no difference in gene expression between the infected WT and C/EBPβ$^{-/-}$ macrophages. Moreover, since there were 26000 genes to test, this meant that 26000 hypothesis tests were needed to be conducted (one corresponding to each t-test). If each test with a $p<0.05$ was considered to be significant, this meant that there was a 5% probability of rejecting the null hypothesis when the null was in fact true. In other words, 5% of the DE genes (1308 genes) would be falsely identified as being differentially expressed. If only one gene were being studied, a 5% margin of error would not be problematic. However, since 26000 genes were being tested, having 1308 false conclusions in one study was unacceptable. Therefore, it was essential to account for multiple testing when identifying differentially expressed genes. Many multiple testing procedures are designed to directly control the FWER. The most common methods include Bonferroni correction, the sequential methods of Hochberg or Holm or the re-sampling-based methods of Westfall & Young (35). Generally, these methods involved adjusting the p-value for each test (i.e. gene), so that even though the critical p-value for the entire data set was still equal to 0.05, each gene was evaluated at a lower p-value. Another multiple testing method is the control of the False Discovery Rate (FDR), where the expected number of false rejections among the rejected hypotheses is controlled by the researcher (36). In general, procedures that control the FWER tend to be more conservative than those that control the FDR. However, statistical significance is not necessarily the same as biological significance and p-values should be used to evaluate the strength of the evidence, rather than being used as an absolute yardstick of significance. Ultimately, what matters most is the biological significance and relevance of the data. Therefore, differentially expressed genes were identified by a paired T-Test where *p*-values were based on 100 random permutations per gene and significance was determined by Standard Bonferroni Correction (37, 38). Differentially expressed genes were defined as those genes whose expression was significantly higher or lower in the C/EBPβ$^{-/-}$ macrophages as compared to the WT in all 4 biological experiments. A total of 1268 genes were identified from the whole mouse genome of approximately 26000 genes to be differentially expressed. Furthermore, 55% of the DE genes were up-regulated, 45% were

down-regulated. Most of the DE genes had relatively small M values, which ranged from -0.8 to 1.2 on a log2 scale, with the majority clustering between 0.2 - 0.6 on a log2 scale (Fig. 20 A). The small M values may have been a consequence of the normalization process or may naturally have been small and not explicitly large due to slight differences in gene expression levels between the WT and C/EBPβ$^{-/-}$ macrophages.

The next important step in the analysis was to choose candidate genes for further study. A natural approach was to select the most highly induced or repressed genes. Selection of the top ten most highly up-regulated or down-regulated genes in the infected C/EBPβ$^{-/-}$ macrophages revealed that the majority were "unknown" genes for which there was neither functional information nor literature (Fig. 20 B). For example, the function or cellular location of the genes for Downs syndrome critical region homolog 6 (Dscr6), SET and MYND domain containing 4 (Smyd4), 1700009J07Rik, 2310020A21Rik, 2900092C05Rik, 4833401D15Rik, 4930563F08Rik, 5830435N17Rik, 8430436L14Rik, A830027B17Rik, B230324K02Rik, D630030L16Rik and K02154 are not known. High mobility group AT-hook 2 (Hmga2) is involved in DNA binding and packaging within the chromosome. It is also involved in the regulation of DNA-dependent transcription. Interleukin 1 family member 6 (Il1f6) is involved in the inflammatory immune response and has cytokine activity. The function of leucine rich repeat containing 6 (Lrrc6) is unknown, but it is tempting to speculate that it may be involved in recognition and/or binding *L. monocytogenes* cell wall products, similar to the leucine rich domains of the TLRs. Regulator of G-protein signalling 5 (Rgs5) is involved in G-protein coupled receptor (GPCR) protein signalling and has GTPase activator activity. G-protein coupled receptor 119 (Gpr119) is involved in the GPCR protein signalling pathway. Vomeronasal 1 receptor B4 (V1rb4) is involved in the GPCR protein signalling pathway and sensory perception of chemical stimulus. Endothelial lipase (Lipg) is involved in the hydrolysis of triacylglycerol, lipids and lipoproteins. Rgs5 and IL-1f6 were considered potential candidates for further study, since they have been shown to play important roles in signal transduction and innate immune responses. Rgs5 is a key regulator of GPCR protein signalling and negatively regulates G protein signalling by acting as a GTPase-activating protein (GAP) for G alpha subunits of G protein coupled receptors (GPCRs) (39). IL-1f6 was shown to be important for pro-inflammatory responses by acting as an IL-1 agonist which in turn activated NF-κB through the orphan IL-1 receptor-related protein 2 (40). However, since the proteins encoded by these genes appeared to act early (upstream) in their signalling pathways, they were not considered good candidates for effecting bacterial killing. In addition, the selection of candidate genes based on the highest fold difference in gene

expression levels would not be the wisest method to use, since the assumption would be made that the bigger the fold difference, the more significant the biological effect. This may not necessarily be true, since it may be possible that a small change in a complex biological system can have a much greater far-reaching effect on the entire system than an overtly large change. For example a small change in the expression levels of a transcription factor can have a far greater biological implication than a large change in the expression levels of a gene involved in protein degradation.

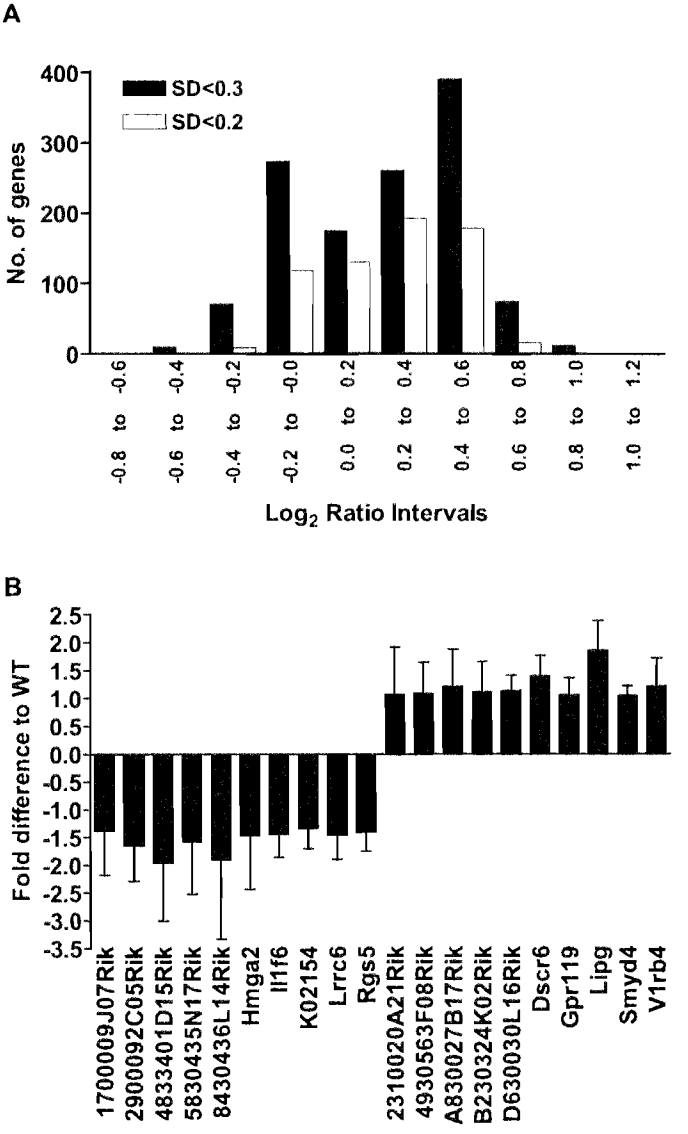


**Figure 20. Differential expression of genes in the C/EBPβ$^{-/-}$ macrophages as compared to WT.** (A) Frequency of M values ($log_2$ ratios) of the differentially expressed genes which has SD<0.2 (filled bars) or SD<0.3 (open bars). (B) The top ten genes in the infected C/EBPβ$^{-/-}$ macrophages with biggest or smallest fold difference in gene expression as compared to WT macrophages.

Moreover, since the microarray data represented only one time-point after infection (4 hours), biological functions could not be inferred upon the unknown genes based on co-clustering with known genes. Clusters based on gene expression data have been shown to be enriched for genes known to be involved in similar biological process, therefore implying that unknown genes in these clusters may also be involved in those processes (41, 42). In addition, since the microarray gene expression data lacked kinetic dimension, candidate genes could not be selected based on interesting expression patterns during the time course of the infection. Instead, the DE genes could only be grouped into four simple patterns of expression during *L. monocytogenes* infection (Fig. 21): Group I genes were down-regulated in both WT and C/EBPβ$^{-/-}$ macrophages, where the degree of down-regulation was either greater or lower in the C/EBPβ$^{-/-}$ macrophages. Group II genes were up-regulated and group III down-regulated in the C/EBPβ$^{-/-}$ macrophages during infection as compared to WT. Group IV genes were up-regulated in both genotypes, but the degree of down-regulation was either greater or lower in the C/EBPβ$^{-/-}$ macrophages as compared to WT controls. However, these simple expression patterns still did not help identify genes that were involved in mediating listericidal activity. A deeper understanding of the biological functions of the DE genes during innate immunity and related processes was needed in order to make an educated decision of which genes to choose for further analysis. However, since there were 1268 DE genes, it would be an overwhelming task to research each individual gene. Therefore, a new strategy, focussing on particular biological functions and characteristics was developed to choose candidate genes.

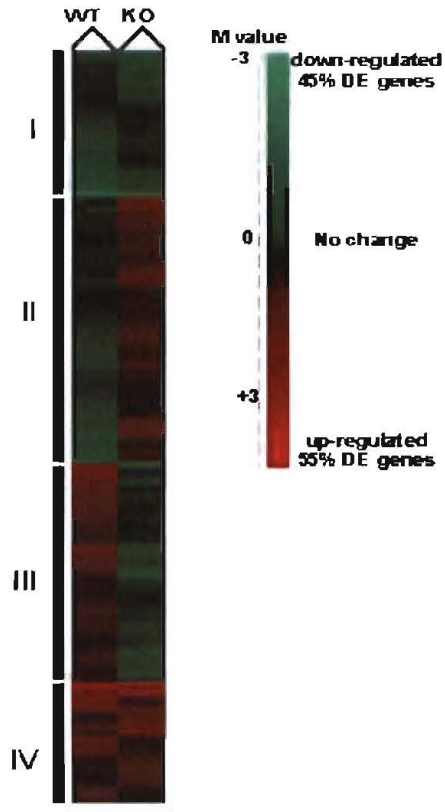


**Figure 21. Hierarchical clustering of differentially expressed based on genes expression values.** Differentially expressed genes were hierarchically clustered in to four groups (I to IV) using Euclidean distance and average linkage. Shown is an Eisen plot where columns represent the average of four WT and C/EBPβ$^{-/-}$ (KO) microarray experiments. Rows represent the average expression ratios of individual genes, which is the ratio of the mRNA levels for the gene in IFN-γ activated macrophages infected with *L. monocytogenes* as compared to untreated macrophages. Genes which have higher levels of their encoding mRNA in IFN-γ activated macrophages infected with *L. monocytogenes* than in the untreated macrophages are defined as up-regulated and are coloured red. Conversely, genes which have lower levels of their encoding mRNA in IFN-γ activated macrophages infected with *L. monocytogenes* than in the untreated macrophages are defined as down-regulated and are coloured green. The intensity of red or green shading is proportional to the level of gene up-regulation or down-regulation respectively. During *L. monocytogenes* infection of IFN-γ activated macrophages, Group I genes are down-regulated in both WT and C/EBPβ$^{-/-}$ macrophages, Group II genes are up-regulated in C/EBPβ$^{-/-}$ but down-regulated in the WT macrophages, Group III genes are down-regulated in the C/EBPβ$^{-/-}$ but up-regulated in the WT macrophages and Group IV genes are up-regulated in both WT and C/EBPβ$^{-/-}$ macrophages.

**7. Focussed Functional Clustering**

Since the aim of the microarray experiment was to identify listericidal genes downstream of C/EBPβ, it was hypothesized that these genes may (i) be transcriptional targets of C/EBPβ and may therefore contain C/EBPβ binding sites in their promoter and/or binding sites for other transcription factors that synergize with C/EBPβ, (ii) be involved in transcription of further downstream effector genes, (iii) be involved in host defense and immunity, (iv) be involved in the production of bactericidal ROI and RNI molecules, (v) be involved in promoting phagosome maturation, phago-lysosome fusion and subsequent lysosome-mediated bacterial killing and/or (vi) be involved in signal transduction of extracellular and intracellular stimuli. A focussed functional clustering strategy was therefore developed (Fig. 22), in which promoter analysis was used to identify potential C/EBPβ target genes and functional data mining of the gene ontology database extracted functional data for each DE gene, describing its cellular localization, biological processes and molecular functions. In addition, the strategy included literature mining of the PubMed database to uncover the roles of the DE genes in host defense and immunity to intracellular pathogens, phagosome maturation, phago-lysosome fusion and signal transduction. After extraction and assignment of functional data, the DE genes would be clustered into the above six "focus" groups based on their gene ontology associations, promoter analysis and previously published functional roles. Candidate genes belonging to 3 or more of the focus groups would then be selected for further analysis. The rationale for selecting genes which intersected with 3 or more (i.e. ≥50%) of the focus functional groups, was that this strategy may increase the probability of selecting candidate genes which have a significant biological impact on the resolution of *L. monocytogenes* infection. For example, the genes that clustered into only one or two of the functional focus groups were comprised mostly of putative C/EBPβ target genes. However, DE genes that intersected with 3 or more of the functional focus groups were found to be enriched for those genes which have already been described in the literature to play a significant role in innate immunity to *L. monocytogenes* (Table 5). Moreover, the significant biological impact for three of these DE genes during *L. monocytogenes* infection has been demonstrated in gene deficient mouse models. For example, mice deficient for IL-1β (21, 43), p47phox (23) and TNFRp55 (20) display increased susceptibility to *L. monocytogenes*. Therefore co-clustering of DE genes with these "high biological impact" genes may therefore highlight which of the 1268 DE genes should be selected for further analysis.

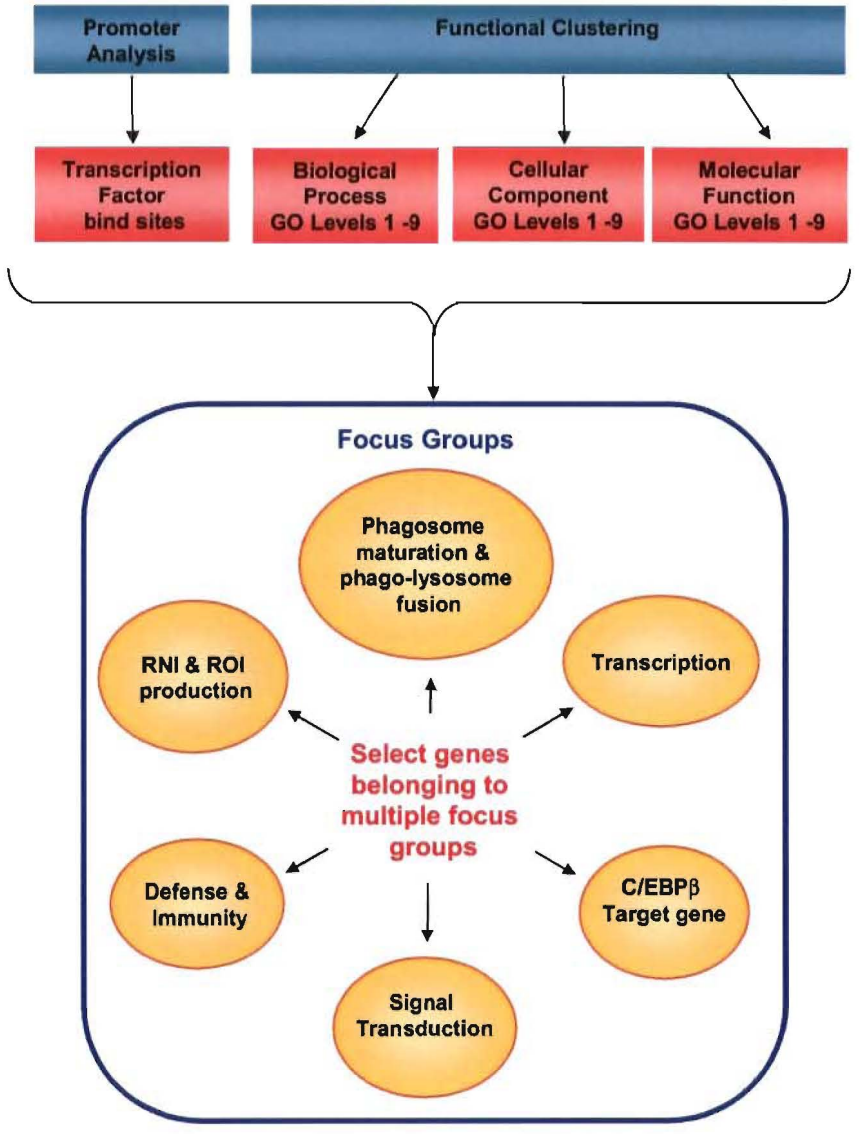


**Figure 22. Focussed Functional Clustering Strategy.** Promoter analysis is used to identify potential C/EBPβ target genes and data mining of the Gene Ontology database extracts data for each DE gene describing its cellular localization, biological processes and molecular functions. In addition, literature mining of the PubMed database is used to uncover the roles of the DE genes in host defense and immunity to intracellular pathogens, phagosome maturation, phago-lysosome fusion and signal transduction. After extraction and assignment of functional data, the DE genes are clustered into the above six "focus" groups based on their functional annotations and genes belonging to 3 or more of the focus groups are selected for further analysis.

**Table 5. The intersection of DE genes between one or more of the functional clustering focus groups**. Listed are the gene accession number, gene symbol, standard deviation (SD) for the average gene expression ratio and the number of functional cluster groups that each gene belongs to. Shaded in light grey are the genes that would have been exlcuded from the candidate DE gene list when using a SD > 0.2 cut off for unreliable data. Genes highlighted in red are reported in the literature to play a role during *L. monocytogenes* infection.

| Accession | Symbol | Occurrence in Functional Cluster Groups | Std Dev < < 0.2 |
|---|---|---|---|
| NM_011103 | PKCδ (44) | 7 | < 0.2 |
| NM_183405 | Cox6b2 | 5 | < 0.2 |
| 8030450C14Rik | ENDASDF | 5 | < 0.2 |
| NM_133225 | Acbd3 | 4 | < 0.2 |
| NM_153319 | Amot | 4 | < 0.2 |
| NM_009725 | Atp5f1 | 4 | < 0.2 |
| NM_172257 | BC023957 | 4 | < 0.2 |
| NM_172599 | D14Ertd436e | 4 | < 0.2 |
| D530030D03Rik | ENDASDF | 4 | < 0.2 |
| C330013F16Rik | ENDASDF | 4 | < 0.2 |
| 9430006E15Rik | ENDASDF | 4 | < 0.2 |
| NM_145546 | Gtf2b | 4 | < 0.2 |
| NM_144513 | Gtl2 | 4 | < 0.2 |
| NM_008349 | Il10rb | 4 | < 0.2 |
| NM_010744 | Il1rl1 | 4 | < 0.2 |
| NM_010562 | Ilk | 4 | < 0.2 |
| NM_147102 | Olfr552 | 4 | < 0.2 |
| NM_080843 | Socs4 | 4 | < 0.2 |
| NM_207543 | V1rd10 | 4 | < 0.2 |
| NM_178066 | 1110012D08Rik | 3 | < 0.2 |
| XM_485446 | 1700125D06Rik | 3 | < 0.2 |
| NM_175216 | 4930506C02Rik | 3 | < 0.2 |
| NM_178936 | 4930577M16Rik | 3 | < 0.2 |
| NM_175163 | 4933416E05Rik | 3 | < 0.2 |
| NM_145562 | 9130213B05Rik | 3 | < 0.2 |
| NM_177790 | A930006D11 | 3 | < 0.2 |
| NM_145415 | AA408296 | 3 | < 0.2 |
| NM_019811 | Acas2 | 3 | < 0.2 |
| NM_013925 | Adat1 | 3 | < 0.2 |
| XM_287445 | AF013969 | 3 | < 0.2 |
| NM_198626 | AI480653 | 3 | < 0.2 |
| NM_144897 | Apoa1bp | 3 | < 0.2 |
| NM_007471 | App | 3 | < 0.2 |
| NM_007477 | Arf2 | 3 | < 0.2 |
| NM_134034 | AW011752 | 3 | < 0.2 |
| NM_173071 | Bai2 | 3 | < 0.2 |
| NM_145402 | BC003277 | 3 | < 0.2 |
| NM_145624 | BC021921 | 3 | < 0.2 |
| NM_198967 | BC023818 | 3 | < 0.2 |
| NM_183217 | BC042698 | 3 | < 0.2 |
| NM_007541 | Bglap1 | 3 | < 0.2 |
| NM_021426 | C030019F02Rik | 3 | < 0.2 |
| NM_007579 | Cacna1b | 3 | < 0.2 |
| NM_019405 | Cetn2 | 3 | < 0.2 |
| NM_009888 | Cfh | 3 | < 0.2 |

| | | | |
|---|---|---|---|
| NM_015730 | Chrna4 | 3 | < 0.2 |
| NM_016877 | Cnot4 | 3 | < 0.2 |
| NM_007792 | Csrp2 | 3 | < 0.2 |
| NM_183223 | D730018G16 | 3 | < 0.2 |
| NM_001003919 | Ddx11 | 3 | < 0.2 |
| NM_013764 | Dguok | 3 | < 0.2 |
| NM_007857 | Dhh | 3 | < 0.2 |
| NM_033374 | Dock2 | 3 | < 0.2 |
| NM_181682 | Dsg1b | 3 | < 0.2 |
| NM_019422 | Elovl1 | 3 | < 0.2 |
| Terg-V5 | ENDASDF | 3 | < 0.2 |
| Myo1a | ENDASDF | 3 | < 0.2 |
| D6Ertd245e | ENDASDF | 3 | < 0.2 |
| D430030G11Rik | ENDASDF | 3 | < 0.2 |
| D130048G10Rik | ENDASDF | 3 | < 0.2 |
| D030067O06Rik | ENDASDF | 3 | < 0.2 |
| C230053E11Rik | ENDASDF | 3 | < 0.2 |
| C030046E11Rik | ENDASDF | 3 | < 0.2 |
| C030002B11Rik | ENDASDF | 3 | < 0.2 |
| BC042494 | ENDASDF | 3 | < 0.2 |
| BC037095 | ENDASDF | 3 | < 0.2 |
| AK081365 | ENDASDF | 3 | < 0.2 |
| AK038840 | ENDASDF | 3 | < 0.2 |
| AK030863 | ENDASDF | 3 | < 0.2 |
| AK009485 | ENDASDF | 3 | < 0.2 |
| AK002970 | ENDASDF | 3 | < 0.2 |
| AJ006521 | ENDASDF | 3 | < 0.2 |
| AF159803 | ENDASDF | 3 | < 0.2 |
| A930019L04Rik | ENDASDF | 3 | < 0.2 |
| 9530020O07Rik | ENDASDF | 3 | < 0.2 |
| 9430040K09Rik | ENDASDF | 3 | < 0.2 |
| 4930553D19Rik | ENDASDF | 3 | < 0.2 |
| 4930447I22Rik | ENDASDF | 3 | < 0.2 |
| NM_146129 | F730014I05Rik | 3 | < 0.2 |
| NM_177320 | F730038I15Rik | 3 | < 0.2 |
| NM_008072 | Gabrd | 3 | < 0.2 |
| NM_010252 | Gabrg1 | 3 | < 0.2 |
| NM_008109 | Gdf5 | 3 | < 0.2 |
| NM_183427 | Glra2 | 3 | < 0.2 |
| Z15022 | IGHV9S3 | 3 | < 0.2 |
| AJ235943 | IGKV4-70 | 3 | < 0.2 |
| NM_145958 | Kbtbd2 | 3 | < 0.2 |
| NM_010663 | Krt1-17 | 3 | < 0.2 |
| NM_133357 | Krtcap1 | 3 | < 0.2 |
| NM_177250 | Lrrn6d | 3 | < 0.2 |
| NM_053251 | MP4 | 3 | < 0.2 |
| NM_181072 | Myo1e | 3 | < 0.2 |
| NM_080849 | Nek8 | 3 | < 0.2 |
| NM_183248 | Nkx6-2 | 3 | < 0.2 |
| NM_146391 | Olfr1058 | 3 | < 0.2 |
| NM_146396 | Olfr1277 | 3 | < 0.2 |
| NM_147068 | Olfr166 | 3 | < 0.2 |
| NM_146749 | Olfr875 | 3 | < 0.2 |
| NM_175094 | Pdhx | 3 | < 0.2 |
| NM_182930 | Plekha6 | 3 | < 0.2 |
| XM_487324 | Polr3a | 3 | < 0.2 |
| NM_007453 | Prdx6 | 3 | < 0.2 |
| NM_198703 | Prkwnk1 | 3 | < 0.2 |
| NM_011220 | Pts | 3 | < 0.2 |
| NM_021326 | Rbak | 3 | < 0.2 |

| | | | |
|---|---|---|---|
| NM_019708 | Scoc | 3 | < 0.2 |
| NM_145581 | Siglec5 | 3 | < 0.2 |
| NM_001002898 | Sirpb | 3 | < 0.2 |
| NM_175283 | Srd5a1 | 3 | < 0.2 |
| NM_020565 | Sult3a1 | 3 | < 0.2 |
| NM_134011 | Tbrg4 | 3 | < 0.2 |
| NM_011582 | Thbs4 | 3 | < 0.2 |
| NM_175274 | Ttyh3 | 3 | < 0.2 |
| NM_011667 | Ube1y1 | 3 | < 0.2 |
| XM_135707 | 0610010K06Rik | 2 | < 0.2 |
| XM_146151 | 1600016N20Rik | 2 | < 0.2 |
| XM_126808 | 1700013G20Rik | 2 | < 0.2 |
| NM_025471 | 1810030N24Rik | 2 | < 0.2 |
| NM_023397 | 1810034K20Rik | 2 | < 0.2 |
| NM_134133 | 2010002N04Rik | 2 | < 0.2 |
| NM_175145 | 2310003P10Rik | 2 | < 0.2 |
| NM_028839 | 2310014H19Rik | 2 | < 0.2 |
| NM_019974 | 2310015I08Rik | 2 | < 0.2 |
| NM_181397 | 2310015N21Rik | 2 | < 0.2 |
| NM_133714 | 2310037I24Rik | 2 | < 0.2 |
| NM_153776 | 2410008J05Rik | 2 | < 0.2 |
| NM_025556 | 2410022L05Rik | 2 | < 0.2 |
| NM_019421 | 425O18-1 | 2 | < 0.2 |
| NM_177307 | 4732474A20Rik | 2 | < 0.2 |
| NM_172468 | 4732481H14Rik | 2 | < 0.2 |
| NM_177769 | 4831417L10 | 2 | < 0.2 |
| NM_029777 | 4930418P06Rik | 2 | < 0.2 |
| NM_183131 | 4930451I11Rik | 2 | < 0.2 |
| NM_029478 | 4930579A11Rik | 2 | < 0.2 |
| NM_172535 | 4932408B21Rik | 2 | < 0.2 |
| NM_173764 | 4932414K18Rik | 2 | < 0.2 |
| NM_198004 | 5133401N09Rik | 2 | < 0.2 |
| NM_172935 | 5730457F11Rik | 2 | < 0.2 |
| NM_173443 | 5730538E15Rik | 2 | < 0.2 |
| NM_134078 | 6330407G04Rik | 2 | < 0.2 |
| NM_198035 | 7030401O21Rik | 2 | < 0.2 |
| XM_355515 | 9230110M18Rik | 2 | < 0.2 |
| XM_488560 | 9530080M15Rik | 2 | < 0.2 |
| NM_177179 | 9930022D16Rik | 2 | < 0.2 |
| XM_488773 | A230028O05Rik | 2 | < 0.2 |
| NM_175079 | A730016F12Rik | 2 | < 0.2 |
| NM_172711 | AA407526 | 2 | < 0.2 |
| NM_007378 | Abca4 | 2 | < 0.2 |
| NM_177470 | Acaa2 | 2 | < 0.2 |
| NM_022816 | Acate3 | 2 | < 0.2 |
| NM_016860 | Actr1a | 2 | < 0.2 |
| NM_011782 | Adamts5 | 2 | < 0.2 |
| NM_013462 | Adrb3 | 2 | < 0.2 |
| NM_199028 | AK122525 | 2 | < 0.2 |
| NM_153066 | Ak5 | 2 | < 0.2 |
| NM_007431 | Akp2 | 2 | < 0.2 |
| NM_001003946 | Als2cr13 | 2 | < 0.2 |
| NM_024204 | Ankrd22 | 2 | < 0.2 |
| NM_145611 | Ankrd25 | 2 | < 0.2 |
| NM_194341 | Aplgbp1 | 2 | < 0.2 |
| NM_019824 | Arpc3 | 2 | < 0.2 |
| NM_178408 | Arrdc1 | 2 | < 0.2 |
| NM_133699 | Atp6v1c2 | 2 | < 0.2 |
| NM_007510 | Atp6v1e1 | 2 | < 0.2 |
| NM_133826 | Atp6v1h | 2 | < 0.2 |

| | | | |
|---|---|---|---|
| NM_178927 | AV344025 | 2 | < 0.2 |
| NM_178638 | B130017P16Rik | 2 | < 0.2 |
| NM_173427 | B230308G19Rik | 2 | < 0.2 |
| NM_178766 | B230315F11Rik | 2 | < 0.2 |
| NM_172742 | BB128963 | 2 | < 0.2 |
| NM_199222 | BC020188 | 2 | < 0.2 |
| NM_201352 | BC024955 | 2 | < 0.2 |
| NM_177601 | BC027828 | 2 | < 0.2 |
| NM_001001326 | BC032266 | 2 | < 0.2 |
| NM_009737 | Bcat2 | 2 | < 0.2 |
| XM_128275 | Brd1 | 2 | < 0.2 |
| NM_172757 | C030036P15Rik | 2 | < 0.2 |
| NM_177842 | C130021I20 | 2 | < 0.2 |
| NM_145540 | C77668 | 2 | < 0.2 |
| NM_009783 | Cacna1g | 2 | < 0.2 |
| NM_009792 | Camk2a | 2 | < 0.2 |
| NM_009835 | Ccr6 | 2 | < 0.2 |
| NM_153098 | Cd109 | 2 | < 0.2 |
| NM_007688 | Cfl2 | 2 | < 0.2 |
| NM_009891 | Chat | 2 | < 0.2 |
| NM_007691 | Chek1 | 2 | < 0.2 |
| NM_138585 | Cherp | 2 | < 0.2 |
| NM_009900 | Clcn2 | 2 | < 0.2 |
| NM_033444 | Clic1 | 2 | < 0.2 |
| NM_009932 | Col4a2 | 2 | < 0.2 |
| NM_007744 | Comt | 2 | < 0.2 |
| NM_011991 | Cops3 | 2 | < 0.2 |
| NM_013715 | Cops5 | 2 | < 0.2 |
| NM_012003 | Cops7a | 2 | < 0.2 |
| NM_013767 | Csnk1e | 2 | < 0.2 |
| NM_016716 | Cul3 | 2 | < 0.2 |
| NM_010010 | Cyp46a1 | 2 | < 0.2 |
| NM_138596 | D13Wsu50e | 2 | < 0.2 |
| NM_023731 | D19Ertd678e | 2 | < 0.2 |
| NM_172490 | D5Ertd135e | 2 | < 0.2 |
| NM_012008 | Ddx3y | 2 | < 0.2 |
| XM_135485 | Dhrsx | 2 | < 0.2 |
| NM_023314 | Eif4el3 | 2 | < 0.2 |
| NM_178736 | Elmod2 | 2 | < 0.2 |
| Fbxl7 | ENDASDF | 2 | < 0.2 |
| F730002C09Rik | ENDASDF | 2 | < 0.2 |
| Drld | ENDASDF | 2 | < 0.2 |
| D930040F23Rik | ENDASDF | 2 | < 0.2 |
| D930016D06Rik | ENDASDF | 2 | < 0.2 |
| D930006K15Rik | ENDASDF | 2 | < 0.2 |
| D730047E02Rik | ENDASDF | 2 | < 0.2 |
| C630016I17Rik | ENDASDF | 2 | < 0.2 |
| C330018A13Rik | ENDASDF | 2 | < 0.2 |
| BC030943 | ENDASDF | 2 | < 0.2 |
| BC027782 | ENDASDF | 2 | < 0.2 |
| B230343A10Rik | ENDASDF | 2 | < 0.2 |
| AK079817 | ENDASDF | 2 | < 0.2 |
| AK045323 | ENDASDF | 2 | < 0.2 |
| AK034422 | ENDASDF | 2 | < 0.2 |
| AK030927 | ENDASDF | 2 | < 0.2 |
| AK008158 | ENDASDF | 2 | < 0.2 |
| A930033M14Rik | ENDASDF | 2 | < 0.2 |
| A930007D18Rik | ENDASDF | 2 | < 0.2 |
| A130079P16Rik | ENDASDF | 2 | < 0.2 |
| 9830137A06Rik | ENDASDF | 2 | < 0.2 |

| | | | |
|---|---|---|---|
| 9430022A06Rik | ENDASDF | 2 | < 0.2 |
| 8430436O14Rik | ENDASDF | 2 | < 0.2 |
| 7330412A13Rik | ENDASDF | 2 | < 0.2 |
| 5830411O07Rik | ENDASDF | 2 | < 0.2 |
| 4930405G09Rik | ENDASDF | 2 | < 0.2 |
| NM_007991 | Fbl | 2 | < 0.2 |
| NM_013911 | Fbxl12 | 2 | < 0.2 |
| NM_028841 | Fbxo23 | 2 | < 0.2 |
| NM_010192 | Fem1a | 2 | < 0.2 |
| NM_011711 | Fmnl3 | 2 | < 0.2 |
| NM_183358 | Gadd45gip1 | 2 | < 0.2 |
| NM_011819 | Gdf15 | 2 | < 0.2 |
| NM_013529 | Gfpt2 | 2 | < 0.2 |
| NM_145929 | Gga1 | 2 | < 0.2 |
| NM_177756 | Glt25d2 | 2 | < 0.2 |
| NM_020273 | Gmeb1 | 2 | < 0.2 |
| NM_010325 | Got2 | 2 | < 0.2 |
| NM_008175 | Grn | 2 | < 0.2 |
| NM_146120 | Gsn (45, 46) | 2 | < 0.2 |
| NM_010388 | H2-DMb2 | 2 | < 0.2 |
| NM_008205 | H2-M9 | 2 | < 0.2 |
| XM_131076 | Hbxip | 2 | < 0.2 |
| NM_008227 | Hcn3 | 2 | < 0.2 |
| NM_133849 | Hrh3 | 2 | < 0.2 |
| NM_018741 | Igfbpl1 | 2 | < 0.2 |
| AJ235934 | IGKV12-66 | 2 | < 0.2 |
| XM_134910 | Ireb2 | 2 | < 0.2 |
| NM_010596 | Kcna7 | 2 | < 0.2 |
| NM_020574 | Kcne3 | 2 | < 0.2 |
| NM_177715 | Kctd12 | 2 | < 0.2 |
| NM_146188 | Kctd15 | 2 | < 0.2 |
| NM_183390 | Klhl6 | 2 | < 0.2 |
| NM_008465 | Kpna1 | 2 | < 0.2 |
| NM_010686 | Laptm5 | 2 | < 0.2 |
| NM_010689 | Lat | 2 | < 0.2 |
| NM_198646 | LOC381062 | 2 | < 0.2 |
| NM_011843 | Mbc2 | 2 | < 0.2 |
| NM_013595 | Mbd3 | 2 | < 0.2 |
| NM_008564 | Mcm2 | 2 | < 0.2 |
| NM_011844 | Mgll | 2 | < 0.2 |
| NM_008598 | Mgmt | 2 | < 0.2 |
| NM_133761 | Mitc1 | 2 | < 0.2 |
| NM_008615 | Mod1 | 2 | < 0.2 |
| NC_004279 | MoV3sS2gp1 | 2 | < 0.2 |
| NM_008209 | Mr1 | 2 | < 0.2 |
| NM_021718 | Ms4a4b | 2 | < 0.2 |
| NM_144843 | Mtmr6 | 2 | < 0.2 |
| NM_008098 | Mtpn | 2 | < 0.2 |
| XM_485520 | Myom3 | 2 | < 0.2 |
| NM_007501 | Neurod4 | 2 | < 0.2 |
| NM_182716 | Nfasc | 2 | < 0.2 |
| S81451 | NFI-X3 | 2 | < 0.2 |
| NM_008706 | Nqo1 | 2 | < 0.2 |
| NM_146818 | Olfr1218 | 2 | < 0.2 |
| NM_207157 | Olfr1333 | 2 | < 0.2 |
| NM_207573 | Olfr1380 | 2 | < 0.2 |
| NM_147082 | Olfr609 | 2 | < 0.2 |
| NM_146665 | Olfr732 | 2 | < 0.2 |
| NM_146419 | Olfr883 | 2 | < 0.2 |
| NM_147105 | Olfr978 | 2 | < 0.2 |

| | | | |
|---|---|---|---|
| NM_011863 | Papss1 | 2 | < 0.2 |
| NM_033609 | Pcqap | 2 | < 0.2 |
| NM_172665 | Pdk1 | 2 | < 0.2 |
| NM_145978 | Pdlim2 | 2 | < 0.2 |
| NM_011822 | Pigq | 2 | < 0.2 |
| NM_013632 | Pnp | 2 | < 0.2 |
| NM_175170 | Pogk | 2 | < 0.2 |
| NM_008905 | Ppfibp2 | 2 | < 0.2 |
| NM_013636 | Ppp1cc | 2 | < 0.2 |
| NM_011625 | Ppp1r13b | 2 | < 0.2 |
| NM_024209 | Ppp6c | 2 | < 0.2 |
| NM_016914 | Prg3 | 2 | < 0.2 |
| XM_131444 | Prpf4 | 2 | < 0.2 |
| NM_011223 | Pxn | 2 | < 0.2 |
| NM_019773 | Rab9 | 2 | < 0.2 |
| NM_053268 | Rasa2 | 2 | < 0.2 |
| NM_133925 | Rbm28 | 2 | < 0.2 |
| NM_145620 | Rnu3ip2 | 2 | < 0.2 |
| NM_009105 | Rsu1 | 2 | < 0.2 |
| NM_172676 | Samd10 | 2 | < 0.2 |
| BC067198 | Samhd1 | 2 | < 0.2 |
| NM_172604 | Scara3 | 2 | < 0.2 |
| NM_133199 | Scn4a | 2 | < 0.2 |
| NM_207214 | Sec10l1 | 2 | < 0.2 |
| NM_009247 | Serpina1e | 2 | < 0.2 |
| NM_018877 | Setdb1 | 2 | < 0.2 |
| NM_175102 | Sf3b5 | 2 | < 0.2 |
| NM_009159 | Sfrs5 | 2 | < 0.2 |
| NM_176846 | Slac2b | 2 | < 0.2 |
| NM_145156 | Slc25a28 | 2 | < 0.2 |
| NM_013901 | Slc39a1 | 2 | < 0.2 |
| NM_145423 | Slc5a8 | 2 | < 0.2 |
| NM_172271 | Slc6a17 | 2 | < 0.2 |
| NM_007514 | Slc7a2 | 2 | < 0.2 |
| NM_146236 | Tceal1 | 2 | < 0.2 |
| NM_009335 | Tcfap2c | 2 | < 0.2 |
| NM_172541 | Tmpit | 2 | < 0.2 |
| NM_011605 | Tmpo | 2 | < 0.2 |
| NM_009397 | Tnfaip3 | 2 | < 0.2 |
| NM_011626 | Tparl | 2 | < 0.2 |
| AY251388 | Trim46 | 2 | < 0.2 |
| NM_009437 | Tst | 2 | < 0.2 |
| NM_001001981 | Utp14b | 2 | < 0.2 |
| NM_009498 | Vamp3 | 2 | < 0.2 |
| NM_013703 | Vldlr | 2 | < 0.2 |
| NM_009518 | Wnt10a | 2 | < 0.2 |
| NM_172993 | Zfp512 | 2 | < 0.2 |
| NM_183154 | Zfyve1 | 2 | < 0.2 |
| XM_127031 | Zfyve26 | 2 | < 0.2 |
| NM_172700 | Zmpste24 | 2 | < 0.2 |
| NM_013859 | Znhit2 | 2 | < 0.2 |
| NM_017461 | 37135 | 1 | < 0.2 |
| NM_172920 | 1100001I19Rik | 1 | < 0.2 |
| NM_024244 | 1200015N20Rik | 1 | < 0.2 |
| XM_128462 | 1700010L19Rik | 1 | < 0.2 |
| NM_023816 | 1700012M14Rik | 1 | < 0.2 |
| XM_132393 | 1700016K13Rik | 1 | < 0.2 |
| XM_358772 | 1810015A11Rik | 1 | < 0.2 |
| XM_126658 | 2310003H01Rik | 1 | < 0.2 |
| NM_025519 | 2310010I16Rik | 1 | < 0.2 |

| | | | |
|---|---|---|---|
| NM_024246 | 2310042N02Rik | 1 | < 0.2 |
| XM_131053 | 2410015C20Rik | 1 | < 0.2 |
| XM_128698 | 2610024N24Rik | 1 | < 0.2 |
| XM_128768 | 4921517J08Rik | 1 | < 0.2 |
| NM_177570 | 4933406A14Rik | 1 | < 0.2 |
| XM_130851 | 4933421B21Rik | 1 | < 0.2 |
| XM_127023 | 4933437F05Rik | 1 | < 0.2 |
| XM_134954 | 5430433E21Rik | 1 | < 0.2 |
| XM_132538 | 5830411G16Rik | 1 | < 0.2 |
| NM_146104 | 6530402N02Rik | 1 | < 0.2 |
| NM_177802 | 9030221C07Rik | 1 | < 0.2 |
| NM_033145 | 9230106L18Rik | 1 | < 0.2 |
| NM_172524 | 9530066K23Rik | 1 | < 0.2 |
| NM_146105 | 9630058J23Rik | 1 | < 0.2 |
| NM_178165 | A230020G22Rik | 1 | < 0.2 |
| XM_132396 | A930033C01Rik | 1 | < 0.2 |
| NM_013455 | Acr | 1 | < 0.2 |
| NM_021895 | Actn4 | 1 | < 0.2 |
| NM_175501 | Adamts12 | 1 | < 0.2 |
| NM_009624 | Adcy9 | 1 | < 0.2 |
| NM_001005847 | Aga | 1 | < 0.2 |
| NM_172754 | AI449175 | 1 | < 0.2 |
| NM_021473 | Akr1a4 | 1 | < 0.2 |
| NM_054080 | Akr1c20 | 1 | < 0.2 |
| NM_175007 | Amph | 1 | < 0.2 |
| NM_007385 | Apoc4 | 1 | < 0.2 |
| NM_029277 | Arhgap12 | 1 | < 0.2 |
| NM_172751 | Arhgef10 | 1 | < 0.2 |
| NM_017402 | Arhgef7 | 1 | < 0.2 |
| NM_026369 | Arpc5 (47) | 1 | < 0.2 |
| NM_080857 | Asb13 | 1 | < 0.2 |
| NM_007517 | Aup1 | 1 | < 0.2 |
| XM_489070 | AW011738 | 1 | < 0.2 |
| NM_021345 | AW742319 | 1 | < 0.2 |
| NM_177280 | B230206H07Rik | 1 | < 0.2 |
| XM_131619 | BC022150 | 1 | < 0.2 |
| NM_172148 | BC028440 | 1 | < 0.2 |
| XM_147687 | BC042761 | 1 | < 0.2 |
| NM_174848 | BC043118 | 1 | < 0.2 |
| NM_172928 | BC056929 | 1 | < 0.2 |
| NM_172502 | BC057552 | 1 | < 0.2 |
| NM_172872 | BC060737 | 1 | < 0.2 |
| NM_025392 | Bccip | 1 | < 0.2 |
| NM_009754 | Bcl2l11 | 1 | < 0.2 |
| NM_172616 | C330027C09Rik | 1 | < 0.2 |
| NM_019704 | C78915 | 1 | < 0.2 |
| NM_007625 | Cbx4 | 1 | < 0.2 |
| NM_019937 | Ccnl1 | 1 | < 0.2 |
| NM_009603 | Chrne | 1 | < 0.2 |
| XM_356089 | Cib3 | 1 | < 0.2 |
| NM_009905 | Clk1 | 1 | < 0.2 |
| NM_007715 | Clock | 1 | < 0.2 |
| NM_009933 | Col6a1 | 1 | < 0.2 |
| NM_198408 | Crhbp | 1 | < 0.2 |
| XM_139502 | Csmd3 | 1 | < 0.2 |
| XM_488510 | Cspg2 | 1 | < 0.2 |
| XM_111693 | D130003B22Rik | 1 | < 0.2 |
| BC046250 | D14Wsu89e | 1 | < 0.2 |
| XM_128587 | D17Wsu92e | 1 | < 0.2 |
| NM_008650 | D230010K02Rik | 1 | < 0.2 |

| | | | |
|---|---|---|---|
| XM_286688 | D630010B17Rik | 1 | < 0.2 |
| NM_172689 | Ddx58 | 1 | < 0.2 |
| NM_026172 | Decr1 | 1 | < 0.2 |
| NM_010046 | Dgat1 | 1 | < 0.2 |
| XM_134573 | Dncli2 | 1 | < 0.2 |
| NM_145919 | Dorz1 | 1 | < 0.2 |
| NM_019466 | Dscr1 | 1 | < 0.2 |
| NM_007886 | Dtnb | 1 | < 0.2 |
| NM_026017 | Dullard | 1 | < 0.2 |
| NM_198093 | Elmo1 | 1 | < 0.2 |
| Tas2r116 | ENDASDF | 1 | < 0.2 |
| Rnu22 | ENDASDF | 1 | < 0.2 |
| Gcap27 | ENDASDF | 1 | < 0.2 |
| D930015M05 | ENDASDF | 1 | < 0.2 |
| D130058E05Rik | ENDASDF | 1 | < 0.2 |
| C130031E09Rik | ENDASDF | 1 | < 0.2 |
| BC060255 | ENDASDF | 1 | < 0.2 |
| AK076321 | ENDASDF | 1 | < 0.2 |
| AK028313 | ENDASDF | 1 | < 0.2 |
| AK007522 | ENDASDF | 1 | < 0.2 |
| A730046J19Rik | ENDASDF | 1 | < 0.2 |
| A430108G06Rik | ENDASDF | 1 | < 0.2 |
| 9530036M11Rik | ENDASDF | 1 | < 0.2 |
| 9130015L21Rik | ENDASDF | 1 | < 0.2 |
| 4930532G15Rik | ENDASDF | 1 | < 0.2 |
| 4930503O07Rik | ENDASDF | 1 | < 0.2 |
| 4930448K12Rik | ENDASDF | 1 | < 0.2 |
| 4930445N06Rik | ENDASDF | 1 | < 0.2 |
| 3110038A09Rik | ENDASDF | 1 | < 0.2 |
| 1700029B22Rik | ENDASDF | 1 | < 0.2 |
| XM_484488 | Ep300 | 1 | < 0.2 |
| XM_110248 | Fbxo11 | 1 | < 0.2 |
| NM_010205 | Fgf8 | 1 | < 0.2 |
| NM_199068 | Foxk1 | 1 | < 0.2 |
| NM_008021 | Foxm1 | 1 | < 0.2 |
| NM_133837 | G431001I09Rik | 1 | < 0.2 |
| NM_010255 | Gamt | 1 | < 0.2 |
| NM_173048 | Gga3 | 1 | < 0.2 |
| NM_027544 | Ggnbp1 | 1 | < 0.2 |
| NM_013531 | Gnb4 | 1 | < 0.2 |
| NM_025331 | Gng11 | 1 | < 0.2 |
| NM_029793 | Golga1 | 1 | < 0.2 |
| NM_145132 | Gpr24 | 1 | < 0.2 |
| NM_022427 | Gpr88 | 1 | < 0.2 |
| NM_026229 | Gpr89 | 1 | < 0.2 |
| NM_010398 | H2-T23 | 1 | < 0.2 |
| NM_011827 | Hcst | 1 | < 0.2 |
| NM_153505 | Hemp1 | 1 | < 0.2 |
| NM_008236 | Hes2 | 1 | < 0.2 |
| XM_133550 | Homer2 | 1 | < 0.2 |
| NM_026820 | Ifitm1 | 1 | < 0.2 |
| L33944 | IGHV1S105 | 1 | < 0.2 |
| J00530 | IGHV1S2 | 1 | < 0.2 |
| NM_170599 | Igsf11 | 1 | < 0.2 |
| NM_008370 | Il5ra | 1 | < 0.2 |
| NM_008376 | Imap38 | 1 | < 0.2 |
| NM_023626 | Ing3 | 1 | < 0.2 |
| NM_008387 | Ins2 | 1 | < 0.2 |
| XM_192925 | Itch | 1 | < 0.2 |
| NM_010655 | Kpna2 | 1 | < 0.2 |

| | | | |
|---|---|---|---|
| NM_015741 | Krtap9-1 | 1 | < 0.2 |
| NM_008562 | Mcl1 | 1 | < 0.2 |
| NM_013597 | Mef2a | 1 | < 0.2 |
| NM_013599 | Mmp9 | 1 | < 0.2 |
| NC_001503 | MMTVgp7 | 1 | < 0.2 |
| NM_010814 | Mog | 1 | < 0.2 |
| NM_016791 | Nfatc1 | 1 | < 0.2 |
| NM_008692 | Nfyc | 1 | < 0.2 |
| NM_027280 | Nkd1 | 1 | < 0.2 |
| NM_172478 | Oatl1 | 1 | < 0.2 |
| NM_146593 | Olfr1111 | 1 | < 0.2 |
| NM_146926 | Olfr477 | 1 | < 0.2 |
| NM_147089 | Olfr572 | 1 | < 0.2 |
| NM_011001 | Olfr58 | 1 | < 0.2 |
| NM_011112 | Papola | 1 | < 0.2 |
| NM_018878 | Paxip1 | 1 | < 0.2 |
| NM_008783 | Pbx1 | 1 | < 0.2 |
| NM_011042 | Pcbp2 | 1 | < 0.2 |
| NM_016688 | Pdcd7 | 1 | < 0.2 |
| NM_008849 | Pit1 | 1 | < 0.2 |
| XM_126961 | Plekhh1 | 1 | < 0.2 |
| NM_011122 | Plod1 | 1 | < 0.2 |
| XM_133979 | Ppfia1 | 1 | < 0.2 |
| XM_131309 | Prdm13 | 1 | < 0.2 |
| XM_139298 | Prkaa1 | 1 | < 0.2 |
| NM_024448 | Rab12 | 1 | < 0.2 |
| NM_024456 | Rab5c | 1 | < 0.2 |
| NM_173781 | Rab6b | 1 | < 0.2 |
| NM_023126 | Rab8a | 1 | < 0.2 |
| XM_132051 | Rhoh | 1 | < 0.2 |
| NM_172716 | Rnf3 | 1 | < 0.2 |
| NM_023372 | Rpl38 | 1 | < 0.2 |
| XM_485277 | Scnm1 | 1 | < 0.2 |
| NM_009147 | Sec23a | 1 | < 0.2 |
| NM_199241 | Sema6d | 1 | < 0.2 |
| NM_011358 | Sfrs2 | 1 | < 0.2 |
| NM_080559 | Sh3bgrl3 | 1 | < 0.2 |
| NM_011403 | Slc4a1 | 1 | < 0.2 |
| NM_009320 | Slc6a6 | 1 | < 0.2 |
| NM_030687 | Slco1a4 | 1 | < 0.2 |
| NM_009213 | Smpd2 | 1 | < 0.2 |
| NM_009225 | Snrpb | 1 | < 0.2 |
| NM_021790 | Solt | 1 | < 0.2 |
| NM_016801 | Stx1a | 1 | < 0.2 |
| NM_011512 | Surf4 | 1 | < 0.2 |
| NM_018802 | Syt8 | 1 | < 0.2 |
| NM_177089 | Tacc1 | 1 | < 0.2 |
| NM_011552 | Tcof1 | 1 | < 0.2 |
| NM_020584 | Terf2ip | 1 | < 0.2 |
| NM_207176 | Tes | 1 | < 0.2 |
| NM_019725 | Tle2 | 1 | < 0.2 |
| NM_153417 | Trpm6 | 1 | < 0.2 |
| NM_009449 | Tuba7 | 1 | < 0.2 |
| NM_199477 | Ubie | 1 | < 0.2 |
| NM_201643 | Ugt1a5 | 1 | < 0.2 |
| XM_356061 | Upf3a | 1 | < 0.2 |
| NM_172465 | Zdhhc9 | 1 | < 0.2 |
| NM_008825 | Pfkfb2 | 7 | < 0.3 |
| NM_013543 | H2-Ke6 | 5 | < 0.3 |
| NM_080729 | Il17e | 5 | < 0.3 |

| | | | |
|---|---|---|---|
| NM_013563 | Il2rg | 5 | < 0.3 |
| NM_146221 | Zfp426 | 4 | < 0.3 |
| NM_011609 | TNFRp55 (20) | 4 | < 0.3 |
| NM_146946 | Olfr50 | 4 | < 0.3 |
| NM_008575 | Mdm4 | 4 | < 0.3 |
| NM_007656 | Kai1 | 4 | < 0.3 |
| NM_008361 | IL-1β (21, 22) | 4 | < 0.3 |
| AF304545 | IGHV1S126 | 4 | < 0.3 |
| NM_010441 | Hmga2 | 4 | < 0.3 |
| NM_008091 | Gata3 | 4 | < 0.3 |
| D730047P14Rik | ENDASDF | 4 | < 0.3 |
| A730006G06Rik | ENDASDF | 4 | < 0.3 |
| NM_144884 | Dyt1 | 4 | < 0.3 |
| NM_016779 | Dmp1 | 4 | < 0.3 |
| NM_133238 | Cd209a | 4 | < 0.3 |
| NM_144835 | B130016L12Rik | 4 | < 0.3 |
| NM_007504 | Atp2a1 | 4 | < 0.3 |
| NM_146119 | 9130404D14Rik | 4 | < 0.3 |
| NM_133983 | 6030411F23Rik | 4 | < 0.3 |
| NM_177607 | 4933430I17Rik | 4 | < 0.3 |
| NM_144801 | 2310076O21Rik | 4 | < 0.3 |
| NM_144953 | 1700019D03Rik | 4 | < 0.3 |
| NM_145492 | Zfp521 | 3 | < 0.3 |
| NM_029498 | Zfp198 (26, 27) | 3 | < 0.3 |
| NM_173399 | Zbtb5 | 3 | < 0.3 |
| NM_024189 | Yaf2 | 3 | < 0.3 |
| XM_135805 | Wdr44 | 3 | < 0.3 |
| NM_053254 | Tle6 | 3 | < 0.3 |
| NM_011490 | Stau1 | 3 | < 0.3 |
| NM_020495 | Slco1b2 | 3 | < 0.3 |
| NM_144856 | Slc22a7 | 3 | < 0.3 |
| NM_011891 | Sgcd | 3 | < 0.3 |
| NM_025436 | Sc4mol | 3 | < 0.3 |
| NM_009057 | Rga | 3 | < 0.3 |
| NM_024457 | Rap1b | 3 | < 0.3 |
| NM_133249 | Ppargc1b | 3 | < 0.3 |
| NM_133167 | Parvb | 3 | < 0.3 |
| NM_023824 | Paqr4 | 3 | < 0.3 |
| NM_008876 | Pld2 (24) | 3 | < 0.3 |
| NM_146418 | Olfr881 | 3 | < 0.3 |
| NM_146548 | Olfr800 | 3 | < 0.3 |
| NM_130866 | Olfr78 | 3 | < 0.3 |
| NM_146353 | Olfr706 | 3 | < 0.3 |
| NM_147073 | Olfr33 | 3 | < 0.3 |
| NM_207576 | Olfr1514 | 3 | < 0.3 |
| NM_207132 | Olfr1471 | 3 | < 0.3 |
| NM_146334 | Olfr1330 | 3 | < 0.3 |
| NM_147062 | Olfr124 | 3 | < 0.3 |
| NM_146630 | Olfr123 | 3 | < 0.3 |
| NM_146921 | Olfr1 | 3 | < 0.3 |
| NM_145209 | Oasl1 | 3 | < 0.3 |
| XM_128696 | Ndufa11 | 3 | < 0.3 |
| NM_181729 | Muc6 | 3 | < 0.3 |
| NM_181852 | Mrpplf4 | 3 | < 0.3 |
| NM_145442 | Mbip | 3 | < 0.3 |
| NM_134152 | Lpxn | 3 | < 0.3 |
| NM_001002011 | Lmna | 3 | < 0.3 |
| AJ231204 | IGKV1-108 | 3 | < 0.3 |
| AF304548 | IGHV1S129 | 3 | < 0.3 |
| NM_183174 | Homez | 3 | < 0.3 |

| | | | |
|---|---|---|---|
| NM_010239 | Fth1 | 3 | < 0.3 |
| NM_008044 | Frda | 3 | < 0.3 |
| NM_008010 | Fgfr3 | 3 | < 0.3 |
| NM_007993 | Fbn1 | 3 | < 0.3 |
| D930046M13Rik | ENDASDF | 3 | < 0.3 |
| D630030B08Rik | ENDASDF | 3 | < 0.3 |
| D0Kist3 | ENDASDF | 3 | < 0.3 |
| C030003H22Rik | ENDASDF | 3 | < 0.3 |
| B230206L02Rik | ENDASDF | 3 | < 0.3 |
| AU044581 | ENDASDF | 3 | < 0.3 |
| AK014142 | ENDASDF | 3 | < 0.3 |
| A130022J21Rik | ENDASDF | 3 | < 0.3 |
| 9830127L17Rik | ENDASDF | 3 | < 0.3 |
| 4930471C06Rik | ENDASDF | 3 | < 0.3 |
| NM_010133 | En1 | 3 | < 0.3 |
| NM_029001 | Elovl7 | 3 | < 0.3 |
| NM_153403 | Eif2c1 | 3 | < 0.3 |
| NM_175540 | Eda2r | 3 | < 0.3 |
| NM_139293 | Ece2 | 3 | < 0.3 |
| NM_175355 | E330013P04Rik | 3 | < 0.3 |
| NM_032418 | Dm15 | 3 | < 0.3 |
| NM_007760 | Crat | 3 | < 0.3 |
| NM_053165 | Clrf | 3 | < 0.3 |
| NM_181858 | Cd59b | 3 | < 0.3 |
| NM_007643 | Cd36 | 3 | < 0.3 |
| NM_153545 | BC023296 | 3 | < 0.3 |
| NM_145597 | BC021367 | 3 | < 0.3 |
| NM_144847 | BC011468 | 3 | < 0.3 |
| NM_007472 | Aqp1 | 3 | < 0.3 |
| NM_130863 | Adrbk1 | 3 | < 0.3 |
| NM_133954 | AA960436 | 3 | < 0.3 |
| NM_177671 | A330090H18 | 3 | < 0.3 |
| NM_177003 | 9630033F20Rik | 3 | < 0.3 |
| NM_182995 | 6330503K22Rik | 3 | < 0.3 |
| XM_141565 | 5530400B04Rik | 3 | < 0.3 |
| NM_182991 | 5330410G16Rik | 3 | < 0.3 |
| NM_176829 | 4931440F15Rik | 3 | < 0.3 |
| NM_178802 | 4732463G12Rik | 3 | < 0.3 |
| NM_181589 | 2610318C08Rik | 3 | < 0.3 |
| NM_133722 | 2210412D01Rik | 3 | < 0.3 |
| XM_145521 | 1810022O10Rik | 3 | < 0.3 |
| NM_183249 | 1100001G20Rik | 3 | < 0.3 |
| NM_011769 | Zim1 | 2 | < 0.3 |
| NM_011766 | Zfpm2 | 2 | < 0.3 |
| NM_009558 | Zfp51 | 2 | < 0.3 |
| NM_019747 | Zfp113 | 2 | < 0.3 |
| NM_139298 | Wnt9a | 2 | < 0.3 |
| NM_009524 | Wnt5a | 2 | < 0.3 |
| NM_011718 | Wnt10b | 2 | < 0.3 |
| NM_011915 | Wif1 | 2 | < 0.3 |
| NM_011693 | Vcam1 | 2 | < 0.3 |
| NM_134245 | V1ri10 | 2 | < 0.3 |
| NM_053230 | V1rb9 | 2 | < 0.3 |
| NM_178635 | Uvrag1 | 2 | < 0.3 |
| NM_181418 | Ushbp1 | 2 | < 0.3 |
| NM_016682 | Uble1b | 2 | < 0.3 |
| NM_008807 | Tulp2 | 2 | < 0.3 |
| NM_173378 | Trp53bp2 | 2 | < 0.3 |
| NM_009054 | Trim27 | 2 | < 0.3 |
| NM_053169 | Trim16 | 2 | < 0.3 |

| | | | |
|---|---|---|---|
| NM_011906 | Tpra40 | 2 | < 0.3 |
| NM_177296 | Tnpo3 | 2 | < 0.3 |
| NM_013694 | Tnp2 | 2 | < 0.3 |
| NM_134131 | Tnfaip8 | 2 | < 0.3 |
| NM_009388 | Tkt | 2 | < 0.3 |
| NM_199154 | Tas2r107 | 2 | < 0.3 |
| NM_011896 | Spry1 | 2 | < 0.3 |
| XM_129130 | Spnb3 | 2 | < 0.3 |
| NM_194355 XM_129018 | Spire1 | 2 | < 0.3 |
| XM_132597 | Smarcad1 | 2 | < 0.3 |
| NM_016769 | Smad3 | 2 | < 0.3 |
| NM_177084 | Slc9a4 | 2 | < 0.3 |
| NM_144852 | Slc7a4 | 2 | < 0.3 |
| NM_078484 | Slc35a2 | 2 | < 0.3 |
| NM_011978 | Slc27a2 | 2 | < 0.3 |
| NM_015747 | Slc20a1 | 2 | < 0.3 |
| NM_013787 | Skp2 | 2 | < 0.3 |
| NM_011377 | Sim2 | 2 | < 0.3 |
| NM_001001144 | Scap | 2 | < 0.3 |
| XM_354544 | Rtdr1 | 2 | < 0.3 |
| NM_145495 | Rin1 | 2 | < 0.3 |
| XM_355286 | Rims1 | 2 | < 0.3 |
| NM_175389 | Rg9mtd2 | 2 | < 0.3 |
| NM_021525 | Rcl1 | 2 | < 0.3 |
| NM_011240 | Ranbp2 | 2 | < 0.3 |
| NM_012025 | Racgap1 | 2 | < 0.3 |
| NM_011969 | Psma7 | 2 | < 0.3 |
| NM_011183 | Psen2 | 2 | < 0.3 |
| NM_008941 | Prss7 | 2 | < 0.3 |
| NM_033573 | Prcc | 2 | < 0.3 |
| NM_178250 | Pramel7 | 2 | < 0.3 |
| NM_008014 | Ppm1g | 2 | < 0.3 |
| XM_129443 | Ppfia4 | 2 | < 0.3 |
| NM_011136 | Pou2af1 | 2 | < 0.3 |
| NM_011636 | Plscr1 | 2 | < 0.3 |
| NM_145629 | Pls3 | 2 | < 0.3 |
| NM_008841 | Pik3r2 | 2 | < 0.3 |
| NM_011082 | Pigr | 2 | < 0.3 |
| XM_203853 | Phpt1 | 2 | < 0.3 |
| NM_008787 | Pcnt2 | 2 | < 0.3 |
| NM_172709 | Otop1 | 2 | < 0.3 |
| NM_146546 | Olfr775 | 2 | < 0.3 |
| NM_147115 | Olfr578 | 2 | < 0.3 |
| NM_146755 | Olfr551 | 2 | < 0.3 |
| NM_146576 | Olfr459 | 2 | < 0.3 |
| NM_146707 | Olfr410 | 2 | < 0.3 |
| NM_146713 | Olfr1342 | 2 | < 0.3 |
| NM_146900 | Olfr1220 | 2 | < 0.3 |
| NM_146772 | Olfr1189 | 2 | < 0.3 |
| NM_146650 | Olfr1166 | 2 | < 0.3 |
| NM_207632 | Olfr1118 | 2 | < 0.3 |
| NM_001003914 | Obscn | 2 | < 0.3 |
| NM_130858 | Nxph3 | 2 | < 0.3 |
| NM_008726 | Nppb | 2 | < 0.3 |
| NM_130456 | Nphs2 | 2 | < 0.3 |
| NM_029561 | Ndfip2 | 2 | < 0.3 |
| NM_010876 | p47phox (23) | 2 | < 0.3 |
| NM_008676 | Nbr1 | 2 | < 0.3 |
| XM_355634 | Myo18b | 2 | < 0.3 |

| | | | |
|---|---|---|---|
| NM_008648 | Mup4 | 2 | < 0.3 |
| NM_138745 | Mthfd1 | 2 | < 0.3 |
| NM_019880 | Mtch1 | 2 | < 0.3 |
| NM_008629 | Msi1h | 2 | < 0.3 |
| NM_019946 | Mgst1 | 2 | < 0.3 |
| NM_008594 | Mfge8 | 2 | < 0.3 |
| NM_139295 | Mcfd2 | 2 | < 0.3 |
| NM_145569 | Mat2a | 2 | < 0.3 |
| NM_133653 | Mat1a | 2 | < 0.3 |
| NM_008928 | Map2k3 | 2 | < 0.3 |
| NM_010728 | Lox | 2 | < 0.3 |
| NM_153404 | Liph | 2 | < 0.3 |
| NM_010700 | Ldlr | 2 | < 0.3 |
| NM_175349 | Ldhal6b | 2 | < 0.3 |
| NM_020268 | Klk27 | 2 | < 0.3 |
| NM_130867 | Kirrel1 | 2 | < 0.3 |
| NM_010612 | Kdr | 2 | < 0.3 |
| NM_010578 | Itgb1 | 2 | < 0.3 |
| NM_133748 | Insig2 | 2 | < 0.3 |
| NM_133193 | Il1rl2 | 2 | < 0.3 |
| AJ231229 | IGKV4-91 | 2 | < 0.3 |
| AJ231222 | IGKV4-68 | 2 | < 0.3 |
| M34983 | IGHV1S53 | 2 | < 0.3 |
| M17575$X06866 | IGHV1S40 | 2 | < 0.3 |
| NM_053088 | Ifitm5 | 2 | < 0.3 |
| NM_008327 | Ifi202b | 2 | < 0.3 |
| NM_015765 | Hspa14 | 2 | < 0.3 |
| NM_010450 | Hoxa11 | 2 | < 0.3 |
| NM_010442 | Hmox1 | 2 | < 0.3 |
| NM_010412 | Hdac5 | 2 | < 0.3 |
| NM_010401 | Hal | 2 | < 0.3 |
| NM_133994 | Gstt3 | 2 | < 0.3 |
| NM_010351 | Gsc | 2 | < 0.3 |
| NM_019518 | Grasp | 2 | < 0.3 |
| NM_013527 | Gdf7 | 2 | < 0.3 |
| XM_284152 | Gal3st4 | 2 | < 0.3 |
| NM_172824 | G630039H03Rik | 2 | < 0.3 |
| NM_013716 | G3bp | 2 | < 0.3 |
| NM_177798 | Frs2 | 2 | < 0.3 |
| NM_053242 | Foxp2 | 2 | < 0.3 |
| NM_199448 | Fez2 | 2 | < 0.3 |
| NM_010191 | Fdft1 | 2 | < 0.3 |
| NM_144960 | Fcamr | 2 | < 0.3 |
| NM_145519 | Farp2 | 2 | < 0.3 |
| NM_175399 | Exosc4 | 2 | < 0.3 |
| NM_175443 | Etnk2 | 2 | < 0.3 |
| U12914 | ENDASDF | 2 | < 0.3 |
| E430002N23Rik | ENDASDF | 2 | < 0.3 |
| E230017H14Rik | ENDASDF | 2 | < 0.3 |
| D930036K23Rik | ENDASDF | 2 | < 0.3 |
| D330050G23Rik | ENDASDF | 2 | < 0.3 |
| D030022P07Rik | ENDASDF | 2 | < 0.3 |
| CC799012 | ENDASDF | 2 | < 0.3 |
| C130036K02 | ENDASDF | 2 | < 0.3 |
| C030012D19Rik | ENDASDF | 2 | < 0.3 |
| BC051572 | ENDASDF | 2 | < 0.3 |
| BC025031 | ENDASDF | 2 | < 0.3 |
| B830032F12 | ENDASDF | 2 | < 0.3 |
| AK029047 | ENDASDF | 2 | < 0.3 |
| AK028167 | ENDASDF | 2 | < 0.3 |

| | | | |
|---|---|---|---|
| AK019732 | ENDASDF | 2 | < 0.3 |
| AK014782 | ENDASDF | 2 | < 0.3 |
| AK009804 | ENDASDF | 2 | < 0.3 |
| AK005257 | ENDASDF | 2 | < 0.3 |
| A930037J23Rik | ENDASDF | 2 | < 0.3 |
| A730014G21Rik | ENDASDF | 2 | < 0.3 |
| A330041B18Rik | ENDASDF | 2 | < 0.3 |
| A230061C15Rik | ENDASDF | 2 | < 0.3 |
| 9530034E10Rik | ENDASDF | 2 | < 0.3 |
| 9330180L10Rik | ENDASDF | 2 | < 0.3 |
| 7530408C15Rik | ENDASDF | 2 | < 0.3 |
| 4930547E14Rik | ENDASDF | 2 | < 0.3 |
| 4930540M03Rik | ENDASDF | 2 | < 0.3 |
| 4930506A18Rik | ENDASDF | 2 | < 0.3 |
| 4930463M05Rik | ENDASDF | 2 | < 0.3 |
| 4930455M05Rik | ENDASDF | 2 | < 0.3 |
| NM_019398 | Ear5 | 2 | < 0.3 |
| NM_011816 | E430034L04Rik | 2 | < 0.3 |
| NM_177310 | E430012M05Rik | 2 | < 0.3 |
| NM_177133 | E330018D03Rik | 2 | < 0.3 |
| XM_130483 | Duox1 | 2 | < 0.3 |
| NM_175647 | Dmrta1 | 2 | < 0.3 |
| NM_144553 | Dlg7 | 2 | < 0.3 |
| NM_207274 | D630004N19Rik | 2 | < 0.3 |
| NM_177657 | D630003M21 | 2 | < 0.3 |
| NM_175514 | D430039N05Rik | 2 | < 0.3 |
| NM_172485 | D130067I03Rik | 2 | < 0.3 |
| NM_138601 | D10Jhu81e | 2 | < 0.3 |
| NM_152809 | Csnk1g3 | 2 | < 0.3 |
| NM_007755 | Cpeb1 | 2 | < 0.3 |
| NM_177751 | Cnksr2 | 2 | < 0.3 |
| NM_008153 | Cmklr1 | 2 | < 0.3 |
| NM_019563 | Cited4 | 2 | < 0.3 |
| XM_146393 | Cilp2 | 2 | < 0.3 |
| NM_173385 | Cilp | 2 | < 0.3 |
| NM_021528 | Chst12 | 2 | < 0.3 |
| NM_139134 | Chodl | 2 | < 0.3 |
| XM_181420 | Cgrefl | 2 | < 0.3 |
| NM_053200 | Ces3 | 2 | < 0.3 |
| NM_007675 | Ceacam10 | 2 | < 0.3 |
| NM_153785 | Cdkl3 | 2 | < 0.3 |
| NM_130904 | Cd209d | 2 | < 0.3 |
| NM_007617 | Cav3 | 2 | < 0.3 |
| NM_007609 | Casp4 | 2 | < 0.3 |
| NM_177759 | C130098D09 | 2 | < 0.3 |
| NM_177875 | C130026L21Rik | 2 | < 0.3 |
| NM_172618 | Btbd9 | 2 | < 0.3 |
| NM_009768 | Bsg | 2 | < 0.3 |
| NM_007553 | Bmp2 | 2 | < 0.3 |
| NM_007532 | Bcat1 | 2 | < 0.3 |
| NM_198667 | BC061212 | 2 | < 0.3 |
| NM_177768 | BC038156 | 2 | < 0.3 |
| XM_131888 | BC034507 | 2 | < 0.3 |
| NM_146256 | BC034099 | 2 | < 0.3 |
| NM_173862 | BC030396 | 2 | < 0.3 |
| NM_145987 | BC025833 | 2 | < 0.3 |
| NM_001004156 | BC023181 | 2 | < 0.3 |
| NM_198609 | BC003885 | 2 | < 0.3 |
| NM_177083 | B430306N03Rik | 2 | < 0.3 |
| NM_020025 | B3galt2 | 2 | < 0.3 |

| XM_130148 | B230208H17Rik | 2 | < 0.3 |
|---|---|---|---|
| NM_174989 | AW046014 | 2 | < 0.3 |
| NM_007505 | Atp5a1 | 2 | < 0.3 |
| NM_023472 | Ankra2 | 2 | < 0.3 |
| NM_011786 | Aloxe3 | 2 | < 0.3 |
| NM_134052 | AL024210 | 2 | < 0.3 |
| NM_178898 | AI894139 | 2 | < 0.3 |
| NM_033526 | AI663987 | 2 | < 0.3 |
| NM_145505 | AI450540 | 2 | < 0.3 |
| NM_007426 | Agpt2 | 2 | < 0.3 |
| NM_145146 | Afm | 2 | < 0.3 |
| NM_007414 | Adprh | 2 | < 0.3 |
| NM_007399 | Adam10 | 2 | < 0.3 |
| NM_011994 | Abcd2 | 2 | < 0.3 |
| NM_133349 | AA407930 | 2 | < 0.3 |
| NM_177578 | A430090E18Rik | 2 | < 0.3 |
| NM_207279 | A330045H12Rik | 2 | < 0.3 |
| NM_173387 | 9630041N07Rik | 2 | < 0.3 |
| NM_175651 | 9630008K15Rik | 2 | < 0.3 |
| NM_177074 | 9330158F14Rik | 2 | < 0.3 |
| XM_127434 | 9030624O13Rik | 2 | < 0.3 |
| NM_172302 | 5730453I16Rik | 2 | < 0.3 |
| XM_484382 | 4930563I02Rik | 2 | < 0.3 |
| NM_152825 | 4930550B20Rik | 2 | < 0.3 |
| XM_142616 | 4930488N24Rik | 2 | < 0.3 |
| XM_127899 | 4930403J22Rik | 2 | < 0.3 |
| XM_130609 | 4921517L17Rik | 2 | < 0.3 |
| NM_133797 | 4833439L19Rik | 2 | < 0.3 |
| XM_132137 | 2310011G06Rik | 2 | < 0.3 |
| XM_130597 | 1700058C13Rik | 2 | < 0.3 |
| NM_173182 | 1600019O04Rik | 2 | < 0.3 |
| NM_176843 | 1110055N21Rik | 2 | < 0.3 |
| NM_025402 | 1110031I02Rik | 2 | < 0.3 |
| NM_029508 | 0610009F02Rik | 2 | < 0.3 |
| NM_009550 | Zfp2 | 1 | < 0.3 |
| NM_172120 | Vps41 | 1 | < 0.3 |
| NM_001001327 | Vkorc1l1 | 1 | < 0.3 |
| NM_009492 | V2r2 | 1 | < 0.3 |
| NM_134218 | V1rh9 | 1 | < 0.3 |
| NM_009470 | Umod | 1 | < 0.3 |
| NM_020285 | Tssc4 | 1 | < 0.3 |
| XM_127444 | Trip13 | 1 | < 0.3 |
| NM_009413 | Tpd52l1 | 1 | < 0.3 |
| NM_133683 | Tmem19 | 1 | < 0.3 |
| NM_144543 | Thy28 | 1 | < 0.3 |
| NM_009369 | Tgfbi | 1 | < 0.3 |
| M62838 M32485 | tea | 1 | < 0.3 |
| NM_011561 | Tdg | 1 | < 0.3 |
| NM_207027 | Tas2r125 | 1 | < 0.3 |
| NM_025303 | Stau2 | 1 | < 0.3 |
| NM_020493 | Srf | 1 | < 0.3 |
| NM_146043 | Spin | 1 | < 0.3 |
| NM_009242 | Sparc | 1 | < 0.3 |
| NM_172339 | Snapc4 | 1 | < 0.3 |
| NM_009222 | Snap23 | 1 | < 0.3 |
| NM_011375 | Siat9 | 1 | < 0.3 |
| NM_177386 | Sfmbt2 | 1 | < 0.3 |
| NM_013658 | Sema4a | 1 | < 0.3 |
| NM_009086 | Rpo1-2 | 1 | < 0.3 |
| NM_013646 | Rora | 1 | < 0.3 |

| | | | |
|---|---|---|---|
| NM_026014 | Ris2 | 1 | < 0.3 |
| NM_177740 | Rgma | 1 | < 0.3 |
| NM_177721 | Ranbp6 | 1 | < 0.3 |
| NM_175211 | Ralgps1 | 1 | < 0.3 |
| NM_026297 | Rabl3 | 1 | < 0.3 |
| NM_019983 | **Rabgef1** (25). | 1 | < 0.3 |
| NM_153559 | Qscn6l1 | 1 | < 0.3 |
| NM_008976 | Ptpn14 | 1 | < 0.3 |
| XM_357441 | Ptafr | 1 | < 0.3 |
| XM_284491 | Ppp2r1b | 1 | < 0.3 |
| XM_358127 | Pira11 | 1 | < 0.3 |
| NM_019781 | Pex14 | 1 | < 0.3 |
| NM_011868 | Peci | 1 | < 0.3 |
| NM_011865 | Pcbp1 | 1 | < 0.3 |
| NM_022321 | Parvg | 1 | < 0.3 |
| NM_177161 | P4ha3 | 1 | < 0.3 |
| NM_146430 | Olfr742 | 1 | < 0.3 |
| NM_146600 | Olfr700 | 1 | < 0.3 |
| NM_147109 | Olfr577 | 1 | < 0.3 |
| NM_146374 | Olfr368 | 1 | < 0.3 |
| NM_146290 | Olfr125 | 1 | < 0.3 |
| NM_153157 | Olfm3 | 1 | < 0.3 |
| XM_129809 | Ogfrl1 | 1 | < 0.3 |
| NM_020610 | Nrip3 | 1 | < 0.3 |
| NM_018787 | Npff | 1 | < 0.3 |
| NM_008693 | Ngfg | 1 | < 0.3 |
| NM_008675 | Nbl1 | 1 | < 0.3 |
| NM_024174 | Mrps23 | 1 | < 0.3 |
| NM_205795 | Mrgprb4 | 1 | < 0.3 |
| XM_484710 | Mocos | 1 | < 0.3 |
| BC057926 | Mmp16 | 1 | < 0.3 |
| NM_008606 | Mmp11 | 1 | < 0.3 |
| NM_145543 | Mclc | 1 | < 0.3 |
| NM_008538 | Marcks | 1 | < 0.3 |
| NM_008519 | Ltb4r1 | 1 | < 0.3 |
| XM_128064 | LOC223672 | 1 | < 0.3 |
| NM_199146 | LOC209387 | 1 | < 0.3 |
| NM_008501 | Lif | 1 | < 0.3 |
| NM_010662 | Krt1-13 | 1 | < 0.3 |
| NM_008450 | Kns2 | 1 | < 0.3 |
| NM_010636 | Klf12 | 1 | < 0.3 |
| NM_177748 | Kirl2 | 1 | < 0.3 |
| NM_033134 | Inpp5e | 1 | < 0.3 |
| NM_011829 | Impdh1 | 1 | < 0.3 |
| NM_008362 | Il1r1 | 1 | < 0.3 |
| NM_008355 | **IL-13** (48, 49) | 1 | < 0.3 |
| NM_027320 | Ifi35 | 1 | < 0.3 |
| NM_178610 | Hrb2 | 1 | < 0.3 |
| NM_013820 | Hk2 | 1 | < 0.3 |
| NM_016956 | Hbb-b2 | 1 | < 0.3 |
| NM_008206 | H2-Oa | 1 | < 0.3 |
| NM_023168 | Grina | 1 | < 0.3 |
| NM_018882 | Gpr56 | 1 | < 0.3 |
| NM_008130 | Gli3 | 1 | < 0.3 |
| NM_008080 | Galgt1 | 1 | < 0.3 |
| NM_172475 | Frmd4a | 1 | < 0.3 |
| NM_175473 | Fras1 | 1 | < 0.3 |
| NM_008239 | Foxq1 | 1 | < 0.3 |
| NM_008260 | Foxa3 | 1 | < 0.3 |
| NM_145927 | Fntb | 1 | < 0.3 |

| | | | |
|---|---|---|---|
| NM_013710 | Fgd2 | 1 | < 0.3 |
| NM_010634 | Fabp5 | 1 | < 0.3 |
| NM_012051 | Etv3 | 1 | < 0.3 |
| Zfp291 | ENDASDF | 1 | < 0.3 |
| Srcasm | ENDASDF | 1 | < 0.3 |
| M11859 | ENDASDF | 1 | < 0.3 |
| Etohd2 | ENDASDF | 1 | < 0.3 |
| E330029E12Rik | ENDASDF | 1 | < 0.3 |
| E030024I16Rik | ENDASDF | 1 | < 0.3 |
| C030014C12Rik | ENDASDF | 1 | < 0.3 |
| B230218P12Rik | ENDASDF | 1 | < 0.3 |
| AK080717 | ENDASDF | 1 | < 0.3 |
| AK008452 | ENDASDF | 1 | < 0.3 |
| A430042F24Rik | ENDASDF | 1 | < 0.3 |
| 9530059O14Rik | ENDASDF | 1 | < 0.3 |
| 9030024J15Rik | ENDASDF | 1 | < 0.3 |
| 8430426J06Rik | ENDASDF | 1 | < 0.3 |
| 8430403D17Rik | ENDASDF | 1 | < 0.3 |
| 5930409G06Rik | ENDASDF | 1 | < 0.3 |
| 4930563J15Rik | ENDASDF | 1 | < 0.3 |
| 4930551O13Rik | ENDASDF | 1 | < 0.3 |
| 4930535L15Rik | ENDASDF | 1 | < 0.3 |
| 4930533K18Rik | ENDASDF | 1 | < 0.3 |
| 4930520A20Rik | ENDASDF | 1 | < 0.3 |
| 4930511E03Rik | ENDASDF | 1 | < 0.3 |
| 4930453H23Rik | ENDASDF | 1 | < 0.3 |
| 2300004M11Rik | ENDASDF | 1 | < 0.3 |
| 1700021F07Rik | ENDASDF | 1 | < 0.3 |
| 1700003G13Rik | ENDASDF | 1 | < 0.3 |
| 1600019K03Rik | ENDASDF | 1 | < 0.3 |
| NM_139138 | Emr4 | 1 | < 0.3 |
| NM_172760 | Elmo3 | 1 | < 0.3 |
| NM_022980 | Dscr1l2 | 1 | < 0.3 |
| NM_023646 | Dnaja3 | 1 | < 0.3 |
| NM_010047 | Dgcr6 | 1 | < 0.3 |
| NM_172464 | Daam1 | 1 | < 0.3 |
| XM_284236 | D630042F21Rik | 1 | < 0.3 |
| NM_010000 | Cyp2b9 (28) | 1 | < 0.3 |
| NM_007764 | Crkl | 1 | < 0.3 |
| NM_019877 | Copz2 | 1 | < 0.3 |
| NM_017477 | Copg | 1 | < 0.3 |
| NM_178599 | Commd8 | 1 | < 0.3 |
| NM_017393 | Clpp | 1 | < 0.3 |
| NM_019701 | Clcnkb | 1 | < 0.3 |
| NM_007390 | Chrna7 | 1 | < 0.3 |
| NM_007693 | Chga | 1 | < 0.3 |
| NM_020006 | Cdc42ep4 | 1 | < 0.3 |
| XM_132882 | Cd69 | 1 | < 0.3 |
| NM_139301 | Catsper1 | 1 | < 0.3 |
| NM_009791 | Calmbp1 | 1 | < 0.3 |
| NM_177259 | C630028C02Rik | 1 | < 0.3 |
| NM_173775 | C230069K22Rik | 1 | < 0.3 |
| NM_178692 | C130074G19Rik | 1 | < 0.3 |
| NM_172142 | AY078069 | 1 | < 0.3 |
| BC025029 | Axot | 1 | < 0.3 |
| NM_152801 | Arhgef6 | 1 | < 0.3 |
| NM_019504 | Ap4b1 | 1 | < 0.3 |
| NM_009663 | Alox5ap | 1 | < 0.3 |
| NM_053156 | Allc | 1 | < 0.3 |
| XM_127049 | Alkbh | 1 | < 0.3 |

| | | | |
|---|---|---|---|
| NM_133884 | AI838661 | 1 | < 0.3 |
| NM_133770 | Adck4 | 1 | < 0.3 |
| NM_009611 | Actl7a | 1 | < 0.3 |
| NM_080633 | Aco2 | 1 | < 0.3 |
| NM_198664 | A630005A06Rik | 1 | < 0.3 |
| NM_175256 | 9530025L16Rik | 1 | < 0.3 |
| XM_109819 | 9330151E16Rik | 1 | < 0.3 |
| NM_177242 | 9130017A15Rik | 1 | < 0.3 |
| NM_175209 | 8430417A20Rik | 1 | < 0.3 |
| NM_207583 | 6430517E21Rik | 1 | < 0.3 |
| NM_024282 | 5830417C01Rik | 1 | < 0.3 |
| XM_134422 | 5730445M16Rik | 1 | < 0.3 |
| NM_172654 | 5330401P04Rik | 1 | < 0.3 |
| NM_172939 | 4921515A04Rik | 1 | < 0.3 |
| NM_177062 | 4833444G19Rik | 1 | < 0.3 |
| NM_172415 | 2810441C07Rik | 1 | < 0.3 |
| NM_029759 | 2410166I05Rik | 1 | < 0.3 |
| NM_172522 | 2410080H04Rik | 1 | < 0.3 |
| XM_355182 | 2010002M12Rik | 1 | < 0.3 |
| XM_110690 | 1810033B17Rik | 1 | < 0.3 |
| XM_133915 | 1190003J15Rik | 1 | < 0.3 |
| NM_025427 | 1190002H23Rik | 1 | < 0.3 |
| XM_128291 | 0610005K03Rik | 1 | < 0.3 |

### 7.1. Promoter Analysis

It was hypothesized that listericidal genes downstream of C/EBPβ may themselves be transcriptionally regulated by C/EBPβ. This transcriptional regulation may be mediated via the direct binding of C/EBPβ of to its consensus binding site in the promoter of the target gene, or via interactions with other transcription factors ($TF_{interacting}$) known to interact with C/EBPβ (Fig. 23). According to the TRANSFAC, BIND, HPRD and Entrez Gene databases, C/EBPβ interacts with 46 other transcription factors (Fig. 24) and has been has been experimentally proven to bind directly to the promoter sequences of 54 genes (Fig. 25). These direct C/EBPβ target genes play important roles in signalling via the cytokine, JAK-STAT, TLR, T cell Receptor (TCR), B cell Receptor (BCR), MAPK and ABC transporter pathways, and are important for several biological pathways including the complement and coagulation cascades, cell cycle, insulin and apoptosis. Moreover, these C/EBPβ target genes also are involved in the biosynthesis and metabolism of glucose, pyruvate, prostaglandins, leukotrienes, glutathione, propanoate, tryptophan, arginine, proline, tyrosine, urea, amino groups, glycerolipid, fatty acids and bile acids. The promoter sequences of the DE genes were therefore searched for potential binding sites for C/EBPβ and for transcription factors that interacted with C/EBPβ. Promoter analysis revealed that only IL-18bp and IL-1β genes contained experimentally proven C/EBPβ binding sites, whereas 18% of the DE genes contained putative C/EBPβ binding sites. Similarly, the promoter sequences for IL-18 binding protein (IL-18bp), Solute carrier family 25, member 36 (Slc25a3), Amyloid beta precursor protein (App), Bone gamma carboxyglutamate protein 1 (Bglap1), Cysteine and glycine-rich protein 2 (Csrp2), IL-1β, Insulin II (Ins2), NADPH dehydrogenase, quinone 1 (Nqo1), Transcription factor AP-2 gamma (Tcfap2c), Choline acetyltransferase (Chat), Alpha-2 type IV collagen (Col4a2), Ferritin heavy chain 1 (Fth1), Heme oxygenase 1 (Hmox1), Vascular cell adhesion molecule 1 (Vcam1), Hemoglobin beta adult major chain (Hbb-b1) and Serum response factor (Srf) contained experimentally proven binding sites for transcription factors that bind C/EBPβ. Moreover, promoter sequences for 47.3% of the DE genes contained putative binding sites for transcription factors known to interact with C/EBPβ e.g. E1A binding protein p300 (Ep300), C/EBPβ, C/EBPα, NF-κB(p50), NF-κB(p65), member of ETS oncogene family 1 (Elk-1), Trans-acting transcription factor 1 (Sp1), runt related transcription factor 1 (Runx1), STATs and the CHOP:C/EBPα dimer. Literature profiling revealed that these interacting transcription factors were found to be involved in biological processes and signalling pathways that were highly relevant in the context of *L. monocytogenes* infection. For example, *L. monocytogenes* has been shown to manipulate the host's actin cytoskeleton,

gap junctions, adherens junction and focal adhesion complexes in order to facilitate its movement through the cytoplasm and cell-cell spread (50, 51). Furthermore, activation of host defense and immunity against *L. monocytogenes* infection requires signalling via JAK-STAT, TLR, MAPK, transforming growth factor beta (TGFβ), TCR, BCR and calcium mediated pathways (44, 52-57). Based on the results of the promoter analysis, DE genes whose promoters' contained putative C/EBPβ binding sites were clustered into the focus group for putative downstream transcriptional targets of C/EBPβ.

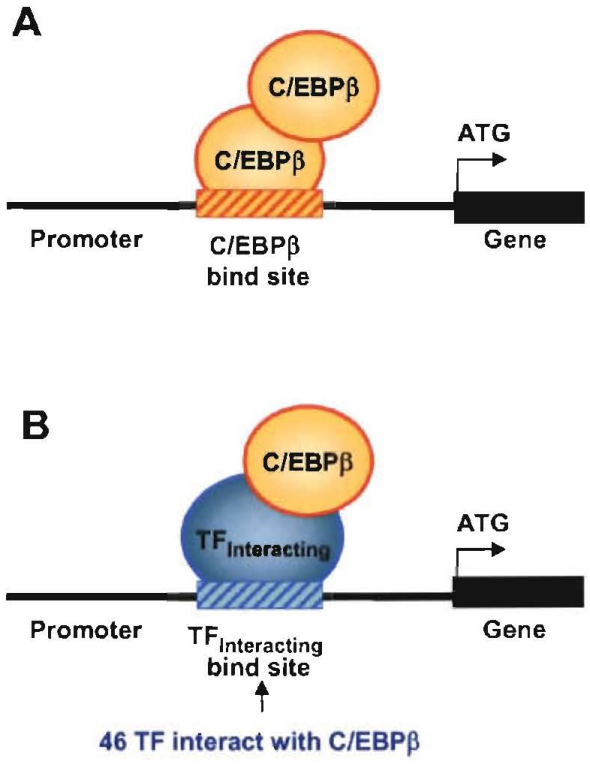


**Figure 23. Direct and indirect transcriptional regulation of C/EBPβ target genes.**

Shown is a simplified representation of how C/EBPβ directly or indirectly regulates transcription of its target genes. (A) Direct transcriptional occurs by the binding of C/EBPβ to its consensus binding site in the promoter of the target gene. (B) Indirect transcriptional regulation by C/EBPβ occurs via protein-protein interactions with other transcription factors (TF) that are bound to their consensus binding site in the promoter ($TF_{interacting}$). According the TRANSFAC, BIND, HPRD and Entrez Gene databases, C/EBPβ interacts with 46 other transcription factors.

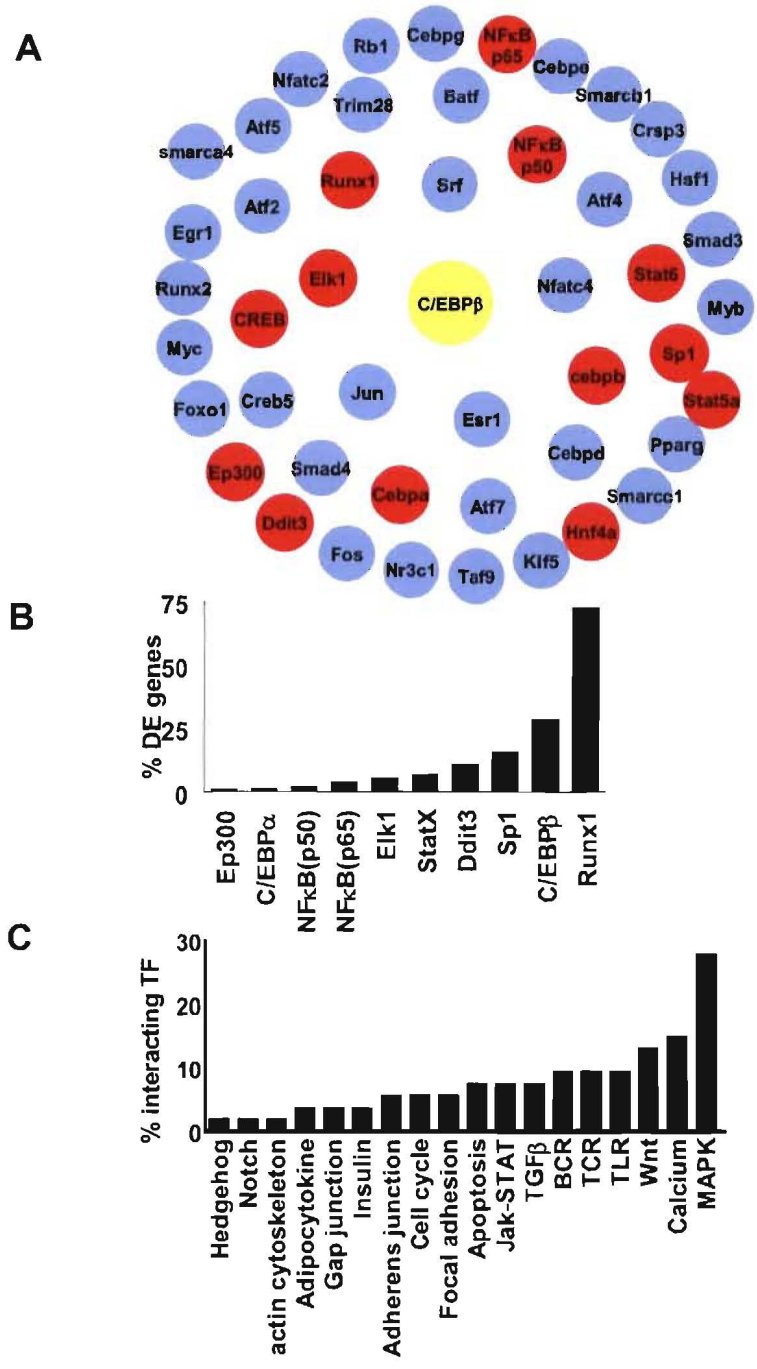


**Figure 24. C/EBPβ interacts with 46 other transcription factors.** (A) Highlighted in red are TF which bind to the promoters of some of the differentially expressed (DE) genes. Putative TF binding sites were identified by P-MATCH analysis. (B) Percentage of DE genes that have putative binding sites in their promoter for the TF highlighted in red. (C) Pathways regulated by the interacting TF and the percentage of interacting TF associated with each pathway.

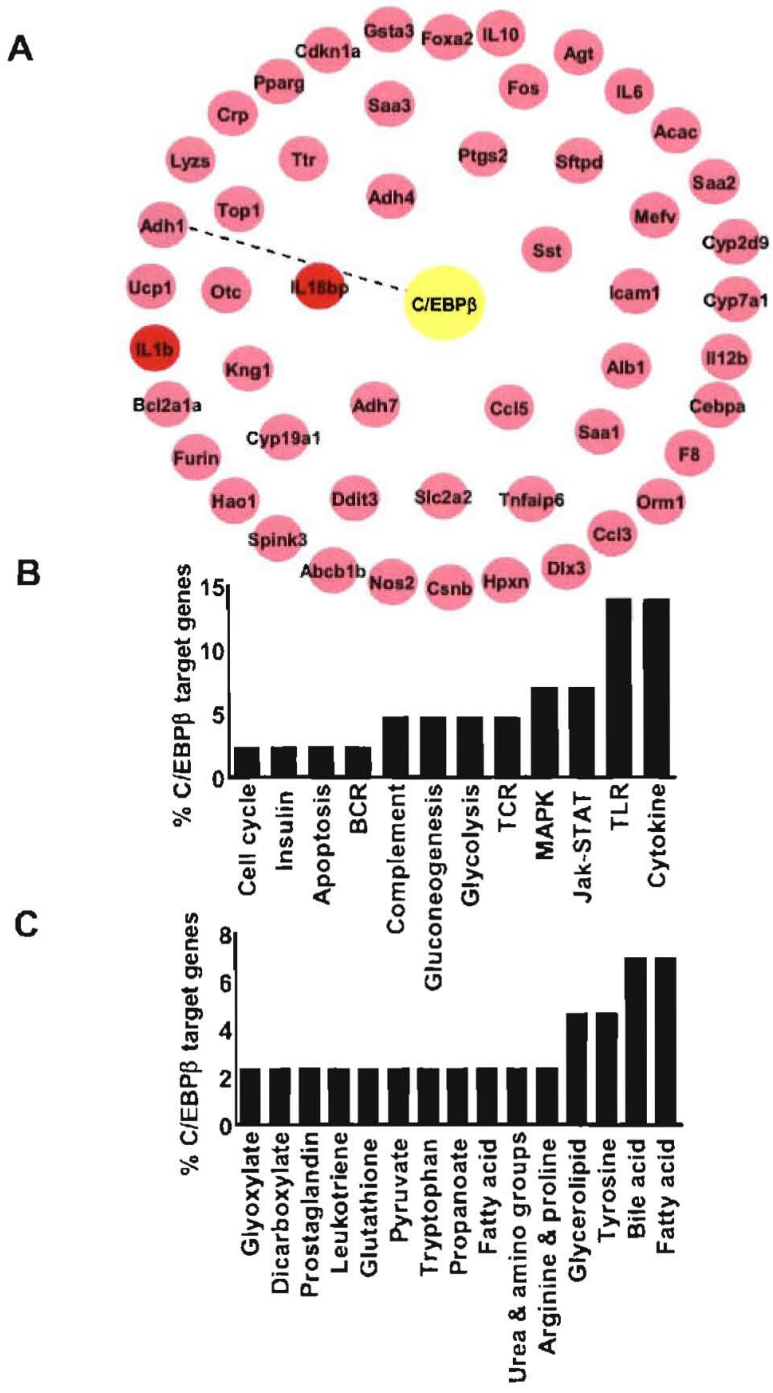


**Figure 25. Fifty-four genes with experimentally proven C/EBPβ binding sites in their promoters.** (A) Direct C/EBPβ target genes listed in the TRANSFAC database as having experimentally proven binding site for C/EBPβ in their promoters. Highlighted in red are DE genes (B) The signalling pathways and (C) metabolic processes regulated by the direct C/EBPβ target genes.

### 7.2. Gene ontology mining and literature profiling

Since 35% of the DE genes were unknown and consequently did not have any gene ontology or published literature, they could not be included in the functional clustering analysis. For those genes with annotation and literature, the gene ontology associations describing their cellular localization, biological processes and molecular functions were downloaded from the Gene Ontology Database using the FatiGOplus program (58). Similarly, literature mining of the PubMed database uncovered roles for the DE genes during host defense and immunity to intracellular pathogens, phagosome maturation, phago-lysosome fusion and signal transduction. The inclusion of genes into each focus group category based on their gene ontology associations was carefully considered (Fig. 26 A, Gene Ontology panel). For example, genes with ontology terms such as immune response, immune pathway signalling, cellular defense, humoral defense and defense response to bacteria were included in the "defense and immunity" focus group. Included in this group, were genes encoding cytokines, chemokines, their cognate receptors, as well as genes involved in the production of nitric oxide, superoxide and reported in literature to play a role in defense against *L. monocytogenes*. Genes in the "RNI and ROI production" focus group included those which had oxidoreductase activity, such as NADPH oxidase, the major enzyme responsible for generating superoxide. In addition, genes involved in binding or transporting potassium, iron and/or chloride and regulation of pH were also included in this focus group. Recently, NADPH oxidase was shown to be involved in a novel bacterial killing mechanism mediated by potassium ion influx in a pH-dependent manner (59-62). Furthermore, potassium, iron and chloride ions have been shown to be elevated in phagosomes containing *Mycobacterium* or *Listeria* and may be important in the restricting the survival of these bacteria (62, 63). Furthermore, DE genes involved in signalling pathways mediated by GPCRs, GTPases, cytokines, mitogen activated protein kinases (MAPKs), Wnt, insulin, hedgehog, growth factors, phosphatidylinositol, neuropeptides, B cell receptor (BCR), T cell receptor (TCR), TLR, notch, integrins, cAMP and calcium were included into the "signal transduction" focus group. Since phagosome maturation and phago-lysosome fusion involved the synergistic interaction of several biological processes, signalling pathways and intracellular organelles (64, 65), DE genes were grouped into the "phagosome maturation and phago-lysosome fusion" focus group if their encoded proteins were (i) reported in literature to play a role in phagosome maturation, (ii) were located within the cytoskeleton or organelles such as the endoplasmic reticulum (ER), Golgi apparatus, endosomes, phagosomes, lysosomes and/or intracellular vesicles, (iii) were involved in the regulation of endocytosis, phagocytosis and/or organization and biogenesis of the actin cytoskeleton, (iv) transported proteins to and/or from

the ER, Golgi apparatus, endosomes, phagosomes, lysosomes and/or intracellular vesicles, and (v) regulated the activity of Rab proteins, especially Rab5a e.g. GTPases, GEFs, GDIs, GAPs, vATPases and PI3kinases.

A comparison of the functional clusters generated for DE genes that had SD<0.2 or SD<0.3, showed that although the number of genes within each cluster was much lower in the SD<0.2 data set as compared to the SD<0.3 set, the overall proportional sizes of the clusters did not differ between the two analyses (Fig.26 A, B). Functional clustering of DE genes with SD<0.3 showed that 4.6% of the annotated DE genes were described as having transcription factor activity or were involved in the regulation of transcription. Similarly, promoter analysis identified that 18% of the annotated DE genes had proven/putative binding sites for C/EBPβ and 47.36% had binding sites for transcription factors that interacted with C/EBPβ. Furthermore, 2.0% of the annotated DE genes were involved in host immunity and defense, 3.1% in the production of ROI, 16.1% in signalling and 8.9% were involved in phagosome maturation and phago-lysosome fusion (Fig. 26 C).

A

| Key | Focus Groups | Gene Ontology |
|---|---|---|
| | Defense & Immunity | • Immune Response<br>• Literature Profile<br>• Defense |
| | RNI & ROI Production | • Oxidoreductase<br>• Iron<br>• Chloride<br>• Postassium<br>• Proton Pump<br>• pH |
| | Transcription | • Transcription activity<br>• Regulation of transcription |
| | Phagosome Maturation & Phago-lysosome Fusion | • Cytoskeleton<br>• Trans Golgi Network<br>• GTPase<br>• Endoplasmic Reticulum<br>• Endosome<br>• Phagosome<br>• Vesicle<br>• Lysosome |
| | Signal Transduction | • Extracellular signalling<br>• Intracellular signalling<br>• BCR & TCR<br>• Calcium<br>• cAMP<br>• GPCRs<br>• Growth Factor<br>• GTP<br>• Hedgehog<br>• Insulin<br>• Integrins<br>• MAPK<br>• Neuropeptide<br>• Phosphatidylinositol<br>• Wnt<br>• Cytokine<br>• Notch<br>• TLR |
| | C/EBPβ Target gene | • Indirect C/EBPb target gene |
| | C/EBPβ Target gene | • Direct C/EBPb target genes |

B

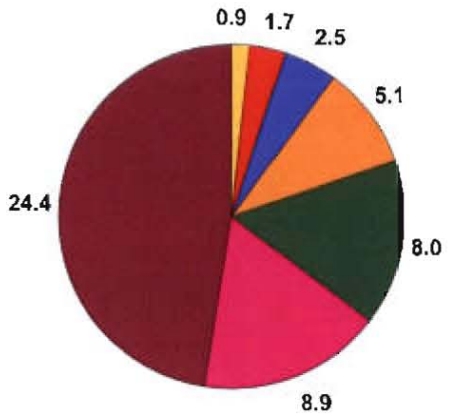


C

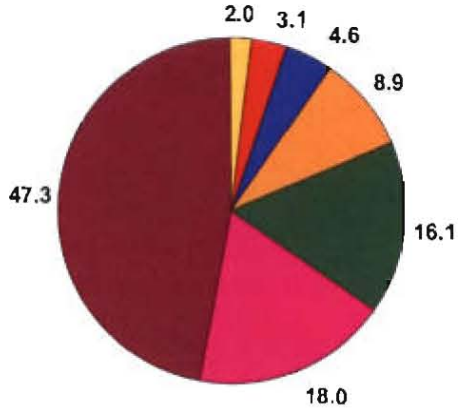


**Figure 26. Clustering of genes into the functional "focus groups".** (A) Promoter analysis, literature and gene ontology mining was used to identify potential C/EBPβ target genes and to extract functional data describing the cellular localization, biological processes and molecular functions for each gene. Shown are the gene ontology terms used to define each category. Genes were then clustered into the "focus groups" based on their functional annotation. (B) Functional clusters for DE genes that have a standard deviation (SD) less than 0.2 and (C) SD less than 0.3. Shown are the percentages of annotated genes belonging to each "focus group".

After clustering the DE genes into the functional "focus groups", genes that clustered into >50% of the functional focus groups were selected for further analysis. Within the set of DE genes that had SD<0.2, only 115 genes clustered into >50% of the functional focus groups. However, key immunological genes which have been shown to play a significant role during defense against *L. monocytogenes,* were excluded due to the SD>0.2 cut off criteria. Since the microarray was an exploratory study, elimination of known and other, as yet, unidentified biologically relevant genes would decrease the probability of fulfilling the aims of the study, which were to identify genes involved in mediating listericidal activity. Therefore, DE genes with SD<0.3 and that clustered into >50% of the functional focus groups were selected for further analysis. Although this strategy increased the number of candidate genes to 220, as compared to the 115 for the SD<0.2 set, it at least did not exclude potentially biologically significant listericidal genes.

Further literature profiling of these genes revealed that several had already been published as playing a role during *L. monocytogenes* infections. For example the C/EBPβ$^{-/-}$ macrophages had down-regulation of IL-1β, RAB guanine nucleotide exchange factor 1 (Rabgef1) and Gelsolin (Gsn) but had higher levels of Phospholipase D2 (Pld2) and p47phox. IL-1β, which was expressed 2-fold lower in the C/EBPβ macrophages, is a potent inflammatory cytokine that is important for early resistance against *L. monocytogenes* infection. Injection of mice with IL-1β prior to intravenous infection with *L. monocytogenes*, resulted in accelerated recovery from infection (66) and studies using monoclonal anti-IL-1β antibodies demonstrated that IL-1β was essential for *L. monocytogenes*-dependent induction macrophage activation (67). Although IL-1β deficient mice showed equivalent resistance as WT mice to *L. monocytogenes* infection (68), obstruction of IL-1β signalling via the blocking of the IL-1R by antibodies or by gene targeting, resulted in highly increased susceptibility to *L. monocytogenes* (21, 43). Moreover, IL-1β has been shown to be important for innate immunity against *M. tuberculosis* (69). Gsn is Ca2+ sensitive protein that plays an important role in *L. monocytogenes* actin-based motility and consequent cell-cell spread. At normal resting intracellular free Ca2+ levels, Gsn is concentrated directly behind motile *L. monocytogenes* at the junction between the actin filament rocket tail and the bacterium, where it was shown to enhance *L. monocytogenes* actin tail disassembly resulting in impaired motility. However, at lowered intracellular free Ca2+ levels, Gsn dissociated from the actin rocket tails and its severing activity was blocked, resulting in lengthening of the *L. monocytogenes* tail lengths and enhanced motility (45). PLD2 is a phosphatidylcholine (PC)-

specific phospholipase that catalyzes the hydrolysis of PC to phosphatidic acid and choline, which are important molecules for cellular processes such as signal transduction, membrane trafficking, secretion, cytoskeletal reorganization, transcriptional regulation, and cell cycle control. During *L. monocytogenes* infection, host polyphosphoinositide-specific phospholipase C (PI-PLC) and PLD2 are induced and activated by bacterial PI-PLC and LLO (24). Moreover, PLD2 has been shown to facilitate that escape of *L. monocytogenes* from macrophage phagosomes (24). Furthermore, p47phox, the cytosolic component of NADPH oxidase, was shown to be important for killing *L. monocytogenes* (23, 70-72). Rabgef forms a complex with Rabep1, which has been shown to be essential for mediating Rab5a functions (25). Rab5a is an IFN-γ effector protein that is important for promoting phagosome maturation, fusion with the lysosome and subsequent bacterial killing (73, 74). *L. monocytogenes* has been shown to delay phagosome maturation by impairing the activity of Rab5a. It does so by preventing the exchange of inactive GDP-bound Rab5a for active GTP-bound Rab5a (75), possibly via manipulation of Rab5a regulating proteins such as guanine nucleotide exchange factors (GEFs). Indeed, Rabgef1, a Rab5a GEF, was down-regulated 0.8 fold in the C/EBPβ$^{-/-}$ macrophages.

PKCδ was selected for further study since it was found to belong to each of the "focus groups" ( transcription, direct or indirect C/EBPβ target gene, signal transduction, defense and immunity, production of ROI and RNI and phagosome maturation and phago-lysosome fusion) in both the SD<0.2 and SD<0.3 data set analyses (Fig. 27). For example, promoter analysis of the first 1000bp upstream of the transcriptional start site revealed several putative C/EBPβ$^{-/-}$ and a NF-κB binding sites, suggesting that PKCδ may be transcriptionally regulated by C/EBPβ. Gene ontology assignments to PKCδ showed that it was involved in humoral defense and intracellular signalling. Literature profiling revealed that PKCδ is involved in several key immune signalling pathways such as NF-κB (76-78), TNF (79, 80), IL-6 (81, 82), IFN-α and IFN-β (83), IFN-γ (84). PKCδ has also been shown to regulate the production of superoxide by phagocyte oxidase (85-87) and to play a role in transcription by phosphorylating the transcription factors STAT1, STAT3 and p300 (88). Furthermore, studies by Wadsworth and Goldfine using rottlerin, a putative specific PKCδ inhibitor, indirectly suggested that PKCδ may play a role in phagosomal escape (24, 44). The role of PKCδ during *L. monocytogenes* infection was therefore further functionally characterized by *in vitro* and *in vivo* infection experiments.

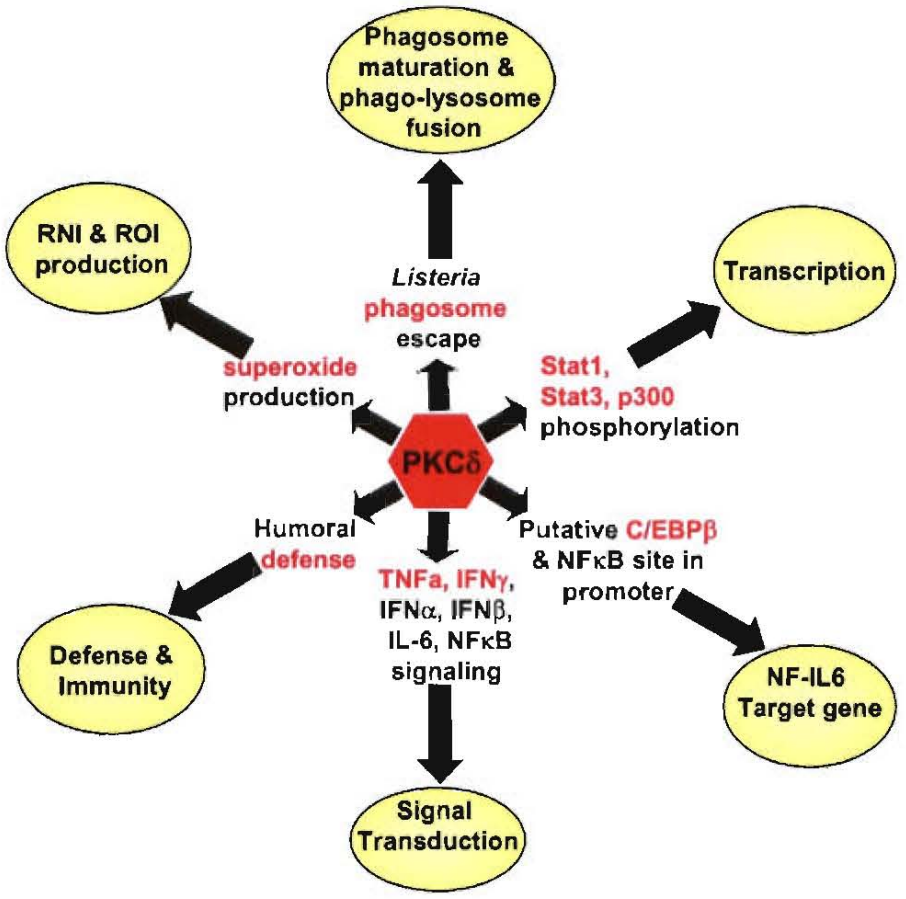


**Figure 27. PKCδ belongs to each functional clustering "focus group".** Promoter analysis revealed that the PKCδ may be a C/EBPβ target gene since its promoter contains a NF-κB and several putative C/EBPβ$^{-/-}$ binding sites. Gene ontology assignments and literature profiling showed that PKCδ was involved in humoral defense and may promote escape of *L. monocytogenes* from the phagosome. PKCδ is involved in regulating key immune signalling pathways such as NF-κB, TNF, IL-6, -α, IFN-β and IFN-γ, regulates the production of superoxide and plays a role in transcription by phosphorylating the transcription factors STAT1, STAT3 and p300.

## DISCUSSION

The anti-listerial transcriptional response of IFN-γ-activated macrophages from WT and C/EBPβ$^{-/-}$ mice was profiled at 4 hours p.i., since this was the earliest time point at which impaired bactericidal activity was observed in the C/EBPβ$^{-/-}$ macrophages. The execution of the microarray experiments went smoothly, with the exception for the hybridization step in which several problems were experienced. The preparation of the high quality cDNA or aRNA with a frequency of incorporation (FOI) of at least 20 dye molecules per 1000 nucleotides is crucial to the success of any microarray experiment. Since the yield aRNA was outstanding (>100μg for each sample) and the FOI was 39-57 dye molecules per 1000 nucleotides of aRNA, the microarray hybridization step was proceeded to with confidence. However, technical variation may have been introduced during the hybridization reaction due to the unintentional incubation of the arrays at 35°C instead of at 42°C. Although no observable non-specific hybridization was detected by eye, unequal hybridization kinetics across the array can not be discounted. Moreover, image analysis of the arrays showed that there were several quality and printing defects resulting in technical systematic variation within and between the arrays. In order to accurately measure differential gene expression, these systematic variations were removed by a sequential normalization procedure recommended by Wit and McClure (7). Probabilistic background correction, print-group LOWESS and slide-scale normalization were used to correct for the high background, spatial hybridization effects and intensity-dependent dye biases within and between arrays. However, despite these efforts to remove as much systematic variation as possible, statistical evaluation of the arrays showed the technical reproducibility within each array was poor as shown by >50% of the replicate spots having SD>0.2. Similarly, the reproducibility between the biological replicate experiments was poor and only 51% of the microarray data was reliable (SD<0.3). In order to improve the reliability and confidence of the microarray data, unreliable or questionable data was removed. However, since the SD>0.2 cut off criteria for reliability, as defined by many researchers (18), removed >60% of the genes from the data set, it was considered too stringent since several known biologically relevant genes were excluded from the data set. Since the microarrays were an exploratory study, it was considered more important to include biologically significant genes for future analyses. Elimination of known and other, as yet, unidentified biologically relevant genes, would decrease the probability of fulfilling the aims of the study, which were to identify genes involved in mediating listericidal activity. Therefore a less conservative value of SD>0.3 was used to remove unreliable data. Although this strategy removed 49%, it did result in better correlation and reproducibility between the biological replicates. Moreover, the outcome of PKCδ being selected as the

prime candidate gene would have been the same, regardless if either the SD<0.2 or SD<0.3 cut off criteria was used, since the SD of the average gene expression ratio for PKCδ in both the WT and KO arrays was less than 0.2. Ideally, the microarray experiments should have been repeated using high quality arrays, however budget limitations did not allow for this.

The systematic variation in the microarray data could have been introduced by several possible sources. For example, technical variation could have been introduced by unintentional differences in conditions during the infection experiment or RNA purification procedures. In addition, slight differences in the mRNA amplification procedure and efficiencies of dye labelling may have added to the variation. RNA amplification was originally developed as a method to expand very small RNA samples to produce enough material for hybridization to microarrays (89). A major concern when deciding to use the mRNA amplification procedure, was that not all mRNAs may amplify equally, which could introduce variation and bias within and between samples. However, studies by several groups have shown that any bias introduced by RNA amplification was minimal (4-6). Moreover, RNA amplification was reported to be actually improve the reliability of array results (5, 6). A major source of technical variation was the printed arrays themselves. Image analysis and visual inspection of the fluorescent array images revealed that there were several printing anomalies. Considerable variation in spot quality and morphology within and between arrays was observed. Not all the spots on printed DNA arrays are perfect and many microarray printing facilities routinely find that 2% of the spots on an array are defective. Unfortunately, in the current study 10% of the spots on the arrays were found to be either printed on top of each other or had merged into each other, resulting in a significant portion of the data becoming unreliable and questionable. Another potential source of variation within and between arrays was the hybridization procedure. The microarray arrays were processed in batches of 2 on different days over a 6 week period during spring. Several problems were experienced with the hybridization process: when adding the denatured labeled aRNA probes to the microarray array, some probes took longer to load than others due to uneven capillary action between the array slide and the coverslip. This difference in loading time could have resulted in some probes cooling and re-annealing. Therefore the degree of denaturation and temperature of the probes may not have been equal for all arrays. In some cases, bubbles formed when the probe was being added due to uneven capillary action and needed to be eased out from under the hybridization coverslip, which may have created unequal hybridization conditions. Moreover, the hybridization apparatus did not hold the hybridization temperature at 42°C, but instead cooled to 35°C over the incubation period. This temperature

fluctuation may have caused unequal hybridization kinetics within and between the arrays. Although sequential normalization of the microarray data removed as much technical variation and systematic biases as possible, there was still considerable "non-biological" variability due to the inclusion of questionable or inconsistent data. In order to reduce the complexity of and variance in the microarray data, the M values for the replicate spots were merged and averaged over all four biological replicate experiments

Even though there were several quality issues, the arrays still contained biologically meaningful data. As reported in literature, genes for several pro-inflammatory cytokines, chemokines and iNOS were significantly up-regulated in both the WT and C/EBPβ$^{-/-}$ activated macrophages during *L. monocytogenes* infection. Moreover, genes involved in macrophage activation, MHC class II presentation and in mediating signalling stimulated by IFN-γ and TNF, were also were significantly up-regulated in macrophages from both genotypes. More significantly, the induction of C/EBPβ was observed only in the WT macrophages and the up-regulation of C/EBPβ target genes such as G-CSF, CLECSF9, IL-12p35 and ISGF3γ was impaired in the C/EBPβ$^{-/-}$ macrophages. C/EBPβ was shown to be essential for the induction of G-CSF during innate immunity against *L. monocytogenes* (29), *Mycobacterium tuberculosis* (30) and *Brucella abortus* (31). Similarly, C/EBPβ was found to be necessary for the induction of CLECSF9 in response to LPS, TNF, IL-6, and IFN-γ stimulation. (32) and IL-12p35 during *Candida albicans* infection (33). In addition, C/EBPβ was shown to play an important role in IFN-γ signaling transduction via its transcriptional control of p48, a component of the ISGF3γ protein complex which is essential for IFN signaling (34). Since biologically relevant data could be extracted from the microarray data, despite the poor performance on a statistical level, the decision was made to go ahead with the data analysis.

Differentially expressed (DE) genes were identified by a paired T-Test where p values were calculated based on permutation and Bonferroni correction rather than distribution, in order to account for Type I Family Wise Error Rate encountered during multiple testing. The Type I error rate in the context of the current study is the probability of identifying genes as being differentially expressed between the WT and C/EBPβ$^{-/-}$ macrophages, when in fact they are not. Differentially expressed genes were defined as those genes whose expression was significantly higher or lower in the C/EBPβ$^{-/-}$ macrophages as compared to the WT in all 4 biological experiments. Five percent (1268 genes) of the mouse genome was identified as

being differentially expressed between the WT and C/EBPβ$^{-/-}$ activated macrophages infected with *L. monocytogenes*. Furthermore, 55% of the DE genes were up-regulated, 45% were down-regulated. The differential expression of these genes may have been be due to either (i) the deletion of C/EBPβ and consequent loss of transcriptional regulation, (ii) IFN-γ stimulation, (iii) infection by *L. monocytogenes* or (iv) a combination of all these parameters. Ideally, microarray experiments using RNA representing each of these individual parameters should have been done, but unfortunately a limited budget did not allow this. Instead, the dependence or independence of candidate DE genes would be determined by quantitative RT-PCR using RNA isolated from these experimental controls e.g. RNA isolated from macrophages treated only with IFN-γ or infected only with *L. monocytogenes*.

Several methods were considered on how to best to choose candidate genes that were potentially involved in mediating listericidal activity. The natural intuitive approach selecting the most highly up- or down-regulated genes, only enriched for genes that acted upstream in immune response signalling pathways rather than downstream, where listericidal activity is mediated. Moreover, this method made the assumption that large differences in gene expression were more biologically significant than small changes, which may not necessarily be true. Furthermore, since the microarray data lacked dimension, genes could not be selected based on interesting expression pattern observed during the time-course of the infection experiment; nor could any functional information be inferred upon the unknown genes based on their co-clustering with known genes. Moreover, the DE genes clustered into four simple patterns of expression only, which still did not help identify potential candidate genes. In depth knowledge of the biological functions of the DE genes during innate immunity was required in order to make an educated decision of which genes to choose. Therefore, a focussed functional clustering strategy was developed, where genes were selected based on particular biological functions and characteristics, rather than gene expression values. Since 35% of the DE genes were unknown and did not have any gene ontology or published literature they could not be included in the functional clustering analysis. Functional clustering of genes with functional information, showed that 4.6% of the annotated DE genes were involved in the regulation of transcription, 2.0% in host immunity and defense, 3.1% in the production of ROI, 16.1% in signalling and 8.9% in phagosome maturation and phago-lysosome fusion. Similarly, promoter analysis revealed that 18.0% of the annotated DE genes were possible direct transcriptional targets of C/EBPβ, while 47.3% of the annotated DE genes had binding sites for transcription factors that interacted with C/EBPβ. The focussed

functional clustering strategy reduced the number of candidate genes from 1268 down to 220 genes. Literature profiling of these 220 candidate genes revealed that several were already published in the literature as playing a role in defense against *L. monocytogenes*.

With hindsight, excluding the "unknown" genes from further analyses was limiting, since some of these genes may have provided novel insight into the RNI/ROI-independent killing pathway against *L. monocytogenes*. The "unknown" genes could have been co-clustered along with the known candidate genes based on the occurrence of functional protein motifs/domains within their encoded proteins. For example, genes encoding proteins that contain GTPase or VPS domains would be of interest since these domains occur within the Rab family of proteins, which are responsible for regulating endocytosis, phagosome maturation and phago-lysosome fusion. Similarly, the "unknown" genes could have been clustered according to the various response elements occurring within their regulatory promoter regions. For example, "unknown" genes that contained an IFN-γ response element within their promoters would most likely be involved in the pro-inflammatory immune response. These putative IFN-γ responsive genes could be grouped with other known IFN-γ response genes into the "Defense and Immunity" cluster. Had these analyses been done, the inclusion of the "unknown" genes in the focused clustering strategy would most likely have changed the percentages of the genes within each cluster. In addition, this more comprehensive analysis may have resulted in a significant enrichment for a particular functional group or activity as compared to the functional groups for the entire gene set. Furthermore, some of these "unknown" genes may have encoded key listericidal proteins. Therefore, due to the limitations of the original strategy, the above proposed analyses will be done in the near future to address these issues.

PKCδ was selected from all the candidate genes for further study since it was found to belong to each of the functional clustering "focus groups". Promoter analysis suggested that PKCδ may be a transcriptionally regulated by C/EBPβ. Gene ontology and literature data mining showed that PKCδ was involved in humoral defense and several key immune signalling pathways such as NF-κB (76-78), TNF (79, 80), IL-6 (81, 82), IFN-α and IFN-β (83), IFN-γ (84). PKCδ has also been shown to regulate the production of superoxide by phagocyte oxidase (85-87) and to play a role in transcription by phosphorylating the transcription factors STAT1, STAT3 and p300. In addition, in B cells stimulated with LPS, PKCδ was shown to negatively regulate C/EBPβ transcriptional activity by phosphorylating C/EBPβ at a serine residue within the DNA binding domain that results in decreased DNA binding activity (90).

Furthermore, studies by Wadsworth and Goldfine using rottlerin, a putative specific PKCδ inhibitor, indirectly suggested that PKCδ may play a role in phagosomal escape by possibly activating PLD2 (24, 44). However, no direct evidence showing a correlation between the listerial phagosomal escape and PKCδ activity was presented. Moreover, the role of PKCδ in innate immunity to intracellular pathogens has not been directly investigated to date. Since the up-regulation PKCδ in the C/EBPβ$^{-/-}$ macrophages was validated by quantitative RT-PCR (discussed in Chapter 5), the role of PKCδ during *L. monocytogenes* infection was therefore further functionally characterized using a PKCδ gene deficient mouse model, rather than rottlerin, since this putative PKCδ specific inhibitor has been reported to non-specifically inhibit several other kinases and non-kinase enzymes (1, 2).

## REFERENCES


1. Tapia, J. A., R. T. Jensen, and L. J. Garcia-Marin. 2006. Rottlerin inhibits stimulated enzymatic secretion and several intracellular signaling transduction pathways in pancreatic acinar cells by a non-PKC-delta-dependent mechanism. *Biochim Biophys Acta 1763:25.*
2. Davies, S. P., H. Reddy, M. Caivano, and P. Cohen. 2000. Specificity and mechanism of action of some commonly used protein kinase inhibitors. *Biochem J 351:95.*
3. Van Gelder, R. N., M. E. von Zastrow, A. Yool, W. C. Dement, J. D. Barchas, and J. H. Eberwine. 1990. Amplified RNA synthesized from limited quantities of heterogeneous cDNA. *Proc Natl Acad Sci U S A 87:1663.*
4. Li, Y., T. Li, S. Liu, M. Qiu, Z. Han, Z. Jiang, R. Li, K. Ying, Y. Xie, and Y. Mao. 2004. Systematic comparison of the fidelity of aRNA, mRNA and T-RNA on gene expression profiling using cDNA microarray. *J Biotechnol 107:19.*
5. Polacek, D. C., A. G. Passerini, C. Shi, N. M. Francesco, E. Manduchi, G. R. Grant, S. Powell, H. Bischof, H. Winkler, C. J. Stoeckert, Jr., and P. F. Davies. 2003. Fidelity and enhanced sensitivity of differential transcription profiles following linear amplification of nanogram amounts of endothelial mRNA. *Physiol Genomics 13:147.*
6. Feldman, A. L., N. G. Costouros, E. Wang, M. Qian, F. M. Marincola, H. R. Alexander, and S. K. Libutti. 2002. Advantages of mRNA amplification for microarray analysis. *Biotechniques 33:906.*
7. Wit, E., and J. D. McClure. 2004. *Statistics for microarrays : design, analysis, and inference.* John Wiley & Sons, Chichester, England ; Hoboken, NJ, USA.
8. R. Development Core Team: R: A language and environment for statistical computing.http://www.R-project.org.
9. Gentleman, R. C., V. J. Carey, D. M. Bates, B. Bolstad, M. Dettling, S. Dudoit, B. Ellis, L. Gautier, Y. Ge, J. Gentry, K. Hornik, T. Hothorn, W. Huber, S. Iacus, R. Irizarry, F. Leisch, C. Li, M. Maechler, A. J. Rossini, G. Sawitzki, C. Smith, G. Smyth, L. Tierney, J. Y. Yang, and J. Zhang. 2004. Bioconductor: open software development for computational biology and bioinformatics. *Genome Biol 5:R80.*
10. Wettenhall, J. M., and G. K. Smyth. 2004. limmaGUI: a graphical user interface for linear modeling of microarray data. *Bioinformatics 20:3705.*
11. Smyth, G. K., J. Michaud, and H. S. Scott. 2005. Use of within-array replicate spots for assessing differential expression in microarray experiments. *Bioinformatics 21:2067.*
12. Smyth, G. K. 2004. Linear models and empirical bayes methods for assessing differential expression in microarray experiments. *Stat Appl Genet Mol Biol 3:Article3.*
13. Chen, Y., E. R. Doughherty, and M. L. Bittner. 1997. Ratio-based decisions and the quantitative analysis of cDNA microarray images. *Biomed. Optics , 2 , 364-374. 2:364.*
14. Yang, Y. H., S. Dudoit, P. Luu, D. M. Lin, V. Peng, J. Ngai, and T. P. Speed. 2002. Normalization for cDNA microarray data: a robust composite method addressing single and multiple slide systematic variation. *Nucleic Acids Res 30:e15.*
15. Cleveland, W. S., B. Kleiner, and J. L. Warner. 1976. Robust statistical methods and photochemical air pollution data. *J Air Pollut Control Assoc 26:36.*
16. Irizarry, R. A., B. M. Bolstad, F. Collin, L. M. Cope, B. Hobbs, and T. P. Speed. 2003. Summaries of Affymetrix GeneChip probe level data. *Nucleic Acids Res 31:e15.*
17. Wu, Y., P. de Kievit, L. Vahlkamp, D. Pijnenburg, M. Smit, M. Dankers, D. Melchers, M. Stax, P. J. Boender, C. Ingham, N. Bastiaensen, R. de Wijn, D. van Alewijk, H. van Damme, A. K. Raap, A. B. Chan, and R. van Beuningen. 2004. Quantitative

assessment of a novel flow-through porous microarray for the rapid analysis of gene expression profiles. *Nucleic Acids Res 32:e123.*

18. Quackenbush, J. 2002. Microarray data normalization and transformation. *Nat Genet 32 Suppl:496.*
19. Churchill, G. A. 2002. Fundamentals of experimental design for cDNA microarrays. *Nat Genet 32 Suppl:490.*
20. Pfeffer, K., T. Matsuyama, T. M. Kundig, A. Wakeham, K. Kishihara, A. Shahinian, K. Wiegmann, P. S. Ohashi, M. Kronke, and T. W. Mak. 1993. Mice deficient for the 55 kd tumor necrosis factor receptor are resistant to endotoxic shock, yet succumb to L. monocytogenes infection. *Cell 73:457.*
21. Havell, E. A., L. L. Moldawer, D. Helfgott, P. L. Kilian, and P. B. Sehgal. 1992. Type I IL-1 receptor blockade exacerbates murine listeriosis. *J Immunol 148:1486.*
22. Rogers, H. W., C. S. Tripp, R. D. Schreiber, and E. R. Unanue. 1994. Endogenous IL-1 is required for neutrophil recruitment and macrophage activation during murine listeriosis. *J Immunol 153:2093.*
23. Endres, R., A. Luz, H. Schulze, H. Neubauer, A. Futterer, S. M. Holland, H. Wagner, and K. Pfeffer. 1997. Listeriosis in p47(phox-/-) and TRp55-/- mice: protection despite absence of ROI and susceptibility despite presence of RNI. *Immunity 7:419.*
24. Goldfine, H., S. J. Wadsworth, and N. C. Johnston. 2000. Activation of host phospholipases C and D in macrophages after infection with Listeria monocytogenes. *Infect Immun 68:5735.*
25. Horiuchi, H., R. Lippe, H. M. McBride, M. Rubino, P. Woodman, H. Stenmark, V. Rybin, M. Wilm, K. Ashman, M. Mann, and M. Zerial. 1997. A novel Rab5 GDP/GTP exchange factor complexed to Rabaptin-5 links nucleotide exchange to effector recruitment and function. *Cell 90:1149.*
26. Sluiter, W., I. Elzenga-Claasen, A. van der Voort van der Kley-van Andel, and R. van Furth. 1984. Differences in the response of inbred mouse strains to the factor increasing monocytopoiesis. *J Exp Med 159:524.*
27. van Furth, R., W. Sluiter, and J. T. van Dissel. 1988. Roles of factor increasing monocytopoiesis (FIM) and macrophage activation in host resistance to Listeria monocytogenes. *Infection 16 Suppl 2:S137.*
28. Garcia Del Busto Cano, E., and K. W. Renton. 2003. Modulation of hepatic cytochrome P450 during Listeria monocytogenes infection of the brain. *J Pharm Sci 92:1860.*
29. Tanaka, T., S. Akira, K. Yoshida, M. Umemoto, Y. Yoneda, N. Shirafuji, H. Fujiwara, S. Suematsu, N. Yoshida, and T. Kishimoto. 1995. Targeted disruption of the NF-IL6 gene discloses its essential role in bacteria killing and tumor cytotoxicity by macrophages. *Cell 80:353.*
30. Sugawara, I., S. Mizuno, H. Yamada, M. Matsumoto, and S. Akira. 2001. Disruption of nuclear factor-interleukin-6, a transcription factor, results in severe mycobacterial infection. *Am J Pathol 158:361.*
31. Pizarro-Cerda, J., M. Desjardins, E. Moreno, S. Akira, and J. P. Gorvel. 1999. Modulation of endocytosis in nuclear factor IL-6(-/-) macrophages is responsible for a high susceptibility to intracellular bacterial infection. *J Immunol 162:3519.*
32. Matsumoto, M., T. Tanaka, T. Kaisho, H. Sanjo, N. G. Copeland, D. J. Gilbert, N. A. Jenkins, and S. Akira. 1999. A novel LPS-inducible C-type lectin is a transcriptional target of NF-IL6 in macrophages. *J Immunol 163:5039.*
33. Gorgoni, B., D. Maritano, P. Marthyn, M. Righi, and V. Poli. 2002. C/EBP beta gene inactivation causes both impaired and enhanced gene expression and inverse regulation of IL-12 p40 and p35 mRNAs in macrophages. *J Immunol 168:4055.*
34. Xiao, W., L. Wang, X. Yang, T. Chen, D. Hodge, P. F. Johnson, and W. Farrar. 2001. CCAAT/enhancer-binding protein beta mediates interferon-gamma-induced p48

(ISGF3-gamma ) gene transcription in human monocytic cells. *J Biol Chem 276:23275.*

35. Dudoit, S., Y. Yang , M. Callow, and T. Speed. 2000. Statistical methods for identifying dierentially expressed genes in replicated cDNA microarray experiments. *Technical report # 578.*
36. Benjamini, Y., D. Drai, G. Elmer, N. Kafkafi, and I. Golani. 2001. Controlling the false discovery rate in behavior genetics research. *Behav Brain Res 125:279.*
37. Pan, W. 2002. A comparative review of statistical methods for discovering differentially expressed genes in replicated microarray experiments. *Bioinformatics 18:546.*
38. Dudoit, S., and T. P. Speed. 2000. A score test for the linkage analysis of qualitative and quantitative traits based on identity by descent data from sib-pairs. *Biostatistics 1:1.*
39. Anger, T., W. Zhang, and U. Mende. 2004. Differential contribution of GTPase activation and effector antagonism to the inhibitory effect of RGS proteins on Gq-mediated signaling in vivo. *J Biol Chem 279:3906.*
40. Towne, J. E., K. E. Garka, B. R. Renshaw, G. D. Virca, and J. E. Sims. 2004. Interleukin (IL)-1F6, IL-1F8, and IL-1F9 signal through IL-1Rrp2 and IL-1RAcP to activate the pathway leading to NF-kappaB and MAPKs. *J Biol Chem 279:13677.*
41. Eisen, M. B., P. T. Spellman, P. O. Brown, and D. Botstein. 1998. Cluster analysis and display of genome-wide expression patterns. *Proc Natl Acad Sci U S A 95:14863.*
42. Tavazoie, S., J. D. Hughes, M. J. Campbell, R. J. Cho, and G. M. Church. 1999. Systematic determination of genetic network architecture. *Nat Genet 22:281.*
43. Labow, M., D. Shuster, M. Zetterstrom, P. Nunes, R. Terry, E. B. Cullinan, T. Bartfai, C. Solorzano, L. L. Moldawer, R. Chizzonite, and K. W. McIntyre. 1997. Absence of IL-1 signaling and reduced inflammatory response in IL-1 type I receptor-deficient mice. *J Immunol 159:2452.*
44. Wadsworth, S. J., and H. Goldfine. 2002. Mobilization of protein kinase C in macrophages induced by Listeria monocytogenes affects its internalization and escape from the phagosome. *Infect Immun 70:4650.*
45. Larson, L., S. Arnaudeau, B. Gibson, W. Li, R. Krause, B. Hao, J. R. Bamburg, D. P. Lew, N. Demaurex, and F. Southwick. 2005. Gelsolin mediates calcium-dependent disassembly of Listeria actin tails. *Proc Natl Acad Sci U S A 102:1921.*
46. Cooper, J. A., and D. A. Schafer. 2000. Control of actin assembly and disassembly at filament ends. *Curr Opin Cell Biol 12:97.*
47. Welch, M. D., J. Rosenblatt, J. Skoble, D. A. Portnoy, and T. J. Mitchison. 1998. Interaction of human Arp2/3 complex and the Listeria monocytogenes ActA protein in actin filament nucleation. *Science 281:105.*
48. Flesch, I. E., A. Wandersee, and S. H. Kaufmann. 1997. Effects of IL-13 on murine listeriosis. *Int Immunol 9:467.*
49. Flesch, I. E., J. Barsig, and S. H. Kaufmann. 1998. Differential chemokine response of murine macrophages stimulated with cytokines and infected with Listeria monocytogenes. *Int Immunol 10:757.*
50. Pizarro-Cerda, J., and P. Cossart. 2006. Subversion of cellular functions by Listeria monocytogenes. *J Pathol 208:215.*
51. Chakraborty, T., F. Ebel, E. Domann, K. Niebuhr, B. Gerstel, S. Pistor, C. J. Temm-Grove, B. M. Jockusch, M. Reinhard, U. Walter, and et al. 1995. A focal adhesion factor directly linking intracellularly motile Listeria monocytogenes and Listeria ivanovii to the actin-based cytoskeleton of mammalian cells. *Embo J 14:1314.*
52. Pamer, E. G. 2004. Immune responses to Listeria monocytogenes. *Nat Rev Immunol 4:812.*

53. Kobayashi, K., L. D. Hernandez, J. E. Galan, C. A. Janeway, Jr., R. Medzhitov, and R. A. Flavell. 2002. IRAK-M is a negative regulator of Toll-like receptor signaling. *Cell 110:191.*
54. Nakane, A., M. Asano, S. Sasaki, S. Nishikawa, T. Miura, M. Kohanawa, and T. Minagawa. 1996. Transforming growth factor beta is protective in host resistance against Listeria monocytogenes infection in mice. *Infect Immun 64:3901.*
55. Repp, H., Z. Pamukci, A. Koschinski, E. Domann, A. Darji, J. Birringer, D. Brockmeier, T. Chakraborty, and F. Dreyer. 2002. Listeriolysin of Listeria monocytogenes forms Ca2+-permeable pores leading to intracellular Ca2+ oscillations. *Cell Microbiol 4:483.*
56. Wadsworth, S. J., and H. Goldfine. 1999. Listeria monocytogenes phospholipase C-dependent calcium signaling modulates bacterial entry into J774 macrophage-like cells. *Infect Immun 67:1770.*
57. Schnupf, P., D. A. Portnoy, and A. L. Decatur. 2006. Phosphorylation, ubiquitination and degradation of listeriolysin O in mammalian cells: role of the PEST-like sequence. *Cell Microbiol 8:353.*
58. Al-Shahrour, F., P. Minguez, J. M. Vaquerizas, L. Conde, and J. Dopazo. 2005. BABELOMICS: a suite of web tools for functional annotation and analysis of groups of genes in high-throughput experiments. *Nucleic Acids Res 33:W460.*
59. Reeves, E. P., H. Lu, H. L. Jacobs, C. G. Messina, S. Bolsover, G. Gabella, E. O. Potma, A. Warley, J. Roes, and A. W. Segal. 2002. Killing activity of neutrophils is mediated through activation of proteases by K+ flux. *Nature 416:291.*
60. Ahluwalia, J., A. Tinker, L. H. Clapp, M. R. Duchen, A. Y. Abramov, S. Pope, M. Nobles, and A. W. Segal. 2004. The large-conductance Ca2+-activated K+ channel is essential for innate immunity. *Nature 427:853.*
61. Rada, B. K., M. Geiszt, K. Kaldi, C. Timar, and E. Ligeti. 2004. Dual role of phagocytic NADPH oxidase in bacterial killing. *Blood 104:2947.*
62. Wagner, D., J. Maser, I. Moric, S. Vogt, W. V. Kern, and L. E. Bermudez. 2006. Elemental analysis of the Mycobacterium avium phagosome in Balb/c mouse macrophages. *Biochem Biophys Res Commun 344:1346.*
63. Wagner, D., J. Maser, B. Lai, Z. Cai, C. E. Barry, 3rd, K. Honer Zu Bentrup, D. G. Russell, and L. E. Bermudez. 2005. Elemental analysis of Mycobacterium avium-, Mycobacterium tuberculosis-, and Mycobacterium smegmatis-containing phagosomes indicates pathogen-induced microenvironments within the host cell's endosomal system. *J Immunol 174:1491.*
64. Vieira, O. V., R. J. Botelho, and S. Grinstein. 2002. Phagosome maturation: aging gracefully. *Biochem J 366:689.*
65. Desjardins, M. 2003. ER-mediated phagocytosis: a new membrane for new functions. *Nat Rev Immunol 3:280.*
66. Cheers, C., Y. F. Zhan, and P. J. Egan. 1990. In vivo IL-1 potentiates both specific and non-specific arms of immune response to infection. *Immunology 70:411.*
67. Rogers, H. W., K. C. Sheehan, L. M. Brunt, S. K. Dower, E. R. Unanue, and R. D. Schreiber. 1992. Interleukin 1 participates in the development of anti-Listeria responses in normal and SCID mice. *Proc Natl Acad Sci U S A 89:1011.*
68. Zheng, H., D. Fletcher, W. Kozak, M. Jiang, K. J. Hofmann, C. A. Conn, D. Soszynski, C. Grabiec, M. E. Trumbauer, A. Shaw, and et al. 1995. Resistance to fever induction and impaired acute-phase response in interleukin-1 beta-deficient mice. *Immunity 3:9.*
69. Juffermans, N. P., S. Florquin, L. Camoglio, A. Verbon, A. H. Kolk, P. Speelman, S. J. van Deventer, and T. van Der Poll. 2000. Interleukin-1 signaling is essential for host defense during murine pulmonary tuberculosis. *J Infect Dis 182:902.*

70. Shiloh, M. U., J. D. MacMicking, S. Nicholson, J. E. Brause, S. Potter, M. Marino, F. Fang, M. Dinauer, and C. Nathan. 1999. Phenotype of mice and macrophages deficient in both phagocyte oxidase and inducible nitric oxide synthase. *Immunity 10:29.*
71. Myers, J. T., A. W. Tsang, and J. A. Swanson. 2003. Localized reactive oxygen and nitrogen intermediates inhibit escape of Listeria monocytogenes from vacuoles in activated macrophages. *J Immunol 171:5447.*
72. Dinauer, M. C., M. B. Deck, and E. R. Unanue. 1997. Mice lacking reduced nicotinamide adenine dinucleotide phosphate oxidase activity show increased susceptibility to early infection with Listeria monocytogenes. *J Immunol 158:5581.*
73. Prada-Delgado, A., E. Carrasco-Marin, G. M. Bokoch, and C. Alvarez-Dominguez. 2001. Interferon-gamma listericidal action is mediated by novel Rab5a functions at the phagosomal environment. *J Biol Chem 276:19059.*
74. Alvarez-Dominguez, C., and P. D. Stahl. 1999. Increased expression of Rab5a correlates directly with accelerated maturation of Listeria monocytogenes phagosomes. *J Biol Chem 274:11459.*
75. Prada-Delgado, A., E. Carrasco-Marin, C. Pena-Macarro, E. Del Cerro-Vadillo, M. Fresno-Escudero, F. Leyva-Cobian, and C. Alvarez-Dominguez. 2005. Inhibition of Rab5a exchange activity is a key step for Listeria monocytogenes survival. *Traffic 6:252.*
76. You, H. J., J. W. Lee, Y. J. Yoo, and J. H. Kim. 2004. A pathway involving protein kinase Cdelta up-regulates cytosolic phospholipase A(2)alpha in airway epithelium. *Biochem Biophys Res Commun 321:657.*
77. Page, K., J. Li, L. Zhou, S. Iasvovskaia, K. C. Corbit, J. W. Soh, I. B. Weinstein, A. R. Brasier, A. Lin, and M. B. Hershenson. 2003. Regulation of airway epithelial cell NF-kappa B-dependent gene expression by protein kinase C delta. *J Immunol 170:5681.*
78. Page, K., J. Li, K. C. Corbit, K. M. Rumilla, J. W. Soh, I. B. Weinstein, C. Albanese, R. G. Pestell, M. R. Rosner, and M. B. Hershenson. 2002. Regulation of airway smooth muscle cyclin D1 transcription by protein kinase C-delta. *Am J Respir Cell Mol Biol 27:204.*
79. Woo, C. H., J. H. Lim, and J. H. Kim. 2005. VCAM-1 upregulation via PKCdelta-p38 kinase-linked cascade mediates the TNF-alpha-induced leukocyte adhesion and emigration in the lung airway epithelium. *Am J Physiol Lung Cell Mol Physiol 288:L307.*
80. Kilpatrick, L. E., J. Y. Lee, K. M. Haines, D. E. Campbell, K. E. Sullivan, and H. M. Korchak. 2002. A role for PKC-delta and PI 3-kinase in TNF-alpha-mediated antiapoptotic signaling in the human neutrophil. *Am J Physiol Cell Physiol 283:C48.*
81. Novotny-Diermayr, V., T. Zhang, L. Gu, and X. Cao. 2002. Protein kinase C delta associates with the interleukin-6 receptor subunit glycoprotein (gp) 130 via Stat3 and enhances Stat3-gp130 interaction. *J Biol Chem 277:49134.*
82. Xu, B., A. Bhattacharjee, B. Roy, G. M. Feldman, and M. K. Cathcart. 2004. Role of protein kinase C isoforms in the regulation of interleukin-13-induced 15-lipoxygenase gene expression in human monocytes. *J Biol Chem 279:15954.*
83. Uddin, S., and L. C. Platanias. 2004. Mechanisms of type-I interferon signal transduction. *J Biochem Mol Biol 37:635.*
84. Deb, D. K., A. Sassano, F. Lekmine, B. Majchrzak, A. Verma, S. Kambhampati, S. Uddin, A. Rahman, E. N. Fish, and L. C. Platanias. 2003. Activation of protein kinase C delta by IFN-gamma. *J Immunol 171:267.*
85. Bey, E. A., B. Xu, A. Bhattacharjee, C. M. Oldfield, X. Zhao, Q. Li, V. Subbulakshmi, G. M. Feldman, F. B. Wientjes, and M. K. Cathcart. 2004. Protein kinase C delta is required for p47phox phosphorylation and translocation in activated human monocytes. *J Immunol 173:5730.*

86. Zhao, X., B. Xu, A. Bhattacharjee, C. M. Oldfield, F. B. Wientjes, G. M. Feldman, and M. K. Cathcart. 2005. Protein kinase Cdelta regulates p67phox phosphorylation in human monocytes. *J Leukoc Biol 77:414.*
87. Yamamori, T., O. Inanami, H. Nagahata, and M. Kuwabara. 2004. Phosphoinositide 3-kinase regulates the phosphorylation of NADPH oxidase component p47(phox) by controlling cPKC/PKCdelta but not Akt. *Biochem Biophys Res Commun 316:720.*
88. Steinberg, S. F. 2004. Distinctive activation mechanisms and functions for protein kinase Cdelta. *Biochem J 384:449.*
89. Yue, H., P. S. Eastman, B. B. Wang, J. Minor, M. H. Doctolero, R. L. Nuttall, R. Stack, J. W. Becker, J. R. Montgomery, M. Vainer, and R. Johnston. 2001. An evaluation of the performance of cDNA microarrays for detecting changes in global mRNA expression. *Nucleic Acids Res 29:E41.*
90. Miyamoto, A., K. Nakayama, H. Imaki, S. Hirose, Y. Jiang, M. Abe, T. Tsukiyama, H. Nagahama, S. Ohno, S. Hatakeyama, and K. I. Nakayama. 2002. Increased proliferation of B cells and auto-immunity in mice lacking protein kinase Cdelta. *Nature 416:865.*

## CHAPTER 5.

## FUNCTIONAL INFECTION STUDIES IN THE PKCδ$^{-/-}$ MOUSE MODEL


### SUMMARY

PKCδ was found by microarray and confirmed by quantitative RT-PCR to be expressed at 1.77 fold higher levels in activated C/EBPβ$^{-/-}$ macrophages infected with *L. monocytogenes* as compared to WT. Functional clustering and literature profiling revealed PKCδ to be the most promising candidate gene since it has been shown to be involved in (1) several critical immune signalling pathways, (2) regulation of superoxide production by phagocyte oxidase, (3) regulation of transcription, (4) may be transcriptionally regulated by C/EBPβ and (5) may be involved promoting listerial escape from the phagosome. In addition, PKCδ was shown to negatively regulate C/EBPβ transcription. Furthermore, since PKCδ was up-regulated in the highly susceptible C/EBPβ$^{-/-}$ macrophages infected with *L. monocytogenes*, as shown by microarray and confirmed by RT-PCR, it was postulated that PKCδ was detrimental to the host during *L. monocytogenes*. However, since this premise has never been directly investigated, the role of PKCδ in innate immunity to intracellular pathogens was investigated using the PKCδ$^{-/-}$ mouse model, rather than rottlerin, since this putative PKCδ specific inhibitor has been reported to non-specifically inhibit several other kinases and non-kinase enzymes (1, 2). PKCδ$^{-/-}$ macrophages infected with *L. monocytogenes* displayed increased bacterial escape from phagosomes and uncontrolled bacterial growth. Despite increased production of iNOS, pro-inflammatory mediators and enhanced neutrophil recruitment, PKCδ$^{-/-}$mice were highly susceptible to *L. monocytogenes* and displayed impaired bactericidal killing, enhanced histopathology and decreased activated macrophage recruitment. PKCδ is therefore critical for confinement of *L. monocytogenes* within phagosomes during innate immunity against *L. monocytogenes*. In contrast, PKCδ$^{-/-}$ mice were able to control *M. tuberculosis* infection as well as WT mice, suggesting that PKCδ is targeted by *L. monocytogenes* in order to facilitate its escape from the phagosome. PKCδ may be part of an unknown listericidal mechanism that is independent of iNOS and pro-inflammatory cytokines that was previously observed in IFN-γ$^{-/-}$, TNFRp55$^{-/-}$, ICSBP$^{-/-}$ and C/EBPβ$^{-/-}$ mice. Using a systems biology approach, a putative role of PKCδ in the unknown listericidal mechanism was uncovered, where PKCδ may function to promote and/or enhance Rab5a activity leading to phagosome maturation, phago-lysosome fusion and bacilli killing.

## RESULTS

### 1. Identification of PKCδ by microarray

The expression levels of PKCδ were found by microarray to be 1.13 fold higher in the C/EBPβ$^{-/-}$ macrophages as compared to WT, which was confirmed by real-time quantitative RT-PCR to be even higher at 1.77 fold (Fig. 1 A). Quantitative RT-PCR of macrophages infected with *L. monocytogenes* stimulated with or without IFN-γ, showed significant induction of PKCδ in the C/EBPβ$^{-/-}$ macrophages as compared to the media control at 4 hours p.i. (Fig. 1 B). The induction of PKCδ by *L. monocytogenes* in the absence IFN-γ stimulation may be due to *L. monocytogenes*-induced transcription of TNF via TLR2 (3) and TLR5 signalling (4). TNF has been shown to induce the expression of PKCδ in a NF-κB dependent manner (5). Moreover, PKCδ itself promotes the nuclear translocation of NF-κB and consequent NF-κB-mediated transcription. Since the transcription of G-CSF is mediated by NF-κB (6), it may be possible that G-CSF acts in a negative feedback regulatory loop to prevent its over-expression by NF-κB. The suppression of NF-κB transcriptional activity by G-CSF may occur via an, as yet unknown mechanism, whereby genes encoding proteins that promote the activation and nuclear translocation of NF-κB e.g. PKCδ, are transcriptionally repressed. Consistent with this hypothesis is the observation that the induction of PKCδ by *L. monocytogenes* alone in infected C/EBPβ$^{-/-}$ macrophages was significantly higher as compared to WT control macrophages (Fig.1.B). The impaired production of G-CSF in the C/EBPβ$^{-/-}$ macrophages, due to the absence C/EBPβ (7), may have resulted in the alleviation of the transcriptional repression of PKCδ by the G-CSF regulatory negative feedback loop. The effect of G-CSF and other C/EBPβ target genes such as IL-12p35, Clecsf9 and ISGF3γ on the transcription of of PKCδ will be further investigated by real-time quantitative RT-PCR in WT and C/EBPβ$^{-/-}$ macrophages. Similarly, the expression levels of PKCδ were higher after IFN-γ stimulation as compared to media controls, but the observed increase was not significant (Fig. 1 C). The apparent decreased levels of PKCδ in untreated C/EBPβ$^{-/-}$ macrophages, although not significant as compared to WT, suggested that PKCδ may be a target gene of C/EBPβ. Gene Ontology (GO) assignments to PKCδ showed that it was involved in humoral defense and intracellular signalling. Literature profiling revealed that PKCδ is involved in several key immune signalling pathways such as NF-κB (8-10), TNF (11, 12), IL-6 (13, 14), IFN-α and IFN-β (15), IFN-γ (16). PKCδ has also been shown to regulate the production of superoxide by phagocyte oxidase (17-19) and to play a role in transcription by phosphorylating the transcription factors STAT1 (16, 20, 21), STAT3 (13, 22, 23) and p300 (24). Furthermore, studies by Wadsworth and Goldfine using rottlerin, a

putative specific PKCδ inhibitor, indirectly suggested that PKCδ may play a role in phagosomal escape (25, 26). However, no direct evidence showing a correlation between the listerial phagosomal escape and PKCδ activity has been reported. In addition, PKCδ was shown to negatively regulate C/EBPβ transcriptional activity by phosphorylating C/EBPβ at a serine residue within the DNA binding domain that results in decreased DNA binding activity (27). Furthermore, since PKCδ was up-regulated in the highly susceptible C/EBPβ$^{-/-}$ macrophages infected with *L. monocytogenes*, shown by microarray and confirmed by RT-PCR, it was postulated that PKCδ was detrimental to the host during *L. monocytogenes*. However, since the role of PKCδ in innate immunity to intracellular pathogens has not been directly investigated to dat, the PKCδ$^{-/-}$ mouse model was used to investigate this premise. The PKCδ$^{-/-}$ mouse model was used, rather than rottlerin, since this putative PKCδ specific inhibitor has been reported to non-specifically inhibit several other kinases and non-kinase enzymes (1, 2).

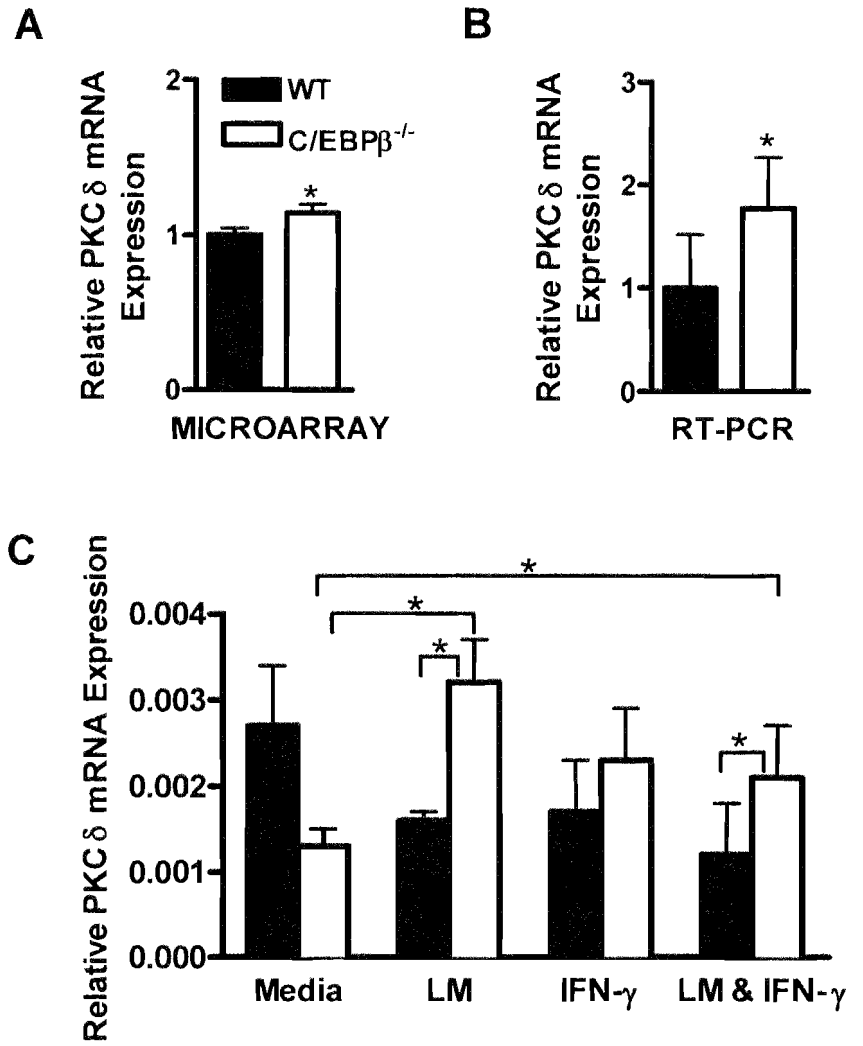


**Figure 1. Up-regulation of PKCδ in activated C/EBPβ$^{-/-}$ macrophages during *L. monocytogenes* infection.** Differential up-regulation of PKCδ in C/EBPβ$^{-/-}$ macrophages (empty bars) as compared to WT (filled bars) as discovered by (A) microarray analysis and (B) confirmed by quantitative RT-PCR. Shown are the averages and SEM of 4 independent biological experiments at 4 hours p.i.. Microarray data is relative to WT and RT-PCR data was normalized to the B2MG housekeeping gene and is relative to the WT average. (C) Quantitative RT-PCR of PKCδ in WT and C/EBPβ$^{-/-}$ macrophages with or without IFN-γ stimulation and infected with *L. monocytogenes* (denoted by LM). Data is relative to the B2MG housekeeping gene and represents the averages and SEM of 4 independent biological experiments at 4 hours p.i. (* $p < 0.5$).

**2. PKCδ$^{-/-}$ macrophages have enhanced bacterial growth and increased bacterial escape from phagosomes**

Since Wadsworth and Goldfine (25) did not directly show a correlation between PKCδ and phagosomal escape nor listericidal activity, IFN-γ-activated PKCδ$^{-/-}$ BMDMs were infected with *L. monocytogenes* and bacilli growth measured at 2, 4, 8 and 12 hours p.i. (Fig. 2 A). Macrophages from WT control mice were able to restrict bacterial growth and reached a steady state plateau at 8 and 12 hours p.i.. Similarly, even though the bacterial load in the PKCδ$^{+/-}$ control macrophages was 4 times significantly higher than in the WT, the PKCδ$^{+/-}$ macrophages were still able to restrict bacterial growth. In contrast, PKCδ$^{-/-}$ macrophages had significantly increased bacterial growth at all time points, with uncontrolled bacilli growth 8 and 12 hours p.i.. To determine if the increased bacterial growth was due to enhanced bacterial escape from phagosomes, BMDMs were infected with *L. monocytogenes* and bacterial escape measured by fluorescent microscopy (Fig. 2 C, D, E, F). WT, PKCδ$^{+/-}$ and PKCδ$^{-/-}$ macrophages contained an equal number of bacteria at 90 minutes, indicating no significant defect with respect to phagocytosis in any of the groups. The number of bacteria associated with actin (red, escaped bacteria) and number of bacteria trapped in the phagosome (green) were scored and the percentage of escape calculated as described in the methods. PKCδ$^{-/-}$ macrophages had 6.5 times greater bacterial escape than the WT and PKCδ$^{+/-}$ controls (Fig. 2 B, 90 minutes p.i.; Fig. 2 C, E). At later time points, significantly more bacteria were associated with actin (Fig. 2 B, 180 and 270 minutes; Fig. 2 D, F) and were in motion (inset, Fig. 2 D) in the PKCδ$^{-/-}$ macrophages as compared to the controls. Taken together these results showed that PKCδ$^{-/-}$ macrophages had impaired listericidal activity due to their inability to confine *L. monocytogenes* within the phagosome, which resulted in enhanced listerial escape and subsequent uncontrolled bacterial growth.

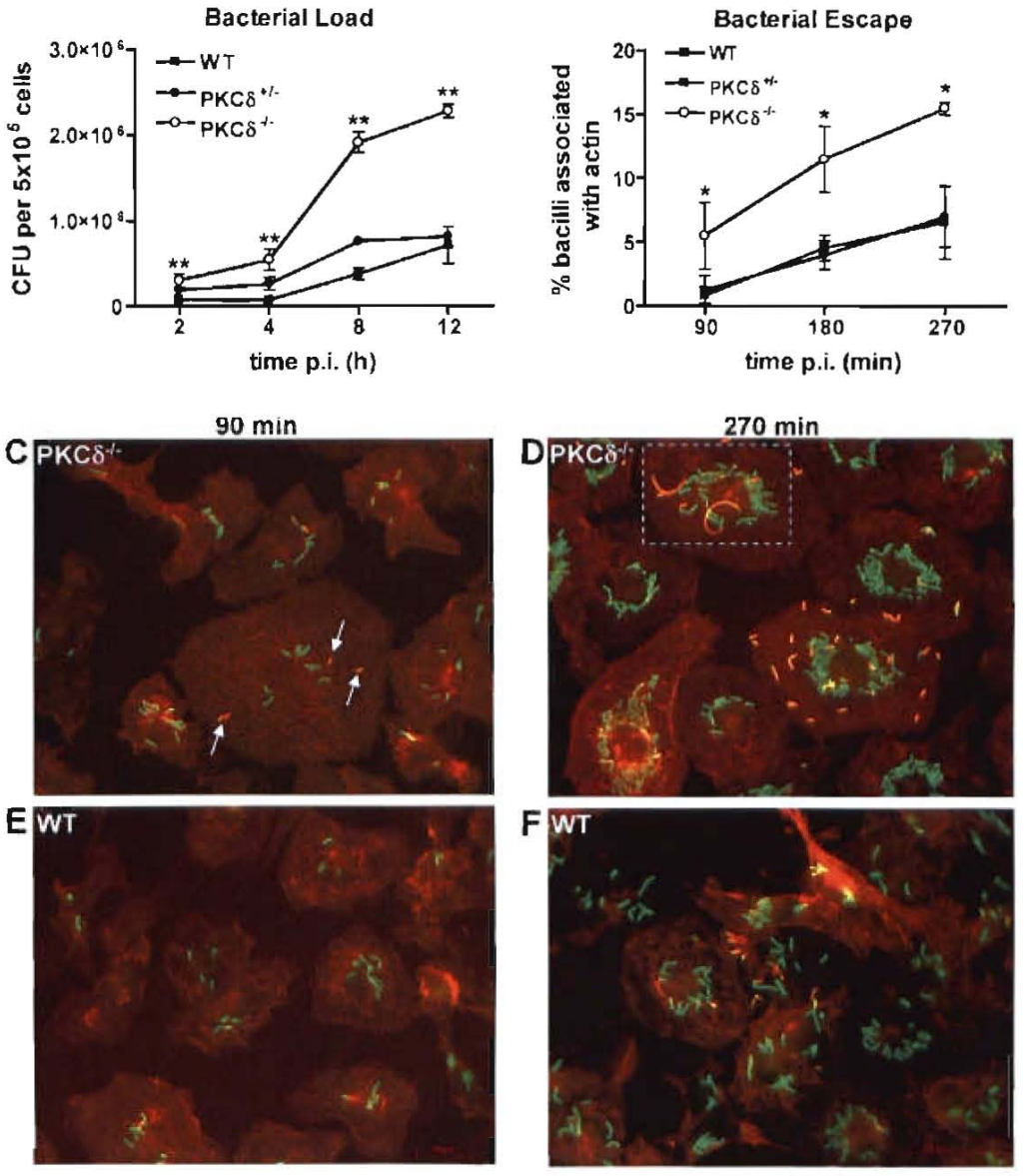


**Figure 2. Enhanced bacterial growth and increased bacterial escape from PKCδ$^{-/-}$ phagosomes.** BMDMs from WT (filled squares), PKCδ$^{+/-}$ (filled circles) and PKCδ$^{-/-}$ (open circles) were infected with *L. monocytogenes*. (A) Bacterial load was determined at 2, 4, 8 and 12 hours p.i.. Results are representative of three independent experiments (B) Quantification of *L. monocytogenes* escape from phagosomes at 90, 180 and 270 minutes p.i. The number of bacteria associated with actin (red) and trapped in the phagosome (green) was scored. Data are averages ± SEM of the means for three independent experiments. Deconvoluting fluorescent microscopy of BMDMs infected with *L. monocytogenes* at 90 minutes (C, E) and 270 minutes (D, F). Escaped bacteria (red) are indicated by arrows. Magnification: X100. Results are representative of three independent experiments (*$p<0.05$; **$p<0.0001$).

### 3. Efficient induction of pro-inflammatory mediators and nitric oxide in *L. monocytogenes*-infected PKCδ$^{-/-}$ macrophages

To determine if the enhanced phagosomal escape and impaired bacterial killing in PKCδ$^{-/-}$ macrophage was a consequence of impaired macrophage activation, the levels of pro-inflammatory cytokines, chemokine MCP-1 and nitric oxide in the supernatant from *L. monocytogenes*-infected macrophages were quantified (Fig. 3). Control PKCδ$^{+/-}$ macrophages produced peak levels of cytokines IL-6, TNF, IL-12p40, IL-12p70 and the chemokine MCP-1 at 8 hours p.i., followed by down-regulation at 12 hours p.i.. In contrast, secretion of cytokines and chemokines from PKCδ$^{-/-}$ macrophages reached peak levels at 12 hours p.i. which were significantly higher as compared to PKCδ$^{+/-}$ controls. Furthermore, nitrite production, representative of nitric oxide, was significantly increased in the PKCδ$^{-/-}$ macrophages at 8 and 12 hours p.i.. In addition, the levels of GM-CSF were found to be similar among the PKCδ$^{-/-}$ and control macrophages, indicating that enhanced cytokine production was not due to enhanced macrophage proliferation. Furthermore, the levels of IFN-γ were found to be similar for PKCδ$^{-/-}$ and control macrophages, indicating comparable levels of activation among all samples. These results demonstrated that in the absence of PKCδ, macrophages were still able to be activated and efficiently produced pro-inflammatory and killing effector molecules such as iNOS in response to the increased bacterial burden, however, they were nevertheless unable to control *L. monocytogenes* bacilli growth (Fig. 2 A).

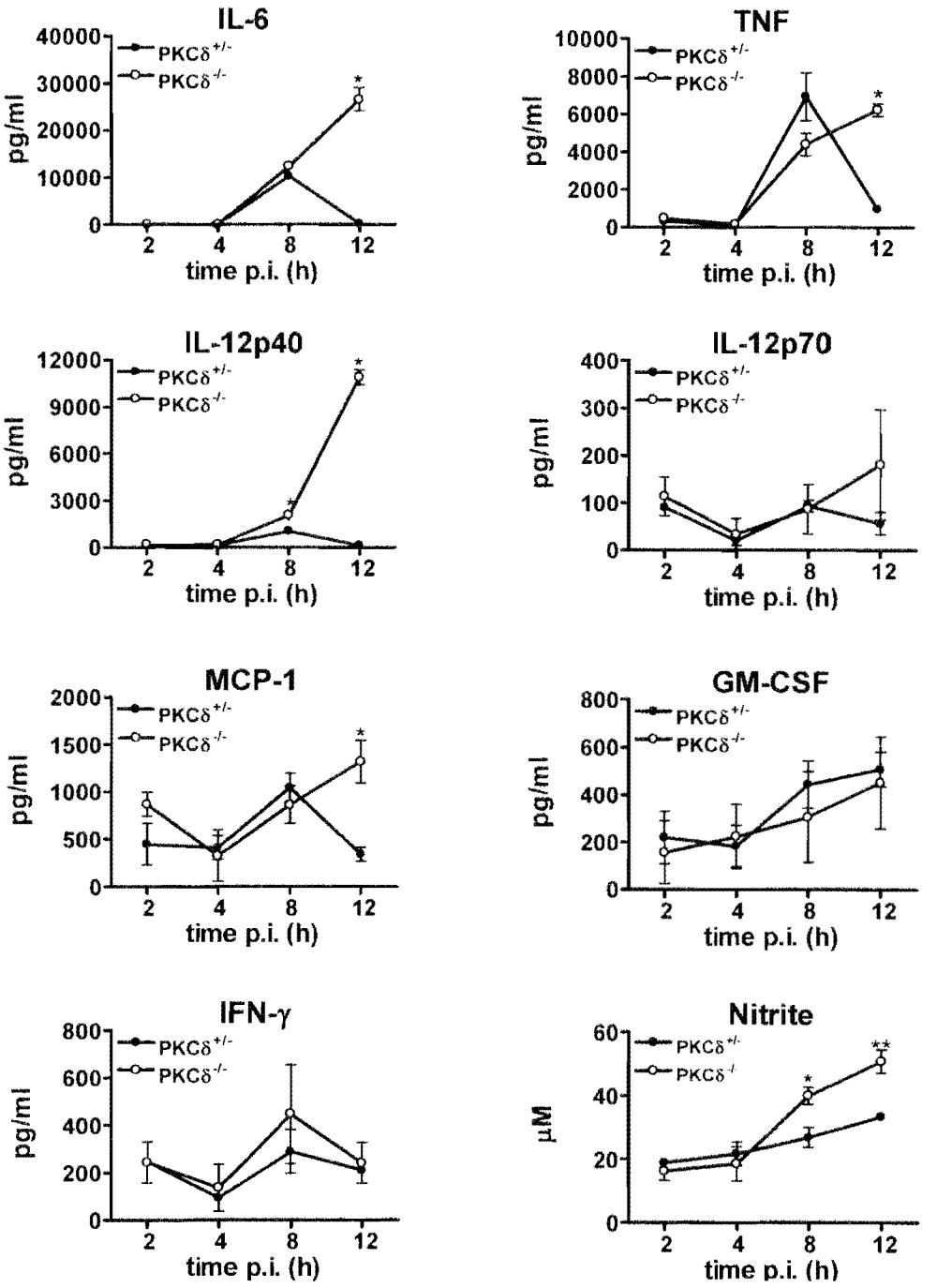


**Figure 3. Efficient induction of pro-inflammatory mediators and iNOS in PKCδ$^{-/-}$ macrophages.** Secretion of cytokines, chemokine MCP-1 and nitrite into culture supernatants by BMDMs from WT (not shown), PKCδ$^{+/-}$ (filled circles), PKCδ$^{-/-}$ (open circles) mice infected with *L. monocytogenes*. Data are represented as means ± SEM of triplicate samples. Results are representative of two independent experiments (* $p<0.05$; ** $p<0.005$).

**4. Increased mortality in *L. monocytogenes*-infected PKCδ$^{-/-}$ mice**

Having shown *in vitro* that PKCδ is involved in controlling *L. monocytogenes* infection in macrophages, the role of PKCδ *in vivo* was investigated. PKCδ$^{-/-}$ mice and their control littermates were infected i.p. with titrated doses of *L. monocytogenes* and mortality was measured (Fig.4). WT mice were able to survive *L. monocytogenes* infection at all doses and had a $LD_{50}$ = 2 x $10^5$ CFU. Furthermore, control PKCδ$^{+/-}$ mice controlled the infection to the same degree as WT, although one out of five mice died at the highest inoculum (2 x $10^4$ CFU). In contrast, PKCδ$^{-/-}$ mice were highly susceptible to *L. monocytogenes* infection and had a $LD_{50}$ of 2 x $10^3$ CFU. Even at a very low dose of 200 CFU, two out of nine PKCδ$^{-/-}$ mice died. IFN-γR$^{-/-}$ mice were included in the mortality study, in order to assess degree of susceptibility of PKCδ$^{-/-}$ mice to *L. monocytogenes* infection. IFN-γR$^{-/-}$ mice have been shown to be extremely susceptible to *L. monocytogenes* and are unable to resist even less than 70 CFU (28). As expected, all the IFN-γR$^{-/-}$ mice died within 5-6 days after infected with 200 CFU, whereas only 22% of the PKCδ$^{-/-}$ mice died within the same period. These results demonstrated that the PKCδ$^{-/-}$ mice had defective innate immune responses and were highly susceptible to *L. monocytogenes* infection, albeit not to the same degree as the IFN-γR$^{-/-}$ mice.

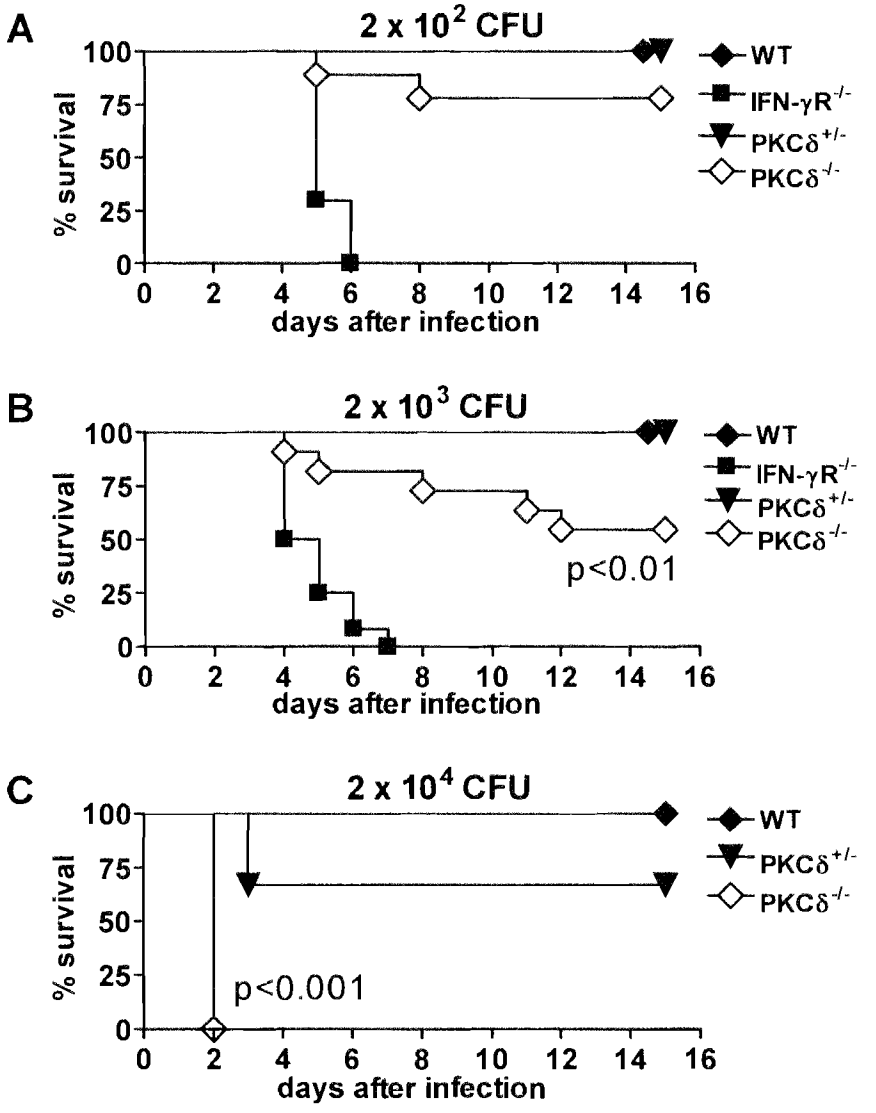


**Figure 4. Enhanced mortality after *L. monocytogenes* infection in the absence of PKCδ.** Mice were infected with either (A) 2 x $10^2$ CFU, (B) 2 x $10^3$ CFU or (C) 2 x $10^4$ CFU of *L. monocytogenes* and mortality measured. Results are representative of 2 independent experiments For (A) n = 7 - 10 mice per group; (B) n=12 mice per group; (C) n=5 mice per group. For (C) 2 PKCδ$^{-/-}$were moribund and 3 PKCδ$^{-/-}$ mice had died 2 days after infection. Moribund mice were sacrificed and used to determine the bacterial burden in liver and spleen. Shown are *p* values comparing the survival curves of WT and PKCδ$^{-/-}$ mice. Survival data was analyzed by Kaplan-Meier using the log-rank test to compare survival data.

**5. Enhanced bacterial burden and increased histopathology in *L. monocytogenes*-infected PKCδ$^{-/-}$ mice**

*L. monocytogenes*-infected PKCδ$^{-/-}$ mice died early after infection (2 days) with a sub-lethal dose for WT mice, indicating a defect in their innate immunity. To verify this hypothesis PKCδ$^{-/-}$, WT and PKCδ$^{+/-}$ control mice were infected with 2 x $10^4$ *L. monocytogenes* and the bacterial burden in liver and spleen was measured at 2 days p.i. (Fig. 5 A, B). The CFU in spleen and liver from PKCδ$^{-/-}$ mice was significantly increased over 3-log fold as compared to their WT and PKCδ$^{+/-}$ control littermates. This indicated that PKCδ$^{-/-}$ mice were defective in their innate immunity and were unable to control bacterial growth resulting in early mortality. Protective immune responses against *L. monocytogenes* involve the proper formation of infiltrating immune cells to form small microabscesses that confine the infection and control bacterial growth. The histopathology of liver (Fig. 5 C, D) was analysed at 2 days p.i.. Haematoxylin and eosin staining showed significantly more abundant microabscesses in PKCδ$^{-/-}$ mice as compared to their littermate controls. The microabscesses from WT mice were small, well defined (Fig. 5 C, WT) and contained only a few bacilli (Fig. 5 D, WT). In contrast, the PKCδ$^{-/-}$ microabscesses were very large, unorganized and contained many polymorphonuclear cells and zones of hepatocellular necrosis (Fig. 5 C, PKCδ$^{-/-}$). Many rod-shaped bacilli were visible in the PKCδ$^{-/-}$ microabscesses (Fig. 5 D, PKCδ$^{-/-}$) whereas the WT and PKCδ$^{+/-}$ microabscesses only contained a few bacteria. Failure to control bacterial growth resulted in necrotic lesions and liver destruction in the PKCδ$^{-/-}$ mice. The size of microabscesses was significantly larger in PKCδ$^{-/-}$ mice as compared to the WT mice (Fig. 5 E). Taken together, histopathology from *L. monocytogenes*-infected PKCδ$^{-/-}$ mice showed significantly more abundant and larger microabscesses than the WT controls, with extensive necrotic lesions, liver parenchymal destruction and bacterial overgrowth.

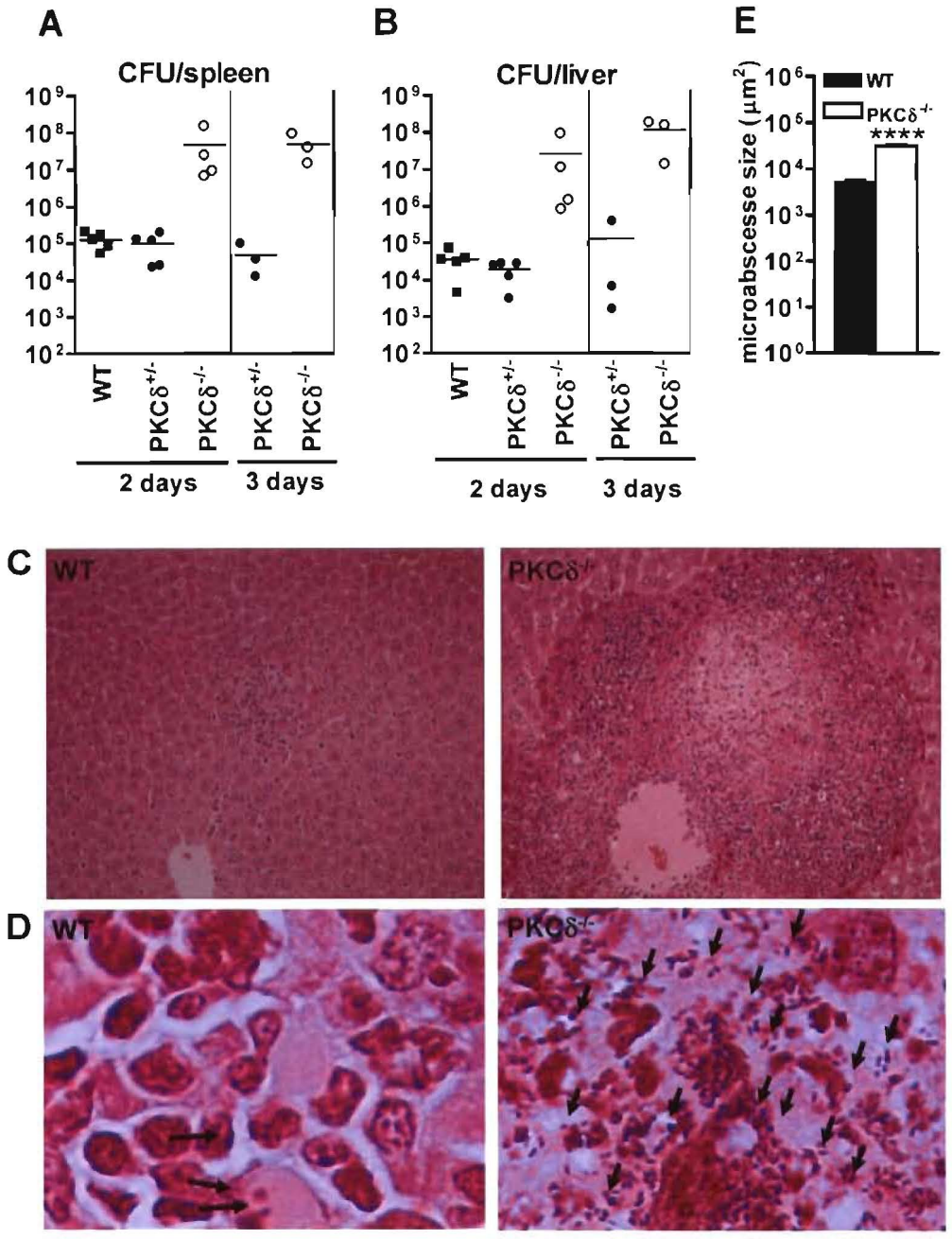


**Figure 5. Increased bacterial burden and histopathology in PKCδ$^{-/-}$ mice.** WT (filled squares), PKCδ$^{+/-}$ (filled circles) and PKCδ$^{-/-}$ (open circles) mice were infected i.p. with 2 x $10^4$ *L. monocytogenes* (n=4 - 5/group). Bacterial load in (A) spleen and (B) liver was determined at 2 and 3 days p.i. (C) Microabscess liver sections were stained with haematoxylin/eosin (C, D) and Gram positive stain (D) which colours *L. monocytogenes* in blue (arrow). Magnifications: C X400; D X1000. All data are representative of two independent experiments. (E) Size quantification of liver microabscesses in control PKCδ$^{+/-}$ (filled bars) and PKCδ$^{-/-}$ (empty bars) mice (***p<0.0001).

**6. Decreased activated macrophages but enhanced neutrophil recruitment in PKCδ$^{-/-}$ mice following *L. monocytogenes* infection.**

Clearance of *L. monocytogenes* involves the proper recruitment of activated macrophages and neutrophils to the site of infection. PKCδ$^{-/-}$ mice and their WT and PKCδ$^{+/-}$ littermate controls were infected with 2 x $10^4$ *L. monocytogenes* CFU and the recruitment of inflammatory cells at 2 days p.i. was analyzed by FACs. PKCδ$^{-/-}$ mice had increased numbers of peritoneal exudate cells (PECs) as compared to their control littermates, indicating no defect in cellular recruitment to the site of infection (Fig. 6). However, PKCδ$^{-/-}$ mice had 10% decreased recruitment of activated macrophages than the controls as shown by MHC class II/MAC1 (Fig. 7 A) and MHC class II/F4/80 (Fig. 7 B) staining. Furthermore, GR1/MAC1 expression was increased in PKCδ$^{-/-}$ mice indicating 30% greater neutrophil recruitment as compared to the controls (Fig. 7 C). These results showed that the PKCδ$^{-/-}$ mice had increased cellular recruitment to the site of infection, with significantly more neutrophils but decreased activated macrophages.

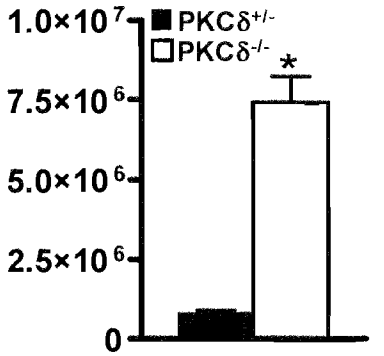


**Figure 6. Yield of recovered peritoneal exudate cells.** Control PKCδ$^{+/-}$ littermates and PKCδ$^{-/-}$ mice was infected with 2 x $10^4$ CFU of *L. monocytogenes*. Two days after infection peritoneal exudate cells (PECs) were recovered and pooled (n=5/group). Data represent the average and SEM of 2 independent experiments of total recovered PECs per mouse (* $p<0.01$).

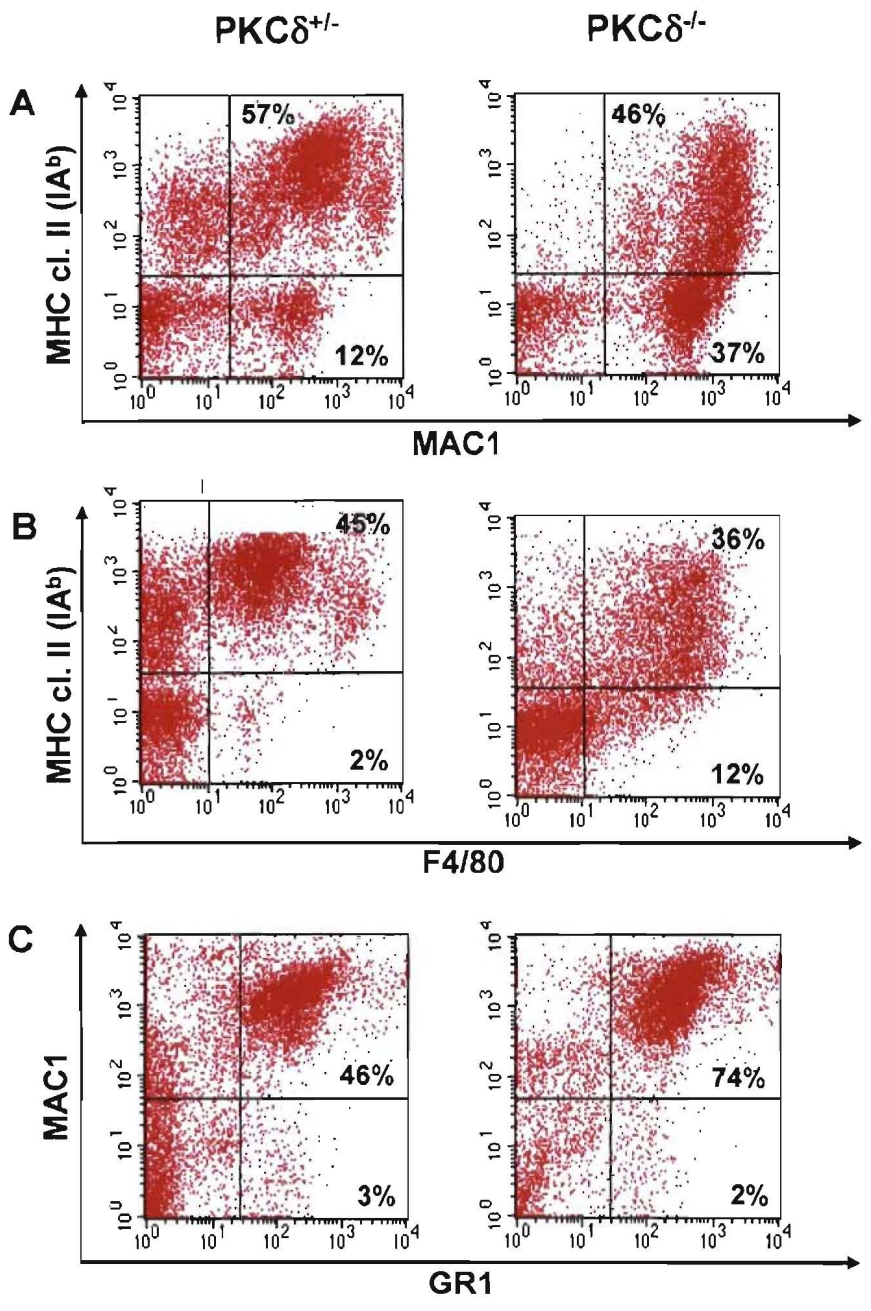


**Figure 7. Decreased activated macrophage and enhanced neutrophil recruitment in PKCδ$^{-/-}$ mice.** FACs analysis of *L. monocytogenes* elicited PECs from PKCδ$^{+/-}$ and PKCδ$^{-/-}$ stained for activated macrophages (A) MHC class II and MAC1, (B) MHC class II and F4/80 and for neutrophils (C) MAC1 and GR1. Numbers represent the percentage of cells in that particular quadrant. Results represent pooled samples n=5/group.

**7. Efficient induction of pro-inflammatory mediators and nitric oxide in *L. monocytogenes*-infected PKCδ$^{-/-}$ mice.**

Serum levels of pro-inflammatory mediators collected 2 and 3 days after infection showed that the PKCδ$^{-/-}$ mice efficiently produced MCP-1, IL-6, TNF, IL12-p40, IL-18 and IFN-γ at levels comparable or significantly higher than the WT (Fig. 8). Similarly, quantitative real-time RT-PCR of infected liver and spleen samples at 2 days (Fig. 9) and 3 days (Fig. 10) p.i. confirmed that the PKCδ$^{-/-}$ mice efficiently induced expression of pro-inflammatory mediators and iNOS at levels greater than their control littermates. The increased MCP-1 expression in PKCδ$^{-/-}$ mice might explain the observed increased cellular recruitment to the site of infection as shown by FACs analysis (Fig. 7). Interestingly, C/EBPβ was highly up-regulated in the PKCδ$^{-/-}$ mice as compared to WT controls. Induction of bactericidal effector, iNOS, was also highly increased in PKCδ$^{-/-}$ mice, however this was not sufficient to reduce the bacterial burden. IL-10, an anti-inflammatory cytokine, was also increased in the PKCδ$^{-/-}$ mice. These results showed that the PKCδ$^{-/-}$ mice had efficient or significantly greater induction of pro-inflammatory mediators and iNOS due to their increased bacterial burden, but were nevertheless unable to control and clear the infection.

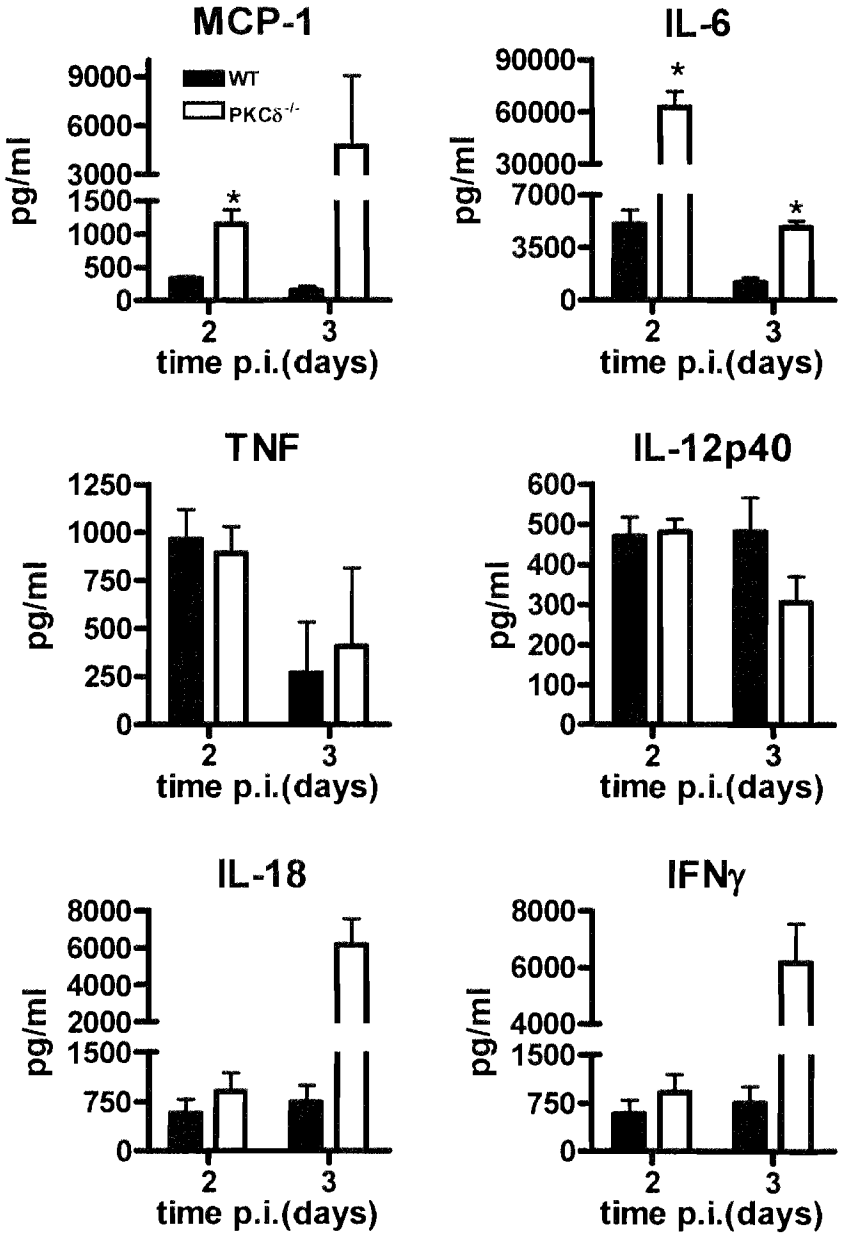


**Figure 8. Efficient production and secretion of pro-inflammatory mediators in PKCδ$^{-/-}$ mice.** Pro-inflammatory mediators were measured by sandwich ELISA in sera of mice at 2 and 3 days after *L. monocytogenes* infection with 2 x $10^4$ CFU. Results are representative of two independent experiments (n=5/group). Data are represented as means ± SEM (* $p<0.05$).

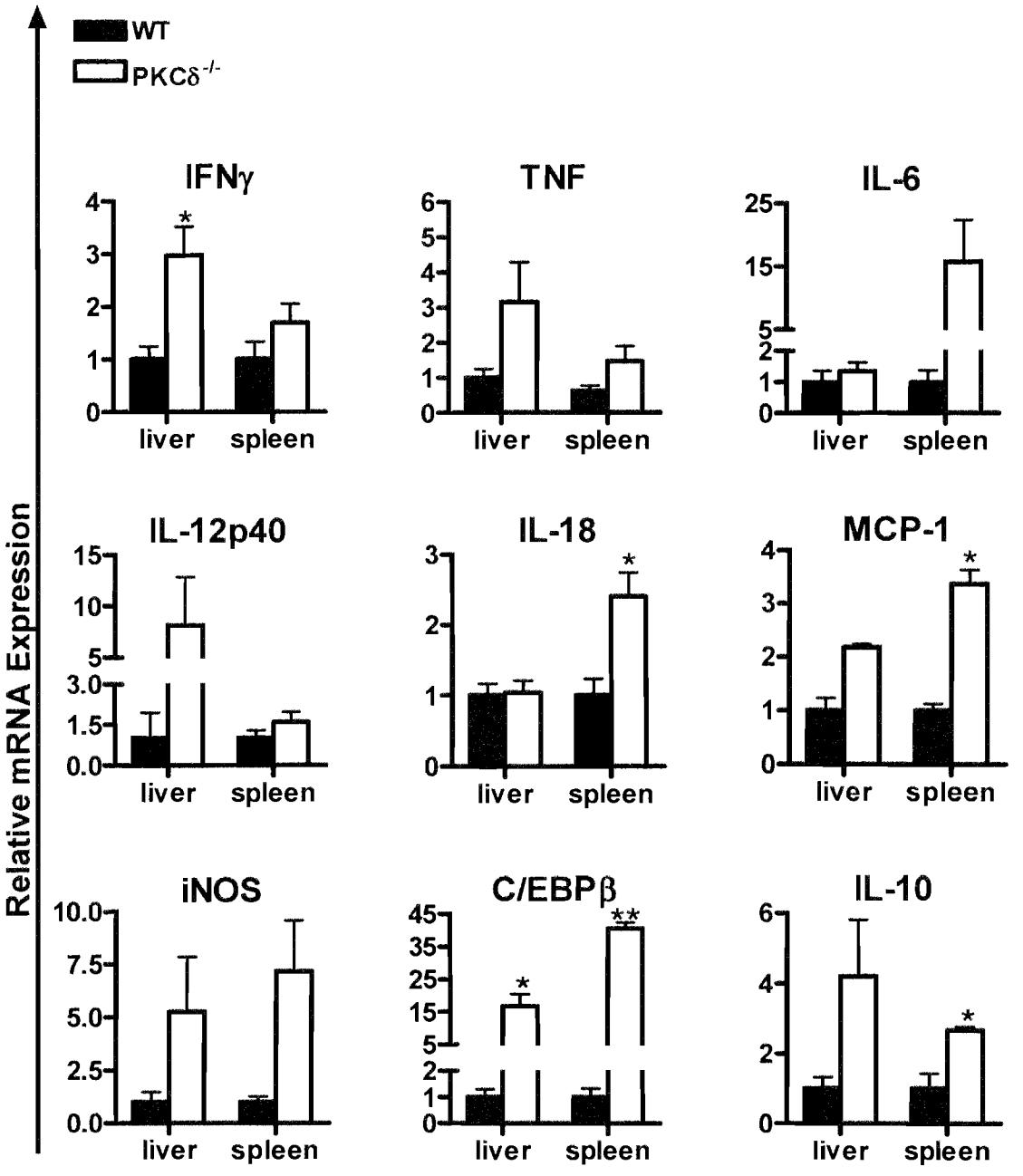


**Figure 9. Efficient induction of pro-inflammatory mediators and iNOS in PKCδ$^{-/-}$mice at 2 days p.i..** Quantitative RT-PCR of pro-inflammatory mediators in livers and spleens of mice at 2 days after *L. monocytogenes* infection with 2 x $10^4$ CFU. Results are representative of two independent experiments (n=5/group). RT-PCR data was normalized to the B2MG housekeeping gene and to the WT average. Data are represented as means ± SEM (* $p<0.05$; ** $p<0.005$).

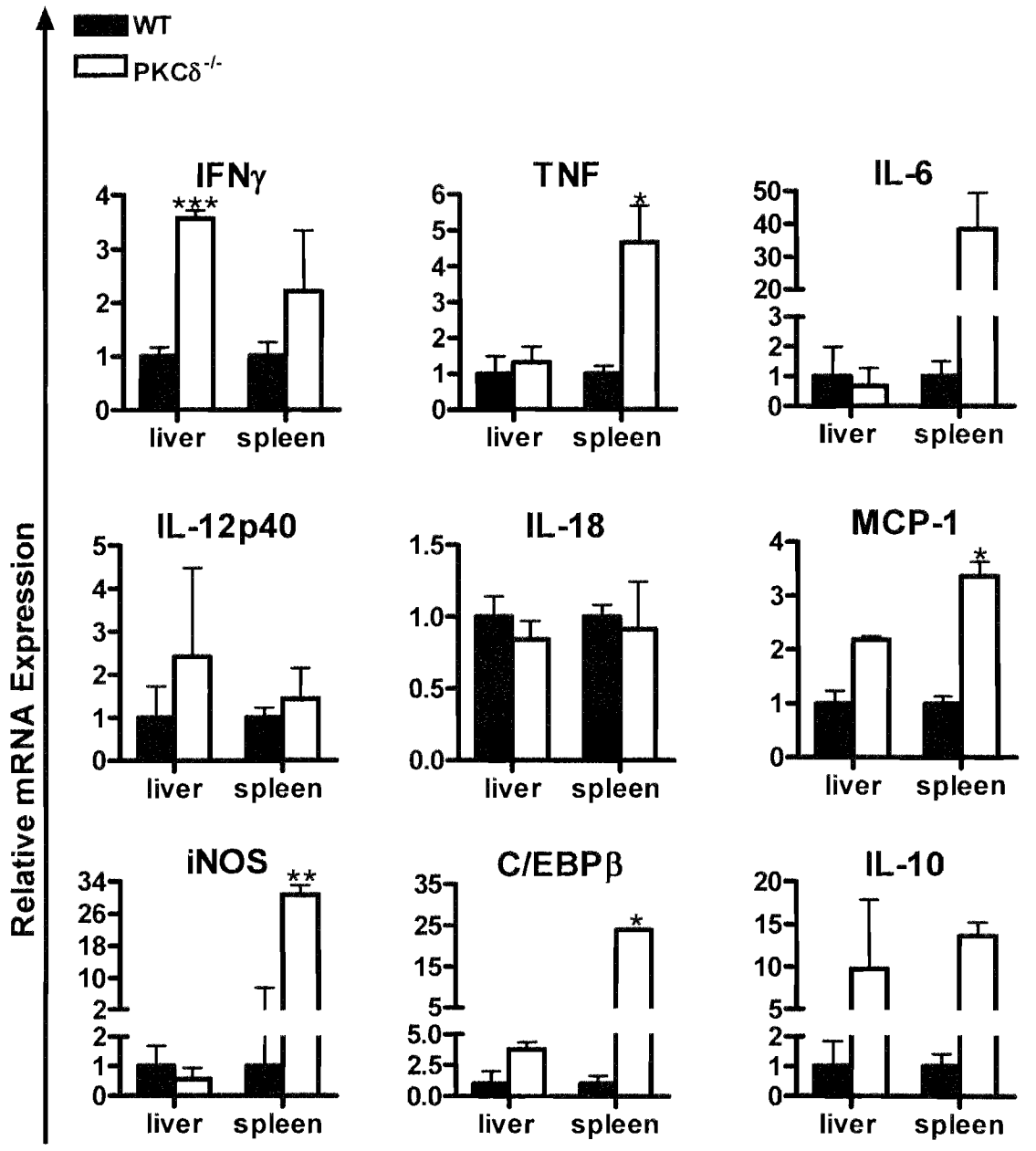


**Figure 10. Efficient induction of pro-inflammatory mediators and iNOS in PKCδ$^{-/-}$mice at 3 days p.i..** Quantitative RT-PCR of pro-inflammatory mediators in livers and spleens of mice at 3 days after *L. monocytogenes* infection with 2 x $10^4$ CFU. Results are representative of two independent experiments (n=5/group). RT-PCR data was normalized to the B2MG housekeeping gene and to the WT average. Data are represented as means ± SEM (* $p<0.05$; ** $p<0.01$; *** $p<0.0001$).

**8. Normal memory response in PKCδ$^{-/-}$ mice following infection**

Clearance of bacilli during secondary *L. monocytogenes* challenge is mediated by protective antigen-specific T cell memory. To determine if immunization of PKCδ$^{-/-}$ mice conferred protection against a subsequent lethal dose of *L. monocytogenes*, PKCδ$^{-/-}$ mice and their control littermates were immunized with a $LD_{50}$ dose of 2 x $10^3$ *L. monocytogenes* CFU. After 2 months, the surviving mice were re-challenged with a secondary lethal dose of 2 x $10^4$ *L. monocytogenes* CFU and the memory response measured by means of bacterial burden in spleen and liver at 2 days after infection. Non-immunized WT and PKCδ$^{+/-}$ control mice efficiently controlled bacterial replication and displayed similar bacterial burden in both organs (Fig. 11). In contrast, non-immunized PKCδ$^{-/-}$ mice displayed uncontrolled bacterial growth with 3 log fold significantly higher CFU in liver and spleen as compared to the controls. Following secondary infection, the bacterial burden decreased by 1-2 log fold in the WT and PKCδ$^{+/-}$ immunized control mice. Surprisingly, immunized PKCδ$^{-/-}$ mice also efficiently cleared this higher dose and the bacterial burden in liver and spleen was reduced to the same level as the WT and PKCδ$^{+/-}$ control mice. Taken together, these results demonstrated that PKCδ was not required for the generation nor for the effector phase of adaptive cell-mediated immune responses to *L. monocytogenes* infection.

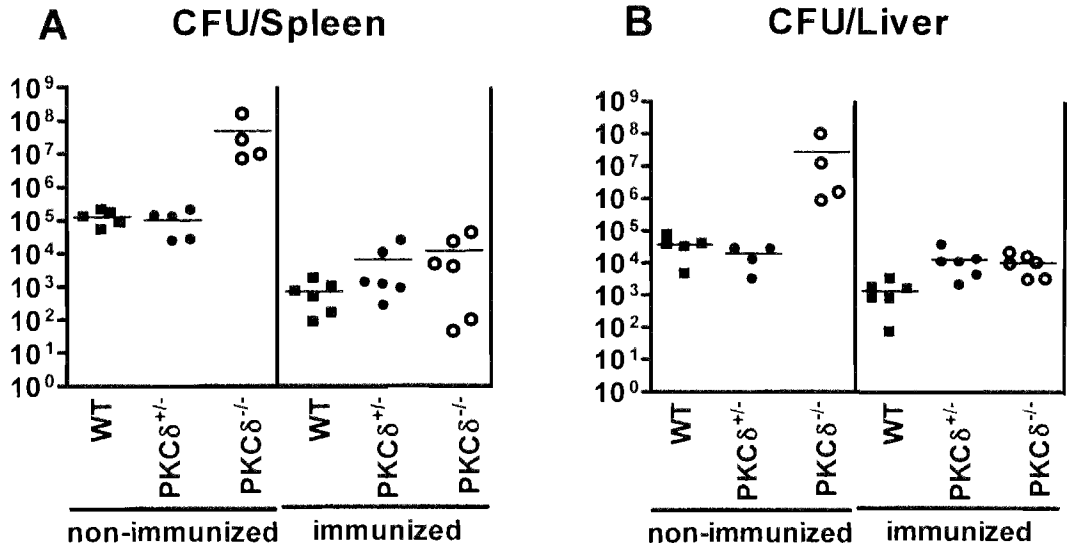


**Figure 11. Normal memory response in PKCδ$^{-/-}$ mice.** Bacterial load in (A) spleen and (B) liver of non-immunized or immunized WT (filled squares), PKCδ$^{+/-}$ (filled circles) and PKCδ$^{-/-}$ (open circles) mice at 2 days p.i. after re-challenge with a lethal dose of 2 x $10^4$ *L. monocytogenes* (n=6/group).

**9. PKCδ$^{-/-}$ are resistant to aerosol *M. tuberculosis* infection.**

To test susceptibility in the absence of PKCδ to another intracellular pathogen, PKCδ$^{-/-}$ mice were infected with *M. tuberculosis* by inhalation. Since C/EBPβ$^{-/-}$ and IFN-γR$^{-/-}$ mice are highly susceptible to *Mycobacterium* (29, 30) they were included as positive controls and as a reference against which to measure the degree of susceptibility in the PKCδ$^{-/-}$ mice. The weight of the mice was monitored weekly and mice sacrificed when they were moribund and had lost ≥ 25% of their initial body weight. The weight of the PKCδ$^{-/-}$ mice increased following infection as compared to their control mice (Fig. 12). In contrast, the C/EBPβ$^{-/-}$ and IFN-γR$^{-/-}$ mice rapidly lost weight after 5 weeks and became cachectic and moribund by 6 and 7 weeks p.i. respectively. The bacterial load in the spleen, liver and lungs of the C/EBPβ$^{-/-}$ and IFN-γR$^{-/-}$ mice was 3 log increased compared to their WT controls (Fig. 13). In contrast, bacterial burden from PKCδ$^{-/-}$ mice were similar to their WT controls at 10 weeks p.i., except for a 1 log increased in the lungs. These data showed that PKCδ was did not play a major role in protection against *Mycobacterium*, since PKCδ$^{-/-}$ mice efficiently controlled *M. tuberculosis infection* as compared to their littermate controls.

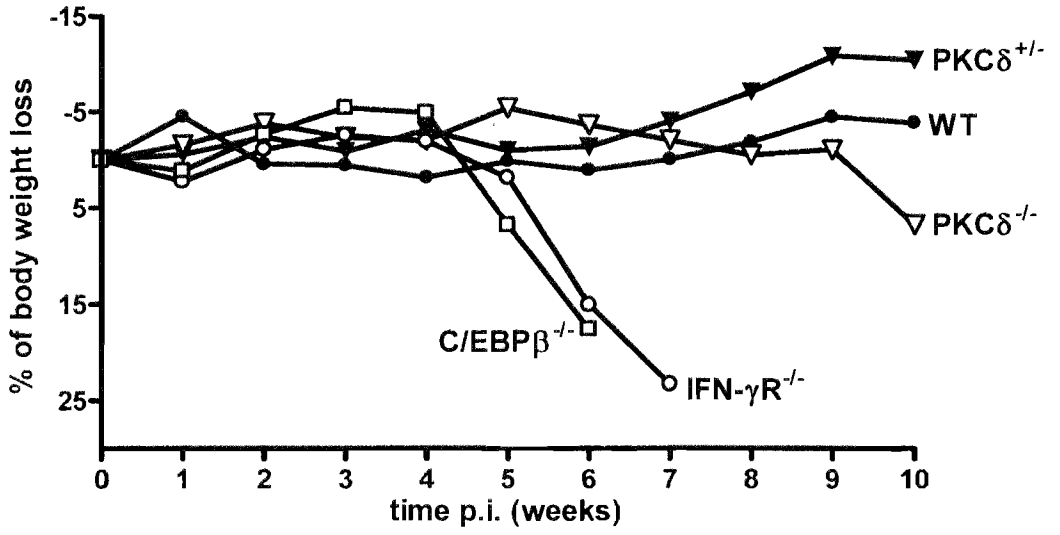


**Figure 12. Percentage body weight loss during *M. tuberculosis* infection.** WT, PKCδ$^{+/-}$, PKCδ$^{-/-}$, IFN-γR$^{-/-}$ and C/EBPβ$^{-/-}$ mice (n=4-6/group) were infected with 100 CFU of *M. tuberculosis* via aerosol. Body weight was monitored weekly and mice were sacrificed once they had lost ≥ 25% of their body weight.

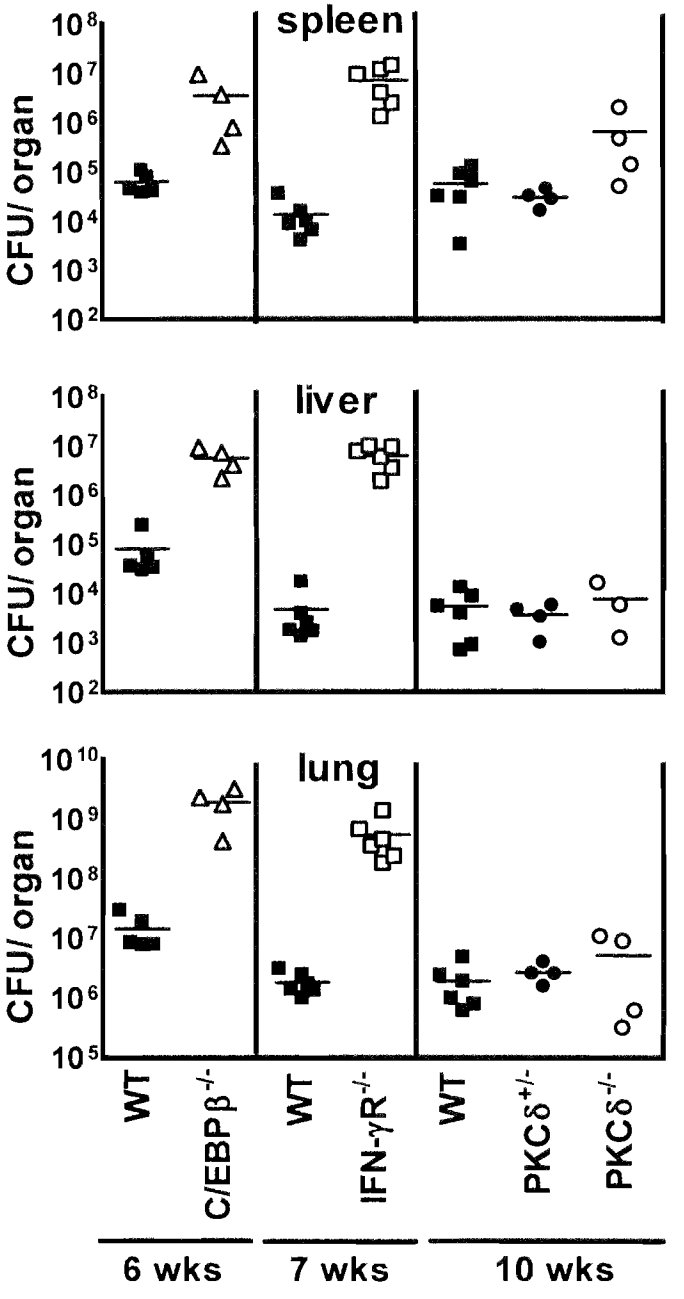


**Figure 13. Resistance to *M. tuberculosis* infection in PKCδ$^{-/-}$ mice.** WT, PKCδ$^{+/-}$, PKCδ$^{-/-}$, IFN-γR$^{-/-}$ and C/EBPβ$^{-/-}$ mice (n=4-6/group) were infected with 100 CFU of *M. tuberculosis* via aerosol. Moribund C/EBPβ$^{-/-}$ and IFN-γR$^{-/-}$ mice were sacrificed at 6 and 7 weeks post infection respectively and their CFUs determined in lung, liver and spleen. WT, PKCδ$^{+/-}$, PKCδ$^{-/-}$ were sacrificed 10 weeks post infection and their bacterial burden was analysed.

**10. Generation and Analysis of a Protein-Protein Interaction Network for PKCδ, Rab5a and G-CSF.**

A systems biology approach was used in order to determine the mechanism whereby PKCδ confined *L. monocytogenes* within macrophage phagosomes. Data from Wadsworth and Goldfine indirectly suggested that PKCδ played a role in promoting listerial escape from the phagosome. In their studies, they showed that inhibition of PKCδ activity by rottlerin, during *L. monocytogenes* infection, resulted in impaired calcium influx into the infected macrophages, which prevented the translocation of PKCβII to early endosomes. Additional experiments blocking PKCβ translocation with hispidin resulted in decreased escape of *L. monocytogenes* from phagosomes. Moreover, pre-treatment of macrophages with calcium channel inhibitors SK&F 96365 and thapsigargin, which block influx of calcium from the extracellular environment or intracellular stores respectively, resulted in 25-30% decreased escape of *L. monocytogenes* from the phagosomes (26). These results therefore indirectly suggested that PKCδ played a role in promoting listerial escape from the phagosome, by facilitating the initial calcium influx into the infected macrophages. Furthermore, additional studies by the same research group showed that LLO and PI-PLC secreted by *L. monocytogenes* during infection induced the activation of host phospholipase C (PLC) and phospholipase D (PLD). Using rottlerin, PKCδ was shown to be responsible for activating PLD resulting in increased escape of the bacilli from the phagosomes, since pre-treatment of the macrophages with the PLD inhibitor, 2, 3-diphosphoglycerate partially inhibited escape from the phagosome (26). PKCδ was therefore considered a detrimental factor during *L. monocytogenes* infections.

However, results of this dissertation indicated that PKCδ played a protective, rather than detrimental role during *L. monocytogenes* infection. PKCδ$^{-/-}$ mice were highly susceptible and displayed increased escape of *L. monocytogenes* from the phagosome. Since phagosomal escape was shown to be dependent on increased cytosolic calcium levels (31), these results suggested that the calcium influx into the infected PKCδ$^{-/-}$ macrophages still took place despite the lack of PKCδ. Other calcium-independent PKC isoforms e.g. PKCε, PKC$\eta$ and PKC$\theta$, may have compensated for the lack PKCδ in the PKCδ$^{-/-}$ macrophages, and stimulated the influx of calcium required for translocation of PKCβII to early endosomes and consequent bacterial escape from phagosomes. If PKCδ did play a detrimental role during infection, the percentage of bacterial escape in the PKCδ$^{-/-}$ macrophages, resulting from the calcium influx compensated for by other PKC isoforms, was expected to be equivalent or slightly reduced as compared to WT macrophages. However, the PKCδ$^{-/-}$ macrophages had 6.5 fold greater

bacterial escape from the phagosomes as compared to WT, suggesting that PKCδ played an additional role other than stimulating inward calcium influxes. For example, PKCδ has been shown to regulate the production of superoxide by phagocyte NADPH oxidase by phosphorylating the enzymes p47phox and p67phox components (17-19). Moreover, since the localized release of superoxide and nitric oxide into the small space of the phagosome was shown to reduce escape of *L. monocytogenes* from the phagosome (32), PKCδ may also function to stimulate the release of superoxide into the phagosome in order to prevent bacterial escape. However, the PKCδ$^{-/-}$ mice displayed higher susceptibility to *L. monocytogenes* than mice deficient for p47phox (p47phox$^{-/-}$) (33), gp91phox (gp91phox$^{-/-}$) (34) and doubly deficient for iNOS and gp91phox (gp91 phox$^{-/-}$/iNOS$^{-/-}$) (35). These results suggested that PKCδ played an additional protective role during infection other than stimulating the production of superoxide (17-19). Experiments by Pizarro-Cerda et al (36) using C/EBPβ$^{-/-}$ mice infected with *B abortus*, demonstrated that C/EBPβ promoted endocytosis and membrane fusion between endosomes and pathogen-containing phagosomes in a G-CSF-dependent manner (36). In these studies, C/EBPβ$^{-/-}$ mice had impaired induction of G-CSF and impaired bacterial killing, however, addition of the G-CSF restored endocytosis and bactericidal activity. C/EBPβ was highly up-regulated in the PKCδ$^{-/-}$ macrophages during *L. monocytogenes* infection, thereby suggesting that PKCδ may act downstream of C/EBPβ in the signaling pathway. It therefore seemed promising that PKCδ may be involved in C/EBPβ mediated regulation of endocytosis, phagosome maturation and consequent bacterial killing. A protein-protein network was created using protein-protein interaction data of PKCδ, G-CSF and Rab5a. All protein-protein interaction data was taken from the BIND, Entrez Gene and HPRD databases which represent experimentally proven interactions. Although no direct interaction between Rab5a and PKCδ has been documented in any of the public databases to date, this interaction can not be discounted. The Cytoscape software programme was used to visualize and analyze the interaction networks (37). The complete network showing all first, second and third neighbour interactions, was very large and complex and the links between PKCδ, G-CSF and Rab5a were unclear (Fig. 14). Therefore only the first and second neighbours and their edges were selected for Rab5a, G-CSF and PKCδ proteins (Figure 15). Although the network is still complex, it can be seen that all the interactions in the signalling network converge on four proteins, RAB GTPase binding effector protein 1 (Rabep1), Angiotensin receptor 1 (Agtr1a), RAS p21 protein activator 1 (Rasa1) and Tuberous sclerosis 2 (Tsc2), which interact with Rab5a directly (Figure 15 A, orange circles). Selecting only those interactions with the shortest "route" linking PKCδ and G-CSF to Rab5a, the

relationship between these players became clearer (Fig. 15 B, C). PKCδ was found to interact directly with "intermediate" proteins such as protein tyrosine kinase 2 beta (Ptk2b), guanine nucleotide binding protein, beta 2, related sequence 1 (Gnb2rs1), Insulin-like growth factor 1 receptor (Igf1r), Insulin receptor (Insr), Rous sarcoma oncogene (Src), Guanine nucleotide binding protein alpha 13 (Gna13) or 14-3-3 gamma (Ywhag), which themselves interacted with the proteins (Rabep1, Agtr1a, Rasa1 and Tsc2) that bound to directly Rab5a. G-CSF interacted only with its receptor, G-CSFR which itself signalled via an additional "layer" of intermediate proteins to Rasa1 and Agtr1a in order to signal to Rab5a. G-CSFR interacted with Spleen tyrosine kinase (Syk), Yamaguchi sarcoma viral oncogene (Lyn), Protein tyrosine phosphatase, non-receptor type 11 (Ptpn11) and JAK1, which in turn interacted with either Hemopoietic cell kinase (Hck), Growth factor receptor bound protein 2 (Grb2), Ptk2b, Src, Insr, Gnb2rs1 or Igf1r to signal to Rasa1, which in turn bound directly to Rab5a. The most direct route for G-CSFR to Rab5a was via JAK2 which interacted with Agtr1a. No direct interaction was found between PKCδ and G-CSF or G-CSFR. However, PKCδ was found to interact with Src homology 2 domain-containing transforming protein C1 (Shc1) which binds G-CSFR (Fig. 15 A). Moreover, PKCδ interacted with several of the "intermediate" proteins involved in G-CSFR interactions e.g. Ptpn11, Insulin receptor substrate 1 (Irs1), Interleukin 6 signal transducer (IL6st), STAT3 and Mucin 1 (Muc1). In order to obtain a clearer picture of which protein interactions were important during *L. monocytogenes* infection, the literature for each interaction was profiled.

Rabep1 has been shown to bind directly to Rab5a via protein-protein interactions with Rabgef1 and the resulting Rabep1:Rabgef1 complex shown to be essential for mediating Rab5a functions (38). Rabep1 is essential for membrane docking and fusion (39), whereas Rabgef1 functions as a specific guanine nucleotide exchange factor for Rab5 and exchanges GDP for GTP (38). Furthermore, Rabgef1 was shown to interact with Ywhag, a 14-3-3 protein which is phosphorylated by PKCδ (40). Ywhag is the gamma isoform of the 14-3-3 family of proteins which are involved in the regulation of most cellular processes, including several metabolic pathways, redox-regulation, transcription, RNA processing, protein synthesis, protein folding and degradation, cell cycle, cytoskeletal organization and cellular trafficking (41). Since 14-3-3 proteins have been shown to acts as "scaffolds" for multi-protein complexes, Ywhag may function to stabilize the Rabep1:Rabgef1 complex, (42). Furthermore, the activity of 14-3-3 proteins is controlled by phosphorylation, which promotes binding to their protein partners (41). Since PKCδ has been shown to phosphorylate Ywhag

(40), it may function to promote the formation the Rabep1:Rabgef1 complex, thereby enhancing Rab5a activity and consequent phagosome maturation, phago-lysosome fusion and bacterial killing. Similarly, the interaction between agonist-activated Agtr1 and Rab5a was shown to promote Rab5a GTP binding and vesicular fusion (43). PKCδ was found to phosphorylate and activate Gna13 (44), an Agtr1 agonist (45). PKCδ may therefore promote Rab5a activity, by driving Agtr1 activation via phosphorylation of Gna13. In contrast, PKCδ may down-regulate the activities of Rasa1 and Tsc2, as both these proteins have been shown to inhibit Rab5a activity. Rasa1 was shown to suppress RAS signalling by stimulating its intrinsic GTPase activity resulting in the inactive GDP-bound form of RAS. The suppressing activity of Rasa1 was controlled by tyrosine phosphorylation or association with tyrosine phosphorylated proteins (46). Since Rab5a is a Ras related protein, its interaction with Rasa1 may promote GTP hydrolysis resulting in suppression of Rab5a activity. To counteract this Rab5a suppressive action, PKCδ may phosphorylate Rasa1 interacting proteins such as Ptk2b, Gnbrs1, Igf1r, Insr, Src, Hck and Grb2, which once phosphorylated may bind to Rasa1 and inhibit its activity. Similarly, Tsc2 has been shown to function as a Rab5 GAP *in vivo* to negatively regulate Rab5-GTP activity in endocytosis (47). Tsc2 interacted with Rab5a via Rabep1 and specifically stimulated the built-in GTPase activity of Rab5a resulting in inactive GDP-bound Rab5a (47). The suppressive activity of Tsc2 was controlled by the binding of 14-3-3 proteins (48) including Ywhag (49). Furthermore, PKCδ has been shown to phosphorylate Ywhag (40), which promoted its binding to its target proteins e.g. Tsc2 (41). PKCδ may therefore down-regulate the Rab5a suppressive function of Tsc2 by phosphorylating Ywhag and thereby promote its binding to Tsc2.

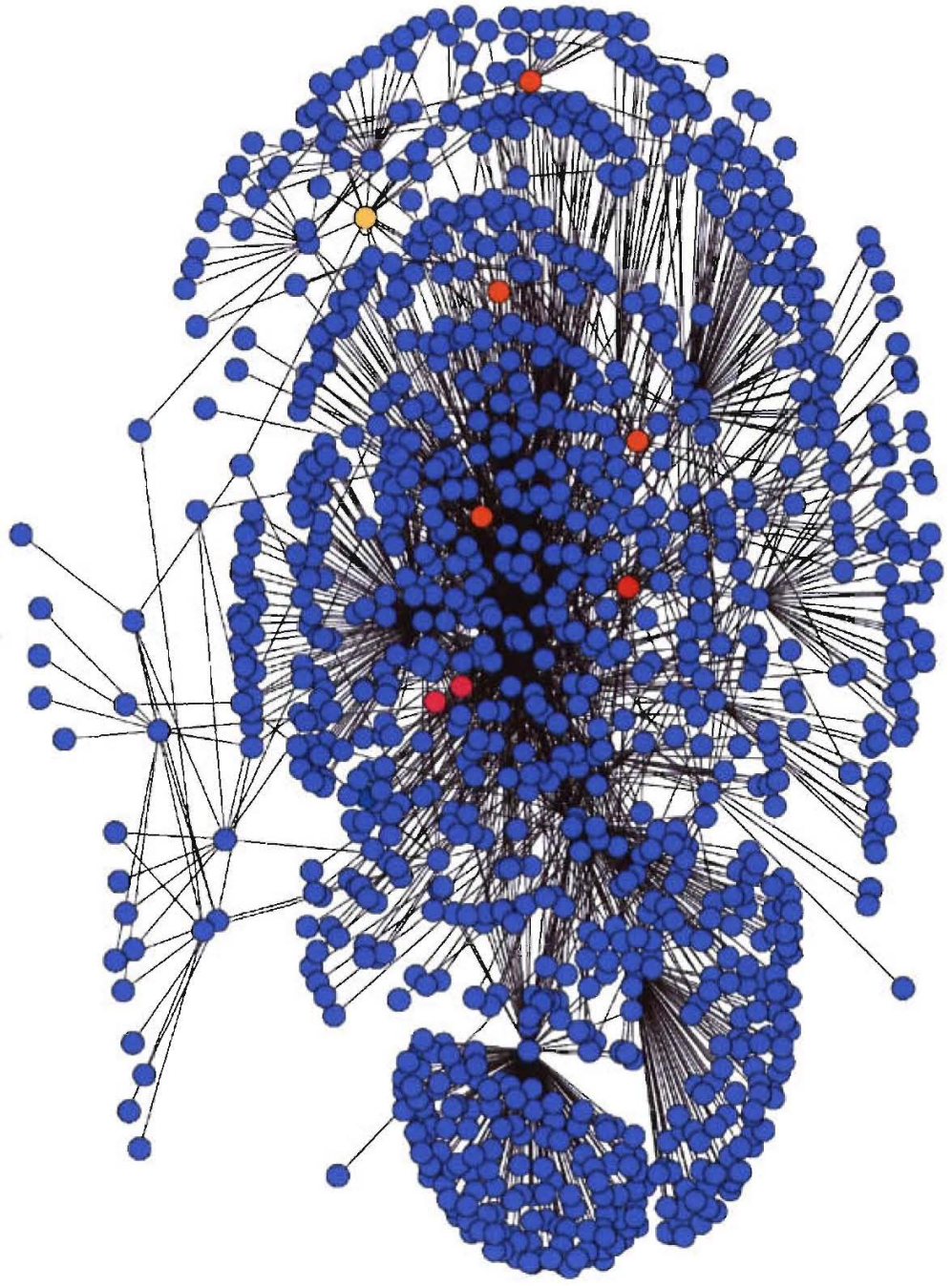

**Figure 14. Protein-Protein Interactions between PKCδ, G-CSF and Rab5a.** Shown are protein-protein interactions between Rab5a (yellow), PKCδ (red), G-CSF (pink), G-CSFR (pink) and their first, second and third neighbour interacting proteins (blue). Proteins are displayed as coloured circles and protein-protein interactions as black lines. Proteins in orange interact directly with Rab5a.

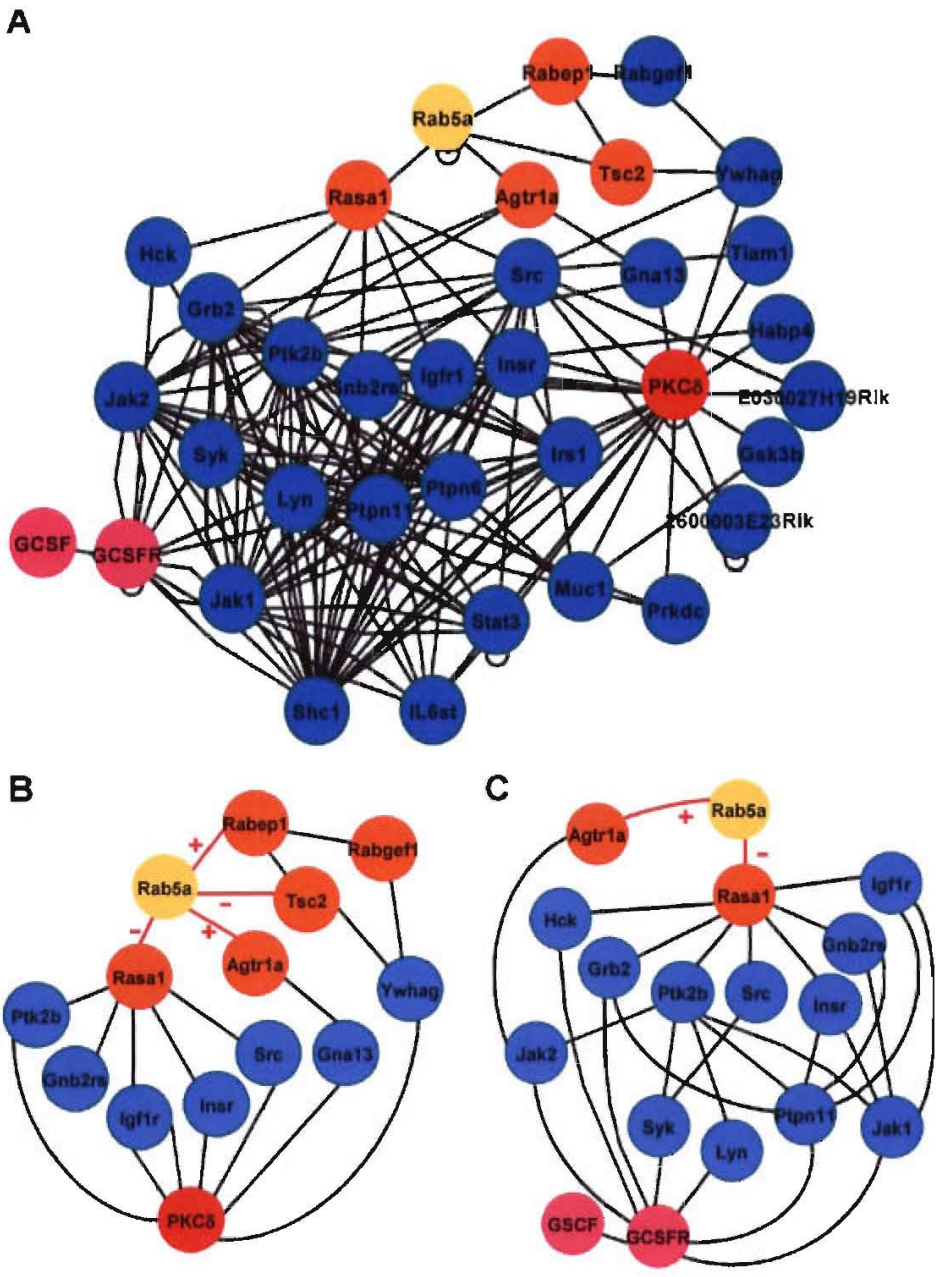


**Figure 15. Putative mechanism of PKCδ and G-CSF regulation of Rab5a activity.** Shown are protein-protein interaction networks of (A) Rab5a, PKCδ, G-CSF and their first and second neighbour interacting proteins. (B) Putative pathway whereby PKCδ (red) signals to Rab5a (yellow) via Rasa1, Agtr1a, Tsc2 and Rabep1 (orange). (C) Putative pathway whereby G-CSF (pink) signals through its receptor, G-CSFR (pink) to Rab5a (yellow) via protein-protein interactions through Rasa1 and Agtr1a (orange circles). Proteins are displayed as coloured circles and interactions as lines. Red lines indicate the direct interactions with Rab5a that either activate (+) or suppress (-) Rab5a activity.

**11. Putative Mechanism whereby PKCδ confines *L. monocytogenes* within phagosomes**

Based on the above protein interactions, literature and hypotheses, PKCδ may therefore indirectly promote Rab5a activity, phagosome maturation, phago-lysosome fusion and subsequent bacterial killing, by promoting the Rab5a-activating functions of Agtr1a and Rabgef1 and by inhibiting the Rab5a-supressing functions of Tsc2 and Rasa1. The following mechanism whereby PKCδ confines *L. monocytogenes* with the phagosome is therefore proposed (Fig. 16 A). During *L. monocytogenes* infection, the secretion of pro-inflammatory mediators such as IFN-γ, IL-1 and IL-6 induces the expression of C/EBPβ (50). Moreover, stimuli such as pro-inflammatory cytokines and LPS activate C/EBPβ by promoting phosphorylation of its transactivation domain (51). Once activated C/EBPβ, translocates to the nucleus where it stimulates the expression of genes involved in oxidative bacterial killing (e.g. iNOS or PKCδ) and/or genes involved in phago-lysosome mediated bactericidal activity e.g. Rab5a, Agtr1a and Rabgef1. Promoter analysis of Agtr1a, G-CSF, iNOS, PKCδ, Rab5a, Rabep1, Rabgef1, Rasa1 and Tsc2 genes revealed that they all contained putative binding sites for C/EBPβ or transcription factors that interacted with C/EBPβ e.g. NF-κB (Fig. 16 B).

In this hypothesis, PKCδ is involved mediating bacterial killing via both the oxidative and phago-lysosome pathways. PKCδ has been previously shown to regulate the activation of phagocyte NADPH oxidase, the multi-protein enzyme complex that generates superoxide (17, 18). However, its hypothesized role in the phago-lysosome pathway is based on (1) the results of this thesis where it was shown to play a crucial role in confining the *L. monocytogenes* within the phagosome, and (2) the hypotheses generated from analysis of the above protein-protein interaction network. In the proposed mechanism, PKCδ indirectly promotes the activation of Rab5a activity by regulating two opposite pathways (Fig. 16 A). The first pathway involves PKCδ phosphorylating the Gnai3 and Ywhag proteins, which in turn enhance and activate Agtr1a and Rabgef1. Once activated, Agtr1a and Rabgef1 subsequently interact directly with Rab5a bound at the phagosome membrane and promote the exchange of Rab5a-GDP for GTP. Upon binding GTP, Rab5a becomes activated and is then able to promote the recruitment iNOS and phagocyte NAPDH oxidase resulting in the localized production of nitric oxide and superoxide into the phagosome (32). Moreover, activated Rab5a promotes phagosome maturation, phago-lysosome fusion and subsequent bacterial killing. The second pathway involves PKCδ indirectly inhibiting the Rab5a-supressing activities of Tsc2 and Rasa1 via its phosphorylation of Ywhag, Ptk2b, Gnb2rs1, Igf1r, Insr, and Src. The binding of phosphorylated Ywhag to Tsc2 and phosphorylated Ptk2b, Gnb2rs1,

Igf1r, Insr, and Src to Rasa1, inhibits their Rab5a suppressing activities. PKCδ therefore plays a central role in synergizing both these pathways in order to promote Rab5a activity and consequent phago-lysosome fusion and bacterial killing.

The gene expression data from the infected WT C/EBPβ$^{-/-}$ macrophages was compared to the proposed mechanism to determine if there was any correlation. Since promoter analysis showed that Agtr1a, Rabgef1, G-CSF, Rasa1, PKCδ, Rab5a, Tsc2 and Rabep1 contained putative C/EBPβ binding sites in their promoters (Fig. 16 B), it was natural to expect that induction of these putative C/EBPβ target genes would be decreased in the infected C/EBPβ$^{-/-}$ macrophages as compared to WT. This was indeed observed for several of the target genes e.g. Rabgef1, Agtr1a, G-CSF, however, Rasa1, Tsc2, PKCδ, Rab5a and Rabep1 were up-regulated (Fig. 16 C). The up-regulation of these genes in the absence of C/EBPβ may be due to compensation by other C/EBP transcription factor family members e.g. C/EBPα, C/EBPδ, C/EBPε or due to alleviation of transcriptional repression by C/EBPβ. Alternative splicing of C/EBPβ mRNA was found to generate long and short forms of the C/EBPβ protein, which had opposite functions: the longer form activated transcription whereas the shorter form, which lacked a trans-activating domain, repressed transcription (52). An example of compensation by other C/EBP family members is demonstrated by the efficient induction of iNOS in the infected C/EBPβ$^{-/-}$ macrophages, even though iNOS has an experimentally proven C/EBPβ binding site in its promoter. Furthermore, the up-regulation of protective factors such as Rab5a, Rabep1 and PKCδ may have been stimulated by the significantly higher bacterial load in the C/EBPβ$^{-/-}$ macrophages. In addition, the up-regulation of the Rasa1 and Tsc2 may have been induced by *L. monocytogenes* itself in order to prevent phagosome maturation.

According to the proposed mechanism (Fig 16 A), despite the enhanced induction of Rab5a, Rabep1 and PKCδ in the C/EBPβ$^{-/-}$ macrophages, PKCδ could not promote the exchange of inactive Rab5a-GDP for active Rab5a-GTP at the phagosome membrane because of the impaired production Agtr1a and Rabgef1 proteins due to the absence of C/EBPβ. In the infected C/EBPβ$^{-/-}$ macrophages, Rabgef1 was significantly down-regulated by 0.76 fold and Agtr1a by 0.71 fold. Moreover, Tsc2 and Rasa1 were up-regulated 1.24 and 1.1 fold respectively in the C/EBPβ$^{-/-}$ macrophages. The consequent increased Rab5a-supressing activity of Tsc2 and Rasa1 may have been be inhibited by PKCδ, which was also up-regulated

by 1.13 fold in the C/EBPβ$^{-/-}$ macrophages. However, although PKCδ could block the Rab5a suppressing activity of Tsc2 and Rasa1, it still could not promote activation of Rab5a via exchange of GDP for GTP. The phagosome maturation and phago-lysosome fusion pathway therefore came to a halt at the "activation of Rab-GDP" step and consequently resulted in increased escape of bacilli from the phagosome and consequent bacterial overgrowth.

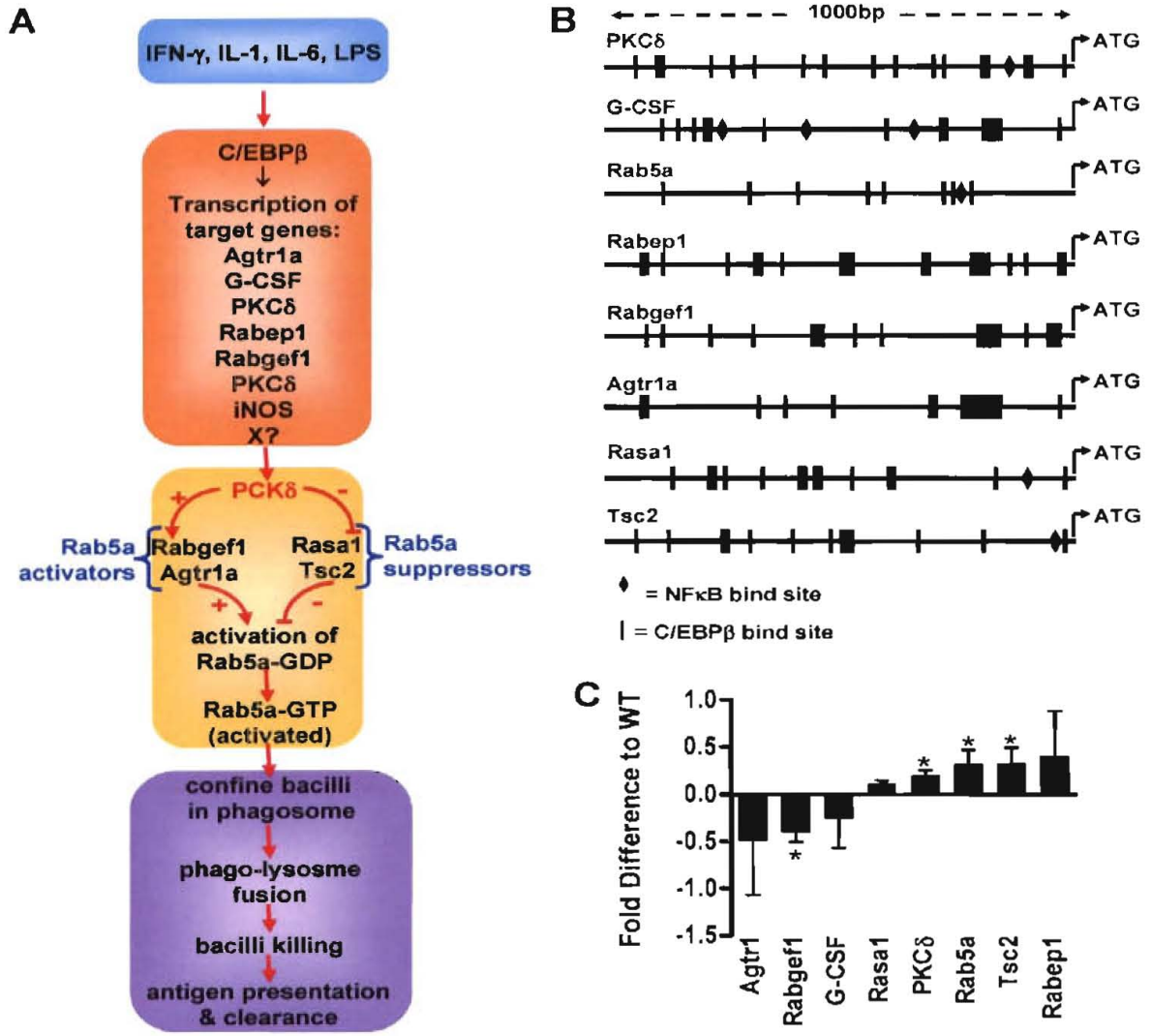


**Figure 16.** (A) Proposed mechanism whereby PKCδ confines *L. monocytogenes* with the macrophage phagosome. (B) Promoters of Rab5a regulating proteins containing putative C/EBPβ ( | ) and/or NF-κB (♦) binding sites; ATG denotes the transcriptional start site. (C) Differential regulation of putative Rab5a regulatory proteins in C/EBPβ$^{-/-}$ macrophages infected with *L. monocytogenes*. Data is relative to WT controls and are the averages and SEM of 4 independent biological experiments at 4 hours p.i. (* $p<0.05$ based on permutation and Bonferroni Correction).

## DISCUSSION

Early control of *L. monocytogenes* infection requires the innate immune response dominated by neutrophils and macrophages, which are the major cells responsible for killing of *L. monocytogenes* (53-55). IFN-γ and TNF are essential for full macrophage activation (56, 57), resulting in enhanced production of cytokines, chemokines and bactericidal molecules such as ROI and RNI. Several *in vivo* infection studies using mice iNOS$^{-/-}$, gp47phox$^{-/-}$, gp91phox$^{-/-}$ and gp91 $^{phox\ -/-}$/iNOS$^{-/-}$ mice showed that bacterial killing took place despite the lack of ROI and RNI (33-35, 58, 59), suggesting that macrophages have an alternative killing mechanism independent of ROI and RNI. This hypothesis was underscored by studies using mice deficient for genes such as IFN-γ (60, 61), IFN-γR (28, 60), ICSBP (62), IRF2 (62), RelB (63), TNFRp55 (64, 65), and C/EBPβ (7). All of these mice were highly susceptible to *L. monocytogenes* despite full macrophage activation and production of pro-inflammatory mediators, ROI and RNI. This hypothetical unknown killing pathway is most likely driven by IFN-γ and TNF, with the most downstream effector being C/EBPβ, since C/EBPβ$^{-/-}$ macrophages expressed normal levels of IFN-γ and TNF (7). Since the effector genes involved in this unknown mechanism would most likely be downstream of C/EBPβ, the transcriptional responses of *L. monocytogenes*-infected WT and C/EBPβ$^{-/-}$ macrophages were compared in order to identify the effector genes.

The transcriptional response of IFN-γ-activated macrophages from WT and C/EBPβ$^{-/-}$ mice infected with *L. monocytogenes* was profiled at 4 hours p.i.. PKCδ was selected as the prime candidate gene because it has been shown to be involved in several critical immune signalling pathways (8-10, 12-19) and may be transcriptionally regulated by C/EBPβ as revealed by promoter analysis. Moreover, studies by Wadsworth and Goldfine indirectly suggested that PKCδ played a role in promoting listerial escape from the phagosome by facilitating the initial calcium influx into the cell required for translocation to early endosomes (25) and by activating host phospholipase D (26). In addition, they showed that bacterial escape from the phagosomes was dependent on increased cytosolic calcium levels (26). These results therefore suggested that PKCδ played a role in promoting listerial escape from the phagosome, by facilitating the initial calcium influx into the infected macrophages. In addition, B cells from PKCδ$^{-/-}$ mice stimulated with LPS showed increased binding of C/EBPβ to DNA due to alleviation of PKCδ phosphorylation of C/EBPβ at a serine residue within the DNA binding domain that results in decreased DNA binding activity (27). Furthermore, PKCδ was up-

regulated in *L. monocytogenes*-infected C/EBPβ$^{-/-}$ macrophages as compared to WT, as shown by microarray and confirmed by RT-PCR. It was therefore postulated that PKCδ was detrimental to the host during *L. monocytogenes* infections since in addition to promoting phagosomal escape of *L. monocytogenes* (25, 26) it also inhibited the transcriptional activity of C/EBPβ (27), which may also result in increased phagosomal escape and impaired listericidal activity as observed in C/EBPβ$^{-/-}$ mice (7).

To test this hypothesis, activated PKCδ$^{-/-}$ macrophages were infected with *L. monocytogenes* and bacterial growth and phagosomal escape measured. From the hypothesis, it was expected that PKCδ$^{-/-}$ macrophages should have decreased levels of phagosomal escape and bacterial load due to enhanced C/EBPβ transcription of effector genes in the absence of PKCδ (27). Surprisingly, PKCδ$^{-/-}$ macrophages had increased bacterial escape from phagosome and uncontrolled bacterial growth, despite enhanced production of iNOS and pro-inflammatory cytokines in response to the high bacterial load. This was unexpected since it opposed *in vitro* data by Wadsworth and Goldfine (25) which indirectly suggested that PKCδ promoted phagosomal escape. This divergence may have resulted from their use of rottlerin at a concentration (25μM) which has been shown to non-specifically inhibit several other kinases (1, 2). Their observations may have been compounded by the non-specific inhibition of other kinases by rottlerin. In this thesis, using PKCδ$^{-/-}$ macrophages, it has been clearly demonstrated that PKCδ is critical for confining *L. monocytogenes* within the phagosome. Moreover, despite having significantly higher expression of C/EBPβ and its expected enhanced transcriptional activity in the absence of PKCδ (27), the PKCδ$^{-/-}$ macrophages were unable to control the growth of *L. monocytogenes*. Data from this thesis clearly shows that PKCδ is protective rather than detrimental during innate immunity to *L. monocytogenes*. Furthermore, PKCδ did not appear to play a critical role in innate immune responses against *M. tuberculosis*, an intracellular bacterium that preferentially resides within the phagosome. PKCδ may therefore be a target that is negatively modulated by *L. monocytogenes* to facilitate its own escape and survival.

The most important finding of this dissertation was that PKCδ was indispensable for confinement of *L. monocytogenes* within the phagosome, since no other PKC isoform compensated for it in the PKCδ$^{-/-}$ macrophages. The enhanced listerial escape and impaired listericidal activity resulted in uncontrolled bacterial growth and dissemination of *L. monocytogenes*, which ultimately led to early death of the PKCδ$^{-/-}$ mice. The increased susceptibility of the PKCδ$^{-/-}$mice was not due to defective induction of pro-inflammatory mediators, since *in vitro* and *ex vivo* quantitation showed that they produced significantly higher levels of nitrite, MCP-1, IFN-γ, TNF, IL-12 and IL-6 than the WT mice in response to the high bacterial load. As expected, the inflammatory response was counter-balanced by the production of IL-10 by the activated macrophages with kinetics similar to that for the pro-inflammatory mediators (66, 67). Furthermore, the massive recruitment of inflammatory cells into the peritoneal cavity and abundant granulomas of PKCδ$^{-/-}$mice indicated that impaired resistance to *L. monocytogenes* was not due to defects in chemokine attraction. However, the number of recruited activated macrophages was 10% lower in the PKCδ$^{-/-}$mice. Furthermore, despite having recruited 30% more neutrophils, which are essential for killing *L. monocytogenes* (53-55), the PKCδ$^{-/-}$mice were still unable to kill and clear the *L. monocytogenes* bacilli, as shown by the significantly increased bacterial burden and histopathology in their spleens and livers. In addition, PKCδ was not required for the generation or for the effector phase of adaptive cell-mediated immune responses to *L. monocytogenes* infection, since immunized PKCδ$^{-/-}$ were able to kill and clear a lethal dose of *L. monocytogenes* as efficiently as the WT controls. PKCδ is therefore a critical component of the innate immune response and is critical for confinement of *L. monocytogenes* within the phagosome. Furthermore, data from this dissertation suggests that PKCδ is involved in similar unknown listericidal mechanism that is independent of iNOS and pro-inflammatory cytokines, that was first observed in IFN-γ$^{-/-}$, TNFRp55$^{-/-}$, ICSBP$^{-/-}$ and C/EBPβ$^{-/-}$ mice.

The key questions arising from this study include (i) what is the mechanism whereby PKCδ confines *L. monocytogenes* within phagosomes, (ii) is PKCδ part of the unknown listericidal mechanism that is independent of RNI and ROI, and if so (iii) where does it fit in this yet undefined pathway? Since phagosomal escape was shown to be dependent on increased cytosolic calcium levels (31) and the PKCδ$^{-/-}$ macrophages had 6.5 fold increased bacterial escape from the phagosome, this indicated that calcium influx into the PKCδ$^{-/-}$ macrophages occurred independently of PKCδ. Moreover, the significantly increased rate of bacterial

escape from the phagosome and higher bacterial load in the PKCδ$^{-/-}$ macrophages, suggested that PKCδ played an additional role other than stimulating inward calcium influxes. Therefore investigation into the interaction between PKCδ and calcium channels was not pursued. Instead, the role of PKCδ within the milieu of the phagosome was focussed upon, since this was the "site of action" where its function to confine the bacilli was effected.

Confinement of bacteria within the phagosome has been shown to be dependent on active GTP-bound Rab5a (68) and the localized release of nitric oxide and superoxide into the phagosomal space (32, 69). However, the actual mechanisms of how this is achieved are not fully elucidated. Active Rab5a promotes phagosome maturation, phago-lysosome fusion and consequent bacterial killing by digestion with lytic enzymes, whereas the release of nitric oxide and superoxide into the small space of the phagosome results in fatal oxidative damage to the bacilli (53-55). Several studies have shown that RNI and ROI are important but not essential for bacterial killing (33-35). Data in this dissertation corroborate these studies, since PKCδ$^{-/-}$ mice were unable to kill and clear the *L. monocytogenes* infection, despite enhanced iNOS production. Since PKCδ has been shown to be important for superoxide production by phagocyte oxidase (17-19), it can be argued that the increased susceptibility of PKCδ$^{-/-}$ mice to *L. monocytogenes* may be due to decreased production of superoxide. However, several lines of evidence suggest that this is not the case. PKCδ$^{-/-}$ mice had a much higher degree of susceptibility to *L. monocytogenes* than p47phox$^{-/-}$ and gp91phox$^{-/-}$ mice: The $LD_{50}$ dose for p47phox$^{-/-}$ mice was only 1 log fold lower than their WT controls (33), whereas for the PKCδ$^{-/-}$ mice it was 2 log fold lower. Similarly, at 2 days p.i., the bacterial burden in the liver and spleen of gp91phox$^{-/-}$ mice were only 1 log fold higher than in the WT. In contrast, the PKCδ$^{-/-}$ mice had 3 log fold higher CFU in the liver and spleen compared to WT controls. In addition, gp91phox$^{-/-}$ mice displayed heightened susceptibility only during the first 2 days of *L. monocytogenes* infection and recovered by day 6. PKCδ$^{-/-}$ mice, on the other hand, were highly susceptible and died by day 3 p.i. (34). These data therefore suggested that PKCδ plays an additional role during *L. monocytogenes* infection, other than stimulating the production of superoxide.

The PKCδ$^{-/-}$ mice were highly susceptible to *L. monocytogenes*, but not to the same extent as observed for extremely susceptible IFN-γR$^{-/-}$, C/EBPβ$^{-/-}$, TNFRp55$^{-/-}$ and ICSBP$^{-/-}$ mice which had $LD_{50}$ doses greater than 3 log fold lower than their WT controls (7, 28, 33, 62). However, the phenotype of PKCδ$^{-/-}$ mice was similar to that observed in C/EBPβ$^{-/-}$ mice, with respect to enhanced bacterial growth and escape despite efficient induction of IFN-γ , TNF and iNOS

(7). It was therefore tempting to speculate that PKCδ may be directly or indirectly involved in the unknown RNI/ROI-independent killing mechanism that was first observed in the IFN-γR$^{-/-}$, TNFRp55$^{-/-}$, ICSBP$^{-/-}$ and C/EBPβ$^{-/-}$ mice (7, 28, 33, 62). Levels of PKCδ were decreased in resting C/EBPβ$^{-/-}$ macrophages as compared to WT, which suggested that it may require C/EBPβ for its expression. Indeed, promoter analyses identified a putative NF-κB and several C/EBPβ binding sites in the promoter of the PKCδ gene. PKCδ may therefore be a direct transcriptional target of C/EBPβ through its C/EBPβ binding sites or an indirect target via its NF-κB binding site, since C/EBPβ interacts with NF-κB subunits p50 (70) and p65 (71). However, PKCδ was efficiently induced by *L. monocytogenes* in activated and non-activated C/EBPβ$^{-/-}$ macrophages. This may be due to the alleviation of transcriptional repression by C/EBPβ, which has been shown to either induce or repress transcription (72, 73) of its target genes. However, since both PKCδ and C/EBPβ are essential for innate immunity to *L. monocytogenes*, it is more likely that other related C/EBP family members transcriptionally compensated for the lack of C/EBPβ during *L. monocytogenes* infection in the C/EBPβ$^{-/-}$ macrophages.

A systems biology approach was used to investigate the mechanism whereby PKCδ confined *L. monocytogenes* within macrophage phagosomes. It was hypothesized that PKCδ may achieve this acting in synergy with G-CSF to promote C/EBPβ mediated regulation of phagosome maturation and phago-lysosome fusion (36). Analysis of the protein-protein interaction network generated the hypothesis that PKCδ indirectly promoted Rab5a activity, phagosome maturation, phago-lysosome fusion and subsequent bacterial killing, by promoting the Rab5a-activating functions of Agtr1a and Rabgef1 and by inhibiting the Rab5a-supressing functions of Tsc2 and Rasa1. Moreover, the microarray gene expression data correlated with the proposed mechanism, since the Rab5a-activating Agtr1a and Rabgef1 were down-regulated in the C/EBPβ$^{-/-}$ macrophages as compared to WT, whereas the Rab5a-supressing Tsc2 and Rasa1 proteins were up-regulated. Although the increased levels of PKCδ may have compensated and repressed the enhanced Rab5a-supressing activities of Rasa1 and Tsc2, it was not able to promote Rab5a activation due to impaired production Agtr1a and Rabgef1 proteins. Therefore phagosome maturation, phago-lysosome fusion and bacterial killing could not take place due the inability to activate Rab5a. Consequently the *L. monocytogenes* bacilli could escape more efficiently from the phagosomes of C/EBPβ$^{-/-}$ macrophages resulting in bacterial overgrowth. Taken altogether, the following hypothetical killing pathway is proposed (Fig. 17):

Since IFN-γ activates the cytocidal or cytostatic potential of macrophages (28, 74) and TNF has phagocytic and bactericidal/bacteriostatic functions (74), both these cytokines would drive the hypothetical killing pathway. IFN-γ would be the first component in the pathway, since IFN-$\gamma^{-/-}$ (60, 61) and IFN-$\gamma R^{-/-}$ (28, 60) mice had impaired induction of TNF. Downstream of IFN-γR would be RelB, a transcription factor belonging to the NF-κB family, since $RelB^{-/-}$ mice efficiently produced IFN-γ but had impaired macrophage activation due to defective induction of TNF (75). Consequently TNF would be downstream of IFN-γ and RelB. The most downstream molecule in this hypothetical pathway would be C/EBPβ, since *L. monocytogenes*-infected macrophages from C/EBPβ$^{-/-}$ mice expressed normal levels of IFN-γ and TNF (7). PKCδ would most likely to be downstream of C/EBPβ in this pathway, since C/EBPβ mRNA was highly up-regulated in the PKCδ$^{-/-}$ mice during the early phase of *L. monocytogenes* infection. This suggested that PKCδ may activate or synergize with, as yet, unknown proteins which are transcriptionally induced by C/EBPβ. Therefore in the PKCδ$^{-/-}$ mice, even though C/EBPβ target genes were expressed, they could not fulfil their function to confine the *L. monocytogenes* within phagosomes due to the absence of PKCδ. Similarly, the C/EBPβ$^{-/-}$ macrophages were unable to prevent listerial escape from the phagosomes despite up-regulation of PKCδ, due to the absence of C/EBPβ target genes in the C/EBPβ$^{-/-}$ macrophages. The proposed hypothetical killing pathway may be initiated by an "IFN-γ module" where IFN-γ binds to the IFN-γR, which in turn activates IFN-γ responsive transcription factors such as STAT1, ICSBP and IRF2. RelB would transcribe TNF, which enters the pathway downstream of the "IFN-γ module" and signals via the TNFRp55 and not TNFRp75, since TNFRp75$^{-/-}$ mice did not exhibit any defects in host defense and inflammatory responses to *L. monocytogenes* (76). Secretion of pro-inflammatory cytokines such as IFN-γ, IL-1 and IL-6 induce expression and activation of C/EBPβ (50, 77). Moreover, IFN-γ activation of mixed-lineage kinases of the mitogen-activated protein kinase (MAPK) family (MLKs), mitogen-activated protein kinase kinase/extracellular signal-regulated protein kinase (MEKs) and extracellular signal-regulated protein kinases (ERKs) phosphorylate and thereby activate C/EBPβ transcription activity (78, 79). The "C/EBPβ module" enters downstream of the "TNF module", where activated C/EBPβ transcribes its target genes which are needed for confinement of bacteria within phagosome e.g. G-CSF, Agtr1a, RAB GTPase binding effector protein 1 (Rabep1) and Rabgef1. Furthermore, transcription of, as yet, unidentified C/EBPβ target genes may themselves be bactericidal or act in concert with other proteins to generate bactericidal molecules. For example, iNOS which generates nitric oxide during pro-inflammatory innate immune response and PKCδ which stimulates production of

superoxide by phagocyte NADPH oxidase (17-19). Downstream of the "C/EBPβ module" is PKCδ which may act in synergy with G-CSF to augment Rab5a activity by promoting the activity of Agtr1 and Rabep1:Rabgef1, while suppressing the activity of Rasa1 and Tsc2. Thereafter phagosome maturation and phago-lysosome fusion occurs resulting in bacterial killing, antigen presentation and clearance by the adaptive immune response. The role of PKCδ in promoting phagosome maturation and phago-lysosome fusion is not implausible, since PKCα has recently been shown to be important for phagosome maturation (80). In addition, activated Rab5a and PKCδ act in concert to recruit phagocyte NADPH oxidase to the phagosome membrane and stimulate the production of superoxide into the phagosome(17, 18, 69). Furthermore, PKCδ may have an additional role in the proposed pathway where it may directly or indirectly modulate the activation of C/EBPβ through phosphorylation of the trans-activation domain. The activity of PKCδ is regulated by phosphorylation of its tyrosine residues in response to different stimuli, and the effect of tyrosine phosphorylation can have many different effects on PKCδ, depending on the biological context e.g. the cell type and nature of the stimulus (81, 82). In B cells stimulated with LPS, PKCδ$^{-/-}$ was shown to inhibit C/EBPβ transcriptional activity by phosphorylating C/EBPβ at a serine residue within the DNA binding domain, resulting in decreased DNA binding activity (27). However, the biological context of B cells stimulated with LPS is very different from IFN-γ activated macrophages infected with *L. monocytogenes*, where PKCδ appears to be a downstream effector of IFN-γ in mediating listericidal activity. Indeed, IL-1β and TNF secreted by IFN-γ activated macrophages induces the transcription of PKCδ (5, 16). Moreover, IFN-γ stimulates the activation of PKCδ, which in turn mediates serine phosphorylation of STAT1 and thereby facilitates transcription of IFN-γ stimulated genes (16). It may therefore be possible that in activated macrophages, PKCδ may activate C/EBPβ through phosphorylation of its transcriptional activation domain; however, this premise would have to be investigated further. Based on this speculation, the higher levels of PKCδ in the C/EBPβ$^{-/-}$ infected macrophages may have functioned to promote C/EBPβ activity and therefore enhance the, as yet, unknown bacterial killing mechanism. It is also possible that PKCδ may indirectly activate C/EBPβ via phosphorylation of other kinases that bind to and activate C/EBPβ. For example, activated PKCδ phosphorylates MEK1 leading to the activation of ERK1/2 (83), which is involved in the activation of C/EBPβ in response to IFN-γ (78).

However, since the PKCδ$^{-/-}$ mice were not as susceptible as IFN-γR$^{-/-}$, STAT1$^{-/-}$, ICSBP$^{-/-}$, IRF2$^{-/-}$, RelB$^{-/-}$, TNFRp55$^{-/-}$ or C/EBPβ$^{-/-}$ mice, it can be argued that PKCδ may not in fact be part of the hypothetical RNI/RO-independent killing pathway. It could be possible that the increased expression of PKCδ in the C/EBPβ$^{-/-}$ during infection by *L. monocytogenes* functioned to enhance the assembly of the phagocyte NADPH oxidase. However, since the PKCδ$^{-/-}$ mice were more susceptible than p47phox$^{-/-}$ or p67phox$^{-/-}$ mice, this suggested that PKCδ played an additional role other than regulating the production of superoxide by phagocyte NADPH oxidase. Alternatively, PKCδ may be involved in a totally separate pathway that functions to confine the bacilli within the phagosome. It can be speculated that PKCδ may activate and/or synergize with, as yet, unidentified proteins to neutralize that activity of listerial LLO and PI-PLC activities, thereby preventing the escape of *L. monocytogenes* from the phagosome. These unknown proteins may themselves be transcriptional targets of C/EBPβ, since the high levels of PKCδ in the infected C/EBPβ$^{-/-}$ macrophages still could not control listerial escape from the phagosome, due to the absence of the unknown proteins. Clearly further studies are required in order to test the above hypotheses and to uncover the mechanism(s) and modes of PKCδ activity in the unknown killing pathway.

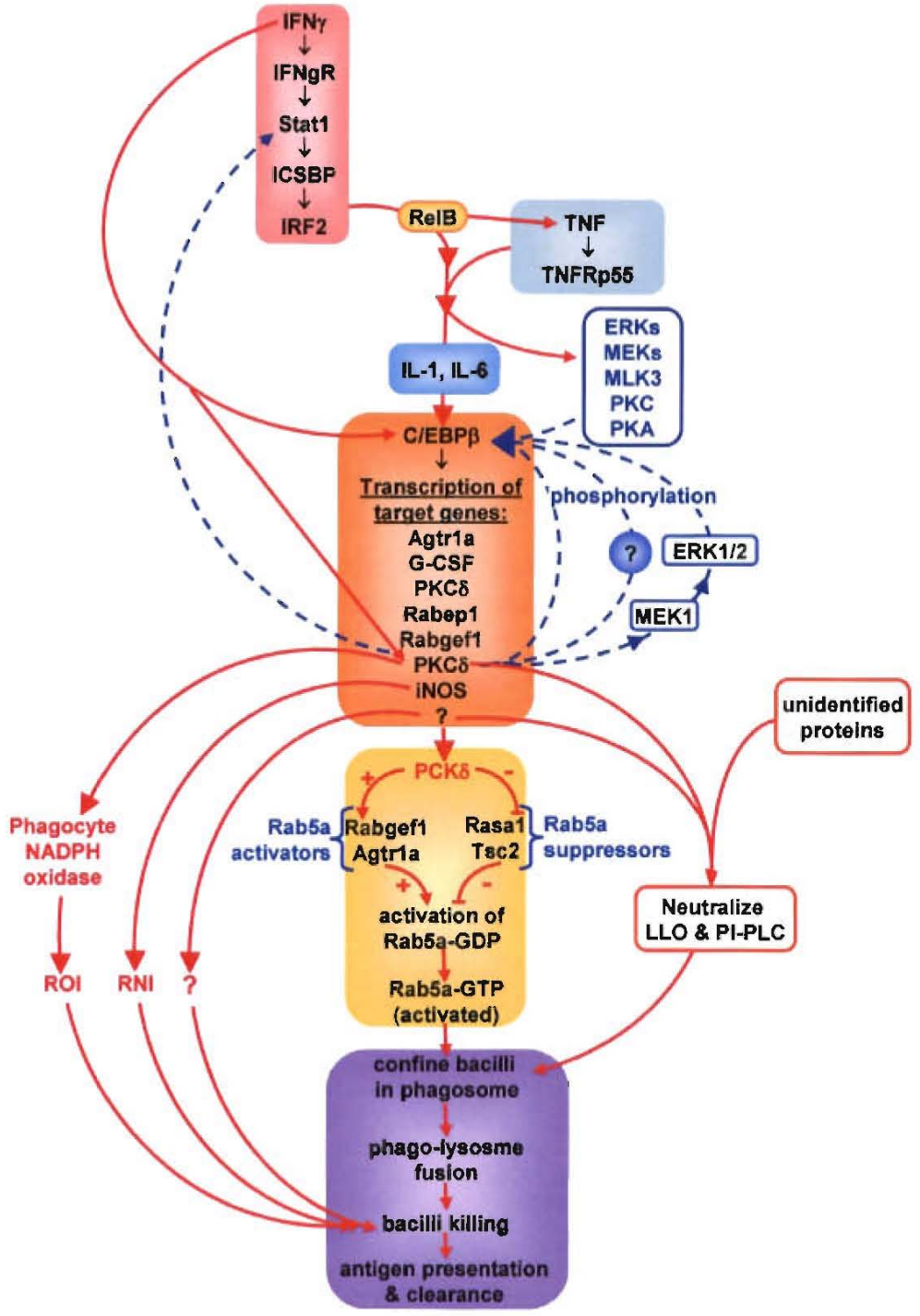


**Figure 17. Role of PKCδ in the hypothetical *L. monocytogenes* killing pathway mediated by IFN-γ, TNF and C/EBPβ that is independent of ROI and RNI.** Solid lines with arrows represent positive (+) regulation; solid lines with blunted ends represent negative (-) regulation; dashed lines represent phosphorylation and activation.

## REFERENCES


1. Tapia, J. A., R. T. Jensen, and L. J. Garcia-Marin. 2006. Rottlerin inhibits stimulated enzymatic secretion and several intracellular signaling transduction pathways in pancreatic acinar cells by a non-PKC-delta-dependent mechanism. *Biochim Biophys Acta 1763:25.*
2. Davies, S. P., H. Reddy, M. Caivano, and P. Cohen. 2000. Specificity and mechanism of action of some commonly used protein kinase inhibitors. *Biochem J 351:95.*
3. Seki, E., H. Tsutsui, N. M. Tsuji, N. Hayashi, K. Adachi, H. Nakano, S. Futatsugi-Yumikura, O. Takeuchi, K. Hoshino, S. Akira, J. Fujimoto, and K. Nakanishi. 2002. Critical roles of myeloid differentiation factor 88-dependent proinflammatory cytokine release in early phase clearance of Listeria monocytogenes in mice. *J Immunol 169:3863.*
4. Way, S. S., L. J. Thompson, J. E. Lopes, A. M. Hajjar, T. R. Kollmann, N. E. Freitag, and C. B. Wilson. 2004. Characterization of flagellin expression and its role in Listeria monocytogenes infection and immunity. *Cell Microbiol 6:235.*
5. Suh, K. S., T. T. Tatunchak, J. M. Crutchley, L. E. Edwards, K. G. Marin, and S. H. Yuspa. 2003. Genomic structure and promoter analysis of PKC-delta. *Genomics 82:57.*
6. Dunn, S. M., L. S. Coles, R. K. Lang, S. Gerondakis, M. A. Vadas, and M. F. Shannon. 1994. Requirement for nuclear factor (NF)-kappa B p65 and NF-interleukin-6 binding elements in the tumor necrosis factor response region of the granulocyte colony-stimulating factor promoter. *Blood 83:2469.*
7. Tanaka, T., S. Akira, K. Yoshida, M. Umemoto, Y. Yoneda, N. Shirafuji, H. Fujiwara, S. Suematsu, N. Yoshida, and T. Kishimoto. 1995. Targeted disruption of the NF-IL6 gene discloses its essential role in bacteria killing and tumor cytotoxicity by macrophages. *Cell 80:353.*
8. You, H. J., J. W. Lee, Y. J. Yoo, and J. H. Kim. 2004. A pathway involving protein kinase Cdelta up-regulates cytosolic phospholipase A(2)alpha in airway epithelium. *Biochem Biophys Res Commun 321:657.*
9. Page, K., J. Li, L. Zhou, S. Iasvovskaia, K. C. Corbit, J. W. Soh, I. B. Weinstein, A. R. Brasier, A. Lin, and M. B. Hershenson. 2003. Regulation of airway epithelial cell NF-kappa B-dependent gene expression by protein kinase C delta. *J Immunol 170:5681.*
10. Page, K., J. Li, K. C. Corbit, K. M. Rumilla, J. W. Soh, I. B. Weinstein, C. Albanese, R. G. Pestell, M. R. Rosner, and M. B. Hershenson. 2002. Regulation of airway smooth muscle cyclin D1 transcription by protein kinase C-delta. *Am J Respir Cell Mol Biol 27:204.*
11. Woo, C. H., J. H. Lim, and J. H. Kim. 2005. VCAM-1 upregulation via PKCdelta-p38 kinase-linked cascade mediates the TNF-alpha-induced leukocyte adhesion and emigration in the lung airway epithelium. *Am J Physiol Lung Cell Mol Physiol 288:L307.*
12. Kilpatrick, L. E., J. Y. Lee, K. M. Haines, D. E. Campbell, K. E. Sullivan, and H. M. Korchak. 2002. A role for PKC-delta and PI 3-kinase in TNF-alpha-mediated antiapoptotic signaling in the human neutrophil. *Am J Physiol Cell Physiol 283:C48.*
13. Novotny-Diermayr, V., T. Zhang, L. Gu, and X. Cao. 2002. Protein kinase C delta associates with the interleukin-6 receptor subunit glycoprotein (gp) 130 via Stat3 and enhances Stat3-gp130 interaction. *J Biol Chem 277:49134.*
14. Xu, B., A. Bhattacharjee, B. Roy, G. M. Feldman, and M. K. Cathcart. 2004. Role of protein kinase C isoforms in the regulation of interleukin-13-induced 15-lipoxygenase gene expression in human monocytes. *J Biol Chem 279:15954.*

15. Uddin, S., and L. C. Platanias. 2004. Mechanisms of type-I interferon signal transduction. *J Biochem Mol Biol 37:635.*
16. Deb, D. K., A. Sassano, F. Lekmine, B. Majchrzak, A. Verma, S. Kambhampati, S. Uddin, A. Rahman, E. N. Fish, and L. C. Platanias. 2003. Activation of protein kinase C delta by IFN-gamma. *J Immunol 171:267.*
17. Bey, E. A., B. Xu, A. Bhattacharjee, C. M. Oldfield, X. Zhao, Q. Li, V. Subbulakshmi, G. M. Feldman, F. B. Wientjes, and M. K. Cathcart. 2004. Protein kinase C delta is required for p47phox phosphorylation and translocation in activated human monocytes. *J Immunol 173:5730.*
18. Zhao, X., B. Xu, A. Bhattacharjee, C. M. Oldfield, F. B. Wientjes, G. M. Feldman, and M. K. Cathcart. 2005. Protein kinase Cdelta regulates p67phox phosphorylation in human monocytes. *J Leukoc Biol 77:414.*
19. Yamamori, T., O. Inanami, H. Nagahata, and M. Kuwabara. 2004. Phosphoinositide 3-kinase regulates the phosphorylation of NADPH oxidase component p47(phox) by controlling cPKC/PKCdelta but not Akt. *Biochem Biophys Res Commun 316:720.*
20. Uddin, S., A. Sassano, D. K. Deb, A. Verma, B. Majchrzak, A. Rahman, A. B. Malik, E. N. Fish, and L. C. Platanias. 2002. Protein kinase C-delta (PKC-delta ) is activated by type I interferons and mediates phosphorylation of Stat1 on serine 727. *J Biol Chem 277:14408.*
21. Kovarik, P., D. Stoiber, P. A. Eyers, R. Menghini, A. Neininger, M. Gaestel, P. Cohen, and T. Decker. 1999. Stress-induced phosphorylation of STAT1 at Ser727 requires p38 mitogen-activated protein kinase whereas IFN-gamma uses a different signaling pathway. *Proc Natl Acad Sci U S A 96:13956.*
22. Jain, N., T. Zhang, W. H. Kee, W. Li, and X. Cao. 1999. Protein kinase C delta associates with and phosphorylates Stat3 in an interleukin-6-dependent manner. *J Biol Chem 274:24392.*
23. Schuringa, J. J., L. V. Dekker, E. Vellenga, and W. Kruijer. 2001. Sequential activation of Rac-1, SEK-1/MKK-4, and protein kinase Cdelta is required for interleukin-6-induced STAT3 Ser-727 phosphorylation and transactivation. *J Biol Chem 276:27709.*
24. Yuan, L. W., J. W. Soh, and I. B. Weinstein. 2002. Inhibition of histone acetyltransferase function of p300 by PKCdelta. *Biochim Biophys Acta 1592:205.*
25. Wadsworth, S. J., and H. Goldfine. 2002. Mobilization of protein kinase C in macrophages induced by Listeria monocytogenes affects its internalization and escape from the phagosome. *Infect Immun 70:4650.*
26. Goldfine, H., S. J. Wadsworth, and N. C. Johnston. 2000. Activation of host phospholipases C and D in macrophages after infection with Listeria monocytogenes. *Infect Immun 68:5735.*
27. Miyamoto, A., K. Nakayama, H. Imaki, S. Hirose, Y. Jiang, M. Abe, T. Tsukiyama, H. Nagahama, S. Ohno, S. Hatakeyama, and K. I. Nakayama. 2002. Increased proliferation of B cells and auto-immunity in mice lacking protein kinase Cdelta. *Nature 416:865.*
28. Dai, W. J., W. Bartens, G. Kohler, M. Hufnagel, M. Kopf, and F. Brombacher. 1997. Impaired macrophage listericidal and cytokine activities are responsible for the rapid death of Listeria monocytogenes-infected IFN-gamma receptor-deficient mice. *J Immunol 158:5297.*
29. Sugawara, I., S. Mizuno, H. Yamada, M. Matsumoto, and S. Akira. 2001. Disruption of nuclear factor-interleukin-6, a transcription factor, results in severe mycobacterial infection. *Am J Pathol 158:361.*
30. Kamijo, R., J. Le, D. Shapiro, E. A. Havell, S. Huang, M. Aguet, M. Bosland, and J. Vilcek. 1993. Mice that lack the interferon-gamma receptor have profoundly altered

responses to infection with Bacillus Calmette-Guerin and subsequent challenge with lipopolysaccharide. *J Exp Med 178:1435.*

31. Wadsworth, S. J., and H. Goldfine. 1999. Listeria monocytogenes phospholipase C-dependent calcium signaling modulates bacterial entry into J774 macrophage-like cells. *Infect Immun 67:1770.*
32. Myers, J. T., A. W. Tsang, and J. A. Swanson. 2003. Localized reactive oxygen and nitrogen intermediates inhibit escape of Listeria monocytogenes from vacuoles in activated macrophages. *J Immunol 171:5447.*
33. Endres, R., A. Luz, H. Schulze, H. Neubauer, A. Futterer, S. M. Holland, H. Wagner, and K. Pfeffer. 1997. Listeriosis in p47(phox-/-) and TRp55-/- mice: protection despite absence of ROI and susceptibility despite presence of RNI. *Immunity 7:419.*
34. Dinauer, M. C., M. B. Deck, and E. R. Unanue. 1997. Mice lacking reduced nicotinamide adenine dinucleotide phosphate oxidase activity show increased susceptibility to early infection with Listeria monocytogenes. *J Immunol 158:5581.*
35. Shiloh, M. U., J. D. MacMicking, S. Nicholson, J. E. Brause, S. Potter, M. Marino, F. Fang, M. Dinauer, and C. Nathan. 1999. Phenotype of mice and macrophages deficient in both phagocyte oxidase and inducible nitric oxide synthase. *Immunity 10:29.*
36. Pizarro-Cerda, J., M. Desjardins, E. Moreno, S. Akira, and J. P. Gorvel. 1999. Modulation of endocytosis in nuclear factor IL-6(-/-) macrophages is responsible for a high susceptibility to intracellular bacterial infection. *J Immunol 162:3519.*
37. Cytoscape. 2005. http://www.cytoscape.org.
38. Horiuchi, H., R. Lippe, H. M. McBride, M. Rubino, P. Woodman, H. Stenmark, V. Rybin, M. Wilm, K. Ashman, M. Mann, and M. Zerial. 1997. A novel Rab5 GDP/GTP exchange factor complexed to Rabaptin-5 links nucleotide exchange to effector recruitment and function. *Cell 90:1149.*
39. Stenmark, H., G. Vitale, O. Ullrich, and M. Zerial. 1995. Rabaptin-5 is a direct effector of the small GTPase Rab5 in endocytic membrane fusion. *Cell 83:423.*
40. Autieri, M. V., and C. J. Carbone. 1999. 14-3-3Gamma interacts with and is phosphorylated by multiple protein kinase C isoforms in PDGF-stimulated human vascular smooth muscle cells. *DNA Cell Biol 18:555.*
41. Kjarland, E., T. J. Keen, and R. Kleppe. 2006. Does isoform diversity explain functional differences in the 14-3-3 protein family? *Curr Pharm Biotechnol 7:217.*
42. Mackintosh, C. 2004. Dynamic interactions between 14-3-3 proteins and phosphoproteins regulate diverse cellular processes. *Biochem J 381:329.*
43. Seachrist, J. L., S. A. Laporte, L. B. Dale, A. V. Babwah, M. G. Caron, P. H. Anborgh, and S. S. Ferguson. 2002. Rab5 association with the angiotensin II type 1A receptor promotes Rab5 GTP binding and vesicular fusion. *J Biol Chem 277:679.*
44. Offermanns, S., Y. H. Hu, and M. I. Simon. 1996. Galpha12 and galpha13 are phosphorylated during platelet activation. *J Biol Chem 271:26044.*
45. Macrez-Lepretre, N., F. Kalkbrenner, J. L. Morel, G. Schultz, and J. Mironneau. 1997. G protein heterotrimer Galpha13beta1gamma3 couples the angiotensin AT1A receptor to increases in cytoplasmic Ca2+ in rat portal vein myocytes. *J Biol Chem 272:10095.*
46. Downward, J. 1992. Regulatory mechanisms for ras proteins. *Bioessays 14:177.*
47. Xiao, G. H., F. Shoarinejad, F. Jin, E. A. Golemis, and R. S. Yeung. 1997. The tuberous sclerosis 2 gene product, tuberin, functions as a Rab5 GTPase activating protein (GAP) in modulating endocytosis. *J Biol Chem 272:6097.*
48. Li, Y., K. Inoki, R. Yeung, and K. L. Guan. 2002. Regulation of TSC2 by 14-3-3 binding. *J Biol Chem 277:44593.*
49. Liu, M. Y., S. Cai, A. Espejo, M. T. Bedford, and C. L. Walker. 2002. 14-3-3 interacts with the tumor suppressor tuberin at Akt phosphorylation site(s). *Cancer Res 62:6475.*

50. Akira, S., H. Isshiki, T. Sugita, O. Tanabe, S. Kinoshita, Y. Nishio, T. Nakajima, T. Hirano, and T. Kishimoto. 1990. A nuclear factor for IL-6 expression (NF-IL6) is a member of a C/EBP family. *Embo J 9:1897.*
51. Trautwein, C., C. Caelles, P. van der Geer, T. Hunter, M. Karin, and M. Chojkier. 1993. Transactivation by NF-IL6/LAP is enhanced by phosphorylation of its activation domain. *Nature 364:544.*
52. Descombes, P., and U. Schibler. 1991. A liver-enriched transcriptional activator protein, LAP, and a transcriptional inhibitory protein, LIP, are translated from the same mRNA. *Cell 67:569.*
53. Pamer, E. G. 2004. Immune responses to Listeria monocytogenes. *Nat Rev Immunol 4:812.*
54. Unanue, E. R. 1997. Inter-relationship among macrophages, natural killer cells and neutrophils in early stages of Listeria resistance. *Curr Opin Immunol 9:35.*
55. Brombacher, F., and M. Kopf. 1996. Innate versus acquired immunity in listeriosis. *Res Immunol 147:505.*
56. Buchmeier, N. A., and R. D. Schreiber. 1985. Requirement of endogenous interferon-gamma production for resolution of Listeria monocytogenes infection. *Proc Natl Acad Sci U S A 82:7404.*
57. Havell, E. A. 1989. Evidence that tumor necrosis factor has an important role in antibacterial resistance. *J Immunol 143:2894.*
58. Jackson, S. H., J. I. Gallin, and S. M. Holland. 1995. The p47phox mouse knock-out model of chronic granulomatous disease. *J Exp Med 182:751.*
59. MacMicking, J. D., C. Nathan, G. Hom, N. Chartrain, D. S. Fletcher, M. Trumbauer, K. Stevens, Q. W. Xie, K. Sokol, N. Hutchinson, and et al. 1995. Altered responses to bacterial infection and endotoxic shock in mice lacking inducible nitric oxide synthase. *Cell 81:641.*
60. Huang, S., W. Hendriks, A. Althage, S. Hemmi, H. Bluethmann, R. Kamijo, J. Vilcek, R. M. Zinkernagel, and M. Aguet. 1993. Immune response in mice that lack the interferon-gamma receptor. *Science 259:1742.*
61. Harty, J. T., and M. J. Bevan. 1995. Specific immunity to Listeria monocytogenes in the absence of IFN gamma. *Immunity 3:109.*
62. Fehr, T., G. Schoedon, B. Odermatt, T. Holtschke, M. Schneemann, M. F. Bachmann, T. W. Mak, I. Horak, and R. M. Zinkernagel. 1997. Crucial role of interferon consensus sequence binding protein, but neither of interferon regulatory factor 1 nor of nitric oxide synthesis for protection against murine listeriosis. *J Exp Med 185:921.*
63. Weih, F., S. K. Durham, D. S. Barton, W. C. Sha, D. Baltimore, and R. Bravo. 1996. Both multiorgan inflammation and myeloid hyperplasia in RelB-deficient mice are T cell dependent. *J Immunol 157:3974.*
64. Pfeffer, K., T. Matsuyama, T. M. Kundig, A. Wakeham, K. Kishihara, A. Shahinian, K. Wiegmann, P. S. Ohashi, M. Kronke, and T. W. Mak. 1993. Mice deficient for the 55 kd tumor necrosis factor receptor are resistant to endotoxic shock, yet succumb to L. monocytogenes infection. *Cell 73:457.*
65. Rothe, J., W. Lesslauer, H. Lotscher, Y. Lang, P. Koebel, F. Kontgen, A. Althage, R. Zinkernagel, M. Steinmetz, and H. Bluethmann. 1993. Mice lacking the tumour necrosis factor receptor 1 are resistant to TNF-mediated toxicity but highly susceptible to infection by Listeria monocytogenes. *Nature 364:798.*
66. Flesch, I. E., and S. H. Kaufmann. 1994. Role of macrophages and alpha beta T lymphocytes in early interleukin 10 production during Listeria monocytogenes infection. *Int Immunol 6:463.*
67. Tripp, C. S., S. F. Wolf, and E. R. Unanue. 1993. Interleukin 12 and tumor necrosis factor alpha are costimulators of interferon gamma production by natural killer cells in

severe combined immunodeficiency mice with listeriosis, and interleukin 10 is a physiologic antagonist. *Proc Natl Acad Sci U S A 90:3725.*

68. Prada-Delgado, A., E. Carrasco-Marin, C. Pena-Macarro, E. Del Cerro-Vadillo, M. Fresno-Escudero, F. Leyva-Cobian, and C. Alvarez-Dominguez. 2005. Inhibition of Rab5a exchange activity is a key step for Listeria monocytogenes survival. *Traffic 6:252.*
69. Prada-Delgado, A., E. Carrasco-Marin, G. M. Bokoch, and C. Alvarez-Dominguez. 2001. Interferon-gamma listericidal action is mediated by novel Rab5a functions at the phagosomal environment. *J Biol Chem 276:19059.*
70. LeClair, K. P., M. A. Blanar, and P. A. Sharp. 1992. The p50 subunit of NF-kappa B associates with the NF-IL6 transcription factor. *Proc Natl Acad Sci U S A 89:8145.*
71. Xia, C., J. K. Cheshire, H. Patel, and P. Woo. 1997. Cross-talk between transcription factors NF-kappa B and C/EBP in the transcriptional regulation of genes. *Int J Biochem Cell Biol 29:1525.*
72. Hanlon, M., L. M. Bundy, and L. Sealy. 2000. C/EBP beta and Elk-1 synergistically transactivate the c-fos serum response element. *BMC Cell Biol 1:2.*
73. Sealy, L., D. Malone, and M. Pawlak. 1997. Regulation of the cfos serum response element by C/EBPbeta. *Mol Cell Biol 17:1744.*
74. Mielke, M. E., S. Ehlers, and H. Hahn. 1993. The role of cytokines in experimental listeriosis. *Immunobiology 189:285.*
75. Weih, F., G. Warr, H. Yang, and R. Bravo. 1997. Multifocal defects in immune responses in RelB-deficient mice. *J Immunol 158:5211.*
76. Peschon, J. J., D. S. Torrance, K. L. Stocking, M. B. Glaccum, C. Otten, C. R. Willis, K. Charrier, P. J. Morrissey, C. B. Ware, and K. M. Mohler. 1998. TNF receptor-deficient mice reveal divergent roles for p55 and p75 in several models of inflammation. *J Immunol 160:943.*
77. Roy, S. K., S. J. Wachira, X. Weihua, J. Hu, and D. V. Kalvakolanu. 2000. CCAAT/enhancer-binding protein-beta regulates interferon-induced transcription through a novel element. *J Biol Chem 275:12626.*
78. Roy, S. K., J. Hu, Q. Meng, Y. Xia, P. S. Shapiro, S. P. Reddy, L. C. Platanias, D. J. Lindner, P. F. Johnson, C. Pritchard, G. Pages, J. Pouyssegur, and D. V. Kalvakolanu. 2002. MEKK1 plays a critical role in activating the transcription factor C/EBP-beta-dependent gene expression in response to IFN-gamma. *Proc Natl Acad Sci U S A 99:7945.*
79. Roy, S. K., J. D. Shuman, L. C. Platanias, P. S. Shapiro, S. P. Reddy, P. F. Johnson, and D. V. Kalvakolanu. 2005. A role for mixed lineage kinases in regulating transcription factor CCAAT/enhancer-binding protein-{beta}-dependent gene expression in response to interferon-{gamma}. *J Biol Chem 280:24462.*
80. Ng Yan Hing, J. D., M. Desjardins, and A. Descoteaux. 2004. Proteomic analysis reveals a role for protein kinase C-alpha in phagosome maturation. *Biochem Biophys Res Commun 319:810.*
81. Steinberg, S. F., and M. A. Sussman. 2005. Cardiac hypertrophy served with protein kinase Cepsilon: delta isoform substitution available at additional cost. *Circ Res 96:711.*
82. Jackson, D. N., and D. A. Foster. 2004. The enigmatic protein kinase Cdelta: complex roles in cell proliferation and survival. *Faseb J 18:627.*
83. Ueda, Y., S. Hirai, S. Osada, A. Suzuki, K. Mizuno, and S. Ohno. 1996. Protein kinase C activates the MEK-ERK pathway in a manner independent of Ras and dependent on Raf. *J Biol Chem 271:23512.*

## CHAPTER 6

## DISCUSSION

In the current study, *L. monocytogenes* was used as a model intracellular pathogen to investigate and identify the genes involved in mediating macrophage bactericidal effector activity. Early control of *L. monocytogenes* infection requires the innate immune response, the primary goal of which is to restrict the proliferation of *L. monocytogenes*, thereby preventing bacterial dissemination into the blood stream, infection of other vital organs and overwhelming sepsis. Activated neutrophils and macrophages are the major cell types responsible for killing of *L. monocytogenes* (1-3). IFN-γ and TNF are key cytokines essential for full macrophage activation (4, 5), resulting in enhanced production of cytokines, chemokines and bactericidal molecules such as inducible nitric oxide and superoxide. Several *in vivo* infection studies using iNOS$^{-/-}$, gp47phox$^{-/-}$, gp91phox$^{-/-}$ and gp91 phox$^{-/-}$/iNOS$^{-/-}$ mice showed that bacterial killing took place despite the lack of nitric oxide and superoxide (6-10), suggesting that macrophages have an alternative killing mechanism independent of these reactive nitrogen- and oxygen- intermediates. This hypothesis was further underscored by studies using mice deficient for genes such as IFN-γ$^{-/-}$ (11, 12), IFN-γR$^{-/-}$ (11, 13), RelB (14), TNFRp55$^{-/-}$ (15, 16) and C/EBPβ$^{-/-}$ (17). All of these mice were highly susceptible to *L. monocytogenes* despite full macrophage activation and production of pro-inflammatory mediators, superoxide and nitric oxide. Since IFN-γ activates the cytocidal or cytostatic potential of macrophages (13, 18) and TNF has phagocytic and bactericidal/bacteriostatic functions (18), this hypothetical killing pathway is most likely activated by these cytokines. IFN-γ would be the first component in the pathway, since IFN-γ$^{-/-}$ (11, 12) and IFN-γR$^{-/-}$ (11, 13) mice had impaired induction of TNF. Similarly, RelB would be downstream of IFN-γ, since mice deficient in this transcription factor efficiently produced IFN-γ but had defective induction of TNF (14). Consequently TNF would be downstream of IFN-γ and RelB. The most downstream molecule in this hypothetical pathway would be C/EBPβ, since the C/EBPβ$^{-/-}$ mice expressed normal levels of IFN-γ and TNF (17). Since IFN-γ stimulation results in the enhanced expression (19, 20) and activation of C/EBPβ (21, 22), and TNF promotes the translocation of C/EBPβ to the nucleus in response to pro-inflammatory cytokine signalling (23), it can therefore be envisaged that IFN-γ and TNF signalling converge on C/EBPβ to transcribe genes required for confinement of *L. monocytogenes* within the phagosome, leading to phago-lysosome fusion and consequent bacterial killing. Macrophage effector genes involved in this unknown mechanism would therefore most likely be downstream of C/EBPβ. C/EBPβ is a transcription factor that is important for macrophage-

mediated antibacterial defenses, Th1 immune responses, anti-tumour defenses, differentiation of various cell types and storage and metabolism of carbohydrates and lipids (22). Furthermore, C/EBPβ$^{-/-}$ mice are highly susceptible to intracellular pathogens such as *Listeria* (17), *Salmonella* (17), *Brucella* (24), *Mycobacterium* (25) and *Candida* (26) due to their inability to confine the pathogen within phagosomes, resulting in impaired listericidal activity. It was therefore postulated that the comparison between the gene expression profiles of WT and C/EBPβ$^{-/-}$ macrophages infected with *L. monocytogenes* would increase the probability of identifying these effector genes, which would be differentially expressed between these two genotypes.

The first part of this study established and optimized the *in vitro* infection of WT and C/EBPβ$^{-/-}$ bone marrow derived macrophages with *L. monocytogenes*. Contrary to most *in vitro* protocols published in literature, the macrophages were simultaneously stimulated with IFN-γ and infected with *L. monocytogenes*, and not pre-activated prior to infection. This particular *in vitro* infection protocol was followed in order to authentically reproduce the biology of the *in vivo* infection experiments, since macrophages do not naturally exist in a pre-activated state. Both WT and C/EBPβ$^{-/-}$ infected macrophages were fully activated and secreted equivalent amounts of pro-inflammatory mediators such as IL-6, IL-12, IL-18, TNF, MCP-1 and nitric oxide. However, despite full macrophage activation C/EBPβ$^{-/-}$ macrophages had 30% more escaped *L. monocytogenes* bacilli in the cytoplasm and uncontrolled bacilli growth as compared to WT. Furthermore, the induction of C/EBPβ target genes G-CSF, CLECSF9, IL-12p35 and ISGF3γ was impaired in the C/EBPβ$^{-/-}$ macrophages (17, 27-29). Comparison of the *in vitro* infection data to that published in the literature confirmed that the *in vitro* infection experiments had successfully mimicked the biology of *in vivo* infections (17, 27-29) and provided a solid foundation on which to base the gene expression profiling experiments.

The second part of the study used comparative DNA microarray analysis to identify genes involved in mediating macrophage listerial activity, which were postulated to be differentially expressed between the infected WT and C/EBPβ$^{-/-}$ macrophages. The transcriptional response of *L. monocytogenes* infected macrophages from WT and C/EBPβ$^{-/-}$ mice was compared at 4 hours p.i. for all four biological experiments. This particular time point was chosen, since it was the earliest instance where a significant difference between WT and C/EBPβ$^{-/-}$ macrophage listericidal activity was observed, due to differential expression of listericidal

genes between the WT and C/EBPβ$^{-/-}$ macrophages. Although the execution of the microarray experiments went smoothly, image analysis revealed that there was significant systematic variation within and between the arrays. This may have been caused by variability in the hybridization procedure as well as by the microarray slides themselves, which had several quality and printing defects. Although sequential normalization within and between arrays removed as much systematic variation as possible from the data, statistical evaluation of the normalized microarray data showed that the technical reproducibility within each array and between replicate experiments was poor. Within each array, more than 50% of the replicated genes had standard deviations (SD) greater than 0.2, which was considered not reproducible (30). Moreover, reproducibility between arrays (biological replicates) was poor since 49% of the genes had SD>0.3 resulting in low correlation coefficients ($R^2$ = 0.000001 - 0.13), which according to Churchill et al indicates that the biological replicates are not reproducible (31). Trimming the unreliable data from the microarray data set improved the reproducibility as shown by the correlation coefficients that were between $R^2$ = 0.2 and $R^2$ = 0.4. However, despite the disappointing performance on statistical level, the microarray data still contained biologically meaningful data. Genes encoding pro-inflammatory cytokines, chemokines, iNOS and genes important for macrophage activation and MHC class II presentation were significantly up-regulated in both the WT and C/EBPβ$^{-/-}$ activated macrophages during *L. monocytogenes* infection. Moreover, the expected impaired induction of C/EBPβ and its target genes, G-CSF, CLECSF9, IL-12p35 and ISGF3γ, was observed in the C/EBPβ$^{-/-}$ macrophages (17, 27, 28, 32). Since the microarray data held biologically relevant information, it was therefore used to search for differentially expressed genes which were postulated to be involved in macrophage effector functions against *L. monocytogenes*. Five percent (1268 out of 25000 genes) of the mouse genome was differentially expressed between the WT and C/EBPβ$^{-/-}$ activated macrophages infected with *L. monocytogenes*. Functional clustering of the DE genes revealed that 2.0% of the DE genes were involved in host immunity and defense, 3.1% in the production of ROI, 4.6% in the regulation of transcription, 16.1% in signalling and 8.9% in phagosome maturation and phago-lysosome fusion. Moreover, 18.0% of the DE genes had putative binding sites for C/EBPβ and 47.3% had binding sites for transcription factors that interacted with C/EBPβ. A focussed functional clustering strategy was used to reduce the number of candidate genes from 1268 down to 220 genes. PKCδ was selected for further study since it possessed all the postulated criteria of a macrophage effector gene: gene ontology and literature data mining showed that PKCδ was involved in humoral defense, immune signalling (33-43), production of superoxide by

phagocyte oxidase (41-43) and regulation of transcription via its phosphorylation of Stat1, Stat3 and p300 (44). Moreover, promoter analysis revealed that it may be directly or indirectly regulated by C/EBPβ. Furthermore, the role of PKCδ in innate immunity to intracellular pathogens has not been investigated to date, except for studies by Wadsworth and Goldfine. Using rottlerin, a putative specific PKCδ inhibitor, data by Wadsworth and Goldfine indirectly suggested that PKCδ played a role in promoting phagosomal escape of *L. monocytogenes* by initiating calcium influx into infected macrophages and by activating PLD2 (45, 46). However, no evidence showing a direct correlation between PKCδ activity and listerial phagosomal escape was reported. In addition, B cells from PKCδ$^{-/-}$ mice stimulated with LPS showed that PKCδ phosphorylation of C/EBPβ negatively regulated its transcriptional activity (47). Furthermore, PKCδ was up-regulated in *L. monocytogenes*-infected C/EBPβ$^{-/-}$ macrophages as compared to WT, as shown by microarray and confirmed by RT-PCR. It was therefore postulated that up-regulation of PKCδ may be detrimental during *L. monocytogenes* infections since it may promote phagosomal escape of *L. monocytogenes* (45, 46) by an unknown mechanism that may involve the inhibition of C/EBPβ transcriptional activity (47), which in C/EBPβ$^{-/-}$ mice resulted in increased listerial escape from the phagosomal (17).

The third part of the current study functionally characterized the role of PKCδ in *L. monocytogenes* infection and addressed the hypothesis that PKCδ played a detrimental role by promoting phagosomal escape. The functional *in vitro* and *in vivo* studies were done using the PKCδ$^{-/-}$ mouse model rather than rottlerin, since this putative PKCδ-specific inhibitor has been shown to non-specifically inhibit several other kinases and non-kinase enzymes (48, 49). PKCδ was found to be important for preventing, rather then promoting, phagosomal escape of *L. monocytogenes*. PKCδ$^{-/-}$ macrophages had a 6.5 fold increased bacterial escape from phagosome and uncontrolled bacterial growth, despite enhanced production of iNOS and pro-inflammatory cytokines. Furthermore, the PKCδ$^{-/-}$ mice were highly susceptible and died 2 days after infection with a sub-lethal dose for WT mice. Although the recruitment of activated macrophages to the site of infection was 10% lower in the PKCδ$^{-/-}$ mice, their susceptibility was not due to impaired macrophage activation, since *in vitro* and *ex vivo* quantitation showed that they produced significantly higher levels of nitric oxide and pro-inflammatory mediators in response to the high bacterial load than did WT mice. Furthermore, their impaired resistance to *L. monocytogenes* was not due to defects in chemokine attraction, since the PKCδ$^{-/-}$mice displayed massive recruitment of inflammatory cells to the site of infection and abundant granulomas in their livers and spleens. In addition, the PKCδ$^{-/-}$mice were still unable

to kill and clear the *L. monocytogenes* despite having recruited 30% more neutrophils, which are essential for killing *L. monocytogenes* (1-3). The current study has therefore clearly demonstrated that PKCδ was indispensable for confinement of *L. monocytogenes* within the phagosome, since no other PKC isoform compensated for it during infection. As a result, the PKCδ$^{-/-}$ mice suffered significantly increased escape of *L. monocytogenes* from the macrophage phagosomes, resulting in bacterial overgrowth, dissemination and early death.

Finally, the question of how PKCδ confined the bacilli within the phagosome was addressed and a hypothesis generated and tested against the microarray gene expression data. Studies by Wadsworth and Goldfine, using rottlerin and calcium channel inhibitors, showed that listerial escape from macrophage phagosomes was dependent on elevated cytosolic calcium levels (50) and that PKCδ was responsible for initiating the first calcium influx into macrophages upon infection with *L. monocytogenes* (45). However, the results from this dissertation clearly showed that PKCδ$^{-/-}$ macrophages had 6.5 fold more escaped *L. monocytogenes* than WT, suggesting that the initial calcium influx into the macrophages upon infection occurred independently of PKCδ. Moreover, the high susceptibility of the PKCδ$^{-/-}$ mice to *L. monocytogenes* suggested that PKCδ played an additional role other than phosphorylating and activating calcium channels.

PKCδ has been shown to be important for superoxide production by phagocyte oxidase (41-43), through its phosphorylation of the enzyme's p47phox and p67phox components. In these studies, lack of phosphorylation by PKCδ resulted in the impaired recruitment of the cytosolic p47phox and p67phox components to the phagosome membrane, where they were to be assembled with other components to form functional phagocyte NADPH oxidase enzyme. Moreover, the localized release of nitric oxide and superoxide into the phagosomal space has been shown to decrease bacterial escape (51). Therefore the increased phagosomal escape and high susceptibility of the PKCδ$^{-/-}$ mice may be due to impaired superoxide production. However, since the PKCδ$^{-/-}$ mice displayed a much higher degree of susceptibility to *L. monocytogenes* than p47phox$^{-/-}$ and gp91phox$^{-/-}$ mice, it suggested that PKCδ may play an additional role other than stimulating the production of superoxide into the phagosome.

It can be envisaged that the RNI/ROI pathway and the phago-lysosome fusion pathway act in concert to confine bacteria within the phagosome and to mediate killing by fusion with the lysosome, which contains bactericidal enzymes that kill and degrade the bacilli. Confinement of bacteria within the phagosome has been shown to be dependent on the recruitment and

assembly of functional NAPDH phagocyte oxidase and nitric oxide synthase at the phagosome membrane and the localized release of nitric oxide and superoxide into the phagosomal space (51, 52). Recruitment of these enzymes is effected by active GTP-bound Rab5a, which translocates Rac2 to the phagosome membrane and regulates its activity. Activated Rac2 in turn governs the assembly and activity of phagocyte NADPH oxidase at the phagosome membrane (52). The process of phagosome maturation, phago-lysosome fusion and subsequent bacterial killing is also regulated by active Rab5a in an IFN-γ dependent manner (52, 53). Active Rab5a causes remodeling of the phagosomal environment and promotes phagosome maturation by enhancing membrane fusion between the pathogen-containing phagosome and endosomes (53). Similarly, experiments by Pizarro-Cerda et al (24) demonstrated that C/EBPβ promoted endocytosis and membrane fusion between endosomes and pathogen-containing phagosomes in a G-CSF-dependent manner (24). However the actual mechanisms of these pathways are not fully elucidated. Since several studies have shown that RNI and ROI are important, but not essential for bacterial killing (6, 8, 9) and that macrophages have an alternative killing mechanism dependent on IFN-γ (11-13), TNF (15, 16) and C/EBPβ$^{-/-}$ (17), it was therefore postulated that this unknown killing pathway may involve the phago-lysosome fusion pathway. In addition, since PKCδ$^{-/-}$ mice were unable to confine and kill the *L. monocytogenes* bacilli, despite full macrophage activation and enhanced production of pro-inflammatory mediators and nitric oxide, it was further postulated that PKCδ may be involved in a similar RNI/ROI-independent unknown listericidal mechanism that was first observed in IFN-γ$^{-/-}$, TNFRp55$^{-/-}$, ICSBP$^{-/-}$ and C/EBPβ$^{-/-}$ mice. Moreover, since PKCδ appeared to act downstream of C/EBPβ, this indicated that PKCδ may be involved in C/EBPβ mediated regulation of endocytosis, phagosome maturation and consequent bacterial killing.

A systems biology approach was used to investigate the mechanism whereby PKCδ confined *L. monocytogenes* within macrophage phagosomes. Analysis of the protein-protein interaction network generated the hypothesis that PKCδ acted in synergy with G-CSF to promote Rab5a activity, phagosome maturation, phago-lysosome fusion and subsequent bacterial killing, by promoting the Rab5a-activating functions of Agtr1a and Rabgef1 and by inhibiting the Rab5a-supressing functions of TSc2 and Rasa1. Moreover, the microarray gene expression data correlated with the proposed mechanism, since the Rab5a-activating proteins Agtr1a and Rabgef1 were down-regulated, whereas the Rab5a-supressing Tsc2 and Rasa1 proteins were up-regulated in the C/EBPβ$^{-/-}$ macrophages as compared to WT. Although the increased levels

of PKCδ may have adequately repressed the increased Rab5a-supressing activities of Rasa1 and Tsc2, it was not able to promote Rab5a activation due to impaired production Agtr1a and Rabgef1 proteins due to the lack of C/EBPβ. Therefore phagosome maturation, phago-lysosome fusion and bacterial killing could not take place due the inability to activate Rab5a. In addition, since transcription of G-CSF was impaired in the C/EBPβ$^{-/-}$ macrophages, activation of Rab5a activity by G-CSF could not take place. Consequently the *L. monocytogenes* bacilli could escape more efficiently from the phagosomes of C/EBPβ$^{-/-}$ macrophages resulting in bacterial overgrowth. This hypothesis could also be extended to the PKCδ$^{-/-}$ mice, where G-CSF may activate Rab5a and inhibit Tsc2 and Rasa1 activities, but not to the same extent as when in synergy with PKCδ.

In addition to promoting Rab5a activity, PKCδ may also act upstream of C/EBPβ in the hypothetical killing where it augments IFN-γ signalling by activating STAT1 (38, 54). In addition, PKCδ may augment the activation of C/EBPβ via phosphorylation of its trans-activation domain, rather than phosphorylation of the DNA binding domain resulting in inhibition of C/EBPβ activity (47). This is not implausible since the activity of PKCδ can vary according to the activation stimulus and cell type (44, 55). For example, in normal cells PKCδ promotes apoptosis and generally suppresses normal cell proliferation, however, in cancer cells, activation of PKCδ inhibits apoptosis and promotes tumour growth (44, 55, 56). Moreover, both PKCδ and C/EBPβ are involved in IFN-γ induced signalling: PKCδ itself is activated by IFN-γ (38) and in turn activates STAT1 by phosphorylation of its serine residue number 727 (38). Similarly, IFN-γ induces the expression and activation of C/EBPβ (19, 20) via MLK3 and/or a MEKK1/MEK1/ERK1/2 signalling cascade to induce transcription of IFN-γ responsive genes (21, 22). Therefore, in the context of IFN-γ activated macrophages infected with *L. monocytogenes*, PKCδ may augment the activation of C/EBPβ via phosphorylation of other kinases that bind to and activate C/EBPβ. For example, activated PKCδ phosphorylates MEK1 leading to the activation of ERK1/2 (57), which is also involved in the activation of C/EBPβ in response to IFN-γ (58). Therefore, the higher levels of PKCδ in the IFN-γ activated C/EBPβ$^{-/-}$ infected macrophages may have functioned to promote C/EBPβ activity in order to enhance macrophage listericidal activity via the alternative RNI/ROI-independent pathway. The concerted action of PKCδ in promoting the localized release of superoxide into the phagosome, the activation C/EBPβ transcriptional activity and the activation of Rab5a activity may therefore augment macrophage listericidal activity via the hypothesized alternative killing pathway. Alternatively, PKCδ may not be involved in

regulating Rab5a activity, and may only serve to activate C/EBPβ transcriptional activity. Moreover, since the PKCδ$^{-/-}$ mice were not as susceptible as IFN-γR$^{-/-}$, RelB, TNFRp55$^{-/-}$ or C/EBPβ$^{-/-}$ mice, it could be possible that PKCδ may not in fact be part of the hypothetical RNI/ROI-independent alternative killing pathway. In this context, PKCδ may confine the *L. monocytogenes* within phagosomes by activating and/or synergizing with, as yet, unidentified proteins to neutralize that activity of listerial LLO and PI-PLC.

Currently further studies are being implemented in order to determine the mechanism whereby PKCδ confines *L. monocytogenes* within phagosomes. Key questions being addressed in the current investigations include (i) if PKCδ phosphorylation of C/EBPβ can activate its transcriptional activity in IFN-γ activated macrophages infected with *L. monocytogenes*, (ii) if *L. monocytogenes* can negatively modulate the activity of PKCδ in order to facilitate its escape from the phagosome, and (iii) if PKCδ can promote activation of Rab5a activity thereby enhancing listericidal activity.

## REFERENCES


1. Pamer, E. G. 2004. Immune responses to Listeria monocytogenes. *Nat Rev Immunol 4:812.*
2. Unanue, E. R. 1997. Inter-relationship among macrophages, natural killer cells and neutrophils in early stages of Listeria resistance. *Curr Opin Immunol 9:35.*
3. Brombacher, F., and M. Kopf. 1996. Innate versus acquired immunity in listeriosis. *Res Immunol 147:505.*
4. Buchmeier, N. A., and R. D. Schreiber. 1985. Requirement of endogenous interferon-gamma production for resolution of Listeria monocytogenes infection. *Proc Natl Acad Sci USA 82:7404.*
5. Havell, E. A. 1989. Evidence that tumor necrosis factor has an important role in antibacterial resistance. *J Immunol 143:2894.*
6. Endres, R., A. Luz, H. Schulze, H. Neubauer, A. Futterer, S. M. Holland, H. Wagner, and K. Pfeffer. 1997. Listeriosis in p47(phox-/-) and TRp55-/- mice: protection despite absence of ROI and susceptibility despite presence of RNI. *Immunity 7:419.*
7. Jackson, S. H., J. I. Gallin, and S. M. Holland. 1995. The p47phox mouse knock-out model of chronic granulomatous disease. *J Exp Med 182:751.*
8. Shiloh, M. U., J. D. MacMicking, S. Nicholson, J. E. Brause, S. Potter, M. Marino, F. Fang, M. Dinauer, and C. Nathan. 1999. Phenotype of mice and macrophages deficient in both phagocyte oxidase and inducible nitric oxide synthase. *Immunity 10:29.*
9. Dinauer, M. C., M. B. Deck, and E. R. Unanue. 1997. Mice lacking reduced nicotinamide adenine dinucleotide phosphate oxidase activity show increased susceptibility to early infection with Listeria monocytogenes. *J Immunol 158:5581.*
10. MacMicking, J. D., C. Nathan, G. Hom, N. Chartrain, D. S. Fletcher, M. Trumbauer, K. Stevens, Q. W. Xie, K. Sokol, N. Hutchinson, and et al. 1995. Altered responses to bacterial infection and endotoxic shock in mice lacking inducible nitric oxide synthase. *Cell 81:641.*
11. Huang, S., W. Hendriks, A. Althage, S. Hemmi, H. Bluethmann, R. Kamijo, J. Vilcek, R. M. Zinkernagel, and M. Aguet. 1993. Immune response in mice that lack the interferon-gamma receptor. *Science 259:1742.*
12. Harty, J. T., and M. J. Bevan. 1995. Specific immunity to Listeria monocytogenes in the absence of IFN gamma. *Immunity 3:109.*
13. Dai, W. J., W. Bartens, G. Kohler, M. Hufnagel, M. Kopf, and F. Brombacher. 1997. Impaired macrophage listericidal and cytokine activities are responsible for the rapid death of Listeria monocytogenes-infected IFN-gamma receptor-deficient mice. *J Immunol 158:5297.*
14. Weih, F., G. Warr, H. Yang, and R. Bravo. 1997. Multifocal defects in immune responses in RelB-deficient mice. *J Immunol 158:5211.*
15. Pfeffer, K., T. Matsuyama, T. M. Kundig, A. Wakeham, K. Kishihara, A. Shahinian, K. Wiegmann, P. S. Ohashi, M. Kronke, and T. W. Mak. 1993. Mice deficient for the 55 kd tumor necrosis factor receptor are resistant to endotoxic shock, yet succumb to L. monocytogenes infection. *Cell 73:457.*
16. Rothe, J., W. Lesslauer, H. Lotscher, Y. Lang, P. Koebel, F. Kontgen, A. Althage, R. Zinkernagel, M. Steinmetz, and H. Bluethmann. 1993. Mice lacking the tumour necrosis factor receptor 1 are resistant to TNF-mediated toxicity but highly susceptible to infection by Listeria monocytogenes. *Nature 364:798.*
17. Tanaka, T., S. Akira, K. Yoshida, M. Umemoto, Y. Yoneda, N. Shirafuji, H. Fujiwara, S. Suematsu, N. Yoshida, and T. Kishimoto. 1995. Targeted disruption of the NF-IL6

gene discloses its essential role in bacteria killing and tumor cytotoxicity by macrophages. *Cell 80:353.*

18. Mielke, M. E., S. Ehlers, and H. Hahn. 1993. The role of cytokines in experimental listeriosis. *Immunobiology 189:285.*
19. Akira, S., H. Isshiki, T. Sugita, O. Tanabe, S. Kinoshita, Y. Nishio, T. Nakajima, T. Hirano, and T. Kishimoto. 1990. A nuclear factor for IL-6 expression (NF-IL6) is a member of a C/EBP family. *Embo J 9:1897.*
20. Roy, S. K., S. J. Wachira, X. Weihua, J. Hu, and D. V. Kalvakolanu. 2000. CCAAT/enhancer-binding protein-beta regulates interferon-induced transcription through a novel element. *J Biol Chem 275:12626.*
21. Roy, S. K., J. D. Shuman, L. C. Platanias, P. S. Shapiro, S. P. Reddy, P. F. Johnson, and D. V. Kalvakolanu. 2005. A role for mixed lineage kinases in regulating transcription factor CCAAT/enhancer-binding protein-{beta}-dependent gene expression in response to interferon-{gamma}. *J Biol Chem 280:24462.*
22. Kalvakolanu, D. V., and S. K. Roy. 2005. CCAAT/enhancer binding proteins and interferon signaling pathways. *J Interferon Cytokine Res 25:757.*
23. Yin, M., S. Q. Yang, H. Z. Lin, M. D. Lane, S. Chatterjee, and A. M. Diehl. 1996. Tumor necrosis factor alpha promotes nuclear localization of cytokine-inducible CCAAT/enhancer binding protein isoforms in hepatocytes. *J Biol Chem 271:17974.*
24. Pizarro-Cerda, J., M. Desjardins, E. Moreno, S. Akira, and J. P. Gorvel. 1999. Modulation of endocytosis in nuclear factor IL-6(-/-) macrophages is responsible for a high susceptibility to intracellular bacterial infection. *J Immunol 162:3519.*
25. Sugawara, I., S. Mizuno, H. Yamada, M. Matsumoto, and S. Akira. 2001. Disruption of nuclear factor-interleukin-6, a transcription factor, results in severe mycobacterial infection. *Am J Pathol 158:361.*
26. Screpanti, I., L. Romani, P. Musiani, A. Modesti, E. Fattori, D. Lazzaro, C. Sellitto, S. Scarpa, D. Bellavia, G. Lattanzio, and et al. 1995. Lymphoproliferative disorder and imbalanced T-helper response in C/EBP beta-deficient mice. *Embo J 14:1932.*
27. Gorgoni, B., D. Maritano, P. Marthyn, M. Righi, and V. Poli. 2002. C/EBP beta gene inactivation causes both impaired and enhanced gene expression and inverse regulation of IL-12 p40 and p35 mRNAs in macrophages. *J Immunol 168:4055.*
28. Matsumoto, M., T. Tanaka, T. Kaisho, H. Sanjo, N. G. Copeland, D. J. Gilbert, N. A. Jenkins, and S. Akira. 1999. A novel LPS-inducible C-type lectin is a transcriptional target of NF-IL6 in macrophages. *J Immunol 163:5039.*
29. Weihua, X., J. Hu, S. K. Roy, S. B. Mannino, and D. V. Kalvakolanu. 2000. Interleukin-6 modulates interferon-regulated gene expression by inducing the ISGF3 gamma gene using CCAAT/enhancer binding protein-beta(C/EBP-beta). *Biochim Biophys Acta 1492:163.*
30. Quackenbush, J. 2001. Computational analysis of microarray data. *Nat Rev Genet 2:418.*
31. Churchill, G. A. 2002. Fundamentals of experimental design for cDNA microarrays. *Nat Genet 32 Suppl:490.*
32. Xiao, W., L. Wang, X. Yang, T. Chen, D. Hodge, P. F. Johnson, and W. Farrar. 2001. CCAAT/enhancer-binding protein beta mediates interferon-gamma-induced p48 (ISGF3-gamma ) gene transcription in human monocytic cells. *J Biol Chem 276:23275.*
33. Kilpatrick, L. E., J. Y. Lee, K. M. Haines, D. E. Campbell, K. E. Sullivan, and H. M. Korchak. 2002. A role for PKC-delta and PI 3-kinase in TNF-alpha-mediated antiapoptotic signaling in the human neutrophil. *Am J Physiol Cell Physiol 283:C48.*
34. Page, K., J. Li, K. C. Corbit, K. M. Rumilla, J. W. Soh, I. B. Weinstein, C. Albanese, R. G. Pestell, M. R. Rosner, and M. B. Hershenson. 2002. Regulation of airway

smooth muscle cyclin D1 transcription by protein kinase C-delta. *Am J Respir Cell Mol Biol 27:204.*

35. Page, K., J. Li, L. Zhou, S. Iasvovskaia, K. C. Corbit, J. W. Soh, I. B. Weinstein, A. R. Brasier, A. Lin, and M. B. Hershenson. 2003. Regulation of airway epithelial cell NF-kappa B-dependent gene expression by protein kinase C delta. *J Immunol 170:5681.*
36. You, H. J., J. W. Lee, Y. J. Yoo, and J. H. Kim. 2004. A pathway involving protein kinase Cdelta up-regulates cytosolic phospholipase A(2)alpha in airway epithelium. *Biochem Biophys Res Commun 321:657.*
37. Novotny-Diermayr, V., T. Zhang, L. Gu, and X. Cao. 2002. Protein kinase C delta associates with the interleukin-6 receptor subunit glycoprotein (gp) 130 via Stat3 and enhances Stat3-gp130 interaction. *J Biol Chem 277:49134.*
38. Deb, D. K., A. Sassano, F. Lekmine, B. Majchrzak, A. Verma, S. Kambhampati, S. Uddin, A. Rahman, E. N. Fish, and L. C. Platanias. 2003. Activation of protein kinase C delta by IFN-gamma. *J Immunol 171:267.*
39. Uddin, S., and L. C. Platanias. 2004. Mechanisms of type-I interferon signal transduction. *J Biochem Mol Biol 37:635.*
40. Xu, B., A. Bhattacharjee, B. Roy, G. M. Feldman, and M. K. Cathcart. 2004. Role of protein kinase C isoforms in the regulation of interleukin-13-induced 15-lipoxygenase gene expression in human monocytes. *J Biol Chem 279:15954.*
41. Yamamori, T., O. Inanami, H. Nagahata, and M. Kuwabara. 2004. Phosphoinositide 3-kinase regulates the phosphorylation of NADPH oxidase component p47(phox) by controlling cPKC/PKCdelta but not Akt. *Biochem Biophys Res Commun 316:720.*
42. Zhao, X., B. Xu, A. Bhattacharjee, C. M. Oldfield, F. B. Wientjes, G. M. Feldman, and M. K. Cathcart. 2005. Protein kinase Cdelta regulates p67phox phosphorylation in human monocytes. *J Leukoc Biol 77:414.*
43. Bey, E. A., B. Xu, A. Bhattacharjee, C. M. Oldfield, X. Zhao, Q. Li, V. Subbulakshmi, G. M. Feldman, F. B. Wientjes, and M. K. Cathcart. 2004. Protein kinase C delta is required for p47phox phosphorylation and translocation in activated human monocytes. *J Immunol 173:5730.*
44. Steinberg, S. F. 2004. Distinctive activation mechanisms and functions for protein kinase Cdelta. *Biochem J 384:449.*
45. Wadsworth, S. J., and H. Goldfine. 2002. Mobilization of protein kinase C in macrophages induced by Listeria monocytogenes affects its internalization and escape from the phagosome. *Infect Immun 70:4650.*
46. Goldfine, H., S. J. Wadsworth, and N. C. Johnston. 2000. Activation of host phospholipases C and D in macrophages after infection with Listeria monocytogenes. *Infect Immun 68:5735.*
47. Miyamoto, A., K. Nakayama, H. Imaki, S. Hirose, Y. Jiang, M. Abe, T. Tsukiyama, H. Nagahama, S. Ohno, S. Hatakeyama, and K. I. Nakayama. 2002. Increased proliferation of B cells and auto-immunity in mice lacking protein kinase Cdelta. *Nature 416:865.*
48. Tapia, J. A., R. T. Jensen, and L. J. Garcia-Marin. 2006. Rottlerin inhibits stimulated enzymatic secretion and several intracellular signaling transduction pathways in pancreatic acinar cells by a non-PKC-delta-dependent mechanism. *Biochim Biophys Acta 1763:25.*
49. Davies, S. P., H. Reddy, M. Caivano, and P. Cohen. 2000. Specificity and mechanism of action of some commonly used protein kinase inhibitors. *Biochem J 351:95.*
50. Wadsworth, S. J., and H. Goldfine. 1999. Listeria monocytogenes phospholipase C-dependent calcium signaling modulates bacterial entry into J774 macrophage-like cells. *Infect Immun 67:1770.*

51. Myers, J. T., A. W. Tsang, and J. A. Swanson. 2003. Localized reactive oxygen and nitrogen intermediates inhibit escape of Listeria monocytogenes from vacuoles in activated macrophages. *J Immunol 171:5447.*
52. Prada-Delgado, A., E. Carrasco-Marin, G. M. Bokoch, and C. Alvarez-Dominguez. 2001. Interferon-gamma listericidal action is mediated by novel Rab5a functions at the phagosomal environment. *J Biol Chem 276:19059.*
53. Alvarez-Dominguez, C., and P. D. Stahl. 1999. Increased expression of Rab5a correlates directly with accelerated maturation of Listeria monocytogenes phagosomes. *J Biol Chem 274:11459.*
54. Uddin, S., A. Sassano, D. K. Deb, A. Verma, B. Majchrzak, A. Rahman, A. B. Malik, E. N. Fish, and L. C. Platanias. 2002. Protein kinase C-delta (PKC-delta ) is activated by type I interferons and mediates phosphorylation of Stat1 on serine 727. *J Biol Chem 277:14408.*
55. Jackson, D. N., and D. A. Foster. 2004. The enigmatic protein kinase Cdelta: complex roles in cell proliferation and survival. *Faseb J 18:627.*
56. Gschwendt, M. 1999. Protein kinase C delta. *Eur J Biochem 259:555.*
57. Ueda, Y., S. Hirai, S. Osada, A. Suzuki, K. Mizuno, and S. Ohno. 1996. Protein kinase C activates the MEK-ERK pathway in a manner independent of Ras and dependent on Raf. *J Biol Chem 271:23512.*
58. Roy, S. K., J. Hu, Q. Meng, Y. Xia, P. S. Shapiro, S. P. Reddy, L. C. Platanias, D. J. Lindner, P. F. Johnson, C. Pritchard, G. Pages, J. Pouyssegur, and D. V. Kalvakolanu. 2002. MEKK1 plays a critical role in activating the transcription factor C/EBP-beta-dependent gene expression in response to IFN-gamma. *Proc Natl Acad Sci U S A 99:7945.*

# CHAPTER 7

## CONCLUSION

The current study addressed the hypothesis that macrophages have an alternative killing mechanism that is independent of superoxide and nitric oxide (1-3) but dependent on IFN-γ (4-6), TNF (7, 8) and C/EBPβ$^{-/-}$ (9). Since the mechanism and the genes involved in this alternative pathway are largely unknown, the aim of this dissertation was to identify these macrophage effector genes and to functionally characterize their role during infection by utilizing gene deficient mouse models.

In the current study, *L. monocytogenes* was used as a model intracellular pathogen for *in vitro* infection of IFN-γ activated bone marrow derived macrophages in order to identify the genes involved in mediating macrophage bactericidal effector activity. In IFN-γ activated macrophages infected with *L. monocytogenes*, IFN-γ and TNF signalling converge on C/EBPβ promoting its transcription, activation and translocation to the nucleus resulting in the transcription of genes required for confinement of *L. monocytogenes* within the phagosome (10-14). Since C/EBPβ$^{-/-}$ mice expressed normal levels of IFN-γ and TNF (9) during *L. monocytogenes* infection, the macrophage effector genes involved in confinement and killing of *L. monocytogenes* were postulated to be downstream of C/EBPβ. Furthermore, comparison between the gene expression profiles of WT and C/EBPβ$^{-/-}$ macrophages infected with *L. monocytogenes* was hypothesized to increase the probability of identifying these effector genes, which would be differentially expressed between the two groups. Comparative gene expression profiling by DNA microarrays between *L. monocytogenes* infected WT and C/EBPβ$^{-/-}$ macrophages, successfully identified 1268 genes to be differentially expressed between the two groups. A focussed functional clustering strategy reduced the number of candidate genes to 220, which were enriched for genes already published to play a protective or detrimental role during role *L. monocytogenes* infections, thereby validating the success of the microarray and data mining strategy.

PKCδ was selected as the prime candidate gene for further study since it possessed all the postulated criteria of a macrophage effector gene. To date, the role of PKCδ in innate immunity to intracellular pathogens has only been investigated by one group, which indirectly demonstrated that PKCδ promoted phagosomal escape (15, 16). However, no evidence showing a direct correlation between PKCδ activity and listerial phagosomal escape was

reported. Moreover, PKCδ phosphorylation of C/EBPβ was shown to negatively regulate the transcription factor's transcriptional activity (17). Furthermore, since PKCδ was up-regulated in *L. monocytogenes*-infected C/EBPβ$^{-/-}$ macrophages as compared to WT, as shown by microarray and confirmed by RT-PCR, it was therefore postulated that up-regulation PKCδ may be detrimental during *L. monocytogenes* infection.

This dissertation provides novel insight into role of PKCδ during innate immunity against *L. monocytogenes*. Functional studies using the PKCδ$^{-/-}$ mouse model uncovered a novel protective role, rather than a detrimental role, for PKCδ in innate immunity against *L monocytogenes*. Data in the current study clearly showed that PKCδ was indispensable for confinement of *L. monocytogenes* within the phagosome, since no other PKC isoform compensated for it in the PKCδ$^{-/-}$ macrophages. The enhanced listerial escape and impaired listericidal activity, despite full macrophage activation and production of nitric oxide, resulted in uncontrolled bacterial growth and dissemination of *L. monocytogenes*, which ultimately led to early death of the PKCδ$^{-/-}$ mice. Furthermore, a systems biology approach was used to investigate the mechanism whereby PKCδ confined *L. monocytogenes* within macrophage phagosomes. It was hypothesized that PKCδ may play a role in the alternative killing mechanism that is independent of superoxide and nitric oxide (1-3) that was first observed in the IFN-γ$^{-/-}$ (4, 5), IFN-γR$^{-/-}$ (5, 6), TNFRp55$^{-/-}$ (7, 8), and C/EBPβ$^{-/-}$ (9) mice. It was envisaged that PKCδ may synergize with G-CSF to activate Rab5a, by promoting the activity of Agtr1a and the Rabep1:Rabgef1 protein complex, and by inhibiting the Rab5a-supressing activity of Tsc2 and Rasa1. Once activated, Rab5a was then able to promote phagosome maturation, phago-lysosome fusion and consequent bacterial killing. Moreover, activated Rab5a has been shown to stimulate Rac2-mediated recruitment, assembly and activation of phagocyte NADPH oxidase at the phagosome membrane, resulting in localized release of superoxide into the phagosome. The concerted action of PKCδ in promoting the localized release of superoxide into the phagosome coupled together with its activation of C/EBPβ and Rab5a, may therefore augment the confinement of the *L. monocytogenes* bacilli within the phagosome and consequent phago-lysosome mediated listericidal activity. Alternatively, PKCδ may function only to activate C/EBPβ transcriptional activity, thereby augmenting C/EBPβ mediated endocytosis and phago-lysosome fusion (18). However, since the PKCδ$^{-/-}$ mice were not as susceptible as IFN-γR$^{-/-}$, RelB, TNFRp55$^{-/-}$ or C/EBPβ$^{-/-}$ mice, PKCδ may not in fact be part of the hypothetical RNI/ROI-independent alternative killing pathway. Instead PKCδ may act in parallel with the hypothetical RNI/ROI-independent alternative

killing pathway to enhance confinement of the bacilli within the phagosome. For example, PKCδ may confine the *L. monocytogenes* within phagosomes by activating and/or synergize with, as yet, unidentified proteins to neutralize that activity of listerial LLO and PI-PLC.

The research undertaken in this dissertation has successfully fulfilled the aims set out at the beginning of the study. Comparative DNA microarray gene expression profiling between infected WT and C/EBPβ$^{-/-}$ macrophages, integrated with a focussed functional clustering strategy, successfully identified candidate genes involved in macrophage effector activity against *L. monocytogenes*. Furthermore, functional characterization of one of these candidate genes, PKCδ, validated and uncovered a novel protective role for PKCδ during *L. monocytogenes* infection, thereby adding new insight into the role of PKCδ during innate immunity to *L. monocytogenes*.

## REFERENCES


1. Endres, R., A. Luz, H. Schulze, H. Neubauer, A. Futterer, S. M. Holland, H. Wagner, and K. Pfeffer. 1997. Listeriosis in p47(phox-/-) and TRp55-/- mice: protection despite absence of ROI and susceptibility despite presence of RNI. *Immunity 7:419.*
2. Dinauer, M. C., M. B. Deck, and E. R. Unanue. 1997. Mice lacking reduced nicotinamide adenine dinucleotide phosphate oxidase activity show increased susceptibility to early infection with Listeria monocytogenes. *J Immunol 158:5581.*
3. Shiloh, M. U., J. D. MacMicking, S. Nicholson, J. E. Brause, S. Potter, M. Marino, F. Fang, M. Dinauer, and C. Nathan. 1999. Phenotype of mice and macrophages deficient in both phagocyte oxidase and inducible nitric oxide synthase. *Immunity 10:29.*
4. Harty, J. T., and M. J. Bevan. 1995. Specific immunity to Listeria monocytogenes in the absence of IFN gamma. *Immunity 3:109.*
5. Huang, S., W. Hendriks, A. Althage, S. Hemmi, H. Bluethmann, R. Kamijo, J. Vilcek, R. M. Zinkernagel, and M. Aguet. 1993. Immune response in mice that lack the interferon-gamma receptor. *Science 259:1742.*
6. Dai, W. J., W. Bartens, G. Kohler, M. Hufnagel, M. Kopf, and F. Brombacher. 1997. Impaired macrophage listericidal and cytokine activities are responsible for the rapid death of Listeria monocytogenes-infected IFN-gamma receptor-deficient mice. *J Immunol 158:5297.*
7. Pfeffer, K., T. Matsuyama, T. M. Kundig, A. Wakeham, K. Kishihara, A. Shahinian, K. Wiegmann, P. S. Ohashi, M. Kronke, and T. W. Mak. 1993. Mice deficient for the 55 kd tumor necrosis factor receptor are resistant to endotoxic shock, yet succumb to L. monocytogenes infection. *Cell 73:457.*
8. Rothe, J., W. Lesslauer, H. Lotscher, Y. Lang, P. Koebel, F. Kontgen, A. Althage, R. Zinkernagel, M. Steinmetz, and H. Bluethmann. 1993. Mice lacking the tumour necrosis factor receptor 1 are resistant to TNF-mediated toxicity but highly susceptible to infection by Listeria monocytogenes. *Nature 364:798.*
9. Tanaka, T., S. Akira, K. Yoshida, M. Umemoto, Y. Yoneda, N. Shirafuji, H. Fujiwara, S. Suematsu, N. Yoshida, and T. Kishimoto. 1995. Targeted disruption of the NF-IL6 gene discloses its essential role in bacteria killing and tumor cytotoxicity by macrophages. *Cell 80:353.*
10. Akira, S., H. Isshiki, T. Sugita, O. Tanabe, S. Kinoshita, Y. Nishio, T. Nakajima, T. Hirano, and T. Kishimoto. 1990. A nuclear factor for IL-6 expression (NF-IL6) is a member of a C/EBP family. *Embo J 9:1897.*
11. Roy, S. K., S. J. Wachira, X. Weihua, J. Hu, and D. V. Kalvakolanu. 2000. CCAAT/enhancer-binding protein-beta regulates interferon-induced transcription through a novel element. *J Biol Chem 275:12626.*
12. Roy, S. K., J. D. Shuman, L. C. Platanias, P. S. Shapiro, S. P. Reddy, P. F. Johnson, and D. V. Kalvakolanu. 2005. A role for mixed lineage kinases in regulating transcription factor CCAAT/enhancer-binding protein-{beta}-dependent gene expression in response to interferon-{gamma}. *J Biol Chem 280:24462.*
13. Kalvakolanu, D. V., and S. K. Roy. 2005. CCAAT/enhancer binding proteins and interferon signaling pathways. *J Interferon Cytokine Res 25:757.*
14. Yin, M., S. Q. Yang, H. Z. Lin, M. D. Lane, S. Chatterjee, and A. M. Diehl. 1996. Tumor necrosis factor alpha promotes nuclear localization of cytokine-inducible CCAAT/enhancer binding protein isoforms in hepatocytes. *J Biol Chem 271:17974.*
15. Wadsworth, S. J., and H. Goldfine. 2002. Mobilization of protein kinase C in macrophages induced by Listeria monocytogenes affects its internalization and escape from the phagosome. *Infect Immun 70:4650.*

16. Goldfine, H., S. J. Wadsworth, and N. C. Johnston. 2000. Activation of host phospholipases C and D in macrophages after infection with Listeria monocytogenes. *Infect Immun 68:5735.*
17. Miyamoto, A., K. Nakayama, H. Imaki, S. Hirose, Y. Jiang, M. Abe, T. Tsukiyama, H. Nagahama, S. Ohno, S. Hatakeyama, and K. I. Nakayama. 2002. Increased proliferation of B cells and auto-immunity in mice lacking protein kinase Cdelta. *Nature 416:865.*
18. Pizarro-Cerda, J., M. Desjardins, E. Moreno, S. Akira, and J. P. Gorvel. 1999. Modulation of endocytosis in nuclear factor IL-6(-/-) macrophages is responsible for a high susceptibility to intracellular bacterial infection. *J Immunol 162:3519.*

## CHAPTER 8

## FUTURE PERSPECTIVES

Currently, the mechanism whereby PKCδ confines *L. monocytogenes* within phagosomes is being investigated. In addition, the putative positive regulation of C/EBPβ by PKCδ and the negative regulation of PKCδ activation by *L. monocytogenes* are also being explored. In addition to PKCδ, several other genes were identified by the microarray and data mining strategy as putative macrophage effector genes. Among these, Rabgef1, PKCβII and the very low density lipoprotein receptor (VLDLR) were selected for further study. Ragbef1 was down-regulated 0.76 fold in the C/EBPβ$^{-/-}$ macrophages as compared to WT. *In vitro* infection studies reported that *L. monocytogenes* suppressed Rab5a function by preventing the exchange of GDP for GTP and that this inhibition by most likely mediated through modulation of Rab5a GEFs (1). However, this premise has never been tested *in vivo* using the Rabgef1 gene deficient mouse model. Similarly, although PKCβII was not differentially expressed between the infected WT and C/EBPβ$^{-/-}$, its putative role in promoting *L. monocytogenes* phagosomal escape (2) has never been validated *in vivo* using the PKCβII$^{-/-}$ mouse model. The very low density lipoprotein receptor (VLDLR), which is important for uptake and metabolism of cholesterol, was down-regulated 0.89 fold respectively in the C/EBPβ$^{-/-}$ macrophages as compared to WT. VLDL binds cholesterol and the uptake of VLDL-bound cholesterol into cells occurs via VLDLR-mediated endocytosis which trafficks the VLDL-bound cholesterol to lysosomes. Enzymatic degradation of the lipoprotein within the lysosome releases the cholesterol, which then represses the activity of microsomal enzyme 3-hydroxy-3-methylglutaryl coenzyme A (HMG CoA) reductase, the major enzyme involved in cholesterol synthesis (3, 4). Although no role was found in the literature for VLDLR during *L. monocytogenes* infection, it can be envisaged that the pathogen may down-regulate the VLDLR gene, since its survival depends on phagosomal escape mediated predominantly by LLO, the activity of which is dependent on cholesterol. Functional studies uncovering and validating the roles of these additional genes in *L. monocytogenes* infections will be implemented utilizing their respective gene deficient mouse models.

## REFERENCES


1. Prada-Delgado, A., E. Carrasco-Marin, C. Pena-Macarro, E. Del Cerro-Vadillo, M. Fresno-Escudero, F. Leyva-Cobian, and C. Alvarez-Dominguez. 2005. Inhibition of Rab5a exchange activity is a key step for Listeria monocytogenes survival. *Traffic 6:252.*

2. Wadsworth, S. J., and H. Goldfine. 2002. Mobilization of protein kinase C in macrophages induced by Listeria monocytogenes affects its internalization and escape from the phagosome. *Infect Immun 70:4650.*

3. Wu, M. K., and D. E. Cohen. 2005. Altered hepatic cholesterol metabolism compensates for disruption of phosphatidylcholine transfer protein in mice. *Am J Physiol Gastrointest Liver Physiol 289:G456.*

4. Gene. http://www.ncbi.nlm.nih.gov/entrez/query.fcgi?db=gene.